ENGINEERING GEOLOGICAL CHARACTERISATION OF THE TORLESSE COMPOSITE TERRANE IN CANTERBURY, NEW ZEALAND WITH REFERENCE TO MECHANISED TUNNELLING

A thesis

submitted in partial fulfilment of the requirements for the degree of

Master of Science in Engineering Geology

at the

University of Canterbury

by

ADAM GRANT IRVINE

2013

UNIVERSITY OF CANTERBURY

Te Whare Wānanga o Waitaha

CHRISTCHURCH NEW ZEALAND

UNIVERSITY OF CANTERBURY

Abstract

The Torlesse composite terrane is an important geological unit in Canterbury, New Zealand, making up the backbone of the Southern Alps. It consists of a large group of rock that exhibits a range of engineering geological conditions. This study has been undertaken to characterise the range in engineering geological conditions throughout the Torlesse of Canterbury in order to develop a rock mass classification scheme specific to this abundant and complex rock type. The classification is aimed to aid in TBM tunnelling assessment in the Torlesse, which enables sub-division of an area or tunnel alignment into rock mass domains. Furthermore the classification enables the prediction of rock masses through geological controls in areas of poor outcrop coverage.

Four sites throughout Canterbury were selected for mapping to represent Torlesse terrane types, metamorphic facies and a range of regional fault settings: the Elliott Fault, Hurunui River, Ashley River Gorge and Opuha Dam. A preliminary desktop study was carried out with a landscape lineation analysis to develop 1) a conceptual geological model at each study site and 2) field mapping sheets to provide a check list to ensure consistency of information collected between outcrops and sites. Lineations and conceptual models identified a series of structural blocks within sites, which were further validated by field mapping. Outcrop field mapping was carried out across selected extents of study sites using the field sheets from the desktop study. Using NZGS (2005) and ISRM (1978) derived parameters, rock mass characteristics, including lithology and defect information, were recorded on the field sheets. A laboratory testing programme on selected outcrop intact rock was undertaken to support field work and later classification development.

Data from field work was plotted to derive rock mass trends. Trends were used to develop a classification framework. It was found the rock mass could be defined by bedding thickness, degree of fracture and the combination of discontinuities such as persistent jointing and shearing, which defined dominant rock mass control. The rock mass could therefore be classified based on: blockiness, defined by bedding thickness and density of non-systematic jointing (fractures); and defect structure, defined by the combination of systematic discontinuities such as persistent jointing and shearing.

The two principle rock mass governing controls were related together on an XY plot to form the conceptual Torlesse rock mass classification (TRC). Six classes encompassing the range of conditions observed in the Torlesse were devised for blockiness and defect structure. Blockiness classes range from: thickly bedded to massive sandstone with slight to moderate fracture, to very thin to thin bedded sandstone that is fragmented. Defect structure classes range from rock masses defined by: dominant systematic, persistent jointing with rare faulting, to rock masses typical of major shear zones, where material geotechnically behaves as a soil with no principle defect sets. Individual outcrop plotting then allowed rock masses typical of each site to be grouped on the TRC.

Clusters of each study sites' outcrops were overlaid to characterise all rock mass types observed throughout this research. This allowed representative identification of eight distinctive rock mass types (Types 1-8) that are indicative of the Torlesse composite terrane of Canterbury. Each type has a series of geological controls that influence the nature of the rock mass. Geological controls can aid in the prediction of rock mass conditions for tunnel alignment selection. The alignment can be divided into rock mass types to allow preliminary assessment of tunnelling conditions.

Lithostructure and proximity to major structures were defined as major rock mass type controls. Lithostructure defines the effect of lithology on bedding thickness and fracturing by non-systematic jointing. Medium to massive bedding as part of rock mass Types 1 and 2 result in the best rock mass. In the sandstone-rich rock mass, systematic jointing dominates with less shearing and faulting and a lower occurrence of short, discrete, non-systematic jointing. Conversely, the thinly bedded Torlesse represented by rock mass Type 5 lacks persistent jointing. This type, being mudstone dominant, fractures more easily, is characterised by short, discrete jointing, and tends to localise faulting, shearing and some folding. Modern tectonic stress fields are also a major control. The size of the tectonic structure can impact different volumes of rock. Rock outside the direct fault zone can also be impacted giving rise to rock mass Type 6. For example, increased levels of shearing are observed in adjacent rock at both the Elliott and Opuha Dam Faults. Rock mass Types 7 and 8 represent the rock masses directly affected by large tectonic structures.

Sub-dividing proposed tunnel alignments by rock mass type allows assessment of tunnelling parameters. Rock mass Types 1 and 2 are expected to represent the best rock mass stability but will be the hardest to excavate. As a result rock bolt, mesh and shotcrete will likely prevent significant block failure through gravity. Rock mass Types 3 and 4 are expected to represent a favourably interlocked rock mass, resulting in an increased penetration rate but whose advance rate is likely to be hindered by the need for more extensive support. Rock mass Types 5-8 are likely to present the worst rock mass conditions. Penetration rates will be high but advance rates are expected to be low, hindered by extensive support installation and the potential need for ground pre-treatment in rock mass Type 8, prior to excavation. Significant potential for failure exists in the poorer rock mass types without adequate support, including running ground. The selection of a shielded or gripper TBM will depend on the proportion and lengths of each TRC rock mass type anticipated along a tunnel alignment.

The opportunity exists for future work to refine and validate the TRC classification through increased data input, more extensive laboratory testing and its application to tunnelling projects. Furthermore it is hoped the TRC can be used for other types of geotechnical applications, at a variety of scales where Torlesse is concerned. To do this the TRC interpretations with respect to rock mass behaviour must be adapted to different scales.

Table of Contents

List of Figures

List of Tables

Acknowledgements

First and foremost I would like to thank Mark Eggers and Marlene Villeneuve. Your continued guidance and support throughout this journey has been invaluable. Thank you for both going out of your way to help with fieldwork, countless discussions, impromptu drop in questions and endless editing despite your busy schedules. I am eternally grateful for your time spent helping me in all aspects of this thesis. Without you guys this thesis would not be at the stage it is at today so a massive thank you. I'd also like to give a huge thanks to David Bell for continued help and discussion throughout this thesis. Your love and passion for the discipline of engineering geology is truly inspiring.

Words cannot express how grateful I am to Emma Griffen. Thank you for giving up your time and taking leave from work to come and wander the hills with me to look at rocks. An even bigger thank you for the countless times you gave up your weekends and nights to help me out. Your GIS and proof reading help has been invaluable and I would not be at the stage I am today without your help. Thank you.

Financial support throughout this thesis has been provided by Pells Sullivan Meynink (PSM) Engineering Consultants, Fraser Geologics (Maurice Fraser) and Integrated Water. Without their presence and support this thesis would not exist. Thank you for giving me the opportunity to carry out this thesis in such an exciting field.

I'd also like to thank the technical staff within the Geology Department at the University of Canterbury, specifically Sacha Baldwin-Cunningham, Cathy Higgins, Rob Spiers, Chris Grimshaw and Stephen Brown. Your help on all aspects of field work and lab testing has been heavily appreciated. You guys are the best!

Thank you to the Department of Conservation for the use of aerial photography. Without it, aspects of this thesis could not be completed. It proved an invaluable resource.

To all my colleagues, friends, flatmates and family, thank you for putting up with me over this incredible journey. It's been a rollercoaster of a ride but I've loved every minute. Thanks for providing endless support and good yarns. Without you guys I would have gone insane and refused to look at another piece or outcrop of Torlesse again. Cheers!

Chapter 1 Introduction

1.1 Context and objectives

This thesis seeks to investigate the engineering geological condition of the Torlesse Composite Terrane of Canterbury, New Zealand. The purpose of the study is to characterise the Torlesse such that the rock mass conditions can be assessed. An outcome of the study is a classification scheme which will provide the framework for investigation and prediction of the Torlesse terrane for mechanised tunnelling. This knowledge will inevitably aid in tunnel selection, specification and design.

Primary objectives of this thesis are to:

- characterise the range of engineering geological conditions expected to be encountered within the Torlesse Composite Terrane of Canterbury, New Zealand
- develop a classification whereby rock mass condition can be assessed
- develop specific engineering geological rock mass types where tunnelling implications can be evaluated
- comment on tunnelling implications.

To meet these objectives engineering geological mapping of outcrops was conducted across four geologically distinctive Torlesse terrane sites across Canterbury; the Elliott Fault, Hurunui River, Ashley River Gorge and Opuha Dam. Data from observational mapping were analysed and the resulting trends were used to develop a conceptual classification diagram from herein to be known as the Torlesse rock mass classification (TRC). A subsequent laboratory programme was developed to help define rock mass character for the TRC and study site locations. Plotting of outcrop data onto the TRC enabled the development of a series of engineering geological rock mass types that enable comment on tunnelling and rock mass conditions. Information gained as a result of this study will also provide a framework and a starting point for future studies to assess rock mass conditions both within the Torlesse rock and other geological settings outside the scope of this study.

1.2 Background

The Torlesse Composite Terrane rock of New Zealand's South Island makes up the backbone of the Southern Alps (Figure 1.1). It consists of a large group of rock whose engineering geological conditions range substantially between localities. The variability in conditions presents a challenge to any engineering projects where Torlesse is involved. It is therefore surprising little work has been published to classify the range in conditions and provide a model whereby rock mass conditions can be adequately assessed.

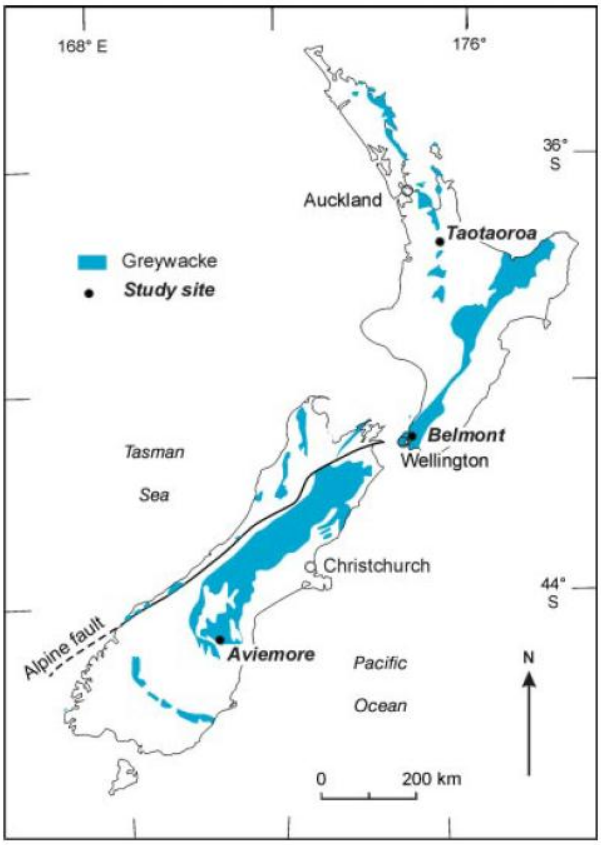

Figure 1.1: Spatial extent of New Zealand's Torlesse Composite Terrane from Read et al. (2000) after Suggate et al. (1978).

Historically tunnelling in Torlesse Composite Terrane in New Zealand has been carried out using traditional drill and blast techniques. Of these tunnels little information has been documented or is readily available. The use of a Tunnel Boring Machine (TBM) represents an opportunity to improve production rates thereby saving time, costs and adding value to projects.

To assess mechanised methods as a viable tunnelling option, the geological setting and rock mass characteristics, including the variability over a larger area than any proposed alignment, must be understood. Mapping of outcrops can provide information that can be applied at depth in context with the geological setting as part of a tunnelling assessment using a rock mass model formulated on the basis of lithostratigraphy and structural style. Furthermore such mapping can provide fast, efficient information across a large area without having to rely on early deployment of specific sub-surface forms of investigation such as drilling boreholes, pilot tunnels or geophysics.

Effectively classifying the rock mass into a series of rock mass types and domains based on lithostratigraphic and structural characteristics can aid in tunnelling projects. Individual rock mass types are used to evaluate which mechanised tunnelling options are most suitable. Furthermore the information gained can enable designers to make preliminary decisions regarding equipment specification, such as gripper design and waste rock disposal. This information is crucial to any mechanised tunnelling project.

At present little information is available that characterises rock mass conditions within the Torlesse suite of rocks. Current classifications typically utilize the Geological Strength Index classification after Hoek et al. (1995) to distinguish domains. The development of a Torlesse-specific classification scheme to characterise the suite of rocks will provide information for the assessment of mechanised tunnelling. The information gained from this research will be invaluable for future tunnelling projects.

1.3 Methodology

1.3.1 Desktop study

Prior to conducting field work a desktop study was carried out in association with a landscape lineation study to develop 1) conceptual geological models and 2) field sheets to record information in the field (Appendix A).

The lineation analysis was carried using a 25m DEM model in conjunction with aerial photography to identify lineations in the landscape. The aim of this analysis was to identify potential faults that could run through the study areas and create changes in the rock mass. Such practices are widely used in assessing regional structure and seismic hazard (Rahiman and Pettinga, 2008, Cortes et al., 1998, Braun, 1982, Boyer and McQueen, 1964, Haman, 1961, Koike et al., 1995, Caran et al., 1982). Rahiman and Pettinga (2008) show that lineaments within the landscape are largely a reflection of intense tectonic fracturing that are emphasised on the ground surface through weathering and erosion process creating topography, drainage patterns and vegetation anomalies. They go on to state such an approach can effectively characterise regional structural patterns providing better understanding of structural and tectonic evolution. Whilst this study does not focus on providing a thorough lineation analysis it has been employed at a basic level to help distinguish and explain rock mass domains.

Conceptual geological models allow existing knowledge to be conveyed in a diagrammatic fashion. The models were constructed to test information gained in the field against existing information to derive structure and rock mass controls. A cross section was created across the extent of the study area. Using the current knowledge held by GNS (Forsyth et al., 2008, Rattenbury et al., 2006) cross sections were created incorporating all major geological information. All major faults and folds were incorporated in conjunction within the lineation study. The structure was inferred onto the cross section and the entirety of the area divided into blocks of expected rock mass. Due to the spatial extent of field areas this was only preformed on the larger field areas.

The aim of constructing the field sheets was to provide a check list and ensure consistency of information collected between outcrops and sites. NZGS (2005) was used as the primary field sheet development source. Information required from NZGS (2005) included weathering, strength, fabric, defect roughness, defect spacing, defect persistence and defect aperture. Using the NZGS (2005) field soil description terms, infill type, strength, thickness and moisture were described. Other information

required in the field was derived from internal documents from Pells Sullivan Meynink (PSM) (2010a, 2010b), after ISRM (1978) and included development of bedding, bedding thickness, degree of fracture, defect waviness (ILA – inter-limb angle and wavelength), defect end and defect termination. Bedding thickness and degree of fracture are important to this study. Bedding thickness in this study refers to the description given in Table 1.1 while, degree of fracture refers to descriptions given in Table 1.2. During mapping it was recorded in the field as the amount of breaks over a metre distance of typical rock.

Table 1.1: Bedding thickness (PSM, 2010b).

Term		Description	Separation of stratification planes
Stratification not recognisable		Massive	-
Stratification more than 20mm apart	Bedded	Very thickly bedded	>2m
		Thickly bedded	0.6 - 2m
		Medium bedded	0.2 - 0.6m
		Thinly bedded	60mm - 0.2m
		Very thinly bedded	20 - 60mm
Stratification planes less than 20mm apart	Laminated	Thickly laminated	6 - 20mm
		Thinly laminated	<6mm

Table 1.2: Degree of fracture (PSM, 2010a).

Descriptive term	Condition of freshly drilled core
Fragmented	The core is comprised primarily of fragments of less than 20 mm and mostly of width less than the core diameter. Generally >50 breaks/metre.
Highly Fractured	Core lengths are generally 20-40 mm with occasional fragments. Generally 25-50 breaks/meter.
Moderately Fractured	Core lengths are generally 30-100 mm with occasional shorter and longer section. Generally 10-30 breaks/metre.
Fractured	Core lengths are generally 80-400 mm with occasional shorter and longer sections. Generally 3-12 breaks/metre.
Slightly Fractured	Core lengths are generally 300-1000 mm with occasional shorter and longer sections. Generally 0-3 breaks/metre.
Unbroken	The core does not contain any natural breaks.

1.3.2 Approach to field mapping

The entirety of the field area was first surveyed to get an estimate of size, volume and the likely time taken to observe and record outcrops. Mapping was conducted at an outcrop scale with the purpose to cover large areas effectively. Mapping was not carried out using scanline techniques as in Cook (2001). Due to constraints only outcrops with relatively easy, safe access were examined. These tended to follow road cuts and river channels through each area. Once the area had been surveyed outcrops were chosen across the extent of the study site. Again constraints dictated what outcrops

could be observed and recorded. Accessibility to any one outcrop was a main constraint. Only outcrops that could be safely accessed were surveyed. From the accessible outcrops the accuracy of information collected dictated selection. Outcrops that were heavily weathered (to the extent defects and lithotypes were difficult to evaluate), dirty or whose height for example meant only limited accuracy, were generally left out of the analysis. Due to the relative time constraint and the need to cover all lithotypes if it was found one outcrop in close proximity to another exhibited very similar characteristics only one was surveyed. Larger outcrops and outcrops where conditions varied substantially (i.e. bedding thickness) were divided up into a series of separate outcrops. The outcrops share the same outcrop number but differ in survey point (i.e. 10a, 10b, 10c etc). Each is treated as its own entity. This enabled any one site to be characterised efficiently.

Each outcrop was surveyed at a distance. All major bedding, jointing, faulting, shearing and other features (i.e. veining) were identified. Once identified the defects character was recorded. Due to the heavy fracturing and need to adequately characterise rock at tunnel scales only surfaces greater than two metres in length were surveyed. Generally one defect from each set was evaluated to effectively characterise the rock over a large area. Typically this surface was dictated by accessibility and the accuracy of information collected as a result. Generally one bedding plane and one jointing plane from each major set were surveyed. Where faults and shears occur as entities each surface over the 2m criteria were surveyed. Other defects were observed to check the validity of the surveying surface. If other surfaces varied substantially in character than the one surveyed, they were in turn surveyed. If it was found all defects were relatively the same but varied to a small extent the average of all surfaces was used.

All surfaces surveyed were checked for infill material. This material included any material that was foreign to the surface. This does not include the obvious shearing a number of mudstone beds had undergone. Characteristics of the outcrop lithology were then examined including colour, lithology and grain size. Combining both defect structure and lithotypes then enabled an adequate characterisation of the outcrop rock mass. All outcrops were located spatially via GPS.

1.3.3 Sample selection

Intact rock was sampled per outcrop for laboratory testing. The aim was to get enough rock for Point Load, Unconfined Compressive Strength (UCS), Brazilian Tensile (BTS), Cerchar Abrasivity (CAI) and fines index testing of breccia and gouge to support the classification of all rock mass types. Each outcrop sampled was noted with the characteristics of that outcrop. Where an outcrop with similar characteristics was observed in close proximity (within 1-2 outcrops) to the original sampled outcrop, samples were not taken. However in more cases than not other factors deemed what rock could be sampled. Only enough rock that could be logistically handled was taken. Many outcrops were too weathered and fractured to obtain adequate rock for testing. Similarly rock for UCS, BTS and CAI

testing was governed primarily by fracture/joint spacing where an adequately sized block for coring could be pried from the outcrop face. In Torlesse this meant a heavy bias toward sandstone for sampling; however every effort was made to try and get a mudstone sample no matter the outcrop. Generally where outcrops needed to be surveyed but no adequately sized block could be sourced for coring; the outcrop was still sampled for point load. At least 5 rocks were sampled per outcrop for point load at random locations across the rock face. Every effort was made to include all lithologies within each outcrop, however in the case of the heavily fragmented mudstone this proved difficult.

Due to the importance of infilling and the need to adequately characterise this material nearly all infill material was sampled. In the case of the Elliott Fault where the whole site remains within a heavy brecciated/gouge zone each major outcrop was divided into a series of survey points where samples were taken. Sampling was rather in the form of bulk disturbed sampling, whereby breccia materials were disaggregated from the outcrop face, or via careful sampling of individual shear planes typically housing gouge. Bulk disturbed samples were typically reserved for major shears and fault zones where a mass of rock primarily acting as soil is present in large volumes. This material includes large greater than 1centimetre rock clasts in association with fines. Material sampled from individual planes was typically fine silt sized sediment such that there was no need to get a voluminous sample to characterise the fines content.

1.3.4 Laboratory work

Tests for both hard rock and fault rock were carried out with the aim to classify the material encountered. Information gained supported development of the TRC and provided information for comment on tunnelling and future works. Testing was performed to evaluate strength, abrasivity, mineralogy, grain shape and the relative size of infill and breccias observed.

Hard rock tests undertaken at the University of Canterbury included:

- Point Load Index testing
- Unconfined Compressive Strength (UCS)
- Brazilian Tensile Strength (BTS)
- Thin section analysis.

Hard rock was also sent to the Trilab laboratory in Brisbane, Australia for the following tests:

- Cerchar Abrasivity Index (CAI)
- P and S wave velocities to asses Young’s Modulus & Poisson Ratio
- Specific energy
- further UCS and BTS using remaining rock samples.

Table 1.3 displays the number of tests carried out per study site. Not enough rock could be cored from the Elliott Fault sample for Trilab testing, similarly not enough rock was available for UCS testing at the University of Canterbury after Ashley Gorge and Opuha Dam sample was sent to Trilab. Raw Trilab results are reproduced in Appendix B and discussed throughout Chapter 3 Site Results.

Table 1.3: Number of lab tests per study site.

	University of Canterbury						Trilab (Brisbane)			
	Point Load Outcrops	**UCS**	**BTS**	**Index**	**XRD**	**Thin Section**	**UCS**	**BTS**	**CAI**	**P & S wave**
Elliott Fault	21	4	30	14	8	3	-	-	-	-
Hurunui River	28	10	27	3	4	2	2	2	2	2
Ashley Gorge	17	-	18	5	7	2	1	2	2	1
Opuha Dam	15	-	16	8	8	2	1	1	1	1

Point load testing was carried using raw lump samples collected from the field. Rocks were point load tested using the suggested methods of Ulusay and Hudson (2007). Testing was carried out per outcrop site with up to 15 tests carried out. Where this was not possible due to poor rock samples, as many tests as possible up to 15 were carried out. The 15 tests per site include localities where more than one lithology was encountered. Generally a minimum of seven tests were undertaken on each lithology however this was often not possible in practice due to mudstone for example not registering results. Where anisotropy (i.e. bedding, banding or foliation) was present rock was point loaded perpendicular and parallel to the assumed plane of weakness. It must be noted however, point load index testing is considered invalid if a sample breaks along defects parallel to loading (Ulusay and Hudson, 2007). To define intact strength however both orientations were tested, however more so perpendicular to anisotropy to define proper intact strength as per accepted standards.

UCS and BTS samples were drilled from large intact rock specimens. Testing was employed to gauge intact strength. UCS and BTS were carried out under the Ulusay and Hudson (2007) suggested methods. Load was applied at 0.2kN/s which ensured failure within the suggested time frame described in Ulusay and Hudson (2007). Core was drilled at 50 mm diametres with sample diametre averaging 49.5 mm. Due to the nature and fracture pattern of the Torlesse core was drilled at 50 mm diametre rather than the widely accepted 54 mm diametre (Ulusay and Hudson, 2007). This minimised the likelihood of encountering sample defects, however in many cases core still fractured along existing defects during drilling. Core was cut to a 100 mm length for UCS to satisfy the 2:1 length diametre ratio outlined in Hendron (1968) to ensure uniform stress distribution. Again this differs from the accepted height to diametre ratio of 2.5-3.0 outlined in Ulusay and Hudson (2007), again employed to minimise the likelihood of sample breakage along existing defects. BTS core was

cut to 25 mm thickness, which is approximately equal to the specimen radius (Ulusay and Hudson, 2007).

Results for UCS and BTS were calculated and reported as MPa, while point load results were calculated and reported as $I_{s(50)}$ (MPa). Using outcrops where both UCS and Point Load testing were undertaken, a multiplier was assessed to allow UCS strength to be estimated where only point load samples could be sourced.

Core samples sent for external testing were cut by Trilab to test specification. BTS core was cut to about 35 mm and UCS to about 135 mm which was also used for P and S wave velocity testing.

To classify the fault rock, material was index tested to determine fines content. Bulk disturbed samples were wet sieved through a 4 mm, 2 mm, 1 mm and less than 1 mm passing. All material was dried in an oven at a constant temperature of 60°C as to not alter any clay mineralogy. Once the sample was completely dry it was weighed and the sediment size proportions obtained. Sediment <1mm in size was divided in half. High definition digital particle size analysis was undertaken on 50% of the sample to work out sediment fine proportions based primarily on particle size. The analysis was carried out using a Saturn DigiSizer II 5205 V1.01. As mentioned the relative size of individual gouge samples from shear planes generally had a large (>95%) fines content, thus there was no need to sieve this material.

To disaggregate the sample into separate particles (un-sieved gouge and oven dried material) Sodium Hexametaphosphate ($(NaPO_3)_6$) was added. Sodium Hexametaphosphate is widely used as a dispersion agent (Gee and Bauder, 1986) and was utilised in this instance to disaggregate the sample. The dispersant also prevented cohesive clay and silt sized particles sticking together. The sediment was mixed until all particles were separated. Some un-sieved raw gouge material did not readily break down upon mixing within the Sodium Hexametaphosphate solution. This material was subjected to ultrasonic vibration for 15 minutes. Generally this was long enough to allow the gouge to disaggregate within the dispersant. Using a disposable pipette with a 2mm tip diametre the material was further mixed (as to mix all sediment size to get a fair representation) and a sample taken. Three tests were run through the DigiSizer per sample. Using the average of all three tests sediment proportions were obtained and grouped based primarily on raw size into sand, silt and clay fractions as to assess the particle size index.

The remaining 50% of the sieved sediment and the raw gouge material was sent for XRD analysis to identify and assess the presence of true clay. The finer sediment fraction of the sieved material was targeted for analysis. Due to the nature of the material at an outcrop scale no material could be taken for soil strength testing.

Analysis of thin section was done primarily to evaluate grain shape, surface structure and mineral content. The latter was carried out through point counting. A minimum of 500 grains were counted over the extent of the thin section slide. Due to the grain size of Torlesse lithotypes only sandstones were analysed. One main aim of this analysis was to quantify quartz content due to its high abrasivity. Quartz, feldspar and lithic fragment ratios were assessed as a means of further classifying the sandstones.

1.3.5 Classification development

All observational field information was input into a spreadsheet. All field data were plotted against each other to identify trends in the rock mass. Information was culled when it was deemed to be truly outlying, showed no definitive trend and was not specifically related to tunnelling implication. Trends were observed, analysed and grouped together to form a series of classes encasing geological information. These classes were then related together to form the basic conceptual TRC diagram. The analysis was first undertaken on the Hurunui River site. After each field site was completed the information used to derive the classes was plotted in the same manner. This was undertaken to validate the original conceptual model. The TRC was then modified to encompass new trends that came to light using the same information.

1.3.6 Rock mass class development

Once all information was analysed and entered into the conceptual TRC each individual outcrop was plotted on the diagram. The plotting of each individual outcrop on the diagram allows the clustering of points to be identified with the idea that each specific cluster relates to a specific unit or type of rock mass. The aim of providing rock mass types enables the different engineering geological conditions to be assessed with each cluster representing a separate rock mass type for which tunnelling implications can be assessed. To enable plotting, each outcrop was assigned a number respective of its placing within the rock mass type. This enabled all information to be plotted on a gradational axis.

In some cases outcrops surveyed may have been smaller than the two metres so no specific defect information was recorded. Using a pictorial gradation outcrops with no defect information were included based on appearance against outcrops with recorded defect information. This allowed gradational numbers to be assigned to these outcrops to allow them to be plotted on the TRC diagram. Outcrops not typical of the bulk volume of Torlesse, i.e. the thin, fault bound red and green mudstone in the Ashley Gorge (Cowan, 1992) were not included in the classification. Whilst the rock mass was recorded during mapping, this material potentially behaves in a different manner and does not fit into the general TRC.

1.4 Key findings

Bedding thickness was found to be a major governing rock mass control. In nearly all cases it was found large bed spacing resulted in the better rock mass. Where bed spacing decreased the fracture density generally increased. Therefore it was found that bedding thickness and associated fracture density were the primary controls on rock mass blockiness which made up the Y axis of the TRC.

Defect structure also dictated rock mass condition. It was found the rock was in better condition where the rock mass was controlled by large, relatively persistent (>2m) jointing. Typically this rock had little to no associated faulting. Where the level of faulting increased the occurrence of large jointing decreased. This made up the X axis of the TRC diagram. The rock mass has been divided into 6 different blockiness and defect structure classes whereby rock mass conditions improve from class 1 through 6.

The plotting of individual outcrops identified eight rock mass types typical of the Torlesse rock mass in the four sites mapped for this study. Rock mass types range from the best possible Torlesse conditions characterised by thickly bedded to massive sandstone with slight to moderate fracturing where persistent >2m jointing controls the rock mass, to the worst rock mass condition represented by sheared rock primarily acting as a soil encasing block sizes less than 2 cm in size. Primary controls dictating the occurrence of the rock mass types were found to be bedding thickness, lithotype volume and proximity to major structures.

Lithostructure defined by relative bedding portions and proximity to major faults were found to be the dominant rock mass character controls throughout the Torlesse examined in this study. The use of this information can better inform rock mass type prediction in association with the TRC.

From the eight rock mass types derived, failure and groundwater issues increase in significance towards the poorer rock mass types (5-8). Failure controlled through simple block release is expected to be the dominant failure mechanism toward the better rock mass types (1-4). Heavy increases in the volume of block failure occurrence through the poorer rock masse types are expected to present issues in association with a significant increase in ground water pressure and inflow. The potential also exists for running ground issues in the poorest fault related rock mass type.

This is expected to dictate TBM selection dependent on project specific rock mass types expected through external use of the TRC. Shielded TBM's as a pose to open gripper TBM's are best suited for rock masses where significant widths of rock mass Types 5-8 are expected. This is largely due to questionable thrust generation and support of the fragmented rock mass types. If rock mass type is dominated by favourable rock mass types (1-2) with lesser zones and widths of poorer rock mass types (5-8), open gripper TBM's may be more viable. If the latter is selected, extensive systematic

support measures are needed within increasing volume toward the poorer rock mass types including the potential need for ground pre-treatment in rock mass Types 7-8 prior to excavation.

1.5 Thesis format

The outline of the thesis is as follows

- Chapter Two details the geological setting for this study, field area localities and discusses current rock mass classifications specific to the Torlesse Composite Terrane.
- Chapter Three describes the conceptual models developed in the desk study and relates them back to observational data. This chapter aims to provide site specific results in order to portray what was observed at each individual study site.
- Chapter 4 introduces the TRC diagram developed and presents a series of Torlesse specific rock mass types presented on the TRC. This chapter presents the TRC, provides a discussion toward the lateral thinking and presents the working TRC diagrams.
- Chapter 5 provides a discussion into Torlesse rock mass controls derived from this research and discusses both tunnelling implication and how this research can be utilised toward mechanised tunnelling.
- Chapter 6 summarises and concludes the thesis. Included are recommendations for future work needed to refine the TRC.

A publication titled "Engineering geological characterisation of the Torlesse Composite Terrane in Canterbury, New Zealand with reference to mechanised tunnelling" was produced for the 19th New Zealand Geotechnical Society (NZGS) Symposium "Hanging by a Thread – Lifelines, Infrastructure and Natural Disasters" to be held in November, 2013. This details the major results and conclusions derived from the thesis and has been located for reference at the back of this thesis (Appendix M).

Chapter 2 Literature review and study areas

2.1 Geological setting

2.1.1 Overall lithology

The Torlesse Composite Terrane rocks of New Zealand dominantly comprise indurated quartzofeldspathic sandstone and mudstone (Cox and Barrell, 2007, Mortimer, 2004). Typically the sandstone is fine to medium grained, poorly to moderately sorted with sub-angular grains. It incorporates lithic fragments of felsic volcanics and is interbedded with massive to finely laminated mudstone (Cox and Barrell, 2007, Forsyth et al., 2008, Mackinnon, 1983).

Compositionally the sandstones are made up of quartz, feldspar and lithic fragments. Mackinnon (1983) discusses the quartz-feldspar-lithic fragment ratio (Q:F:L) to be approximately 29:47:24. The quartz present is generally monocrystalline and the feldspar dominantly plagioclase at a 5:1 ratio over potassium feldspar (Mackinnon, 1983). The relative proportion between sandstone and mudstone lithologies ranges substantially between localities (Richards and Read, 2007). It must be noted that the Torlesse examined in this study is relatively fresh, unweathered rock that differs on varying scales from other Torlesse regions i.e. Wellington's weathered greywacke as examined in Pender (1996).

Deposition of the Torlesse accumulated near the margin of Gondwana initially as sediments in mid to deep water submarine fans, marine shelves or terrestrial environments (Cox and Barrell, 2007, Mackinnon, 1983, Howell, 1981, Andrews, 1974, Forsyth et al., 2008). Typically the material is late Carboniferous to early Cretaceous in age and has been progressively imbricated and deformed during the uplift of Gondwana in an accretionary wedge plate tectonic setting (Cox and Barrell, 2007). The general source material is derived from both volcanics and erosion of latter uplifted Torlesse (Mackinnon, 1983).

The sandstone mudstone sequences are distinctively interbedded with bedding ranging in size from massive to very thin. Burial and deformation of the material has caused the Torlesse to undergo low-grade prehnite-pumpellyitc facies metamorphism (Forsyth et al., 2008). This has resulted in mineral alteration, increased induration and localised development of cleavage in mudstones (Cox and Barrell, 2007). Lower grade zeolite facies metamorphism is present and observed in the Ashley River Gorge (Figure 2.1) (Adams, 2003, Forsyth et al., 2008).

Veining, dominantly quartz, is common in the lithology on varying scales. Stewart (2007) discusses through petrographic examination veining formed in association with increased induration and slight metamorphism more so in the massive sandstone member. As discussed by de Ronde et al. (2001) some veining like that at Benmore Dam post dates low grade regional metamorphism. Veining also increases in close proximity to major structures. Ward (2000) discusses increasing veining as distance towards a major structure decreases indicating extensive fluids in association with faulting. It is

discussed in the literature this veining has often been annealed or recrystallised (Stewart (2007) after Watters (1965)) most likely due to continued fault and fluid movement. It is further discussed by Stewart (2007) that calcite veining over the last three to five million years has been more prevalent in association with block faulting along major faults.

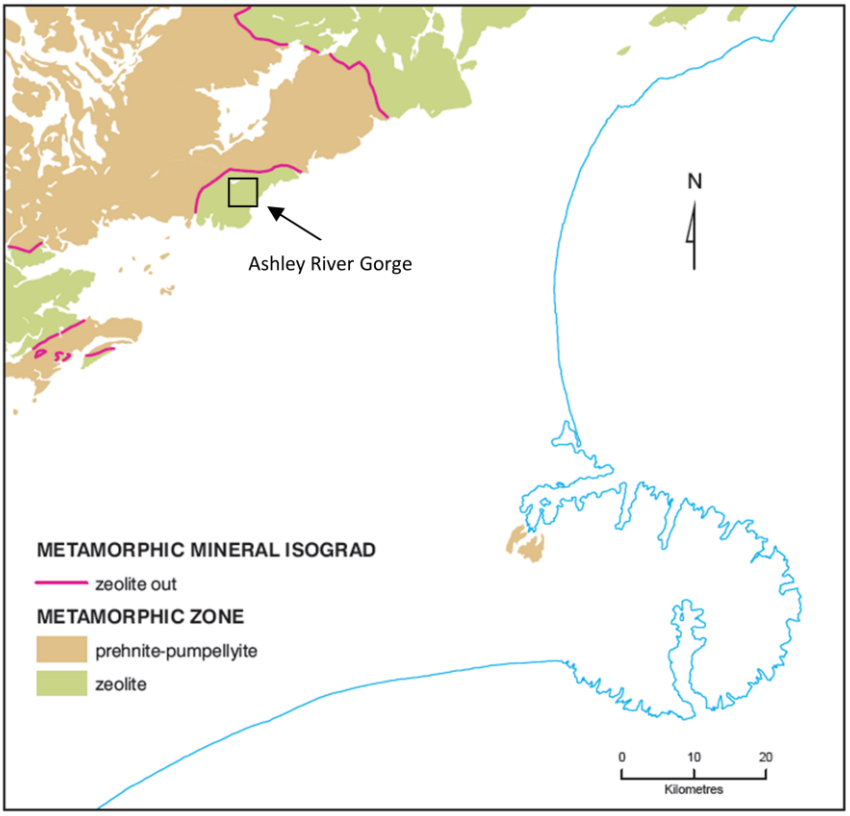

Figure 2.1: Torlesse Composite Terrane metamorphic facies, Canterbury, New Zealand, modified from Forsyth et al. (2008).

Other minor lithologies are tectonically incorporated and interbedded into the Torlesse deposits. They include chert, basalt, limestone, pebble conglomerates and red and green mudstones of which some formed the crustal substrate the Torlesse was deposited (Mortimer, 2004). During accretion the deposition substrate has been tectonically incorporated into the sandstone-mudstone sequence.

2.1.2 Tectonic setting

The Canterbury region of the South Island forms a part of the broad plate boundary collision zone between the Pacific and Australian plates. The Alpine Fault and the Marlborough Fault System (MFS) make up the structural grain of the South Island and represent the modern day plate boundary (Figure 2.2). It is recognised as an oblique dextral strike-slip transform linkage between the opposite dipping convergent subduction zones (Pettinga et al., 2001). Approximately 70% of the plate boundary motion is accommodated by this narrow high strain zone (Eusden et al., 2011, Norris and Cooper, 2001). The MFS includes the Wairau, Awatere, Clarence and Hope Faults which strike north-east/south-west. Whilst this makes up the modern day plate boundary it has been discussed in numerous works the

current plate boundary is experiencing a southward migration in the loci of strike-slip displacements, widening the plate boundary (Eusden et al., 2011, Little and Jones, 1998, Wallace et al., 2007, Pettinga et al., 2001, Little and Roberts, 1997, Furlong and Kamp, 2009). This is due to the general Pacific plate convergence in a southward direction with the southernmost Hope Fault carrying the highest slip rate (Figure 2.2) (Pettinga et al., 2001, Wallace et al., 2007, Little and Jones, 1998, DeMets et al., 1990). The Porters Pass – Amberley Fault Zone (PPAFZ) is considered to be the latest addition to the southward progression of strike-slip displacements (Cowan, 1992, Noble, 2011). Between the two entities is the North Canterbury Block (NCB) of Wallace et al. (2007). The NBC incorporates a series of northeast trending structures and is termed a "thrust wedge" by Pettinga et al. (2001), (Noble, 2011). It is discussed by Pettinga et al. (2001) the thrust wedge represents a series of back-thrusts off the Alpine Fault (Figure 2.3) that previously made up a constricted plate boundary during the early Pleistocene. Tippett and Kamp (1993) discuss the heavy exponential increase in elevation toward the Alpine Fault is the result of south-eastward tilting of the Pacific plate which has ramped up in response to oblique convergence and crustal shortening. Sites for this study reside within the MFS, PPAFZ and NBC.

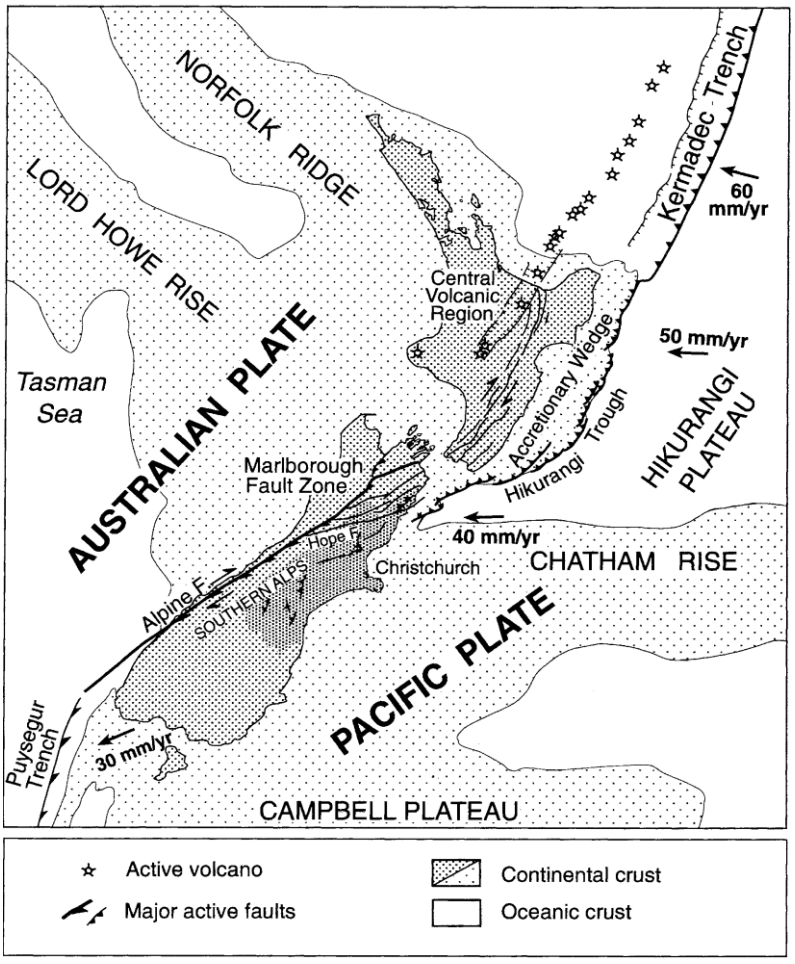

Figure 2.2: Tectonic setting of the current Australian-Pacific plate boundary (Pettinga et al., 2001). Note the convergence rates derived from DeMets et al. (1990).

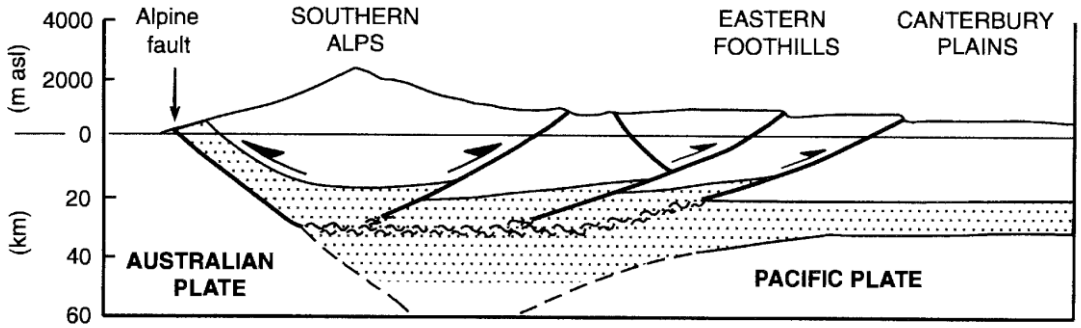

Figure 2.3: Thrust wedge schematic from Pettinga et al. (2001) modified after Norris et al. (1990) and Kleffmann et al. (1998).

The consequent ramping of Torlesse rock up the Alpine Fault back thrusts has caused an unroofing structure to develop. As discussed, unroofed rock westward of the NCB at higher elevations is expected to be much older and may differ structurally. All study sites concerned in this study reside in or near the Canterbury foothills where elevation is relatively small in comparison. As such this study may be less applicable to unroofed, older Torlesse.

2.1.3 Rock mass structure

Several periods of deformation are recognised prior to the formation of the current plate boundary (Whitehouse and Bradshaw, 1988). In response the Torlesse is now intensely deformed. Structurally the rocks are highly folded, faulted and commonly out of sequence (Cox and Barrell, 2007). Bedding is known to dip very steeply, generally dipping westward and changes strike at 1-4km intervals about steeply plunging folds and faults (Mortimer, 2004, Cox and Barrell, 2007). Crush zones within Torlesse associated with faulting are common and in some cases are large enough to be mapped on the GNS 1:250000 map series (see Rattenbury et al. (2006), Forsyth et al. (2008), Cox and Barrell (2007)). The mudstone beds are typically more susceptible to deformation and as a result significant layer parallel shearing is very common along bedding. This is termed the 'Broken Formation' (Rattenbury et al., 2006) and is typically a main control on rock mass character.

Significant boudinage is common within the loosely termed 'Broken Formation'. Rattenbury et al. (2006) state that the Torlesse in locations has preferentially developed zones of deformed rocks whereby layer parallel extension has resulted in the pinching and swelling of beds forming sandstone boudins within heavily sheared mudstone. Beetham and Watters (1985) also discuss this phenomenon in their North Island Torlesse study and describe it as if the mudstone member has flowed around the sandstone member creating boudins.

The effects of large scale faulting on Torlesse are well documented in the literature. Large crush zones are present around faults whereby rock has been mechanically sheared in a brittle sense. Numerous works for example have been carried out on the Hope Fault (see 2.1.2 Tectonic setting) located within Torlesse (Ward, 2000, McMorran, 1991, Freund, 1971). All authors discuss a preferential crush zone

of up to 800 m coupled with damage zones in excess of four kilometres wide. Crush zones are described as absent of all visible bedding whereby rock is intensely sheared (McMorran, 1991). Within this region the block size rarely exceeds two to three centimetres in length and is light green to light grey in colour due to alteration. Typically the crushed zone rock mass has low cohesive strength and high permeability (McMorran, 1991). Within the crush zones rotated pods of intact rock are common whereby rock surrounding the blocks has been sheared around the more intact rock (Ward, 2000). McMorran (1991) also describes a zone of fault gouge adjacent to the fault zone that is very soft and easily remoulded. Generally the hanging wall exhibits a wider crush zone (Ward, 2000). Ward (2000) goes onto to describe up to seven zones of characteristic fault rock of varying deformation spatially related to the main Hope Fault trace (Figure 2.4). This information can directly feed into this study to predict likely rock mass characteristics around fault zones. Faulting and shearing at smaller outcrop scales are not well examined in the literature within Torlesse based on the extensive population of joint dominated rock masses. It is mentioned by Stewart (2007) that faults and shears within the rock mass influence the volume, character and orientation of adjacent defects. This is observed at varying shear scales, therefore observation at large scale structures can be loosely transferred to smaller scale structures.

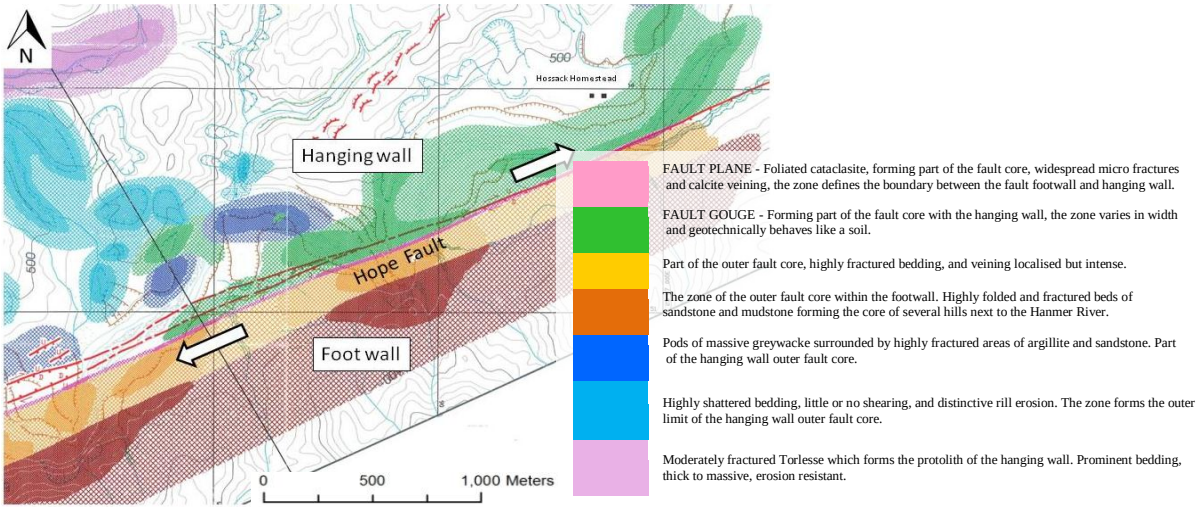

Figure 2.4: Hope Fault fracture zones at The Hossack, east Hanmer basin, North Canterbury modified after Ward (2000).

2.1.4 Discontinuities

Discontinuities vary substantially in character. Table 2.1 from Richards and Read (2007) summarises different defect characteristics. Typically jointing has very low persistence whilst bedding and shearing have relatively high persistence (Figure 2.5). The rock mass has a large number of defects (Figure 2.6) and is unusual in the fact it has high intact strengths in combination with low persistent jointing (Richards and Read, 2007). Read and Richards (2007) report average defect spacings of 60-200mm with most block sizes less than 0.01m³, ranging from 0.00036-0.0081m³ (Cook, 2001).

Mansergh (1968) describes joint spacings of <10mm in shattered zones up to 300mm in better rock masses (Stewart, 2007). Generally these values increase in sandstone. Defect surfaces are typically poor ranging from planar smooth to planar rough (Richards and Read, 2007). Where present, infilling material is typically inactive clays (Read and Richards, 2007) defined by Cook (2001) as low plasticity, thin clay deposited by water or wind in fresh unweathered greywacke defects. Stewart (2007) states because of this the infilling is likely to have little engineering significance. Other infilling types are recorded in much less quantity by Cook (2001) and are discussed by Stewart (2007) to be of little significance. Due to the close spacing and lack of significant infill thickness defect strength is not considered to be influenced by infilling (Stewart, 2007).

Table 2.1: Summary of defect characteristics from Richards and Read (2007) studies on Torlesse

	Bedding[1]	Vein[1]	Joint	Sheared zone	Crushed zone[2]
Physical description	Defect where parting is parallel with rock texture	Defect with secondary mineralisation	Defect with little or no displacement	Roughly parallel sided zone with closely spaced joints	Roughly parallel sided zone with angular fragments including clay and/or gouge
Proportion	0–8%	0–10%	80–100%	0–2%	0–2%
Spacing	10 mm–5 m	Where present: 10 mm–2 m	20–600 mm	Where present: 1–20 m	Where present: 1–20 m
Persistence	<2 m–>10 m	<1 m–<10 m	<1 m–10 m	10–>100 m	10–>100 m
Width	n/a	n/a	n/a	<1 m	<2 m
Filling	Clean or silt/clay infill where relaxed	Secondary mineralisation (e.g. calcite or zeolite)	Clean or silt/clay infill where relaxed	n/a	n/a

[1] Not considered a defect where bedding is textural only (has no parting) or vein is annealed.
[2] Fault is a generic term for crushed zones with development of gouge from significant tectonic displacement and may be >2 m wide.

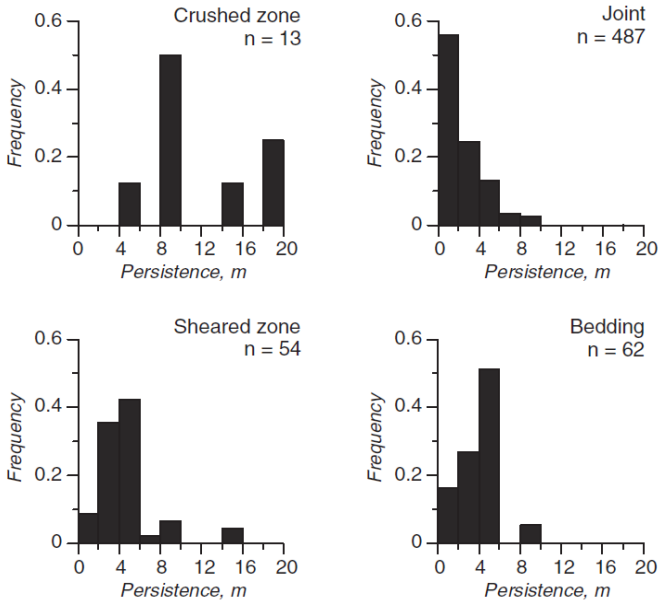

Figure 2.5: Summary of defect persistence values in Torlesse (Richards and Read, 2007).

Jointing is the most common defect with up to six different joint sets in any one outcrop (Figure 2.6). Cook (2001) reports 90% of recorded scanline defects were joints. Similarly Read and Richards (2007) report that >90% of total discontinuities are joints. It is discussed by Read and Richards (2007) that more than 50% of joints have persistence lengths less than 500mm with approximately 80% of all

jointing terminating against other discontinuities. This creates a tightly interlocked rock mass giving higher resistance to compression or shear loads (Read and Richards, 2007). It is further discussed that these attributes result in better mechanical properties than other rock masses of similar quality based on conventional classification systems. It was found by Cook (2001) that the dominant, most common jointing is sub-parallel to bedding. Other joint sets were found to orientate orthogonal to bedding. Because of this Stewart (2007) discusses "the best classes of rock are only likely to be blocky at best with more irregular block sizes and small block sizes in areas of poorer quality". The effect on jointing of increasing proximity to large scale structures is also discussed by Stewart (2007). He states more joint sets are likely to be superimposed in the rock mass in close proximity to large scale structures where changing rock mass conditions are expected.

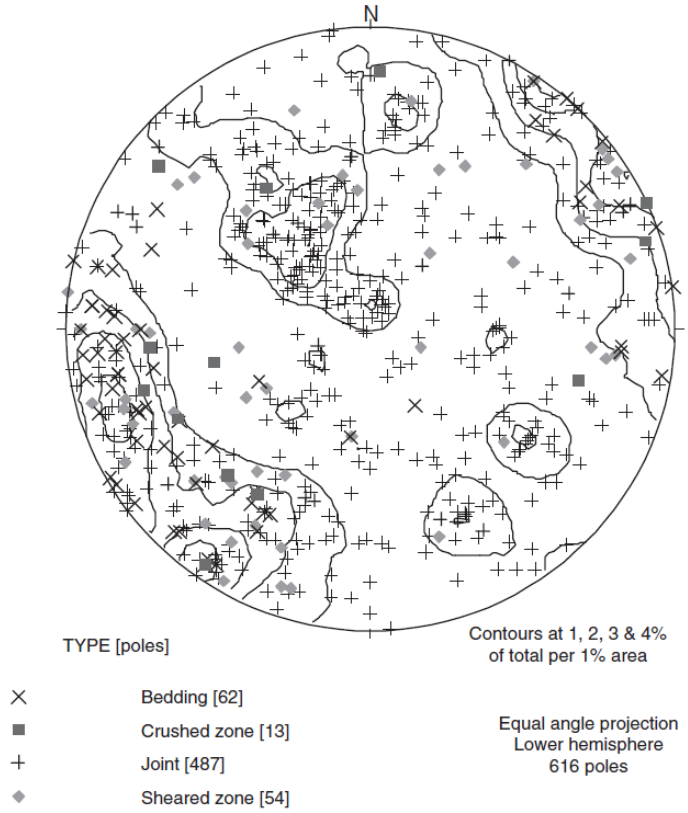

Figure 2.6: Discontinuity steronet of Torlesse discontinuities (Richards and Read, 2007).

2.1.5 Intact strength

The Torlesse sandstone member has very high intact strength. Unconfined compressive strengths of up to 350 MPa are reported by Read et al. (2000) with unweathered rock mass strengths above 100 MPa (Richards and Read, 2007). Typically the intact strength is related to grain size with coarser sandstones incorporating higher strengths with less deformation (Stewart, 2007). Cook (2001) discusses that a wide variation in sandstone strength is most likely due to the high quartz ratio whereby sandstone gives a wide range of strength values compared to consistent mudstone strength values due to the smaller grain size. Point load conversion factors of 23 and 11 for sandstone and

mudstone respectively are reported by Read and Richards (2007), however it is noted high variability in sandstone conversion factors exist with the factor value ranging from 14-31.

Stewart (2007) provides a thorough review of work carried out in Torlesse strength testing. The tables presented in this section include data derived from authors sourced by Stewart (2007). He notes most of the UCS tests are unpublished results completed by the Institute of Geological and Nuclear Sciences (GNS) for which he gives no reference.

Typically homogenous sandstone is the strongest in all forms of testing with UCS strengths of up to 347.4 MPa recorded at Belmont quarry (Table 2.2). The difference in strength between lithologies is well demonstrated with a maximum UCS value in mudstone of 97.4 MPa. Interbedded samples are relatively weak although have higher strength values than the mudstone member. Brazilian Tensile strength tests carried out by Read et al. (1999) shed a similar result whereby the mudstone has a much weaker tensile strength than the sandstone member (Table 2.3).

Table 2.2: UCS results from Torlesse literature (Stewart, 2007, pg.121-122).

Sandstone location	Mean UCS (MPa)	Std dev	# of tests	Max	Min	Author
Belmont	244.7	66.7	18	347.4	144.3	Cook (2001) + GNS (unpub.)
Aviemore	200.9	85.1	5	282.1	62.0	Cook (2001) + GNS (unpub.)
Whitehall	103.0	-	1	-	-	Cook (2001) + GNS (unpub.)
Taotaoroa	168.0	-	1	-	-	Cook (2001) + GNS (unpub.)
Benmore	187.0	-	1	-	-	Robinson (1957)
Rangipo	129.3	60.3	10	206.3	33.4	Hegan (1977)
Globe Progress Mine, Reefton	92.0	47.8	15	165.7	12.1	Clark (1996)
Ruataniwha	175.7	34.9	15	234.0	117.0	Read et al. (1998)
Motu	166.1	164.9	2	282.7	49.5	Read et al. (1998)
Plimmerton Quarry	196.1	77.3	5	281.4	104.0	Read et al. (1998)
Karapiro dam	130.3	50.6	2	166.0	94.5	Hegan (1998)
Moawhango	92.2	38.6	3	125.8	50.1	Hancox (1975)
Mudstone location						
Belmont	62.8	20.1	10	97.4	35.9	Cook (2001)
Rangipo	74.2	21.1	2	89.1	59.3	Hegan (1977)
Karapiro dam	9.1	4.0	2	11.9	6.3	Hegan (1998)
Moawhango	80.8	10.8	3	92.8	71.7	Hancox (1975)
Interbedded location						
Belmont	115.7	-	1	-	-	Cook (2001)
Rangipo	109.6	48.5	10	195.8	20.8	Hegan (1977)
Globe Progress Mine, Reefton	30.3	12.2	4	46.5	18.0	Clark (1996)
Moawhango	85.0	18.6	3	105.8	69.7	Hancox (1975)

Table 2.3: Brazilian Tensile strengths recorded in Read et al. (1999) from Stewart (2007, pg.123).

Location	Rock type	Mean σ1 (MPa)	Std dev	# of tests	Max	Min
Aviemore	sandstone	-19.34	5.81	5	-12.96	-24.93
Belmont	sandstone	-18.77	5.07	15	-9.26	-25.38
Belmont	sandstone	-6.63	2.78	4	-3.89	-10.50

Point load index testing results displayed in Table 2.4 have been converted to a UCS value using a conversion factor of 24 for sandstone and 11 for mudstone. The same strength trend between lithologies is shown. Note the point load sample type. Typically the diametral core tests have higher MPa values. Cook (2001) attributed the difference to a sample bias toward core rock being the better of the rock masses. In Cook (2001), samples from Aviemore presented foliation planes. As seen in Table 2.4 point load index tests were conducted parallel and perpendicular to the fabric. Results indicate the foliation planes have a significant effect on the strength of Torlesse rocks. When a load is applied perpendicular to the foliation planes the rock exhibits higher strengths. In contrast when a load is applied parallel to the foliation planes the rock fractures along the weakness planes at significantly lower strengths. Cook (2001) reported anisotropy ratios of 2.9 for lump samples and 2 for core samples suggesting medium anisotropy (Ramamurthy, 1993). This differs from typical sandstones that exhibit lower results between isotropic and low anisotropy (Ramamurthy, 1993, Stewart, 2007).

Table 2.4: Point Load strength testing from Torlesse literature (Stewart, 2007, pg.127-128)

Sandstone location	**Mean UCS (MPa)**	**Std dev**	**# of tests**	**Max**	**Min**	**Author**	**Sample**	**Orientation**
Belmont	222.1	44.5	15 (221)	280.8	158.4	Cook (2001)	Irregular	Perpendicular
	260.7	20.5	8 (13)	284.1	221.8	Cook (2001)	Core	Perpendicular
	161.4	-	1	-	-	Cook (2001)	Core	Parallel
Aviemore	225.4	29.7	6 (82)	273.6	192.0	Cook (2001)	Irregular	Perpendicular
	116.0	56.7	3 (10)	180.0	72.0	Cook (2001)	Irregular	Parallel
	241.5	64.0	2 (6)	286.7	196.2	Cook (2001)	Core	Perpendicular
	127.1	64.8	2 (11)	172.9	81.3	Cook (2001)	Core	Parallel
Taotaoroa	213.3	30.2	20	241.9	174.2	Cook (2001)	Irregular	Perpendicular
	232.7	21.7	4	251.1	208.8	Cook (2001)	Core	Perpendicular
Whitehall	250.6	29.2	10	271.2	229.9	Cook (2001)	Irregular	Perpendicular
Globe Progress Mine, Reefton	155.8	-	1	-	-	Cook (2001)		
Ohau Bridge	217.5	24.7	2	235.0	200.0	Read et al. (1998)		
Terrace Tunnel, Wellington	110.0	-	1	-	-	Read et al. (1998)		
Motu	133.6	83.2	8	237.0	43.0	Read et al. (1998)		
Karapiro dam	159.0	31.6	4	192.0	132.0	Hegan (1998)		
Mudstone location								
Belmont	43.4	13.1	33	55.4	29.5	Cook (2001)	Irregular	Perpendicular
	68.5	19.3	14	101.9	35.1	Cook (2001)	Core	Perpendicular

Table 2.4 (continued): Point Load strength testing from Torlesse literature (Stewart, 2007, pg.127-128)

Mudstone location	Mean UCS (MPa)	Std dev	# of tests	Max	Min	Author	Sample	Orientation
Belmont	18.6	-	1	-	-	Cook (2001)	Core	Parallel
Taotaoroa	41.4	-	1	-	-	Cook (2001)	Irregular	Perpendicular
	46.3	-	1	-	-	Cook (2001)	Core	Perpendicular
Whitehall	60.7	-	1	-	-	Cook (2001)	Irregular	Perpendicular
Karapiro dam	11.4	7.48	2	23.1	4.4	Hegan (1998)		

2.1.6 Terrane types

The Torlesse Composite Terrane rocks of the South Island, New Zealand are sub divided into three main terrane types (Figure 2.7). The terrane types are subdivided based primarily on age, however, they can also be distinguished by petrography, geochemistry and conglomerate class composition (Mackinnon, 1983, Andrews and Field, 1987, Roser and Korsch, 1999, Wandres et al., 2004) . The Rakaia terrane is the oldest of the terranes, predominantly Permian to Triassic in age (Cox and Barrell, 2007). It occurs as the largest Torlesse terrane by area (Figure 2.7). It is widely deformed and arguably monotonous (Mortimer, 2004). It is discussed by (Mortimer, 2004) that the steep dipping features and the west facing bedding in association with fossil zones younging toward the east indicate deformation of the Rakaia terrane in an east-facing accretionary wedge. Some parts of the Rakaia terrane have been further metamorphosed into semi-schist and schist (Cox and Barrell, 2007).

The Pahau terrane exists toward the northeast and is the younger of the terrane types. It is differentiated from the Rakaia terrane by the third (sub) terrane in the study region, the Esk Head Belt (Silberling et al., 1988, Bradshaw et al., 1980, Bradshaw, 1973). The Esk Head Belt is described as a zone that is more sheared than other terrane members (Rattenbury et al., 2006). The bulk volume of the Esk Head Belt contains both Rakaia and Pahau Torlesse, however, distinguishing the terrane from the Rakaia and Pahau are the associated blocks of melange, including exotic limestone, chert and basalt (Rattenbury et al., 2006). The Esk Head Belt is offset by major faults making up the Marlborough Fault System (Figure 2.7). The major faulting represents the north-south contact with the eastward contact progressively grading into Pahau terrane through several kilometres of sheared rock incorporating exotic material (Silberling et al., 1988). The level of deformation within the belt is highly variable due to the level of tectonism (Rattenbury et al., 2006). Significant levels of bed shearing in the mudstone member (Broken Formation) and significant boudinage of the sandstone exist in the Esk Head Belt. Preferential erosion of the mudstone member has resulted in hill crests with numerous pinnacles (Rattenbury et al., 2006). Other lithologies occur in major fault zones more so than in other terrane types and include chert, green-grey sandstone, red mudstone, igneous rock and limestone (Rattenbury et al., 2006).

Many different models have been proposed explaining how the Esk Head Belt came to be i.e. Mackinnon (1983) and Cawood (1984). However it is agreed the Esk Head formed in response to the coming together of the Caples and Torlesse terranes (later to be Rakaia terrane) in a subduction/collision event, exhuming the Rakaia terrane in the late Triassic, early Jurassic. This model explains the submarine basalts and seafloor limestone present in the terrane.

Deposition is said to have resumed in the late Jurassic and continued into the Cretaceous after the exhumation of the Rakaia. During this time sediment was sourced from active volcanics and the now exposed Rakaia terrane forming the younger Pahau terrane (Mackinnon, 1983). The Pahau terrane is comparable to other terrane types in both lithologic content and structure (Mortimer, 2004). The sandstone member is slightly lighter in colour, slightly less indurated and has a more sugary appearance in comparison to the Rakaia terrane (Forsyth et al., 2008, Rattenbury et al., 2006). It also differs by containing more carbonaceous material, conglomerate bands and volcanic rocks. It is also noted that the Pahau terrane contains on average a higher percentage of sedimentary and volcanic lithic fragments than other members (Forsyth et al., 2008). Rocks can be further divided into sub units based on fossil assemblages; however the structure and lithotypes do not differ significantly enough to treat them as separate entities within this study.

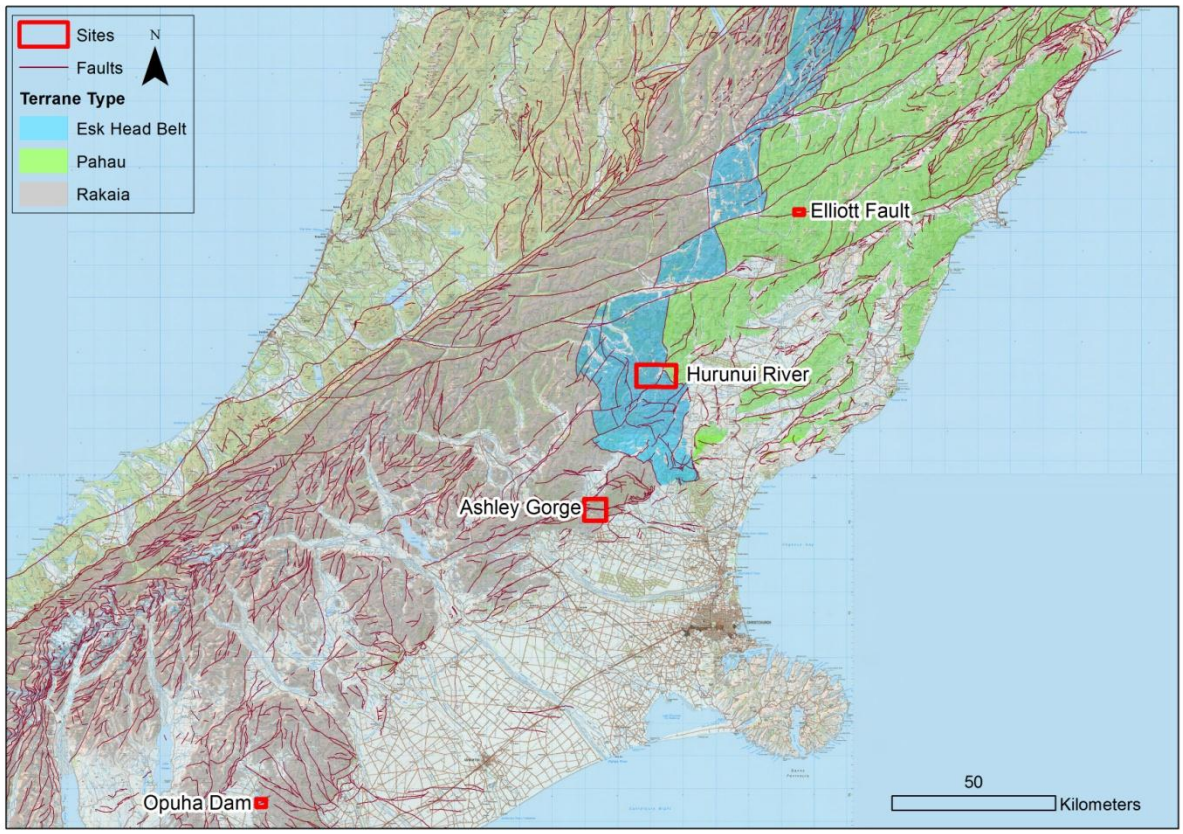

Figure 2.7: Torlesse Composite Terrane types showing structural grain of Canterbury, New Zealand. Data sourced and modified from Rattenbury et al. (2006), Nathan et al. (2002), Forsyth et al. (2008) and Cox and Barrell (2007). Imagery from LINZ.

2.2 Study areas

Study areas were chosen on the basis of obtaining a good representation across the suite of Torlesse rock. Sites were selected in all terrane types, metamorphic facies and structural style to characterise the variations in the Torlesse rock mass.

2.2.1 Elliott Fault

The active Elliott Fault is located within the larger MFS. Regionally it lies within North Canterbury, with the area concerned for this study residing north of Hanmer Springs, Canterbury. It occurs as a splay off the larger through-going dextral Clarence Fault and has a trace length of approximately 60 km. Both the Clarence and Elliott Faults are dominantly situated within the Pahau Torlesse terrane (Figure 2.8) (Rattenbury et al., 2006). A total of 13 outcrops were mapped (Appendix C.1). The Elliott Fault is of interest to this study as the Clarence River has cut a well defined cross section perpendicular to the main Elliott trace. It provides an example of the effect a major structure can have on Torlesse rock mass characteristics.

The current Clarence-Elliott duplex which makes up a part of the MFS acts as a component of the strike-slip transfer zone between the west-facing Hikurangi subduction margin in the northeast and the east-dipping oblique-slip Alpine Fault to the southwest as previously discussed (Eusden et al., 2011, van Dissen and Nicol, 2009). The Elliott Fault dips northwest and creates a large upthrown northern block suggesting some reverse movement in addition to strike-slip motion (Eusden et al., 2011). It has been proposed by Eusden et al. (2011) through their mechanical modelling that prior to the current day strike-slip velocity field, the area was experiencing an oblique compressional velocity field. They propose that under the current day stress regime, the model results in topographic subsidence of the upthrown northern block, rather than uplift which explains the current day topography. It is assumed that the change in velocity fields is due to the southeast migration in the loci of strike-slip displacements across younger faults in the Quaternary (Eusden et al., 2011, Little and Jones, 1998, Wallace et al., 2007). It should therefore be assumed that the rock mapped in this study has experienced two significant stress regimes. Numerous surficial expressions are recorded along the extent of the Elliott Fault and mechanically altered rock is visible at two sites within the field area described as fault gouge by Eusden et al. (2011).

2.2.2 Hurunui River

The Hurunui River site similarly lies in North Canterbury approximately 20 km from the small township of Hurunui. The entirety of the study site is located adjacent to Lake Sumner Forest Park. The area predominantly lies within Esk Head Belt terrane however the upper right hand corner of the study site is situated within Pahau terrane (Figure 2.9) (Rattenbury et al., 2006). The area directly crosses the reverse Esk Fault (GNS, 2004, Rattenbury et al., 2006) and encompasses relatively high volumes of exotic volcanics. Bordering the study site to the east is the Waitohi Downs Fault (GNS,

2004). Although this fault does not cross the mapping area, the potential exists for the structure to have an influence on the surrounding rock mass. A total of 38 outcrops were mapped (Appendix C.2).

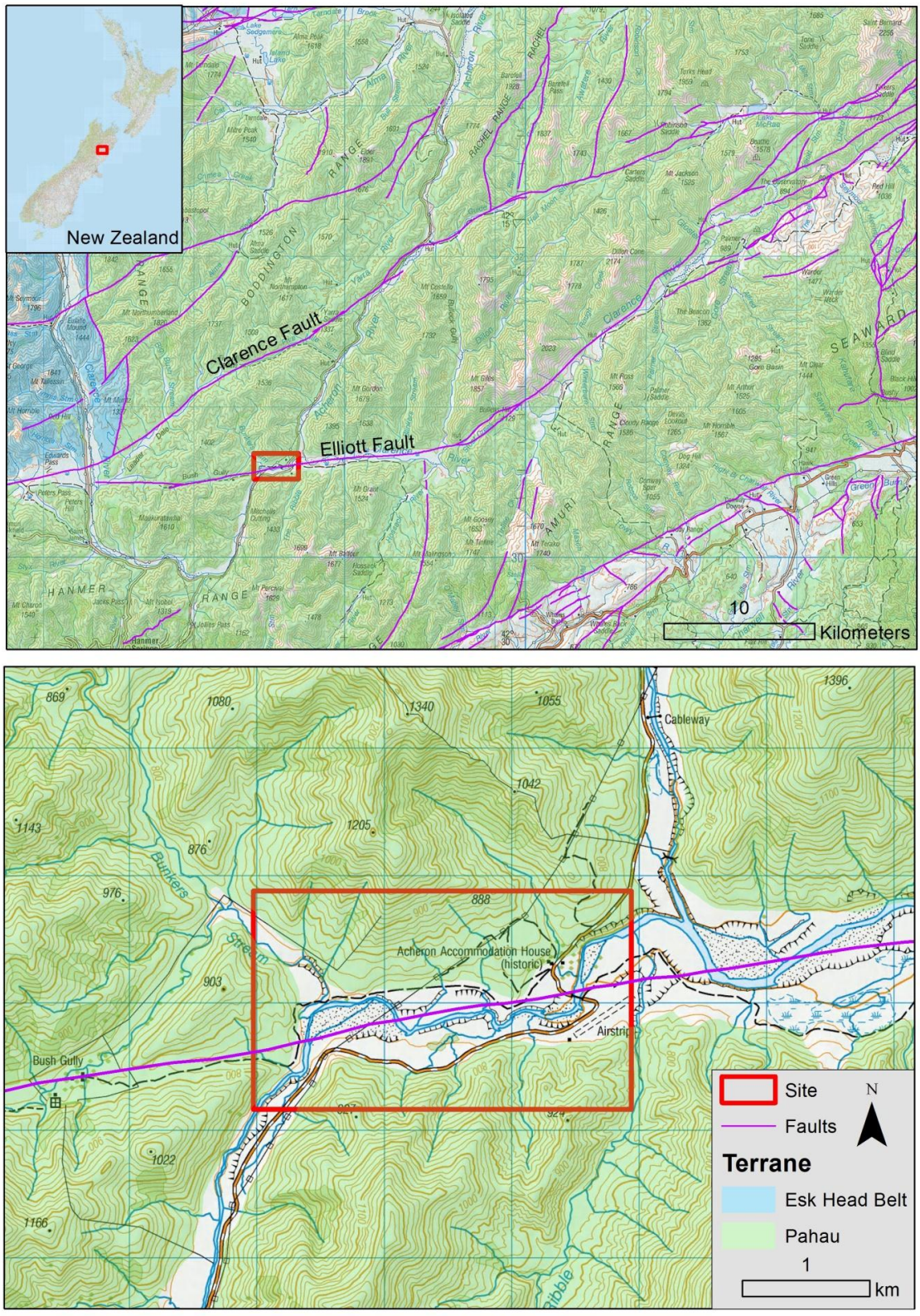

Figure 2.8: Elliott Fault regional (top) and study site (bottom). Data sourced from Rattenbury et al. (2006). Imagery from LINZ.

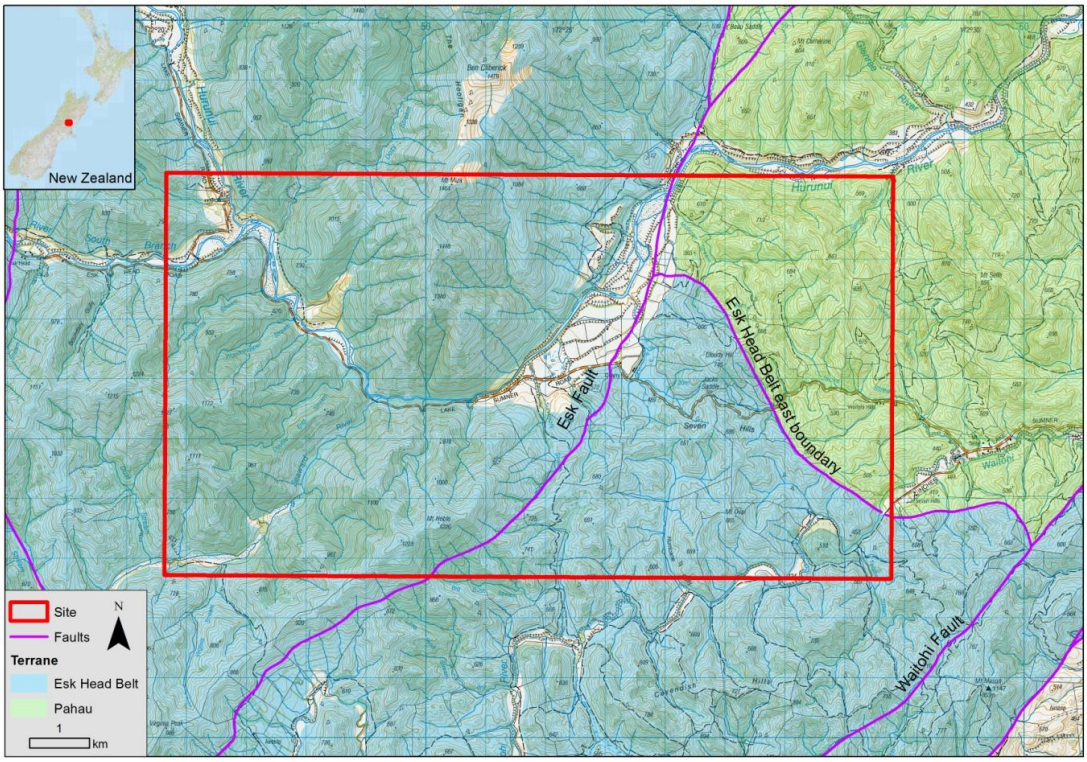

Figure 2.9: Hurunui River study site. Data sourced from Rattenbury et al. (2006). Imagery from LINZ.

2.2.3 Ashley River Gorge

The Ashley River Gorge lies westward of Christchurch approximately 8 km from the local township of Oxford. The Ashley River Gorge is a deeply incised river valley that meanders through mountainous terrain. The area is situated within the Rakaia terrane and is cut by several large faults that make up part of the PPAFZ (Figure 2.10) (Forsyth et al., 2008). The Lees Valley Fault runs along the western end of the study area and has a reverse sense most likely controlling the initial topography between Lees Valley and the Ashley Gorge. The Townshend Fault meets with the Coopers Creek Fault toward the middle of the gorge. The Faults then continue as the Glentui Fault (Forsyth et al., 2008). Sense of movement along these structures is dextral (GNS, 2004). The intersection of the two faults lies approximately on Lees Valley Road and create a 250 m wide crush zone that preferentially follows a band of red and green mudstone (Cowan, 1992). The Ashley Gorge Fault runs across the eastern range front contact with the Canterbury Plains sediment. Its relative sense is unknown but most likely has a reverse dextral component controlling topography. The structural grain of the area is related to the PPAFZ (Forsyth et al., 2008). A total of 57 outcrops were mapped (Appendix C.3).

2.2.4 Opuha Dam

The Opuha Dam study site is located in South Canterbury, approximately 12 km from the township of Fairlie. The entirety of the site is located within the Rakaia Terrane (Figure 2.11) (Cox and Barrell, 2007). The Dam construction offers rock exposures in an area that otherwise does not have good outcrop coverage. The relative age of the dam also offers relatively fresh rock. The Opuha Dam fault

protrudes the bottom of the Opuha Dam (Figure 2.11) (Cox and Barrell, 2007). It is characterised by two main argillaceous crush zones with lower rock strength and stiffness (Pickens and Grimston, 2001). A total of 11 outcrops were mapped (Appendix C.4).

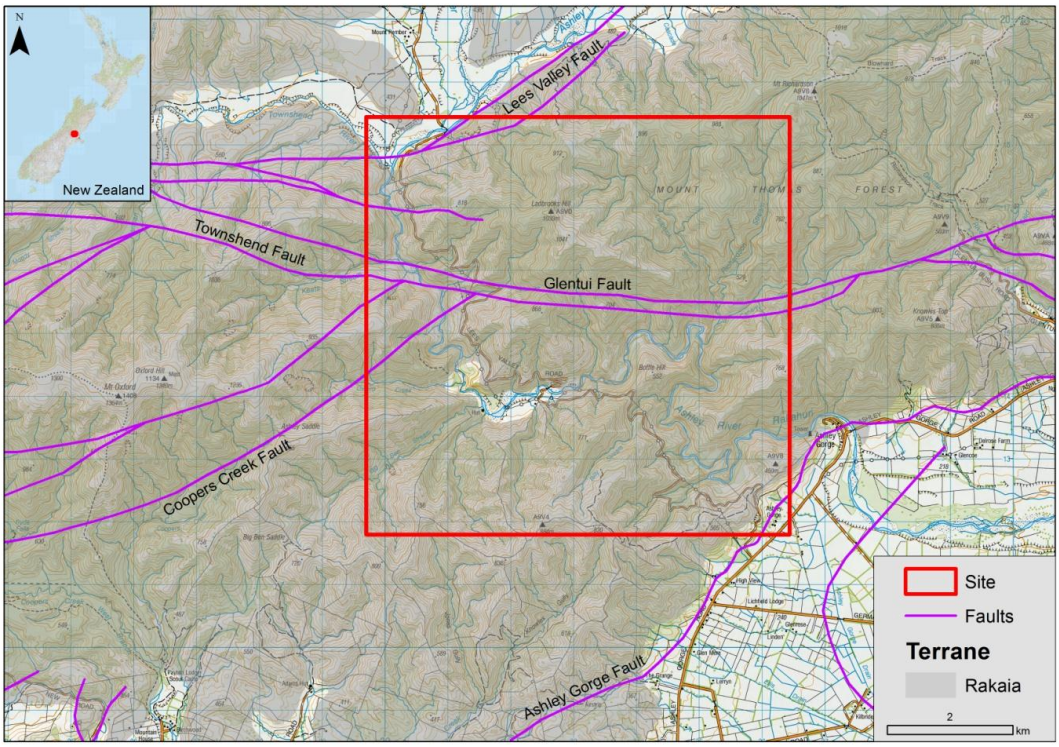

Figure 2.10: Ashley River Gorge study site. Data sourced from Forsyth et al. (2008). Imagery from LINZ.

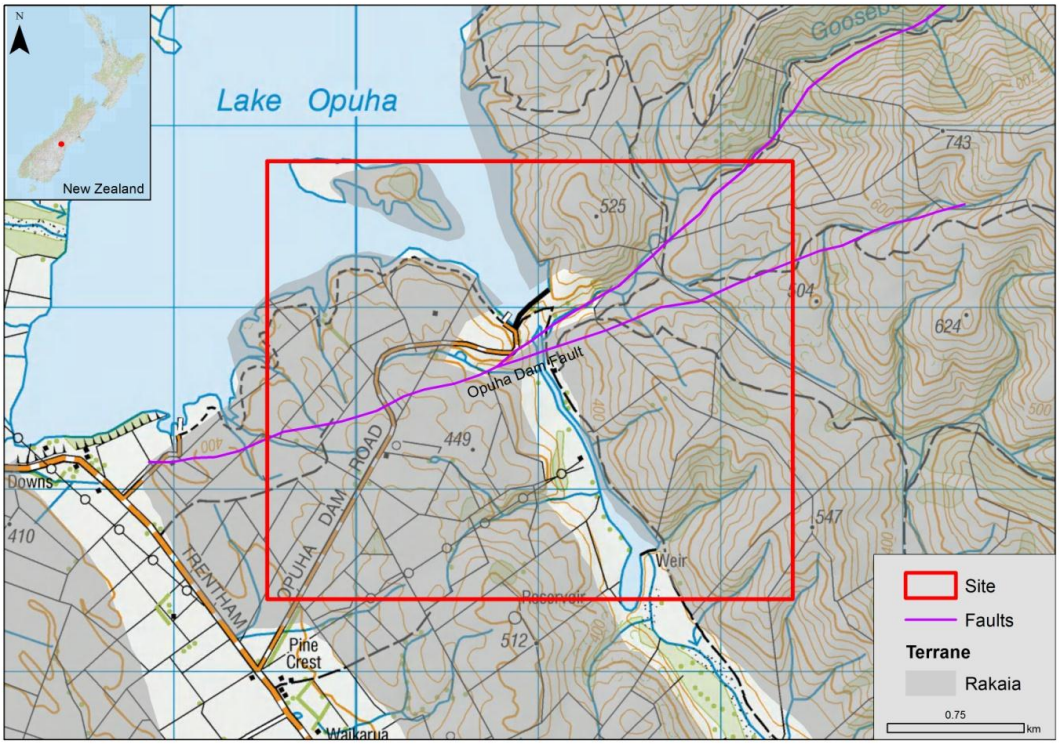

Figure 2.11: Opuha Dam study site. Data sourced from Cox and Barrell (2007). Imagery from LINZ.

2.3 Rock mass classification

Although little work has been done on Torlesse classification, recent works have been carried out by Richards and Read (2007), Read and Richards (2007), Read et al. (2000), Cook (2001) and Stewart (2007). Their works have been primarily concerned with New Zealand Torlesse rock mass characteristics and classification, whereby strength and structure has been examined mainly for input into failure criterions. Study sites for all works have been concentrated around three sites 1) Aviemore Dam, located on the Waitaki River, South Island 2) Belmont Quarry, located in the Hutt Valley, lower North Island and 3) Taotaoroa Quarry, Cambridge, Waikato.

Using engineering geological mapping of exposures at Aviemore Dam, Belmont Quarry and Taotaoroa Quarry, Read et al. (2000) devised a five class classification system (Table 2.5). The classification system, primarily based on lithology, intact strength and defect character, is presented as a table with the corresponding classes presented as a series of descriptive terms. It is noted by the authors that Class II is the dominant type of Torlesse rock mass.

Table 2.5: Read et al. (2000) five class descriptive classification of Torlesse.

Class	Lithology	Strength	Defects	Comments
I	Homogeneous or faintly bedded medium-grained sandstone. Fine-grained sandstone with some widely spaced interbeds of mudstone.	Extremely strong to very strong	Joint spacing >150 mm, typically 200–300 mm, surfaces rough to smooth. Sheared, crushed or shattered zones generally absent.	Little indication of major tectonic deformation in rock mass.
II	Fine or very fine-grained sandstone with mudstone laminae. Interbedded sandstone and mudstone. Mudstone/sandstone with coarse podding.	Very strong to strong	Joint spacing 60–200 mm, surfaces rough to slickensided. Minor narrow (<300 mm wide) sheared, crushed or shattered zones.	Rock mass may contain minor very widely spaced zones of sheared and crushed rock.
III	Mudstone with extensive recrystallisation. Interbedded sandstone and mudstone, often with podding and some veining.	Strong to moderately strong	Joint spacing <100 mm, surfaces smooth to slickensided. Narrow (<300 mm wide) sheared, crushed, or shattered zones.	Characterized by closely spaced defects (may be shattered) or recrystallised rock mass.
IV	Interbedded sandstone and mudstone, often with extensive podding. Mudstone or very fine sandstone with extensive veining.	Strong to moderately strong	Joint spacing <60 mm, surfaces smooth to clay-lined. Sheared zones with crushed zones (typically <500 mm wide), and may contain thin (<25 mm) gouges.	Characterised by very closely spaced fractures with sheared zones (i.e. shattered and sheared rock mass with some crushed zones associated with fault zones).
V	Mudstone or fine sandstone (rock material generally sheared and crushed).	Strong to moderately strong (or n/a)	Joint spacing <20 mm, surfaces slickensided to clay-lined. Generally sheared or crushed zones which contain gouges.	Characterised by very or extremely closely spaced fractures with crushed zones and gouges (i.e. crushed rock mass associated with major faulting).

Classification based on rock mass in the unweathered (fresh) or fresh-stained state.
Podding refers to the disruption of bedding into irregular lenses or pods. Recrystallisation refers to recementation of the rock mass and is often accompanied by veining.

Read et al. (2000) overlaid the five classes onto the Geological Strength Index (GSI, after Hoek et al. (1998)). GSI is an input into a system for estimating rock mass strength and is based on defect surface condition and structure, which were considered by Read and Richards (2007) to be the main variables of Torlesse. The five class system overlay visually demonstrates where each of Read et al. (2000) classes plotted (Figure 2.12). They discuss that assigning a GSI value through the classification provides better linkages with engineering geological mapping and rock mass descriptors. It then allows the Torlesse-specific information to be imputed into the Generalised Hoek-

Brown Failure Criterion (Hoek et al., 2002) for example. However they note that the use of the descriptive table should remain in use since assigning a single value does not represent the complexity of the Torlesse rock mass. The gradational boundaries act to accommodate some of this complexity and variability between classes. It is further noted by Read and Richards (2007) that significant variation is common in the same domains.

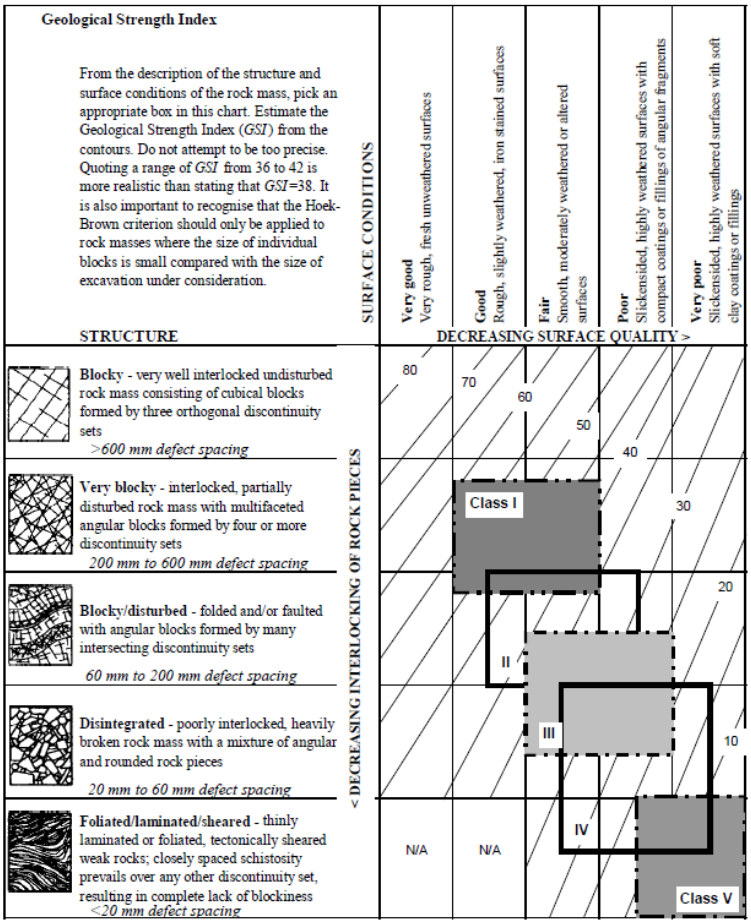

Figure 2.12: Read et al. (2000) five class Torlesse classification scheme after Hoek et al. (1998) GSI chart.

Included in the authors' work is an assessment of the Generalised Hoek-Brown failure criterion with respect to New Zealand Torlesse. It is discussed by Read et al. (2000) that the Generalised Hoek-Brown Failure Criterion leads to unrealistically high predictions of rock mass strength for better quality rock masses and lower predictions for poorer quality rock masses. They go on to note that failure criterion inputs for strength testing and observed performance need calibration in association with refinement of a rock mass classification that acknowledges defect spacing more specifically than the GSI.

The use of external classification systems is not included within this study, specifically the widely used Rock Mass Rating system (RMR, after Bieniawski (1989)) and the Tunnelling Quality Index (Q, after Barton et al. (1974)). However the potential exists for further work to be carried out using

information derived from this study. Read and Richards (2007) discuss that the use of these conventional classifications are not well suited in New Zealand's Torlesse. Whilst they provide good information on rock mass classification for engineering purposes, their use in the Torlesse is not well suited due to high intact strength and low defect persistence in a closely jointed rock mass (Read and Richards, 2007). It is further discussed by Read and Richards (2007) that a comprehensive engineering geological description to characterise the Torlesse is the preferred approach. It provides directed linkage to the RMR or GSI that can be implemented into the Generalised Hoek-Brown Failure Criterion as discussed.

Further work was undertaken by Cook (2001) who classified a series of structural domains in the Torlesse from the Belmont Quarry. His structural domains, shown in Table 2.6 were chosen based on the likely strength properties of the rock mass (Stewart, 2007). Domains were derived from engineering geological distinction rather than via a structural-geological assessment of the rock mass present. The boundaries between domains were derived from field observation of joint spacing, mineral veining and joint patterns (Stewart, 2007). Nonetheless it provides a useful cross section of rock mass types across the Torlesse.

Table 2.6: Torlesse structural domains as defined by Cook (2001).

Domain	Description
I – Fractured mudstone	Black sheared/crushed zone (~20 cm thick) in contact with light grey sandstone; zone consist of black, sticky clay material (gouge) with angular clasts of mudstone rock; heavily mineralised white sandstone lies against this sheared/crushed zone.
II – very slightly weathered sandstone	Rusty orange yellow coating on surface of rock (iron staining); well-jointed rock mass containing irregular blocks.
III – Sheared crushed sandstone	Numerous sheared and crushed areas; the rock mass outside of these areas is very closely jointed (<20mm spacing), with clay and sand infilling very narrow joint apertures (2-3 mm); seepage is common.
IV(a) – Heavily mineralised sandstone	Closely jointed (~20-30 mm spacing) sandstone rock mass with occasional mudstone beds; thin (2-3 mm) zeolite veins anastomise through the sandstone; small blocky fabric to the rock mass structure.
IV – Blocky sandstone	Blocky jointed greywacke rock mass containing well sheared mudstone beds; occasional persistent mineral veining (zeolite/prehnite/quartz); some major sheared planes cut through the rock mass and consist of a light grey sticky clay material (fault gouge); large (25-50m^2) failure planes are apparent and are generally joint controlled; minor seepage associated with shear planes.
V – Fault junction	Adjacent fault plane: Attitude is 64 SW 147; 70 mm thick greeny/grey gouge zone (SW side of plane) lies directly against the fault plane and a zone of crushed greeny sandstone lies against this; terminates against above plane on Batter C-D.
VI – Irregular jointed sandstone	Joints sets become more developed away from fault plane; the rock mass closer to the fault is more sheared and has a greeny appearance (chlorite mineralisation); low angle shear zones and thickish (100 – 150 mm) low angle quartz veins are commonly persistent; green sandstone lenses (200 mm thick and up to 1m long) are also apparent.

Hoek et al. (1998) and Marinos and Hoek (2000) recognised the significant engineering challenges associated with heterogeneous, highly deformed, flysh-like materials whereby use of the conventional GSI chart is not well suited. Flysh-like materials consist of alternations of strong and weak clastic sediments (Marinos and Hoek, 2000). Similar to the Torlesse of New Zealand it is characterised by alternating sandstone and more fine grain layers i.e. mudstone. Thickness of the sandstone ranges from centimetres to metres and the relative proportion between the two lithotypes differ between localities (Marinos and Hoek, 2000). It is noted that the rock mass can be mechanically altered by faulting to soil-like material with alteration of both the competent and non-competent members (Marinos and Hoek, 2001). Due to the number of engineering projects concerned with this type of rock mass, a variation of the GSI chart was developed in order to estimate GSI values (Figure 2.13). Despite this study not being primarily concerned with GSI, the values from the Marinos and Hoek (2000) modification of the GSI chart may represent a better system to classify the Torlesse of New Zealand outside of this study.

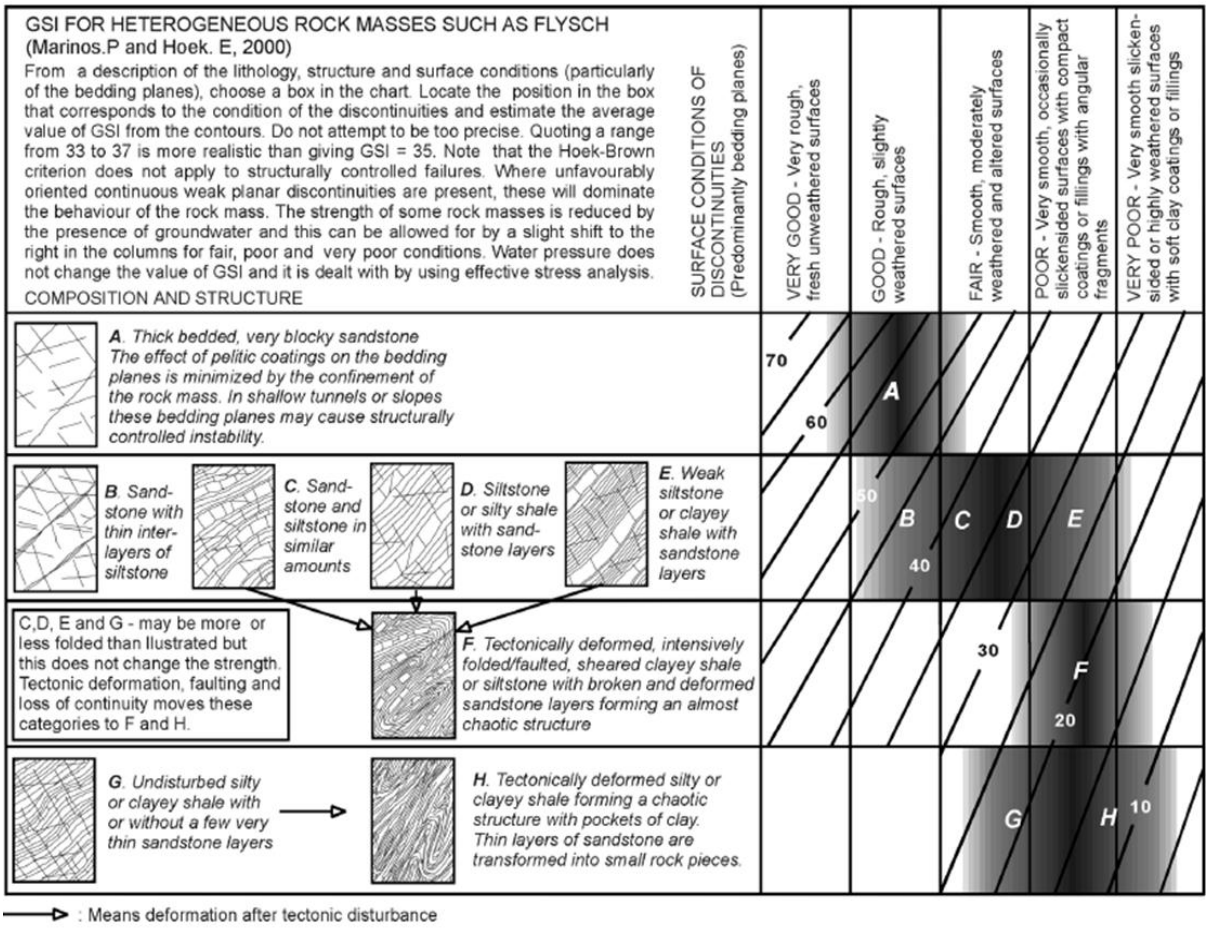

Figure 2.13: GSI chart for heterogeneous rock masses (Marinos and Hoek, 2000).

2.4 Torlesse engineering works

A number of works, including dams (i.e. Aviemore, Benmore) and rail/road tunnels, around New Zealand have been constructed within Torlesse. Of the constructions very little information regarding

Torlesse is readily available. In recent history no documented projects specific to Torlesse have been undertaken. Of late however, work has been done on the North Bank Tunnel Project located on the lower Waitaki River. The project proposes to take water from Lake Waitaki and divert it through a 34 km tunnel to generate power before discharging it back in the lower Waitaki River (URS, 2008). The scheme runs through Rakaia terrane and crosses a series of faults (URS, 2008). Current knowledge held by URS (2008) through desktop and preliminary geologic mapping is consistent with this study. Their mapping found a series of new faults with associated zones of shearing and associated deformation. To classify the rock mass the Read et al. (2000) descriptive classification was used for the purposes of underground support prediction. They state that the majority of work will be carried out in Class III Torlesse, described as blocky/disturbed to disintegrated using the GSI overlay.

URS (2008) assumes 50% of the lithology encountered is likely to be argillite. They also state the argillite will be the dominant control on stability and support requirements. Support requirements are given based upon a rock bolts, mesh and shotcrete system with steel sets and shotcrete used in zones of poorer ground. 90% of the excavation will be carried out by full face TBM which will be open, have a closed face cutting head and have rear loading cutters. They state that advance rates will likely be constrained by support rather than penetration rate and overbreak of the excavation will be minimal based on the close spacing and low persistence of jointing.

Other engineering works not directly related to this study include the Otira Viaduct constructed in Torlesse. The project provides a good volume of literature and reports related to Torlesse. Work concentrated around the geology found predominantly thick sandstone interbedded with thin argillite beds. Minor crush and shear zones were also found in areas particularly concentrated sub-parallel with bedding (PCA, 1994, Paterson, 1987). Some areas were found to be highly tectonised with the sandstone and mudstone intimately mixed. It was further noted by PCA (1994) that the geological structure of the rock is highly complex and unpredictable.

Chapter 3 Site results

The aim of this chapter is to assess observed trends through desktop study information, field mapping and laboratory testing to independently portray rock mass conditions at each site. Lineation analysis and conceptual models for select sites are paired with observed rock mass character to derive the main characteristics at each site. Understanding what controls each rock mass highlights trends and information that will inevitably feed into a classification system.

3.1 Elliott Fault

3.1.1 Lineation analysis

Lineation analysis of the Elliott Fault revealed a number of lineaments parallel with the main fault trace defined by GNS (Rattenbury et al., 2006). Lengths of the lineaments differ and some dwindle out or disappear beneath the active river channel (Appendix D.1). Results of the basic analysis reveal a diffuse zone of deformation around the major fault zone.

3.1.2 Rock mass

Raw Elliott Fault mapping results are reproduced in Appendix D.2. Rock mass conditions vary substantially across the study site. A greater level of deformation is observed within the hanging wall of the main fault trace, which has been uplifted (Eusden et al., 2011). The foot wall, conversely, has less deformation and hosts more evidential bedding. A 250 m extent of rock mass along the hanging wall is affected by faulting. Conversely, approximately 60 m of rock has been affected on the foot wall side. Rock examined outside these zones within the foot wall is in relatively good condition and gives little structural indication of regional scale faulting.

3.1.2.1 Rock mass conditions in relation to proximity to the main fault trace

Rock around the main Elliott Fault trace is deformed to different levels. Within the main fault zone different rock mass types can be observed. The rock mass existing at an approximate 50 m width on the hanging wall and an approximate 10 m width on the footwall, is the weakest of the material described as stiff to very stiff with no bedding recognisable (Figure 3.1). This is located either side of the main active fault trace. The material is clast supported with no apparent clast rotation. The rock can be readily disaggregated from the rock face by shovel and crushed into silty sandy gravel by hand. Similar to the Ward (2000) fault gouge distinction, the disaggregated material geotechnically behaves as a soil. In-situ however the rock mass appears tightly interlocked (Figure 3.1, left). It is dominated by incipient fracturing with block sizes rarely exceeding 2 cm.

Dominantly located within the hanging wall, rock outside the main fault rock zone differs in properties. No bedding can be recognised and the rock is still fragmented (outcrops 10a, 10b, 5d, Figure 3.2). The top 10-20 cm of weathered sun baked material is readily removed. Approximately 25 cm into the face the rock becomes more indurated incorporating greater volumes of intact rock and

has notable fragmented, rotated blocks up to a metre in size. Rock can be disaggregated from the face with a rock hammer and clasts collected can be broken by hand. Small scale shear planes can be identified within the sheared rock mass.

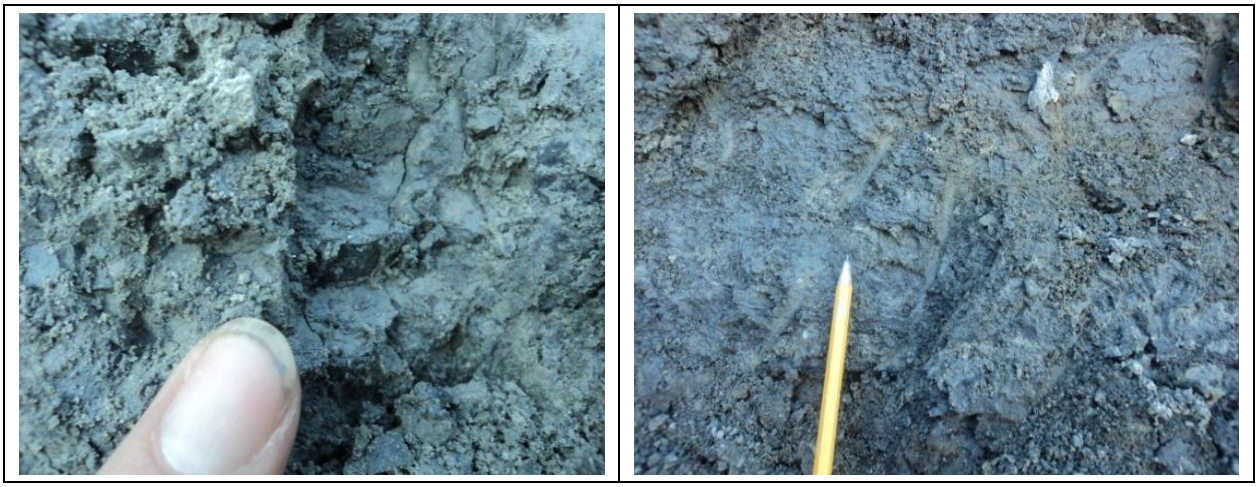

Figure 3.1: Main fault zone rock. Note the heavy incipient fracturing. Left: outcrop 10c; right: outcrop 5g.

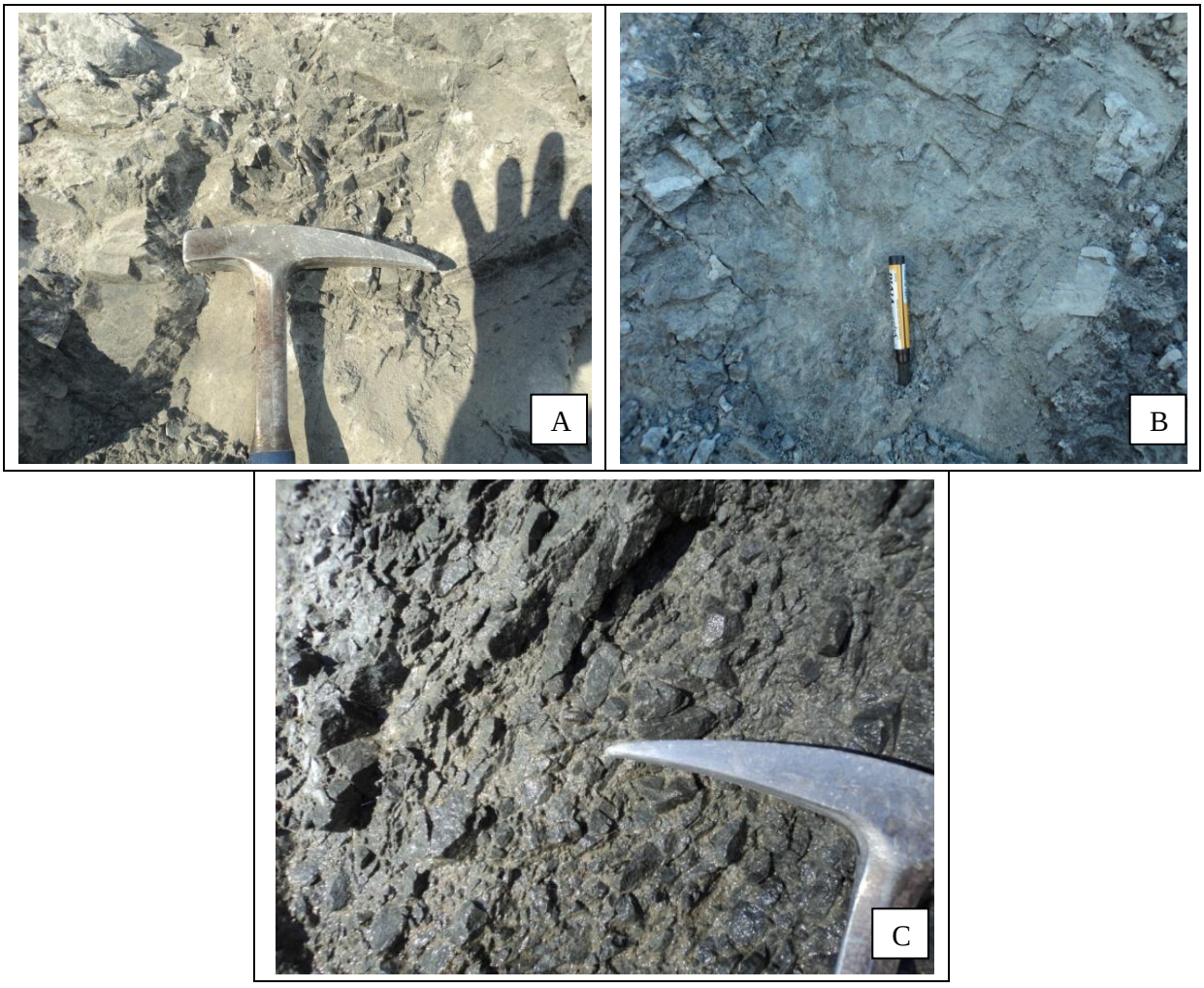

Figure 3.2: Secondary rock mass appearance. A: outcrop 10a; B: outcrop 5d; C: cleaned surface, outcrop 13a.

Immediately away from the main trace bedding was recognisable. Observations at outcrop 9a and 10d show notable bedding which remains fragmented with the largest clast sizes approximately 10 cm in length. Mudstone within this zone is fragmented to a higher degree than the interbedded sandstone.

Immediately outside this zone, only observed within the foot wall, is a zone where rock mass improves (outcrop 10e). The rock mass is still predominantly fragmented with pockets of highly fractured rock. Intact blocks greater than 10 cm are common. Faults and shears up to 70 cm in width (Figure 3.3A & B) dominate the rock mass and likely relieve some rock mass stress during fault rupture. A large, more intact, rotated block in excess of 5 m in length is observed within this zone (Figure 3.3C). Bedding and jointing patterns differ from surrounding rock and the block is bound by two distinctive shears. Non persistent, less than 2 m jointing is observed but the rock mass is predominantly controlled by apparently random fractures.

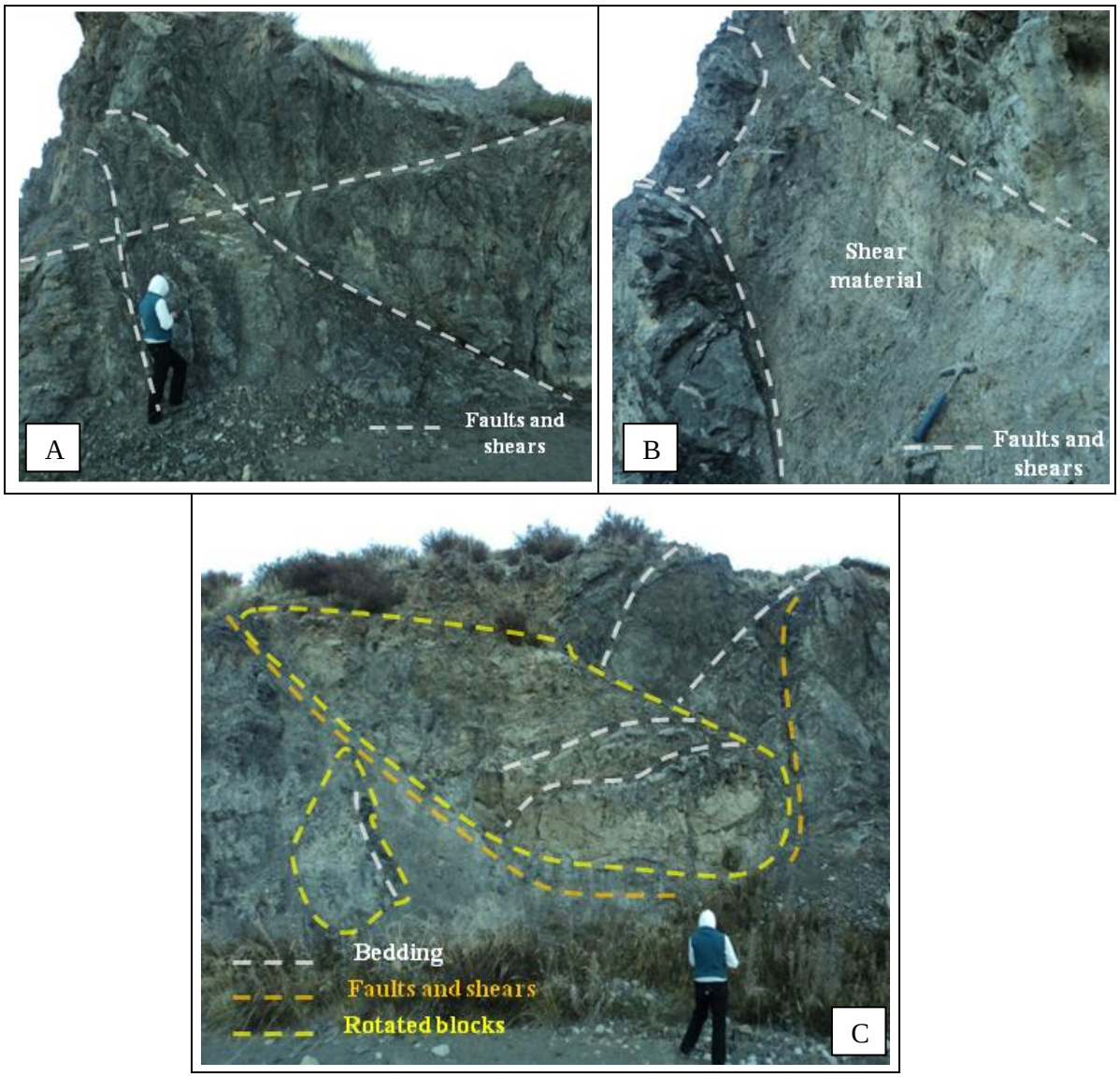

Figure 3.3: Outcrop 10e. A: shear cluster in the fragmented rock mass; B: large shear material present in the zone; C: large rotated blocks with bedding and shearing indicated.

Fault footwall rock, some 110 m outside the main zone of faulting is in relatively good condition and does not give any indication of structural damage. A large proportion of thinly bedded sandstone-mudstone sequences are observed (outcrops 1a-e, 3a, see Appendix D.3). The bedding displays gradational changes from fine to coarser sandstone and mudstone (Figure 3.4). The thin bedding is in relatively good condition, however, it remains highly fractured to fragmented. Other thinly interbedded rock (outcrop 5b) has distinctive bedding planes and the rock mass appeared worse as a result. Two main shear zones in excess of 2 m were observed within thinly bedded members away from the active trace (Figure 3.5). More intact rock of greater thicknesses was observed (4a, 5k, 6a, 6b, 12a). This rock mass is the best observed in the study site. Degree of fracturing is dominantly moderate to highly fractured and there is no indication of ground water. Persistent jointing is identified within the range of bedding thicknesses at the Elliott Fault which differs from jointing patterns observed elsewhere (Appendix D.3).

Figure 3.4: Gradational bedding within the thinly bedded members at outcrop 3a, Elliott Fault.

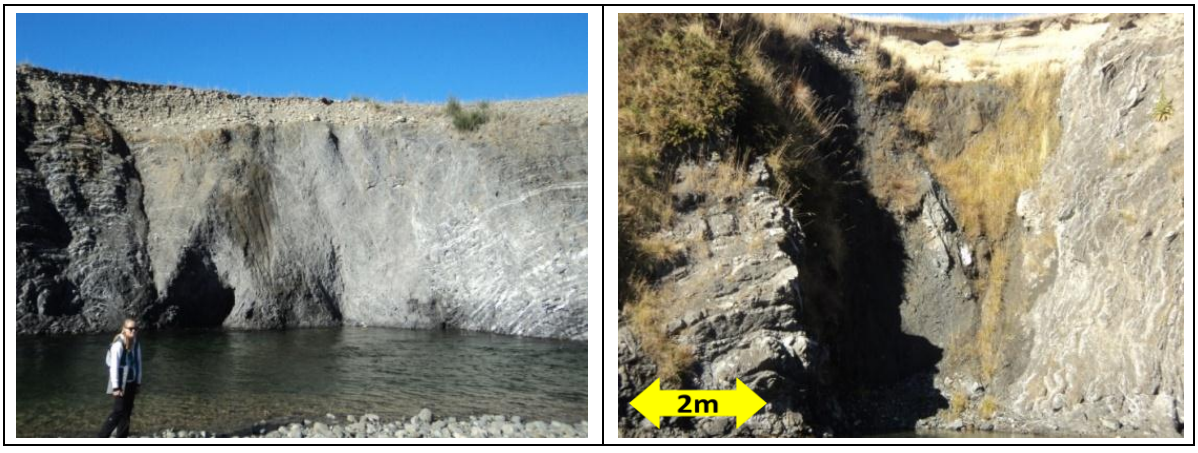

Figure 3.5: Large scale shearing within thinly bedded members away from the active fault trace. Left: outcrop 1c; right: outcrop 8b.

3.1.2.2 Discontinuity condition

Smaller outcrop scale faults and shears are concentrated within the thinly bedded members (see Appendix D.3). These faults and shears are infilled 75% of the time, commonly with lineated mudstone, sand fractions and gravel (Figure 3.6) less than 10 cm in width (Figure 3.7). This excludes the main fault zone widths at 100 m. Joint, bedding and fault/shear shape is dominantly linear with little variation (Figure 3.8) and are dominantly clean. Defect roughness is commonly undulating across all defects (Figure 3.9).

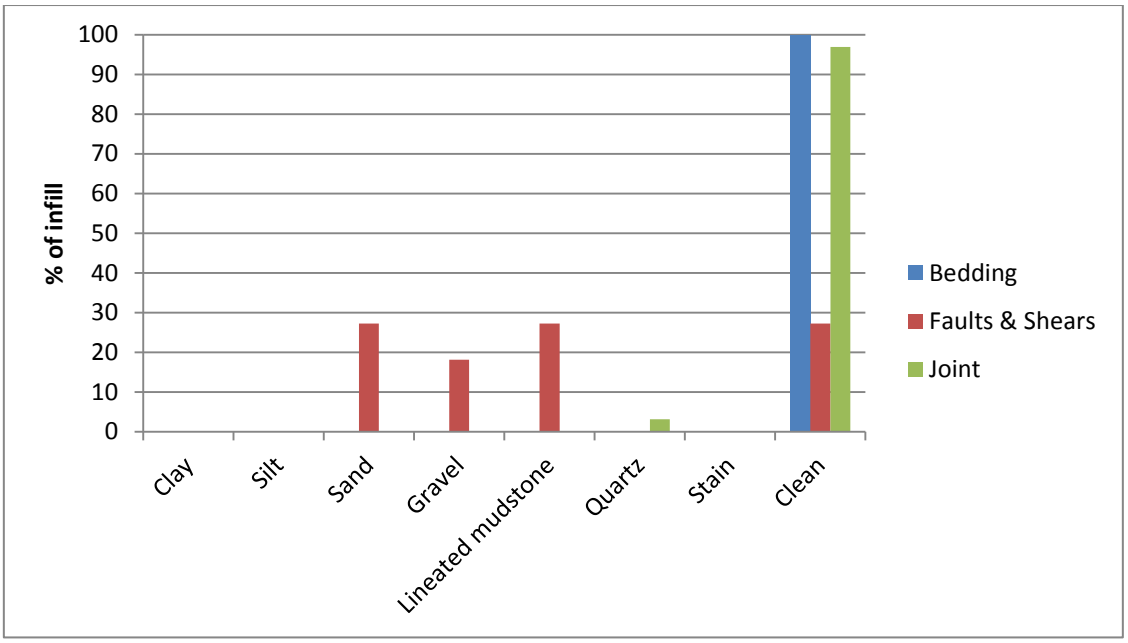

Figure 3.6: Elliott Fault infilling type and percentage as a total of all infill lithology per defect type.

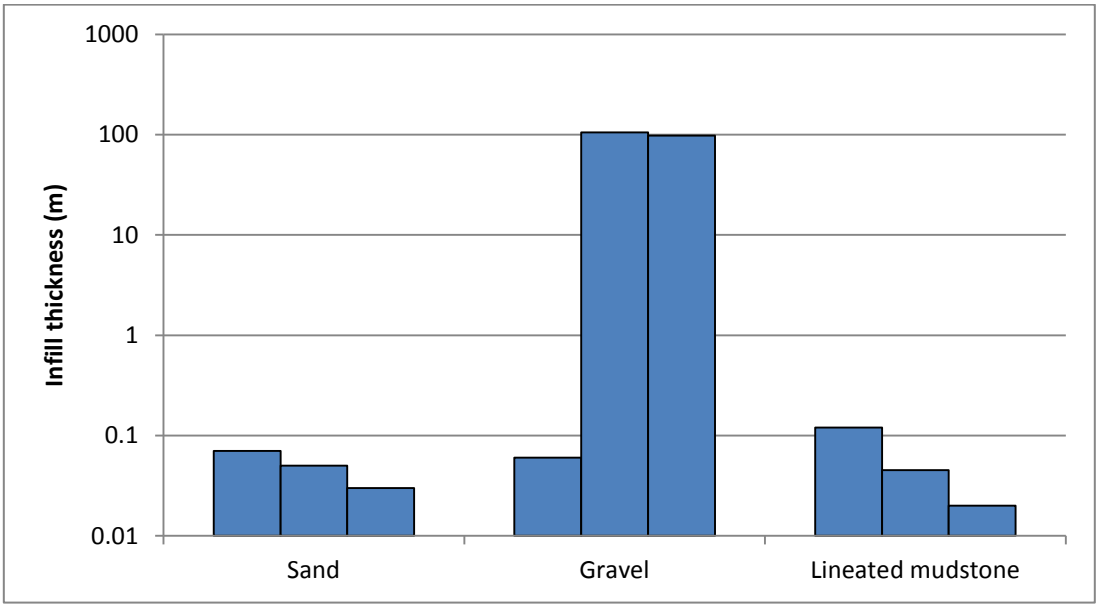

Figure 3.7: Elliott Fault shear and fault infill thickness.

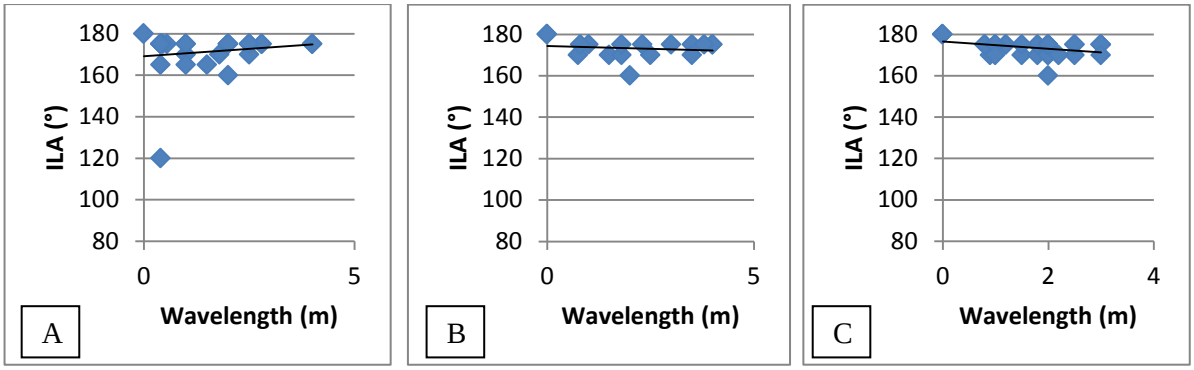

Figure 3.8: Elliott Fault defect waviness defined by interlimb angle (ILA) and wavelength (m). A: bedding; B: faults/shears; C: jointing.

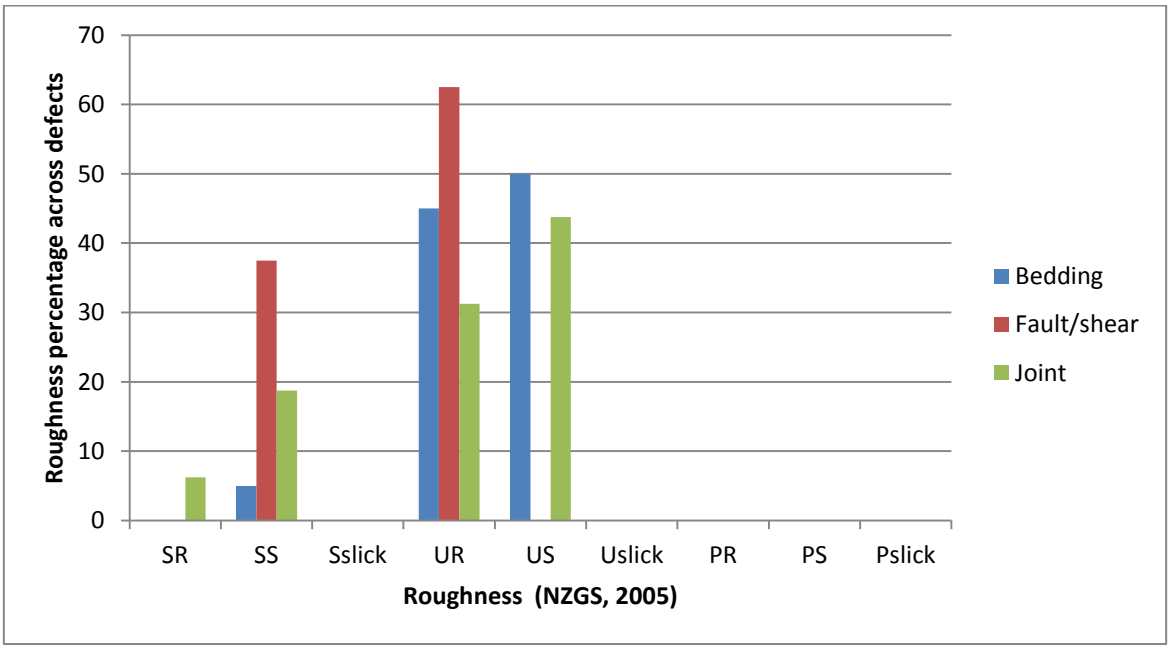

Figure 3.9: Elliott Fault surface roughness percentage across defects.

Two dominant bedding orientations were derived (Appendix D.4). Variation is likely due to localised faulting. Bedding strike and dip direction remains relatively consistent. One dominant dip/dip direction joint cluster is identified at 60°/225°, sub-parallel with bedding. Shearing remains independent at random orientations.

3.1.3 Laboratory testing

3.1.3.1 UCS

Intact hard rock testing was carried out on a number of samples from the Elliott Fault. Table 3.1 summaries Unconfined Compressive Strength results for the four lump samples from which adequate core was able to be drilled. Full results and calculations are reproduced in Appendix D.5. Results indicate an average strength of 135 MPa. Failure mode was predominantly violent disintegration with multiple extension and fracture failure defined by (Szwedzicki, 2007). Samples taken from locations

where no evidence of large scale faulting was observed were relatively stronger in comparison to rock taken from outcrop 5k, bordering the major fault.

Table 3.1: Elliott Fault UCS results.

Outcrop	UCS (MPa)	Failure mode (Szwedzicki, 2007)
6a	165.53	Multiple extension & fracture – Disintegration
6a	130.81	Simple extension & multiple fracture – Disintegration
5k	87.87	Multiple extension & fracture – Disintegration with 5-10% break along existing defects
4a	150.6	Simple extension with 100% break along existing quartz vein

3.1.3.2 BTS

Thirty indirect Brazilian Tensile Strength tests were carried out across nine outcrops (see Appendix D.6). Testing was largely restricted to intact rock and as a result may over estimate tensile strengths. A distinction between clean failure through the rock substance, representing intact strength, and existing defect failure, better representing rock mass strength have been given.

The fine sandstone sample appeared to have greater average intact and existing defect failure strengths (Table 3.2). In comparison, fine to medium sandstone had lower average clean and existing failure strengths. Results further indicate thickly to massively bedded sandstones typical of outcrop 6a tend to have the highest average intact tensile strengths with a lower average tensile strengths for failure along existing defect. In contrast the thinly bedded members typical of 1e and 3a on average have lower intact strengths averaging 15 MPa, but higher existing defect failure strengths of 13 MPa.

A trend can also be derived from proximity to the Elliott Fault. Outcrop 5a and 5k were observed to be relatively intact however exhibited low tensile strengths averaging 14 MPa. Higher strength samples tended to fail along a number of planes parallel to loading defined as multiple extension by Szwedzicki (2007). Conversely lower strengths tended to fail in a simple extension sense.

Table 3.2: Elliott Fault average Brazilian Tensile strengths.

	Clean failure (MPa)	Existing defect failure (MPa)
Fine sandstone	20.25	11.47
Fine to medium sandstone	11.35	6.83
Massive - thick bedding	17.14	8.23
Medium to very thin bedding	14.78	12.57
Direct fault bordering rock	13.66	7.82

3.1.3.3 Point load

Point load index testing was carried out per outcrop. Raw results and calculations are reproduced in Appendix D.7. Table 3.3 summarises point load index strength results produced as averages per bedding thickness, lithology and fault affected rock. Thickly bedded sandstone is the strongest sandstone both intact and when failing along defects. This result is consistent throughout different intact strength testing. Mudstone remains the weakest lithotype with direct intact fault affected rock having similar strengths to the thinly bedded member. Little variation was shown over mudstone strengths across the study site despite changes in bedding thickness and proximity to faulting. An average point load to UCS sandstone conversion factor of 28 was worked out from Elliott Fault outcrops were point load and UCS sample was collected. No mudstone conversion factor was obtained due to the lack of mudstone sample for UCS testing.

Table 3.3: Elliott Fault average point load index strength results.

	Average I_{s50} (MPa)	
Failure	**Clean break**	**Existing break**
Thin bedding (sandstone)	3.65	1.45
Thick bedding (sandstone)	5.64	3.89
Faulted rock (sandstone)	3.92	1.6
Intact faulted rock (sandstone)	4.98	1.68
Fine to medium sandstone	4.77	2.25
Fine sandstone	4.18	1.67
Mudstone	3.02	0.94

3.1.3.4 Fines index testing

Fines index testing across the Elliott Fault was carried out as a systematic cross section line along the two main faulted rock outcrops 5 and 10. Table 3.4 and Table 3.5 differentiate fines content through sieve and laser sizing analysis. Raw laser sized calculations are reproduced in Appendix D.8. The decrease of gravel and increase of fines percentage, particularly clay is well correlated with the lineation analysis where lineations including the main Elliott Fault trace intersect closely with outcrop 5h and 5j. Similarly the increase in fines content toward the major fault zone supports observations of a number of different rock mass zones around the major fault zones previously discussed.

Table 3.4: Fines index testing results for outcrop 5 cross section samples. Increasing proximity to the fault from left to right.

	5c	**5d**	**5e**	**5f**	**5g**	**5h**	**5i**	**5j**
Passing	%	%	%	%	%	%	%	%
>4mm	78.16	74.67	43.32	51.57	51.81	41.38	59.92	40.56
>2mm (Gravel)	8.54	11.47	13.33	10.4	18.9	10.17	19.4	9.84

Table 3.4 (continued): Fines index testing results for outcrop 5 cross section samples. Increasing proximity to the fault from left to right.

	5c	5d	5e	5f	5g	5h	5i	5j
	%	%	%	%	%	%	%	%
>1mm (C-M sand) (sieving & laser)	7.98	9.98	15.32	10.23	21.60	15.10	15.95	11.55
<200 microns (Fine sand)	1.2	1.82	4.37	11.86	1.63	9.47	1.23	11.81
<60 microns (Silt)	3.32	1.73	19.08	12.88	4.92	18.73	2.73	22.23
<2 microns (Clay)	0.79	0.33	4.58	3.07	1.14	5.14	0.78	4.02

Table 3.5: Fines index testing results for outcrop 10 cross section samples. Increasing proximity to the fault from left to right.

	9a	11a	10a	10b	10c	10e (shear zone)
Passing	%	%	%	%	%	%
>4mm	88.18	71.37	59.49	45.27	39.2	56.41
>2mm (Gravel)	4	10.79	15.27	15.14	15.04	16.63
>1mm (C-M sand) (sieving & laser)	5.47	10.79	18.69	29.75	19.08	14.29
<200 microns (Fine sand)	0.66	2.36	0.7	4.46	13.6	0
<60 microns (Silt)	1.31	3.97	4.62	4.3	10.9	9.8
<2 microns (Clay)	0.38	0.72	1.23	1.07	2.19	2.87

3.1.3.5 XRD and thin section analysis

XRD was undertaken to validate the occurrence of true clay from the clay sized fraction targeting the finer fraction of sieved material (Table 3.6). From the finer fraction a maximum of 15% true clay defined by Kaolinite and Illite was identified. Similarly to the sieve analysis, outcrops defined as the main fault trace, i.e. 10c and 5j show the highest percentage of true clay. It must be noted however, clay volume at 15% true clay from material less than 1 mm is relatively minor.

Table 3.6: Elliott Fault XRD analysis of infill material less than 1 mm.

Sample outcrop	Quartz (%)	Albite (%)	Kaolinite (%)	Illite (%)
10a	60	30	10	Trace
10c	50	35	10	5
10e (shear zone)	60	30	5	5
5e	65	25	5	5
5g	65	25	5	5
5h	60	30	5	5
5i	55	30	5	10
5j	55	30	10	5

Thin section work was carried out on two fine to medium grained sandstones either side of the study area and a third fine grained sandstone section to define QFL ratios (Table 3.7). Of interest is the relatively high lithic to quartz and feldspar ratio. This classifies the greywacke as a Lithic Greywacke (Boggs (2001) after Pettijohn et al. (1987)). Grains are typically angular to sub-angular and feldspars tend to be discoloured in both plane polarised light (PPL) and cross polarised light (CPL). Millimetre scale boudinage is observed in thin section from sample 9a. A finer matrix is observed (mudstone) 'flowing' around both pockets of coarser sandstone and individual crystals.

Table 3.7: Elliott Fault QFL ratios derived from thin section point counting.

Sample #	Quartz %	Feldspar %	Lithic fragments %
1e	19	32	49
5c	27	30	43
9a	24	26	50

3.2 Hurunui River

3.2.1 Lineation analysis

A general structural northeast-southwest grain of lineaments was observed. 14 lineaments were observed throughout the large lineation analysis area (Appendix E.1). The eastward topography of the study site appears increasingly chaotic in visual appearance compared to the west. As a result no definitive landscape lineations were derived in the westward study area whereas lineations tended to cluster around the more eastward chaotic topography. This area, as previously described, marks the transition from Esk Head Belt to Pahau Torlesse terrane. The transition between the two terranes is described as a gradation through several kilometres of sheared rock incorporating exotic material (Silberling et al., 1988) which is reinforced with the relative level of lineation observed.

3.2.2 Conceptual model

The conceptual model defined two rock mass zones across the Hurunui site (Figure 3.10). The cross section of the study site crosses a number of lineaments including the Esk Fault, defined by A-A" (refer to Appendix E.1). The two blocks identified incorporate the lineaments observed and as a result distinguish the more chaotic eastward zone, termed the Mount Noble Structural Zone (MNSZ) from the less sheared westward zone termed the Hurunui River Block (HRB).

The HRB is expected to be in much better rock mass condition with consistent bedding dip/dip direction toward the southeast. Lineations defining potential structures increase toward the Esk Fault. Using the Read et al. (2000) Torlesse specific classification previously described, rock mass conditions are expected to be dominated by class III Torlesse with occasional better zones of class II & poorer zones of class IV. The occurrences of class V discrete crush zones of varying thickness should be anticipated and potentially concentrate around the lineations identified.

Rock Mass Zone	Hurunui River Block	Mount Noble Structural Zone
Geology	Esk Head Belt Torlesse terrane.	Esk Head Belt Torlesse terrane with some Pahau Torlesse terrane toward the northeast. This zone incorporates the Esk Fault and exotic melange is expected.
Rock Mass Conditions with reference to Read et al. (2000) classification classes	Anticipated to be dominated by class III greywacke with occasional better zones of class II & poorer zones of class IV; some widely spaced (>0.5km apart) class V discrete crush zones are also possible.	Zone topographically appears more chaotic (see lineation analysis). Class III greywacke with frequent class IV brecciated rock & class V crushed rock associated with major fault & sheared zones spaced approximately 0.5km apart. Potential fault gouge is possible.
Groundwater	Some compartmentalisation of groundwater associated with relatively wider spaced faults & shears.	Lineation can be observed within the chaotic topography. A number of small scale closely spaced shear zones associated with the transition into Pahau terrane are likely to compartmentalise groundwater. Higher pore pressures are expected in this zone than the Hurunui Block.

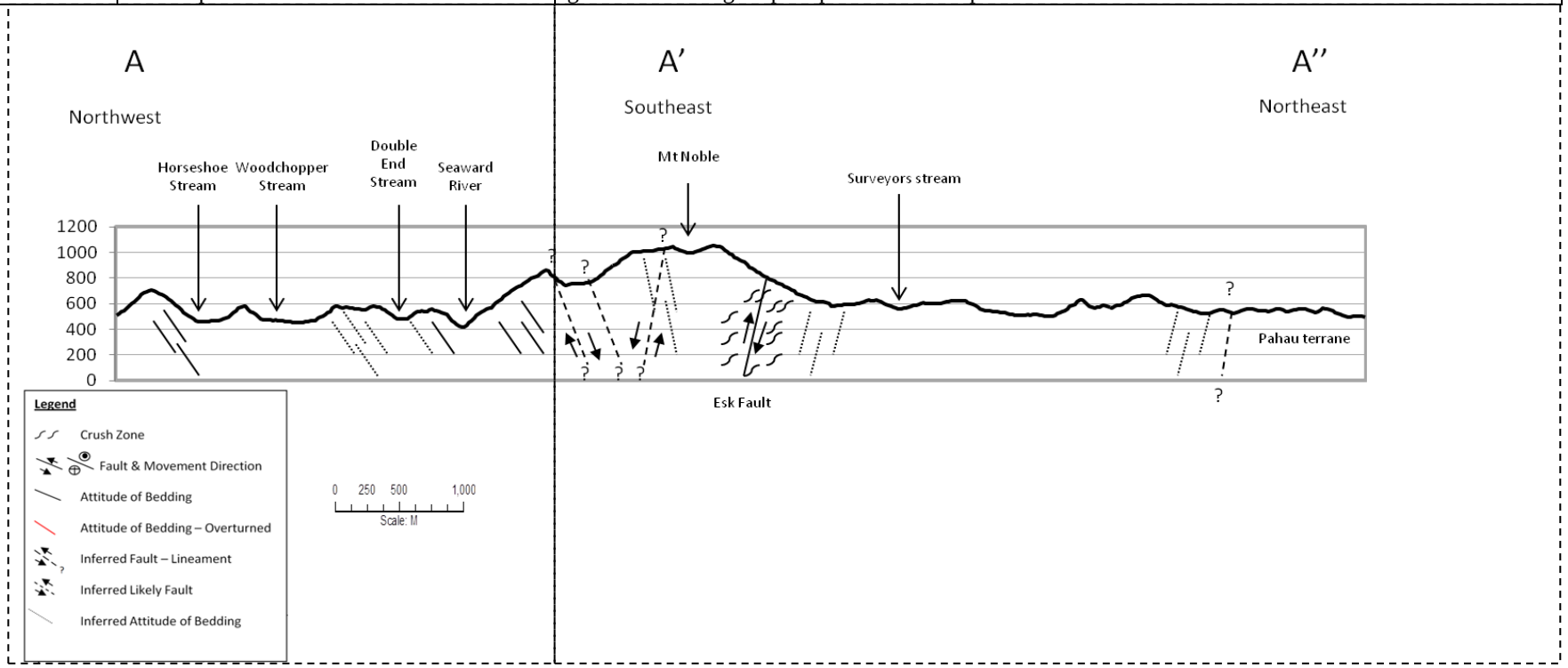

Figure 3.10: A-A'' conceptual cross section model showing faults, structure and rock mass zones derived from the lineation analysis and Rattenbury et al. (2006).

Poorer rock mass condition is likely to be expected in the MNSZ. The zone incorporates the regional Esk Fault structure and houses a number on lineaments only three of which, including the Esk Fault, cross the section line. Again, utilising the Read et al. (2000) classification, the rock mass is anticipated to be class III Torlesse with frequent class IV brecciated rock and class V crushed rock associated with zones of more sheared rock (Silberling et al., 1988). Bedding is likely to be more disturbed, changing dip direction from the southeast to the southwest. Significant Broken Formation is expected throughout both blocks which characteristically define the Esk Head Belt Torlesse terrane.

3.2.3 Rock mass

Raw mapping results are reproduced in Appendix E.2. Distinctive rock mass zones are present throughout the Hurunui River site. Observations are divided into the Hurunui River Block (HRB) and the Mount Noble Structural Zone (MNSZ).

3.2.3.1 Hurunui River Block

The HRB was confirmed as the better rock mass. Medium spaced bedding to massive sandstone was dominantly paired with thinly interbedded mudstone (Appendix E.3). Degree of fracturing was generally moderately to highly fractured. Mudstone bedding was typically thin, however, some mudstone beds of greater thickness were observed within the HRB (Figure 3.11A). Due to the relative strength of the mudstone, abundant small scale faults and shears tended to concentrate in the member (Figure 3.11A). Despite bedding thickness, mudstone bedding remained fragmented with greater than 50 breaks per metre (Figure 3.11B). Within fragmented centimetre scale mudstone blocks hairline incipient fracturing was observed (Figure 3.11C).

Thinly interbedded sandstone and mudstone was observed at outcrops 13 through 14 in the HRB. Outcrop scale faulting and folding tended to concentrate within the thinly bedded members (Appendix E.3). The degree of faulting and folding was much more abundant in comparison to the thinly bedded rock mass previously described at Elliott Fault (Figure 3.12A & B). The thinly bedded outcrops tended to contain the worst rock mass conditions through the HRB, and were typically fragmented in fracture density (Figure 3.12C). A lineation was observed running directly perpendicular to this site (Appendix E.1) and may account for the increase in outcrop scale faulting. Sandstone lithologies in the thinly bedded members are fine grained, however, fine to medium grained sandstone is still present in select beds.

Abundant small centimetre scale boudinage was observed within the very thin interbedding observed at outcrops 14a and b. Similar boudinage was observed at outcrop 12a. The outcrop however is described as thickly bedded sandstone and mudstone defined by sharp bedding contact. Encased within the mudstone matrix, centimetre scale angular sandstone fragments are observed (Figure 3.12D). Due to the sharp bedding contacts, sandstone boudins likely originate from thin to very thinly

bedded sandstone layering within the mudstone. The entirety of the mudstone unit encasing the sandstone boudins is now homogenous with no evidential bedding defect.

Figure 3.11: A: very thickly bedded mudstone with heavy shearing indicated; B: fragmented nature of the mudstone lithotype; C: incipient fracturing occurring within fragmented mudstone blocks.

Differing to typical thinly bedded characteristics, outcrop 13b had two distinct persistent joint sets despite a highly fractured to fragmented fracture density. The rock mass was still heavily controlled by non-persistent fracturing, however, the larger persistent jointing controlled the release of blocks from the outcrop face having limited control on the rock mass.

Persistent jointing (greater than 2 m) throughout the HRB was exceedingly abundant. Jointing is concentrated within the thicker bedded members (Appendix E.3). Generally the rock mass was in better condition where the presence of persistent jointing controlled the rock mass (Figure 3.13A & B). It must be noted the occurrence of less persistence jointing is still present and still has some control on the overall rock mass. The effect of the jointing volume creates rock mass types which are predominantly blocky (Figure 3.13C). Despite the better overall rock mass conditions creating large blocks, incipient hairline fractures, similar to mudstone are observed (Figure 3.13D & E).

Figure 3.12: A & B: folding and faulting concentration in the thinly bedded member; C: fragmented fracture density; D: centimetre scale sandstone boudinage encased in mudstone matrix.

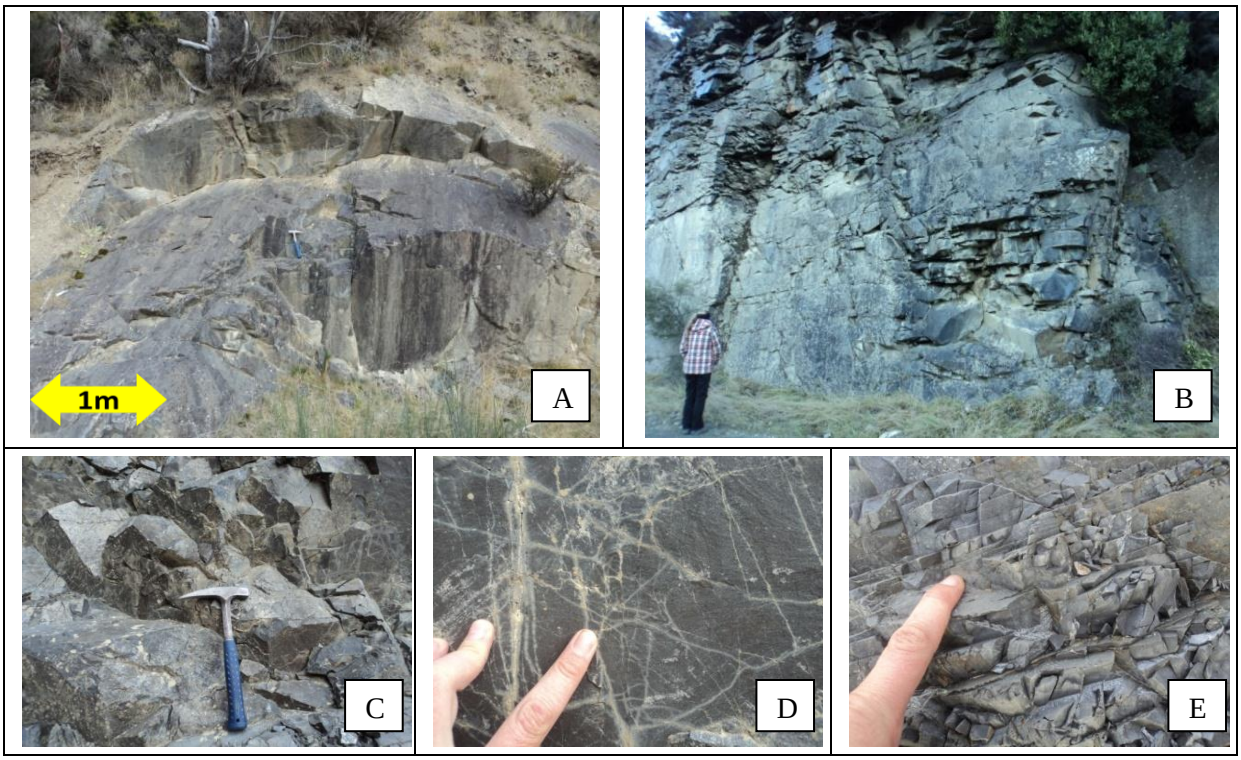

Figure 3.13: A & B: outcrops 5b and 17a rock masses controlled by persistent jointing; C: blocky rock mass. Note the level of low persistent jointing; D & E: incipient fracturing examined in good rock masses.

3.2.3.2 Mount Noble Structural Zone

The MNSZ tended to have a higher concentration of thinner bedded members resulting in an average fractured density of highly fractured to fragmented (outcrops 18a-23d). The rock mass is in overall worse condition in comparison to the HRB. Heavy boudinage from centimetre to metre scale was observed throughout the MNSZ and tended to concentrate around the thin to medium bedded sandstones (Figure 3.14). Exotic melange in the form of volcanic pods were observed in this zone and tended to occur at random localities throughout the Torlesse in the MNSZ.

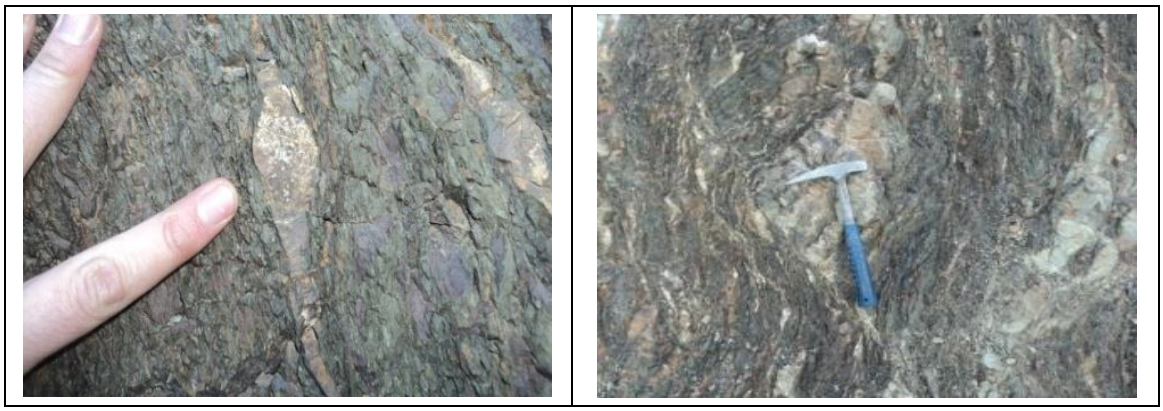

Figure 3.14: Examples of varying scales of boudinage observed in the MNSZ.

Outside the Esk Head Belt zone defined by Rattenbury et al. (2006) (outcrops 24a-29a) conditions improved dramatically where the Pahau terrane was encountered. Fracture density subsequently decreased to an average of moderately fractured with some outcrops described as fractured. Bedding thickness in the Pahau terrane was relatively random with a range of thickness also observed.

Due to the nature of thinner, medium bedding thickness in the MNSZ (excluding the Pahau terrane), persistent jointing greater than two metres in length was not encountered. Shears and faulting however tended to concentrate within the member further increasing the degree of fracture. This observation confirms the Silberling et al. (1988) zone of more sheared rock as the Esk Head Belt grades into Pahau terrane.

Fragmented, layer parallel sheared mudstone is indicative of the Broken Formation (after Rattenbury et al. (2006)). It was observed in all mudstone bedding throughout both structural blocks regardless of bedding thickness, however was more evident within the thinner mudstone member. Typically fracture was lineated parallel with bedding indicating layer parallel shearing (Figure 3.15). Due to the level of weathering, slickenside was not easily observed to confirm this hypothesis. Broken Formation was observed throughout the whole study site, however was more evident within the MNSZ.

Figure 3.15: Broken formation observed throughout the Hurunui River study site.

3.2.3.3 Discontinuity condition

Little indication of groundwater condition was given throughout the entirety of the study site. Outcrop 15a had the only indication of ground water condition (Figure 3.16). Defect surfaces were wet and water was observed dripping from relatively open, horizontal jointing.

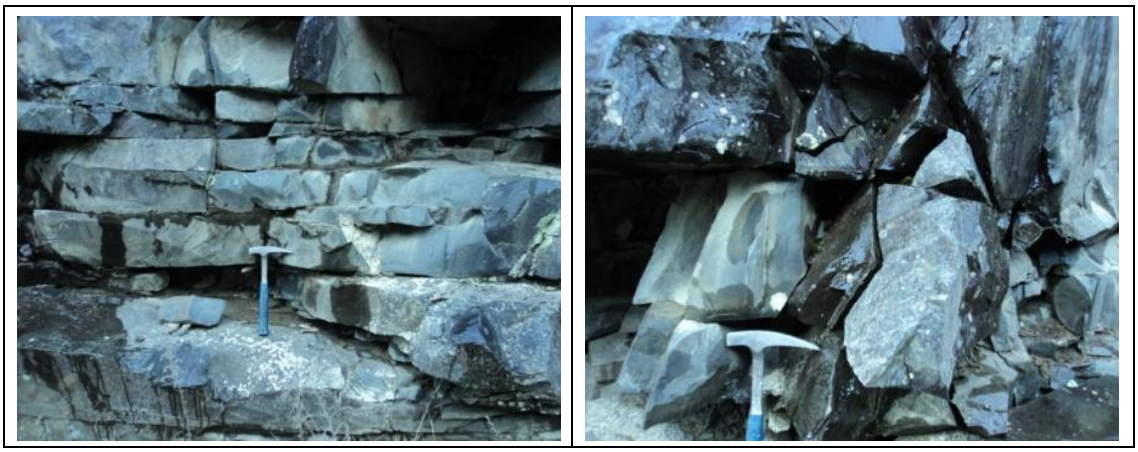

Figure 3.16: Indication of ground water nature flowing through open horizontal jointing.

Similar to the Elliott Fault site occurrence of infilling was dominant toward faults and shears. Bedding remained clean ignoring the development of fragmented mudstone not foreign to the surface (Figure 3.17). Jointing was dominantly clean. Defect staining should be anticipated where groundwater is likely to be flowing through interconnected defects where adequate aperture exist. The lack of groundwater flowing through surficial outcrops and extended periods of surface weathering has meant evident stained surfaces are rare. Silt is the dominant infilling fraction. Plastic, clay sized gouge was observed in some select faults and shears (Figure 3.18). The material exhibited clay properties with slight plasticity. The material was moist and hosted millimetre scale intact granules. The material occurred in zones less than 10 cm in size and has been termed gouge. Faulting and subsequent infilling was particularly abundant throughout outcrop 23 which may be related to external influences.

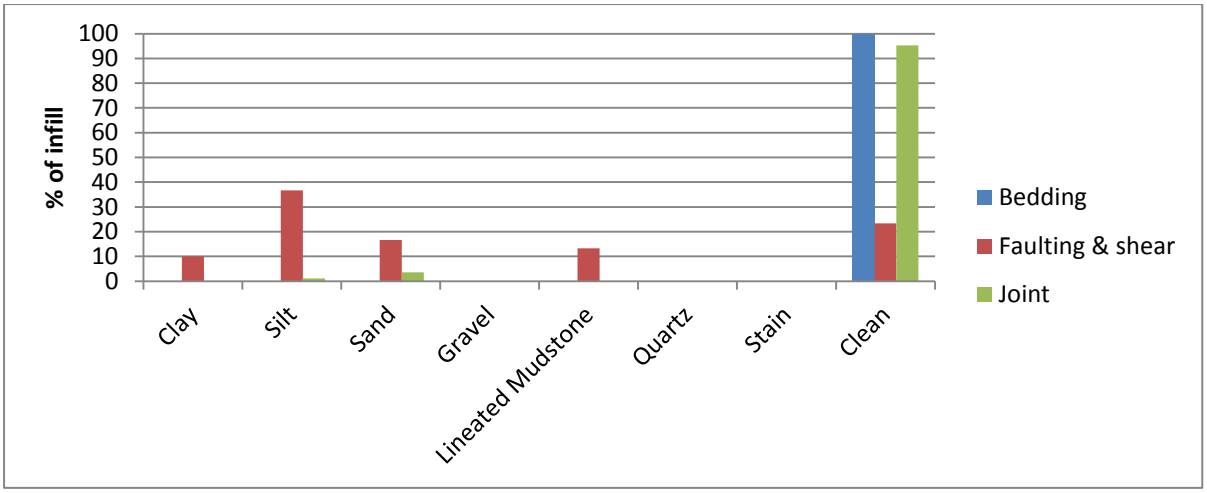

Figure 3.17: Hurunui River infilling type and percentage as a total of all infill lithology per defect type.

Figure 3.18: Clay fault gouge. Left: outcrop 18a; right: outcrop 23b (sample 23b – clay).

Defect waviness slightly differed from the Elliott Fault site. Bedding and jointing defects remained relatively linear, however due to the level of historic tectonisation in the area, bedding and to a lesser extent jointing, increased in waviness at higher persistence (Figure 3.19). Of interest is the distinct low wavelength and interlimb angle of bedding defects. These are characterised by the waviness of boudinage bedding particularly in the MNSZ and the heavy folding of thinly bedded sandstone down to 90° in one occurrence. Fault and shear defects are shown to become increasingly wavier at higher persistence. Discontinuity roughness is dominantly undulating, however stepped and planar surfaces are observed without slickensides (Figure 3.20).

Shear and joint orientation is random and steronet plots tend to shotgun across the Hurunui River. Four well defined bedding orientations are observed in the Hurunui (Appendix E.4). Further analysis suggested different bedding orientations between structural blocks likely offset by the Esk Fault. In both structural zones bedding orientations alternate over 180° which is well defined by structural zone steronets (Appendix E.4). Well defined 180° alternations are likely a result of folded bedding limps across numerous fold axes.

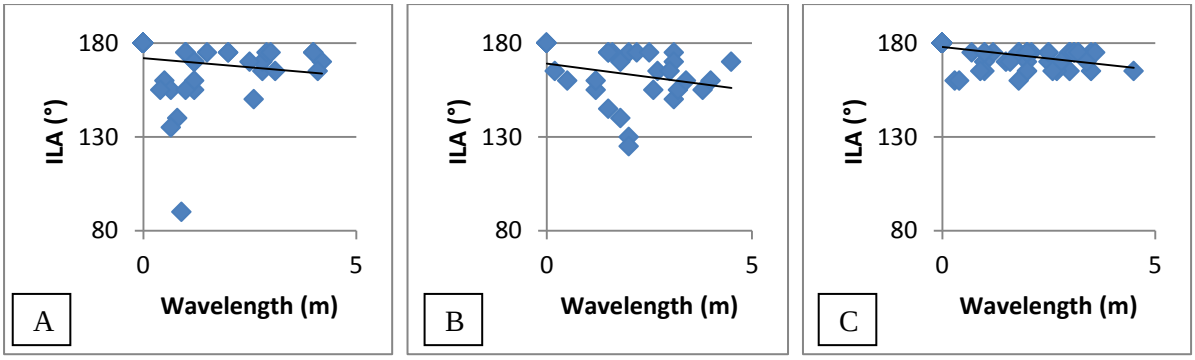

Figure 3.19: Hurunui River defect waviness defined by interlimb angle (ILA) and wavelength (m). A: bedding; B: faults/shears; C: jointing.

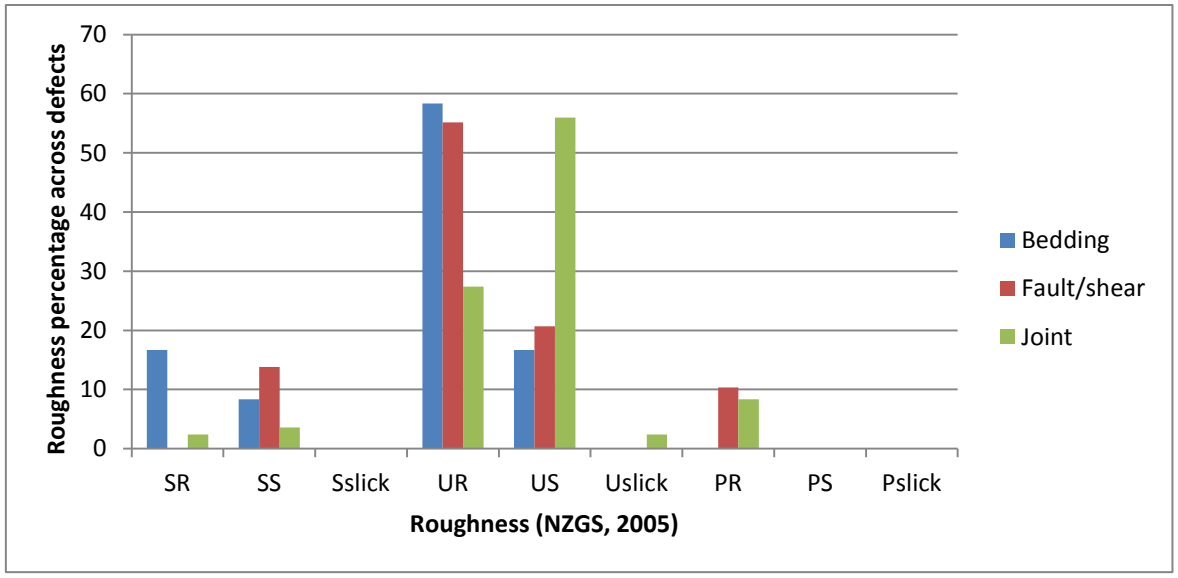

Figure 3.20: Hurunui River defect roughness percentage across defects.

3.2.4 Laboratory testing

3.2.4.1 UCS

The relatively good rock mass throughout the site meant sample for coring was readily obtained. Rock had high intact rock strengths from the 12 Hurunui samples UCS tested (Table 3.8). Due to the relative lower occurrence of fractures and shears in the HRB compared to the MNSZ, sampling for coring (USC, BTS, and CAI) was typically restricted to the HRB. The overall UCS average strength is 169 MPa. Ignoring samples with significant breaks along existing discontinuities, intact rock strengths average 210 MPa. Similarly ignoring clean (substance) UCS breaks may give some indication of the overall rock mass strength which averaged 90 MPa. A fine grained sample from outcrop 13c was the only sample that differed from the medium to fine grain size of other samples. As previously described, the thinly bedded outcrop exhibited a number of shears and was highly fractured to fragmented in fracture density. Under unconfined load the sample failed at 35.63 MPa with approximately 80% breakage along existing defects. Appendix E.5 reproduces raw UCS results and

calculations. Specific energy (MJ/m³) was obtained through Trilab analysis of UCS samples. Outcrop 5b had a specific energy of 0.028 MJ/m³ and outcrop 29a, 0.024MJ/m³.

Table 3.8: Hurunui River UCS results.

Outcrop	UCS (MPa)	Failure mode (Szwedzicki, 2007)
2a	251.47	Multiple extension & fracture – Disintegration
1b	162.02	Multiple extension & fracture – Disintegration
2b	165.74	Multiple extension with some indication (5%) of break along a perpendicular quartz vein
4a	196.25	Multiple extension & fracture – Disintegration
5b	221.60	Multiple extension & fracture – Disintegration
7a	121.00	Multiple extension with ~20% break along existing oxidised joint
10a	96.6	Simple extension with 100% break along existing quartz vein parallel with loading
11a	110.13	Multiple fracture with 80% break along existing oxidised and quartz coated fractures
13c	35.63	Multiple fracture with 80% break along existing oxidised fractures
16a	207.36	Multiple extension & fracture with some indication of shear powder – Disintegration
29a	232	Trilab tested – Disintegration
5b	233	Trilab tested – Disintegration

3.2.4.2 BTS

Brazilian Tensile Strength testing was carried out on samples from 16 outcrops with 29 tests (including Trilab testing) carried out (see Appendix E.6). Testing was restricted to medium-fine grained sandstone, typically thickly bedded to massive with only one fine grained sample.

Similar to UCS testing, intact rock strength is reported as the average of samples that broke cleanly through the substance upon loading. Rock mass strength indication for comparison with intact strength is reported as the average strength of samples that broke along existing defects. Overall strengths averaged 16 MPa with clean breakage averaging 25 MPa and breakages along existing defects averaging 11 MPa.

Further dividing samples into bedding thickness demonstrates the thicker bedded members have higher strengths on average (18 MPa) in comparison to the thinner bedded members including medium bedding, averaging 13 MPa. Typically, the thinner bedded members tended to break more readily along existing defects and as a result only one sample broke cleanly through the substance. As a result the thinly bedded members with breaks along existing defects averaged 10 MPa in comparison to thickly bedded samples that broke along existing defects averaging 12 MPa. Intact thickly bedded members averaged 25 MPa. Higher strength rock samples tended to fail along a number of planes parallel to loading defined as multiple extension by Szwedzicki (2007). Conversely lower strengths tended to fail in a simple extension sense.

3.2.4.3 Cerchar abrasivity and ultrasonic velocity

Cerchar Abrasivity Index (CAI) was carried out on two samples (5b and 29a). Average CAI values were given as 3.77 and 3.56 respectively. The rock is classed as very abrasive according to Käsling et al. (2007).

Through P and S wave velocity dynamic Young's Modulus (GPa) and Poisson's Ratios were derived as 50.1 GPa and 0.17 for 5b and 51.5 GPa and 0.17 for 29a, respectively. Young's modulus and Poisson's ratios derived for the two samples indicate the sandstone material is exceedingly stiff and brittle in comparison to common sandstone values.

3.2.4.4 Point load

Point load index testing results were sub-divided into representative domains to demonstrate trends. Results have been divided into clean substance break, indicative of intact strength, and existing defect breaks, more indicative of overall rock mass strength. Raw results are reproduced in Appendix E.7.

Fine to medium sandstone had the highest intact I_{s50} strength (Table 3.9). Fine sandstone and mudstone remained the weakest lithologies. The thickly bedded sandstone member had the highest overall existing defect break I_{s50} strength and the second highest intact I_{s50} strength. An indicative trend was found further validating the existence of two distinct rock mass zones within the Hurunui River site. HRB point load results across all bedding thickness and lithotypes show on average higher strengths than the adjacent more sheared MNSZ. An average sandstone point load to UCS conversion factor of 32 was worked out from outcrops were point load and UCS sample was collected. No mudstone conversion factor was obtained due to the lack of mudstone sample for UCS testing.

Table 3.9: Hurunui River average point load Is_{50} (MPa) results.

	Clean break (I_{s50} (MPa))	Existing break (I_{s50} (MPa))
Thick bedding (sandstone overall)	6.06	2.64
Thin bedding (sandstone overall)	5.76	1.92
Thick bedding (sandstone HRB)	6.49	2.81
Thin bedding (sandstone HRB)	6.18	1.85
Thick bedding (sandstone MNSZ)	4.53	1.13
Thin bedding (sandstone MNSZ)	5.39	2.21
F-M Sandstone (sandstone Overall)	6.14	2.58
F-M Sandstone (sandstone HRB)	6.65	2.72
F-M Sandstone (sandstone MNSZ)	5.19	1.9
Fine Sandstone	3.75	1.47
Mudstone	2.8	0.64

3.2.4.5 Fines index testing

Fines index testing for the Hurunui was undertaken on three fault and shear infill samples obtained from outcrops 23b and 30a. Two samples from 23b were taken from separate fault planes described as clay with some sand and silty sand. Outcrop 30a's sample was sourced from a shear plane and described as a silt with some sand according to NZGS (2005).

Table 3.10 presents the infill materials fines content derived from sieve and laser sizing analysis. The clay sample from 23b was only analysed through digital laser sizing. Results show minor levels of clay sized particles in 23b and 30a. Other fines contents are relatively similar. The second test from outcrop 23b described as clay revealed more voluminous clay content of 15.2% of total defect infill material. This is likely a function of greater movement along the select discontinuity in comparison to the other defect infill sampled. Raw results and calculations are reproduced in Appendix E.8.

Table 3.10: Hurunui River fines index testing results.

	23b	**23b - clay**	**30a**
Passing	**%**	**%**	**%**
>4mm	23.7	-	37.34
>2mm (Gravel)	14.57	-	17.19
>1mm (C-M sand) (sieving & laser)	26.01	15.00	23.27
<200 microns (Fine sand)	9.66	14.1	5.78
<60 microns (Silt)	21.9	55.7	14.44
<2 microns (Clay)	4.16	15.2	1.98

3.2.4.6 XRD and thin section analysis

XRD results show little to no true clay in any sample (Table 3.11). 23b and 30a show 5% clay defined by Illite. The sample 23b clay fraction showed only a trace of true clay despite sieve analysis revealing significant levels of clay sized particle. Similarly, field descriptions defined it exhibiting geotechnical properties of clay. Only a limited amount of infilling material was sourced from 18a. As a result the material was only analysed through XRD analysis. The material described as clay with slight plasticity is identical to material of sample 23b. In similar fashion no true clay was identified from the sample.

Table 3.11: Hurunui River XRD analysis of infill material less than 1 mm.

Sample outcrop	**Quartz (%)**	**Albite (%)**	**Kaolinite (%)**	**Illite (%)**
23b	60	35	Trace	5
23b - clay	65	35		Trace
30a	75	25	Trace	
18a	70	25		5

Point counting was carried out on two Hurunui River samples. Two additional thin sections of very thinly bedded samples from outcrops 14a and 14b were analysed to observe texture of the heavily sheared mass.

Consistent QFL ratios were derived across the site (Table 3.12). Rock type is defined as a Feldspathic Greywacke (Boggs (2001) after Pettijohn et al. (1987)). Quantities of matrix (~14%), opaque minerals (<2%), mica, chlorite and calcite (<1%) were additionally observed. Grains are typically sub-angular. Feldspar exhibited slight discolouration in cross polarised light but is largely unweathered.

Within the fine sandstone matrix of 14a, calcite veins up to 1 mm in width are observed. The calcite is defined by high relief, high birefringence and bold 120/60° cleavage paired with multiple twinning. Thin section sample 14b is dominantly a mudstone. Very fine sandstone boudinage is observed within the mudstone matrix. A volcanic 'flow banded' deformation texture is exhibited within the sedimentary member in one distinct orientation. The mudstone is heavily discoloured and oxidised.

Table 3.12: Hurunui River QFL ratios derived from thin section point counting.

Sample #	Quartz %	Feldspar %	Lithic fragments %
1a	36	38	26
26a	35	43	23

3.3 Ashley River Gorge

3.3.1 Lineation analysis

13 Lineaments were distinguished across the Ashley River Gorge. The evolution and deep incision of the mountainous terrane enabled many large scale lineations to be identified (Appendix F.1). Generally these tended to follow drainage patterns; however lineations were identified across some scarps and distinctive topography. A general northeast-southwest structural grain was identified, similar to the Hurunui River lineation analysis, which follows the general NE-SW trend of known faults in the area.

3.3.2 Conceptual model

Similar to the Hurunui River site, two rock mass zones have been distinguished across the Ashley River Gorge site (Figure 3.21). The cross section extends across the extent of the study site (A-A', see Appendix F.1) and incorporates the Lees Valley Fault, Glentui Fault, its associated crush zone and the Ashley Gorge Fault as defined by (Forsyth et al., 2008).

The Ladbrooks Hill Block (LHB) is distinguished from the Lower Ashley Gorge Block (LAGB) by structural and landscape evolution. The westward LHB is expected to be more tectonically evolved and as a result rock mass is expected to be deformed to greater levels. Incorporated within this block

Rock Mass Zone	Ladbrooks Hill Block	Lower Ashley Gorge Block
Geology	Rakaia Terrane Torlesse greywacke with characteristics of Esk Head Melange within the Glentui Fault Zone	Rakaia Terrane Torlesse greywacke
Rock Mass Conditions with reference to Read et al. (2000) classification classes	Rock is anticipated to be of class II - III between fault zones. Within the crush zones of faults clay gouge is expected. The rock mass within these regions is expected to be as low as class IV-V. This block is expected to be more mature, thrust zone and is likely to be more dissected that the lower Ashley Gorge Block	Rock is anticipated to be predominantly class II with regions of class III. Minimal crush zones around faults should be expected of class IV to V. This block is less mature and thus a better rock mass should be expected than the Ladbrooks Hill Block
Groundwater	Groundwater will likely be controlled by crush zones around faults and compartmentalisation between structures is likely. This will have implications on pore pressures.	Groundwater will be controlled predominantly by the rock mass with compartmentalisation being of a lesser issue however is still likely to be expected due to the potential for clay gouge.

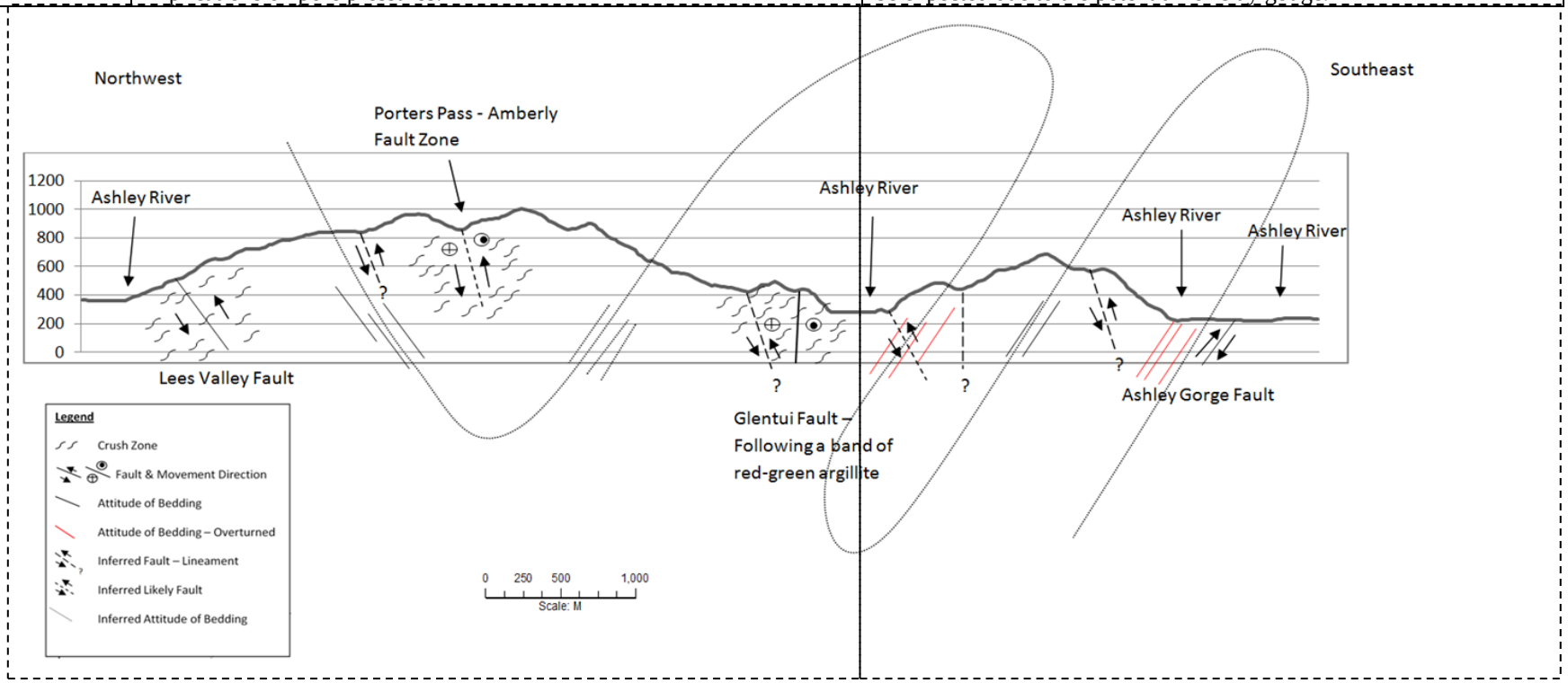

Figure 3.21: A -A' conceptual cross section model showing faults, structure and rock mass zones derived from the lineation analysis and Forsyth et al. (2008).

is the subsequent 250 m crush zone formed around the Glentui Fault. Other crush zones on smaller scales are present around the Lees Valley Fault and a PPAFZ unidentified splay as per fault attributes from Forsyth et al. (2008). Characteristics of Esk Head Melange is expected to be encountered in the block particularly along the band of red and green mudstone from which the Glentui Fault runs (Cowan, 1992). Using Read et al. (2000) Torlesse classification, rock within the LHB is anticipated to be class II to III between faults and class IV-V around major structures.

The LAGB is anticipated to be in better condition. The bulk of the block does not incorporate any major fault structures or subsequent crush zones defined by (Forsyth et al., 2008). River morphology between the two structural blocks varies (Appendix F.1). The river channel in the LHB tends to follow a relatively linear meandering path. Conversely river morphology within the LAGB changes course and runs through large looping meanders, dissimilar to the LHB. Subsequently the region is likely to be less tectonically evolved, in better condition and, as a result, the rock mass is expected to be favourable. Minor crush zones should still be expected as defined through the lineation analysis. The bulk of the block is expected to be class II with regions of class III. Poorer zones of class IV and V should be anticipated on smaller scales than the LHB around structures, particularly those identified within the lineation analysis.

3.3.3 Rock mass

Raw mapping data is reproduced in Appendix F.2. Discussion is provided based on the understanding the influence of large scale fault structures has implications on rock mass conditions. The Ashley River Gorge site presents a large range in condition. The numerous large scale faults that pass through the area have effects on different scales. Overall average rock mass quality did not vary significantly between the two blocks identified within the desktop study. Rock within the LHB varied greatly in condition. Generally sandstone was always medium to massive in bedding. Interestingly no thinly interbedded rock was observed in the block. Of the sandstone member, rock fracturing ranged from moderately fractured to fragmented with faulting having spatial influence on the rock mass. Overall the thick to massive sandstone member was in slightly better condition in the LAGB. Significant volumes of thinly interbedded outcrops were, however, observed in the LAGB. The thinly bedded members were heavily deformed, faulted and folded.

3.3.3.1 Impact of large faults

Large scale fault affected rock was observed at numerous outcrops, dominantly within the LHB block. Outcrops 1a and 2a related to the PPAFZ Lees Valley Fault splay and had very similar characteristics to those identified throughout the Elliott Fault site (Figure 3.22). Similar to the secondary fault rock at the Elliott Fault site, outcrop 1a was heavily fragmented, had numerous small scale shear planes and no bedding could be recognised. Significant shear bound, more intact blocks

were identified in outcrop 2a, similar to Elliott Fault outcrop 10e previously described (Section 3.1.2 Rock mass).

Figure 3.22: Rock mass fault related structure. Left: fragmented rock mass, outcrop 1a; right: more intact block within a fragmented matrix, outcrop 2a.

Metre scale zones of direct fault material were examined throughout the site. Outcrop 51a lies perfectly on a lineation identified in this study. It appears to follow a thinly interbedded sequence striking parallel with bedding. A massive sandstone unit has been thrust over the thin interbeds (Figure 3.23A). All rock concerned with this zone is fragmented, the mudstone to a higher degree. The thin interbeds are heavily folded with heavy clustering of centimetre scale faults offsetting bedding (Figure 3.23B). A 3 cm black gouge material was observed along the primary slip plane (Figure 3.23C & D). The material described as clay sized has slight plasticity and likely has mudstone origins. Material immediately either side of the zone (20 cm) is silt sized and encompasses mudstone fragments (Figure 3.23E). The material becomes slightly plastic upon the addition of water and geotechnically behaves as a soil similar to immediate fault material observed at the Elliott Fault site.

Similar characteristics are expressed in outcrops 38a and 42a (Figure 3.24). In both cases large scale faulting is restricted to the thinly bedded member with a more thickly bedded unit thrust above. The thinly bedded members are fragmented and distorted. The massive hanging wall sandstone at outcrop 42a is in very good condition remaining very strong. A gouge material similar to 51a occurs along the primary fault zone for up to 30 cm before heavily chaotic thinly bedded rock can be recognised. Faulting and shearing on metre scales is observed within the Glentui crush zone defined by outcrop 45a. The outcrops rock is entirely fragmented despite bedding thickness.

An approximately 1 m shear is observed running layer parallel along a thickly bedded mudstone (outcrop 13a, Figure 3.25). The mudstone material is described as a firm gouge and is lineated parallel to bedding. Sandstone bordering the mudstone bed has a 4 m crush zone before rock mass condition improves but remains fragmented.

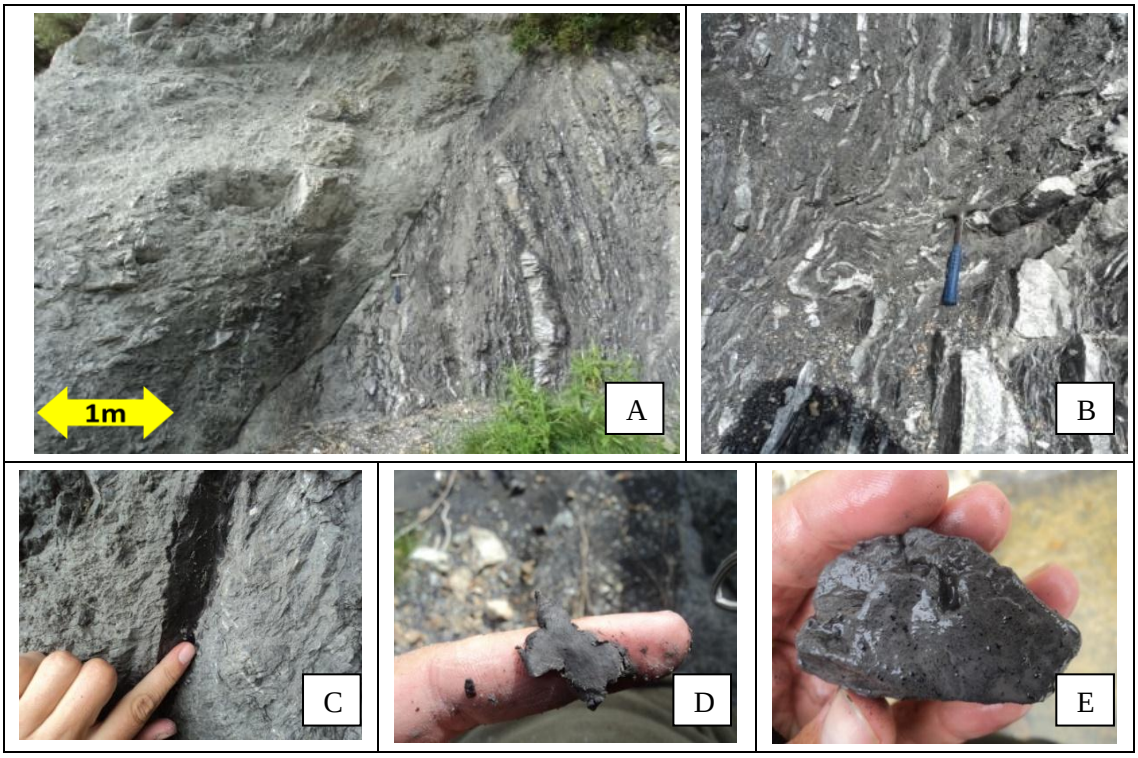

Figure 3.23: Outcrop 51a fault rock. A: main fault zone; B: distort, highly chaotic thin interbedding; C: black, clay sized gouge along the primary slip plane; D: gouge material; E: fault breccia material.

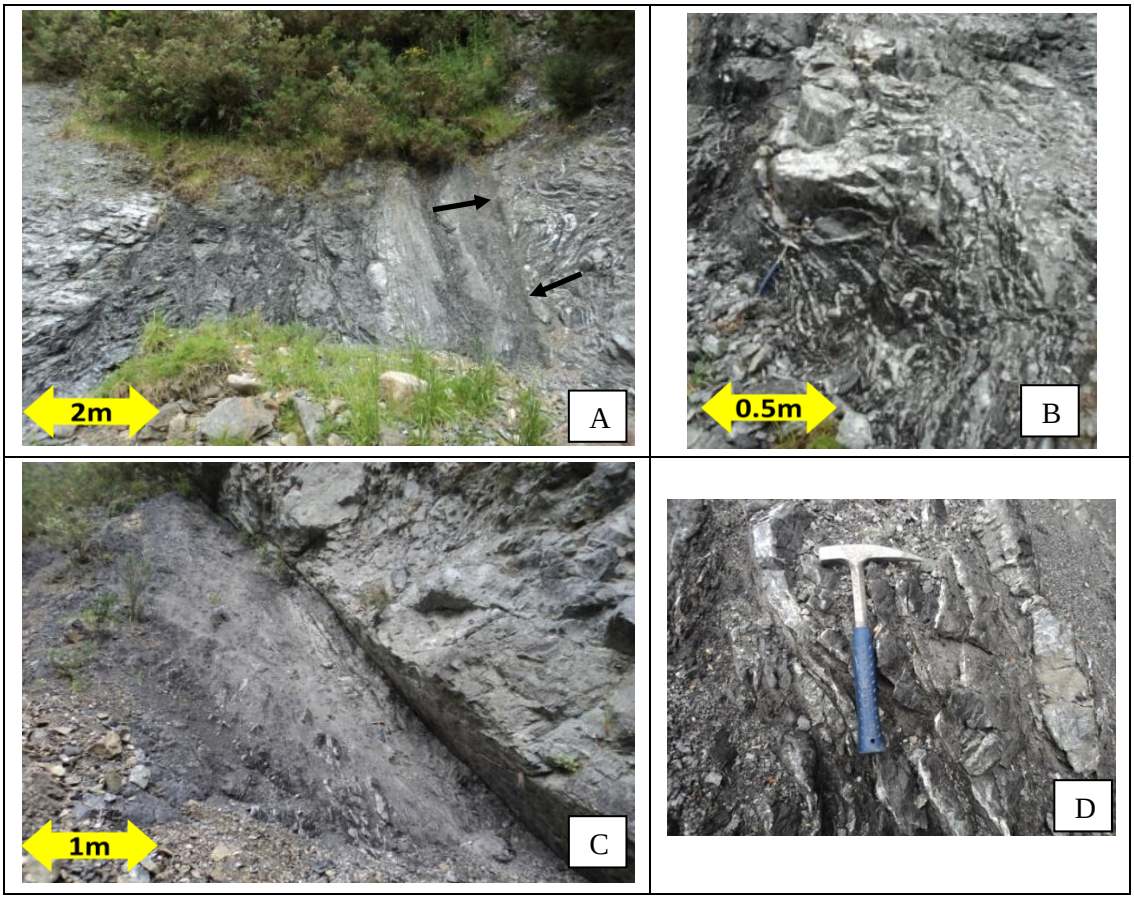

Figure 3.24: A & B: outcrop 38a fault rock (note distinct boundary between fault rock and thin interbedding indicated); C & D: outcrop 42a fault rock bound by intact favourable massive sandstone.

Figure 3.25: Left: mudstone bedding shear; right: firm mudstone shear material.

Numerous outcrops observed within the Ashley River Gorge had unusual rock mass characteristics not observed in the Hurunui River or Elliott Fault sites. Numerous outcrops were heavily fractured to fragmented with increased levels of faulting and shearing irrespective of bedding thickness (Figure 3.26A – D).

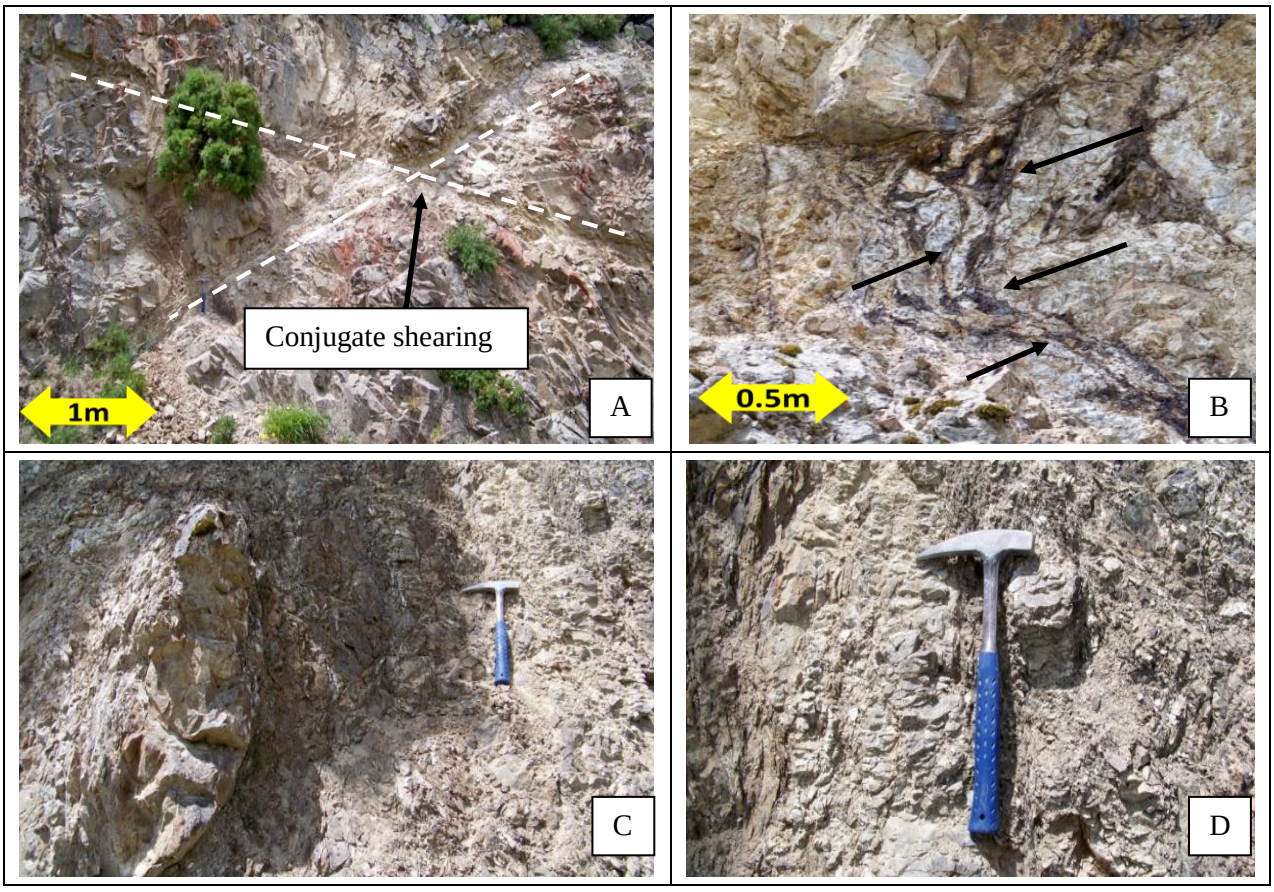

Figure 3.26: Heavily fractured to fragmented rock masses with numerous outcrop scale faults and shears distorting and forming boudins in the thinner bedded member. A & B: Outcrop 7b with shearing and folding indicated; C & D: Outcrop 8a fragmentation and boudinage.

3.3.3.2 Rock outside the influence of large faults

Joint controlled rock masses are observed similar to other study sites and present the best rock mass conditions. This included medium to massive bedding thickness which forms a relatively blocky rock mass between the persistent jointing and bedding defects (Figure 3.27).

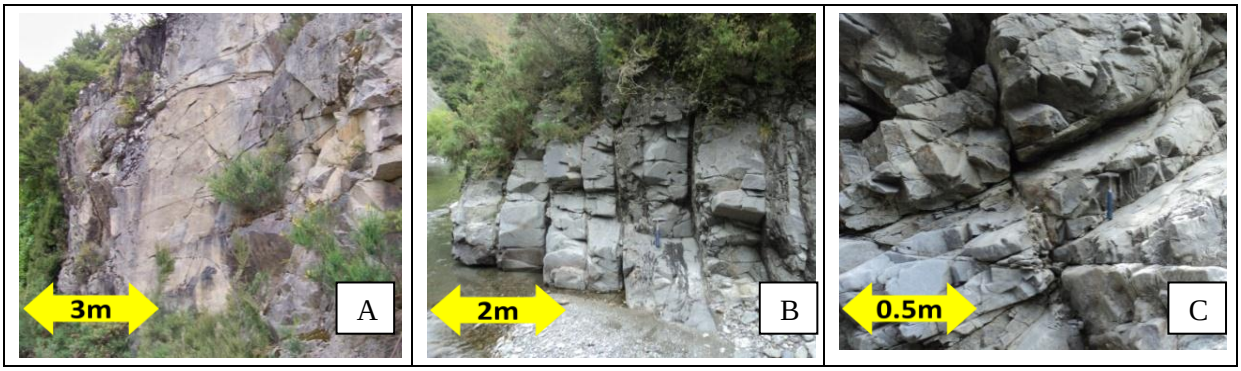

Figure 3.27: Joint controlled rock masses. A: outcrop 18a; B: outcrop 37a; C: outcrop 54a.

Thick bedded members controlled by non-persistent jointing occur in equal portions to the best, thickly bedded rock masses controlled by persistent jointing. These outcrops tend to distort thin bedding forming sandstone boudinage (Figure 3.28A & B). Where faulting volume increases in thicker sandstone units, mudstone present is commonly dragged along the fault plane giving rise to lineated mudstone infilling type along faults and shears (Figure 3.28C & D).

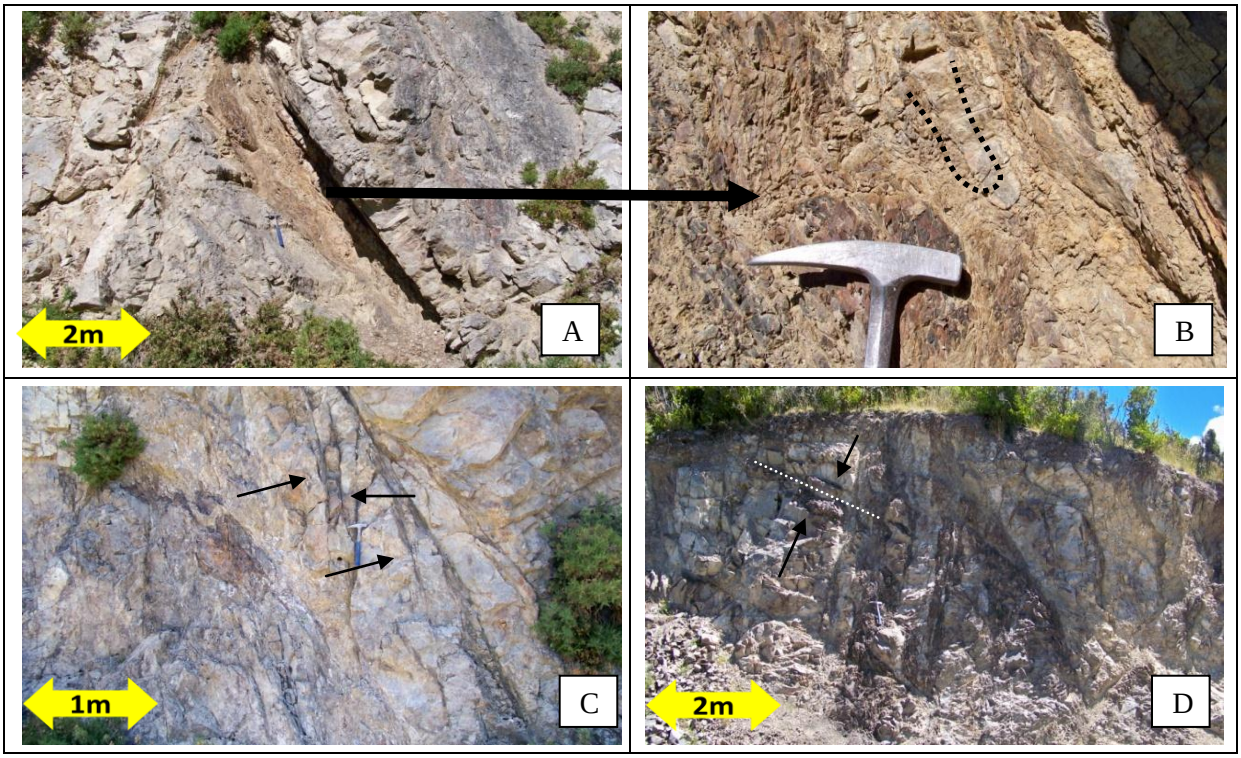

Figure 3.28: A: outcrop 6a thin interbedding bound by thick sandstone units; B: outcrop 6a subsequent boudinage formation indicated, note the thin interbedded weathering profile; C: outcrop 7a and 15a note the dragging of mudstone unit into the faults.

Thin interbedding, restricted to the LAGB ranged in condition (Figure 3.29). Similar to other study sites faulting and folding concentrates in this member. Differing is the occurrence of better condition highly fractured to fragmented thin interbedding (Figure 3.29A – D). Similar to Elliott Fault observations, some thin interbedding had alternating fine to fine medium sandstone. Gradational banding was observed and as a result the rock mass was more favourable (Figure 3.29B). Similar to other sites boudinage is observed within the thin interbedding despite lithology (Figure 3.29C). It is noted that thin interbeds have wavier shapes (Figure 3.29D). Observed within the better condition, thinly interbedded member was incipient fracturing, similar to that observed elsewhere. Because the best thinly bedded rock masses are observed in the river bed, it is possible the river is actively cleaning the rock face, not allowing weathering to develop along incipient fracturing. Thinly bedded road outcrops, which on observation present poor, fragmented, faulted, folded conditions, appear worse as a result (Figure 3.29E & F).

Figure 3.29: Characteristics of thinly interbedded sandstone mudstone observed at Ashley River Gorge; A & B: outcrop 28a; C: outcrop 30a; D: outcrop 33b; E outcrop 22a; F: outcrop 20a.

The mudstone member, similar to other sites, is always fragmented (Figure 3.30). Layer parallel shearing is also observed particularly between thicker sandstone units as they readily squash, shear and deform the mudstone beds (Figure 3.30A). Fragmented mudstone with higher strengths were observed within the river bed (Figure 3.30B). Clustering of faults, shears and quartz veining are observed in some thicker mudstone units (Figure 3.30D & E). The effect of this is a more heavily fragmented, deformed rockmass than mudstone observed elsewhere.

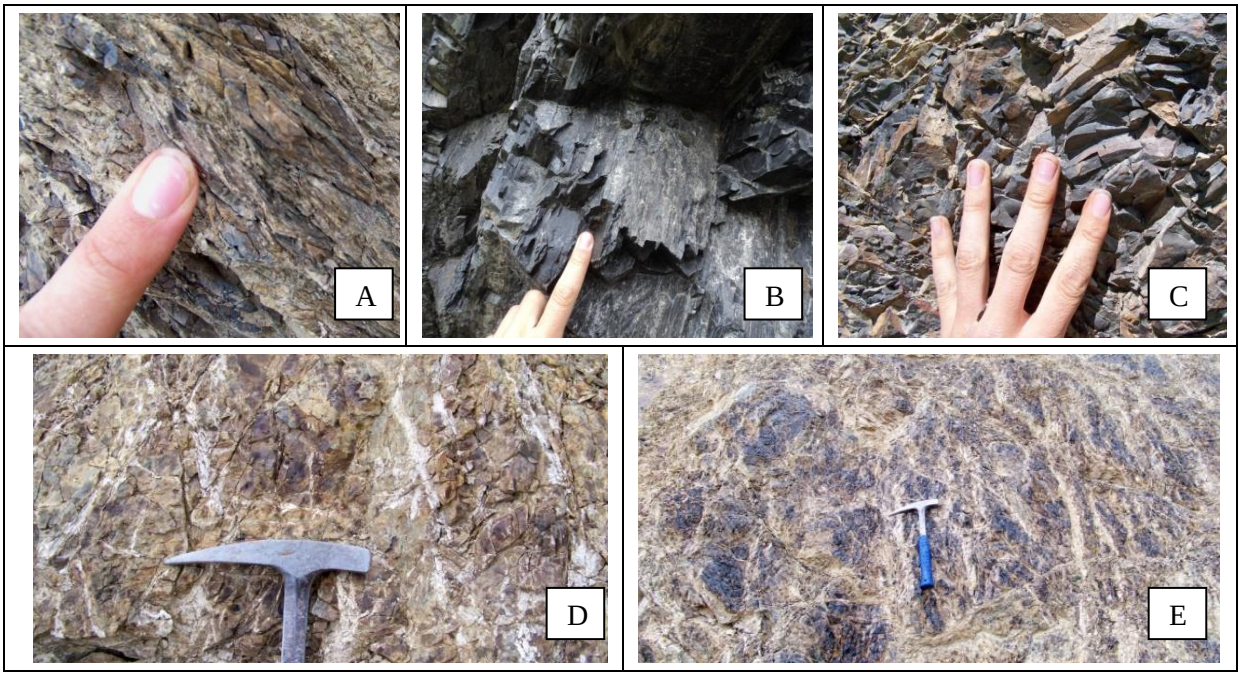

Figure 3.30: Ashley River Gorge mudstone character; A: fragmented, lineated mudstone of outcrop 14a; B: higher strength, fragmented mudstone character of outcrop 41a; C: mudstone fragmentation of outcrop 24a; D & E: clustering of faults, shears and veining within thicker mudstone units (outcrop 23a).

Red, green and black mudstone was observed along the Glentui Fault crush zone (Figure 3.31). The material was not directly concerned with this study, however of note was cleaved black mudstone. The black mudstone is fragmented and cleavage planes have developed parallel to bedding. Of similar character, the green mudstone has developed schistosity planes in response to faulting. It is likely the formation of the planes have formed at depth before uplift to the current elevation.

Figure 3.31: Green and cleaved black mudstone observed along the Glentui Fault crush zone.

Bedding thickness throughout the Ashley Gorge was comparable to other sites. Sandstone bedding thickness is variable with very thick bedding occurring more than 30% of the time. Thinly bedded sandstone, similar to other sites, only occurs in association with thinly bedded mudstone. Persistent jointing (>2 m) was concentrated in the thicker beds while faults and shears tended to be more voluminous toward the more thinly bedded members (Appendix F.3).

3.3.3.3 Discontinuity condition

Condition varied between discontinuities. Defects generally became wavier at higher wavelengths (Figure 3.32). Bedding was the waviest defect. Generally the trend is exaggerated by the tendency of the more thinly bedded member to bend and fold more readily. Faults and shears remained relatively wavy. Joint defect was generally linear at both the Hurunui and Elliott sites. Here, however, the interlimb angle of jointing tends to decrease at higher wavelengths. Average surface roughness tends to be undulating (Figure 3.33). Differing from other sites, the Ashley River Gorge incorporates greater volumes of planar roughness. No trend exists between defect type and surface roughness.

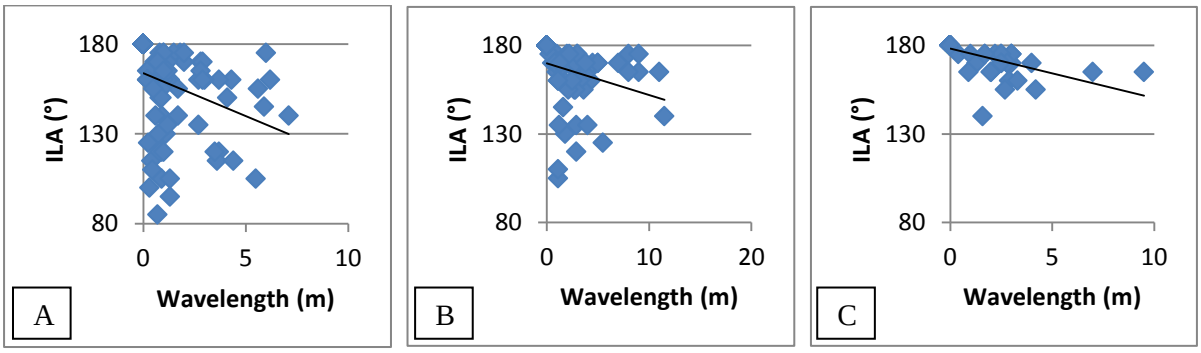

Figure 3.32: Ashley River Gorge defect waviness defined by interlimb angle (ILA) and wavelength (m). A: bedding; B: faults/shears; C: jointing.

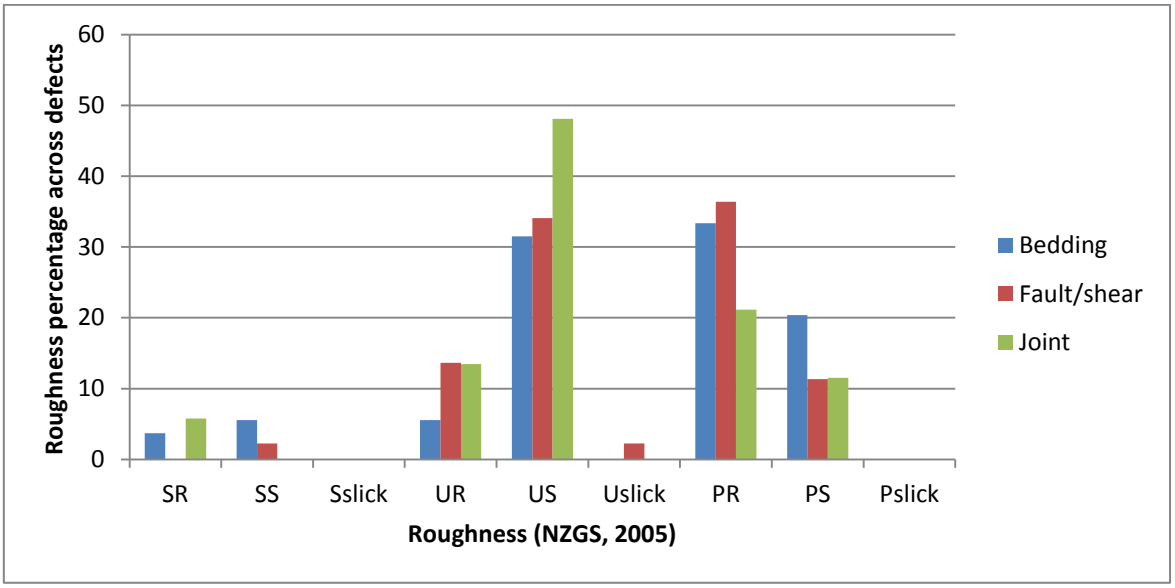

Figure 3.33: Ashley River Gorge surface roughness percentage across defects.

Similar to other areas, infill is dominated by faulting and shearing, particularly by finer silt sized particles (Figure 3.34). Infill thickness toward the finer infill sediment (clay, silt and sand) is generally thinner on average in comparison to gravel infill (Figure 3.35). Jointing is generally clean with infilling of quartz and surface staining relating to historical flow through the interlinked permeable pathways created by jointing. Bedding defect remains dominantly clean.

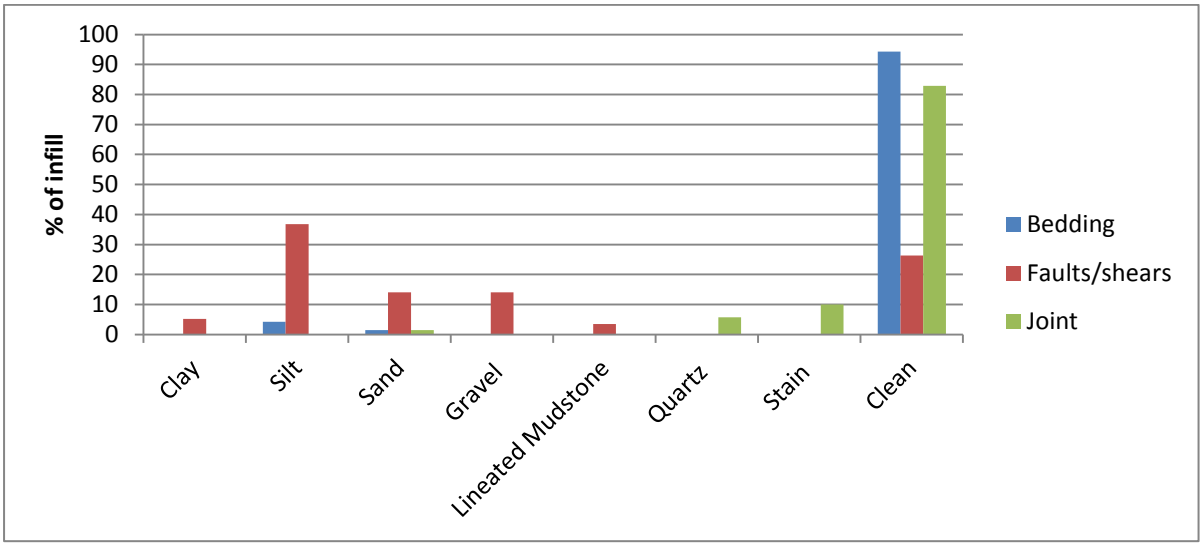

Figure 3.34: Ashley River Gorge infilling type and percentage as a total of all infill lithology per defect type.

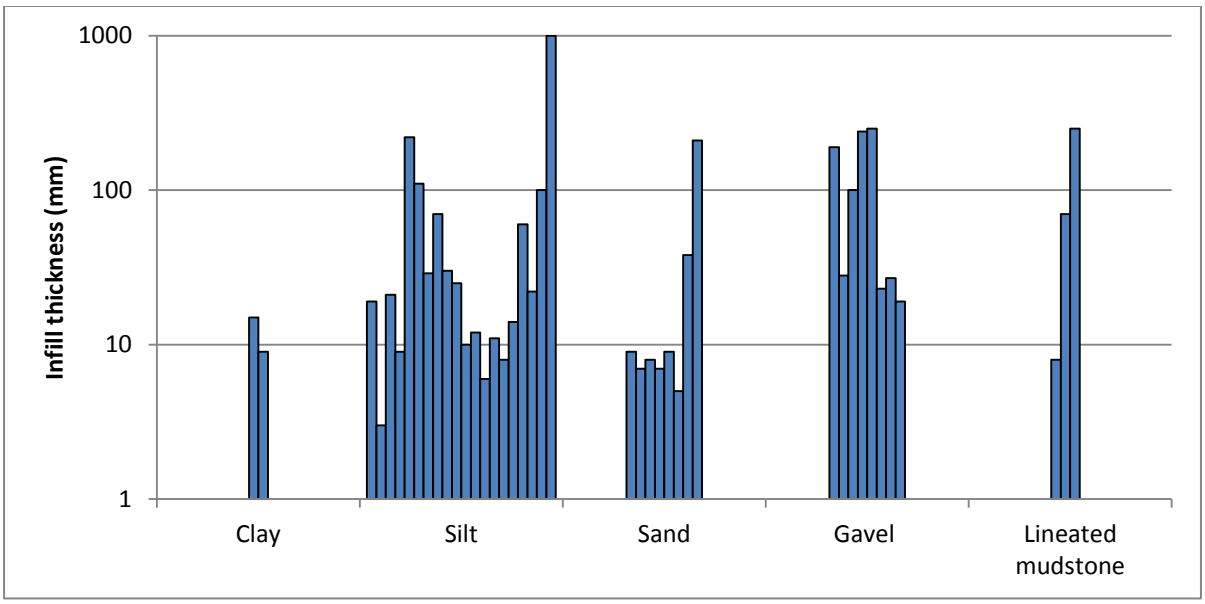

Figure 3.35: Ashley River Gorge fault and shear infill thickness.

Similar to the Hurunui River alternations between two general bedding plane orientations is observed (Appendix F.4). It is likely alternations in orientation are related to folding, similar to that identified in the conceptual model. Two joint sets are identified through steronet analysis at 44°/338° and 69°/037°. Shearing remains independent and random in orientation.

3.3.4 Laboratory testing

3.3.4.1 UCS and BTS

Intact rock strengths at the Ashley were significantly weaker than experienced at the Hurunui River or Elliott Fault. Numerous sites across the area were able to be sampled for coring, however, adequately sized core for UCS testing was sent to Trilab for external testing. One UCS test was conducted by Trilab resulting in a strength of 146 MPa, cleanly failing through the substance by disintegration. Specific energy is derived from the sample as 0.031 MJ/m^3 through Trilab analysis.

Core was sourced from smaller intact lump samples and Trilab core off cuts for BTS testing. 20 BTS tests were carried out over five outcrops (Appendix F.5). Fine to medium sized sandstone had the highest average intact strengths of 13 MPa while three fine sandstone tests shed average intact strengths of 8 MPa. Samples failing along existing defects were not significantly lower than intact strengths with average strengths of 11 MPa for fine to medium sandstone. Bedding thickness similar to other sites has an effect on strength but not as clearly defined with thick and very thick strengths averaging 13 MPa and medium beds 10 MPa. No thinly bedded sample was sourced. Generally samples tended to fail through low energy simple extension (Szwedzicki, 2007). Overall strengths were much weaker than experienced at both the Hurunui River and Elliott Fault sites.

3.3.4.2 Cerchar abrasivity and ultrasonic velocity

Cerchar Abrasivity Index (CAI) was carried out by Trilab on two samples (4a and 21a). Average CAI values were given as 4.35 and 3.51 respectively. The rock is further classed as extremely to very abrasive according to Käsling et al. (2007).

P and S wave velocities were performed by Trilab on outcrop sample 21a. Dynamic Young's Modulus (GPa) and Poisson's Ratio were derived as 44.4 GPa and 0.26 respectively. The Young's modulus result indicates the sandstone material of the Ashley River Gorge is relatively stiff, however not to the same degree as the Hurunui River. A Poisson's ratio of 0.26 remains indicative of typical sandstone lithology and has higher elasticity than the Hurunui River sample.

3.3.4.3 Point load

Point load index strengths have been sub-divided and reported into bedding thickness and lithologies for all rock, LHB rock and LAGB rock (Table 3.13). Rock anisotropy in sample was observed generally along thin interbedding within fine sandstone and mudstone. Rock was point load tested at either orientation and reported.

The occurrence of fine sandstone has not been distinguished throughout both structural blocks as I_{s50} values remain relatively similar. Similar to the previous study sites, thickly bedded fine to medium sandstone was generally the strongest. Of interest were results derived for thin interbedded sandstone

which had similar strength values. Generally the LAGB had higher strengths across bedding thickness and lithology ranges validating desk and field observation. Rock anisotropy existed within the Ashley River Gorge site as gradational cross bedding (Table 3.13). No significant difference in strength was found between samples loaded parallel and perpendicular to bedding fabric. Raw point load data and calculations are reproduced in Appendix F.6. An average point load to UCS conversion factor of 20 was derived from the Ashley River Gorge sandstone. No mudstone conversion factor was obtained due to the lack of mudstone sample for UCS testing.

Table 3.13: Ashley River Gorge average point load I_{s50} (MPa) results per bedding thickness, lithology, structural block and anisotropy.

		Clean break	Existing break
	Thick bedding (sandstone overall)	4.85	2.03
	Thin bedding (sandstone overall)	4.94	2.25
	Thick bedding (sandstone LHB)	4.65	1.88
	Thin bedding (sandstone LHB)	4.44	2.17
	Thick bedding (sandstone LAGB)	7.52	5.41
	Thin bedding (sandstone LAGB)	5.49	2.33
	F-M Sandstone (sandstone Overall)	5.35	2.45
	F-M Sandstone (sandstone LHB)	5.04	2.27
	F-M Sandstone (sandstone LAGB)	6.82	4.27
	Fine Sandstone	3.67	1.36
	Mudstone	2.74	0.58
Parallel	**Fine Sandstone**	5.96	2.4
	Mudstone	4.08	0.15
Perpendicular	**Fine Sandstone**	4.84	1.56
	Mudstone	1.47	0.37

3.3.4.4 Ashley River Gorge strength variation discussion

On average the Ashley River Gorge has significantly lower intact strengths in comparison to other field sites. This was largely attributed to difference in metamorphic facies. As previously described the Ashley River Gorge is located within a zone of lower grade zeolite facies metamorphism. As a result intact rock strengths are significantly lower than all other sites located within low grade prehnite-pumpellyitc metamorphic zones. As discussed by Forsyth et al. (2008), low grade prehnite-pumpellyitc facies metamorphism resulted in mineral alteration, increased induration and local development of cleavage in mudstone. It is possible the better condition mudstone observed within the Ashley River Gorge is a direct result of this.

3.3.4.5 Fines index testing

Fines index testing for the Ashley Gorge was carried out on fault rock from outcrops 1a, 13a, 38a, 42a, 51a and on infill sampled from defects at outcrop 5a and 45a. Material taken from 5a, 13a and 45a was dominantly fine thus required no need for wet sieve analysis.

Table 3.14 presents fines content derived by wet sieve and laser sizing analysis. 100% of fines material taken from defect surfaces 5a and 45a were silt and clay sized. Similarly material taken from the thick mudstone shear (13a) had 55% silt fines and a large proportion (45%) of clay sized particle. Shear material sourced from large fault zones observed in the region (38a, 42a, 51a) were reasonably coarse. Sand and silt sized fractions were dominant, indicating the grinding of rock through fault movement. Clay sized fractions remained under 6% of the total sample. Non-direct fault sample taken from outcrop 1a had dominant clasts greater than 4 mm. This is representative of secondary fault rock similar to Elliott Fault (i.e. 10a) discussed in Section 3.1.3. Raw results and calculations are reproduced in Appendix F.7.

Table 3.14: Ashley River Gorge fines index percentages derived from wet sieve analysis and laser sizing.

	1a	5a	13a	38a	42a	45a	51a
Passing	**%**	**%**	**%**	**%**	**%**	**%**	**%**
>4mm	63.7	-	-	32.2	5.7	-	11.02
>2mm (Gravel)	15.1	-	-	11.7	8.2	-	9.89
>1mm (C-M sand) (sieving & laser)	12.2	-	-	17.1	30.2	-	41.85
<200 microns (Fine sand)	3.0	-	-	9.23	20.6	-	12.21
<60 microns (Silt)	5.1	68.6	54.7	26.0	29.3	66.1	20.24
<2 microns (Clay)	1.0	31.4	45.3	3.82	6.0	33.9	4.78

3.3.4.6 XRD and thin section analysis

Similar to other sites, clay content is relatively small with generally less than 10% of total sample volume representing true clay (Table 3.15). Quartz and Albite Feldspar is dominant in all samples. Of interest are the results of outcrop 42a. 25% of the total fines sample is clay defined by 10% Kaolinite, 10% Montmorillonite and 5% Illite. This true clay content is significantly higher than other samples. Outcrops 5a, 13a and 45a previously described as clay dominant material was found to have small concentrations.

Point counting to define QFL ratios was restricted to fine to medium sandstone. Two different bedding thickness and locations (outcrop 2a and 28a) were analysed with QFL ratio results shown in Table 3.16. The rock is further classified as a Feldspathic Greywacke. Grains are sub-angular and feldspars commonly discoloured in plane polarized light and cross polarized light. Calcite veining (3%) is observed within outcrop sample 28a along with additional matrix (11%), opaque mineral (3%)

and Mica mineral (1%). Approximately 16% of outcrop sample 2a is made up of matrix, defined by material too fine to see under the microscope with no grain shape.

Table 3.15: Ashley River Gorge XRD analysis of infill material less than 1 mm.

Sample outcrop	Quartz (%)	Albite (%)	Kaolinite (%)	Montmorillonite (%)	Illite (%)
1a	65	30	5	-	Trace
5a	80	20	Trace	-	Trace
13a	75	20	5	-	Trace
38a	50	40	10	-	Trace
42a	40	35	10	10	5
45a	70	20	5	-	5
51a	50	40	10	-	Trace

Table 3.16: Ashley River Gorge thin section QFL ratios derived from thin section point counting.

Sample #	Quartz %	Feldspar %	Lithic fragments %
2a	29.3	45.1	25.6
28a	32.1	50.6	17.3

Additional thin sections were made to observe textures of boudinage (17a) and red/green mudstone (9a, 10a). Observation of the thinly interbedded outcrop sample 17a revealed sandstone clasts encased within a mudstone matrix on millimetre to micron scale. Similar 'flow banding' type texture of mudstone are observed. This creates lineations parallel with flow direction. Commonly the sandstone clasts are distorted and folded indicating significant shear stress has acted on the rock.

Red and green mudstone clasts of outcrop 9a and 10a are completely deformed. Heavy quartz veining is present from millimetre to micron scale. Veins are dissected by numerous other veins indicating multiple infilling events. The quartz veins are subsequently completely folded and faulted at micro scales giving the rock a completely chaotic appearance under the microscope. The folding of the quartz veins indicates plastic deformation after quartz deposition likely to be related directly to faulting along the PPAFZ splays in the area.

3.4 Opuha Dam

Due to the spatial extent of the study site and subsequent lack of existing information at that scale, no lineation analysis or conceptual geological model was carried out or developed.

3.4.1 Rock mass

Similar to the Ashley River Gorge a range in conditions were experienced. Raw mapping data is reproduced in Appendix G.1 for reference. Sandstone was dominantly very thick to massive typically

associated with very thin to thin mudstone. Due to the Opuha Dam Fault, shear/fault occurrence was not restricted to any one bedding thickness. Similar to other sites, jointing clustered around the more thickly bedded members (Appendix G.2). Rock in close proximity to the Opuha Dam Fault splays tended to be more fractured. Rock at greater distances from the fault structures tended to have persistent joint controlled rock mass conditions. The Opuha Dam fault has two splays. The largest splay, defined by a 4.5 m crush zone, is observed within outcrops 5b and 7a (Figure 3.36A & B) with the smaller secondary 1.5 m crush zone located at outcrops 2a and 4b (Figure 3.36C& D). Similar to the Elliott Fault the majority of deformation is concentrated within the hanging wall (Figure 3.36A).

3.4.1.1 Influence of the Opuha Dam Fault

Within the main fault zone differing rock mass blocks are observed. A distinct plane bordering two different rock mass zones is observed at outcrop 5b and 7a (Figure 3.36A). The defect is infilled with black silt to clay sized material that has slight plasticity upon the addition of water. This infill, also observed within the secondary splay (Figure 3.36D), is observed along similarly orientated planes between 5b and 7a and likely represents the fault's primary slip plane, creating the ground-up infill observed. Two differing rock mass zones either side of the plane are identified as a more intact block bound by another distinctive linear defect to the right and a more fragmented rock, typical of other study sites fault rock that is readily eroded to the left (Figure 3.36A).

The leftward zone (Figure 3.36A) has similar characteristics to major faults and shears examined at other sites. Geotechnically it appears to behave as a soil and is easily eroded. It is described as silt with variations of sand and clay fraction, firm to hard in strength. The rock mass to the right (Figure 3.36A) borders the main movement plane and is defined by a 3 m fragmented crushed zone with notable centimetre scale shears. Located within the hanging wall of the fault, it has similar characteristics to the secondary fault rock observed at the Elliott Fault (10a). Intact blocks however differ by being up to 15 cm. Likely due to the smaller fault size, the rock here remains in better condition than the Elliott Fault. The linear defect bordering this zone to the more intact rock to the far right likely accommodated limited movement in historic rupture and defines the main fault zone affected crush rock.

Bordering the main shear zone at outcrop 7b is a very thin to thin sequence of sandstone-mudstone. The rock mass is entirely fragmented. Mudstone has developed cleavage parallel to slip and has interlimb angles of 100° across 50 cm wavelengths (Figure 3.37). The material observed is very similar to the shear bordering thin interbedding members observed in select Ashley Gorge outcrops. Lump samples can be readily broken by hand.

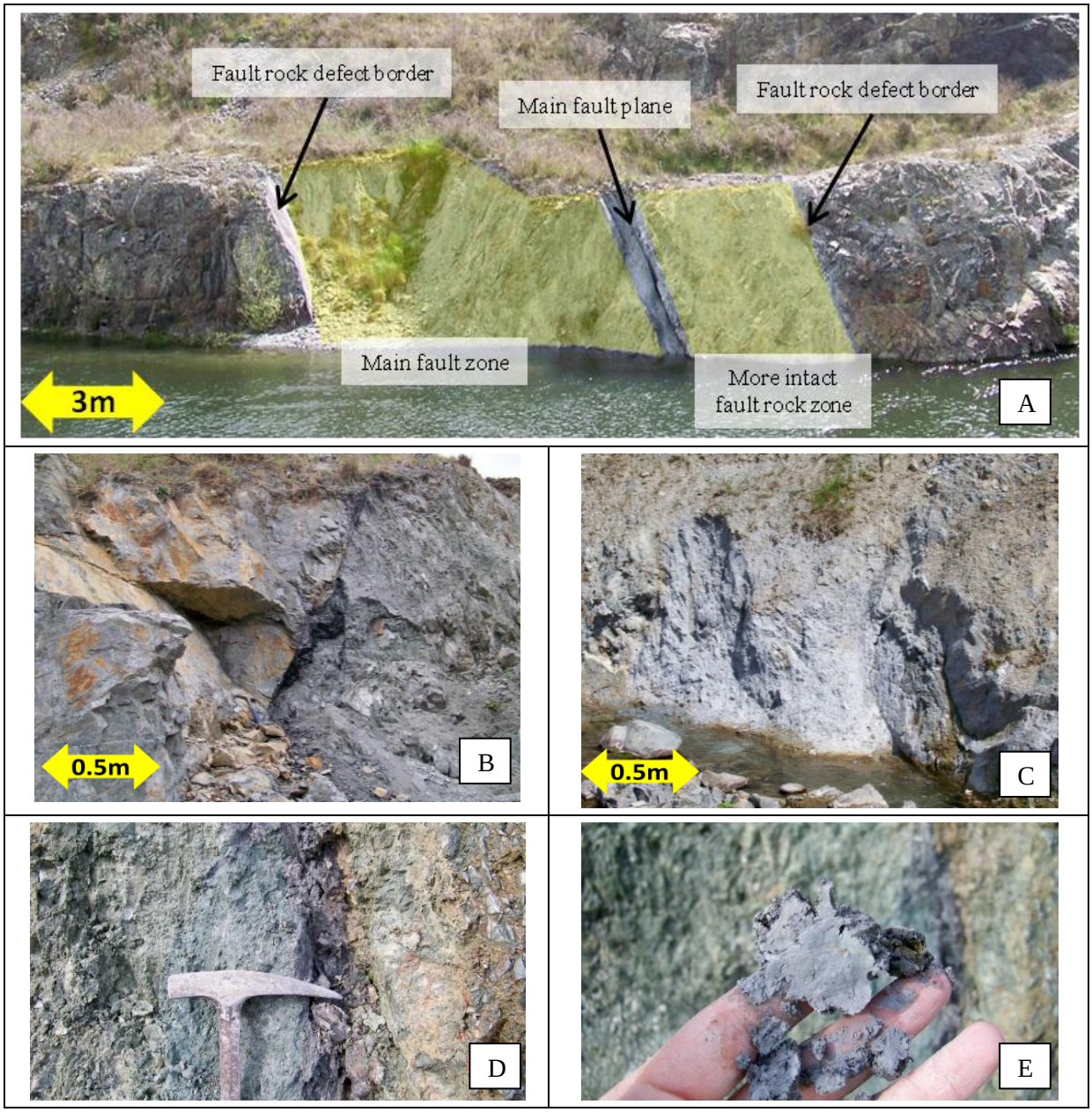

Figure 3.36: Direct fault related material. A: outcrop 7a with rock mass zones indicated; B: outcrop 5b fault plane; C: outcrop 4b 1.5m shear; D & E: outcrop 2a infill material.

Figure 3.37: Left: wavy thinly interbedded lithotype bordering the Opuha Dam Fault, outcrop 5a; right: cleaved mudstone, outcrop 5a.

Rock immediately outside this zone is in relatively good condition. Outcrops 5a and 4a are very thickly bedded to massive, are generally controlled by persistent jointing and have moderate to high fracturing (Figure 3.38A & B). Crush shear zones (<70 cm wide) are observed (Figure 3.38B & C). Material within the shears generally comprises rock fragments of coarse gravel size and does not directly influence surrounding intact rock. At closer scales the rock mass is relatively blocky defined by a moderate to high degree of fracturing.

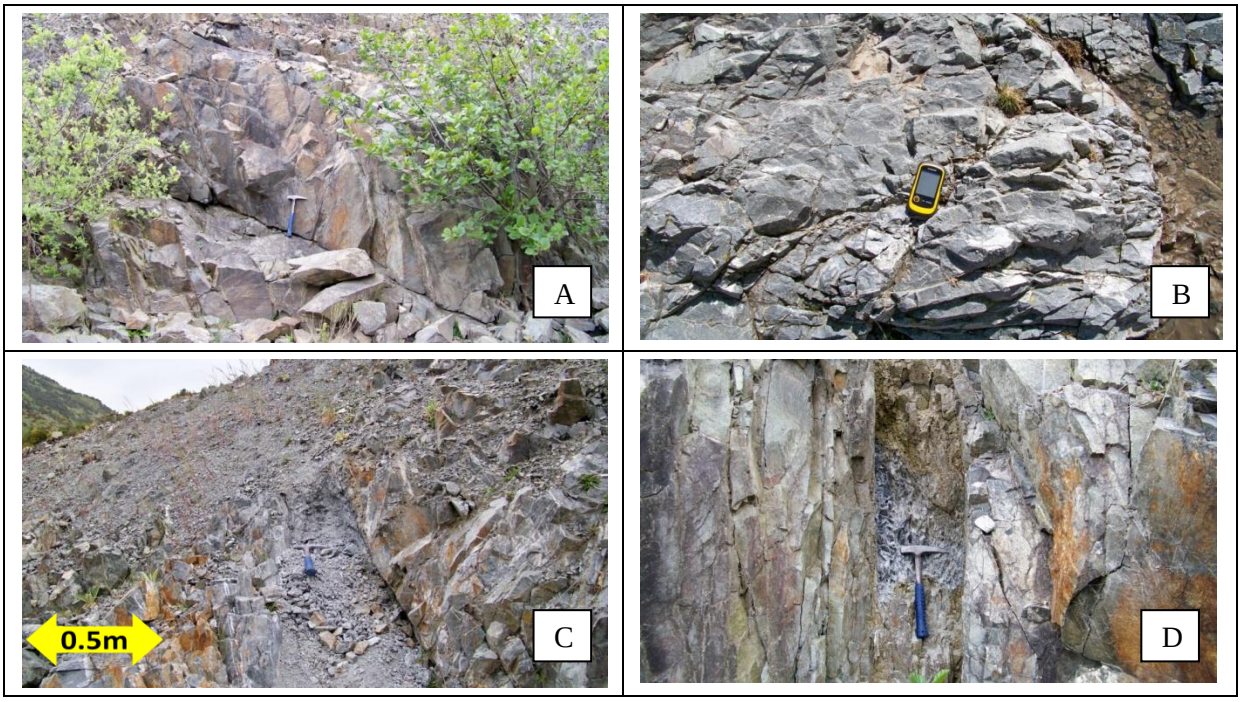

Figure 3.38: A & B: favourable blocky rock mass bordering the main Opuha Dam Fault (outcrop 5a, 4a respectively) C & D: Localised shearing defined by outcrop 5a.

3.4.1.2 Discontinuity conditions

An abundance of outcrop scale shear infill is observed throughout the site. An increased level of shearing and subsequent infilling is directly observed at the Opuha Dam and with increasing proximity to the main structures. Of note is the profusion of quartz and calcite infilling and veining along shear fabric and discrete non persistent fracture (Figure 3.39). Numerous veins infilling joints are found in massive to very thick beds. Calcite veining observed at outcrops 3a, 6a, 6b is typically weathered, reflecting each outcrop's surface weathering profile. The calcite material is weathered such that it occurs as sandy silt (Figure 3.39D). Similarly the calcite material was identified occurring as powder in shears and localised crush zones (Figure 3.39A). Quartz veins are also observed in fresh rock occurring in good condition (Figure 3.39C). Again, this only occurs in close fault proximity, indicating faulting has some direct influence on the level of quartz veining. Other infilling observed is dominantly silt sized, largely restricted to faults and shears generally less than 10 mm (Figure 3.40 & Figure 3.41). Bedding remains entirely clean and jointing infill is dominantly restricted to quartz infill.

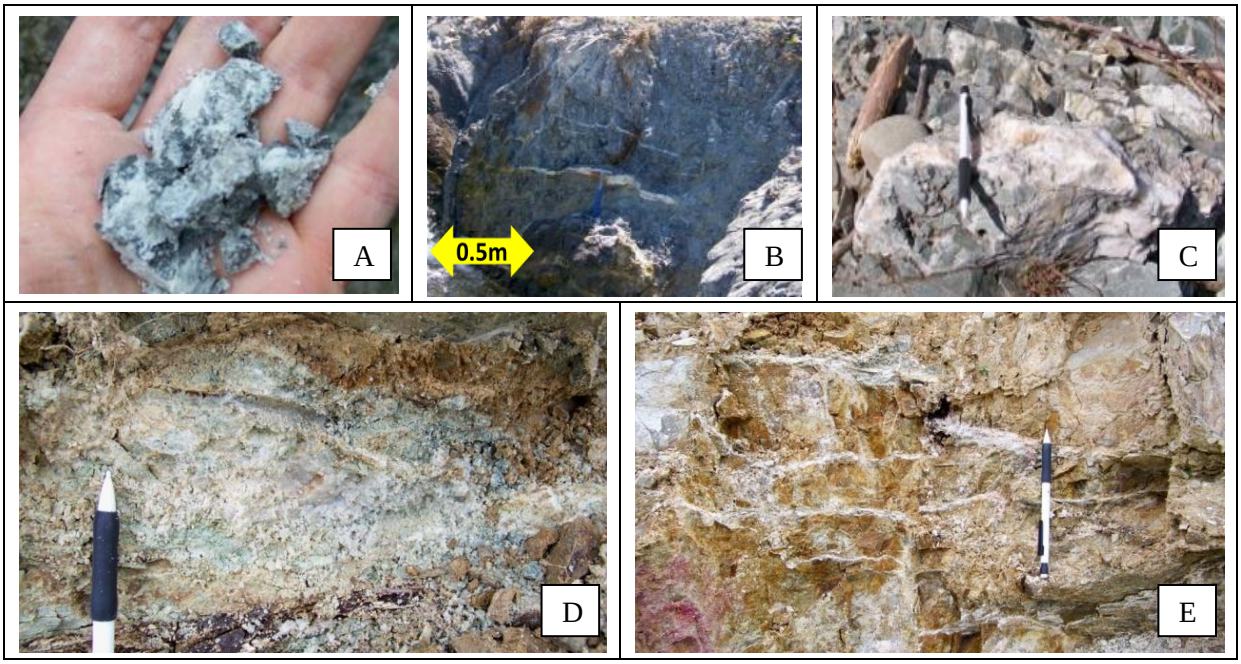

Figure 3.39: A: outcrop 5a shear material calcite powder coating; B & C: intact quartz veining up to 10cm in width; D & E: nature of calcite infilling along jointing (outcrop 3a).

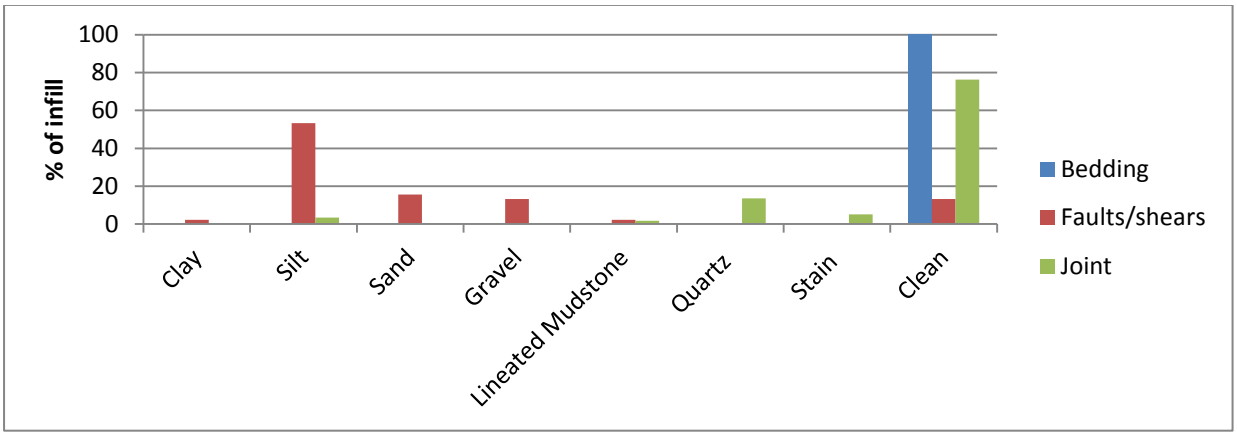

Figure 3.40: Opuha Dam infilling type and percentage as a total of all infill lithologies per defect type.

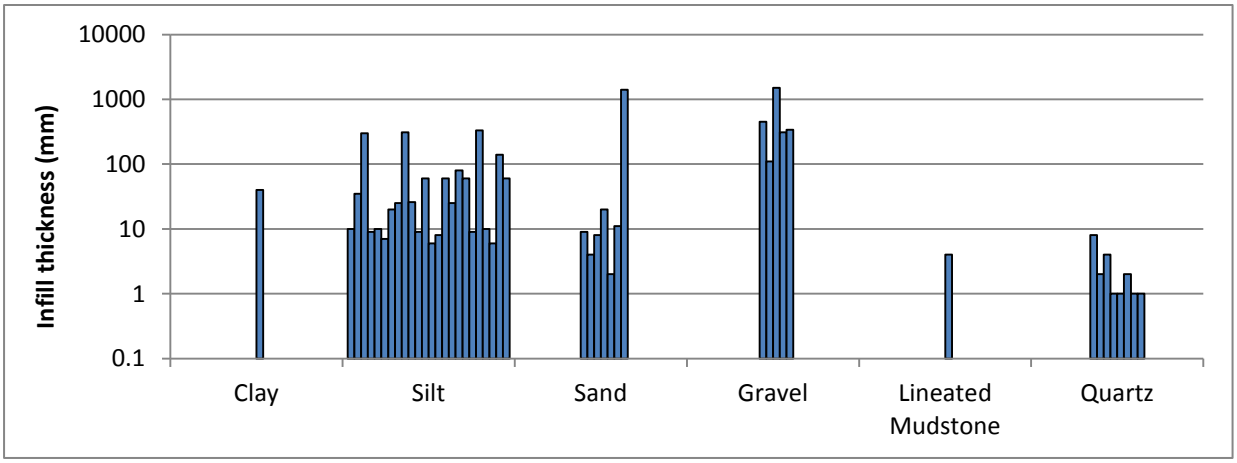

Figure 3.41: Opuha Dam fault and shear infill thickness.

Mudstone occurrence at the Opuha Dam Fault was relatively rare but where it does occur, similar characteristics to all other sites were observed. The rock mass remains fragmented. In the one thickly bedded mudstone unit boudinage was observed of a medium bedded sandstone unit (Figure 3.42).

Figure 3.42: Mudstone occurrence at Opuha Dam (outcrop 1f).

With increasing distance away from the fault zone, rock mass conditions improved i.e. outcrop 1g, 1h, 9a and to a lesser extent 8a. The rock mass was characterised by persistent jointing where blocky character was observed. This presented the most favourable conditions at the Opuha Dam study site (Figure 3.43).

Figure 3.43: Left: joint controlled rock mass at outcrop 1g; right: blockiness nature of persistent jointing observed at outcrop 9a.

Defect shape does not differ substantially from shape observed at other study areas. Bedding is relatively linear whilst faults/shears and to a lesser extent jointing increase waviness with increasing wavelengths (Figure 3.44). Roughness, similar to other sites, has no trend relating to defect type. Defect surfaces are dominantly undulating in shape with bedding and jointing surfaces commonly planar (Figure 3.45).

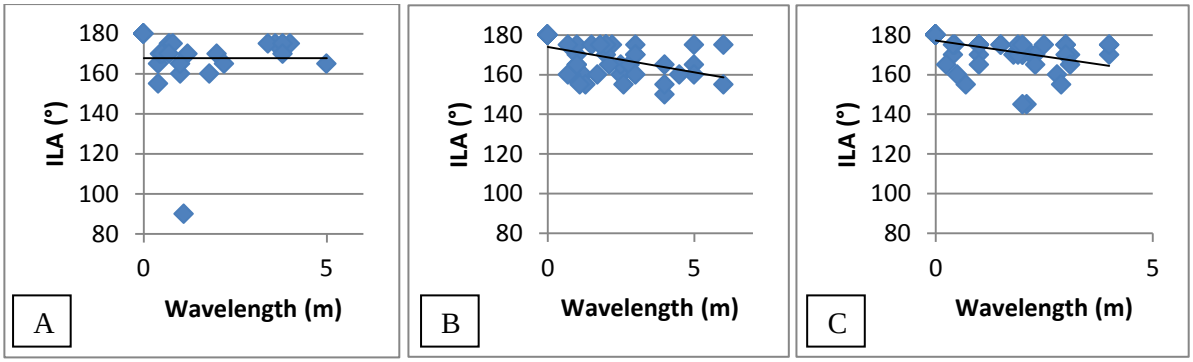

Figure 3.44: A: Opuha Dam defect waviness defined by interlimb angle (ILA) and wavelength (m). A: Bedding; B: faults/shears; C: jointing.

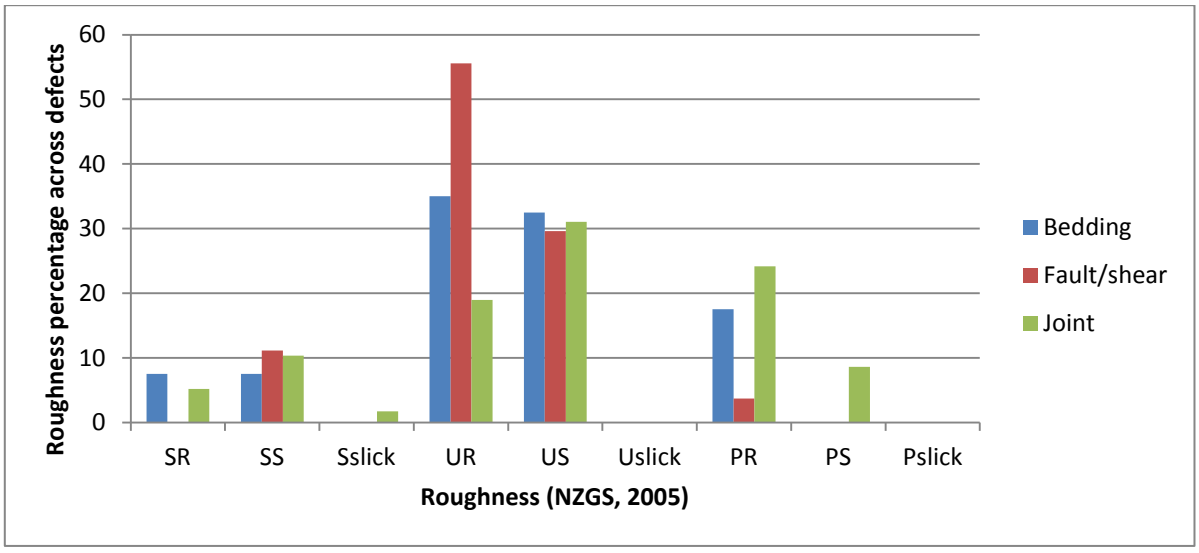

Figure 3.45: Opuha Dam surface roughness percentage across defects.

Bedding orientation is generally consistent with slight variation likely related to the Opuha Dam Fault orientated at 70°/211° (Appendix G.3). One well defined persistent joint set is identified at 28°/038°. Of interest is the dominant shear orientation of 79°/140°.

3.4.2 Laboratory testing

3.4.2.1 UCS and BTS

Due to the small spatial area of the study site, limited suitable lump samples for coring were able to be sourced. Core obtained for intact strength testing was sent to Trilab. Trilab preformed one UCS test with an intact rock strength of 189 MPa and failure through disintegration. Specific energy calculated for the sample is 0.026 MJ/m^3 through Trilab analysis.

Smaller lump samples for drilling and core cut-offs of adequate size allowed BTS testing to be done. A total of 17 tests were carried out across five outcrops restricted to the best jointed outcrops. Raw results and calculations are reproduced in Appendix G.4. Out of 17 tests only 1 test failed along an

existing discontinuity. All tests preformed were on fine to medium sandstone, generally thickly bedded to massive with one BTS carried out on a medium bedded outcrop defined by outcrop 6b. An average strength of 21 MPa was derived across all rock. The sample that broke along an existing defect indicated a strength of 9 MPa. The medium bedded test returned a strength of 14 MPa. Failure modes comprised both simple and multiple extension.

3.4.2.2 Cerchar abrasivity and ultrasonic velocity

Cerchar Abrasivity Index (CAI) was carried out on one sample (5a) by Trilab. An average CAI value of 4.27 was given. This rock is classified as extremely abrasive according to Käsling et al. (2007). P and S wave velocities also preformed on outcrop sample 1h. Dynamic Young's Modulus (GPa) and Poisson's Ratio were derived as 52.4 GPa and 0.26 respectively. The Young's modulus value remains very high for sandstone and indicates the rock is very stiff. A Poisson's ratio of 0.26 remains indicative of typical sandstone lithology.

3.4.2.3 Point load

Similar to other sites, fine to medium grained and thickly bedded sandstone have the highest intact point load strengths (Table 3.17). Thinly bedded sandstone intact strengths do not differ substantially from the thicker member indicating bedding thickness does not have a bearing on intact strength. Of note, however, breakage along existing defects renders the thinly bedded member the poorer rock mass. Rock located within gravel infilled shears, commonly with associated veining (calcite & quartz) was found to have the weakest intact strengths. No differentiation between fine grained sandstone and mudstone was derived for intact strength. Fine sandstone, however, had higher strengths when failure occurred along existing defects. Mudstone, however, which is typically the more weathered member, had existing defect failure strengths comparable to sheared rock indicating its relative weakness. Raw results and calculations are reproduced in Appendix G.5 for reference. An average point load to UCS conversion factor of 27 was derived for sandstone across the Opuha Dam site. No mudstone conversion factor was obtained due to the lack of mudstone sample for UCS testing.

Table 3.17: Opuha Dam average point load I_{s50} (MPa) results per bedding thickness, lithology and shear rock.

	Clean break	Existing break
Thick bedding (sandstone overall)	6.51	3.23
Thin bedding (sandstone overall)	5.53	1.41
F-M Sand	6.88	3.69
Fine Sandstone	3.66	1.36
Mudstone	3.32	0.44
Shear rock (sandstone)	2.09	0.48

3.4.2.4 Fines index testing

Five samples were analysed using wet sieve and laser sizing analysis, four from outcrops directly concerned with the Opuha Dam Fault. A further three fines dominated samples were laser sized, one from defect infill and two from clay gouge zones within the main fault zones previously discussed.

Results are given in Table 3.18. Clay sized particle content in fines material less than 1 mm is less than 10%. Of interest is the dominance of silt sized infill material across all samples analysed. Silt is particularly abundant with increased levels of clay sized particle in the two fault gouge zones.

Of note was the 50/50 split of sandstone and mudstone clasts, identified in the lab, making up the main Opuha Dam crush breccia zone. This indicates faulting concentrated primarily within the thin interbedded sequence. Appendix G.6 presents raw fines data and calculations.

Table 3.18: Opuha Dam fines index percentages derived from wet sieve analysis and laser sizing.

	1c	1h	2a	2a - clay	4b	5b	7a	7a - clay
Passing	**%**	**%**	**%**	**%**	**%**	**%**	**%**	**%**
>4mm	11.9	-	26.0	-	31.0	31.3	14.2	-
>2mm (Gravel)	15.4	-	15.5	-	12.4	14.6	7.2	-
>1mm (C-M sand) (sieving & laser)	22.5	44.1	17.4	40.5	17.8	18.4	22.2	-
<200 microns (Fine sand)	12.3	1.3	11.3	0.4	10.9	10.8	10.4	-
<60 microns (Silt)	32.7	44.8	24.9	45.6	23.1	22.4	38.9	72.9
<2 microns (Clay)	5.1	9.8	5.1	13.5	4.9	2.5	7.2	27.1

3.4.2.5 XRD and thin section analysis

Clay content differed between the Opuha Dam and other sites examined. Generally infill material from Opuha Dam had higher true clay contents than other sites, commonly up to 25% defined by Kaolinite, Montmorillonite and Illite (Table 3.19). No significant difference in true clay content is distinguished between main zones of fault gouge (<20%) and smaller scale defect infill (<25%).

Of interest is the significant increase in Montmorillonite, only observed elsewhere in one Ashley River Gorge sample. Contents up to 10% represent a change in condition between sites. Significant levels of calcite were found in the main Opuha Fault zone sample 5b. As discussed by Stewart (2007), calcite veining has been more common over the last three to five million years and is more prevalent in association with block faulting.

Two thin sections were analysed by point counting across the Opuha Dam site. Both were very thickly bedded to massive sandstones. Sample 4a was weathered to a higher degree and as such incorporated unidentifiable material recorded as matrix (33.4% by volume).

Table 3.19: Opuha Dam XRD analysis of infill material less than 1 mm.

Sample outcrop	Quartz (%)	Albite (%)	Kaolinite (%)	Montmorillonite (%)	Illite (%)	Calcite %
1c	60	15	5	10	10	-
1h	70	15		10	5	-
2a	65	20	5	5	5	-
2a – clay	75	10	Trace	10	5	-
4b	60	25	5	5	5	-
5b	40	10	5	10	10	25
7a	70	20	5	5	Trace	-
7a - clay	70	10	5	10	5	-

QFL ratios are reported in Table 3.20. Results indicate Feldspathic Greywacke lithology. Thin section sample from 4b mudstone and 1d sandstone were analysed to define textures and crystal habit. It both sections voluminous, high birefringence calcite veining on millimetre to micron scale was observed. Calcite and quartz veining are observed cross cutting each other. Calcite veining tends to cross cut quartz veining more often, indicating a younger age. It must be noted however some evident quartz veins are also observed cross cutting calcite veining to a lesser degree indicating some recent quartz veining activity. Both forms of veining are orientated in one distinct orientation in both samples. This indicates some form of shear present to allow micro-fracture to develop parallel with $\sigma 1$ which subsequently allows fault fluid to migrate.

Crystal grains are sub-angular in nature and commonly bound by up to 12% fine matrix material. The effects of feldspar weathering can be observed under thin section. Some feldspar has rough surface appearances and commonly discoloured under plane polarized light. A weathering rind can also be observed on select feldspar crystals. Lithic fragments represent the most chemically weathered material and are commonly too fine to identify minerals. It must be noted the rock sourced for thin section analysis remains relatively fresh, likely indicative of occurrence at depth.

Table 3.20: Opuha Dam thin section QFL ratios derived from thin section point counting.

Sample #	Quartz %	Feldspar %	Lithic fragments %
9a	33	42	26
4a	32	39	29

Chapter 4 TRC conceptual classification

4.1 TRC development

The objective of developing a rock mass classification specific to the Torlesse is to convey patterns or trends in rock mass condition. These patterns can then be linked to geological controls to help predict rock mass condition for engineering projects, in particular to assist tunnelling studies.

Trends were identified by systematically plotting all information derived from field mapping against each other for each site. Where rock mass conditions displayed clear relationships they were further examined to assess the geological relationships leading to these trends. These were then used together to develop the classification framework.

This was an iterative process fundamentally driven by using geological field observations to come up with ideas to test on what the important factors that control change in Torlesse rock mass condition.

4.2 Overall rock mass trends

The framework for the Torlesse rock mass classification (TRC) needs to convey rock mass trends experienced throughout all study sites. The purpose of this section is to deliver the main rock mass trends throughout all study sites as a framework for the development of the TRC. Site specific trends have been further analysed to strengthen or weaken trends for input into the TRC framework.

4.2.1 Patterns supporting the TRC framework

The main indicators of rock mass change were found to be blockiness and defect structure. Blockiness describes the general shape and size of blocks defined principally by bed thickness and fracture density while defect structure describes the occurrence of persistent jointing and localised shears through to regional scale faulting; that is, systematic defects. Of importance to both rock mass trends is lithostructure, defined as the percentage occurrence of sandstone and mudstone and the relative difference in bedding thickness between the two lithotypes.

4.2.1.1 Bedding thickness proportion

From the trend analysis a major governing control on rock mass character was found to be bedding thickness and the proportion of sandstone to mudstone. Sandstone bedding proportion is variable across the Torlesse (Figure 4.1 left). Generally the sandstone member is more voluminous toward the thicker beds however the trend is weak, while very thinly bedded sandstone is relatively rare.

In excess of 65% of mudstone encountered in the field was very thin to thin in thickness (Figure 4.1, right). Thicker mudstone beds are relatively rare likely due to the depositional environment at the time of deposition. However due to the heavily fractured nature and subsequent increase in surface area, the mudstone is prone to accelerated weathering and erosion. As a result thicker mudstone beds that

may be present could be obscured and hidden from surface outcrop exposure. Generally very thin and thin sandstone beds only occur interbedded with very thin to thinly bedded mudstone.

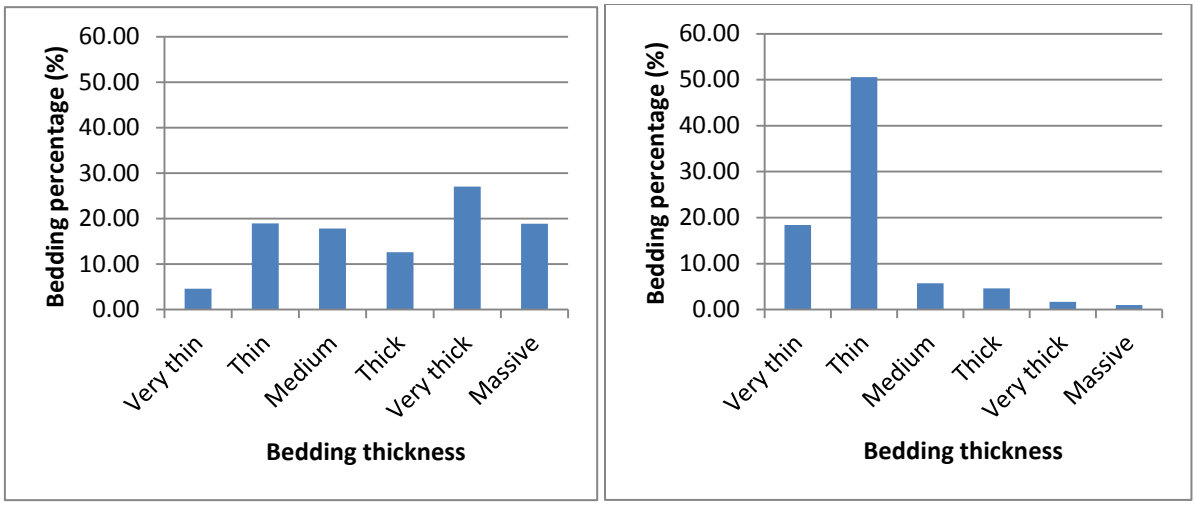

Figure 4.1: Left: sandstone bedding proportion; right: mudstone bedding proportion.

4.2.1.2 Blockiness

The trend analysis shows size and shape of blocks is fundamentally controlled by bedding thickness. It was generally found that a larger sandstone bedding thickness results in a better rock mass (Figure 4.2). This is due not only to the relatively large spacing between bedding partings but also this rock tended to have a lower degree of fracturing.

As the proportion of mudstone generally increases toward the thinner bedded units fracturing increased (Figure 4.2). Very thinly bedded rock masses are nearly always fragmented in fracture density where mudstone portions are highest. As the occurrence of mudstone decreases toward the thicker bedded units fracturing decreases in density (Figure 4.3). Therefore, it was found bedding thickness and associated fracture density were the primary controls on rock mass blockiness. The trend is further strengthened by excluding fault related rock from the analysis. In nearly all cases the mudstone member has fragmentation greater than 50 breaks per metre.

4.2.1.3 Defect structure

The occurrence of persistent jointing, faults and shears was also found to dictate rock mass condition. Rock is in better fractured condition where the rock mass was controlled by large, relatively persistent (>2 m) jointing (Figure 4.4). Typically this rock had little to no associated faulting. Where the level of faulting increased the occurrence of large, persistent jointing decreased to the point where discrete, non-persistent joints control rock mass character.

As such a differentiation can be made between defects which can be described as systematic and non-systematic based on their relative persistence and their ability to form defect sets. Systematic joints tend to form sets of varying spacing and control the release of blocks. Non-systematic joints are short,

discrete and generally of random orientation, although a portion of these defects do cluster in broadly defined sets. In this study they are described as fractures, and are differentiated from persistent joints (>2 m in this study) that typically form better defined sets. It must be noted there is always some degree of non-systematic jointing (fracturing) present in all Torlesse rock mass types including types that contain dominant defect sets.

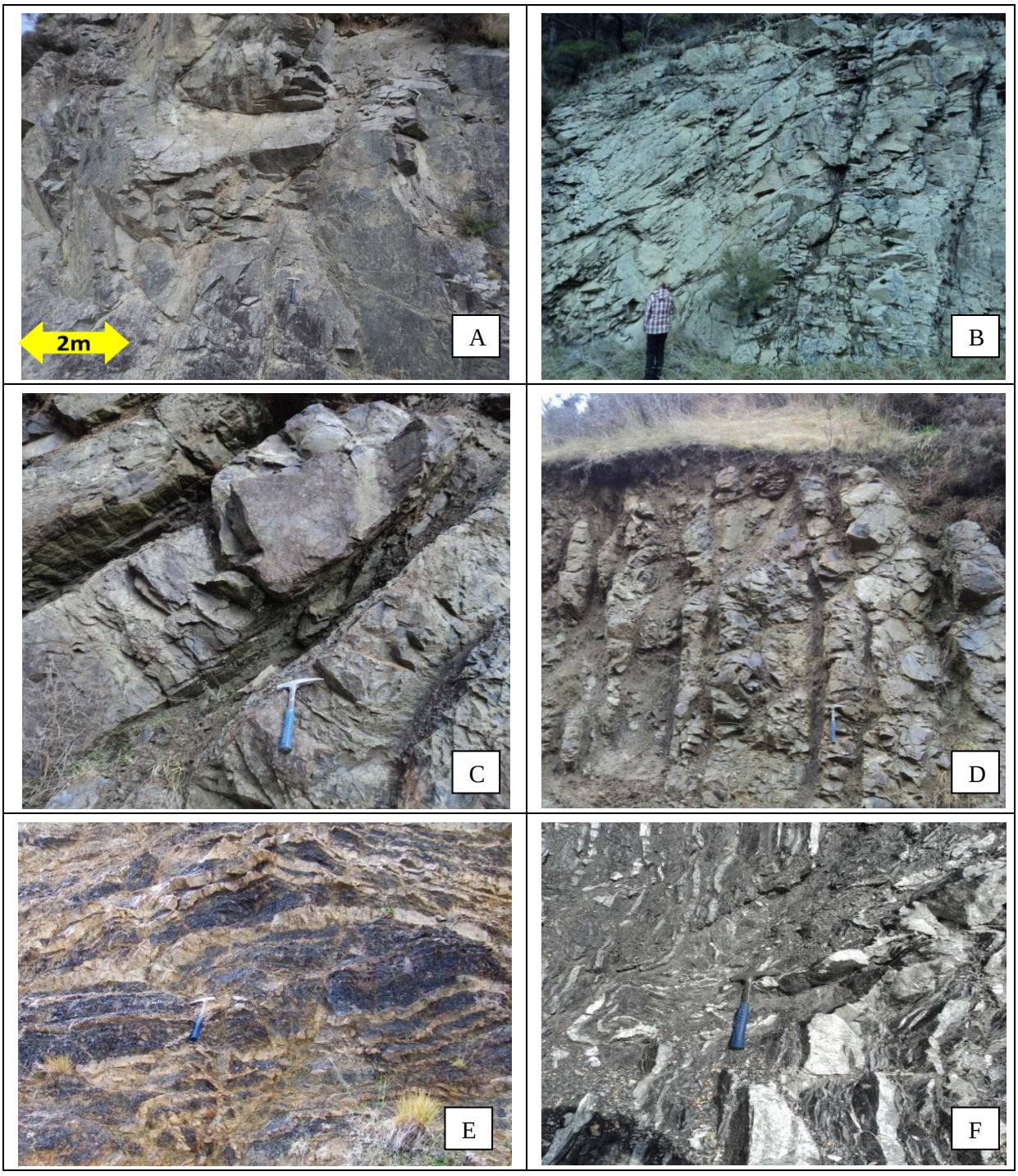

Figure 4.2: A: Hurunui outcrop 7a, thick/thin sandstone/mudstone; B: Hurunui outcrop 16a, thick/thin sandstone/mudstone; C: Hurunui outcrop 26a, medium/thin sandstone/mudstone; D: Hurunui outcrop 29a, medium/thin sandstone/mudstone; E: Ashley outcrop 25a, thin/thin sandstone/mudstone; F: Ashley outcrop 51a thin/very thin sandstone/mudstone.

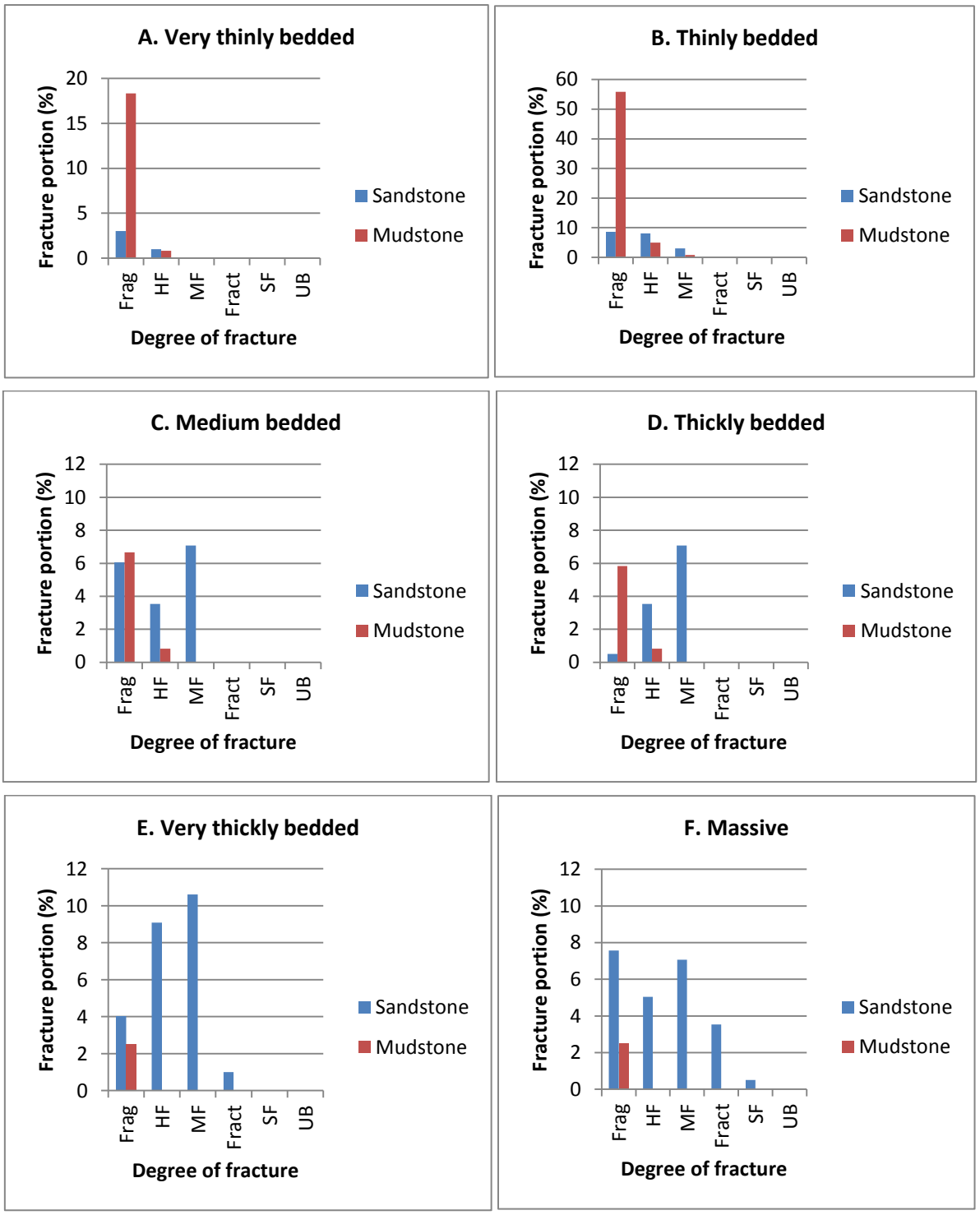

Figure 4.3: Degree of fracture according to bedding thickness. Frag = fragmented, HF = highly fractured, MF = moderately fractured, Fract = fractured, SF = slightly fractured, UB = Unbroken.

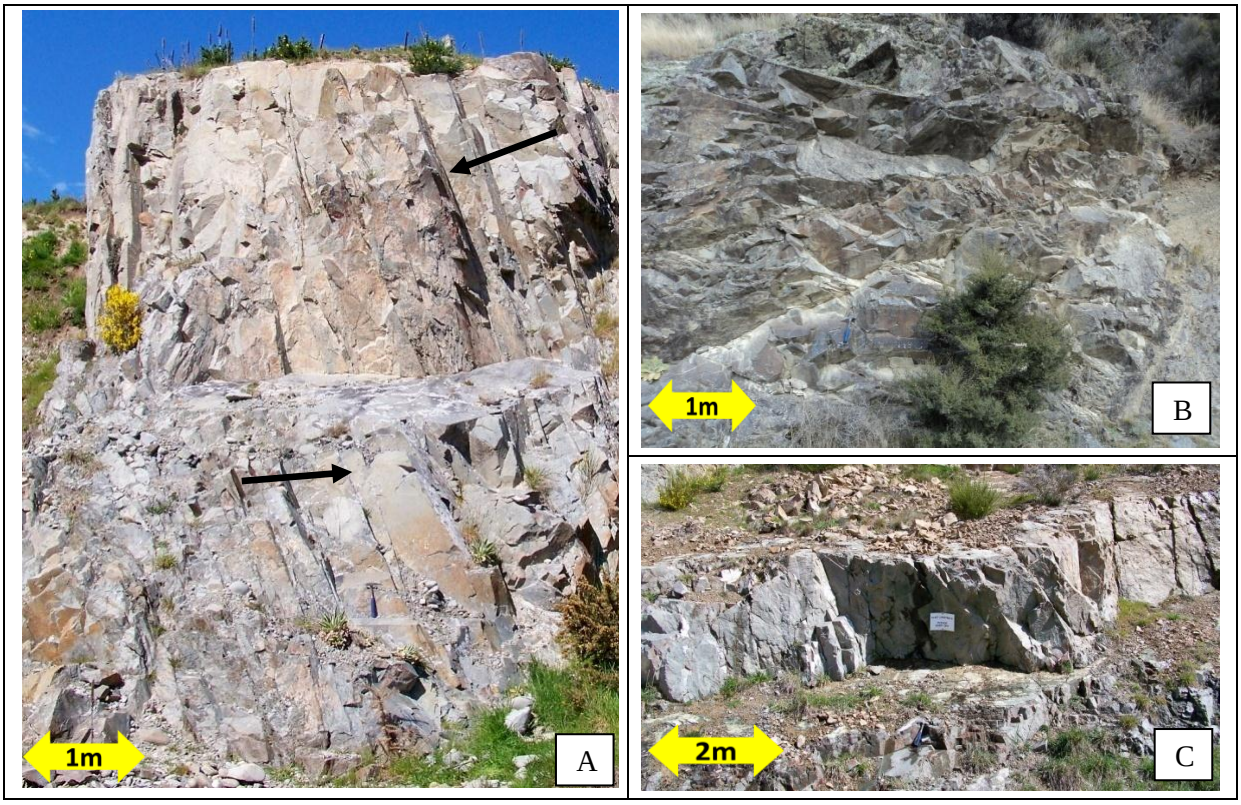

Figure 4.4: A: Opuha 9a massive sandstone with persistent rock mass dominated jointing indicated; B: Hurunui 5a very thick/thin alternating sandstone mudstone; C: Opuha 1g massive sandstone.

4.2.2 Relationship between blockiness and defect structure

A relationship between bedding thickness and defect structure was found. Typically shears and faults on a variety of scales tend to localise in the thinly bedded members (Figure 4.5 & Figure 4.6). In contrast the more thickly bedded members tend to resist faulting and contain a greater amount of persistent jointing.

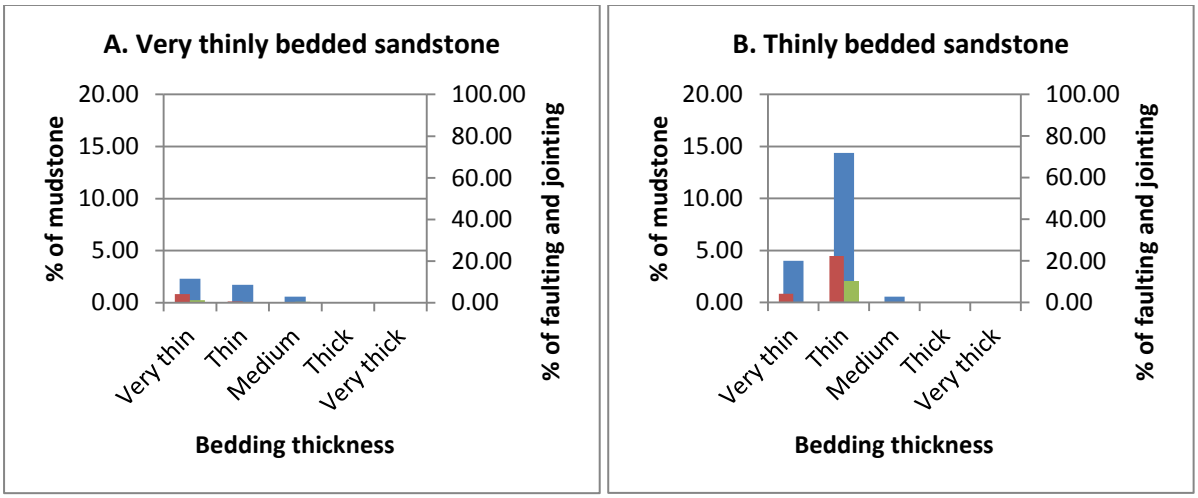

Figure 4.5: Overall mudstone bedding proportion with associated joint and fault occurrence as a percentage of independent defect. Mudstone bedding percentage = blue, faulting/shearing = red and jointing = green.

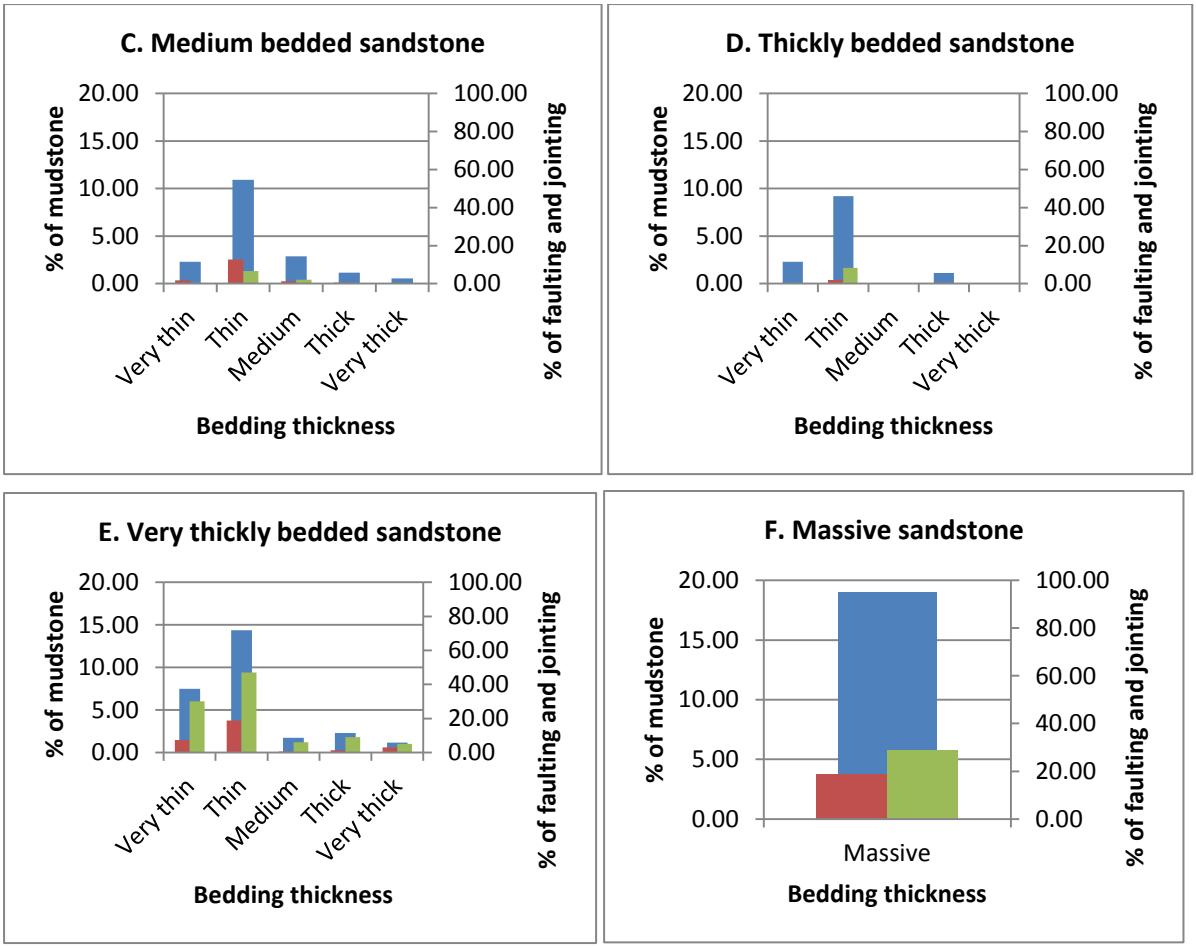

Figure 4.5 (continued): Overall mudstone bedding proportion with associated joint and fault occurrence as a percentage of independent defect. Mudstone bedding percentage = blue, faulting/shearing = red and jointing = green.

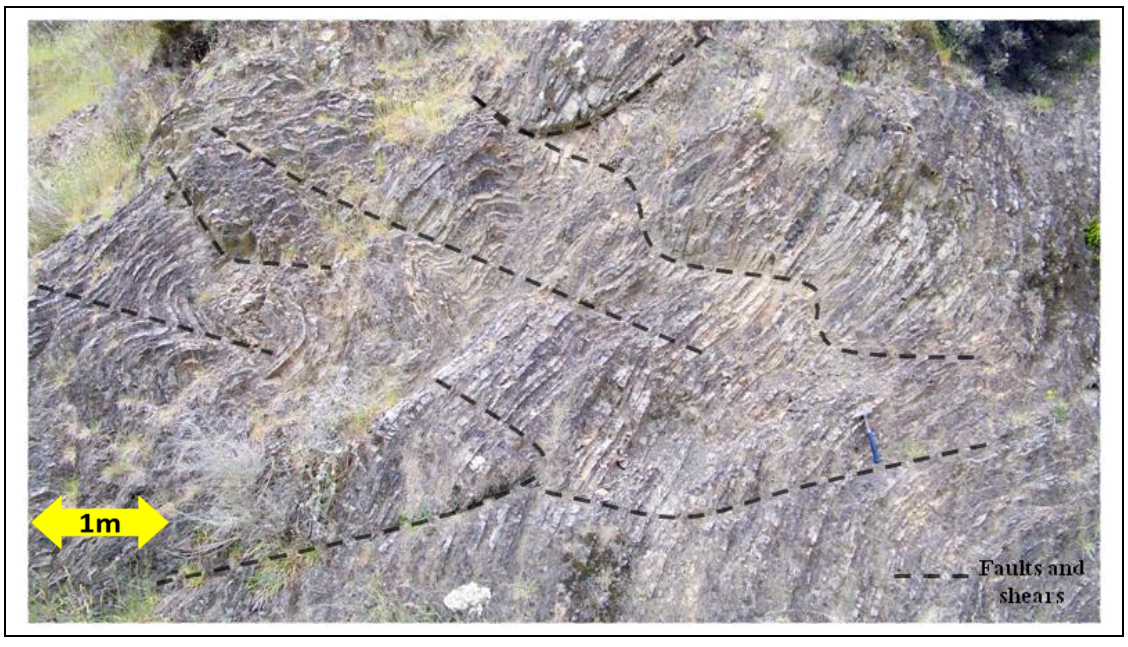

Figure 4.6: Top: Ashley 22a very thinly interbedded sandstone-mudstone sequence with abundant faults and shears indicated; bottom: Hurunui 13c thin interbedded sandstone-mudstone sequence with faults and shears indicated.

Figure 4.6 (continued): Top: Ashley 22a very thinly interbedded sandstone-mudstone sequence with abundant faults and shears indicated; bottom: Hurunui 13c thin interbedded sandstone-mudstone sequence with faults and shears indicated.

4.2.3 Variations to rock mass trends

Due to the nature and complexity of the Torlesse rock mass, the general trends exhibited do not always hold true everywhere. In a few localities the thinly bedded member is in reasonably good condition, however fracturing still remains moderate to high (Figure 4.7). Similarly in some cases thickly bedded members have high levels of fracturing (Figure 4.7).

The trends expressed differ in proximity to major fault and shear structures. The rock mass within major fault zones has a high fracture density irrespective of bedding thickness (Figure 4.8). Whilst faulting tends to concentrate within the thinly bedded members, where a significant stress field is present faulting will occur irrespective of bedding thickness. Bedding defects in main fault zones is commonly absent and as such, is described as massive for plotting purposes. The better quality rock mass bordering the main fault zone exhibits increased levels of outcrop scale shearing and faulting. The magnitude of this increase in shearing around major structures differs according to fault size.

Figure 4.7: Left: Ashley 28a thin interbedded, moderately to highly fractured sandstone-mudstone; Right: Hurunui 14c very thickly bedded, highly fractured sandstone.

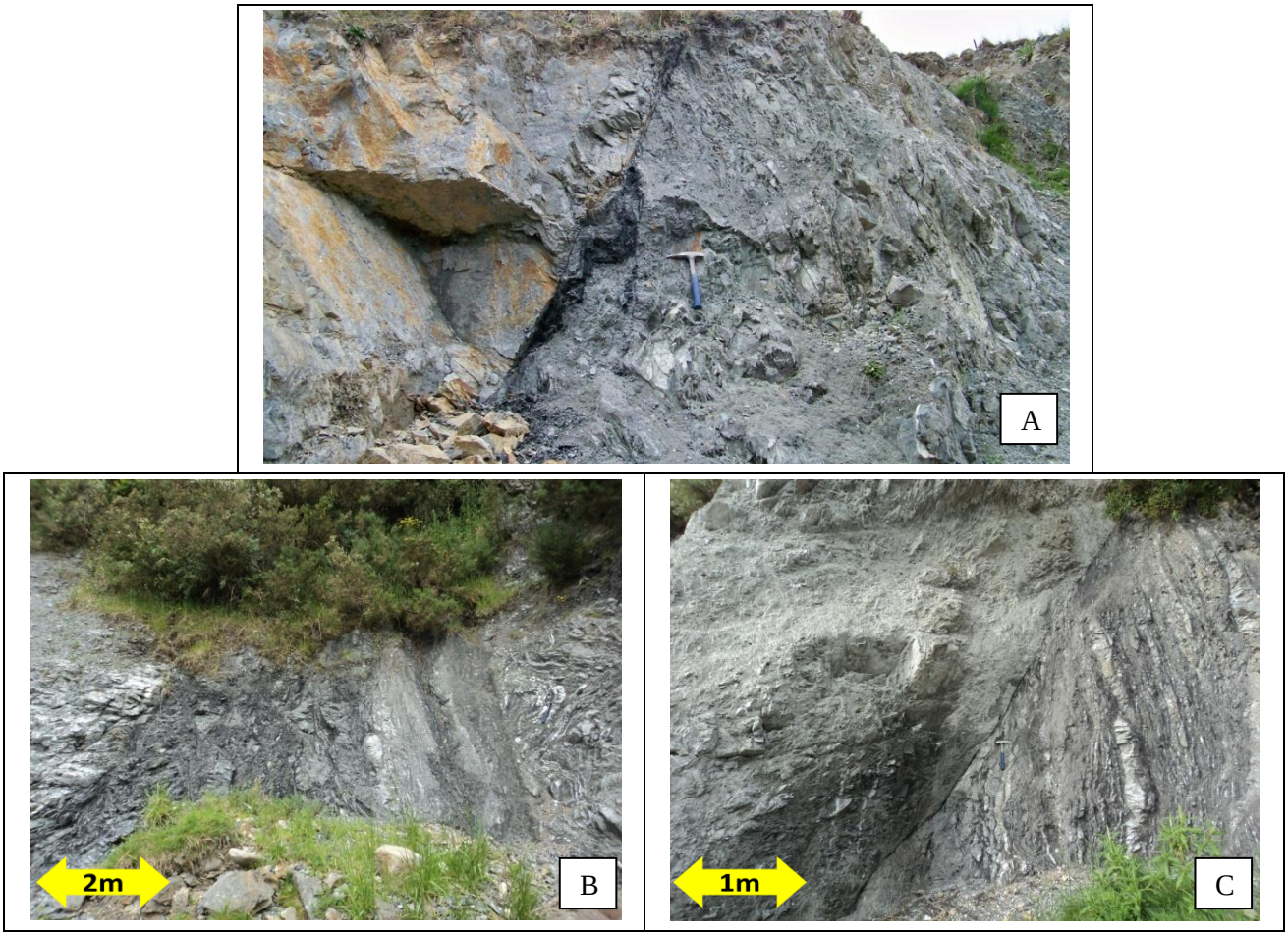

Figure 4.8: A: Opuha Dam Fault located in very thickly bedded sandstone; B & C: examples of large Ashley Gorge structures located within thin interbedded sequences (left, Ashley 38a, right, Ashley 51a).

4.2.4 Poorly correlated rock mass trends

4.2.4.1 Influence of scale

No relationship was found between many rock mass variables collected in the field. Due to outcrop and tunnel scale mapping, and the need to cover large areas in a relatively short amount of time outcrops were not mapped using scanline or line mapping techniques such as used by Cook (2001). In previous studies (Read and Richards, 2007, Richards and Read, 2007, Read et al., 2000, Cook, 2001) authors have described to some detail the presence of non-persistent, discrete, interlocked jointing that likely forms high rock mass strengths at smaller scales. This study took to undertake investigation of other rock mass controls and influences at larger scales. The presence of low persistence jointing is still significant and recorded via degree of fracture through this study, however larger scale controls and influences need to be conveyed for anticipation of ground behaviour.

Spacing of jointing greater than two metres in length was found to have a minimal influence on the rock mass. Generally wider joint spacings (>2 m) are expected to lead to better quality rock masses. Cook (2001) concluded that defect spacing between low persistence jointing is a main controlling factor in the Torlesse rock mass. Read et al. (2000) discuss that this attribute is required for a rock mass classification that addresses defect spacing more specifically than the GSI. At scales examined in this study, joint spacing and persistence were very loosely related. It is expected defect spacing subsequently decreases toward the poor rock masses to the point where non-persistent (<2 m) joints, similar to that described in the literature, are a major feature of the rock mass. Due to complexity of the rock mass, particularly at scanline scales, irregular, non-persistent defect spacing remains a hard characteristic to quantify. Therefore, the degree of fracturing, recorded as the number of low persistence joints crossing a one metre section, was used in this study to characterise defect spacing. The results indicate this method served the purpose well given the application intended in this study.

4.2.4.2 Defect condition and intact strength

No significant relationship was derived for defect condition or intact strength. A large variation in defect roughness character was observed throughout all defect types, irrespective of blockiness or defect structure. Similarly, no significant difference was observed through intact rock strengths between different bedding thicknesses irrespective of lithology. It was therefore found intact rock strength and defect condition did not have any significant control on rock mass character. Despite this, a slight variation was observed in intact strengths between Torlesse terrane types, further discussed in Section 5.2.3. This has slight implications respective of Torlesse terrane, however is not considered a major, overall rock mass governing control.

4.3 Conceptual classification system

Blockiness and defect structure, as described in sections 4.2.1.2 and 4.2.1.3 respectively make up the dominant Torlesse controlling attributes. The relationship exhibited between blockiness and defect structure (Section 4.2.2) was taken and related together to form the conceptual Torlesse rock mass classification (TRC). To allow plotting, further analysis revealed blockiness and defect structure could each be grouped into six representative rock mass classes encasing the range in conditions experienced and related together as per relationships derived to form an XY plot. Due to the nature of the Torlesse rock mass it became clear some regions of the TRC would not have any plotting.

4.3.1 Rock mass classes

The two principal rock mass controls, blockiness and defect structure, were related together on an XY plot to form the conceptual TRC. To further develop and define the blockiness classes, bed spacing and degree of fracture were plotted per outcrop (Appendix H). The data were then grouped into six rock mass categories (A-F, Table 4.1) of similar condition ranging from thickly bedded to massive sandstone with slight to moderate fracture, to very thin to thinly bedded sandstone that is fragmented (Table 4.1).

Observational trends in conjunction with defect structure analysis (Appendix D.3, E.3, F.3 and G.2) were used to derive six defect structural rock mass categories (1-6, Table 4.1). Each outcrop was grouped into a class according to jointing and faulting occurrence. Outcrops for which no defects satisfied the greater than 2 m criteria but for which there was blockiness information were classified using the pictorial gradation (Appendix I) discussed in Section 1.3.6. Categories describing both blockiness and defect structure were formulated such that rock mass conditions deteriorate from Class A to F and 1 through 6, respectively. The nature of the class labels allows any one outcrop to be categorised into a representative block by quoting a blockiness and defect structure class i.e. A3, E5 etc. To enable defect structure to be quantified, ISRM (1978) spacing descriptions have been used (Table 4.2).

Table 4.1: Blockiness and defect structure classes.

Blockiness		
Class	**Lithostructure**	**Fracture Density (section 1.3.1)**
A	Massive to thickly bedded sandstone	Slightly to moderately fractured
B	Medium bedded sandstone	Moderately to highly fractured
C	Massive to very thickly bedded sandstone	Highly fractured
D	Thinly bedded sandstone	Moderately to highly fractured
E	Massive to medium bedded sandstone	Fragmented
F	Thinly to very thinly bedded sandstone and mudstone	Fragmented

Table 4.1 (continued): Blockiness and defect structure classes.

Defect Structure		
Class	**Dominant Structure (refer to ISRM (1978))**	**Secondary Components**
1	Persistent joints, moderate (rarely close) to very wide spacing	Shears and faults are rare
2	Persistent joints, moderate (rarely close) to very wide spacing	Shears and faults, very to extremely wide spacing
3	Persistent joints (moderate to very wide spacing, rarely close) and shears/faults (very to extremely wide spacing) in approximately equal portions	
4	Shears and faults, wide to extremely wide spacing	Persistent joints, moderate to very wide spacing
5	Shears and faults, moderate to wide spacing	Persistent joints are rare
6	Brecciated rock with very close to widely spaced sheared and crushed zones typical of major fault zones	

Table 4.2: ISRM (1978) defect spacing classification.

Description	Spacing
Extremely close spacing	< 20 mm
Very close spacing	20–60 mm
Close spacing	60-200 mm
Moderate spacing	200-600 mm
Wide spacing	600-2000 mm
Very wide spacing	2000-6000mm
Extremely wide spacing	> 6000 mm

To allow representative plotting each axis of the TRC is treated as a gradational axis across any one blockiness or defect condition class. Combinations of attributes making up the classes were assigned a number related to where that individual outcrop rock mass plotted in respect to the overall class. This allowed a true gradation of improving/worsening rock mass condition through each category.

4.3.2 Nature of the TRC

An objective of the classification is to characterise the variability in condition of the Torlesse through individual outcrop assessment. Observations show that the mudstone member has consistently thin bedding, which is often fragmented and whose contact with sandstone is typically sheared. The sandstone member makes up a larger proportion of the rock mass by volume and exhibits a higher degree of variability in condition. As such, the classification attempts to capture variability in the sandstone member while incorporating the typical mudstone characteristics. Additionally at a tunnelling scale the mudstone lithotype in some instances could be of lower importance than for large scale road cuts, for example, where the mudstone beds could act as problematic large scale discrete failure planes.

The idea of the classification is to characterise the variability across individual outcrops. The sandstone member makes up the bulk of the rock mass and hence is responsible for a large part of variability in the Torlesse condition. As such the classification is dominantly concerned with the sandstone member as an easier way of presenting data. The descriptions have thus been set up to concentrate on sandstone condition due to its abundance. As a result mudstone has been left out of the descriptions, however remains an important rock mass attribute. The mudstone has very consistent thin bedding and a fragmented degree of fracture which allows typical mudstone character to be derived per rock mass type.

4.3.3 Conceptual TRC development and validation

The conceptual TRC (Figure 4.9) was devised on the basis of observed rock mass trends prior the plotting of individual outcrops to check its validity. In relating blockiness and defect structure together to form the TRC, the best rock mass blockiness conditions defined by class A and B were rarely expected to have a defect structure of class 5 or 6 where the rock mass is controlled by major faulting. Therefore, the top right hand corner is not included in the classification. An interpretation termed 'rock bordering major fault zones' was implemented as an indicator of increasing proximity toward a major structure to capture the range in rock masses experiencing increased levels of faulting and shearing that would plot on or near the XY truncation curve (i.e. Opuha and Elliott).

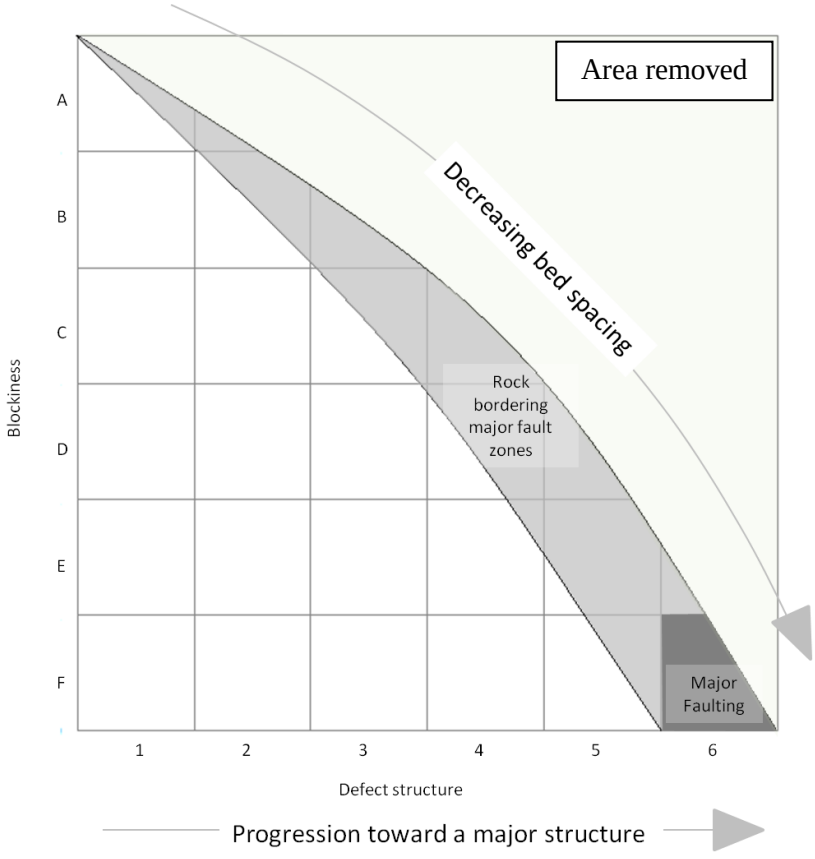

Figure 4.9: Conceptual TRC diagram.

The final classification (Figure 4.10) also removed the bottom left region out where poor blockiness classes (E & F) combine with favourable defect structures (class 1 & 2). The removal of these regions concludes that these combinations are not likely in a Torlesse rock masses. This final form of the TRC was validated by plotting individual site data, although, the overall plotting area of the TRC increased in size. The XY truncation curve was shifted to the right to accommodate better than expected rock masses, such as at the Opuha Dam, which exhibit favourable blockiness class whilst incorporating higher degrees of outcrop faulting and shearing.

It was found the majority of outcrops plotting in "rock bordering major fault zones" were located within close spatial proximity to major faults or lineations identified in the desktop study. Some outcrops located in this region, however, have no apparent relation to the occurrence of major faulting. For this reason the "rock bordering major fault zones" interpretation should be only used as a general indicator to identify potential for increasing proximity to major structures and will not always hold true due to the complex nature of the Torlesse Composite Terrane.

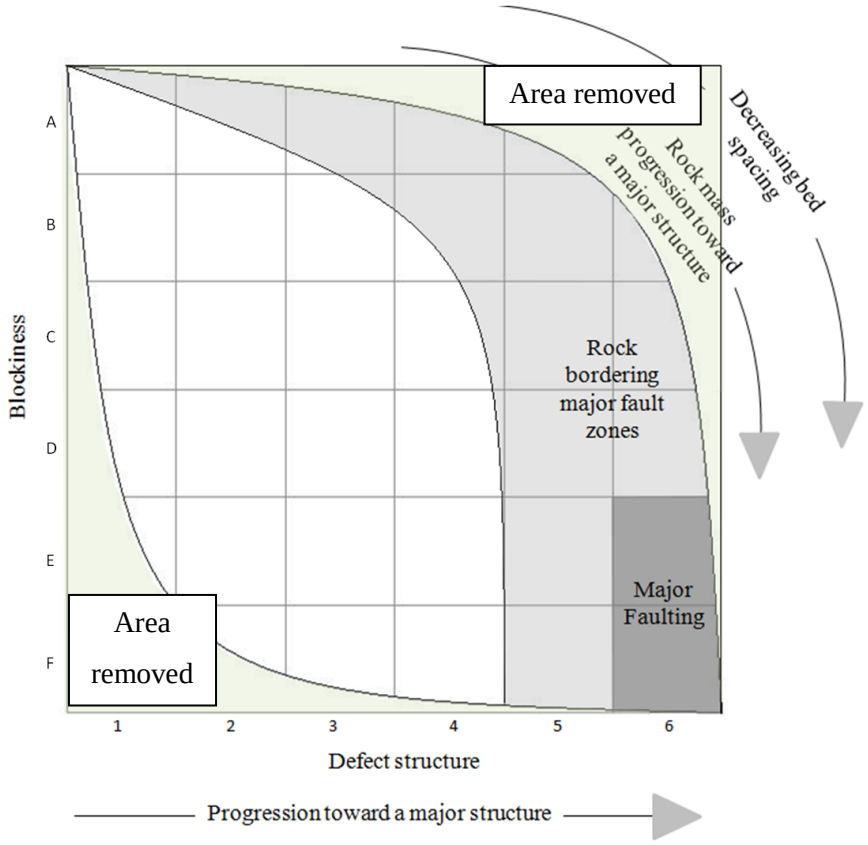

Figure 4.10: Final TRC conceptual model plot.

4.4 Study site TRC

Plotting of data from individual study sites was undertaken as a check and validation procedure of the conceptual TRC. Furthermore the plotting of individual outcrops from each study site allows representation of the variation in rock mass conditions.

4.4.1 Elliott Fault TRC

The Elliott Fault TRC plot (Figure 4.11) shows a general gradation toward a major structure with increasing levels of shearing and faulting toward the principal slip zone. Four major clusters were identified in the data. Cluster 1 is generally characterised by thick sandstone with minimal shearing. Rock here is controlled by persistent, systematic, planar jointing. Cluster 2 represents a transition zone between the main zones of movement and relatively intact rock of cluster 1. A higher degree of shearing is present with minor amounts of persistent jointing. The rock mass here is dominantly controlled by incipient, low persistent (<2 m) fracturing. Points tend to cluster around blockiness class D and do not present within the rock mass bordering major fault zones region despite close spatial proximity to the Elliott Fault. The cluster represents the thin interbedded outcrops located on the fault footwall. Due to regional stress likely accommodated by the major fault zone, persistent jointing within the member occurs in equal proportions in association with outcrop scale shearing. Cluster 3 represents the completely fragmented rock mass that borders the main fault zone of heavily sheared rock. Cluster 4 represents the worst rock mass conditions observed, in which the rock is completely fragmented and behaves as a soil. Rill erosion is present at every site where this rock mass type is observed. More intact centimetre to metre sized blocks bound by sheared material are common.

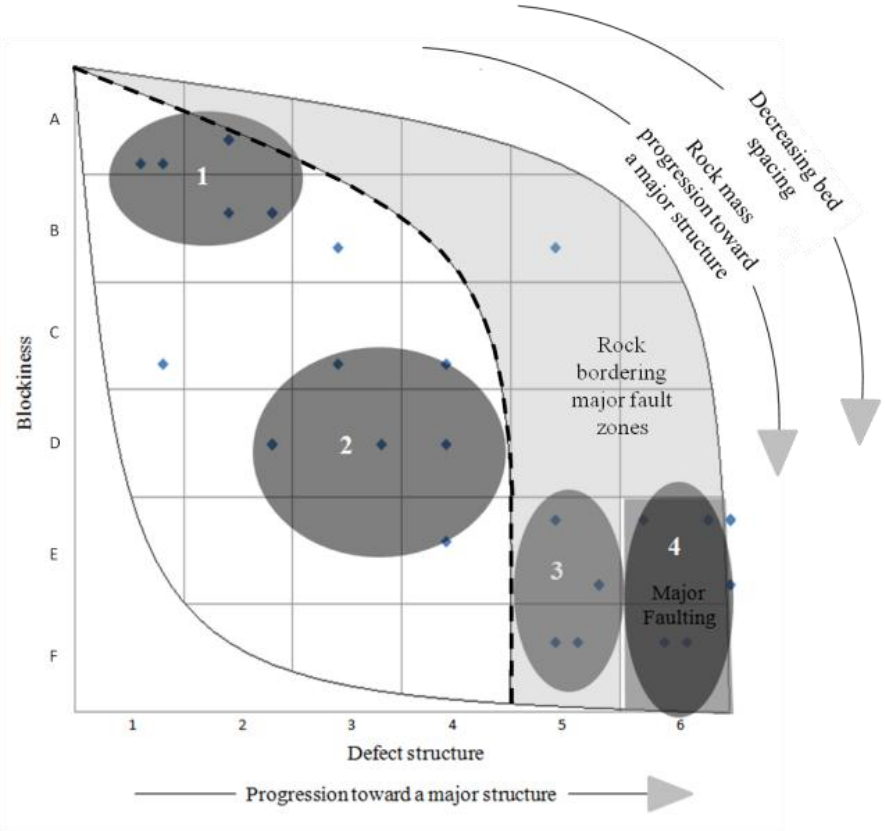

Figure 4.11: Elliott Fault TRC plot and subsequent rock mass classes.

4.4.2 Hurunui River TRC

The Hurunui River represented the best rock mass conditions in this study despite its locality in the Esk Head Belt, described as a zone of more sheared rock than other terranes (Rattenbury et al., 2006). Five rock mass clusters are present in the Hurunui TRC (Figure 4.12). Cluster 1 represents the bulk of the data and has similar characteristics cluster 1 at the Elliot fault. Cluster 2 represents a more fractured rock mass representing an increasing occurrence of low persistent (<2 m) joints with medium spaced to massive bedding. The rock mass still contains some persistent joints, however, small discrete joints also have an effect on the rock mass, making the cluster transitional between systematic and non-systematic joint control. Cluster 3 represents rock masses similar to cluster 2, however, with increased levels of faulting indicative of potential for increasing proximity to a major structure. It is however unclear in the Hurunui if these structures exist. Typically cluster 3 is representative of the Mount Noble Structural Zone, indicating increasing likelihood that the rock mass character is due to nearby structures based on the amount of faulting and shearing discussed in Section 3.2.3. Cluster 4 is characterised by thin bedding that is dominantly faulted and sheared. Persistent jointing is very uncommon and low persistent fracturing dominates the rock mass. Cluster 4 represents the best quality thinly interbedded sandstone and mudstone observed throughout the site. Cluster 5 represents fragmented rock masses where some persistent jointing is present but only has minimal influence on the fragmented rock. The rock mass typically has a high degree of faulting and shearing irrespective of bedding thickness.

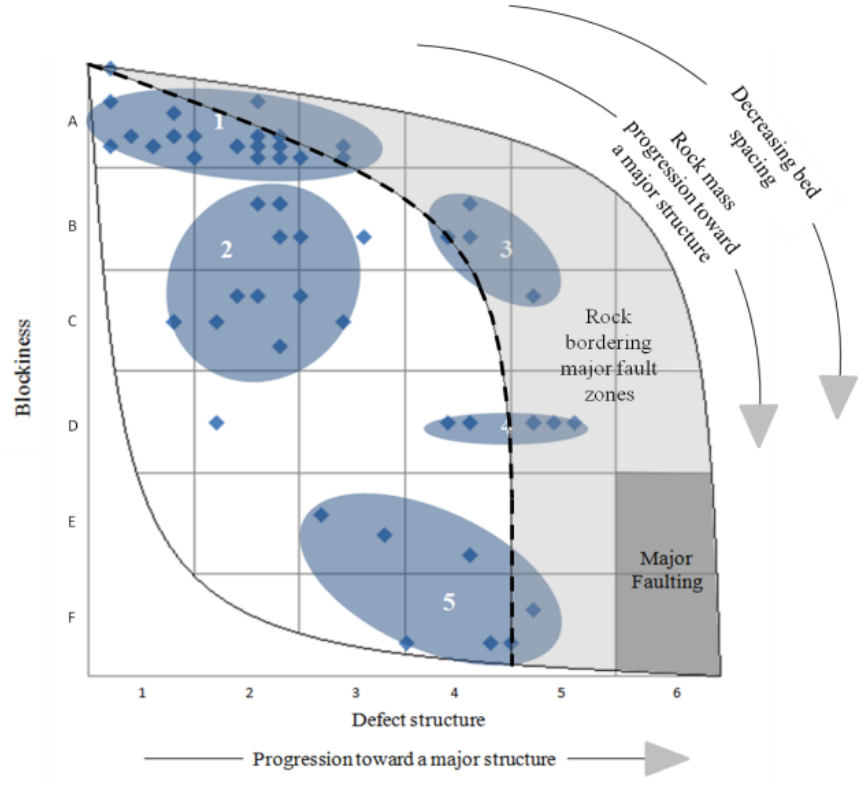

Figure 4.12: Hurunui River TRC plot and subsequent rock mass classes.

4.4.3 Ashley River Gorge TRC

The Ashley River Gorge site represents a broad cross section across rock mass conditions seen at all the study sites. Eight clusters are identified on the Ashley Gorge TRC (Figure 4.13). All clusters have comparable clusters exhibited at other sites. Cluster 1 presents the best systematic joint controlled rock mass similar to other 1st clusters. Cluster 2 represents the same blockiness as cluster 1 but with faulting and persistent dominant jointing in equal measures. This rock mass is indicative of increasing proximity of the rock mass to major structures where blockiness is retained with increasing presence of shears and faults, but the rock mass remains dominantly controlled by systematic jointing. Cluster 3 represents a more fractured rock mass with shearing that does not differ substantially from clusters 1 and 2. Cluster 4 represents highly fractured thick to massive Sandstone with abundant shearing typically found near major fault zones. Cluster 5, similar to Elliott Fault cluster 2, represents the best quality thin bedding rock mass conditions that incorporate a higher degree of shearing. Cluster 6, similar to Hurunui cluster 5, represents fragmented rock masses with prevalent shearing and some distinct persistent jointing. Cluster 7, equivalent to Elliott Fault cluster 3 represents the range of fragmented bedding thickness subjected to abundant faulting or areas boarding a major fault zone. Cluster 8 represents the main fault zones with the same fault zone characteristics as at other sites. In the Ashley River Gorge these fault zones tend to localise in the thinly bedded member.

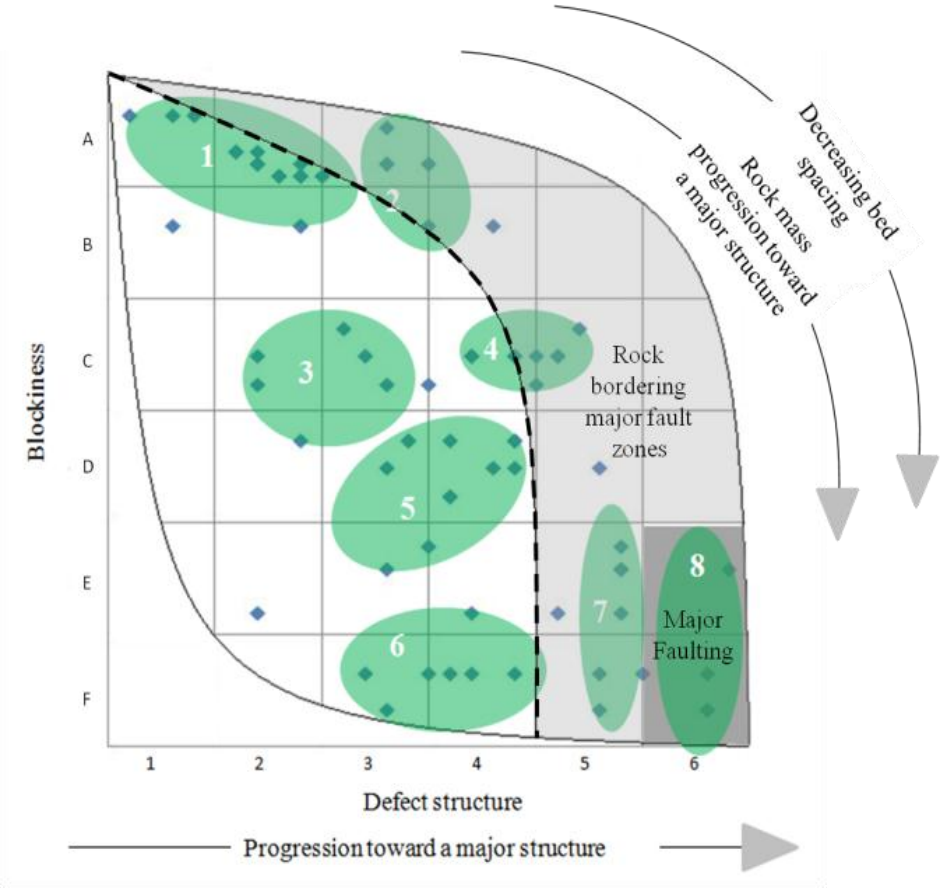

Figure 4.13: Ashley River Gorge TRC plot and subsequent rock mass classes.

4.4.4 Opuha Dam TRC

Large ranges in conditions are observed on the Opuha Dam TRC (Figure 4.14) due to the Opuha Dam Fault and its smaller size on a regional scale compared with the Elliot Fault. Cluster 1, similar to 1st clusters at other sites, represents the same rock mass characteristics and represents the best rock mass. Cluster 2 represents a similar thickly bedded blockiness to cluster 1, however, an increase in the level of small scale shearing is present due to its close proximity to the main Opuha Dam Fault. The rock mass in cluster 2 remains dominantly controlled by systematic jointing. Cluster 3 has a higher degree of fracturing in similar thickly bedded sandstone with the same level of increased shearing exhibited in cluster 2. This cluster represents a transition between systematic, persistent joint controlled rock masses and rock masses controlled by non-systematic, non-persistent discrete fractures, faulting and shearing. Cluster 4 is interesting because it represents a fragmented rock mass with numerous shears and persistent jointing. Due to the level of fragmentation the outcrops are controlled by discrete, incipient fracturing. Persistent jointing still exists, however, which has a limited control on rock mass condition. Cluster 5 is equivalent to Elliott Fault cluster 4 and Ashley River Gorge cluster 8, and represents the fault crush zones. The material here primarily acts as a soil with intact blocks rarely exceeding 2 cm in size. Small scale (<10 cm) zones of slightly plastic gouge material could be differentiated from cluster 5 by colour and texture along primary slip zones. This material is primarily silt sized brown material with no intact rock. The colour suggested mudstone origins.

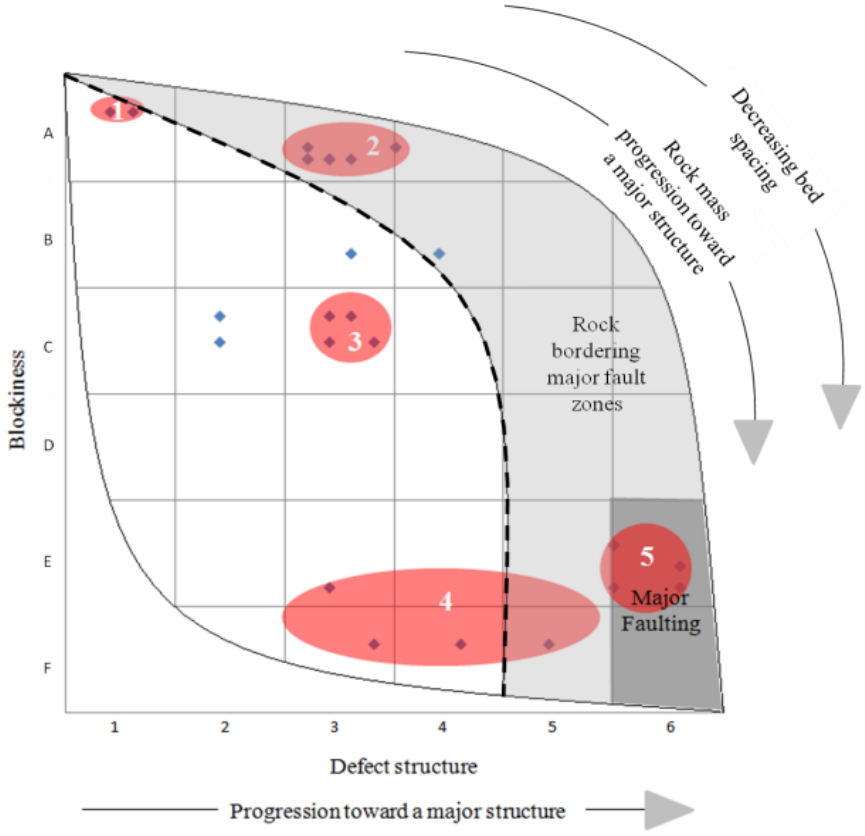

Figure 4.14: Opuha Dam TRC plot and subsequent rock mass classes.

4.5 Overall rock mass TRC and Types

Identifying clustering in the TRC allows characterisation of the range in rock mass conditions likely to be encountered within a tunnel section. Each study site's TRC clusters were overlaid onto the TRC diagram to represent the range in rock mass conditions and to identify equivalent clusters across the different sites (Figure 4.15). The purpose of identifying common clustering was to test if there are any consistent trends in rock mass distribution across the Torlesse Composite Terrane. There is an expectation however, projects concerned with TRC use will independently plot their own data to identify site specific rock mass types and not solely rely on types derived from this study. It remains possible future TRC work will show similar rock mass patterns but equally other rock mass types may be derived, being of benefit to the overall TRC.

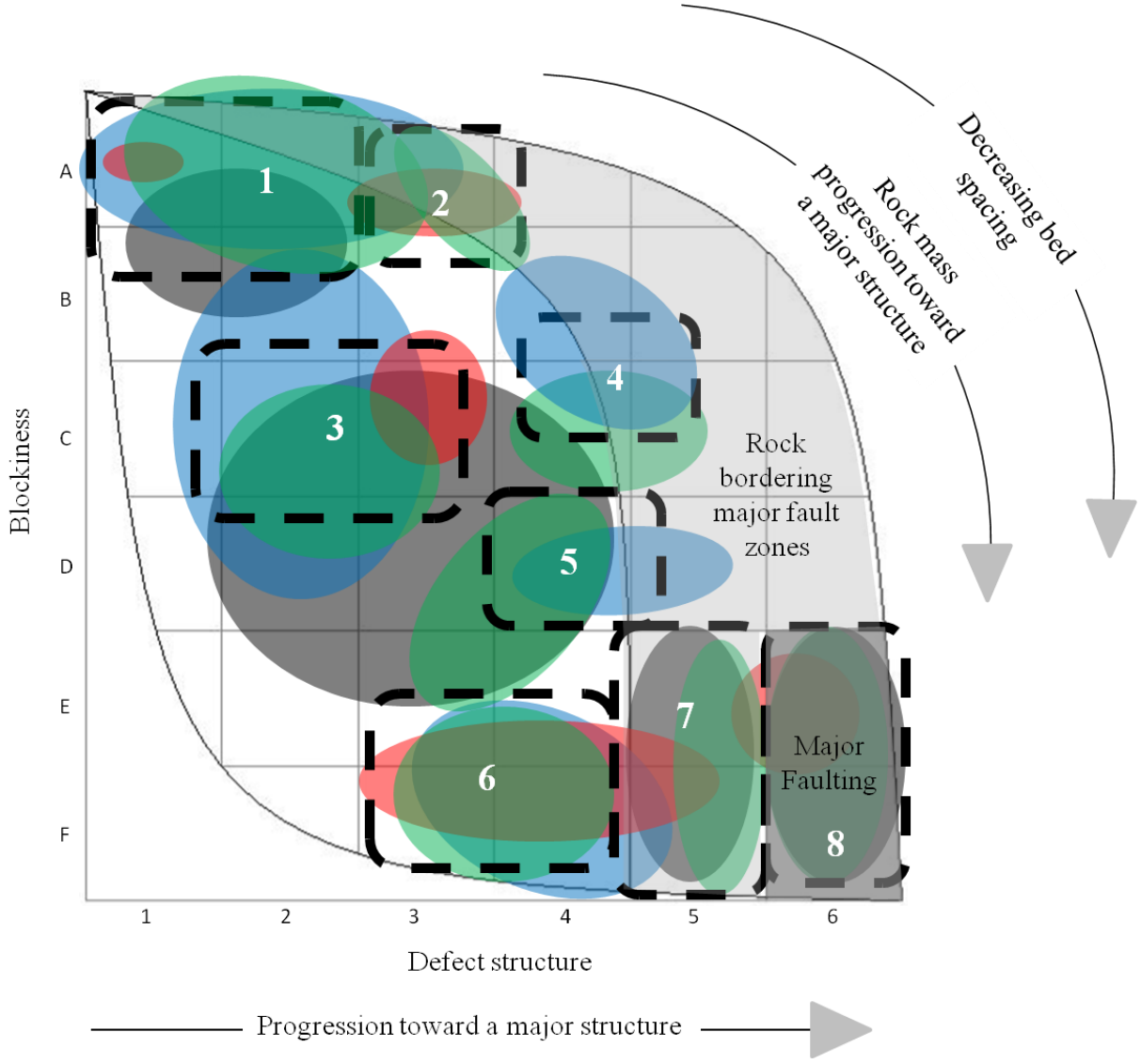

Figure 4.15: TRC plot of individual outcrop clusters.

To quantify defect structure character, subsequently allowing the TRC characterisation to be more user friendly and easier to domain rock mass type in the field, spacing terms presented in ISRM

(1978) have been used to describe defect spacing in rock mass types (Section 4.3.1). Eight rock mass types were differentiated (Table 4.3).

Table 4.3: Rock mass type characteristics.

Type	Bedding & Lithology	Sandstone Fracture	Defect structure (spacing based on ISRM (1978)
1	Thick to massive sandstone generally associated with thin, rarely thick, mudstone	Slight to moderate	Persistent, moderate (rarely close) to very wide spaced joints with rare faults and shears
2	Thick to massive sandstone generally associated with thin, rarely thick, mudstone	Slight to moderate	Moderate to very wide spaced, common persistent jointing with wide to extremely wide faults/shears commonly in equal portions
3	Medium to massive sandstone associated with dominantly thin, often very thin or medium, rarely thick, mudstone	High	Dominant, persistent joints, moderate (rarely close) to very widely spaced with shears and faults, very to extremely wide spacing, sometimes in equal portions
4	Medium to massive sandstone associated with dominantly thin, often very thin or medium, rarely thick, mudstone	High	Dominant, wide to extremely wide shears and faults, with persistent jointing (sometimes rare) moderate to very wide in spacing
5	Thin sandstone associated with dominantly thin, commonly very thin mudstone	Moderate to high	Dominant, wide to extremely wide shears and faults, with infrequent persistent jointing moderate to very wide in spacing
6	Very thin to massive sandstone & mudstone	Fragmented	Persistent, (rarely close) moderate to very widely spaced jointing with very wide to extremely wide shears/faults in equal & shear/fault favouring portion
7	Very thin to massive sandstone & mudstone	Fragmented	Shears and faults, moderate to widely spaced, with rare occurrences of persistent jointing
8	Very thin to massive sandstone & mudstone	Fragmented	Brecciated rock with very close to widely spaced sheared and crush zones typical of major fault zones

4.5.1 Type 1

Type 1 is the best possible rock mass within the Torlesse Composite Terrane observed across the study sites. The TRC defines the zone as a slight to moderately fractured, thickly bedded to massive sandstone outcrop. Controlling the rock mass is the presence of persistent, moderately to very widely spaced jointing (Figure 4.16). Non-persistent, discrete jointing is present within this type as observed in Figure 4.16, however, it has limited influence on outcrop character. Faults and shears are rare.

4.5.2 Type 2

Type 2 represents the same sandstone bedding thickness and fracture density as Type 1, but contains increased occurrence of outcrop scale faulting and shearing within the better quality rock mass (Figure 4.17). Systematic jointing, largely related to bedding thickness of blockiness class A, controls the rock mass (Figure 4.17). The rock mass type is also predominantly located within the zone defined by increasing proximity to major fault zones, incorporating the increase in outcrop scale shears and

faulting observed directly at both the Elliott and Opuha Dam Fault sites. Outcrops that plot as Type 2 may indicate a need for further investigation into potential faults and shears of significant scale.

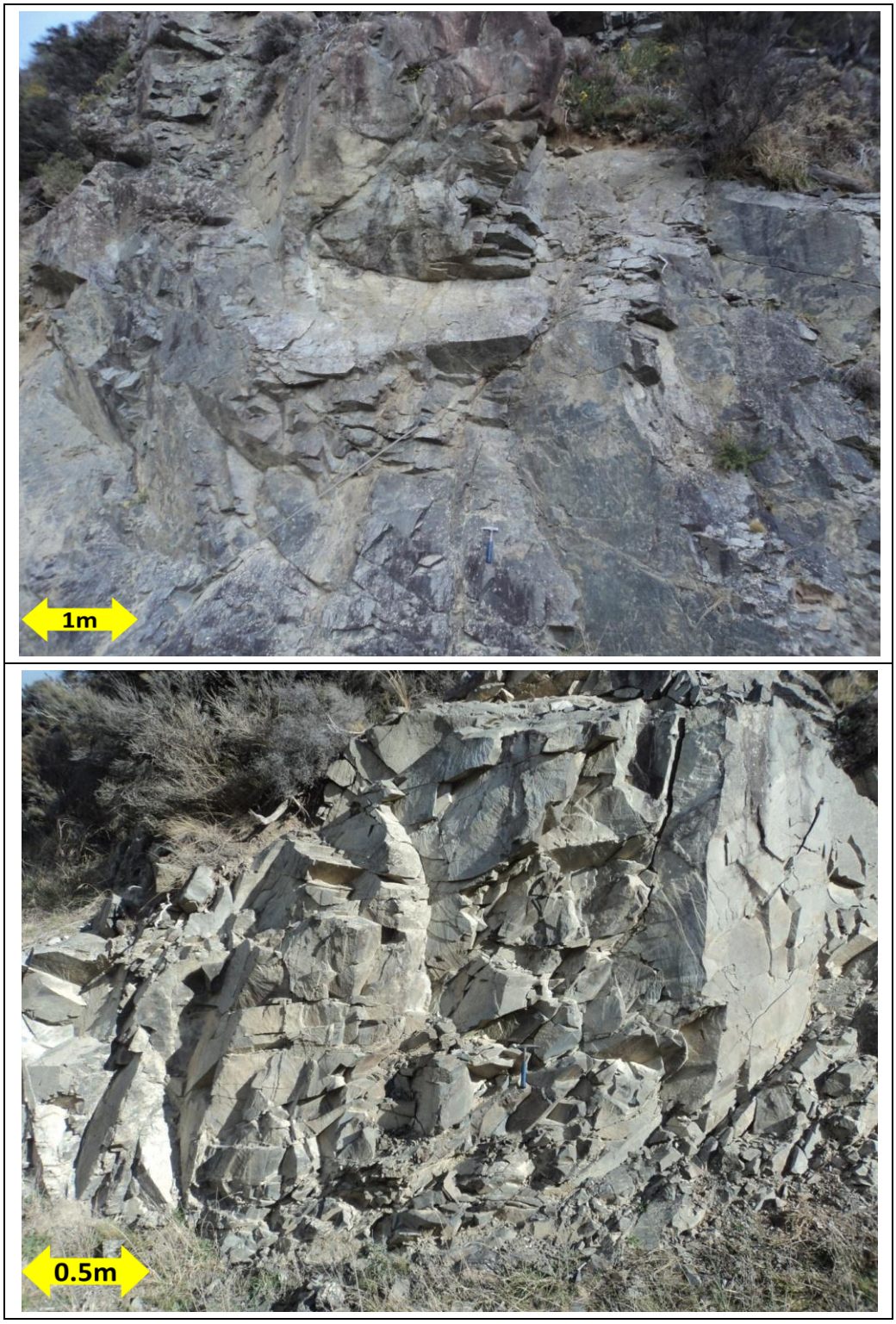

Figure 4.16: Best joint controlled rock masses typical of the range in conditions from (top) Hurunui outcrop 7a, through to (bottom) Hurunui outcrop 3b.

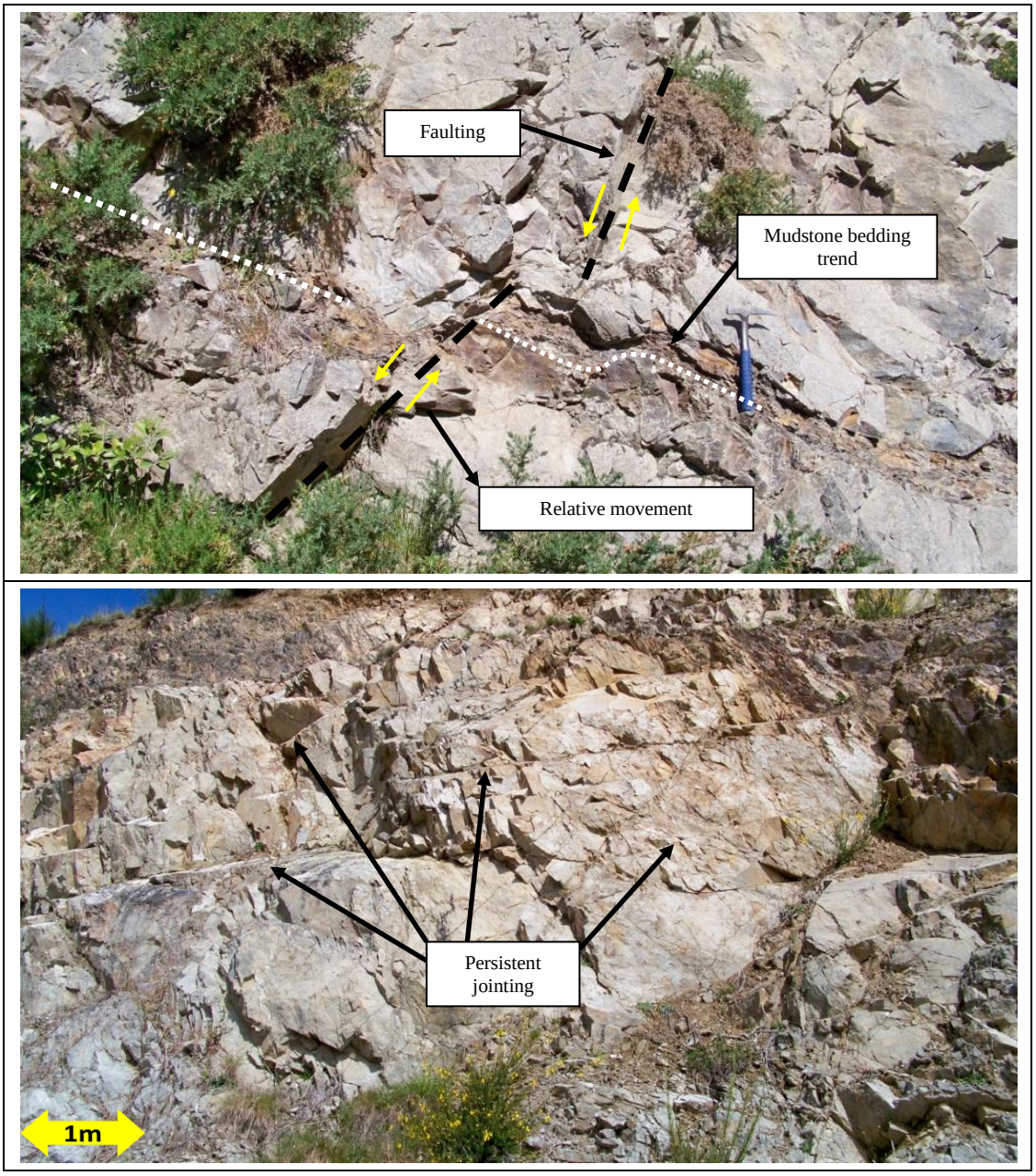

Figure 4.17: Rock masses typical of Type 2. Top: Ashley outcrop 6a. Note the occurrence of mudstone offsetting faults typical of Type 2; bottom: Opuha outcrop 1e, jointing indicated.

4.5.3 Type 3

Type 3 represents a large spread in point clustering. Generally bedding thickness is medium to massive. The rock mass is highly fractured. Generally, dominant jointing defined by defect structure classes 2 and 3 controls the rock mass (Figure 4.18). The occurrence of faulting and shearing increases toward defect structure class 3 where jointing, faulting and shearing occur in relatively equal proportions. The presence of short, discrete jointing is more common in Type 3 than in better rock mass types (Figure 4.18).

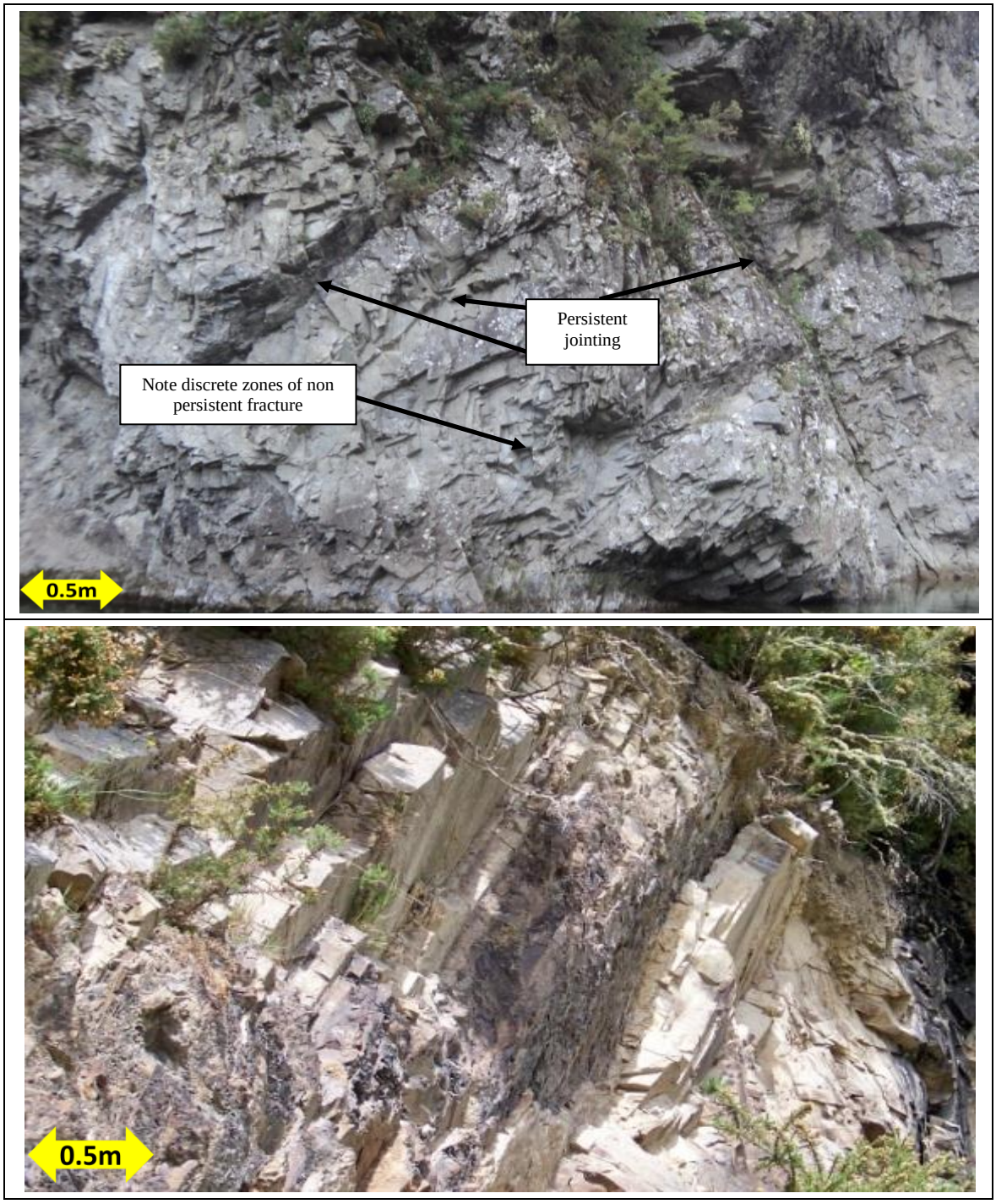

Figure 4.18: Typical rock masses of Type 3: top: Ashley outcrop 43a. Note the existence of discrete, non persistent fracturing around persistent jointing indicated; bottom: Ashley outcrop 21a. Note existence of medium bedding thickness in relatively good highly fractured rock mass.

4.5.4 Type 4

Type 4 rock mass was the least commonly observed type in this study. It is defined by medium to massive bedding with high fracturing, similar to Type 3 (Figure 4.19). What differentiates Type 4 is the occurrence of dominant, wide to extremely wide shears and faults (Figure 4.19A) occurring readily with persistent jointing (sometimes rare) at moderate to very wide in spacing. The rock mass type lies within the zone defined by increasing proximity to major structures, however, observation

from the Hurunui River suggests outcrops plotting in this block may not be necessarily due to nearby faulting. The rock mass has a rubbley appearance and mudstone is commonly dragged into faults and shears (Figure 4.19B - C) causing lineated mudstone infill.

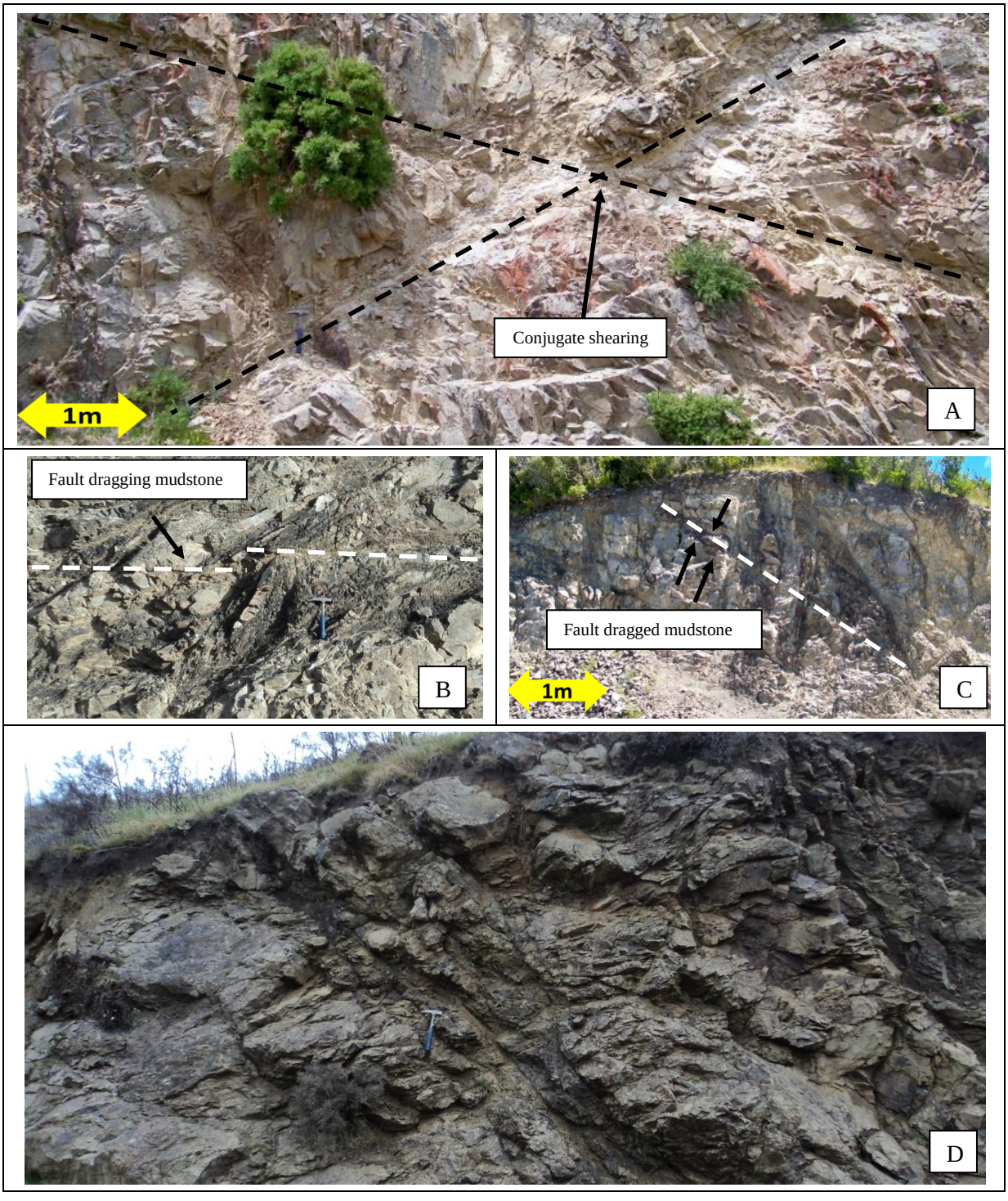

Figure 4.19: Rock masses typical of Type 4. A: Ashley outcrop 7b, conjugate shears; B: Hurunui outcrop 2a, mudstone infilled fault, distorting medium bedding; C: Ashley outcrop 15a, fault dragged mudstone; D: rubbley, faulted rock mass of Hurunui outcrop 23d.

4.5.5 Type 5

Type 5 represents the best rock mass of the thinly bedded blockiness classes. Whilst the mudstone is fragmented, incipient fracturing remains tight and is accompanied by moderate to highly fractured thin sandstone (Figure 4.20). Faulting and shearing tend to be dominant over persistent jointing. Due to the nature of the thinly bedded material, however, only limited amounts of persistent jointing are observed. This persistent jointing does not appear to have great influence on the rock mass. Discrete fracturing, characterised by moderate to high fracturing, interconnects bedding defects, thereby is likely to be controlling the rock mass.

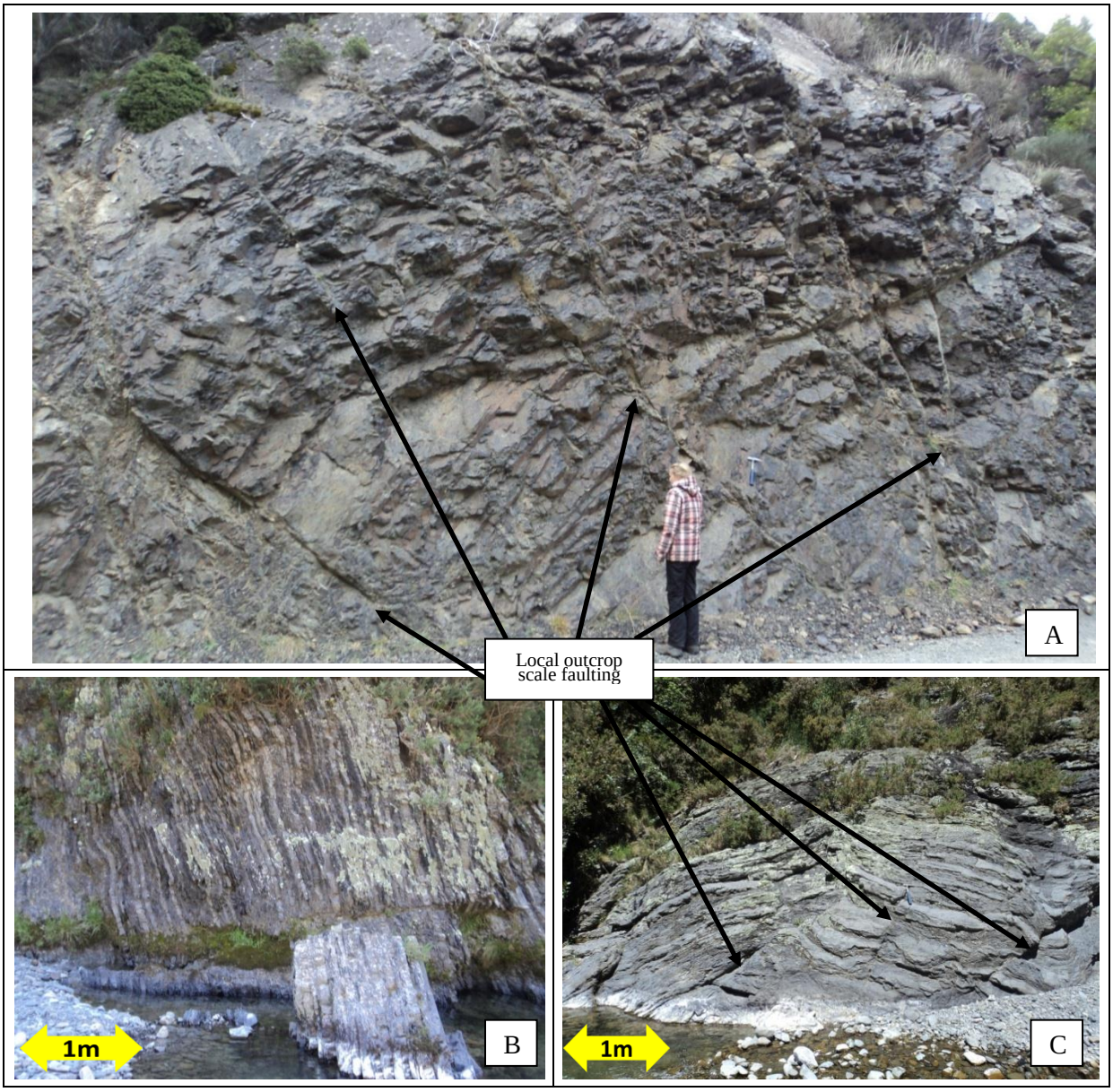

Figure 4.20: Moderate to highly fractured thin interbedding typical of rock mass Type 5. A: Hurunui outcrop 13a; B: Ashley outcrop 34a; C: Ashley outcrop 29a.

4.5.6 Type 6

Type 6 represents fragmented very thin to massive sandstone and mudstone. Persistent, (rarely close), moderate to very widely spaced jointing commonly occurs with very wide to extremely widely spaced shears and faults. Generally both persistent joints and shears/faults occur in relatively equal proportion. The fragmented nature of the material, however, controls the rock mass rather than persistent jointing. The nature of the fracturing is discrete, non-persistent jointing that creates an interlocked rock mass (Figure 4.21A & B). Boudinage is also common in this type (Figure 4.21C).

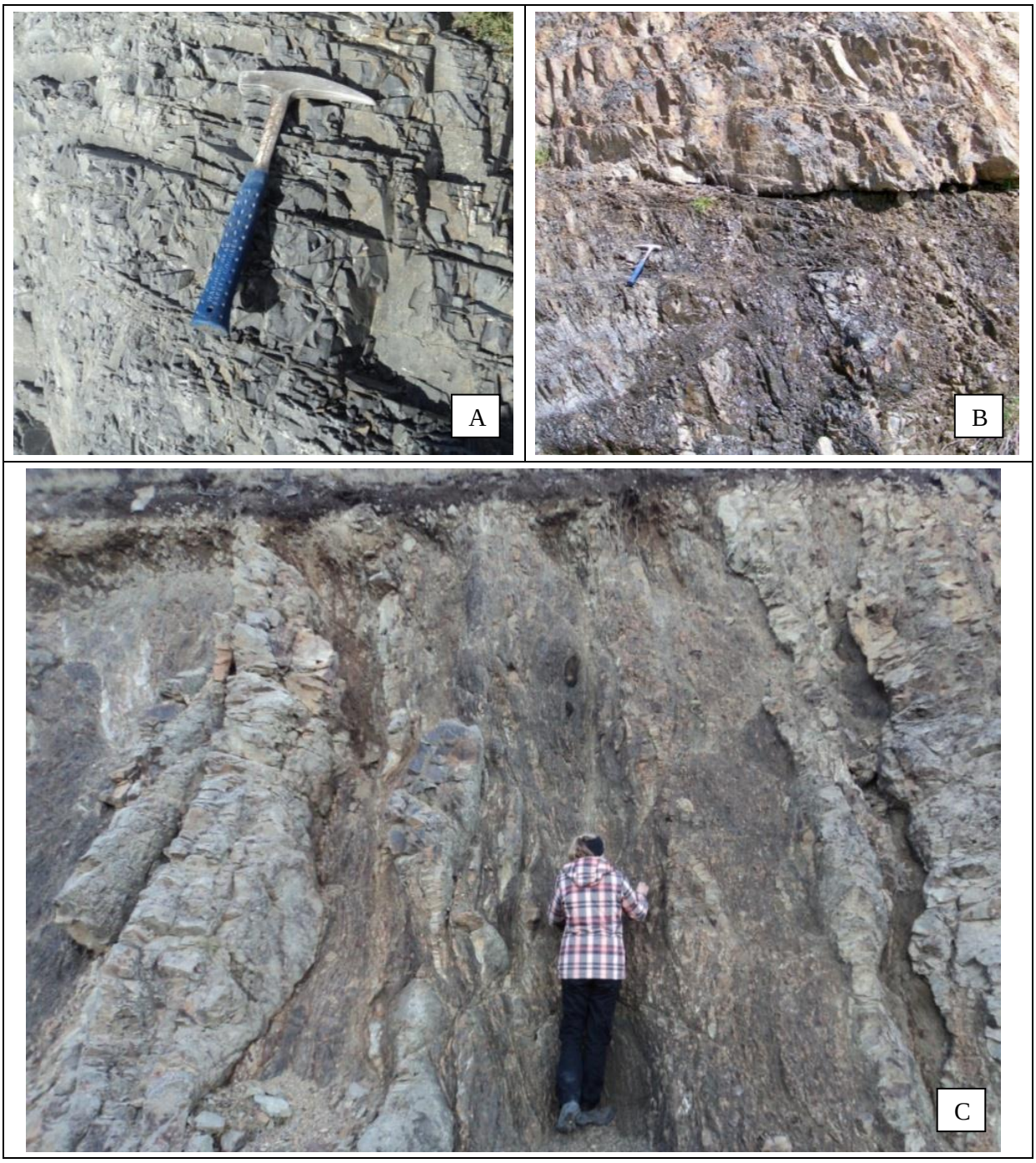

Figure 4.21: Fragmented rock masses typical of Type 6. A: Hurunui outcrop 21a; B: Opuha outcrop 1f. Note the occurrence of mudstone-sandstone discontinuity defining a fault; C: Hurunui outcrop 21a.

4.5.7 Type 7

The occurrence of any jointing greater than two metres in length is rare in Type 7. The rock mass is described as fragmented and is commonly folded and faulted (Figure 4.22), making up the bulk of thinly interbedded material within the study. As previously discussed, faulting and shearing observed on varying scales tends to concentrate within the thin bedding (Figure 4.22). More often than not Type 7 rock masses are related to major structures, identified by GNS, lineation analysis and field mapping, and plot within the "rock bordering major fault zones" area. Fragmented rock masses directly bordering major fault zones are defined by outcrop plotting close to rock mass Type 8 on the TRC and are displayed in Figure 4.22 (C & D). Directly related to faulting, these outcrops are heavily fragmented, indurated masses with numerous small scale faults and shears.

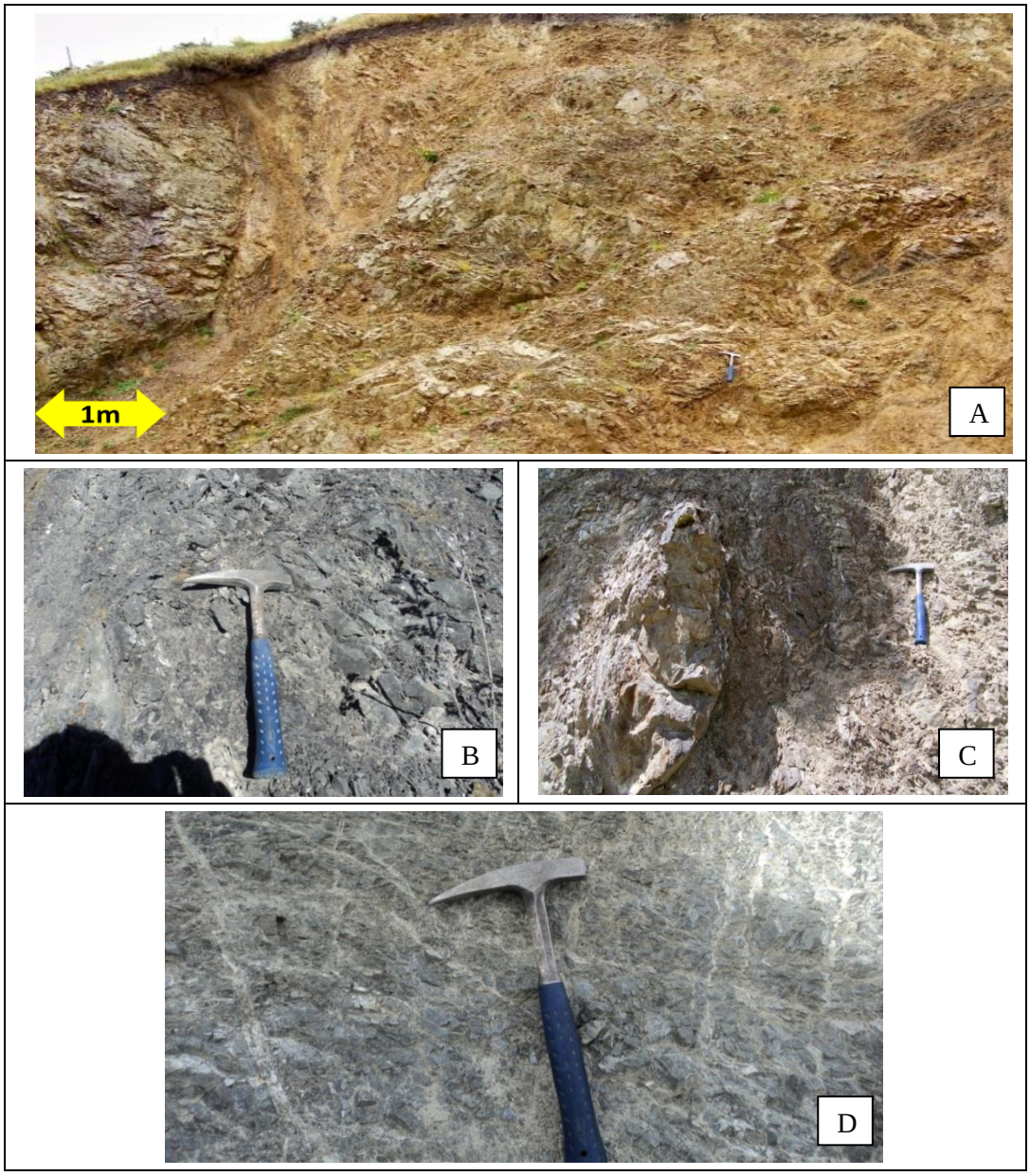

Figure 4.22: Fragmented, heavily sheared rock masses typical of Type 7. A: Ashley outcrop 27b; B: Elliott outcrop 9a; C: Ashley outcrop 8a; D: Ashley outcrop 1a.

4.5.8 Type 8

This rock mass type is the worst encountered throughout the study (Figure 4.23). Bedding defects are barely recognisable, but where so, represents the range in bedding thickness of both sandstone and mudstone. Incipient fracturing, rarely exceeding a few centimetres in length, controls the rock mass character. Localised shear zones within the mass are typically very close to widely spaced. More intact blocks of typically fragmented rock are observed within the fault rock zone. Geotechnically the main fault zone is likely to behave as a soil. Different types of fault rock have been observed to make up the zone and include a <20 cm firm fault (mudstone) gouge, softer gravel sized material able to be ground up by hand into a sandy silt and a more intact fragmented rock where clasts can be broken by hand.

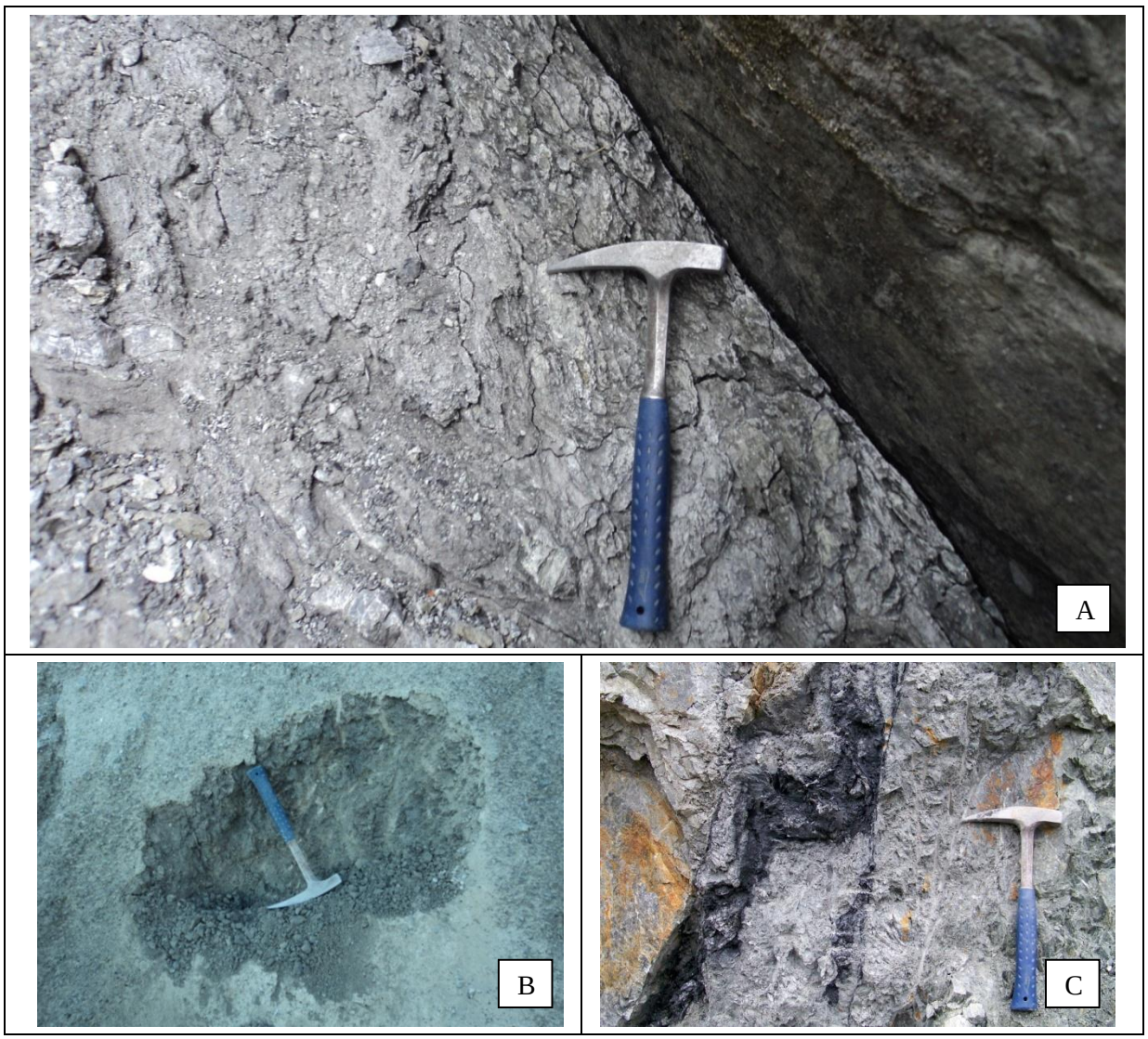

Figure 4.23: Fault related gouge and breccia material typical of rock mass Type 8. A: Ashley outcrop 45a; B: Elliott outcrop 1c; C: Opuha outcrop 5b.

4.6 Rock mass condition discussion

4.6.1 Lithology and bedding

Typical lithology proportions for different rock mass types are presented in Table 4.4. Ranges are given assuming maximum and minimum bedding thickness according to rock mass type description. This was undertaken on the assumption any tunnel alignment will likely be bored perpendicular to bedding, as per the nature of Torlesse steep bedding dips. The maximum percentage given will however change as a function of tunnel and bedding orientation. Typical percentage of lithologies is also presented as observed in this study. Due to the range in bedding thickness in the poorer rock mass types, typical percentage portions are variable.

Table 4.4: Lithology proportions across rock mass types.

Rock mass Type	Fine to medium sandstone portion		Mudstone portion	
	% range	Typical %	% range	Typical %
1	75-100	95	0-25	5
2	75-100	95	0-25	5
3	50-100	90	0-50	<10
4	50-100	90	0-50	<10
5	30-70	50	30-70	50
6	30-100	Variable	0-70	Variable
7	30-100	Variable	0-70	Variable
8	30-100	Variable	0-70	Variable

Interbedded fine and fine to medium grained sandstone is present throughout rock mass Type 5. It is therefore likely mudstone portion will occur less than 50% of the time at select localities. Thicker mudstone beds occurring less than 15% of total mudstone are typically observed in the more thickly bedded sandstone. This will locally increase the mudstone proportion but due to the wide spatial extent of thick mudstone beds, ranges given will likely be retained. Sandstone is, therefore, dominant over mudstone within Canterbury's Torlesse Composite Terrane. This conclusion likely differs from other spatial localities including the 50% and dominant argillite occurrence reported by URS (2008) and Richards and Read (2007) in the Waitaki. This information is important and aids in assessing quantities of poorer mudstone rock mass that will likely require additional support needs.

4.6.2 Defect persistence and block size

Dominant jointing as part of rock mass Type 1, 2 and 3 replicate the Stewart (2007) findings that the best rock mass classes are blocky at best with irregular, smaller block sizes in areas of poorer quality rock. Throughout all rock mass types, non-persistent, discrete jointing less than 2 m in length occurs to different extents and always tends to have some impact on rock mass character. Cook (2001) found the nature of all jointing to be sub-systematic (ISRM, 1978) indicating high proportions of joints terminating against other defects. In this study the presence of persistent jointing in rock mass Types 1 and 2 leads to equal amounts of systematic and non-systematic jointing. In the more fragmented rock mass types jointing becomes more non-systematic.

The effect on this low persistence, high termination joint nature creates an interlocked rock mass which may lead to higher shear strength as described by Read and Richards (2007). This ranges across rock mass types respective of persistent jointing/degree of fracture defect termination. Rock mass Types 1-4 are expected to be interlocked, however more so in rock mass Types 3 and 4 as a function of low persistent fracture density. The lower density of fracture is the principal control which makes rock mass Type 1 and 2 a better rock mass however. For this reason interlock is considered to be more important in the higher fracture density rock mass types which will dominantly control rock mass strength. Poorer interlocking conditions are expected as rock mass types become fragmented in nature towards rock mass Type 8.

Degree of fracture has obvious implications on block size, which is an important parameter for TBM tunnelling and waste rock disposal. Table 4.5 presents average block size according to rock mass type based on average degree of fracture and observation in the field.

Table 4.5: Average intact block sizes across rock mass types.

Rock mass Type	Block size
1	Range from 300-400 mm in the best rock masses to 50 mm in poorer quality rock masses
2	Range from 300-400 mm in the best rock masses to 50 mm in poorer quality rock masses
3	Typical range from 30-70 mm with 100 mm blocks common in the best rock mass
4	Typical range from 30-70 mm with 100 mm blocks common in the best rock mass
5	Typical range from 30-70 mm with 100 mm blocks common in the best rock mass
6	Typically <20 mm with 40 mm – 50 mm blocks in better quality rock
7	Typically <20 mm with 40 mm – 50 mm blocks in better quality rock
8	Dominantly <20mm. Blocks of 50 mm can be observed within the fault matrix intact blocks

4.6.3 Defect condition

Defect condition is the most important aspect of the Torlesse rock mass that will inevitably control shear strength and any potential failure within the rock mass. Surface roughness and infill primarily control the initial shear strength within the rock mass. Waviness only becomes significant under stress and strain conditions at which shearing of the asperities occurs and the shear strength of the joint is subsequently controlled by waviness (Patton, 1966). For this reason further analysis was carried out to identify defect characteristics typical of each defect structure class (Appendix J). No significant rock mass trends were derived across defect conditions. As such it is important that data on defect condition is collected at each specific project site rather than relying on any published information as typical trends. Typical trends per defect structure class were derived however and are summarised in Table 4.6. General trends include:

- Bedding – degree of waviness increases in defect Class 4 and 5 rock where shearing is the major influence,
- Persistent joints – little change in condition between defect classes,
- Shears and faults – width of sheared zones and the degree of waviness both increase as the influence of shearing and crushing intensifies from Class 1 to 6.

Table 4.6: Typical condition of systematic defects (fresh rock).

Defect Type	Roughness (2^{nd} order asperities)	Infill	Waviness (1^{st} order asperities)	
			Inter-limb angle	Wavelength
Bedding	Undulating smooth or rough, some planar smooth	Clean	170-180° (gentle), some 150-170° (open); becoming 90-180° from Class 4 (close to gentle)	0.5-4m, usually ~2m
Joints	Undulating smooth or rough, some planar smooth or rough	Clean	170-180° (gentle), some 150-170° (open)	0.2-3m, usually ~2m
Shears	Sheared zone contacts undulating smooth or rough	Class 2-3: fragmented rock ~10-100mm wide Class 4: fragmented rock in a silty/sandy matrix up to 300mm wide Class 5-6: clay/silt/sand up to 2m wide	Class 2: 170-180° (gentle) Class 3 & 4: 150-180° (open to gentle) Class 5 & 6: 90-180° (close to gentle)	0.5-12m, usually ~3m

The infill width of shear and fault zones generally exceed surface roughness amplitude resulting in lower defect shear strengths. Infill less than 3 mm is assumed to have potential for roughness asperities to be in contact resisting shear stress. Defects with infill of 3 mm or greater are therefore assumed to have lower shear strength. Of the approximate 75% fault and shear surfaces infilled, approximately 95% are infilled with material in excess of 3 mm. It is therefore likely infill material will control initial shear strength. Bedding and jointing have relatively clean defects indicating shear

stress will be controlled by surface roughness. Bedding and jointing roughness has relatively favourable undulating rough surfaces however a greater amount of planar surfaces indicate a poor pattern of surface conditions throughout the Torlesse.

4.6.4 Intact strength

Intact rock strength between rock mass types does not represent any significant trend. Thinly interbedded and fine grained sandstone, for example, commonly has comparable results to thickly bedded, fine to medium grained sandstone. Due to the nature of the classification system, a range of different bedding thickness, fracture density and defect nature are encountered. Providing intact strength values defined by UCS, BTS and PLT for each class or type is not sensible. However trends and strength values presented throughout Chapter 3 can allow preliminary prediction in association with other published studies on Torlesse intact rock strength. Strength variation is primarily due to weathering indicating intact strength is not a factor helping identify changes in rock mass character.

Chapter 5 Comparisons with other classifications and application to tunnelling

5.1 Torlesse rock mass classification

5.1.1 Project classification

The goal of the TRC is to provide a method of describing and classifying the range of rock mass conditions in the Torlesse Composite Terrane for mechanised tunnelling. To enable TRC analysis, it is envisioned mapping at any new project area will be concerned with identifying and describing outcrop characteristics. This information can then be plotted onto the TRC and project specific rock mass types identified. On this basis geological controls discussed throughout this chapter can be assessed and predictions made on distribution of rock mass types across an area or tunnel alignment. Hence mapping is not directly concerned with rock mass type, but rather blockiness and defect structure classes for TRC plotting. As noted, observation and recording of other factors including project specific defect condition for example needs to be carried out in association for shear strength estimates. Ultimately then, rock mass type mapping across an area can be carried after TRC rock mass type identification.

As mentioned, each mappable rock mass type has a series of geological controls and likely defect conditions, discussed throughout this chapter. Rock mass types can then be predicted in areas, for example, with low outcrop coverage prior to more invasive forms of investigation such as boreholes. This enables preliminary assessment of tunnelling performance and targeted site investigation planning.

All areas mapped throughout this study were subdivided up into a series of rock mass zones relating to outcrops with correlatable rock mass types. Outcrops plotting within each defined rock mass type on the TRC were overlaid on top of the study site. Manual grouping and mapping of locations was undertaken to define different rock mass zones (Appendix K). An example is given in Figure 5.1 from the Opuha Dam rock mass type mapping. Due to the complex nature of the rock mass and at practical mapping scales, no one zone will be solely concerned with one rock mass type. Whilst it can be done at smaller mapping scales (i.e. Elliott Fault and Opuha Dam sites) it is more practical at this scale to characterise zones based on dominant and minor rock mass types. The trend and orientation of different rock mass zones have been related to faulting, lineation, terrane and bedding defined rock mass controls.

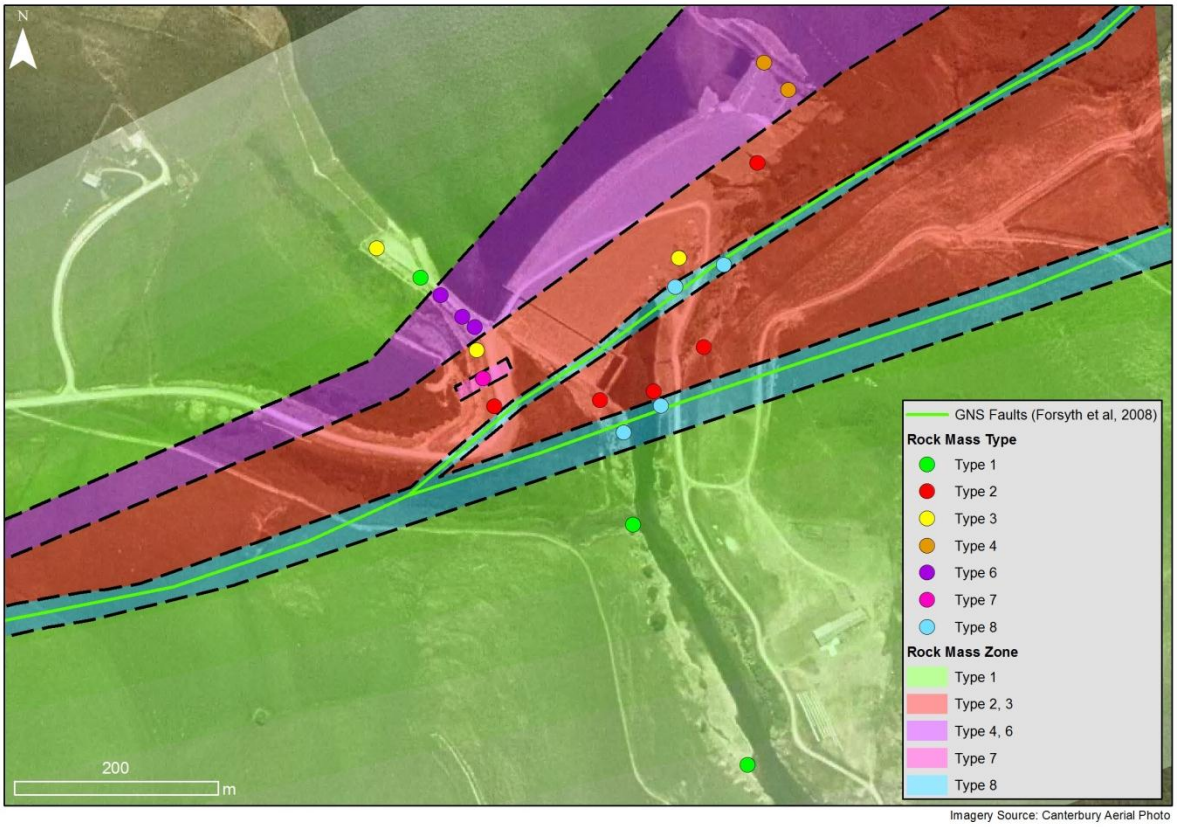

Figure 5.1: Opuha Dam rock mass type mapping example reproduced from Appendix J.4. Imagery from Canterbury Aerial Photo.

5.1.2 Comparison with the Read et al. (2000) classification

The TRC conceptual classification differs from other classifications including the Read et al. (2000) system. Both classifications are set up with a different end purpose. The main use of the Read et al. (2000) classification is to portray general conditions that are expected to be universal throughout the Torlesse. The main aim of the TRC scheme is not solely concerned with portraying typical rock masses but rather presents means of setting up a system to allow each project to identify their own rock mass types. As demonstrated through individual site analysis, rock mass types vary substantially between localities respective of regional change in lithostructure and tectonic setting. For this reason the large variability in Torlesse had to be captured to a higher degree (Section 4.2.4.1) than examined in Read et al. (2000) five class system. Similarly mapping needed to include other rock mass controlling attributes not assessed through their classification, specifically, bedding thickness and proportion of fault to joint occurrence derived through this study.

The rock mass classes defined by Read et al. (2000) can be compared to rock mass types derived in this study to enable parallels to be drawn between this newly developed scheme and the existing scheme (Table 5.1). To accomplish this, the Read et al. (2000) defect descriptions and values have been correlated to the degree of fracture in the TRC blockiness classes. It must be noted the Read et al. (2000) defect spacings are given per joint set and any one section analysed for degree of fracture

estimation may have multiple joint set breaks occurring within it. This has been taken into account when comparing the two schemes. Some correlation exists between schemes which appear to be sensible. For example, Read et al. (2000) states class II, which is correlated to TRC Type 3, is the dominant type of Torlesse greywacke encountered. Similarly the bulk type of Torlesse encountered in this research was rock mass Type 3.

Table 5.1: Comparison between Read et al. (2000) rock mass classes and rock mass types derived through this study.

TRC rock mass type for four study areas	Read et al. (2000) classification class
Type 1	Class I
Type 2	Class I – Class II
Type 3	Class II
Type 4	Class II – Class III
Type 5	Class IV
Type 6	Class IV – V
Type 7	Class V
Type 8	Class V

5.2 Controls on rock mass condition

Using rock mass types derived in Chapter 4, rock mass controls can be examined in association with desktop study information, lineation analysis and field observation. Effectively understanding what controls each rock mass in specific outcrops allows prediction of rock mass conditions in other areas. Specifically, any potential tunnel alignment can be sub-divided into the rock mass types derived from project or site-specific investigations (similar to Appendix K). This allows preliminary assessment of tunnelling conditions per type and allows selection of optimal tunnel alignment and comment on tunnelling implications such as support measures, equipment specification, advance rates, and groundwater inflow.

5.2.1 Lithostructure

The dominant Torlesse rock mass control is lithostructure, specifically the effect of lithology on bedding thickness and fracturing by non-systematic jointing. Medium to massive bedding as part of rock mass Types 1 and 2 tends to result in the best rock mass conditions. In the relatively sandstone-rich rock mass, systematic jointing tends to dominate with less shearing, faulting and a lower occurrence of short, discrete, non-systematic jointing, although there is always some degree of fracturing present. The thinly bedded Torlesse represented by rock mass Type 5, conversely, tends to lack dominant persistent (>2 m) jointing. This type, being mudstone dominant, fractures more easily. Faulting, folding and shearing tend to concentrate in the member further influencing character by non-

systematic short, discrete jointing. Based on field observation and general rock strength testing, the more thinly bedded member tends to incur the poorest rock mass. The effect of bedding lithology, bedding spacing, fracture density and defect structure combines to form the lithostructural control on rock mass condition.

5.2.1.1 Mudstone occurrence

The bulk occurrence of mudstone bedding is within the thinly bedded units (rock mass Types 5-7). Throughout the study higher proportions of mudstone equate to poorer rock mass conditions. Mudstone at all sites examined in this study is fragmented. Broken Formation (after Rattenbury et al. (2006)) is often found in literature to be observed within the Hurunui River Esk Head Belt terrane. The mudstone within the Esk Head Belt is sheared to a higher degree than at other sites and, as a result, tends to be lineated parallel with bedding to a higher degree. This phenomenon is also observed at other sites examined in this study and all mudstone observed has been sheared to a certain extent. This is partly represented by its characterisation as fragmented.

Being the weaker of the Torlesse lithologies, the mudstone across all rock mass types has appeared to localise and accommodate stress within the rock mass and is therefore typically highly strained. Numerous stress fields have been present over the complex tectonic history of the Torlesse. It is likely the rock mass has accommodated stress by deforming the weaker mudstone bedding. As reported by Rattenbury et al. (2006) the mudstone has undergone layer parallel extension. The primary stress direction when perpendicular to bedding has effectively compressed the mudstone bedding. Deformation concentrates within the mudstone as a direct result of differing stiffness properties. This has fragmented the rock mass and resulted in the pinching and swelling of mudstone bedding forming boudinage where the more incompetent mudstone has undergone plastic flow (Ramberg, 1955). This is observed throughout this study, however, at significant levels only within medium to very thinly bedded members.

5.2.1.2 Bedding deformation

Where stress is unable to be accommodated by bed deformation it is likely movement has occurred along bedding defects causing slip and subsequent development of bed parallel mudstone cleavage. The effect is jointing in both lithologies, described in this study as incipient fracturing, forming sub-parallel with bedding in more thickly bedded sandstone units, as described by Cook (2001). This model explains the lack of large scale boudinage and heavy evidential shearing of mudstone layers between thicker, stronger sandstone units, particularly evident in the Esk Head Belt Broken Formation. Furthermore, due to the complex formation history of the Esk Head Belt, it is likely layer parallel shearing and boudinage may be more abundant in this terrane than elsewhere.

The concentration of stress within the thinly interbedded units and subsequent mudstone fragmentation has caused the thinly interbedded sandstone units (rock mass Types 5-7) to fracture to

higher degrees than thicker sandstone units (rock mass Types 1-4). Whilst mudstone rock mass proportion is the dominant controlling factor in thin interbedding, it has caused discrete non-persistent jointing, described in this study as fracture, to also concentrate within the thin sandstone units. Due to the concentration of stress and subsequent concentration of faulting and shearing within the thinly interbedded units, the rock mass is highly fractured to fragmented. The effect of this is a rock mass which is controlled by discrete, low persistent jointing.

Cook (2001) describes the dominant joint orientation sub-parallel to bedding throughout the Torlesse, only observed here in the thicker bedded units. The absence of sub-parallel jointing in thinly bedded units is likely related to stress parallel to bedding being accommodated by bedding shear rather than the need to form a sub-parallel joint set.

Where rock mass stress and strain is accommodated by both mudstone and thin interbedded layers (Types 5-7), more thickly bedded rock masses in close spatial proximity are likely to be in better condition (Types 1-4). This is observed within the Ashley River Gorge LAGB structural zone. Significant volumes of thinly interbedded outcrops were observed in the LAGB. Generally the area has less tectonic influence through large scale faulting. The thinly bedded units are heavily deformed, faulted and folded, while the thicker bedded units within the same structural block are in more favourable condition. It is likely the thinly interbedded unit has historically preferentially accommodated the stress fields throughout the regions evolution. As a result the thicker bedded member has been less stressed and is observed to be in better condition. This could explain the lack of large scale faulting observed and the slightly better rock mass condition in the LAGB.

5.2.1.3 Intact strength

Despite clear differences in observational rock mass strengths, no significant change was found in intact strength between rock mass types excluding Type 8. Due to the heavy fracture density of the thinly bedded units, strength testing was largely restricted to point load testing. Of the thinly bedded samples, a very high proportion tended to fail along existing defects. The thinly bedded member tended to have overall lower strengths when failing along existing defects compared to the thicker units. However, clean intact strength failures were very similar for different bedding thicknesses. The thicker bedded units were stronger overall but only by an average of 0.4 MPa $I_{s(50)}$ across all sites. Variation may be due to differing levels of surface weathering between the more fractured thinly bedded members and the more thickly bedded members.

5.2.1.4 Weathering effect

The thinly bedded Torlesse (rock mass Types 5-7) represents a more weathered rock mass at road exposures. This is likely related to the highly fractured to fragmented degree of fracture, large amounts of hairline incipient fracturing and stress relaxation along defects toward the free face increasing surface volume available for weathering. This is further supported by the thinly bedded

rock on the Ashley River bed appearing in more favourable intact condition. In this location rock is actively cleaned by fluvial process not allowing prolonged weathering. The level of faulting is still high in comparison to the thicker bedded members and the rock is still described as highly fractured to fragmented. Implications of this suggest the thinly bedded rock mass at depth, similar to the thinly bedded units observed in the Ashley River bed will initially be coherent and relatively intact and may not necessarily be physically weathered.

5.2.1.5 Anisotropy

The rock mass is in better intact condition where mudstone is absent from thin interbedding (rock mass Type 5). This is directly observed at the Elliott Fault and Ashley River Gorge. Generally alternations through gradational bedding occur between fine and fine to medium grained sandstone. As a result no defined bedding parting (defect) is present. The lack of defined, well developed bedding planes likely allows the rock mass to behave more as a homogenous mass accounting for a more favourable rock mass condition. This differs in comparison to other cases of thin interbedding where both mudstone and definitive bedding planes are present.

This is further supported in rock exhibiting apparent anisotropy in the form of gradational banding and cross bedding by the lack of difference in I_{s50} results loaded parallel and perpendicular to anisotropy. Intact strength values averaged 4.9 I_{s50} (MPa) for homogenous rock compared to 5.96 I_{s50} (MPa) for samples loaded parallel and 4.84 I_{s50} (MPa) for samples loaded perpendicular to anisotropy. Due to the lack of bedding parting (defect) of anisotropy (bedding, foliation, etc.), no one fabric acts as a plane of weakness when subjected to loading. It must be noted, however, anisotropy observed in this study was rare due to the scale of observation and only restricted to depositional banded fabric from gradational sediment changes. The lack of strength difference between loadings at different fabric orientations suggests gradational banding is not true anisotropy. Cook (2001) suggests that anisotropy has direct implications on intact strength. Cook (2001) goes on to state samples where minor foliation planes are present, an anisotropy ratio of 2.9 (perpendicular $I_{s(50)}$ to parallel $I_{s(50)}$) was derived, showing that they lead to a significant reduction of intact rock strength.

5.2.2 Fault proximity

Fault proximity has a significant effect on rock mass condition at varying scales. The effect of a closer proximity to a major fault on rock mass structure is evident within both Elliott Fault and Opuha Dam study site TRC diagrams. Closer proximity generally encompasses a movement from better rock mass types toward types where localised shearing is the dominant defect type. The size of tectonic structure can also impact on different volumes of rock. The Elliott Fault zone, for example, directly affects about 200 m width of rock whereas the Opuha Dam Fault only directly affects about 4 m width.

5.2.2.1 Large scale fault fracturing and localised outcrop shearing

Analysis of fragmented, more thickly bedded units not observed at other outcrops revealed close proximity to faults and lineations in the Ashley River Gorge (Figure 5.2). This has significant implications in predicting rock mass zones with increasing proximity to faults (outcrops 24-27) and crush zones (outcrops 45a, 8a etc). Typically localised shearing and faulting is prevalent as a result.

Localised outcrop shearing is also observed at the Opuha Dam and Elliott Fault sites. In conjunction, abundant landscape lineation at the Elliott Fault site defines a zone of diffused deformation around major fault zones. Due to the heavy jointing and fracture of the Torlesse, stress within a typical rock mass can be accommodated by movement along many planes. Therefore no one plane may accommodate all rock mass stress. Increasing fines content toward the Elliott Fault and potential lineament structures could validate this conclusion and point to subsequent zones of increased shearing. It is therefore important to identify lineations and increases in outcrop shearing giving rise to rock mass Types 2, 4 and 7 as an indication of increasing structure proximity.

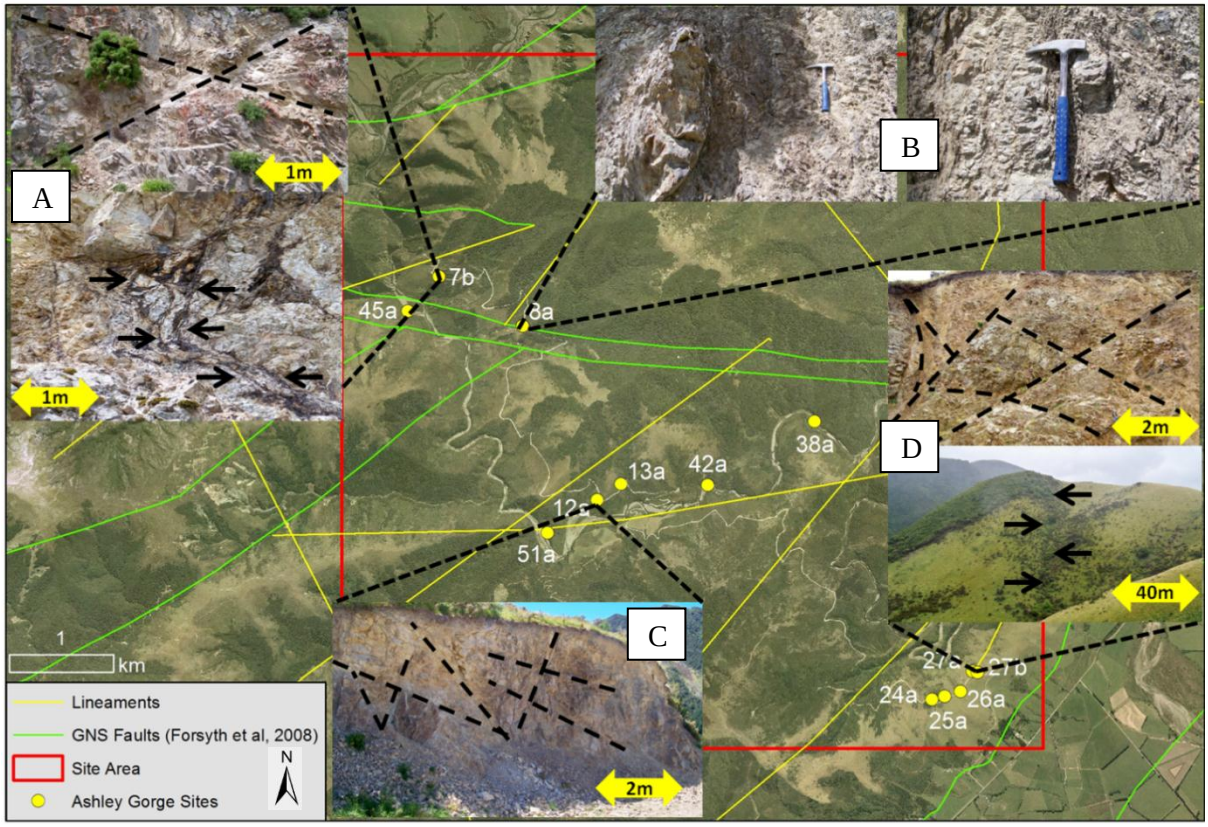

Figure 5.2: Ashley River Gorge lineament analysis with outcrops representing various lineament and fault related outcrop structures defined through dashed black lines and arrows. A: outcrop 7b; B: outcrop 8a; C: outcrop 12a; D: outcrop 27b and observed field lineation (see arrows). Imagery from Canterbury Aerial Photo.

5.2.2.2 Veining

Veining is present throughout all sites but is more abundant at the Opuha Dam site in response to block faulting (Stewart, 2007). Coupled with this is the presence of Montmorillonite within Opuha

Dam defect infill, only observed once outside the study site. Montmorillonite commonly forms as a volcanic weathering or hydrothermal alteration product. This suggests the circulation of fluids at some stage in the evolution of the site geology. It is unclear if fluid circulating and subsequent alteration is a direct result of faulting or if external influences have caused circulation along the permeable pathway created by faulting. It is however plausible frictional heating caused by fault movement has heated water in the system causing it to circulate through pre-existing and newly developed fault fractures. The heated water is likely to dissolve pre-existing veins and precipitate the minerals in the colder country rock upon cooling. This creates what we see as a cluster of veining concentrated around major structures. Based on the relative strength and description of veining, it is likely the occurrence of veining is detrimental to the overall rock mass.

5.2.2.3 Intact strength

Intact rock mass strength was significantly lower at the Elliott Fault site despite differing rock mass types. It is unclear if the difference in intact strength is a direct result of fault influence or due to Elliott Fault rock located within the Pahau terrane which is generally accepted as the less indurated terrane type (Rattenbury et al., 2006). This has direct consequences for the validation of regional rock mass controls and has direct TBM excavation implications.

5.2.2.4 Improving rock

Thin interbedding in the presence of large structures had more favourable, highly fractured to fragmented condition (rock mass Type 5). This was observed at the Hurunui (outcrop 13a, lineation), Elliott Fault (outcrop 1 variants and 3a) and to a lesser extent throughout the Ashley River Gorge site. Similarly the mudstone appeared in more intact, fragmented condition to mudstone observed elsewhere. It is likely regional and rock mass stress fields have been accommodated by the main zone of faulting. As a result the weaker, thin interbedding has resisted significant deformation through folding and fracturing. Outcrop scale faulting still tends to concentrate with the rock mass where a higher occurrence is observed in comparison with more thickly bedded members in similar tectonic settings. It must be noted thinly interbedded units directly bordering large scale structures (i.e. Ashley River structures) are heavily deformed with small scale faulting tending to dominant.

A gradation of improving rock mass types generally occurs away from the main zone of faulting irrespective of bedding thickness. It should be assumed more deformation exists on the hanging wall both observed in this study and in Ward (2000) study on Torlesse damage zones at the Hope Fault. In the case of the Elliott Fault it is likely the pop-up block previously discussed from Eusden et al. (2011) has experienced a greater thrust displacement and as such has moved heavily in relation to the fault footwall. The result is a more fragmented rock on the hanging wall side which extends for greater distances.

5.2.2.5 Fault structure variation

The difference in fault structure should also be quantified. The Elliott Fault for example is likely to have historically carried the bulk of the MFS slip in combination with the Clarence Fault prior the transition of strike-slip displacement southward. In conjunction, the compressional stress fields the Elliott Fault has experienced likely contribute to the large lateral extent of deformation. Rock mass character is expected to differ in scale to the PPAFZ splays located within the Ashley River Gorge for example. The PPAFZ is considered the latest addition to the southward progression of strike slip movements across the plate boundary. It is therefore less mature and accordingly its associated rock mass should have better conditions as a result. The North Canterbury Block of Wallace et al. (2007), termed a thrust wedge, previously made up a constricted plate boundary (Pettinga et al., 2001). It is likely to have experienced a similar tectonic environment to the Elliott Fault and thus some similarities in rock mass structure likely occur.

5.2.2.6 Ward (2000) fault rock comparison

Observation and division of fault rock by Ward (2000) were very similar to observations made at the Elliott Fault throughout rock mass Type 7 and 8. Both the gouge and main fault zone rock observed in this study correspond to the fault plane and fault gouge distinction by Ward (2000) which reside within the hanging wall in both studies. Due to the small size of Ashley Gorge and the Opuha Dam faults, it is expected a thicker, more significant zone of direct fault gouge may be present along larger structures i.e. the Elliott Fault, however this is not directly observed. This is primarily due to the greater slip rates and more mature evolution of the larger fault zones releasing a greater amount of energy and subsequently pulverising, shearing and breaking up greater volumes of rock. More intact rock outside this zone i.e. Elliott Fault outcrop 10e, is similar to Ward (2000) two rock mass zones within the Hope Fault footwall. The better rock mass conditions observed in the footwall outside of this zone were not however observed by Ward (2000). Ward (2000) also describes highly shattered bedding within the hanging wall which was only observed away from the main Elliott trace. The use of Ward (2000) can provide more detailed descriptions of rock masses encountered in rock mass Types 7 and 8.

5.2.3 Terrane type

Differences between Torlesse terrane types were derived throughout this research. This is largely due to the difference in composition and complex tectonic history. The Rakaia terrane is older and as a result has experienced longer periods of tectonic deformation and metamorphism resulting in increased induration and outcrop deformation. Excluding the Ashley River Gorge whose intact rock strength is a direct result of metamorphic facies, the Rakaia terrane sandstone averaged 6.0 I_{s50} (MPa) in comparison to the Pahau averaging 5.3 I_{s50} (MPa). Therefore variation in tunnelling condition is likely to exist between terranes and must also be factored when applying the TRC.

One major difference between terrane types was found to be composition defined through thin section point counting. Pahau terrane had a higher lithic occurrence in comparison to the Rakaia terrane. Mackinnon (1983) discusses compositional differences in source rock. The Rakaia terrane is indicative of a volcanic/plutonic arc system where high levels of feldspar are sourced. The Pahau terrane conversely has higher lithic occurrence with less quartz and feldspar where increased lithic fragments have been sourced from exhumed Rakaia terrane. This has a direct influence on abrasivity and likely has an effect on intact strength. Rock sourced from the Rakaia terrane was found to be on the low end of extremely abrasive (Käsling et al., 2007) with an average CAI value of 4. CAI for the Esk Head Belt was found to be 3.77 and 3.56 for the Pahau terrane, classified as very abrasive according to (Käsling et al., 2007). Literature suggests higher abrasivity indexes are related to quartz content (West, 1989, Yaralı et al., 2008), rock strength (Al-Ameen and Waller, 1994) and grain size (Yaralı et al., 2008). Due to the relatively similar grain size, differences in abrasivity are likely due to quartz content and rock strength which has significant implications on TBM cutter wear and advance rates.

Due to the complex tectonic history of the Torlesse different levels of tectonic deformation are recognised between terranes. The Rakaia terrane has undergone and experienced greater uplift and stress regimes than the younger Pahau terrane whose source was partly Rakaia. Therefore the Rakaia terrane is expected to be deformed to a higher level. However due to the lack of observation of Pahau terrane away from major faulting, no definitive conclusions can be derived as to difference in overall deformation as a result of this study. The small segment of Pahau terrane examined at the Hurunui River however was in good condition and represented a well defined change in rock mass condition from the more sheared Esk Head Belt terrane into Pahau.

The Pahau terrane is however locally deformed to higher degrees. Modern day tectonics is more prevalent within the Pahau terrane than the Rakaia. The MFS, which is defined as part of the plate boundary, directly resides within the Pahau terrane. Outside the influence of modern day tectonics, the Pahau terrane is expected to remain in better condition.

The Esk Head belt was found to exhibit the best quality rock in this study. It was expected the Esk Head Belt formation would have resulted in a heavily deformed rock mass. This was true to an extent within the MNSZ which is defined as the more sheared rock mass gradating into the Pahau terrane. Within the HRB the best rock mass conditions were observed. It is unclear why these two distinct zones occur. It is possible stress fields have been accommodated within the more sheared MNSZ resulting in the better rock mass observed within the HRB. The more severe exhumation, collision and metamorphism may also play a part to increase induration within the HRB rock mass which has subsequently resulted in less deformation and higher intact strengths.

5.3 Applications to tunnelling

The use of the derived rock mass controls can aid in the division of an area or tunnel alignment into a series of rock mass types. The aim of this section is to build on this knowledge and comment on implications to tunnelling across the range of rock mass types derived from the TRC.

5.3.1 Rock mass versus structurally controlled failure

Due to the high fracture density of the Torlesse a number of rock mass failure mechanisms are possible. The different in-situ and induced stress states around the excavation will lead to a variety of failure mechanisms (Table 5.2), depending on the rock mass and defect condition. It is discussed by Stewart (2007) spacing and orientation determine the ability of the rock mass to deform or fail without fracturing of the intact rock. Therefore the volume, persistence and orientation of discontinuities, as defined throughout this study have important influences upon failure modes. These attributes will inevitably control failure mechanisms through kinematic failure along one or more singular planes or involve whole rock mass failure, i.e. combination of intact breakage and sliding along multiple defects (Stewart, 2007). Table 5.2 presents ground mass behavioural types (ASG, 2010) correlated to rock mass types. The table is intended to give an indication of potential failure mechanisms within each rock mass type.

Toward the better rock mass types (1-4) failure is likely to occur along singular planes, respective of defect surface condition, rather than whole rock mass failure as a result of fracture and lithostructure. The size of blocks will vary however (section 4.6.2), as a response to increasing fracture density and bedding thickness. Due to the density of fracturing, failure through intact rock is unlikely. Of primary concern is planar slide failure through behavioural Types 1-3 (Table 5.2). Due to the regional steep dip of the Torlesse, unfavourable defect orientations are likely irrespective of tunnel boring orientation. This becomes more of an issue toward the better rock mass types (1-4) were thick bedding is concerned. At larger bedding thicknesses the mudstone bounding sandstone beds are typically sheared, squashed and fragmented. The weaker mudstone bedding thus has the potential to act as slide boundaries. Paired with dominant jointing orientated sub-parallel to bedding (Cook, 2001) potential exists for release joints to be present at unfavourable orientations, respective of tunnel orientation.

As discussed by previous authors (Read and Richards, 2007, Stewart, 2007, Cook, 2001) the nature of non-persistent joints commonly create favourable interlocked rock masses (Type 1 & 4). It is stated “such rock masses are tightly interlocked giving higher resistance to compression or shear loads than more dilated masses” (Read and Richards, 2007). It is discussed by Singh et al. (2002), closely interlocked masses typical of rock mass Types 3 and 4 are likely to fail through splitting or shearing of intact rock at low defect dip angles (10-30°) and through rotation and sliding failure at higher defect dip angles (Figure 5.3). Due the relative high intact strengths examined both here and in the literature suggests the unlikelihood of significant failure through splitting and shearing at low joint

inclinations. It is likely however, small scale dislodgment of blocks from the tunnel roof due to high levels of fracture will occur irrespective of stress (behaviour Types 1-3, Table 5.2). It must be noted the variable orientation of defects will dictate failure were combinations of mechanisms may be present. The short persistence of defects further suggests limited excavation overbreak.

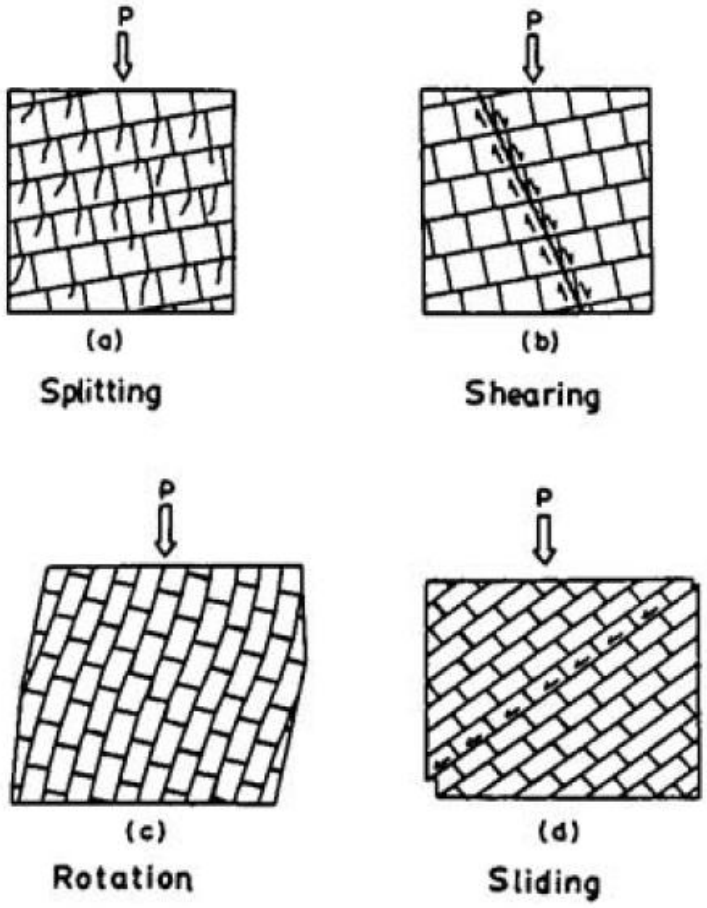

Figure 5.3: Modes of failure in regularly jointed rock masses (Singh et al., 2002).

Failure within defects Types 5-7 will likely occur through the release of small blocks between incipient, non-persistent fracturing and jointing. Due to the heavily fractured nature of the rock mass, no one plane will act to accommodate all movement. The increased occurrence of infilled persistent faulting and shearing may present stability issues around areas of more fragmented rock where ravelling failure is possible (Table 5.2). It is also likely these thin zones, if unlined, will preferentially erode forming negative relief which will have further failure implication. Due to fracture density, potential exists in rock mass Types 6-8 to experience voluminous stress induced failure and crown failure (Table 5.2) if adequate support is not installed. Dependant on rock mass Type 8 cohesion, the potential exists for running and swelling ground due to the complete incipient fractured nature.

Spalling prior to rock disintegration was directly observed during UCS testing for this study and was also described in Cook (2001). Due to the high intact strengths and high stiffness defined through

Young's modulus and Poisson's ratios, the intact rock under high stress may be prone to spalling along tunnel walls in rock mass Types 1-5 (Table 5.2).

Table 5.2: Ground mass behavioural types (modified from ASG (2010)).

Basic categories of Behaviour Types		Description of potential failure modes/mechanisms during excavation of the unsupported ground	Rock mass types with potential to experience the respective behaviour
1	Stable	Stable ground with the potential of small local gravity induced falling or sliding of blocks	1-4
2	Potential of discontinuity controlled block fall	Voluminous discontinuity controlled, gravity induced falling and sliding of blocks, occasional local shear failure on discontinuities	1-7
3	Shallow failure	Shallow stress induced failure in combination with discontinuity and gravity controlled failure	1-7
4	Voluminous stress induced failure	Stress induced failure involving large ground volumes and large deformation	6-8
5	Rock burst	Sudden and violent failure of the rock mass, caused by highly stressed brittle rocks and the rapid release of accumulated strain energy	1-5
6	Buckling	Buckling of rocks with a narrow spaced discontinuity set, frequently associated with shear failure	3-6
7	Crown failure	Voluminous overbreaks in the crown with progressive shear failure	6-7
8	Ravelling ground	Ravelling of dry or moist, intensely fractured, poorly interlocked rocks or soil with low cohesion	5-7
9	Flowing ground	Flow of intensely fractured, poorly interlocked rocks or soil with higher water content	8
10	Swelling ground	Time dependant volume increase of the ground caused by physical-chemical reaction of ground and water in combination with stress relief	8
11	Ground with frequently changing deformation characteristics	Combination of several behaviours with strong local variations of stresses and deformations over longer sections due to heterogeneous ground (i.e. in heterogeneous fault zones; block-in-matrix rock, tectonic melanges	1-8

5.3.2 Groundwater implications

No significant of groundwater seepage was observed through outcrop observation. This is likely due to observation of outcrops above the water table. Cook (2001) suggests increased permeability around faults and shears defined by increased seepage. This is likely based on raw observation of a more fractured rock mass and increased potential for permeability around major faulted zones directly observed in this study. In this study permeability is likely to be higher in fragmented rock mass Types 6 and 7 near fault zones. Rock mass Type 8 will likely be less permeable, with flow restricted to the fractured mass around the black gouge material described. This is likely to create compartmentalisation of different ground water levels between structures. It must be noted however the lack of any significant fines (i.e. clay) content in a variety of fault zone infill materials suggests some permeability may be possible. Therefore groundwater inflow within rock mass Type 8 should be anticipated.

Cook (2001) states the tight nature and surficial infilling of open joints prevents water from entering into the system. The tightness of jointing examined in this study suggests jointing at depth may be tight and as a result may limit seepage. It is expected, however, that seepage through all rock mass types will occur due to the interconnection and termination of defects against one another. All groundwater flow within the Torlesse rock mass is expected to be controlled by secondary permeability due to the low matrix porosity of the intact rock.

At depth larger groundwater head is expected to cause issues around major fault zones were significant pore pressure can develop. The significant head and development of pore pressures will decrease effective stress on defects. This will lead to decreased shear strength in areas of significant ground water flow.

5.4 Implications to TBM implementation

The aim of this section is to present general comment and basic reference towards TBM implementation and specification specifically related to Torlesse and the rock mass types derived in this study. The purpose of this section is not to provide a thorough review or assess detailed specification parameters but rather present lateral thinking towards these applications.

5.4.1 Excavatability

Due to the high degree of fracturing observed in this study, in general, penetration rates are likely to be favourable. Rock mass Types 1 and 2 represent the best rock mass overall but will have lower penetration rates due to low fracture density and high intact rock strength. The formation and propagation of radial cracks from the cutterhead will be important in the formation of chip fragments in intact blocks between joints and will be closely related to the tensile strength. Cutter wear will also be high due to the high abrasivity of the material. Large block sizes present in these rock mass types are expected to have the potential to damage cutterhead from face fallout leading to cutterhead seizure and fallout blocks can be dragged around the cutting face increasing excavation overbreak (Nelson, 1993) . Specific energy testings on intact rock, typically from the best rock mass types (1-4), showed little variance in results between sites and are likely to overestimate the excavation energy required to excavate rock by not taking defects and external rock mass controls into account.

Due to the degree of fracture and increase in local shearing, higher penetration rates are expected in rock mass Types 3-7. However, high penetration rates in these units may be offset by increasing support needs (Barton, 2000). Issues surrounding rock jams, cutter head seizure and gripper problems could also be significant in these rock mass types. Due to the high density of fracturing in rock mass Types 3-7, cutterhead excavation will tend to rip closely spaced fracture rather than directly fracture the intact rock. As a result cutterheads are expected to last longer and require fewer changes. It must be noted however abrasion remains the dominant parameter for cutter change. The ability of rock

mass Types 6 and 7 to provide sufficient resistance for grippers against the walls is questionable and needs further investigation before defining machine specification and support measures.

Within rock mass Types 5-7 higher portions of heavily fractured to fragmented mudstone and fine sandstone is expected to be less abrasive, benefiting cutter bearing life, cutterhead wear and general excavatability (NTH, 1994). Higher fragmented volumes of rock, typical of rock mass Types 5-7 tend to flow more easily past cutterheads, generating heat and allowing self sharpening of cutters (NTH, 1994).

Rock mass Type 8 is expected to pose the most significant challenge to tunnelling in the Torlesse rock mass. It is not unusual for a TBM to achieve three times the penetration rate in a softer rock compared to a hard rock using the same TBM (Fawcett, 1993). Support measures, rather than penetration rate, will dictate TBM advance rates through rock mass Type 8. Issues typically encountered in faulted rock include (after Barton (2000)):

- Muck jams in the muck bucket and along the conveyors
- Rock or soil loads on the shield causing thrust loss, steering problems and delayed access to areas needing reinforcement or support
- Erosion of fault debris, invert burial and flooding
- Chimney formation and block falls due to high water inflows and erosion in faulted rock
- Damage to linings caused by fault void collapse.

Water inflow represents another significant challenge in Torlesse rocks. The nature of fracturing and jointing suggest significant secondary permeability is possible. Interpretation suggests rock joints are expected to be tight under high stress conditions. Under low stress conditions permeability is expected to increase and significant groundwater issues are likely. High flow rate is detrimental to any TBM design. As such groundwater inflow rates need to be properly estimated for the design of mucking and slurry systems for example. Other issues are likely to exist with high groundwater inflow including exaggerated overbreak and chimney formations (Barton, 2000).

5.4.2 Machine design

Due to the complex nature of the Torlesse and the variability in rock mass condition, different machine designs will suit different rock mass types. It is therefore critical thorough mapping using the TRC to classify tunnel alignments is carried out. Results and lengths of different rock mass types will heavily influence which TBM will be best suited for rock mass conditions. In rock mass Types 1 & 2 gripper TBM's are probably best suited. They provide the highest advance rates and allow for support installation close to the working face (Barton, 2000). In rock mass Types 3-4 gripper TBM's may be appropriate, but require a finger shield to allow bolting and steel sets to be installed with support from the shield (Barton, 2000).

A shielded TBM is likely suited to rock mass Types 5-8. Adequate TBM thrust is unlikely to be generated by grippers against the fragmented tunnel walls so precast segment installation for support and thrust is advantageous. Significant groundwater inflow and potential for large erosion and kinematic failure exists. Support in wet, unstable rock masses is difficult (Nelson, 1993) and the support advantage from precast concrete segments may be the best option. The advantage of shield TBM's full face excavation may also provide additional support to the working face through the likes of slurry support which may be beneficial in rock mass Type 7 and 8 for example (Maidl et al., 2012).

Variability along anyone alignment is typical of Torlesse. It is therefore likely a section will encounter all conditions. If any one alignment length is dominated by rock mass Types 1 and 2 with lesser zones of rock mass Types 5-8, no more than 3-5 m long occurring as individual zones for example, a gripper TBM is likely to be best suited. Conversely however, if a section length is to be dominated by poorer rock mass conditions with extensive fault zones, a shielded TBM with the added advantage of precast concrete segment thrust generation will be best suited.

Despite overall machine design, probe drilling equipment at the front of the TBM to anticipate zones of poorer ground condition (rock mass Types 7 & 8) will likely be advantageous. Furthermore, optimum cutter spacing relating to joint and fracture occurrence along the alignment needs to be carefully selected (Maidl et al., 2008, Rostami and Ozdemir, 1993).

5.4.3 Support requirements

Support requirements from herein are presented respective of machine design and rock mass type expected.

5.4.3.1 Open gripper TBM

Systematic support is needed if gripper TBM's are employed. The better rock mass Types 1 & 2 are not expected to present major failure or stability concerns. Limited overbreak and wedges are the most likely types of instability and support measures are likely to be a combination of systematic rock bolting, mesh with the addition of shotcrete in areas of poorer quality. Mudstone bedding throughout all rock mass types will likely require a shotcrete cover or another form of final liner to prevent weathering and erosion. Furthermore tunnel alignment with respect to bedding orientation will dictate rock bolt orientation to minimise bedding-controlled planar sliding. In rock mass Types 3 & 4, increased support type and occurrence will be required to prevent shallow failure of blocks. Therefore more extensive support measures should be employed which may encompass more closely spaced rock bolts and thicker shotcrete in poor rock mass areas.

Due to bed spacing of rock mass Type 5 and heavy fracturing of rock mass Types 6-7 intensive support measures are likely needed. These zones may act as permeable pathways, necessitating ground pre-treatment prior to excavation, such as groundwater depressurisation, to dissipate pore

water pressures and increase effective rock mass strength. In some cases there may be a need to pre-treat rock through pre-injection of grouting to reduce leakage, increase deformation modulus and increase shear strength, resulting in a better rock mass (Barton, 2000). Full shotcrete coverage is likely needed to ensure stability in pair with an extensive rock bolt and steel set plan. It must be noted however these zones have to be relatively thin (up to 5 m) if gripper TBM's are employed due to inadequate gripper thrust and face support requirements unless significant ground pre-treatment is carried out. Therefore the width of extensive support requirements will not be great.

Intensive support measures including ground pre-treatment are likely needed if rock mass Type 8 is encountered along a gripper TBM drive. However case by case variants will dictate to what extent this is needed. Fault zone width for example needs to be constrained i.e. Elliott Fault vs. Opuha lateral deformation zones. Pre-investigation and probe drilling ahead of the working face should predict when boring comes within close proximity to faulting. The main issue is the relatively short stand up time likely to be experienced in fault rock under stress. If not adequately supported and pre-treated, the machine can become stuck or tunnel collapse can occur. In cases like this, which have potential to be derived in fault related Torlesse rock masses, the installation of steel arches with heavy lagging may be required (Barton, 2000). As discussed by Barton (2000) stabilisation of fault rock material similar to that of rock mass Type 8 can be achieved through 1) spiling, 2) pre-injection of cement or grout (discussed), 3) forepoling and 4) jet piling. Shotcrete is unlikely to be effective and rock bolts will not be able to generate the tension needed to work effectively in rock mass Type 8 conditions.

Dependant on the final liner of the tunnel it may be necessary to overbore fault zones to accommodate extra support/lining than better quality surrounding rock. In rock mass Types 6-8 full liner installation is expected regardless of tunnel purpose. Tunnel use will however dictate what type of final liner is to be implemented.

5.4.3.2 Shielded TBM

Where wide regions of poor rock mass types (5-8) are expected, shielded TBM's are best suited. The shield prevents progressive failure of fragmented rock and precast concrete segments provide tunnel support which eliminates the need for questionable thrust generation off poorer rock mass types. Groundwater inflow issues are also reduced with elimination of extensive support in areas of high groundwater inflow (i.e. rock mass Types 6-7). Extensive reinforcement of segments is likely needed under areas of high stress i.e. faulted rock at depth. It is expressed by Barton (2000) even a shielded TBM with concrete element ring building may be stopped by conditions exhibited by rock mass type 8. The fault rock observed in this study tended to be relatively cohesive in cliff stand up. Literature however suggests this same rock mass should be relatively non-cohesive in nature, defined by the degree of fracture. It is therefore likely pre-injecting of grout ahead of the working face will need to be employed to strengthen the fault rock (Barton, 2000). An effect of this is to prevent settlement

damage caused by reduced pore pressures upon excavation and drainage (Barton, 2000). Furthermore controlled drainage of the rock mass type should be employed. The dissipation of pore water pressure will subsequently strengthen the rock. Erosion of fault rock fines and subsequent failure of rotated blocks within the fault matrix will therefore be minimised.

5.4.4 Advance rates

Depending on individual rock mass types concerned through a tunnel alignment, advance rates will be restricted by excavatability or support measures. It must be noted, however, TBM machine specification will alter rates (Türtscher and Leitner, 2010). In rock mass Types 1 and 2 advance rates will likely be restricted and controlled by excavatability of the intact rock. Because of the need to propagate fracturing through extremely to very abrasive medium to fine grained sandstone, cutters will need to be replaced more often decreasing advance rates. Due to lower intact strength, increased fracture pattern and decreased abrasivity a significantly higher penetration rate is expected in the mudstone member. Despite the high penetration rate of the mudstone, advance rates remain relatively similar due to the increased need for extra support.

Penetration and advance rates are expected to be constrained by support measures rather than excavatability in rock mass Types 3 to 8. Sandstone still remains very abrasive so frequent cutter change is expected despite less radial crack propagation and high degrees of defect ripping. Towards the poorer rock mass types, increased levels of shearing and subsequent gouge infill will be favourable to penetration rates (Wanner and Aeberli, 1979), however detrimental to advance rates due to support needs. Average advance rates in rock mass Type 8 are likely to be severely impacted where there is a need for ground pre-treatment prior to excavation and slow penetration rate to allow additional support measures to be installed during excavation.

Anisotropy in the rock mass is expected to alter penetration rates. Bedding strike to tunnel drive orientation for example will heavily influence both advance and penetration rates. Tunnel drive perpendicular to bedding will encounter both lithotypes (dependant on relative proportion and depositional lithofacies) and will likely result in differing penetration and advance rates respective of lithology and rock mass type. Conversely a tunnel drive parallel with bedding will result in differing lengths of lithology and rock mass types encountered. If tunnel drive is parallel to a thicker mudstone bed for example high penetration rates are expected with significantly lower advance rates based on extensive support needs. Penetration rates along a thicker sandstone bed conversely are anticipated to be less, but advance rates will likely be comparable due to the less significant need for extensive support measures despite slower excavation. Penetration and advance rates are also likely to vary at depth. It is reported in the literature tight jointing at depth proved not to change penetration rates in comparison to more intact rock (Wanner and Aeberli, 1979).

5.5 TRC forms for future mapping

A blank TRC can be found in Appendix L.1 for mapping in Torlesse. Furthermore Appendix L.2 contains overlays of each rock mass type derived from this study over the blank classification. This allows comparison between project derived rock mass types and rock mass types derived from this study.

Chapter 6 Summary and conclusions

6.1 Thesis merit and objectives

Torlesse Composite Terrane is a dominant rock unit in the geology of New Zealand, particularly in Canterbury, and as such is encountered in many engineering projects. Despite widespread distribution there is relatively little description in the literature on the engineering geology of the Torlesse, especially for the assessment of mechanised tunnelling. Past work by Read et al. (2000), Richards and Read (2007), Read and Richards (2007), Cook (2001) and Stewart (2007) typically address New Zealand greywacke rock mass characterisation and classification, where strength and structure have been examined mainly for input into existing failure criteria. To extend this knowledge to the application of tunnelling, this study undertook to characterise the range of engineering geological conditions in the Torlesse exposed in Canterbury to help assess the geological controls on tunnel selection, specification and design.

This study set out to 1) define the range of engineering geological conditions across the Torlesse, 2) develop a classification whereby rock mass condition can be assessed, 3) use this to define rock mass classes indicative of Torlesse and 4) to use this to comment on Torlesse tunnelling implication. An outcome of the study includes a framework for the classification of Torlesse rock mass conditions. This classification is based on trends analysed from mapping data collected from four geologically distinct sites across a range of terrane types and regional structural locations in Canterbury: the Elliott Fault, Hurunui River, Ashley River Gorge and Opuha Dam. It differs from existing classifications such as Read et al. (2000) where lithostructure, specifically the lithological control on bedding spacing and density of short, discrete non-systemic jointing, is emphasised together with the occurrence of systematic defects.

6.2 Methodology

Prior to field mapping a desktop study was carried out in association with a landscape lineation study to develop 1) a conceptual geological model at select sites and 2) field mapping sheets to provide a check list to ensure consistency of information collected between outcrops and sites. Information recorded on the mapping sheets during field mapping included weathering, intact strength, defect type and orientation, bedding fabric, defect roughness, spacing, persistence, aperture, infill type, strength, thickness and moisture according to NZGS (2005). Bedding thickness, degree of fracturing, defect waviness (ILA – inter-limb angle and wavelength), defect end condition and termination parameters were collected according to PSM (2010a) and (2010b). Outcrop lithology was observed including colour, lithology and grain size. Sampling for lab testing was carried out on selected outcrops to obtain a representation of intact rock characteristics and spatial extent across the entire study site.

6.3 Rock mass site results

Sites chosen across the study defined different rock masses. As a direct result of faulting the rock mass at the Elliott Fault and Opuha Dam ranged in condition. At both sites a main zone of crushing was observed. Immediately outside of this zone conditions improved steadily on different scales. Deformation was concentrated within the hanging wall with favourable rock masses observed generally dependant on fault size at varying scales away from the main fault zone. An increase in localised shearing and mineral veining was observed in rock adjacent to the principle slip zone.

Two distinct structural zones were defined through lineation and conceptual model development in both of the larger field areas, the Ashley River Gorge and Hurunui River. The Hurunui River had two distinct structural zones defined by a more favourable HRB and a more sheared, fractured MNSZ. Rock mass character and strength differ between them. The Ashley River Gorge contains two structural blocks with slight variation in rock mass character, the LHB and the LAGB.

Thin interbedding across all structural zones was found to be highly fractured, faulted and folded, tending to concentrate deformation. In comparison, thicker sandstone beds tended to present less fracture and higher levels of persistent jointing. As the level of deformation increased in the more thickly bedded units, localised faulting increased and the occurrence of persistent systematic jointing decreased.

Sandstone is typically associated with the best rock mass conditions across this study. The mudstone, conversely, tended to always be fragmented and deformed. Rock mass strength varied across field sites as the result of external rock mass influence. Infilling of defects was dominantly restricted to faults and shears. Minimal clay contents were derived for fine infill material, dominantly described as silt fraction, despite displaying some geotechnical characteristics of clay due to heavy pulverisation.

6.4 Torlesse rock mass classification (TRC)

Field data were plotted to identify trends in the rock mass. It was found that bedding thickness, degree of fracture and the occurrence of persistent jointing vs. faults and shears were rock mass controlling trends. Trends were analysed and common characteristics grouped together to form a series of rock mass classes, which, when combined, form a conceptual classification diagram. Plotting of individual outcrops from each study site on the classification enabled clusters to be identified indicative of different types of Torlesse rock mass condition.

Rock mass condition was divided into two categories: blockiness and defect structure (Table 6.1). Blockiness describes the general shape and size of blocks defined by bed thickness and fracture density. In nearly all cases thicker bedding was associated with a better quality rock mass. Where bed thickness decreased, the fracture density generally increased. Bedding distribution is closely related to

lithology whereby bed thickness decreased as the proportion of mudstone relative to sandstone increased. As such lithostructure appears to be a major control on rock mass condition in the Torlesse.

Defect structure describes the occurrence of systematic jointing and localised shears through to regional scale faulting. The rock mass with the best condition typically had little to no associated faulting and is controlled by relatively persistent (>2m long) jointing. As the level of shearing and faulting increased, the occurrence of persistent, systematic jointing appeared to decrease. A higher occurrence of shearing and faulting was typically related to rock mass lithologies with a larger proportion of mudstone to sandstone, that is, in more closely bedded rock masses.

Categories describing both blockiness and defect structure were formulated such that rock mass conditions deteriorate from Class A to F and 1 through 6, respectively. Categories were plotted against each other to form a conceptual model termed the Torlesse rock mass classification (TRC) as shown in Figure 6.1. The overlay of individual site clusters identified 8 rock mass Types indicative of the Torlesse Composite Terrane. A zone termed 'rock bordering major fault zones' was overlaid as an indicator of increasing proximity toward a major structure. While a vast majority of outcrops plotting in this region are related to large scale faulting, the trend does not hold true in all circumstances and as such should only be used as an indicator.

Table 6.1: Blockiness and defect structure classes.

Blockiness		
Class	Lithostructure	**Fracture Density**
A	Massive to thickly bedded sandstone	Slightly to moderately fractured
B	Medium bedded sandstone	Moderately to highly fractured
C	Massive to very thickly bedded sandstone	Highly fractured
D	Thinly bedded sandstone	Moderately to highly fractured
E	Massive to medium bedded sandstone	Fragmented
F	Thinly to very thinly bedded sandstone and mudstone	Fragmented
Defect Structure		
Class	Dominant Structure	Secondary Components
1	Persistent joints, moderate (rarely close) to very wide spacing	Shears and faults are rare
2	Persistent joints, moderate (rarely close) to very wide spacing	Shears and faults, very to extremely wide spacing
3	Persistent joints (moderate to very wide spacing, rarely close) and shears/faults (very to extremely wide spacing) in approximately equal portions	
4	Shears and faults, wide to extremely wide spacing	Persistent joints, moderate to very wide spacing
5	Shears and faults, moderate to wide spacing	Persistent joints are rare
6	Brecciated rock with very close to widely spaced sheared and crushed zones typical of major fault zones	

Rock mass Type 1 and 2 present the best rock mass conditions. The rock mass is generally thick to massive in bed spacing with slight to moderate fracture. High persistent jointing (greater than 2 m) controls the rock mass character. Rock mass conditions deteriorate through rock mass Types 3 and 4

where fracture density and the presence of faulting and shearing increase. Increased levels of faulting and shearing paired with decreasing bed spacing define poorer rock mass Types 5-7. The rock mass is heavily fractured to fragmented in fracture density and the presence of persistent jointing becomes rare. Rock mass type 8 defines major fault affected rock which is fragmented in nature with no principle defects recognisable.

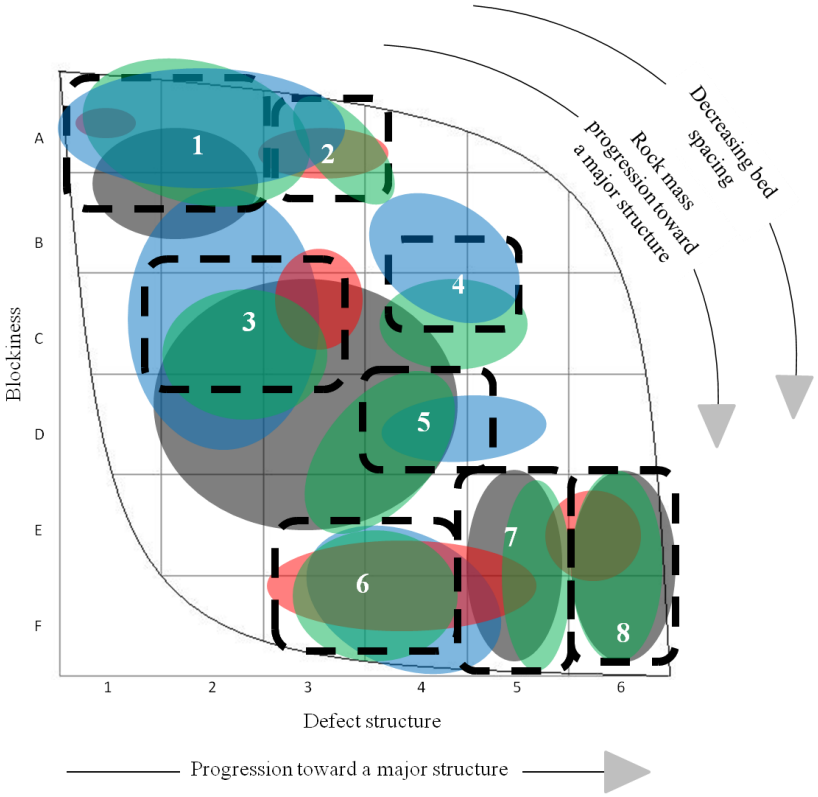

Figure 6.1: TRC classification with study site clustering and division of typical Torlesse rock mass types.

6.5 Rock mass control

Understanding geological controls can aid in the prediction of rock mass conditions. A dominant control in the Torlesse identified in this study is lithostructure, specifically the effect of lithology on bedding thickness and fracturing by non-systematic jointing. The distribution of mudstone bands is a major control on bedding thickness. Mudstone, being the weaker of the lithotypes, appears to localise and accommodate stress within the rock mass and is therefore typically highly strained. The result is fracturing to the point of fragmentation of mudstone beds and localised shearing of the contacts with the stiffer sandstone interbeds.

Medium to massive bedding as part of rock mass Types 1 and 2, result in the best rock mass conditions. In the relatively sandstone rich rock mass, systematic jointing tends to dominate with less shearing and faulting and a lower occurrence of short, discrete, non-systematic jointing, although there is always some degree of fracturing present. Conversely, the thinly bedded Torlesse represented by rock mass Type 5 lacks persistent jointing. This type, being mudstone dominant, fractures more

easily, is therefore characterised by short, discrete jointing and tends to localise faulting, shearing and some folding.

Modern tectonic stress fields are also a major control. This is shown in the TRC by the number of outcrops plotting within rock mass Types 7 and 8. The size of tectonic structure can impact on different volumes of rock. The Elliott Fault zone, for example, directly affects around 200 m width of rock whereas the Opuha Dam Fault only directly affects an approximate 4 m width. Rock outside the direct fault zone can also be impacted giving rise to Type 6 conditions. For example, increased levels of shearing are observed in adjacent rock masses at both the Elliott and Opuha Dam Faults. Proximity to major faulting has a large influence on fracture density and is related to differences in stress fields throughout the complex tectonic history of the Torlesse.

Other, less significant, rock mass controls were observed throughout this study. Differences between terrane type including deformation, strength and abrasivity were attributed to differences in composition and tectonic history. The older Rakaia terrane is more deformed, slightly stronger and has higher quartz and feldspar percentages than the lithic-rich Pahau terrane relating to material source during deposition. Differences in levels of metamorphism also gave rise to metamorphic rock mass control. The Ashley River Gorge was located within a zone of lower grade zeolite facies metamorphism in comparison to other sites where low grade prehnite-pumpellyitc facies metamorphism resulted in mineral alteration and increased induration. The result was intact strength values significantly lower in the Ashley River Gorge than other sites. Rock mass Types 3 and 4, which cannot be assigned specific rock mass controls, represent a transition from the best to worst rock mass conditions. Both lithostructure and major faulting may have an influence without a definitive control being obvious.

6.6 TBM implications

Due to the need for extensive support measures and questionable thrust generation in the poorer rock mass types, a shielded TBM is likely to be best suited for the range of Torlesse greywacke rock masses. Thrust will be generated from the precast concrete segmental lining, which will also provide rock mass support. It must be noted however, individual sites are likely to vary and use of the TRC should be utilised to best predict rock masses for TBM specification. The decision between a gripper TBM and a shielded TBM will depend on the proportion of the tunnel expected to be in rock mass Types 5-8, and the length of each occurrence of the poorest rock mass Types (7-8).

TBM excavation across the Torlesse Composite Terrane is expected to be reasonably favourable, however, large variation according to rock mass type is expected. Rock mass Types 1 and 2 are expected to be most stable but the hardest to excavate. High sandstone proportion, abrasivity, intact strength and dominance of widely-spaced jointing are expected to result in low penetration rates.

Support measures, penetration and advance rates are influenced by TBM specification. In better rock mass types where gripper TBM's are likely to be best suited, localised gravity-induced failure dictates relatively simple rock bolt, mesh and shotcrete support. The level of support needed increases in the more fractured rock mass Types 3 and 4 where penetration rates are likely to be higher. The potential exists here for a more favourable interlocked rock mass with higher shear strengths than rock mass types 1 and 2. The need for additional support to mitigate a higher occurrence of gravity-induced failure, however, is likely to restrict advance rates. Rock mass Types 5-8 are expected to result in the highest penetration rates due to the heavily fractured to fragmented fracture density but the lowest advance rates based on the need for installation of robust support measures. Extensive failure is likely, particularly in rock mass Type 8, where running ground may become an issue. For this reason shielded TBM's are best suited for poorer rock mass types where full precast concrete segments provide support and thrust generation. Due to the high density of fracturing associated with rock mass Types 5-8, cutterhead excavation will tend to rip along existing defects, rather than induce fractures through intact rock, prolonging cutter life. Dependant on machine selection ground pre-treatment may be necessary prior to excavation.

6.7 Future work

It is anticipated that as more data is collected from future studies the classification scheme will be improved to assist the design of tunnels. Mapping was largely restricted to road and main river channels and as such underground mapping and comparison to rock mass behaviour during tunnelling will validate this classification scheme and its relationship to tunnel specification and design.

More extensive laboratory testing including further TBM testing is needed to define intact and rock mass strength throughout each rock mass type. Cutter Life Index (CLI) and Drilling Rate Index (DRI) testing could be performed to define and allow more accurate TBM comment and design, especially in rock mass Types 1 & 2, where chipping will dominate. A significant issue exists regarding how to best define overall rock mass strength in this complex, heavily jointed, high intact strength rock mass. Rock mass in-situ shear testing, similar to Stewart (2007), could provide further means of relating rock mass Types to rock mass strength and behaviour.

It is hoped the TRC can also be used as a tool enabling rock mass behaviour prediction for other applications, such as slopes. To allow this the TRC needs to be tested at a variety of scales to determine rock mass type implications for rock mass behaviour at different scales.

At present the classification attempts to capture variability in the sandstone member while incorporating the typical mudstone characteristics which hinders use of the TRC on different project scales. In the next iteration of the TRC, work could be done to define sandstone to mudstone proportion and variation based on correlation with a depositional lithofacies system.

Although not directly examined in this thesis the use of external classifications will likely benefit the development or the TRC. Information collected from this study allows use of the Rock Mass Rating (RMR) (Bieniawski, 1989), and Tunnelling Quality Index (Q) (Barton et al., 1974) classification systems. Future tunnelling projects are likely to use both the RMR and Q systems which present a unique opportunity for correlation with the TRC. Furthermore the opportunity to further develop the TRC for input into the widely accepted Hoek-Brown failure criterion exists. If each rock mass type can be assigned values up to 100 (i.e. similar to the Geological Strength Index (GSI, (Hoek et al., 2002)), direct input into the failure criterion in place of the GSI may be possible.

The relative age and maturity of sheared zones also needs to be addressed to better predict rock mass conditions in rock mass Type 8. Future studies will include differentiating conditions of sheared zones related to older, inactive fault zones from younger, active faulting. The older sheared zones can be recemented or annealed potentially giving rise to higher shear strengths.

6.8 Conclusion

Variability in engineering geological condition of the Torlesse Composite Terrane specific to Canterbury, New Zealand, has been assessed in this thesis. Four study sites were selected to represent all three Torlesse terranes and regional structure conditions with the resulting mapping information analysed to observe rock mass trends. It was found that bedding thickness, fracture density and defect structure were the differentiating characteristics across the range of rock mass conditions in the Torlesse. These attributes were related to form the Torlesse rock mass classification (TRC). Each individual outcrop per site was plotted on the TRC to derive rock mass types with clustering of points used to highlight zones indicative of the range in Torlesse rock mass conditions. Eight rock mass types were identified ranging from massive sandstone controlled by systematic persistent jointing to incipient fractured, brecciated and shear dominated fault rock. Lithostructure and tectonic stresses resulting in major to regional scale faults are the key influences on rock mass conditions. Rock mass types and associated geological controls enable the prediction of rock mass behaviour during excavation to relate to TBM selection and design. As such excavatability of the Torlesse is expected to be favourable but the need for extensive support measures for the poorer rock mass types will likely restrict advance rates. As a result shielded TBMs with precast concrete segmental liners are likely to be best suited to the overall terrane. However mapping using the TRC will dictate machine requirements on a case by case basis. There is scope for use of an open gripper TBM if significant amounts of rock mass Type 1 and 2 are present with lesser zones of poorer rock mass types along the alignment. The TRC can be directly used in the grouping and characterisation of Torlesse Composite Terrane. Furthermore it can be directly used through mapping for tunnel alignment selection and further assessment of tunnelling implications. To allow external TRC use, a blank TRC diagram has been produced in Appendix L.

References

Adams, C. 2003. K-Ar geochronology of Torlesse Supergroup metasedimentary rocks in Canterbury, New Zealand. *Journal of the Royal Society of New Zealand,* 33**,** 165-187.

Al-Ameen, S. & Waller, M. 1994. The influence of rock strength and abrasive mineral content on the Cerchar Abrasive Index. *Engineering Geology,* 36**,** 293-301.

Andrews, P. B. 1974. Deltaic sediments, Upper Triassic Torlesse Supergroup, Broken River, North Canterbury. *New Zealand Journal of Geology and Geophysics,* 17**,** 881-905.

Andrews, P. B. & Field, B. 1987. *Lithostratigraphic nomenclature for the Upper Cretaceous and Tertiary sequence of central Canterbury, New Zealand,* New Zealand Geological Survey.

ASG 2010. Guideline for the geotechnical design of underground structures with conventional excavation. *Ground characterization and coherent procedure for the determination of excavation and support during design and construction.* Austrian Society for Geomechanics.

Barton, N. 2000. *TBM tunnelling in jointed and faulted rock,* Taylor & Francis.

Barton, N., Lien, R. & Lunde, J. 1974. Engineering classification of rock masses for the design of tunnel support. *Rock mechanics,* 6**,** 189-236.

Beetham, R. D. & Watters, W. A. 1985. Geology of Torlesse and Waipapa terrane basement rocks encountered during the Tongariro Power Development project, North Island, New Zealand. *New Zealand Journal of Geology & Geophysics,* 28**,** 575-594.

Bieniawski, Z. 1989. Engineering rock mass classifications. *New York: John Wiley and Sons*.

Boggs, S. 2001. *Principles of sedimentology and stratigraphy,* Upper Saddle River, N.J, Prentice Hall Englewood Cliffs.

Boyer, R. & McQueen, J. 1964. Comparison of mapped rock fractures and airphoto linear features. *Photogrammetric Engineering,* 30**,** 630-635.

Bradshaw, J. 1973. Allochthonous Mesozoic fossil localities in melange within the Torlesse rocks of North Canterbury. *Journal of the Royal Society of New Zealand,* 3**,** 161-167.

Bradshaw, J., Andrews, P. & Adams, C. Carboniferous to Cretaceous on the Pacific margin of Gondwana: The Rangitata phase of New Zealand. Fifth International Gondwana Symposium, 1980 Wellington, New Zealand. Rotterdam, The Netherlands, A. A. Balkema, 217-221.

Braun, O. 1982. A structural synthesis of Brazil, based on the study of major lineaments derived from remote sensing imagery interpretation. *Photogrammetria,* 37**,** 77-108.

Caran, S. C., Woodruff, C. M. & Thompson, E. J. 1982. *Lineament Analysis and Inference of Geologic Structure: Examples from the Balcones Ouachita Trend of Texas,* Bureau of Economic Geology, University of Texas at Austin.

Cawood, P. A. 1984. The development of the SW Pacific margin of Gondwana: correlations between the Rangitata and New England orogens. *Tectonics,* 3**,** 539-553.

Clark, P. 1996. *Rock mass characterisation for the open pit mine at Globe-Progress, Reefton.* Master of Science, unpublished thesis, University of Canterbury, Christchurch, New Zealand.

Cook, G. K. 2001. *Rock mass structure and intact rock strength of New Zealand greywackes.* Master of Science, unpublished thesis, University of Canterbury, Christchurch, New Zealand.

Cortes, A., Maestro, A., Soriano, M. & Casas, A. 1998. Lineaments and fracturing in the Neogene rocks of the Almazan Basin, northern Spain. *Geological Magazine,* 135**,** 255-268.

Cowan, H. A. 1992. *Structure, seismicity and tectonics of the Porter's Pass-Amberley fault zone, North Canterbury, New Zealand.* Doctor of Philosophy, unpublished thesis, University of Canterbury, Christchurch, New Zealand.

Cox, S. C. & Barrell, D. J. A. 2007. *Geology of the Aoraki Area,* Institute of Geological & Nuclear Sciences, Lower Hutt, New Zealand.

de Ronde, C. E. J., Sibson, R. H., Bray, C. J. & Faure, K. 2001. Fluid chemistry of veining associated with an ancient microearthquake swarm, Benmore Dam, New Zealand. *Bulletin of the Geological Society of America,* 113**,** 1010-1024.

DeMets, C., Gordon, R. G., Argus, D. & Stein, S. 1990. Current plate motions. *Geophysical Journal International,* 101**,** 425-478.

Eusden, J. D., Upton, P., Eichelberger, N. & Pettinga, J. R. 2011. The Dillon and Acheron sinistral faults, Marlborough Fault System, New Zealand: field studies and mechanical modelling. *New Zealand Journal of Geology and Geophysics,* 55**,** 91-102.

Fawcett, D. F. 1993. The effects of rock properties on the economics of full face TBMs. In Hudson et al. (eds). *Comprehensive rock engineering,* Ch. 10(4)**,** 293-311. UK: Pergamon.

Forsyth, P. J., Jongens, R. & Barrell, D. J. A. 2008. *Geology of the Christchurch area,* Institute of Geological and Nuclear Sciences, Lower Hutt, New Zealand.

Freund, R. 1971. *The Hope fault: a strike slip fault in New Zealand,* New Zealand Geological Survey Bulletin, 86.

Furlong, K. P. & Kamp, P. J. 2009. The lithospheric geodynamics of plate boundary transpression in New Zealand: Initiating and emplacing subduction along the Hikurangi margin, and the tectonic evolution of the Alpine Fault system. *Tectonophysics,* 474**,** 449-462.

Gee, G. W. & Bauder, J. W. 1986. Particle-size analysis. *Methods of soil analysis: Part 1—Physical and mineralogical methods***,** 383-411.

GNS. 2004. *New Zealand Active Fault Database* [Online]. Available: http://data.gns.cri.nz/af/detail.jsp [Accessed 26/03/13 2013].

Haman, P. J. 1961. *Lineament analysis on aerial photographs: examplified in the North Sturgeon Lake Area, Alberta,* PJ Haman.

Hancox, G. T. 1975. Tongariro Power Development. Moawhango diversion completion report on the engineering geology of the Moawhango dam. NZ Geological Survey report EG213.

Hegan, B. Engineering geological aspects of Rangipo underground powerhouse. Papers Presented to the Symposium on Tunnelling in New Zealand, Hamilton, 1977, 1977. Institution of Professional Engineers New Zealand, 6.

Hegan, B. D. 1998. Mighty River Power. Unpublished test data.

Hendron, A. J. 1968. *Rock mechanics in engineering practice,* Ed. Stagg & Zienkiewicz. Wiley.

Hoek, E., Carranza-Torres, C. & Corkum, B. 2002. Hoek-Brown failure criterion-2002 edition. *Proceedings of NARMS-TAC***,** 267-273.

Hoek, E., Kaiser, P. K. & Bawden, W. F. 1995. *Support of underground excavations in hard rock,* Taylor & Francis Group.

Hoek, E., Marinos, P. & Benissi, M. 1998. Applicability of the geological strength index (GSI) classification for very weak and sheared rock masses. The case of the Athens Schist Formation. *Bulletin of Engineering Geology and the Environment,* 57**,** 151-160.

Howell, D. G. 1981. Submarine fan facies in the Torlesse terrane, New Zealand. *Journal, Royal Society of New Zealand,* 11**,** 113-122.

ISRM 1978. *Suggested methods for the quantitative description of discontinuities in rock masses,* International Society for Rock Mechanics. Pergamon Press.

Käsling, H., Thiele, I. & Thuro, K. 2007. Abrasivitätsuntersuchungen mit dem Cerchar-Test–eine Evaluierung der Versuchsbedingungen. *Veröffentlichungen von der,* 16**,** 229-235.

Kleffmann, S., Davey, F., Melhuish, A., Okaya, D., Stern, T. & Sight, T. 1998. Crustal structure in the central South Island, New Zealand, from the Lake Pukaki seismic experiment. *New Zealand Journal of Geology and Geophysics,* 41**,** 39-49.

Koike, K., Nagano, S. & Ohmi, M. 1995. Lineament analysis of satellite images using a segment tracing algorithm (STA). *Computers & Geosciences,* 21**,** 1091-1104.

LINZ. NZ Topo50. Land Information New Zealand.

Little, T. A. & Jones, A. 1998. Seven million years of strike-slip and related off-fault deformation, northeastern Marlborough fault system, South Island, New Zealand. *Tectonics,* 17**,** 285-302.

Little, T. A. & Roberts, A. P. 1997. Distribution and mechanism of Neogene to present-day vertical axis rotations, Pacific-Australian plate boundary zone, South Island, New Zealand. *Journal of Geophysical Research,* 102**,** 20447-20,468.

Mackinnon, T. C. 1983. Origin of the Torlesse terrane and coeval rocks, South Island, New Zealand. *Geological Society of America Bulletin,* 94**,** 967-985.

Maidl, B., Herrenknecht, M., Maidl, U. & Wehrmeyer, G. 2012. *Mechanised shield tunnelling,* Berlin, Germany, Ernst & Sohn.

Maidl, B., Schmid, L., Ritz, W. & Herrenknecht, M. 2008. *Hardrock tunnel boring machines,* Wiley-VCH.

Mansergh, G. D. 1968. Summary Report of the Aviemore foundations. Unpublished NZ Geological Survey (Christchurch) report.

Marinos, P. & Hoek, E. GSI: a geologically friendly tool for rock mass strength estimation. Proc. GeoEng2000 Conference, Melbourne, 2000. 1422-1442.

Marinos, P. & Hoek, E. 2001. Estimating the geotechnical properties of heterogeneous rock masses such as flysch. *Bulletin of Engineering Geology and the Environment,* 60**,** 85-92.

McMorran, T. J. 1991. *The Hope Fault at Hossack Station East of Hanmer Basin, North Canterbury.* Master of Science, unpublished thesis, University of Canterbury, Christchurch, New Zealand.

Mortimer, N. 2004. New Zealand's geological foundations. *Gondwana Research,* 7**,** 261-272.

Nathan, S., Rattenbury, M. S. & Suggate, R. P. 2002. *Geology of the Greymouth area,* Institute of Geological & Nuclear Sciences, Lower Hutt, New Zealand.

Nelson, P. 1993. TBM performance analysis with reference to rock properties. *Comprehensive rock engineering,* 4**,** 261-292.

Noble, D. P. 2011. *Tectonic Geomorphology and Paleoseismicity of the Northern Esk Fault, North Canterbury, New Zealand.* Master of Science, unpublished thesis, University of Canterbury, Christchurch, New Zealand.

Norris, R., Koons, P. & Cooper, A. 1990. The obliquely-convergent plate boundary in the South Island of New Zealand: implications for ancient collision zones. *Journal of Structural Geology,* 12**,** 715-725.

Norris, R. J. & Cooper, A. F. 2001. Late Quaternary slip rates and slip partitioning on the Alpine Fault, New Zealand. *Journal of Structural Geology,* 23**,** 507-520.

NTH 1994. Full face tunnel boring. [In Norwegian: Fullprofilboring av tunneler.] Prosjektrapport anleggsdrift 1-94. Trondheim: NTH.

NZGS 2005. Field Description of Soil and Rock. *Guidelines for the field classification and description of soil and rock for engineering purposes.* New Zealand Geotechnical Society Inc.

Paterson, B. 1987. Engineering geology assessment of alternative highway options at the Zig Zag and Otira Gorge, Arthur's Pass. *New Zealand Geological Survey report EG409.*

Patton, F. D. Multiple modes of shear failure in rock. 1st ISRM Congress, 1966.

PCA 1994. SH73 Otira Viaduct & Approaches, Engineering Geological Report on Design Investigations. Paterson & Coates Associates. Prepared for Beca Carter Hollings and Ferner Ltd.

Pender, M. Aspects of Geotechnical Behaviour of Some NZ Materials. 7th Australia New Zealand Conference on Geomechanics: Geomechanics in a Changing World: Conference Proceedings, 1996. Institution of Engineers, Australia, 21.

Pettijohn, F. J., Potter, P. E. & Siever, R. 1987. *Sand and sandstone,* Springer Verlag.

Pettinga, J. R., Yetton, M. D., Van Dissen, R. J. & Downes, G. 2001. Earthquake source identification and characterisation for the Canterbury region, South Island, New Zealand. *Bulletin of the New Zealand Society for Earthquake Engineering,* 34**,** 282-317.

Pickens, G. & Grimston, J. 2001. The Opuha Dam project. *ANCOLD BULLETIN***,** 41-52.

PSM 2010a. PSM Guideline for Rock Description. Internal document: Pells Sullivan Meynink.

PSM 2010b. PSM Guideline Geotechnical Line Mapping. Internal document: Pells Sullivan Meynink.

Rahiman, T. I. & Pettinga, J. R. 2008. Analysis of lineaments and their relationship to Neogene fracturing, SE Viti Levu, Fiji. *Geological Society of America Bulletin,* 120**,** 1544-1555.

Ramamurthy, T. 1993. Strength and modulus responses of anisotropic rocks : in: Comprehensive rock engineering. Vol. 1, ed J.A. Hudson, (Pergamon). *International Journal of Rock Mechanics and Mining Sciences & Geomechanics Abstracts,* 31**,** 313-329.

Ramberg, H. 1955. Natural and experimental boudinage and pinch-and-swell structures. *The Journal of Geology***,** 512-526.

Rattenbury, M., Townsend, D. & Johnston, M. 2006. *Geology of the Kaikoura area,* Institute of Geological and Nuclear Sciences, Lower Hutt, New Zealand.

Read, S. & Richards, L. 2007. Characteristics and classification of New Zealand greywackes. *Rock Mechanics: Meeting Society's Challenges and Demands, Two Volume Set.* Taylor & Francis.

Read, S., Richards, L. & Perrin, N. Applicability of the Hoek–Brown failure criterion to New Zealand greywacke rocks. Proceeding 9th international society for rock mechanics congress, Paris, 1999. 655-660.

Read, S. A., Richards, L. & Perrin, N. D. 2000. Assessment of New Zealand greywacke rock masses with the Hoek-Brown failure criterion. *GeoEng2000, Melbourne***,** 20-24.

Read, S. A. L., Richards, L. R. & Perrin, N. D. 1998. Engineering parameters of closely-jointed rocks – Mapping and strength testing of greywacke from Aviemore and Belmont. Institute of Geological & Nuclear Sciences science report 98/19.

Richards, L. & Read, S. 2007. New Zealand greywacke characteristics and influences on rock mass behaviour. *The Second Half Century of Rock Mechanics, Three Volume Set.* Taylor & Francis.

Robinson, J. V. 1957. Benmore Power Project: - Argillite Rock Modulus. Unpublished Central laboratories report, 3rd Oct, 1957.

Roser, B. P. & Korsch, R. J. 1999. Geochemical characterization, evolution and source of a Mesozoic accretionary wedge: The Torlesse terrane, New Zealand. *Geological Magazine,* 136**,** 493-512.

Rostami, J. & Ozdemir, L. A new model for performance prediction of hard rock TBMs. Proceedings of the Rapid Excavation and Tunneling Conference, 1993. Society for Mining, Metallogy & Exploration Inc, 793-793.

Silberling, N. J., Nichols, K. M., Bradshaw, J. D. & Blome, C. D. 1988. Limestone and chert in tectonic blocks from the Esk Head subterrane, South Island, New Zealand. *Geological Society of America Bulletin,* 100**,** 1213-1223.

Singh, M., Rao, K. & Ramamurthy, T. 2002. Strength and deformational behaviour of a jointed rock mass. *Rock Mechanics and Rock Engineering,* 35**,** 45-64.

Stewart, S. W. 2007. *Rock mass strength and deformability of unweathered closely jointed New Zealand greywacke.* Doctor of Philosophy, unpublished thesis, University of Canterbury, Christchurch, New Zealand.

Suggate, R. P., Stevens, G. R. & Te Punga, M. T. 1978. *The geology of New Zealand,* EC Keating, Government Printer.

Szwedzicki, T. 2007. A hypothesis on modes of failure of rock samples tested in uniaxial compression. *Rock Mechanics and Rock Engineering,* 40**,** 97-104.

Tippett, J. M. & Kamp, P. J. 1993. The role of faulting in rock uplift in the Southern Alps, New Zealand. *New Zealand Journal of Geology and Geophysics,* 36**,** 497-504.

Türtscher, M. & Leitner, W. 2010. Penetration, Meißel-verschleiß und Vor-triebsgeschwindigkeit für TBM-Vortriebe im Festgestein.

Ulusay, R. & Hudson, J. A. 2007. *The complete ISRM suggested methods for rock characterization, testing and monitoring: 1974-2006,* Commission on Testing Methods, International Society of Rock Mechanics.

URS. 2008. *North Bank Tunnel Project - Summary of Pre-feasibility Study* [Online]. Christchurch, New Zealand. Available: http://www.meridianenergy.co.nz/assets/PDF/What-we-do/Our-projects/North-Bank-Hydro-project/NBTPROJECTSummaryReport11Nov08.pdf [Accessed 22/02 2013].

van Dissen, R. & Nicol, A. 2009. Mid-late Holocene paleoseismicity of the eastern Clarence Fault, Marlborough, New Zealand. *New Zealand Journal of Geology and Geophysics,* 52**,** 195-208.

Wallace, L. M., Beavan, J., McCaffrey, R., Berryman, K. & Denys, P. 2007. Balancing the plate motion budget in the South Island, New Zealand using GPS, geological and seismological data. *Geophysical Journal International,* 168**,** 332-352.

Wandres, A. M., Bradshaw, J. D., Weaver, S., Maas, R., Ireland, T. & Eby, N. 2004. Provenance analysis using conglomerate clast lithologies: A case study from the Pahau terrane of New Zealand. *Sedimentary Geology,* 167**,** 57-89.

Wanner, H. & Aeberli, U. Tunnelling machine performance in jointed rock. 4th ISRM Congress, 1979.

Ward, S. J. 2000. *The Physical, Chemical and Mineralogical Properties of a Fault Zone: The Hope Fault, East Hanmer Basin, New Zealand.* Master of Science, unpublished thesis, University of Canterbury, Christchurch, New Zealand.

Watters, W. A. 1965. Petrographic examination of rock specimens from Aviemore dam. Unpublished NZ Geological Survey report.

West, G. 1989. Rock abrasiveness testing for tunnelling. *International Journal of Rock Mechanics and Mining Sciences,* 26**,** 151-160.

Whitehouse, I. E. & Bradshaw, J. 1988. *Reconnaissance bedrock geology of upper Rakaia River, Canterbury*, New Zealand Geological Survey.

Yaralı, O., Yaşar, E., Bacak, G. & Ranjith, P. 2008. A study of rock abrasivity and tool wear in Coal Measures Rocks. *International Journal of Coal Geology*, 74**,** 53-66.

Appendices

Appendix A: Field sheets

Field sheets developed for use of recording information in the field.

| A.1 Coherent rock and bedding | | |

A.2 Defect structure

Outcrop #	Photo	Defect type	Orientation		Spacing (m)	Persistence (m)	Aperture (mm)	Infilling type	Infilling strength	Infill moisture	Infill thickness (mm)	Roughness
			Dip	Dip direction								

A.2 Defect structure (cont)

| Waviness | | |

A.3 Soil description for infill

Outcrop #	Fraction (name)	Colour	Structure	Strength: NZGS (2005)	Strength: PSM (2010a, 2010b) Non-cohs	Moisture	Grading	Sorting	Plasticity*	Weathering	Other (Shatter zone width, schmidt)

A.4 Breccia fabric descriptions

Outcrop #	Fabric support	Fabric arrangment	Fabric (random - lineated?)	Matrix vs. cement	Rotation angle	Rounding	Clast size	Alteration	Grain size*	Other

Appendix B: Trilab reports

Raw Trilab Torlesse rock reports including Brazilian Tensile Strength, Uniaxial Compressive Strength (and Stress Strain Plot), Cerchar Abrasivity Index and Ultrasonic Velocity testing including test parameters. Note some Trilab sample names have been reproduced incorrectly. See corrections below.

Old sample name	New sample name
Hurunui River H-29-A	Hurunui River 29a
Hurunui River H-56-A	Hurunui River 5b
Ashley Gorge A.219	Ashley Gorge 21a
Ashley Gorge A.49	Ashley Gorge 4a
Opuha Dam O.1.H	Opuha Dam 1h
Opuha Dam O.5.A	Opuha Dam 5a

Trilab
Soil Rock Calibration

Brisbane
346A Bilsen Road,
Geebung
QLD 4034
Ph: +61 7 3265 5656

Perth
2 Kimmer Place,
Queens Park
WA 6107
Ph: +61 8 9258 8323

INDIRECT TENSILE - BRAZILIAN TEST REPORT

Test Method: QMRD Q185

Client	Pells Sullivan Meynink Pty Ltd	**Report No.**	13020222-BR
Project	TBM Research - NZ	**Test Date**	27/02/2013
		Report Date	07/03/2013

Sample No.	13020222	13020223	13020224	13020225	13020226	-
Client ID	1 - Hurunui River - H-29-A	2 - Hurunui River - H-56-A	3 - Ashey Gorge - A.219	4 - Ashey Gorge - A.4.9	5 - Opuna Dam - O.5.A	-
Depth (m)	Not Supplied	Not Supplied	Not Supplied	Not Supplied	Not Supplied	-
Description	-	-	-	-	-	-
Wet Density (t/m^3)	2.63	2.67	2.64	2.60	2.65	-
Moisture Content (%)	0.1	0.2	0.5	0.5	0.1	-
Specimen Length (mm)	35.7	37.2	35.0	35.6	34.9	-
Specimen Diameter (mm)	49.4	49.5	49.4	49.4	49.6	-
Mode of Failure	Axial Splitting	Axial Splitting	Axial Splitting	Axial Splitting	Axial Splitting	-
Test Duration (min:sec)	5:14	5:32	4:20	2:59	3:37	-
TENSILE STRENGTH (MPa)	29.00	24.37	16.10	14.97	21.24	-

NOTES/REMARKS:

Sample/s supplied by the client

Accredited for compliance with ISO/IES 17025.
The results of the tests, calibrations, and/or measurements included in this document are traceable to Australian/National Standards.

Tested at Trilab Brisbane Laboratory.

Authorised Signatory

C. Channon

NATA ACCREDITED FOR TECHNICAL COMPETENCE

Laboratory No. 9926

Trilab
Soil Rock Calibration

Brisbane
346A Bilsen Road,
Geebung
QLD 4034
Ph: +61 7 3265 5656

Perth
2 Kimmer Place,
Queens Park
WA 6107
Ph: +61 8 9258 8323

CERCHAR ABRASIVITY INDEX TEST REPORT

ASTM D7625 - 10 Standard Test Method for Laboratory Determination of Abrasiveness of Rock Using the Cerchar Method

Client	Pells Sullivan Meynink Pty Ltd	**Report No.**	13020223-CERC
Project	TBM Research - NZ	**Test Date**	6/03/2013
		Report Date	7/03/2013
Client ID	2 - Hurunui River - H-56-A	**Depth (m)**	Not Supplied
Description		**Sample Type**	Single Individual Rock Core Specimen

SAMPLE DETAILS

Sample Diameter (mm):	49.4	**Moisture Content (%):**	0.2
Sample Height (mm):	36.3	**Dry Density (t/m^3)**	2.66
Surface Type :	Smooth (Saw Cut) Surface	**Wet Density (t/m^3)**	2.67

RESULTS OF TESTING

Hardness of Tip Used	16 HRC	Hardness of Tip Used	40 HRC	Hardness of Tip Used	57 HRC
Average Diameter (mm)	*CAI	Average Diameter (mm)	*CAI	Average Diameter (mm)	*CAI
0.51	**5.50**	**0.40**	**4.45**	**0.31**	**3.56**

Linear Relationship between Tip Hardness and CAI

CAI = (-0.0422 x HRC) + 6.0935

Average CAI (HRC55) = 3.77

Classification : High abrasiveness

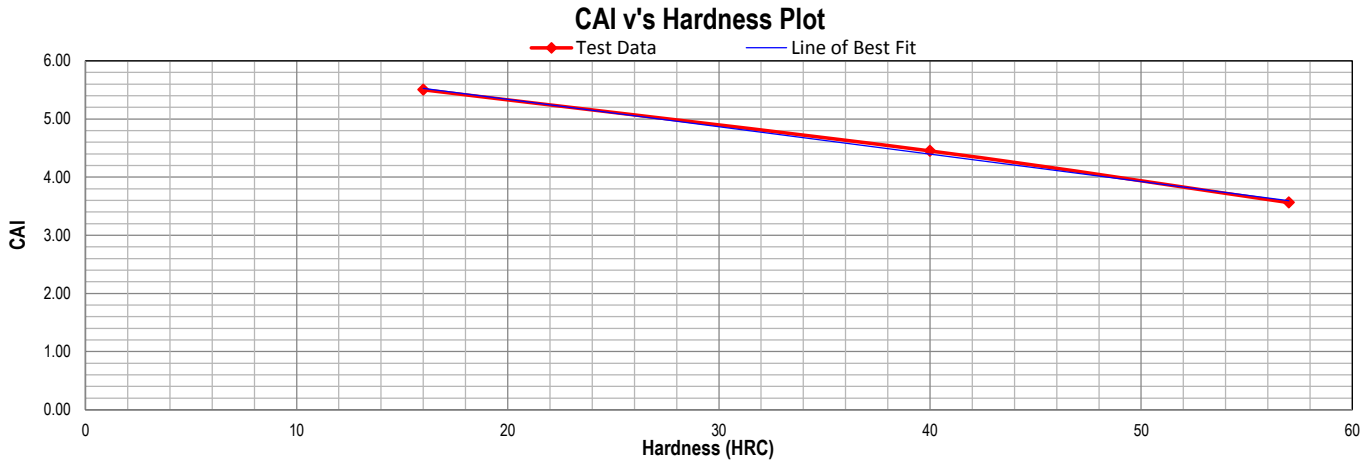

Remarks:

Sample/s supplied by client

* CAI values corrected for smooth surface.

Laboratory No. 9926

Trilab
Soil Rock Calibration

Brisbane
346A Bilsen Road,
Geebung
QLD 4034
Ph: +61 7 3265 5656

Perth
2 Kimmer Place,
Queens Park
WA 6107
Ph: +61 8 9258 8323

CERCHAR ABRASIVITY INDEX TEST REPORT

ASTM D7625 - 10 Standard Test Method for Laboratory Determination of Abrasiveness of Rock Using the Cerchar Method

Client	Pells Sullivan Meynink Pty Ltd	**Report No.**	13020223-CERC
Project	TBM Research - NZ	**Test Date**	6/03/2013
		Report Date	7/03/2013
Client ID	2 - Hurunui River - H-56-A	**Depth (m)**	Not Supplied
Description		**Sample Type**	Single Individual Rock Core Specimen

RESULTS OF TESTING

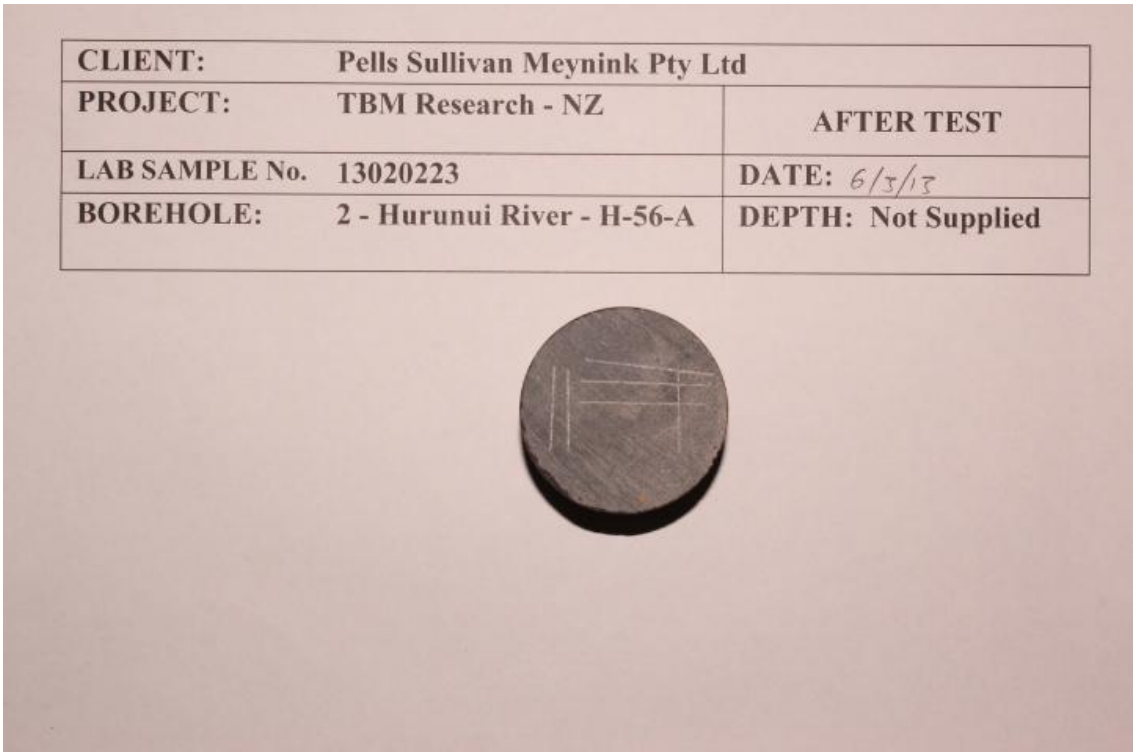

Remarks:

Sample/s supplied by client

* CAI values corrected for smooth surface.

Trilab
Soil Rock Calibration

Brisbane
346A Bilsen Road,
Geebung
QLD 4034
Ph: +61 7 3265 5656

Perth
2 Kimmer Place,
Queens Park
WA 6107
Ph: +61 8 9258 8323

UNIAXIAL COMPRESSIVE STRENGTH & DEFORMATION TEST REPORT

Test Method: AS 4133.4.3.1

Client	Pells Sullivan Meynink Pty Ltd	**Report No.**	13020223-MOD
Project	TBM Research - NZ	**Test Date**	26/02/2013
		Report Date	27/02/2013
Client ID	2 - Hurunui River - H-56-A	**Depth (m)**	Not Supplied
Description	-	**Sample Type**	Single Individual Rock Core Specimen

Uniaxial Compressive Strength 233 MPa

	Young's Modulus	Poisson Ratio	
Tangent	53.7 GPa	0.108	from 9 % to 21 % of Max UCS
Secant	52.8 GPa	0.108	from 0 % to 21 % of Max UCS

Axial Stress vs Strain Plots

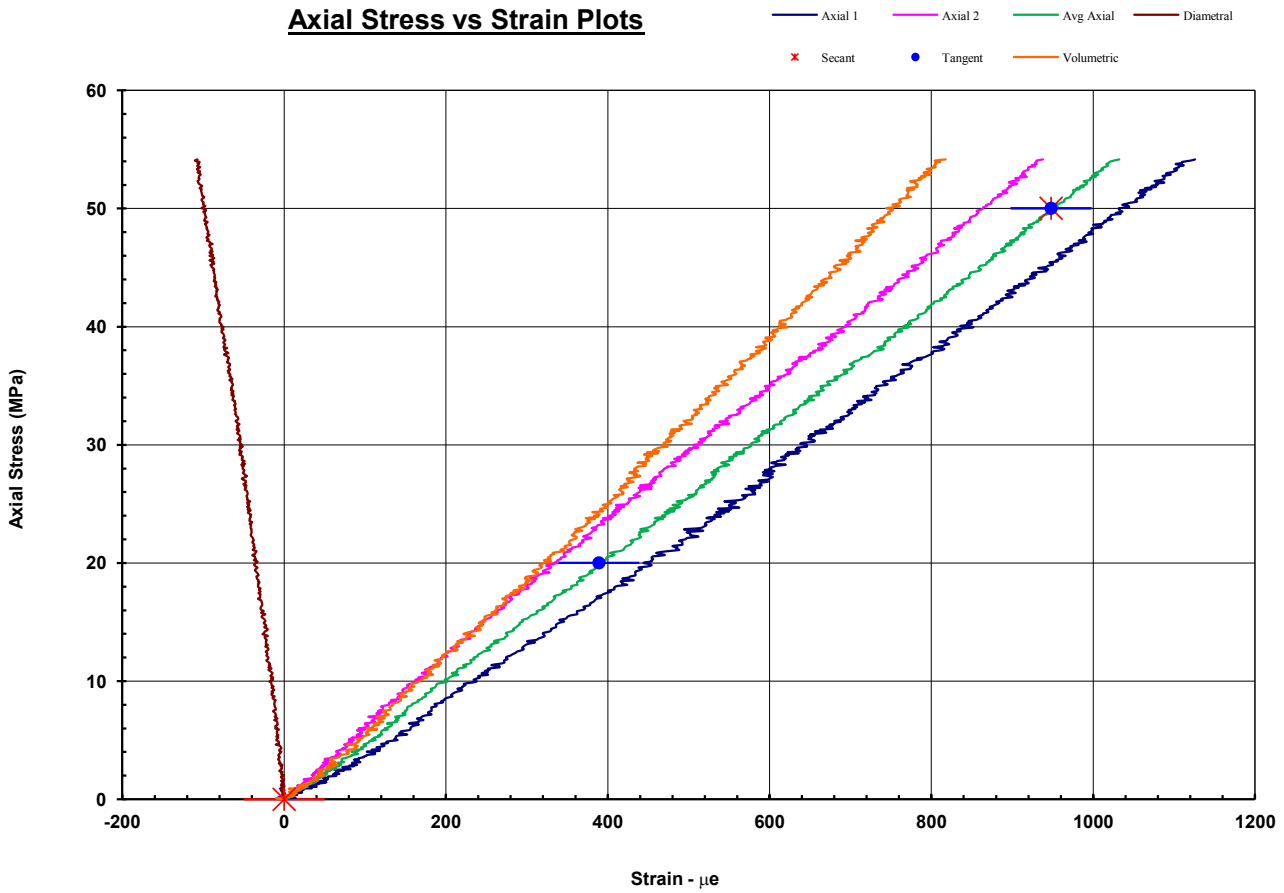

Notes/Remarks: Tested as received.

Sample/s supplied by client

Graph not to scale

Accredited for compliance with ISO/IES 17025.
The results of the tests, calibrations, and/or measurements included in this document are traceable to Australian/National Standards.

Tested at Trilab Brisbane Laboratory.

Authorised Signatory
J. Russell

NATA ACCREDITED FOR TECHNICAL COMPETENCE

Laboratory No. 9926

Trilab
Soil Rock Calibration

Brisbane
346A Bilsen Road,
Geebung
QLD 4034
Ph: +61 7 3265 5656

Perth
2 Kimmer Place,
Queens Park
WA 6107
Ph: +61 8 9258 8323

UNIAXIAL COMPRESSIVE STRENGTH & DEFORMATION TEST REPORT

Test Method: AS 4133.4.3.1

Client	Pells Sullivan Meynink Pty Ltd	**Report No.**	13020223-MOD
Project	TBM Research - NZ	**Test Date**	26/02/2013
		Report Date	27/02/2013
Client ID	2 - Hurunui River - H-56-A	**Depth (m)**	Not Supplied
Description	-		

Uniaxial Compressive Strength 233 MPa

Average Sample Diameter (mm)	49.3	Moisture Content (%)	0.2
Sample Height (mm)	133.8	Wet Density (t/m^3)	2.67
Duration of Test (min)	10.38	Dry Density (t/m^3)	2.66
Rate of Loading (MPa/min)	22.47	Bedding (°)	Nil
Mode of Failure	Disintegration	Test Apparatus	Kelba 1000kN Load Cell
Specific Energy (MJ/m^3)	0.028		

Specific energy determined from area under curve between 0 and 1,032με

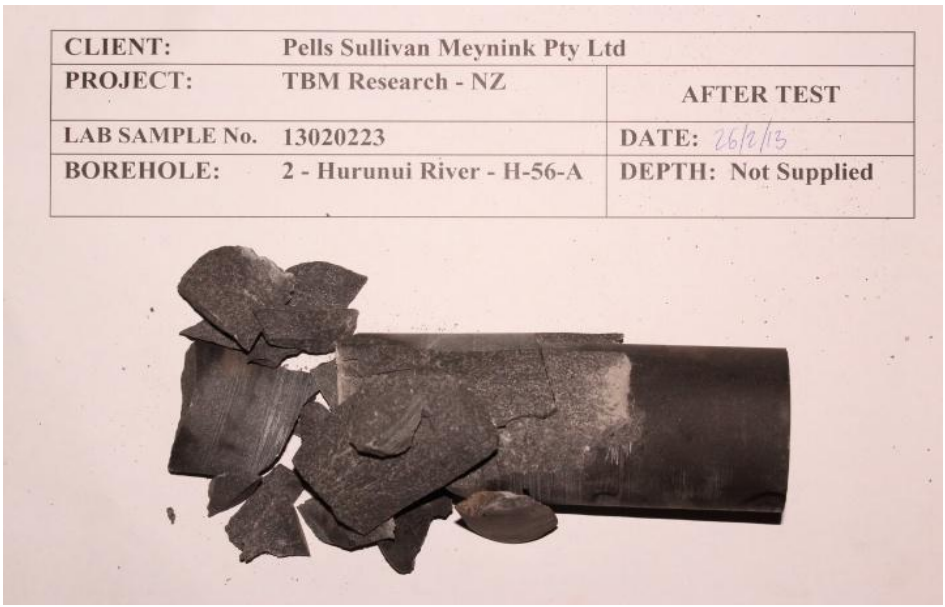

Photo not to scale

Notes/Remarks:

Accredited for compliance with ISO/IES 17025.
The results of the tests, calibrations, and/or measurements included in this document are traceable to Australian/National Standards.

Tested at Trilab Brisbane Laboratory.

Authorised Signatory
J. Russell

NATA ACCREDITED FOR TECHNICAL COMPETENCE

Laboratory No. 9926

Trilab
Soil Rock Calibration

Brisbane
346A Bilsen Road,
Geebung
QLD 4034
Ph: +61 7 3265 5656

Perth
2 Kimmer Place,
Queens Park
WA 6107
Ph: +61 8 9258 8323

DETERMINATION OF THE ULTRASONIC VELOCITY OF ROCK

Test Method: ASTM D2845 - 08 - Determination of Pulse Velocities and Ultrasonic Elastic Constants of Rock

Client	Pells Sullivan Meynink Pty Ltd	**Report No.**	13020223- SON
Project	TBM Research - NZ	**Test Date**	25/02/2013
		Report Date	25/02/2013
Client ID	2 - Hurunui River - H-56-A	**Depth (m)**	Not Supplied
Description		**Sample Type**	Single Individual Rock Core Specimen

Sample and Test Details

Average Sample Diameter (mm)	49.3	Couplant	Honey
Sample Height (mm)	133.8	Probe Type	63.6mm "P" & "S" Wave
Sample Density (t/m^3)	2.67	Test Apparatus	GCTS- ULT 100 - Ultrasonic Velocity
Applied Axial Stress (MPa)	1.0		

Test Results

"P" Velocity (m/s)	4481		
"P" Arrival Time (µsec)	43.7	Young's Modulus (GPa)	50.1
"S" Velocity (m/s)	2837	Poisson's Ratio	0.17
"S" Arrival Time (µsec)	68.0		

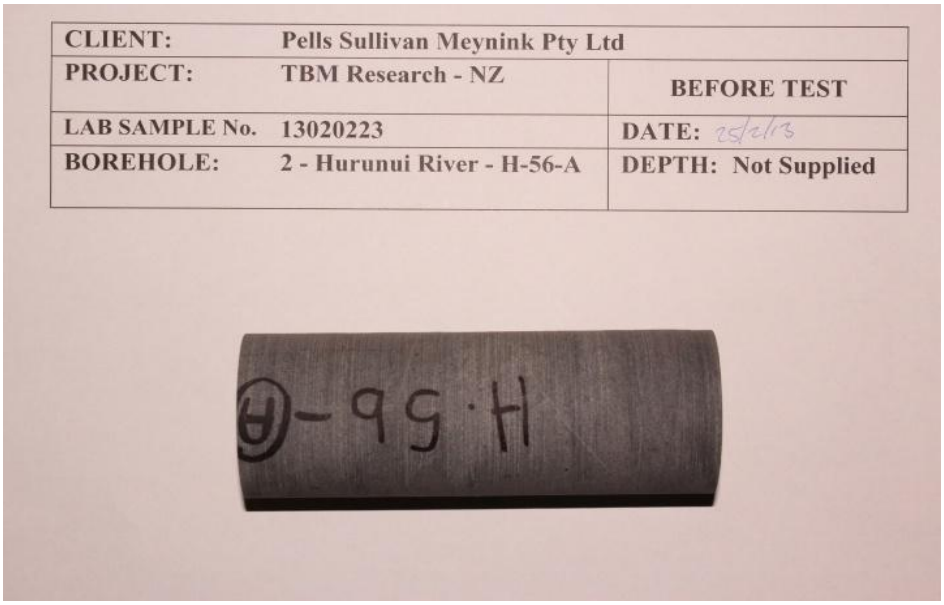

Notes/Remarks:

Sample/s supplied by client Photo not to scale Tested as received

Trilab
Soil Rock Calibration

Brisbane
346A Bilsen Road,
Geebung
QLD 4034
Ph: +61 7 3265 5656

Perth
2 Kimmer Place,
Queens Park
WA 6107
Ph: +61 8 9258 8323

DETERMINATION OF THE ULTRASONIC VELOCITY OF ROCK

Test Method: ASTM D2845 - 08 - Determination of Pulse Velocities and Ultrasonic Elastic Constants of Rock

Client	Pells Sullivan Meynink Pty Ltd	**Report No.**	13020223- SON
Project	TBM Research - NZ	**Test Date**	25/02/2013
		Report Date	25/02/2013
Client ID	2 - Hurunui River - H-56-A	**Depth (m)**	Not Supplied
Description			

"P" WAVEFORM

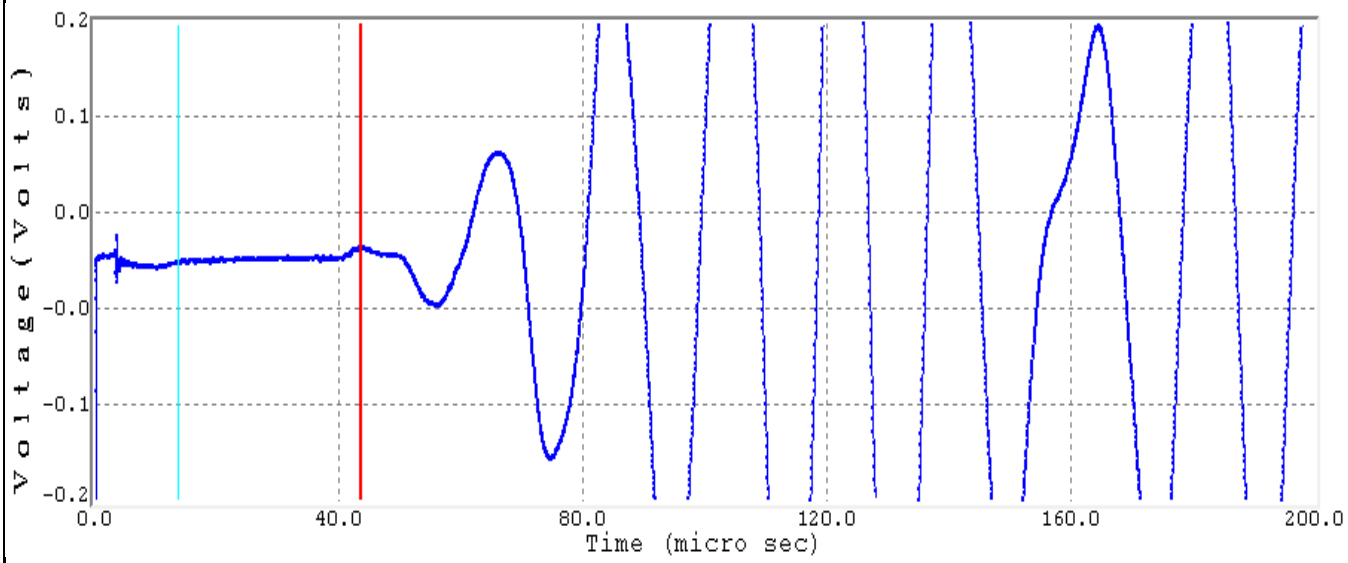

"S" WAVEFORM

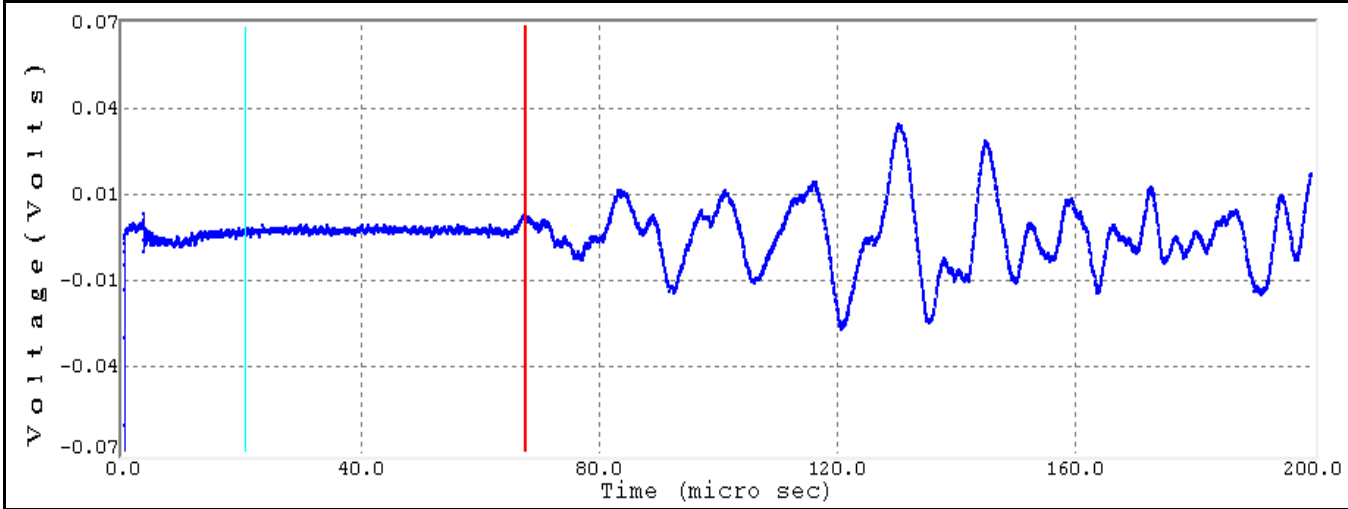

Notes/Remarks:

Sample/s supplied by client

Trilab
Soil Rock Calibration

Brisbane
346A Bilsen Road,
Geebung
QLD 4034
Ph: +61 7 3265 5656

Perth
2 Kimmer Place,
Queens Park
WA 6107
Ph: +61 8 9258 8323

CERCHAR ABRASIVITY INDEX TEST REPORT

ASTM D7625 - 10 Standard Test Method for Laboratory Determination of Abrasiveness of Rock Using the Cerchar Method

Client	Pells Sullivan Meynink Pty Ltd	**Report No.**	13020222-CERC
Project	TBM Research - NZ	**Test Date**	6/03/2013
		Report Date	7/03/2013
Client ID	1 - Hurunui River - H-29-A	**Depth (m)**	Not Supplied
Description		**Sample Type**	Single Individual Rock Core Specimen with existing defect

SAMPLE DETAILS

Sample Diameter (mm):	49.4	**Moisture Content (%):**	0.1
Sample Height (mm):	35.9	**Dry Density (t/m^3)**	2.62
Surface Type :	Smooth (Saw Cut) Surface	**Wet Density (t/m^3)**	2.63

RESULTS OF TESTING

Hardness of Tip Used	16 HRC	Hardness of Tip Used	40 HRC	Hardness of Tip Used	57 HRC
Average Diameter (mm)	*CAI	Average Diameter (mm)	*CAI	Average Diameter (mm)	*CAI
0.55	5.95	0.45	4.93	0.32	3.67

Linear Relationship between Tip Hardness and CAI

CAI = (-0.0662 x HRC) + 7.1962

Average CAI (HRC55) = 3.56

Classification : High abrasiveness

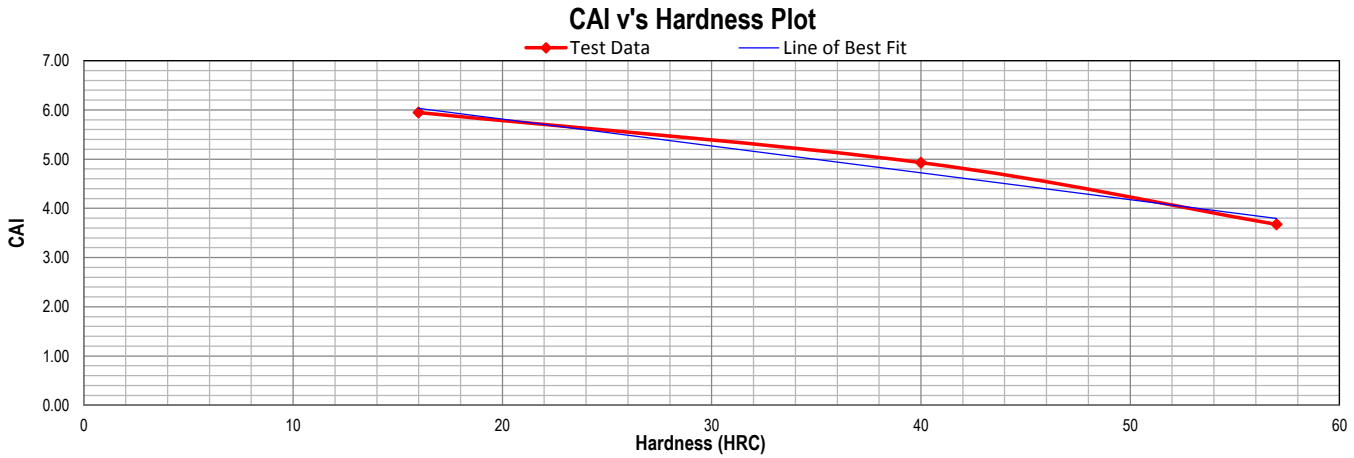

Remarks:

Sample/s supplied by client

* CAI values corrected for smooth surface.

Laboratory No. 9926

Trilab
Soil Rock Calibration

Brisbane
346A Bilsen Road,
Geebung
QLD 4034
Ph: +61 7 3265 5656

Perth
2 Kimmer Place,
Queens Park
WA 6107
Ph: +61 8 9258 8323

CERCHAR ABRASIVITY INDEX TEST REPORT

ASTM D7625 - 10 Standard Test Method for Laboratory Determination of Abrasiveness of Rock Using the Cerchar Method

Client	Pells Sullivan Meynink Pty Ltd	**Report No.**	13020222-CERC
Project	TBM Research - NZ	**Test Date**	6/03/2013
		Report Date	7/03/2013
Client ID	1 - Hurunui River - H-29-A	**Depth (m)**	Not Supplied
Description		**Sample Type**	Single Individual Rock Core Specimen with existing defect

RESULTS OF TESTING

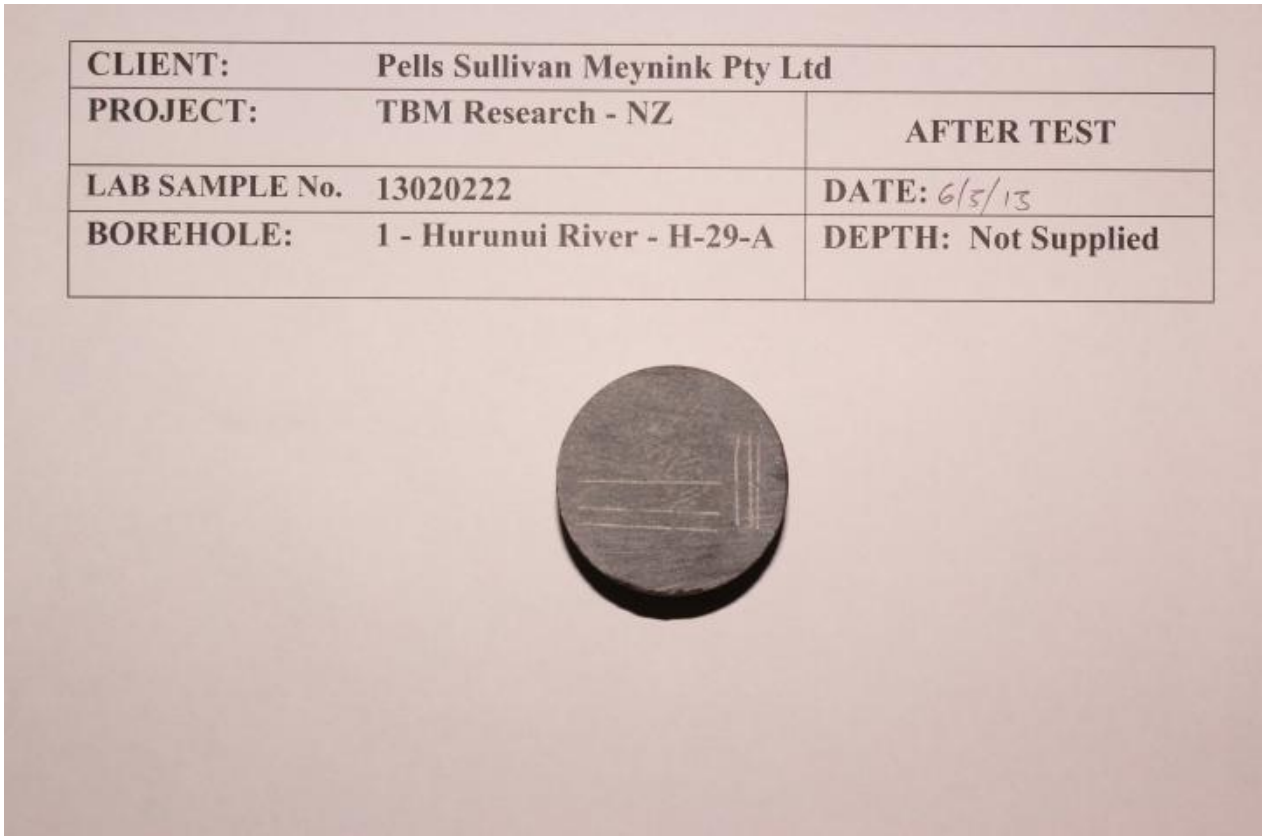

Remarks:

Sample/s supplied by client

* CAI values corrected for smooth surface.

Trilab
Soil Rock Calibration

Brisbane
346A Bilsen Road,
Geebung
QLD 4034
Ph: +61 7 3265 5656

Perth
2 Kimmer Place,
Queens Park
WA 6107
Ph: +61 8 9258 8323

UNIAXIAL COMPRESSIVE STRENGTH & DEFORMATION TEST REPORT

Test Method: AS 4133.4.3.1

Client	Pells Sullivan Meynink Pty Ltd	**Report No.**	13020222-MOD
Project	TBM Research - NZ	**Test Date**	26/02/2013
		Report Date	27/02/2013
Client ID	1 - Hurunui River - H-29-A	**Depth (m)**	Not Supplied
Description	-	**Sample Type**	Single Individual Rock Core Specimen

Uniaxial Compressive Strength 232 MPa

	Young's Modulus	Poisson Ratio	
Tangent	58.4 GPa	0.079	from 9 % to 22 % of Max UCS
Secant	58.3 GPa	0.083	from 0 % to 22 % of Max UCS

Axial Stress vs Strain Plots

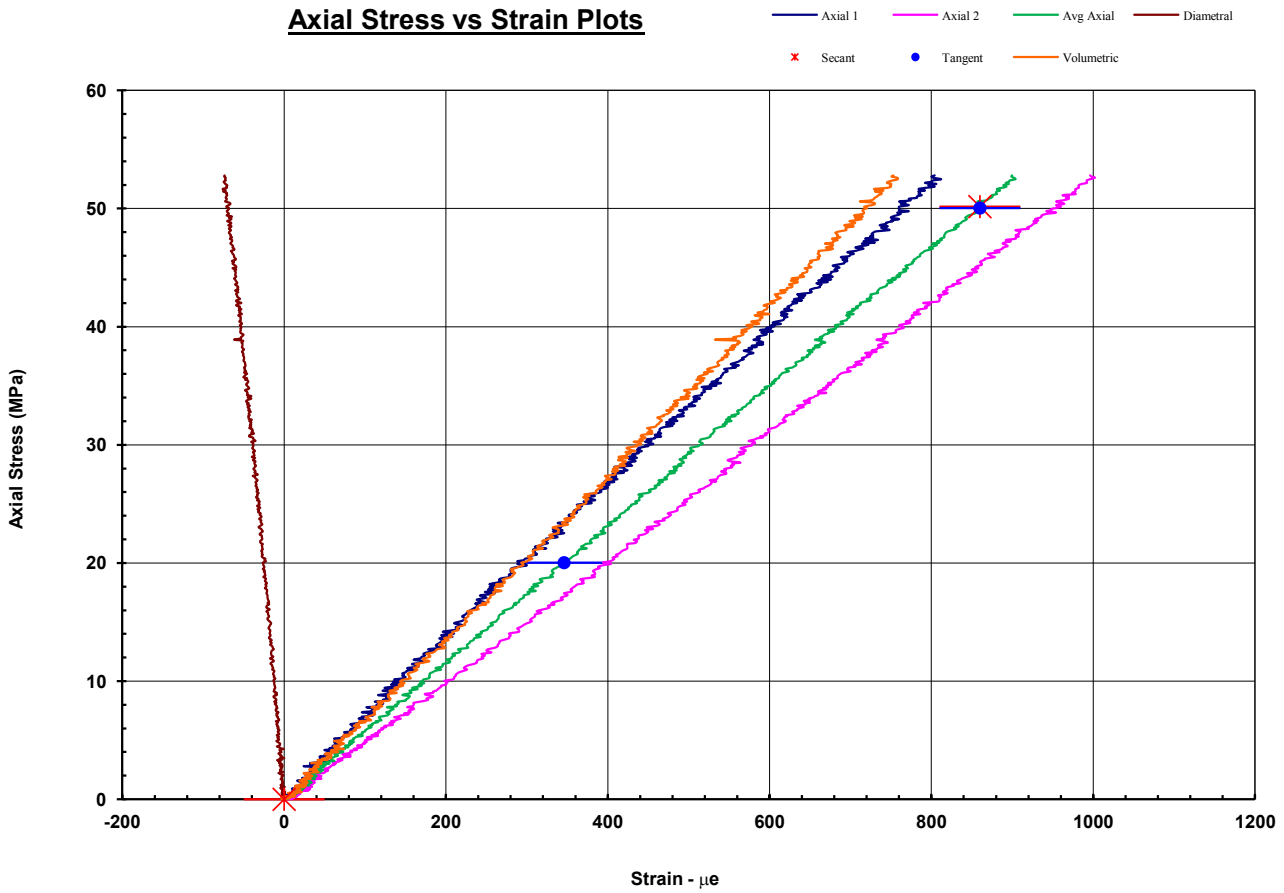

Notes/Remarks: Tested as received.

Sample/s supplied by client

Graph not to scale

Accredited for compliance with ISO/IES 17025.
The results of the tests, calibrations, and/or measurements included in this document are traceable to Australian/National Standards.

Tested at Trilab Brisbane Laboratory.

Authorised Signatory
J. Russell

NATA ACCREDITED FOR TECHNICAL COMPETENCE

Laboratory No. 9926

Trilab
Soil Rock Calibration

Brisbane
346A Bilsen Road,
Geebung
QLD 4034
Ph: +61 7 3265 5656

Perth
2 Kimmer Place,
Queens Park
WA 6107
Ph: +61 8 9258 8323

UNIAXIAL COMPRESSIVE STRENGTH & DEFORMATION TEST REPORT

Test Method: AS 4133.4.3.1

Client	Pells Sullivan Meynink Pty Ltd	**Report No.**	13020222-MOD
Project	TBM Research - NZ	**Test Date**	26/02/2013
		Report Date	27/02/2013
Client ID	1 - Hurunui River - H-29-A	**Depth (m)**	Not Supplied
Description	-		

Uniaxial Compressive Strength 232 MPa

Average Sample Diameter (mm)	49.4	Moisture Content (%)	0.2
Sample Height (mm)	129.3	Wet Density (t/m^3)	2.66
Duration of Test (min)	10.87	Dry Density (t/m^3)	2.66
Rate of Loading (MPa/min)	21.37	Bedding (°)	Nil
Mode of Failure	Disintegration	Test Apparatus	Kelba 1000kN Load Cell
Specific Energy (MJ/m^3)	0.024		

Specific energy determined from area under curve between 0 and 904με

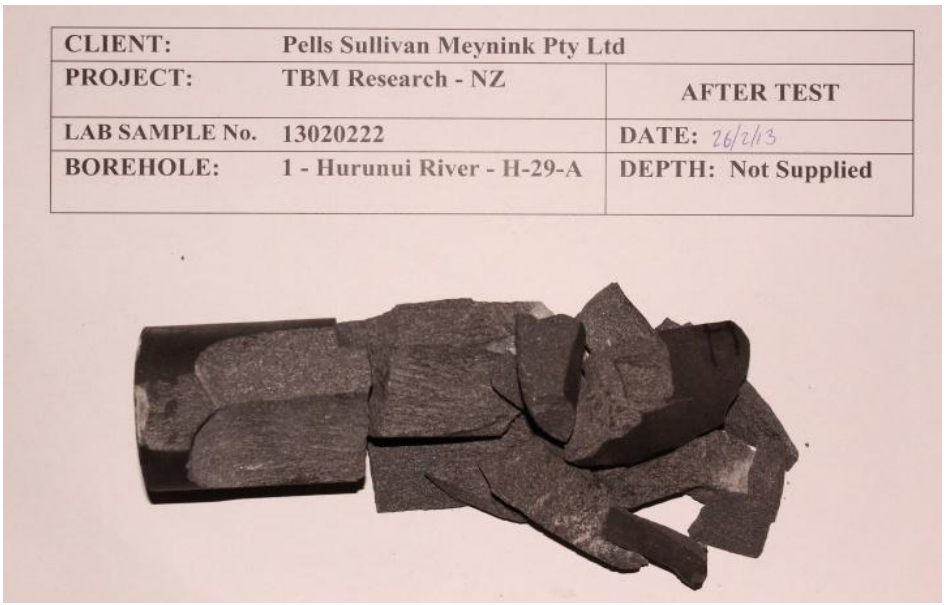

Photo not to scale

Notes/Remarks:

Accredited for compliance with ISO/IES 17025.
The results of the tests, calibrations, and/or measurements included in this document are traceable to Australian/National Standards.

Tested at Trilab Brisbane Laboratory.

Authorised Signatory
J. Russell

NATA ACCREDITED FOR TECHNICAL COMPETENCE

Laboratory No. 9926

Trilab
Soil Rock Calibration

Brisbane
346A Bilsen Road,
Geebung
QLD 4034
Ph: +61 7 3265 5656

Perth
2 Kimmer Place,
Queens Park
WA 6107
Ph: +61 8 9258 8323

DETERMINATION OF THE ULTRASONIC VELOCITY OF ROCK

Test Method: ASTM D2845 - 08 - Determination of Pulse Velocities and Ultrasonic Elastic Constants of Rock

Client	Pells Sullivan Meynink Pty Ltd	**Report No.**	13020222- SON
Project	TBM Research - NZ	**Test Date**	25/02/2013
		Report Date	25/02/2013
Client ID	1 - Hurunui River - H-29-A	**Depth (m)**	Not Supplied
Description	-	**Sample Type**	Single Individual Rock Core Specimen

Sample and Test Details

Average Sample Diameter (mm)	49.4	Couplant	Honey
Sample Height (mm)	129.3	Probe Type	63.6mm "P" & "S" Wave
Sample Density (t/m^3)	2.66	Test Apparatus	GCTS- ULT 100 - Ultrasonic Velocity
Applied Axial Stress (MPa)	1.0		

Test Results

"P" Velocity (m/s)	4549		
"P" Arrival Time (µsec)	42.3	Young's Modulus (GPa)	51.5
"S" Velocity (m/s)	2879	Poisson's Ratio	0.17
"S" Arrival Time (µsec)	65.6		

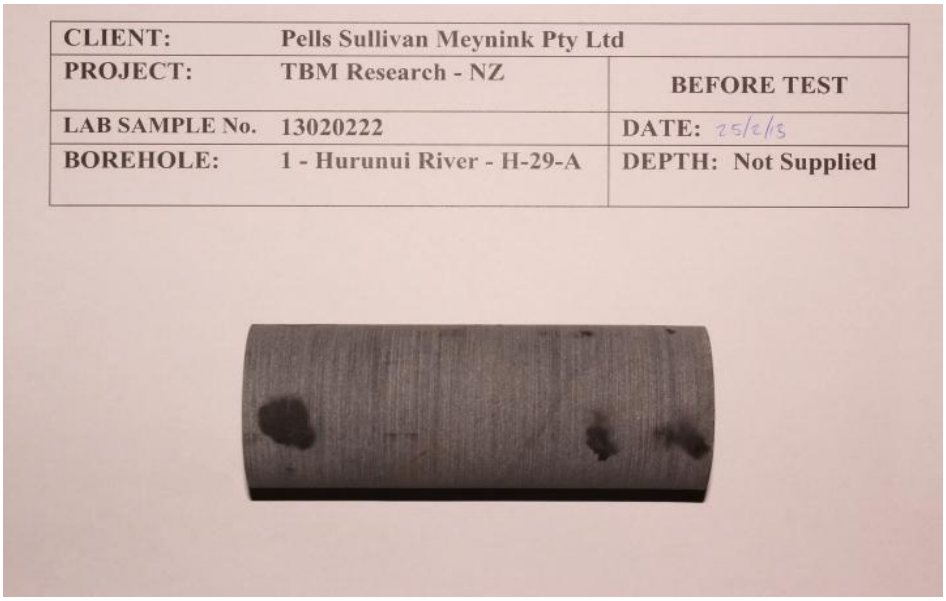

Notes/Remarks:

Sample/s supplied by client Photo not to scale Tested as received

Trilab
Soil Rock Calibration

Brisbane
346A Bilsen Road,
Geebung
QLD 4034
Ph: +61 7 3265 5656

Perth
2 Kimmer Place,
Queens Park
WA 6107
Ph: +61 8 9258 8323

DETERMINATION OF THE ULTRASONIC VELOCITY OF ROCK

Test Method: ASTM D2845 - 08 - Determination of Pulse Velocities and Ultrasonic Elastic Constants of Rock

Client	Pells Sullivan Meynink Pty Ltd	**Report No.**	13020222- SON
Project	TBM Research - NZ	**Test Date**	25/02/2013
		Report Date	25/02/2013
Client ID	1 - Hurunui River - H-29-A	**Depth (m)**	Not Supplied
Description	-		

"P" WAVEFORM

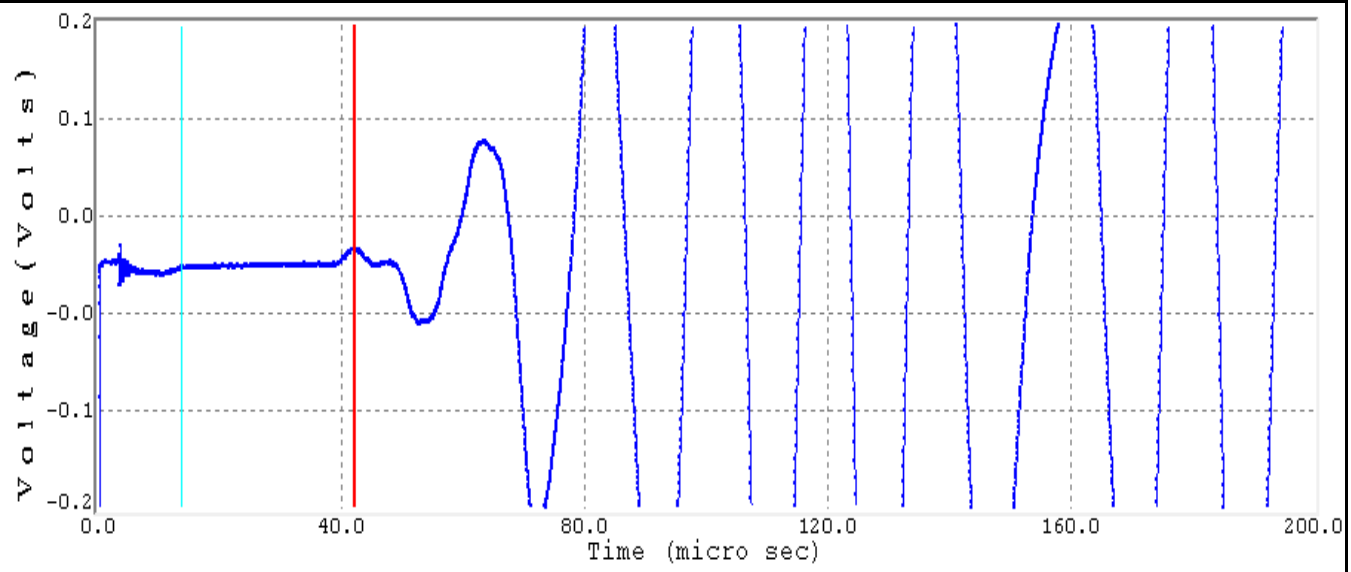

"S" WAVEFORM

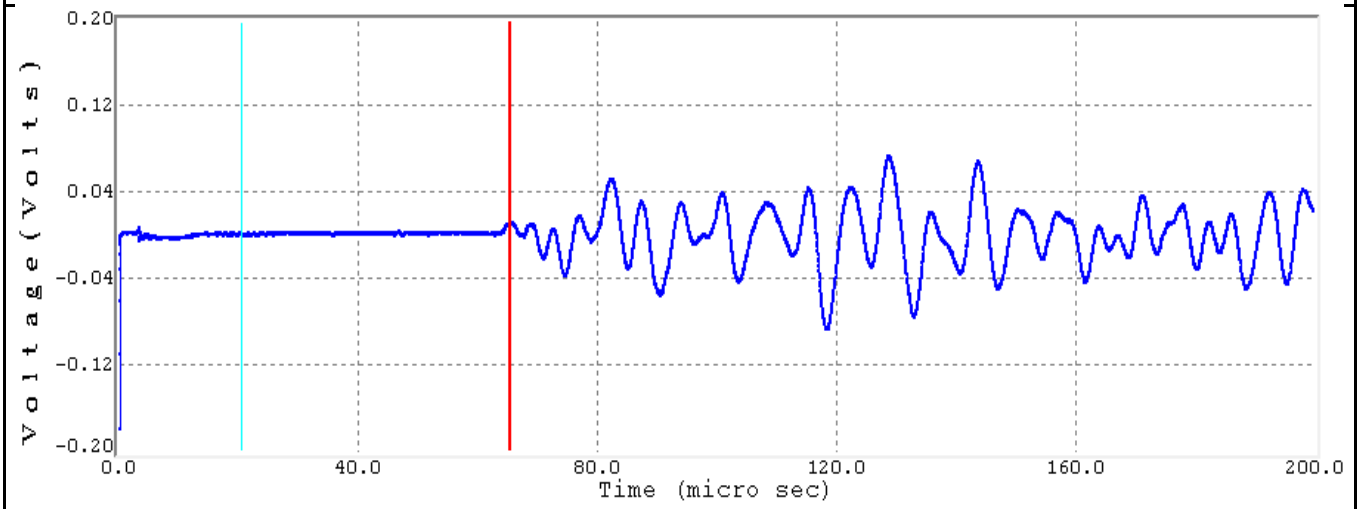

Notes/Remarks:

Sample/s supplied by client

Trilab
Soil Rock Calibration

Brisbane
346A Bilsen Road,
Geebung
QLD 4034
Ph: +61 7 3265 5656

Perth
2 Kimmer Place,
Queens Park
WA 6107
Ph: +61 8 9258 8323

CERCHAR ABRASIVITY INDEX TEST REPORT

ASTM D7625 - 10 Standard Test Method for Laboratory Determination of Abrasiveness of Rock Using the Cerchar Method

Client	Pells Sullivan Meynink Pty Ltd	**Report No.**	13020225-CERC
Project	TBM Research - NZ	**Test Date**	6/03/2013
		Report Date	7/03/2013
Client ID	4 - Ashey Gorge - A.4.9	**Depth (m)**	Not Supplied
Description		**Sample Type**	Single Individual Rock Core Specimen

SAMPLE DETAILS

Sample Diameter (mm):	49.4	**Moisture Content (%):**	0.3
Sample Height (mm):	23.2	**Dry Density (t/m^3)**	2.58
Surface Type :	Smooth (Saw Cut) Surface	**Wet Density (t/m^3)**	2.59

RESULTS OF TESTING

Hardness of Tip Used	16 HRC	Hardness of Tip Used	40 HRC	Hardness of Tip Used	57 HRC
Average Diameter (mm)	*CAI	Average Diameter (mm)	*CAI	Average Diameter (mm)	*CAI
0.50	**5.43**	**0.37**	**4.13**	**0.35**	**3.92**

Linear Relationship between Tip Hardness and CAI

CAI = (-0.0214 x HRC) + 5.5236

Average CAI (HRC55) = 4.35

Classification : Extreme abrasiveness

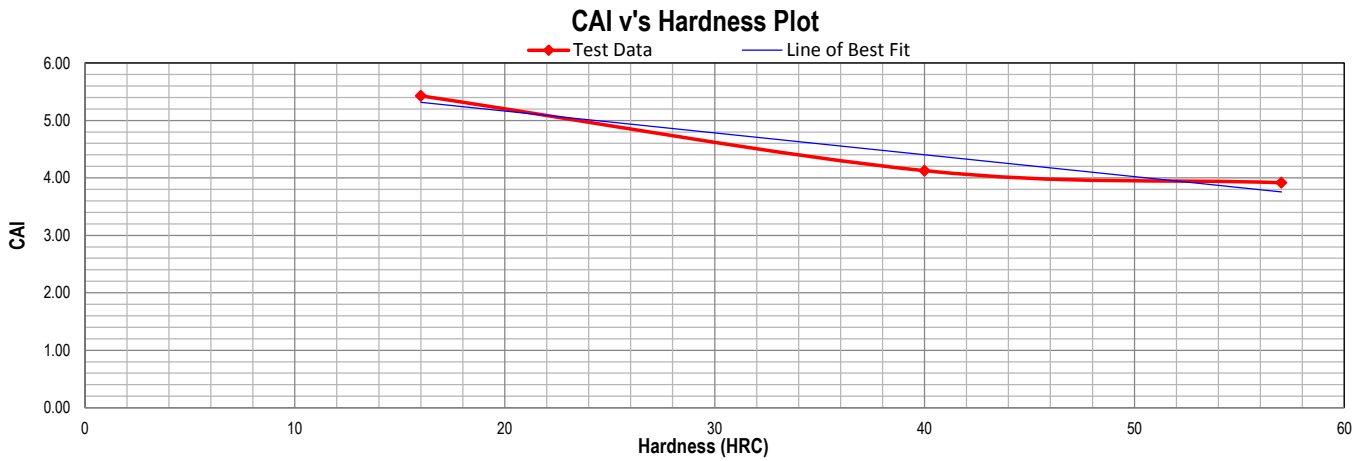

Remarks:

Sample/s supplied by client

* CAI values corrected for smooth surface.

Trilab
Soil Rock Calibration

Brisbane
346A Bilsen Road,
Geebung
QLD 4034
Ph: +61 7 3265 5656

Perth
2 Kimmer Place,
Queens Park
WA 6107
Ph: +61 8 9258 8323

CERCHAR ABRASIVITY INDEX TEST REPORT

ASTM D7625 - 10 Standard Test Method for Laboratory Determination of Abrasiveness of Rock Using the Cerchar Method

Client	Pells Sullivan Meynink Pty Ltd	**Report No.**	13020225-CERC
Project	TBM Research - NZ	**Test Date**	6/03/2013
		Report Date	7/03/2013
Client ID	4 - Ashey Gorge - A.4.9	**Depth (m)**	Not Supplied
Description		**Sample Type**	Single Individual Rock Core Specimen

RESULTS OF TESTING

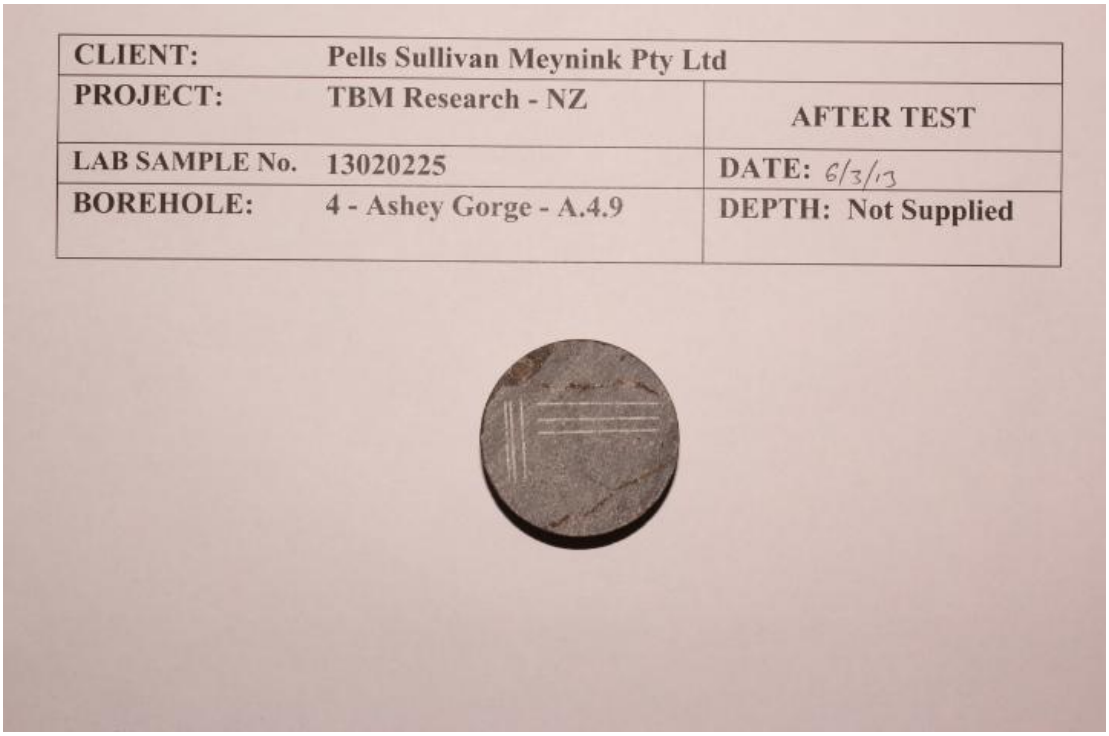

Remarks:

Sample/s supplied by client

* CAI values corrected for smooth surface.

Trilab
Soil Rock Calibration

Brisbane
346A Bilsen Road,
Geebung
QLD 4034
Ph: +61 7 3265 5656

Perth
2 Kimmer Place,
Queens Park
WA 6107
Ph: +61 8 9258 8323

CERCHAR ABRASIVITY INDEX TEST REPORT

ASTM D7625 - 10 Standard Test Method for Laboratory Determination of Abrasiveness of Rock Using the Cerchar Method

Client	Pells Sullivan Meynink Pty Ltd	**Report No.**	13020224-CERC
Project	TBM Research - NZ	**Test Date**	6/03/2013
		Report Date	7/03/2013
Client ID	3 - Ashey Gorge - A.219	**Depth (m)**	Not Supplied
Description		**Sample Type**	Single Individual Rock Core Specimen

SAMPLE DETAILS

Sample Diameter (mm):	49.5	**Moisture Content (%):**	0.6
Sample Height (mm):	18.7	**Dry Density (t/m^3)**	2.47
Surface Type :	Smooth (Saw Cut) Surface	**Wet Density (t/m^3)**	2.49

RESULTS OF TESTING

Hardness of Tip Used	16 HRC	Hardness of Tip Used	40 HRC	Hardness of Tip Used	57 HRC
Average Diameter (mm)	*CAI	Average Diameter (mm)	*CAI	Average Diameter (mm)	*CAI
0.50	5.47	0.39	4.33	0.28	3.29

Linear Relationship between Tip Hardness and CAI

CAI = (-0.049 x HRC) + 6.2041

Average CAI (HRC55) = 3.51

Classification : High abrasiveness

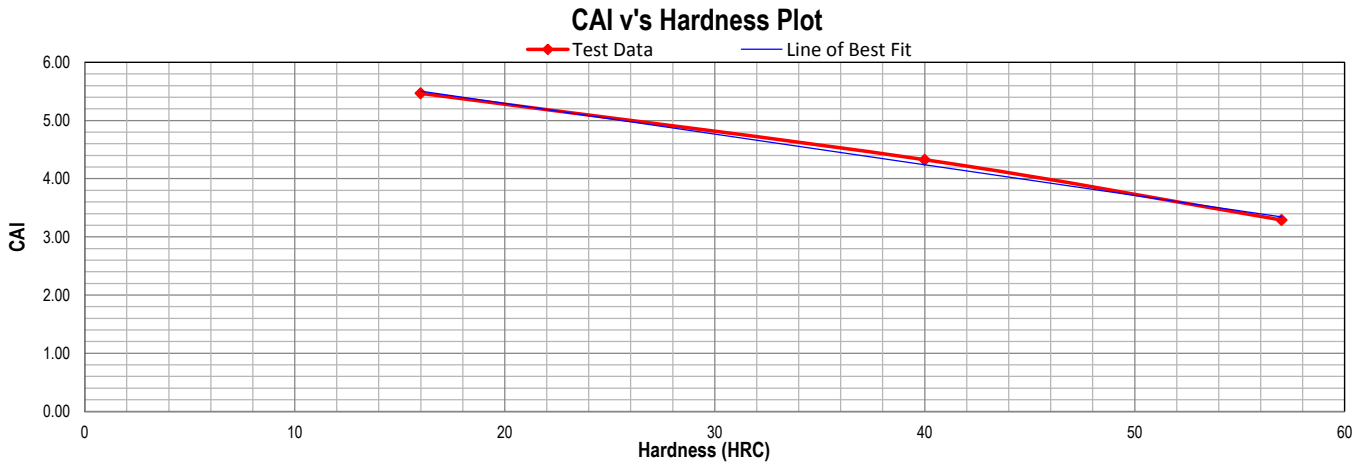

Remarks:

Sample/s supplied by client

* CAI values corrected for smooth surface.

Laboratory No. 9926

Trilab
Soil Rock Calibration

Brisbane
346A Bilsen Road,
Geebung
QLD 4034
Ph: +61 7 3265 5656

Perth
2 Kimmer Place,
Queens Park
WA 6107
Ph: +61 8 9258 8323

CERCHAR ABRASIVITY INDEX TEST REPORT

ASTM D7625 - 10 Standard Test Method for Laboratory Determination of Abrasiveness of Rock Using the Cerchar Method

Client	Pells Sullivan Meynink Pty Ltd	**Report No.**	13020224-CERC
Project	TBM Research - NZ	**Test Date**	6/03/2013
		Report Date	7/03/2013
Client ID	3 - Ashey Gorge - A.219	**Depth (m)**	Not Supplied
Description		**Sample Type**	Single Individual Rock Core Specimen

RESULTS OF TESTING

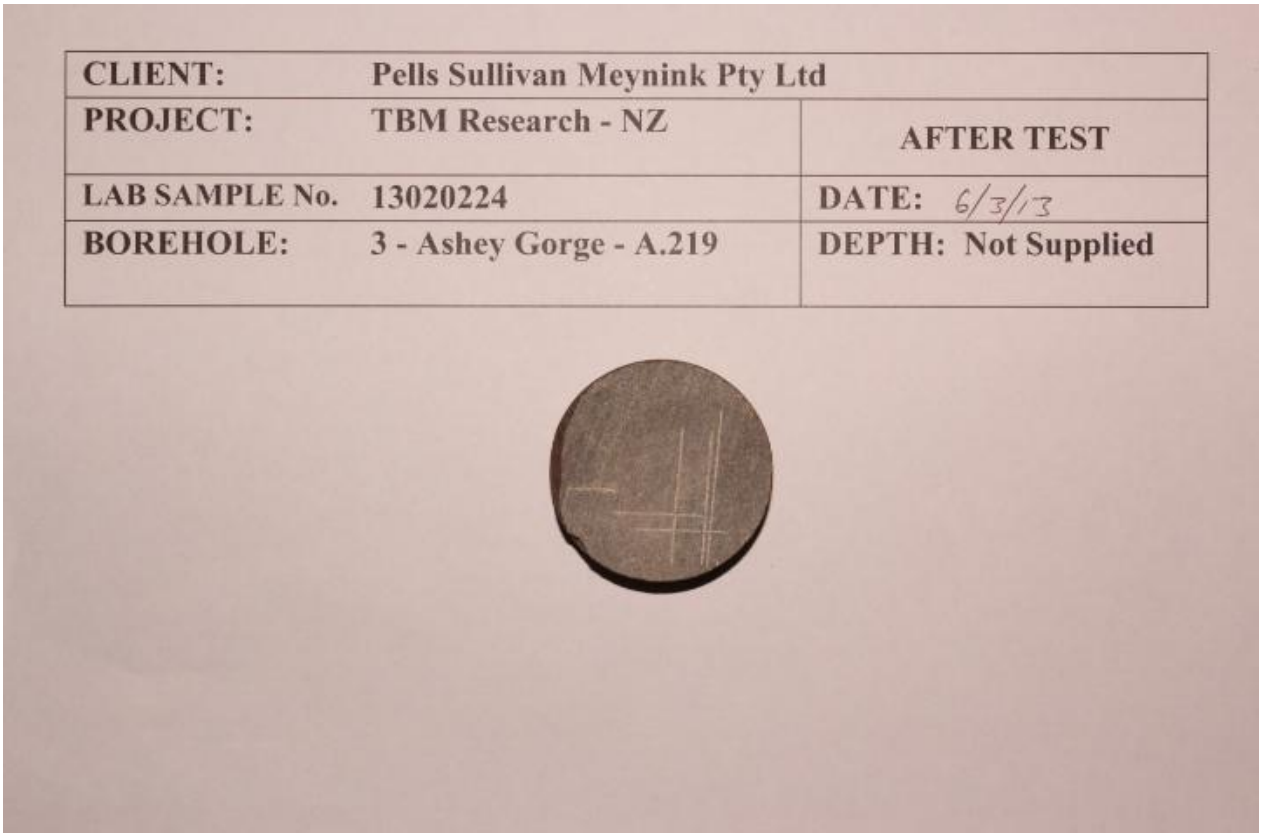

Remarks:

Sample/s supplied by client

* CAI values corrected for smooth surface.

Trilab
Soil Rock Calibration

Brisbane
346A Bilsen Road,
Geebung
QLD 4034
Ph: +61 7 3265 5656

Perth
2 Kimmer Place,
Queens Park
WA 6107
Ph: +61 8 9258 8323

UNIAXIAL COMPRESSIVE STRENGTH & DEFORMATION TEST REPORT

Test Method: AS 4133.4.3.1

Client	Pells Sullivan Meynink Pty Ltd	**Report No.**	13020224-MOD
Project	TBM Research - NZ	**Test Date**	26/02/2013
		Report Date	27/02/2013
Client ID	3 - Ashey Gorge - A.219	**Depth (m)**	Not Supplied
Description	-	**Sample Type**	Single Individual Rock Core Specimen

Uniaxial Compressive Strength 146 MPa

	Young's Modulus	Poisson Ratio	
Tangent	46.6 GPa	0.114	from 14 % to 34 % of Max UCS
Secant	45.7 GPa	0.115	from 0 % to 34 % of Max UCS

Axial Stress vs Strain Plots

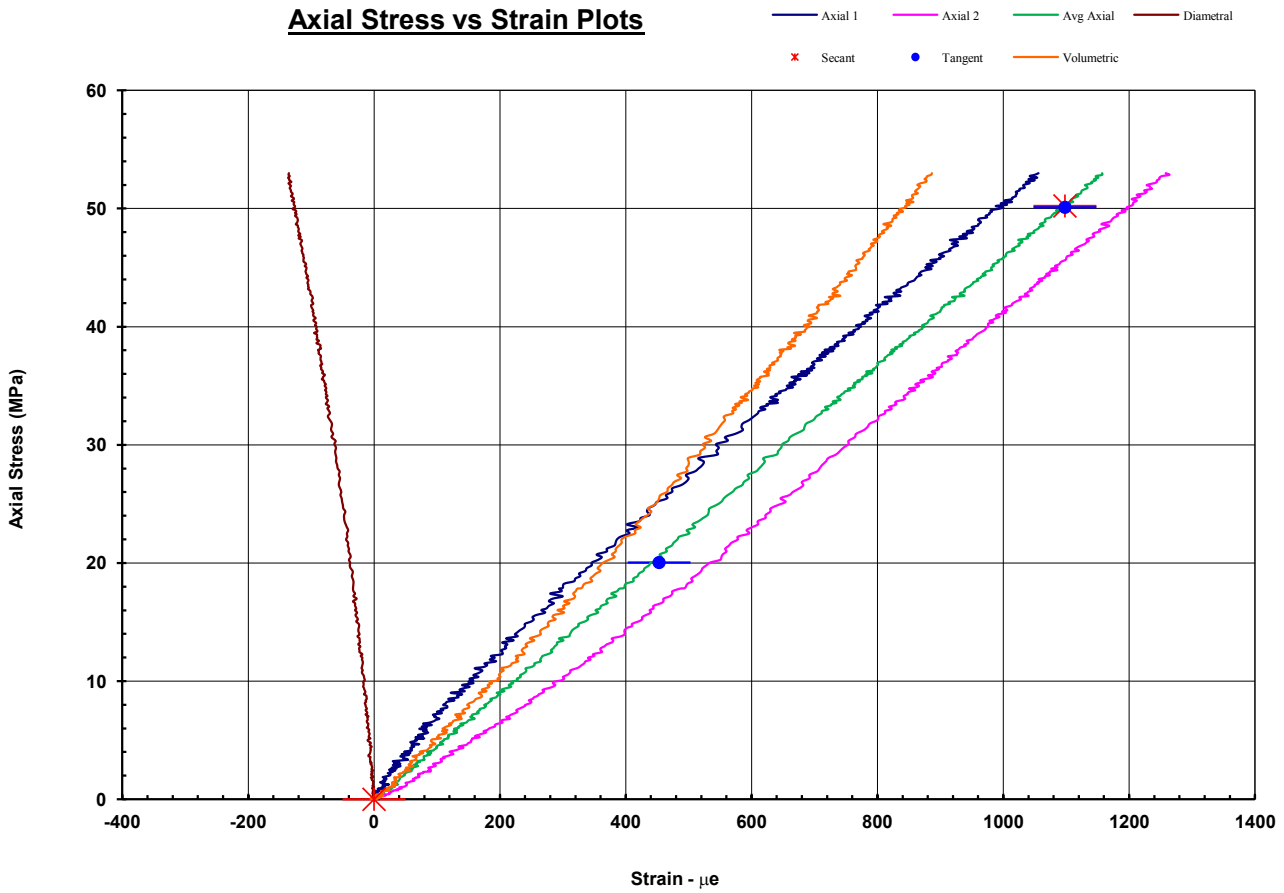

Notes/Remarks: Tested as received.

Sample/s supplied by client

Graph not to scale

Accredited for compliance with ISO/IES 17025.
The results of the tests, calibrations, and/or measurements included in this document are traceable to Australian/National Standards.

Tested at Trilab Brisbane Laboratory.

Authorised Signatory
J. Russell

NATA ACCREDITED FOR TECHNICAL COMPETENCE

Laboratory No. 9926

Trilab
Soil Rock Calibration

Brisbane
346A Bilsen Road,
Geebung
QLD 4034
Ph: +61 7 3265 5656

Perth
2 Kimmer Place,
Queens Park
WA 6107
Ph: +61 8 9258 8323

UNIAXIAL COMPRESSIVE STRENGTH & DEFORMATION TEST REPORT

Test Method: AS 4133.4.3.1

Client	Pells Sullivan Meynink Pty Ltd	**Report No.**	13020224-MOD
Project	TBM Research - NZ	**Test Date**	26/02/2013
		Report Date	27/02/2013
Client ID	3 - Ashey Gorge - A.219	**Depth (m)**	Not Supplied
Description	-		

Uniaxial Compressive Strength 146 MPa

Average Sample Diameter (mm)	49.4	Moisture Content (%)	0.5
Sample Height (mm)	135.0	Wet Density (t/m^3)	2.63
Duration of Test (min)	10.10	Dry Density (t/m^3)	2.62
Rate of Loading (MPa/min)	14.43	Bedding (°)	Nil
Mode of Failure	Disintegration	Test Apparatus	Kelba 1000kN Load Cell
Specific Energy (MJ/m^3)	0.031		

Specific energy determined from area under curve between 0 and 1,157με

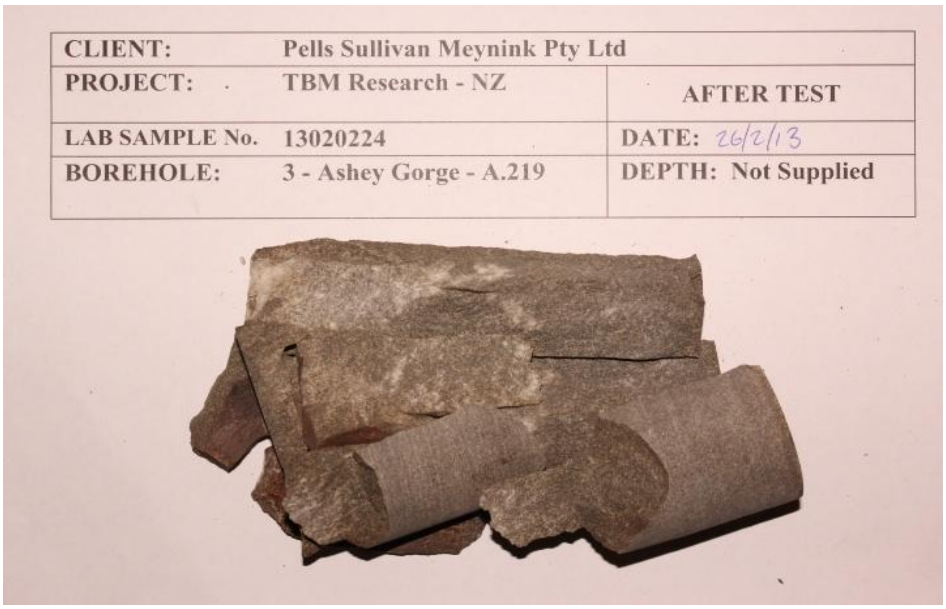

Photo not to scale

Notes/Remarks:

Accredited for compliance with ISO/IES 17025.
The results of the tests, calibrations, and/or measurements included in this document are traceable to Australian/National Standards.

Tested at Trilab Brisbane Laboratory.

Authorised Signatory
J. Russell

NATA ACCREDITED FOR TECHNICAL COMPETENCE

Laboratory No. 9926

Trilab
Soil Rock Calibration

Brisbane
346A Bilsen Road,
Geebung
QLD 4034
Ph: +61 7 3265 5656

Perth
2 Kimmer Place,
Queens Park
WA 6107
Ph: +61 8 9258 8323

DETERMINATION OF THE ULTRASONIC VELOCITY OF ROCK

Test Method: ASTM D2845 - 08 - Determination of Pulse Velocities and Ultrasonic Elastic Constants of Rock

Client	Pells Sullivan Meynink Pty Ltd	**Report No.**	13020224- SON
Project	TBM Research - NZ	**Test Date**	25/02/2013
		Report Date	25/02/2013
Client ID	3 - Ashey Gorge - A.219	**Depth (m)**	Not Supplied
Description	-	**Sample Type**	Single Individual Rock Core Specimen

Sample and Test Details

Average Sample Diameter (mm)	49.4	Couplant	Honey
Sample Height (mm)	135.0	Probe Type	63.6mm "P" & "S" Wave
Sample Density (t/m^3)	2.63	Test Apparatus	GCTS- ULT 100 - Ultrasonic Velocity
Applied Axial Stress (MPa)	1.0		

Test Results

"P" Velocity (m/s)	4521		
"P" Arrival Time (µsec)	43.7	Young's Modulus (GPa)	44.4
"S" Velocity (m/s)	2592	Poisson's Ratio	0.26
"S" Arrival Time (µsec)	72.8		

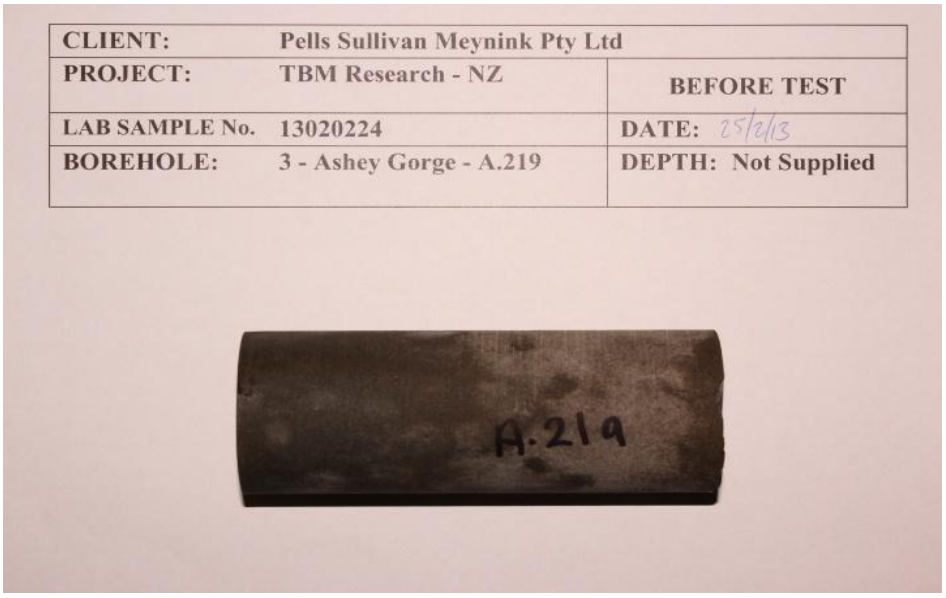

Notes/Remarks:

Sample/s supplied by client Photo not to scale Tested as received

Trilab
Soil Rock Calibration

Brisbane
346A Bilsen Road,
Geebung
QLD 4034
Ph: +61 7 3265 5656

Perth
2 Kimmer Place,
Queens Park
WA 6107
Ph: +61 8 9258 8323

DETERMINATION OF THE ULTRASONIC VELOCITY OF ROCK

Test Method: ASTM D2845 - 08 - Determination of Pulse Velocities and Ultrasonic Elastic Constants of Rock

Client	Pells Sullivan Meynink Pty Ltd	**Report No.**	13020224- SON
Project	TBM Research - NZ	**Test Date**	25/02/2013
		Report Date	25/02/2013
Client ID	3 - Ashey Gorge - A.219	**Depth (m)**	Not Supplied
Description	-		

"P" WAVEFORM

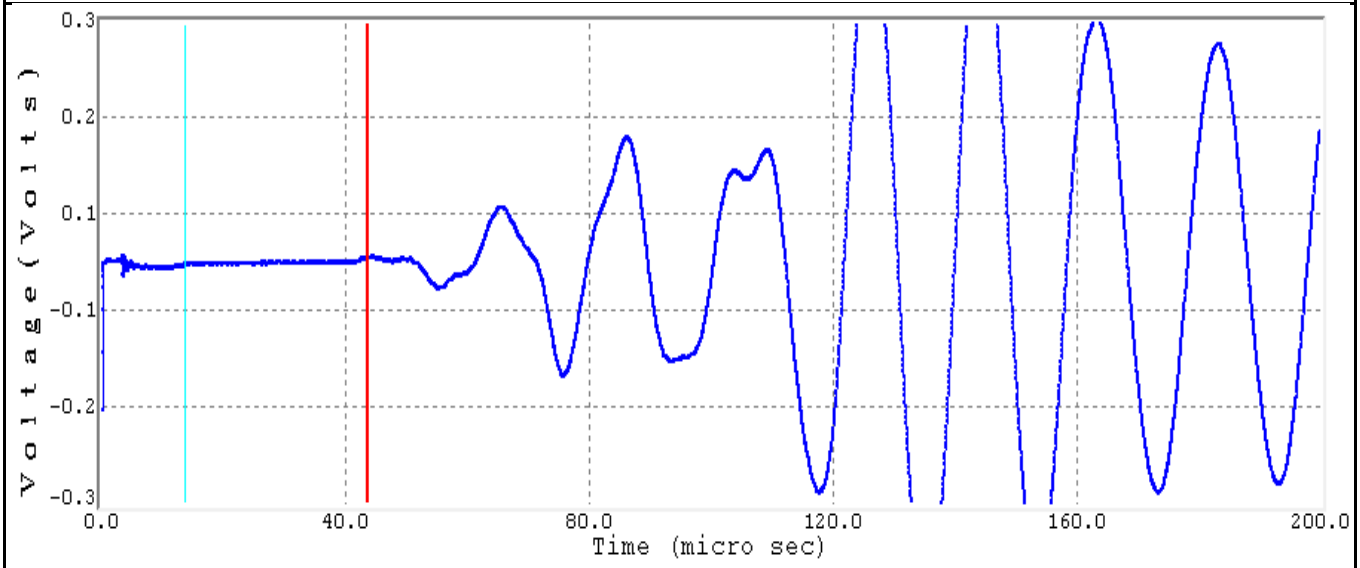

"S" WAVEFORM

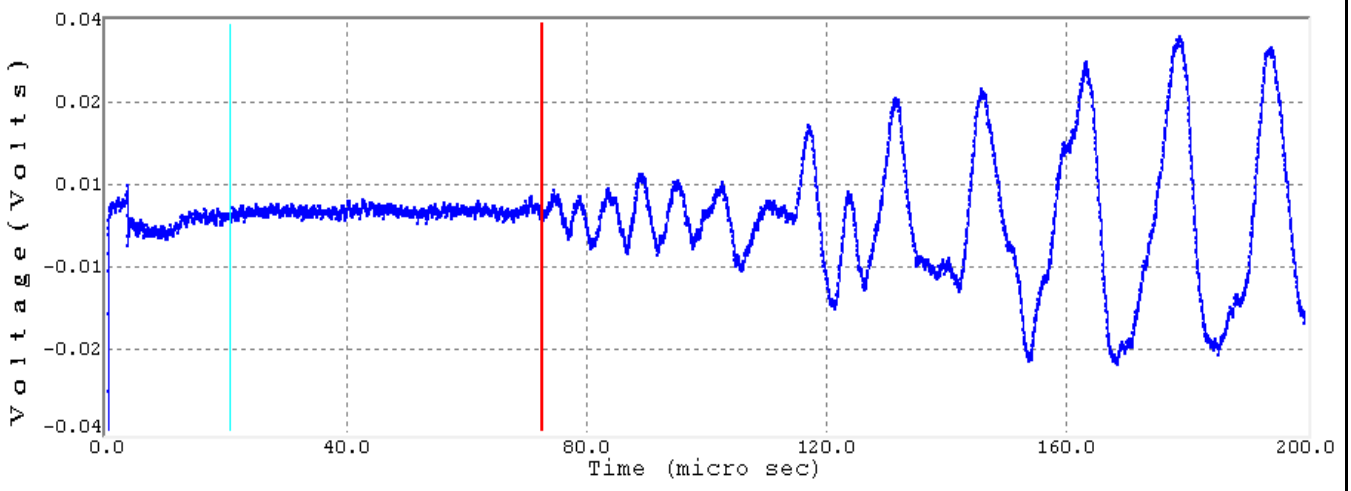

Notes/Remarks:

Sample/s supplied by client

Trilab
Soil Rock Calibration

Brisbane
346A Bilsen Road,
Geebung
QLD 4034
Ph: +61 7 3265 5656

Perth
2 Kimmer Place,
Queens Park
WA 6107
Ph: +61 8 9258 8323

CERCHAR ABRASIVITY INDEX TEST REPORT

ASTM D7625 - 10 Standard Test Method for Laboratory Determination of Abrasiveness of Rock Using the Cerchar Method

Client	Pells Sullivan Meynink Pty Ltd	**Report No.**	13020226-CERC
Project	TBM Research - NZ	**Test Date**	6/03/2013
		Report Date	7/03/2013
Client ID	5 - Opuna Dam - O.5.A	**Depth (m)**	Not Supplied
Description		**Sample Type**	Single Individual Rock Core Specimen

SAMPLE DETAILS

Sample Diameter (mm):	49.5	**Moisture Content (%):**	0.1
Sample Height (mm):	62	**Dry Density (t/m^3)**	2.65
Surface Type :	Smooth (Saw Cut) Surface	**Wet Density (t/m^3)**	2.65

RESULTS OF TESTING

Hardness of Tip Used	16 HRC	Hardness of Tip Used	40 HRC	Hardness of Tip Used	57 HRC
Average Diameter (mm)	*CAI	Average Diameter (mm)	*CAI	Average Diameter (mm)	*CAI
0.50	**5.41**	**0.45**	**4.93**	**0.38**	**4.23**

Linear Relationship between Tip Hardness and CAI

CAI = (-0.0326 x HRC) + 6.0638

Average CAI (HRC55) = 4.27

Classification : Extreme abrasiveness

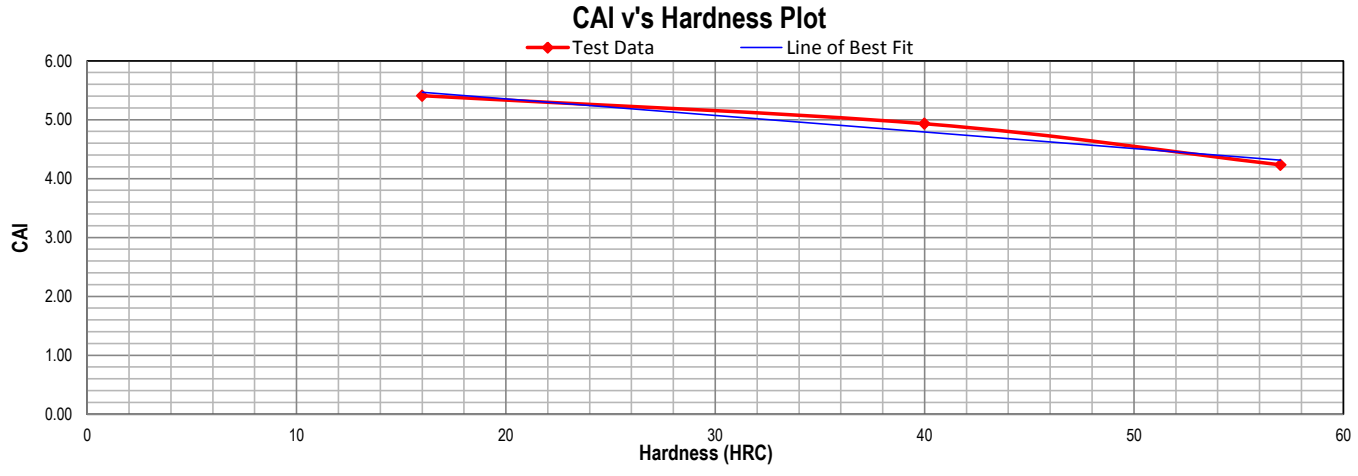

Remarks:

Sample/s supplied by client

* CAI values corrected for smooth surface.

Trilab
Soil Rock Calibration

Brisbane
346A Bilsen Road,
Geebung
QLD 4034
Ph: +61 7 3265 5656

Perth
2 Kimmer Place,
Queens Park
WA 6107
Ph: +61 8 9258 8323

CERCHAR ABRASIVITY INDEX TEST REPORT

ASTM D7625 - 10 Standard Test Method for Laboratory Determination of Abrasiveness of Rock Using the Cerchar Method

Client	Pells Sullivan Meynink Pty Ltd	**Report No.**	13020226-CERC
Project	TBM Research - NZ	**Test Date**	6/03/2013
		Report Date	7/03/2013
Client ID	5 - Opuna Dam - O.5.A	**Depth (m)**	Not Supplied
Description		**Sample Type**	Single Individual Rock Core Specimen

RESULTS OF TESTING

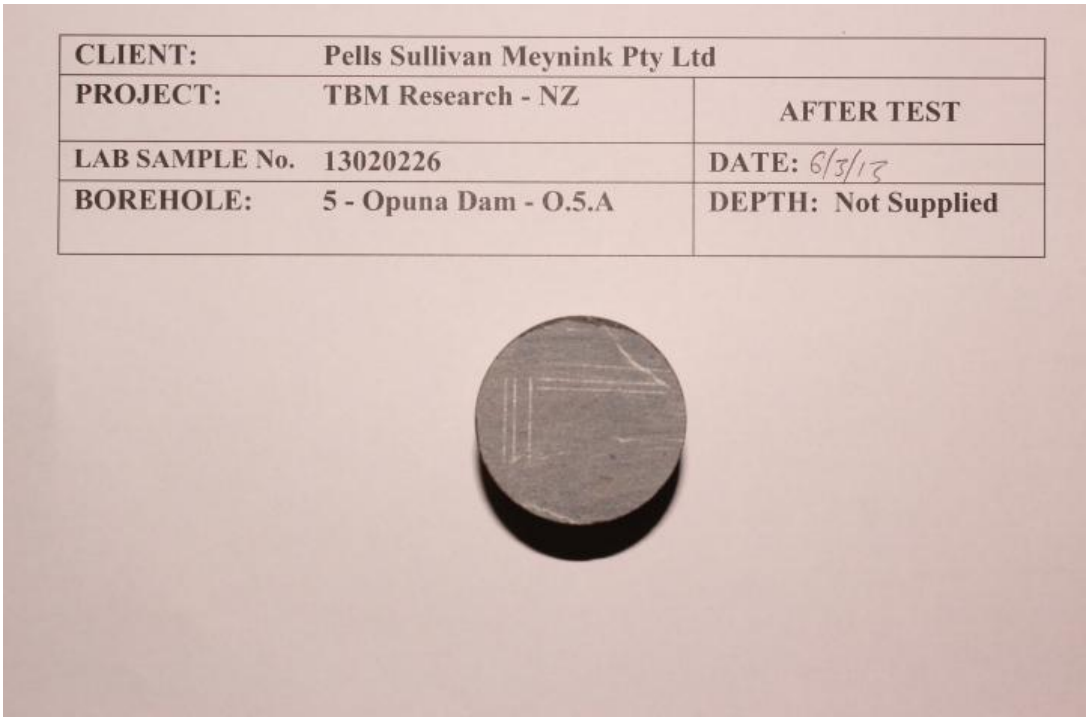

Remarks:

Sample/s supplied by client

* CAI values corrected for smooth surface.

Trilab
Soil Rock Calibration

Brisbane
346A Bilsen Road,
Geebung
QLD 4034
Ph: +61 7 3265 5656

Perth
2 Kimmer Place,
Queens Park
WA 6107
Ph: +61 8 9258 8323

UNIAXIAL COMPRESSIVE STRENGTH & DEFORMATION TEST REPORT

Test Method: AS 4133.4.3.1

Client	Pells Sullivan Meynink Pty Ltd	**Report No.**	13020227-MOD
Project	TBM Research - NZ	**Test Date**	26/02/2013
		Report Date	27/02/2013
Client ID	6 - Opuna Dam - O.1.H	**Depth (m)**	Not Supplied
Description	-	**Sample Type**	Single Individual Rock Core Specimen

Uniaxial Compressive Strength 189 MPa

	Young's Modulus	Poisson Ratio	
Tangent	60.1 GPa	0.189	from 11 % to 26 % of Max UCS
Secant	55.8 GPa	0.189	from 0 % to 26 % of Max UCS

Axial Stress vs Strain Plots

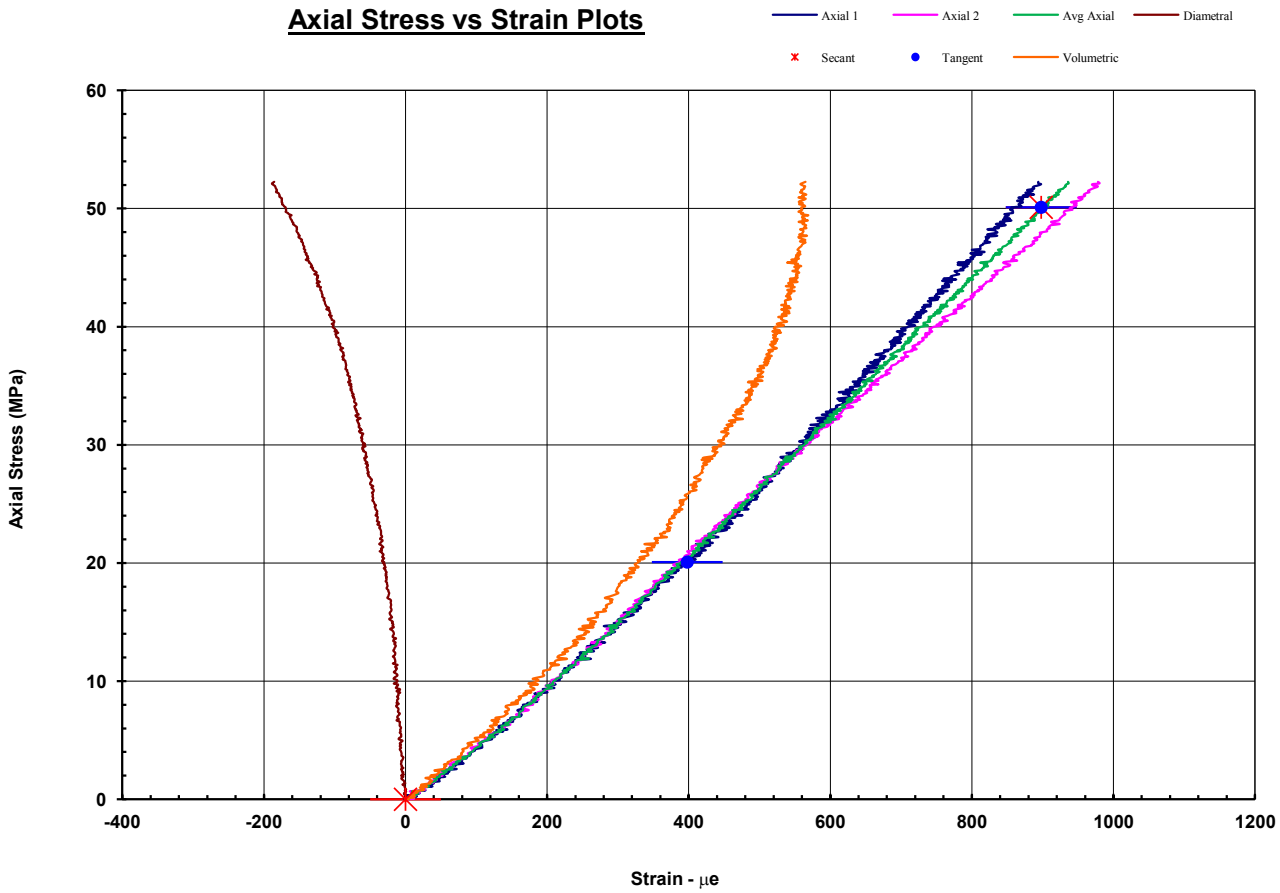

Notes/Remarks: Tested as received.

Sample/s supplied by client

Graph not to scale

Accredited for compliance with ISO/IES 17025.
The results of the tests, calibrations, and/or measurements included in this document are traceable to Australian/National Standards.

Tested at Trilab Brisbane Laboratory.

Authorised Signatory
J. Russell

NATA ACCREDITED FOR TECHNICAL COMPETENCE

Laboratory No. 9926

Trilab
Soil Rock Calibration

Brisbane
346A Bilsen Road,
Geebung
QLD 4034
Ph: +61 7 3265 5656

Perth
2 Kimmer Place,
Queens Park
WA 6107
Ph: +61 8 9258 8323

UNIAXIAL COMPRESSIVE STRENGTH & DEFORMATION TEST REPORT

Test Method: AS 4133.4.3.1

Client	Pells Sullivan Meynink Pty Ltd	**Report No.**	13020227-MOD
Project	TBM Research - NZ	**Test Date**	26/02/2013
		Report Date	27/02/2013
Client ID	6 - Opuna Dam - O.1.H	**Depth (m)**	Not Supplied
Description	-		

Uniaxial Compressive Strength 189 MPa

Average Sample Diameter (mm)	49.4	Moisture Content (%)	0.1
Sample Height (mm)	135.1	Wet Density (t/m^3)	2.70
Duration of Test (min)	8.28	Dry Density (t/m^3)	2.70
Rate of Loading (MPa/min)	22.78	Bedding (°)	Nil
Mode of Failure	Disintegration	Test Apparatus	Kelba 1000kN Load Cell
Specific Energy (MJ/m^3)	0.026		

Specific energy determined from area under curve between 0 and 937με

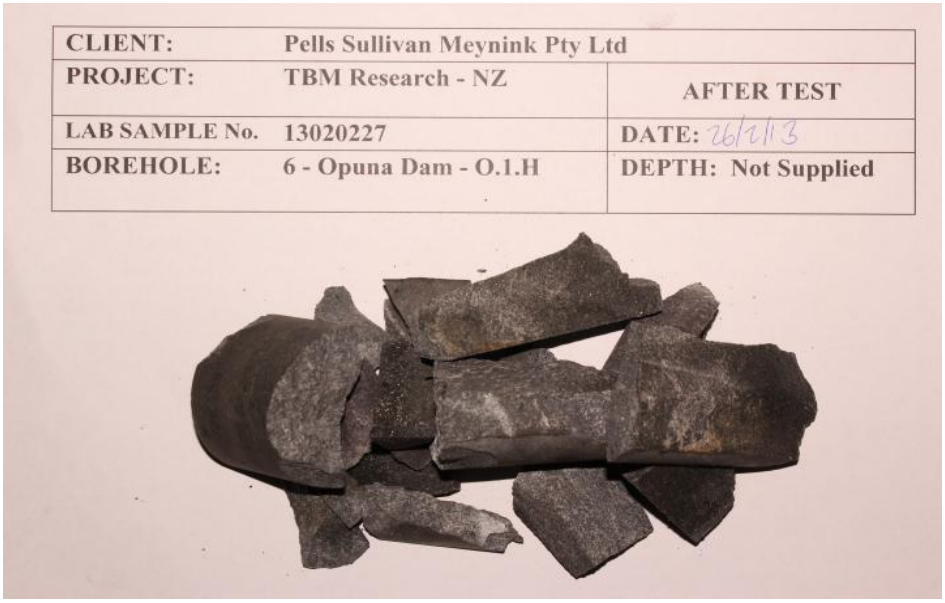

Photo not to scale

Notes/Remarks:

Accredited for compliance with ISO/IES 17025.
The results of the tests, calibrations, and/or measurements included in this document are traceable to Australian/National Standards.

Tested at Trilab Brisbane Laboratory.

Authorised Signatory
J. Russell

NATA ACCREDITED FOR TECHNICAL COMPETENCE

Laboratory No. 9926

Trilab
Soil Rock Calibration

Brisbane
346A Bilsen Road,
Geebung
QLD 4034
Ph: +61 7 3265 5656

Perth
2 Kimmer Place,
Queens Park
WA 6107
Ph: +61 8 9258 8323

DETERMINATION OF THE ULTRASONIC VELOCITY OF ROCK

Test Method: ASTM D2845 - 08 - Determination of Pulse Velocities and Ultrasonic Elastic Constants of Rock

Client	Pells Sullivan Meynink Pty Ltd	**Report No.**	13020227- SON
Project	TBM Research - NZ	**Test Date**	25/02/2013
		Report Date	25/02/2013
Client ID	6 - Opuna Dam - O.1.H	**Depth (m)**	Not Supplied
Description	-	**Sample Type**	Single Individual Rock Core Specimen

Sample and Test Details

Average Sample Diameter (mm)	49.4	Couplant	Honey
Sample Height (mm)	135.1	Probe Type	63.6mm "P" & "S" Wave
Sample Density (t/m^3)	2.70	Test Apparatus	GCTS- ULT 100 - Ultrasonic Velocity
Applied Axial Stress (MPa)	1.0		

Test Results

"P" Velocity (m/s)	4902		
"P" Arrival Time (µsec)	41.4	Young's Modulus (GPa)	53.4
"S" Velocity (m/s)	2807	Poisson's Ratio	0.26
"S" Arrival Time (µsec)	68.9		

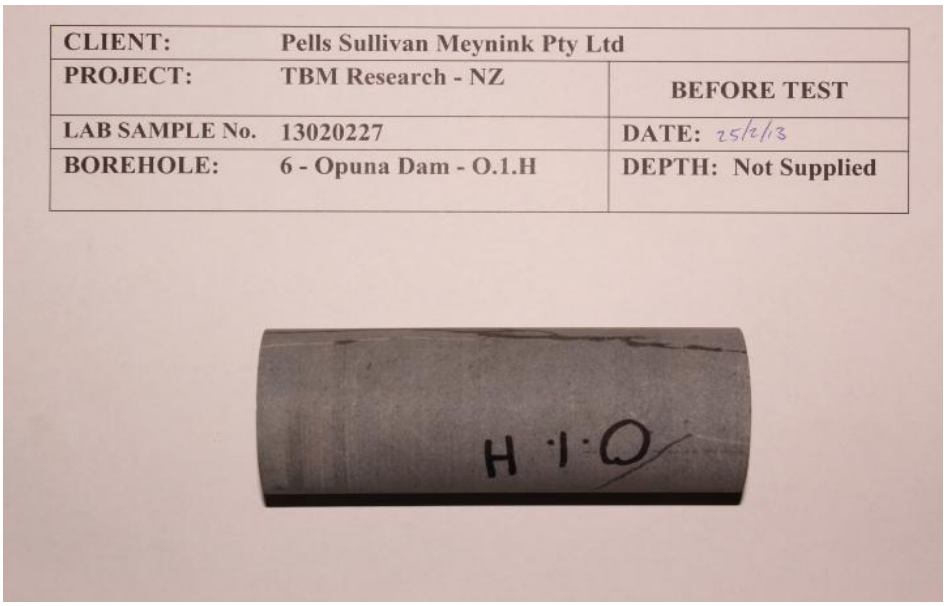

Notes/Remarks:

Sample/s supplied by client Photo not to scale Tested as received

Trilab
Soil Rock Calibration

Brisbane
346A Bilsen Road,
Geebung
QLD 4034
Ph: +61 7 3265 5656

Perth
2 Kimmer Place,
Queens Park
WA 6107
Ph: +61 8 9258 8323

DETERMINATION OF THE ULTRASONIC VELOCITY OF ROCK

Test Method: ASTM D2845 - 08 - Determination of Pulse Velocities and Ultrasonic Elastic Constants of Rock

Client	Pells Sullivan Meynink Pty Ltd	**Report No.**	13020227- SON
Project	TBM Research - NZ	**Test Date**	25/02/2013
		Report Date	25/02/2013
Client ID	6 - Opuna Dam - O.1.H	**Depth (m)**	Not Supplied
Description	-		

"P" WAVEFORM

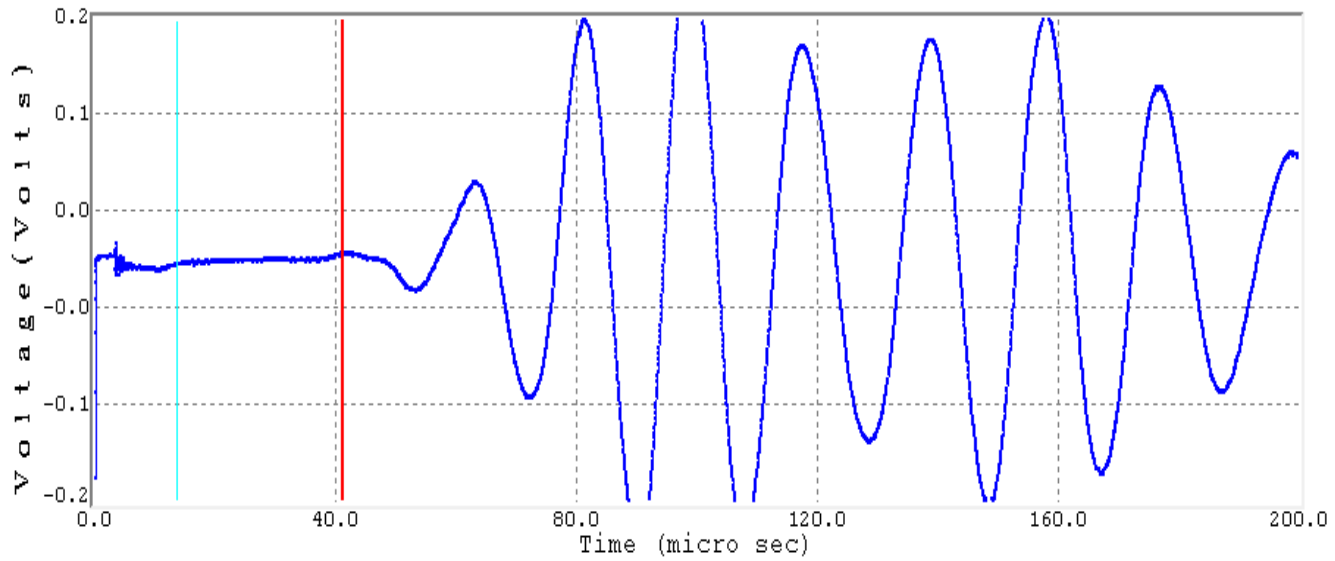

"S" WAVEFORM

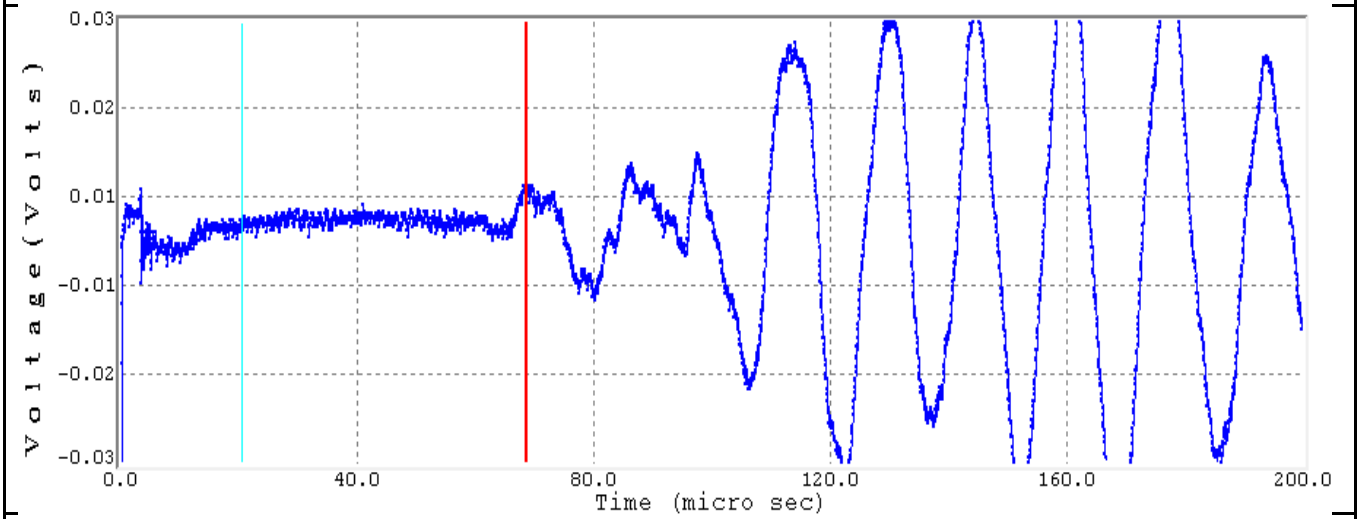

Notes/Remarks:

Sample/s supplied by client

Appendix C: Study site outcrop localities

Outcrop locations surveyed across the spatial extent of each study site.

C.1 Elliott Fault sites

Elliott Fault sites

GNS Faults (Rattenbury et al, 2006)

N

13a 5a 5b 5c 5d 5e 5f 5g 5h 5i 5j 5j.1 5k

50 m

10a 10b 10c 10d 10e 12a 6a 6b

50 m

1e 1e 1d 1c 1b 1a

50 m

2a 9a 11a 3a 7a 4a 8a 8b

500 m

Imagery Source: Canterbury Aerial Photo

Hururui River sites

GNS Faults (Rattenbury et al, 2006)

C.2 Hururui River sites

N

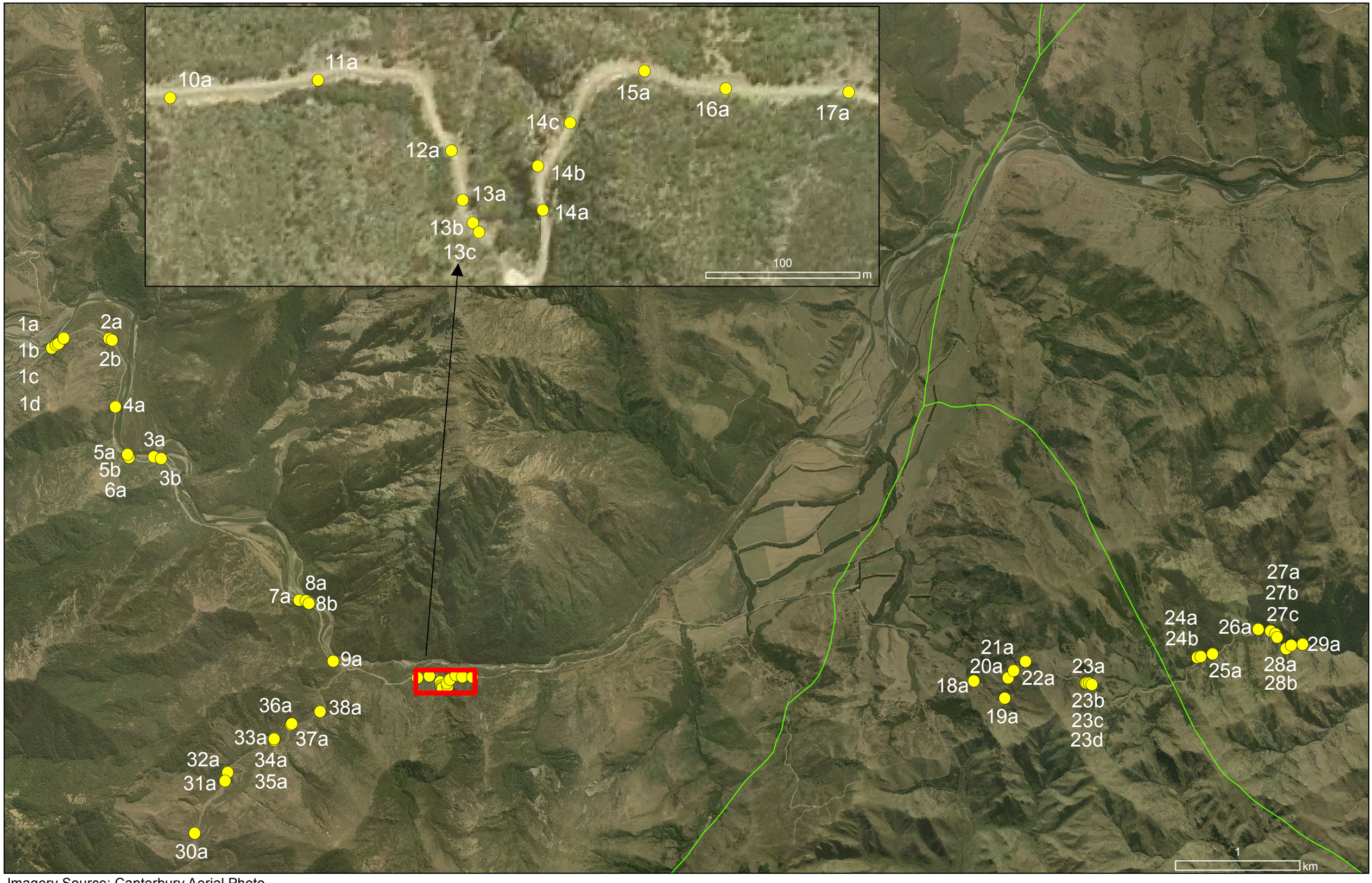

Imagery Source: Canterbury Aerial Photo

Ashley Gorge sites

GNS Faults (Forsyth et al, 2008)

C.3 Ashley River Gorge sites

N

13A
12A
42A
41A
40A
43A
43B
14A
200 m

1A
2A
3A
44A
7A
7B
45A
8A
46A
9A
10A
47A
49A
48A
11A
50A
51A
15A
16A
17A
18A
19A
20A
21A
36A
38A
39A
37A
1 km

200 m
4A
57A
56A
5A
55A
6A
54A
53A
52A

35A
34A
28A
33B
29A
33A
30A
22A
31A
32A
27A
27B
23A
25A
26A
24A
200 m

Imagery Source: Canterbury Aerial Photo

C.4 Opuha Dam sites

Opuha Dam sites

GNS Faults (Cox & Barrell, 2007)

N

1 km

100 m

Text

1H 1G 1F 1E 1D 1C 1B 1A

2B 2A 4B 4A

6B 6A 3A

5A 5B 7C 7A 7B 8A 9A

11A 10A

Imagery Source: Canterbury Aerial Photo

Appendix D: Elliott Fault

Results derived from the lineation analysis, raw mapping data, analysis, raw lab testing data and calculations for the Elliott Fault study site.

D.1 Elliott Fault lineation analysis

Landscape lineation derived from aerial photography and DEM analysis.

D.1 Elliot Fault - lineation analysis

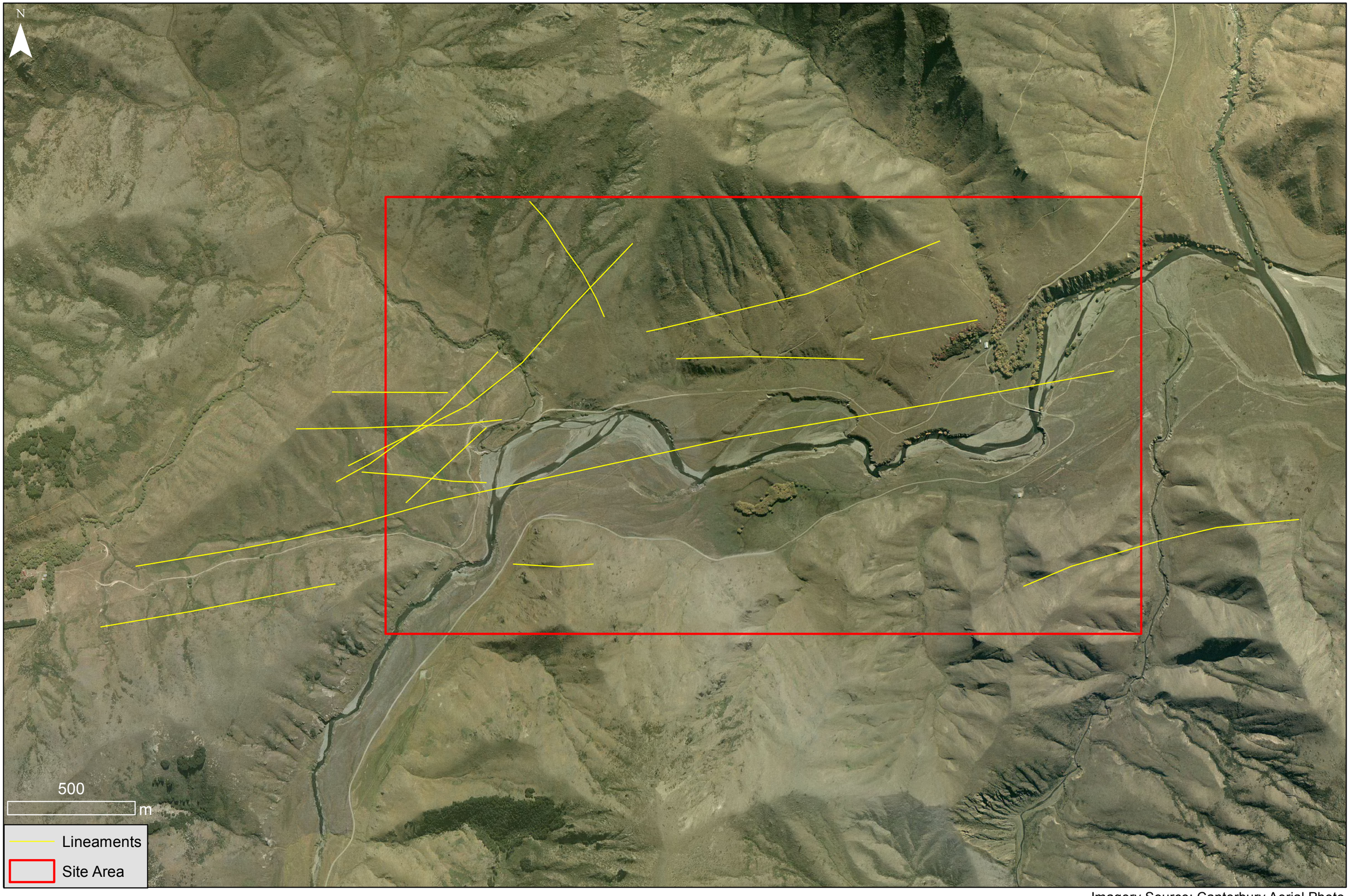

Imagery Source: Canterbury Aerial Photo

D.2 Elliott Fault raw mapping data

Mapping per field data sheets (Appendix A). Where data is missing, blanked out or ranges from other sites, information has been unobtainable due to access issues, poor rock/defect conditions, recording prior to the continual modification of the field sheets or previous recording of the defect (i.e. 1 x bedding plane between two lithologies).

D.2.1 Elliott Fault - Coherent Rock and bedding

Outcrop #	Weathering	Colour	Bedding fabric	Bedding thickness	Bedding development	Grain size	Rock name	Strength (rebound)	Strength (hammer)	Strength (MPa)	Dip	Dip direction	Raw field notes
1a	Sw-Mw	L-GY	M	Thin	VW		Sandstone				42	26	
1a	Sw-Mw	D-GY	M	Thin	VW		Mudstone				42	26	
1b	Sw	L-GY	M	Medium	VW		Sandstone				15	2	
1b	Sw	D-GY	M	Thin	VW		Mudstone				18	4	
1c				Thin			Mudstone						Note: Shear ~2m but as like 8b bedding can be inferred
1c	Hw-Cw	L-GY	M	Thin	MP-D		Sandstone						
1d	Sw-Mw	L-GY	M	Thin	VW		Sandstone				60	60	
1d	Sw-Mw	D-GY	M	Thin	VW		Mudstone				62	40	
1e	Sw	D-GY	M	Thin	VW		Mudstone	26, 32, 42	MS	52, 68, 100	55	40	
1e	Sw	L-GY	M	Thin	VW	F-M	Sandstone	42, 24, 38	MS	105, 47, 88	58	42	
2a	Sw-Mw	L-GY	M	Thick	WD	F-M	Sandstone	40, 42	S-VS	100, 105	30	80	
2a	Sw-Mw	D-GY	M	Thin	WD		Mudstone	20, 12	MS	40, 28	55	121	Note - Effect of degree of fracture on Schmidt hammer
3a	Sw-Mw	L-GY	M	Medium	WD	F-M	Sandstone	32, 24, 38, 52	VS	68, 47, 88, 170	60	93	
3a	Mw	D-GY	M	Thin	WD		Mudstone	20, 20, 26, 24	MS-S	40, 40, 52, 47	72	87	
3a	Mw	L-GY		Thin	VW	Fine	Sandstone				65	89	
4a	Mw	L-GY	M	Medium	D	F-M	Sandstone	50, 46	VS	150, 130	42	45	
4a	Mw	D-GY	M	Medium	D		Mudstone	14	MS	30	70	35	
5a	Mw	L-GY	M	Medium	VW	F-M	Sandstone	12, 20, 20	MS	28, 40, 40	71	125	
5a	Mw	D-GY-BR	M	Medium	VW		Mudstone	12	W-MS	28	73	127	
5b	Hw	OX-B	M	Thin	VW		Mudstone	10	W-MS	25	81	336	Too weathered
5b	Mw-Hw	L-GY	M	Thin	VW	F-M	Sandstone	20	MS	40	85	338	
5c	Mw-Hw	L-GY	M	Medium	WD-D	F-M	Sandstone	26, 20	VW	52, 40	79	134	
5c	Mw-Hw	D-GY	M	Medium	WD-D		Mudstone	20	VW	40	82	136	
5d	Hw	L-GY	M	Medium	WD	F-M	Sandstone		H-VW		51	119	
5d	Hw	D-GY	M	Thin	WD		Mudstone		H-VW				
5e	Hw-Cw	L-GY	M	Massive	M	F-M	Breccia		VS-H				Rotated coherent rock
5f	Hw-Cw	L-GY	M	Massive	D-M	F-M	Breccia		VS-H				
5g	Hw-Cw	L-GY	M	Massive	M		Breccia		S				less coherent - more clay, no intact clasts to describe
5h	Mw-Cw	L-GY	M	Massive	M	F-M	Breccia		VS-H				more coherent - harder clasts inside soft rock - to weak to measure strength
5i	Hw-Cw	L-GY	M	Massive	M	F-M	Breccia		VS-VW				Note: Massive fabric with incipient fracture
5j	Hw	D-GY	M	Massive	D-MP		Breccia		H-VW				Note: Massive fabric with incipient fracture, mudstone present
5j.1	Hw	L-GY	M	Medium	D	F-M	Breccia sand		VW				Note: Massive fabric with incipient fracture, Breccia with mud and sand present
5j.1	Hw	D-GY	M	Thin	D		Breccia mud		H-VS				Breccia with mud and sand present - grading/sorting of massive - bed folded
5k	Sw-Mw	L-GY	M	Thick	VW	F-M	Sandstone	56, 34, 16, 40	VW	180, 70, 34, 98	66	294	
5k	Sw-Mw	D-GY	M	Thick	VW		Mudstone	12, 11, 15	VW	28, 26, 32	69	300	
6a	Sw	L-GY	M	Thick	WD	F-M	Sandstone	40, 38, 22	S	100, 88, 44	54	149	
6b	Sw	L-GY	M	Thick	VW	F-M	Sandstone						To dangerous for measurements, sandstone hard intact
6b	Sw	D-GY	M	Thin	VW		Mudstone						Mudstone fragmentation/shear - see photo. Some medium sand in better condition than v thin mud
7a	Mw	L/D GY	M	Massive	D		Sandstone						No access to face
8a	Sw	L-GY	M	Thick	VW		Sandstone				43	65	Note: No access to face - dip/dip direction sighted
8a	Sw-Mw	D-GY	M	Thin	VW		Mudstone				66	79	Note: No access to face - dip/dip direction sighted
8b	Sw	L-GY	M	Thin	VW		Sandstone						Thin beds heavily deformed and folded
8b	Sw	D-GY	M	V thin	VW		Mudstone						No consistent D/DD
9a	Mw	L-GY	M	Thin	WD-D	F-M	Sandstone	44, 9, 35, 32	MS	110, 20, 78, 65	66	206	
9a	Mw	D-GY	M	Thin	WD-D		Mudstone	9, 10	VW	20, 26	68	204	
9a	Hw-Cw	L/D GY	M	M	D-M		Breccia		VW				Note - clast size = longest axis
10a	Hw	L-GY	M	M	M	F-M	Breccia S/M		VW				Some bedding in rotated blocks, description = breccia
10a	Mw	L-GY	M	M	M	F-M	Sandstone	18, 38, 16, 17	MS	38, 88, 34, 36			Rebound from block, Breccia = unregister on Schmidt, block still FRAG
10b	Hw-Cw	D-GY	M	M	M		Breccia S/M		H-VW				Note: Weathering = disintegration - Little to no colour change
10c	Hw-Cw	D-GY	M	M	M		Breccia S/M		VW-H				30cm into slope = pieces of intact - photo 3909 - 3912
10d	Mw-Hw	L-GY	M	Med	M-D	F-M	Breccia S	38, 47, 48, 42	MS-VW	88, 130, 140, 105			20cm into slope = pieces of intact - photo 3913 - 3914
10d	Mw-Hw	D-GY	M	Thin	M-D		Breccia M		VW				Bedding barely obvious - No plane to take dip/dip direction
10e	Mw	L-GY	M	V thick	M-D	F-M	Sandstone B	48, 41, 40, 50	S-MS	140, 100, 98, 150	70	75	Bedding barely obvious and where it is changes dip considerable over short distances
10e	Mw	D-GY	M	Thin	M-D		Mudstone B	21, 31, 32	VW	42, 65, 68	75	50	Can't get reading on fragmented mudstone for Schmidt (Schmidt = intact mudstone)
10e	Mw	L/D-GY	M	Thin	D		Block S/M						Rotated block in better condition that surrounding rock
11a	Hw	D-GY	M	M	MP		Breccia M		H-VW				
13a	Hw	D-GY	M	Massive	VWD		Mudstone B		S-VS				Bedding to disturbed to get accurate dip/dip direction
13a	Hw	L-GY	M	Massive	VWD		Sandstone B		S-VS				Both sandstone and mudstone present

D.2.2 Elliott Fault - Defect structure

		Orientation								Waviness										
Outcrop #	Defect type	Dip	Dip Direction	Spacing (m)	Persistence (m)	Aperture	Infilling type	Infilling strength	Roughness	Wavelength (m)	Interlimb angle (ILA, °)	Ends	End termination	Strength (rebound)	Strength (hammer)	Strength (MPa)	Water	Weathering	Degree of fracture	Raw field notes
1a	Bedding	40	24	0.2	20					2.5	175	2	C				Dry	Sw-Mw	HF	Sandstone/mudstone interbed
1a	Joint	68	220	3.5	4					3	175	1	O				Dry	Sw-Mw	HF	
1a	Joint	72	205	3.5	4.5					3	175	1	O				Dry	Sw-Mw	HF	
1a	Joint	76	354	1	2.5					1.5	170	1	O				Dry	Sw-Mw	HF	
1b	Fault	25	6		25					0	180	2	C				Dry	Sw	MF	
1b	Joint	65	220	2.2	2.5					0	180	1	O				Dry	Sw	MF	
1b	Joint	64	239	2.2	2					0	180	1	O				Dry	Sw	MF-HF	Rock becoming more heavily fractured toward shear
1b	Joint	56	238	2.5	5					3	175	2	C				Dry	Sw	MF-HF	
1b	Joint	65	352	2	4.5					2.5	175	1	R				Dry	Sw	MF-HF	
1b	Joint	64	327	2	3					2	175	0	R				Dry	Sw	MF-HF	
1b	Bedding	15	2	0.1-0.3	25					4	175	2	C				Dry	Sw	MF-HF	
1b	Bedding	18	4	0.1-0.3	35					2.5	170	2	C				Dry	Sw	MF-HF	Becoming more weathered toward the shear
1c	Fault	82	155		7					3.5	175	2	C				Dry	Hw	F	
1c	Fault	72	148		7.5					0.75	170	2	C				Dry	Hw	F	
1c	Joint	60	264	0.5	5.5					2.5	170	2	C				Dry	Hw	F	By weathering definition - Note no colour change
1d	Joint	62	175	2.8	7.5					1.8	170	2	C				Dry	Sw-Mw	HF	
1d	Joint	62	184	2.8	7.5					2	170	2	C				Dry	Sw-Mw	HF	
1d	Shear	68	351	3	9					4	175	2	C				Dry	Sw	HF	
1d	Shear	70	345	2.2	5					4	175	2	O				Dry	Sw	HF	
1d	Shear	85	340	2	4.8					3	175	1	D				Dry	Sw	HF	
1d	Shear	72	145	2	3.9					0	180	2	C				Dry	Sw	HF	
1d	Joint	84	114	1.8	4					2	170	1	D				Dry	Sw-Mw	HF	
1d	Joint	46	289	3	4.2					2	175	1	R				Dry	Sw-Mw	HF	
1d	Fault	50	130		3					1	175	0	R				Dry	Sw-Mw	HF	
1d	Joint	54	265	3	5					1.8	175	2	C				Dry	Sw-Mw	HF	
1d	Shear	55	317	2	4					2.3	175	2	C				Dry	Sw-Mw	HF	
1e	Bedding	62	51	0.2	10		Kl	Nil	SU	0.4	175	2	C	52, 26, 52, 42, 28	MS	160, 54, 160, 105, 58	Dry	Sw	MF-HF	Schmidt hammer values against sandstone
1e	Joint	59	220	2	3.8		Kl	Nil	SU	1.2	175	2	C	18, 44, 34	MS	37, 110, 75	Dry	Sw	MF-HF	Mudstone rejects
1e	Joint	59	231	2	6.5		Kl	Nil	SU	1.2	175	2	C	38, 30	MS	90, 62	Dry	Sw	MF-HF	
1e	Shear	22	210		2.8		Sheared Ms	Very Weak	RU	0.8	175	2	C		VW		Dry	Sw	MF-HF	
1e	Bedding	55	40	0.2	30				SU	0.55	175	2	C	30, 46, 28, 22	S-VS	64, 130, 58, 44	Dry	Sw	MF	
1e	Joint	61	222	2	5.5				SU	1.5	175	2	C	12, 12	MS-S	28, 28	Dry	Sw	MF	
1e	Joint	60	228	2	6				SU	1	175	2	C	22, 28	MS-S	44, 58	Dry	Sw	MF	
1e	Bedding	58	42	0.1-0.3	20				SU	0.4	175	2	C		S		Dry	Sw	MF	
1e	Shear	39	192		8		Med Sand	Very Weak	RU	1.8	170	2	C		VW		Dry	Sw	MF	
2a	Bedding	30	80	1	10		Some Quartz	Weak	RU	4	175	1	O	40, 42	MS-S	98, 100	Dry - Moist	Sw-Mw	MF-F	
2a	Bedding	55	121	1	8				RU	1	170	2	C	20, 12	MS-S	40, 28	Dry - Moist	Sw-Mw	HF-F	
2a	Joint	51	194	1	15				RU	0.9	170	1	O	18	MS	37	Dry	Sw-Mw	MF	
3a	Bedding	60	93	0.3-1	7				SU	2	175	2	C	32, 24, 38, 52	VS	67, 46, 89, 160	Dry	Sw-Mw	MF	Sandstone
3a	Bedding	72	87	0.3	8				RU	1	175	2	C	20, 20, 26, 24	MS	40, 40, 53, 46	Dry	Mw	HF	Mudstone
3a	Bedding	87	86	0.1-0.3	7				SU	1	165	1	O	36, 32, 16, 14	VW	80, 67, 35, 31	Dry	Sw-Mw	HF-F	Sandstone
3a	Joint	55	233	0.25	3				SS	2	175	2	C	42, 50	VS	100, 150	Dry	Sw-Mw	HF	
3a	Joint	80	210	0.35	5				SU	0	180	2	C	14, 26, 30, 44	MS-VS	31, 53, 64, 115	Dry	Sw-Mw	MF-HF	Fragmented mudstone - unregistered on Schmidt
3a	Joint	80	26	0.3	3.5				SU	0.8	175	1	R	46, 34, 46, 30	MS-VS	130, 74, 130, 64	Dry	Sw-Mw	MF	Sandstone
3a	Shear	40	130		4		Lineated Mudstone	Hard	RU	1.5	160	2	C		V-STIFF		Dry-Moist	Mw-Hw	F	Lineated fragmented mudstone along shear
4a	Bedding	42	45	0.1-0.3	2.5				RU	0.4	165	1	O	50, 14, 46	VS	150, 31, 130	Dry	Sw-Mw	MF	Sandstone/Mudstone
4a	Joint	50	266	0.1-1	3				RU	3	170	1	R	20, 12	MS	40, 28	Dry	Mw-Hw	MF-HF	
4a	Fault	70	254		4				SS	1.5	170	2	C	12	MS	28	Dry	Mw	MF-HF	
4a	Joint	76	154	0.1-1	3				RS	2.2	170	1	O	28, 18, 18, 41	MS	58, 37, 37, 104	Dry	Mw	MF-HF	
4a	Bedding	70	35	0.2	3				RU	0	180	1	D	28, 41, 53	Sand - VS, Mud - W-VW	58, 104, 170	Dry	Mw	Mf-HF	
5a	Bedding	71	125	0.2-0.4	1				RU	0.45	175	1	O	12, 20, 20	MS	28, 40, 40	Dry	Mw	HF-F	
5a	Joint	49	152	0.3	2				SU	0.8	175	2	C	34, 46, 26, 32	S-VS	73, 130, 53, 68	Dry	Sw	HF-F	
5b	Bedding	76	336	0.1-0.2	3				RU	2	160	1	O	12 - Reject	W-MS	28	Dry	Mw-Hw	F	
5b	Shear	40	149		5		Silty sandy gravel	Hard	SS	2.5	170	1	O		V-STIFF		Moist	Mw-Hw	F	
5c	Bedding	75	134	0.03-0.4	3				SU	1.8	170	1	O	26, 20	VW	53, 40	Dry	Mw-Hw	HF-F	
5c	Joint	55	50	0.3	2				SS	2	160	1	O	20	VW	40	Dry	Mw-Hw	HF-F	Quartz infilling, slickenside, gouge fabric in select shear/fault
5d	Bedding	51	119	0.05-0.4	2.5				SS	0.4	175	0	O		VW-VS		Dry	Hw	F	
5k	Bedding	66	294	0.3-1	1.2				SU	1	175	2	C	26, 18	MS-S	53, 37	Dry	Sw-Mw	HF	Note: Clean off by River
6a	Bedding	54	149	1	2.5				US	2	175	2	C	40, 38, 22	S	100, 88, 44	Dry	Sw	MF	
6a	Joint	19	126	0.1-0.3	3				UR	1	175	1	O	48, 26, 12	MS-S	140, 54, 28	Dry	Sw	MF-HF	
6b	Bedding			0.4	2.5				UR	0	180	0	O				Dry	Sw	MF-HF	Site photographed - Not accessible for long - Mud HF-F
7a	Bedding			1.5-2	3					2.8	175	1	O				Moist	Sw-Mw	MF	7a = Site not accessible
7a	Bedding			0.4-1.5	2.5					1.5	165	1	O				Dry	Mw-Hw	HF	7a = Site not accessible - Mud
7a	Joint			0.3-0.5	1.5	3				2.5	175	1	O				Wet	Sw-Mw	MF-HF	7a = Site not accessible
7a	Joint			0.4	2					2	175	1	O				Dry	Sw-Mw	MF-HF	7a = Site not accessible
8a	Bedding	43	65	1	3					2.5	175	1	O				Dry	Sw-Mw	MF-HF	
8a	Bedding	66	79	0.1-0.7	3.2					0.4	120	1	O				Dry	Mw	HF-F	
8a	Joint	60	251	1	3.5					2	175	1	O				Dry	Sw-Mw	MF	
8b	Shear				6		Breccia - No access	Very Weak				2	C				Wet	Hw-Cw	F	Running water from soil/rock interface, massive with no orientation/waviness able to be recorded
9a	Bedding	66	206	0.1-0.2	1.8				US	0.4	175	0	R		W		Dry	Mw	HF-F	
9a	Joint	54	300	0.3	1.4				UR	1	175	1	O	17, 48	W	36, 140	Dry	Mw	F	

10d	Bedding	31	155	0.2-0.7	2.8				US	2.8	175	1	O		S-VW		Dry	Mw-Hw	F	
10e	Bedding			0.2-0.4	3					2.5	175	1	D	31, 35, 18	MS-VW	64, 78, 38	Dry	Mw	F	Mud = VW
10e	Block bedding	75	129	0.2-0.4	1.8				UR	2	175	0	R	34, 26, 14, 15	S-VW	74, 52, 30, 32	Dry	Mw	HF-F	Mud = VW
10e	Joint	90	345	2	3.5				UR	1	170	2	C	55, 52, 26	VS-VW	185, 160, 52	Dry	Mw	F	Mud = VW
10e	Shear	72	105		4.2		7cm sand/silt w/ lineated mud	Hard	SS	3.8	175	2	C		S-VW		Dry	Mw	F	Mud = VW
10e	Shear	33	112		4.8		5cm sand/silt w/ lineated mud	S-H	UR	1.8	175	2	C		MS-VW		Dry	Mw	F	Mud = VW
10e	Shear	28	130		4		Lineated mud	S-H	UR	3.5	170	2	C		MS		Dry	Mw	F	
10e	Shear	10	342		3				SS	2	160	1	D		MS		Dry	Mw	F	

D.2.3 Elliott Fault - Soil descriptions of infill

				Strength							
Outcrop #	Fraction (name)	Colour	Structure	NZGS	PSM Non-cohs	Moisture	Grading	Sorting	Plasticity*	Weathering	Raw field notes
1c		L-GY	HOMO/Fis/block			Moist				Hw-Cw	6.4m wide
5e	Silty Sandy Gravel	L-GY	HOMO/Fis/block	VS-H	Compact	Dry	WG	PS		Hw-Cw	
5f	Silty Sandy Gravel	L-GY	HOMO/Fis/block	VS-H	Compact	Dry	WG	PS		Hw-Cw	
5g	Silty Sandy Gravel	L-GY	HOMO/Fis	S	Compact	Dry	WG	PS		Hw-Cw	
5h	Silty Sandy Gravel	L-GY	HOMO/Fis/block	S-VS	Compact	Dry	WG	PS		Mw-Cw	
5i	Silty Sandy Gravel	L-GY	HOMO/Fis	H-VW	Compact	Dry	WG	PS		Hw-Cw	
5j	Silty Sandy Gravel	L/D GY	HOMO/Fis/block	VW - H	Compact	Dry/Moist	WG	PS		Hw	
5j.1	Silty Sandy Gravel	L/D GY	HOMO/Fis/Block	VW	Compact	Dry	WG	PS		Hw	
9a	Silty Sandy Gravel	L/D GY	Bedding/Fis/Block	H-VW	Co/Ce	Dry	WG	PS		Hw-Cw	
10a	Silty Sandy Gravel	L-GY	HOMO/Fis/block/bed	H	Compact	Moist	WG	PS		Hw	
10b	Silty Sandy Gravel	L-GY	HOMO/Fis/block	VS-H	Lo/Co	Moist	WG	PS		Hw-Cw	Most L-GY but some D-GY
10c	Silty Sandy Gravel	L/D GY	HOMO/Fis/block	S-VS	Lo/Co	Moist	WG	PS		Hw-Cw	Slickenside on quartz joints
10d	Gravel with some Sand	L/D GY	Bedding/Fis	H-VW	Co/Ce	Dry	WG	PS		Mw-Hw	Bedding with mud and sand
11a	Silty Sandy Gravel	D-GY	HOMO/Fis/block	VS-VW	Lo/Co	Moist/Wet	WG	PS		Hw	
13a	Silty Sandy Gravel with minor clay	D-GY	Thin-Medium	S-VS	Compact	Moist	WG	PS		Hw	Bedding present
8b		L-GY	HOMO			Moist				Hw-Cw	No access

D.2.4 Elliott Fault - Breccia fabric descriptions

Outcrop #	Fabric support	Fabric arrangement	Fabric (random - lineated?)	% Clast >1mm to matrix	% of clasts >2mm	Matrix vs. cement	Rotation angle	Rounding	Clast size	Alteration	Grain size*	Raw field notes
1c			R			M						No access
2a	Clast	Crackle	R	95	90	M		Angular	2x4x5cm to silt			
5e	Clast	Crackle	R	95	85	M		Angular	1cm to silt			Coherent Rock with bedding inside
5f	Clast	Crackle	R	95	90	M		Angular	5cm to silt			Larger rock clasts
5g	Clast	Crackle	R	95	90	M		Angular	1cm to silt			Becoming softer
5h	Clast	Crackle	R	95	90	M		Angular	1cm to silt			1cm clasts up to 10cm
5i	Clast	Crackle	R	95	90	M		Angular	1cm to silt			
5j	Clast	Crackle	R	95	90	M		Angular	1cm to silt			
5j.1	Clast	Crackle	R	95	90	M		Angular	1cm to silt			
9a	Clast	Crackle	R	95	90	M		Angular	10cm to silt			
10a	Clast	Crackle	R	95	85	M		Angular	1cm to silt			
10b	Clast	Crackle	R	90	80	M		Angular	1cm to silt			
10c	Clast	Crackle	R	90	80	M		Angular	1cm to silt			
10d	Clast	Mosaic	R/L	100	99	M		Angular	5cm - Silt			Separation through relax? - Mudstone lineated
10e	Clast	Mosaic	R/L	100	99	M/C		Angular	5cm - Sand			Some quartz veining
11a	Clast	Crackle	R	95	90	M		Angular	2cm-silt			Cohesive clay like substance beside more intact rock
13a	Clast	Crackle	R	90	85	M		Angular	2cm-silt			Multiple 1cm-5cm shear zones in rock - still coherent rock observed
8b			R			M						No access

D.3 Bedding thickness portions with joint and fault occurrence

Bedding thickness across the study site with joints and faults/shears presented as percentage occurrence respective of bedding thickness.

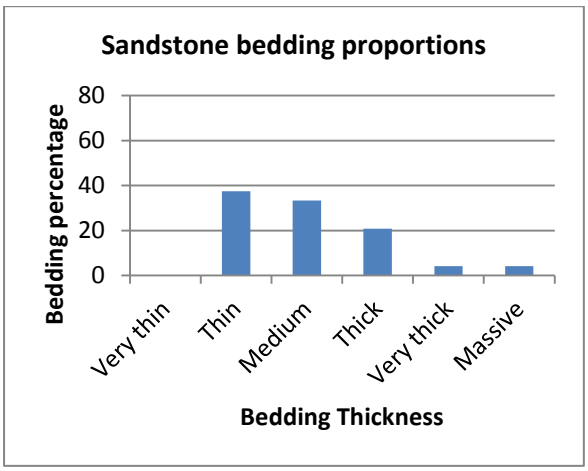

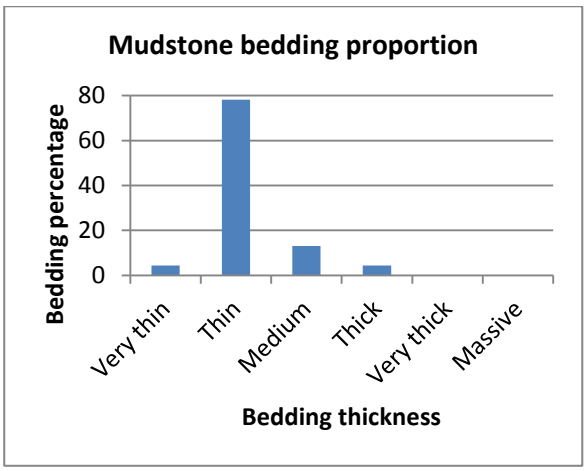

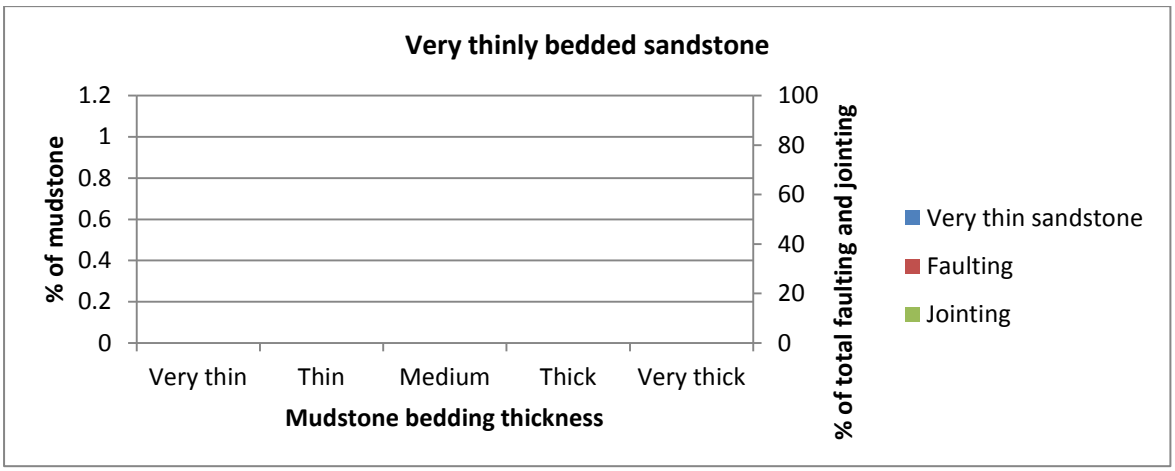

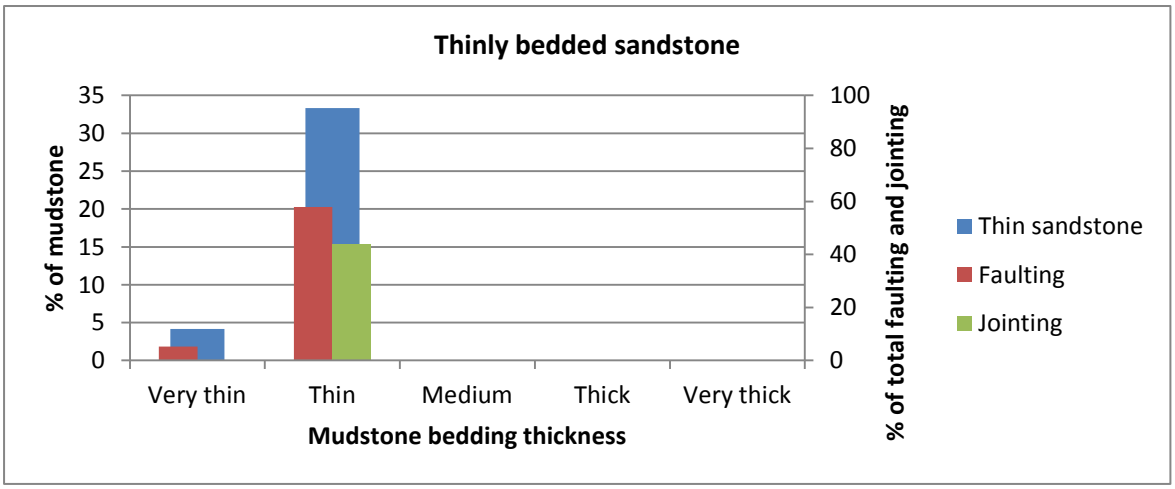

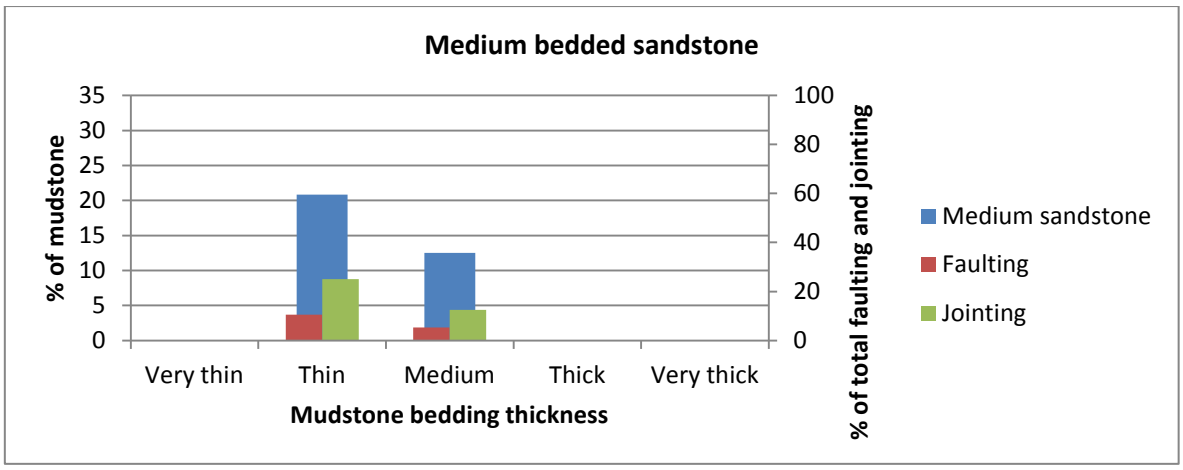
Medium bedded sandstone
% of mudstone
35
30
25
20
15
10
5
0
100
80
60
40
20
0
% of total faulting and jointing
Very thin
Thin
Medium
Thick
Very thick
Mudstone bedding thickness
Medium sandstone
Faulting
Jointing

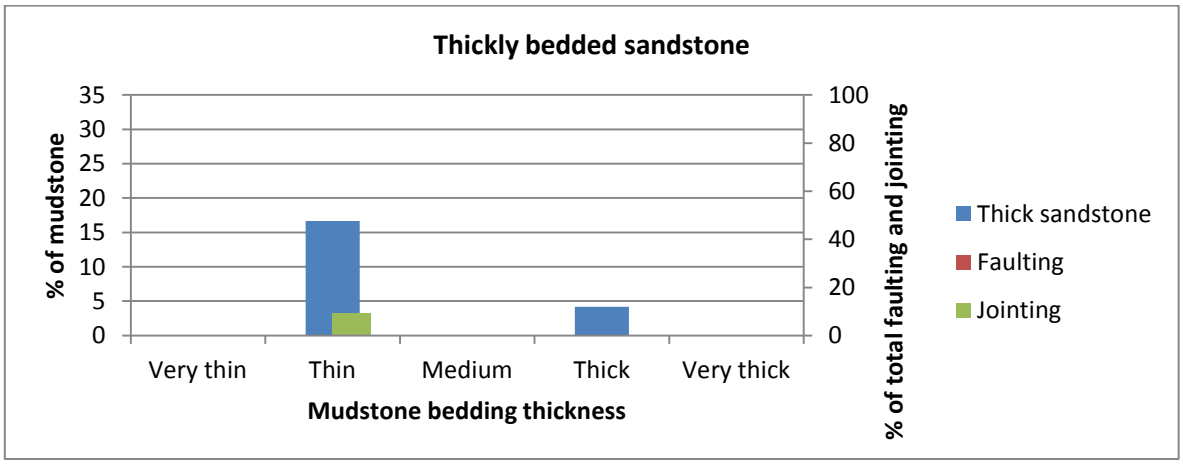
Thickly bedded sandstone
% of mudstone
35
30
25
20
15
10
5
0
100
80
60
40
20
0
% of total faulting and jointing
Very thin
Thin
Medium
Thick
Very thick
Mudstone bedding thickness
Thick sandstone
Faulting
Jointing

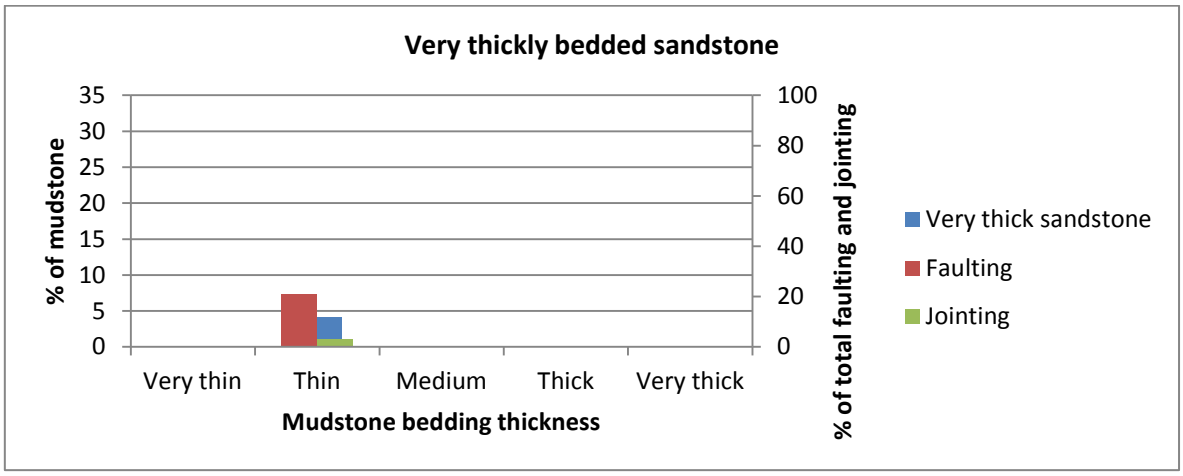
Very thickly bedded sandstone
% of mudstone
35
30
25
20
15
10
5
0
100
80
60
40
20
0
% of total faulting and jointing
Very thin
Thin
Medium
Thick
Very thick
Mudstone bedding thickness
Very thick sandstone
Faulting
Jointing

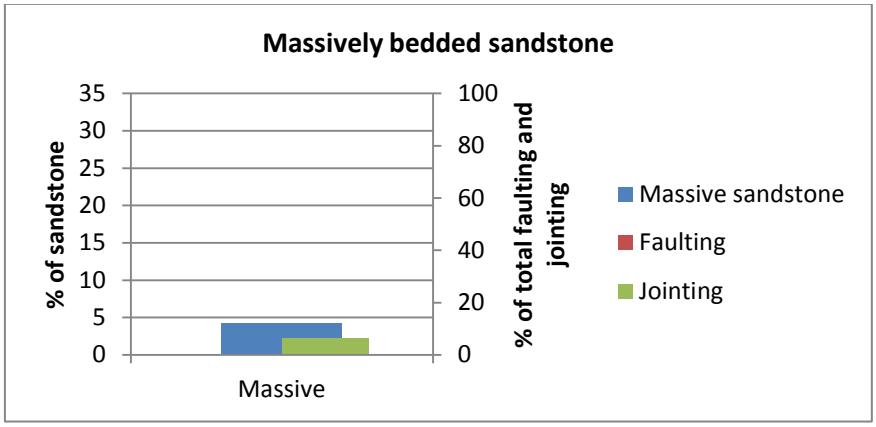
Massively bedded sandstone
% of sandstone
35
30
25
20
15
10
5
0
100
80
60
40
20
0
% of total faulting and jointing
Massive
Massive sandstone
Faulting
Jointing

D.4 Elliott Fault steronet analysis

Steronet dip/dip direction analysis of bedding, jointing and faults/shears respectively, showing pole and cluster plots.

Bedding poles

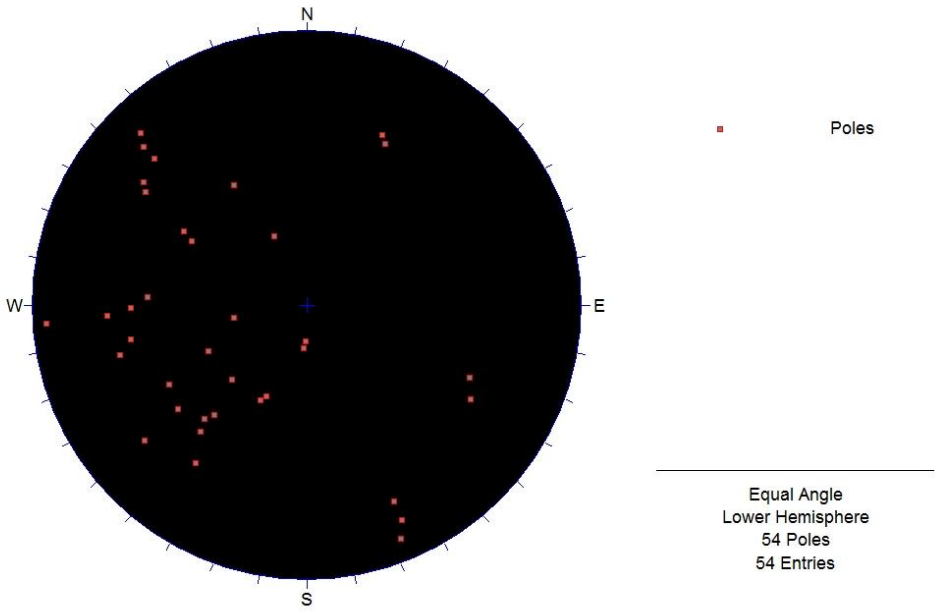

Bedding cluster

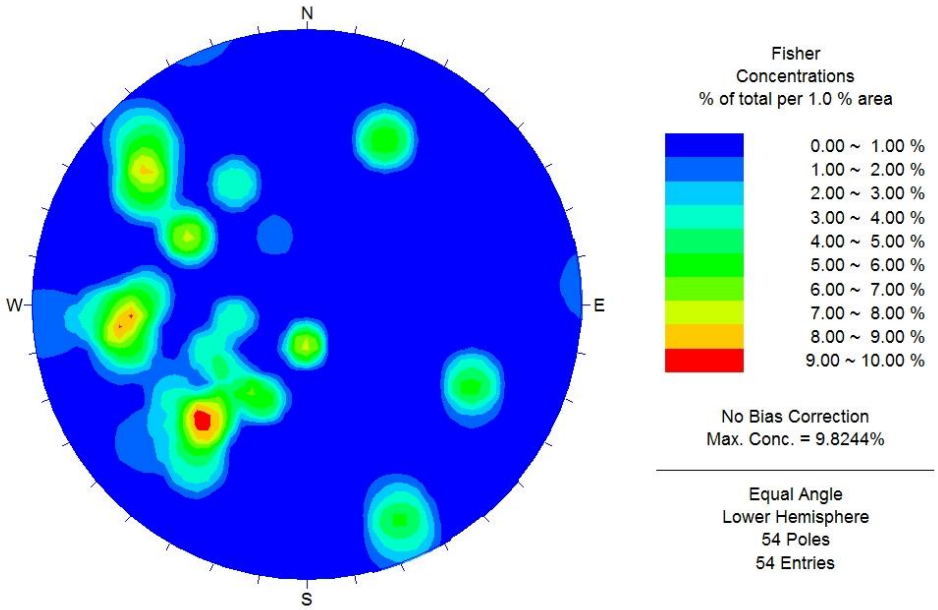

Jointing poles

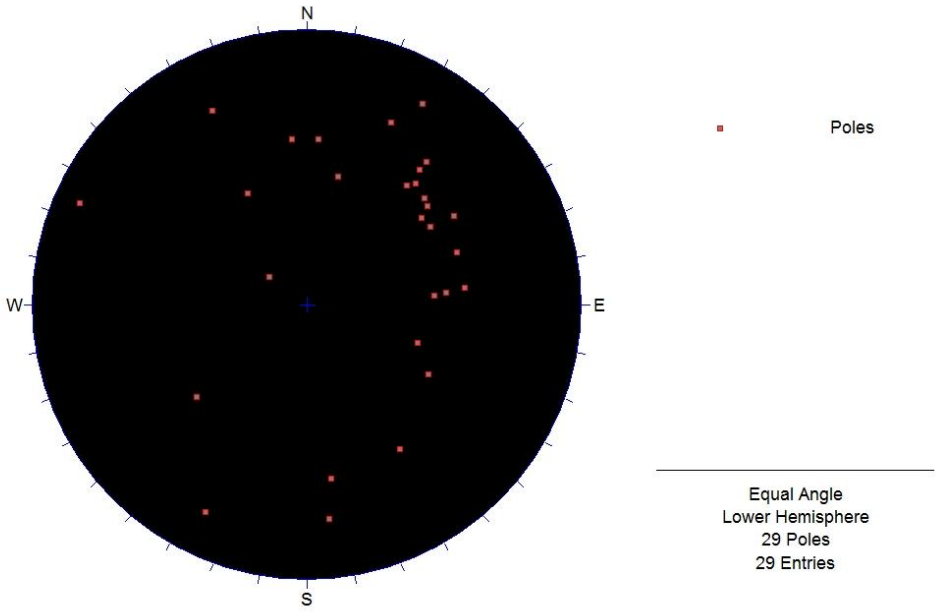

Jointing cluster

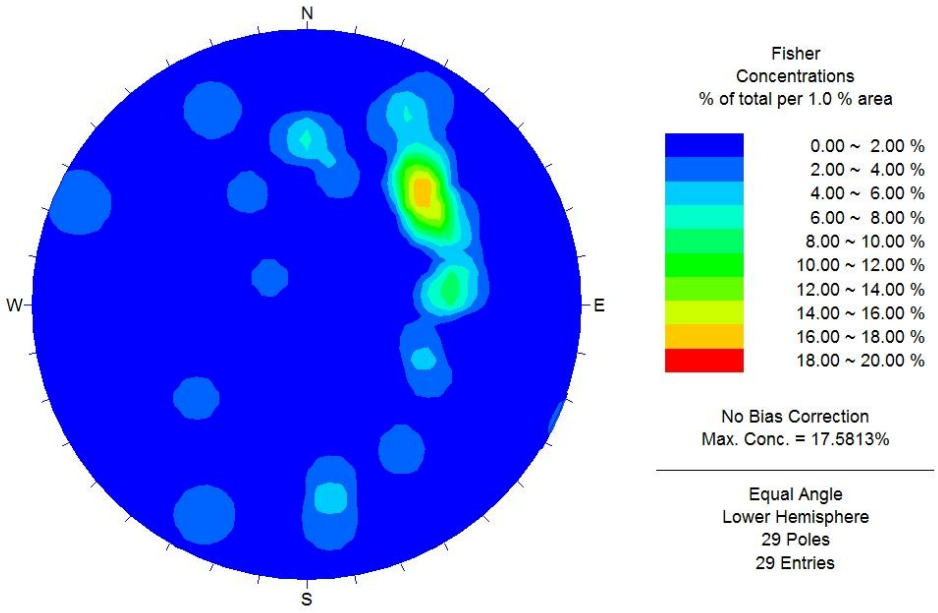

Faulting/shearing poles

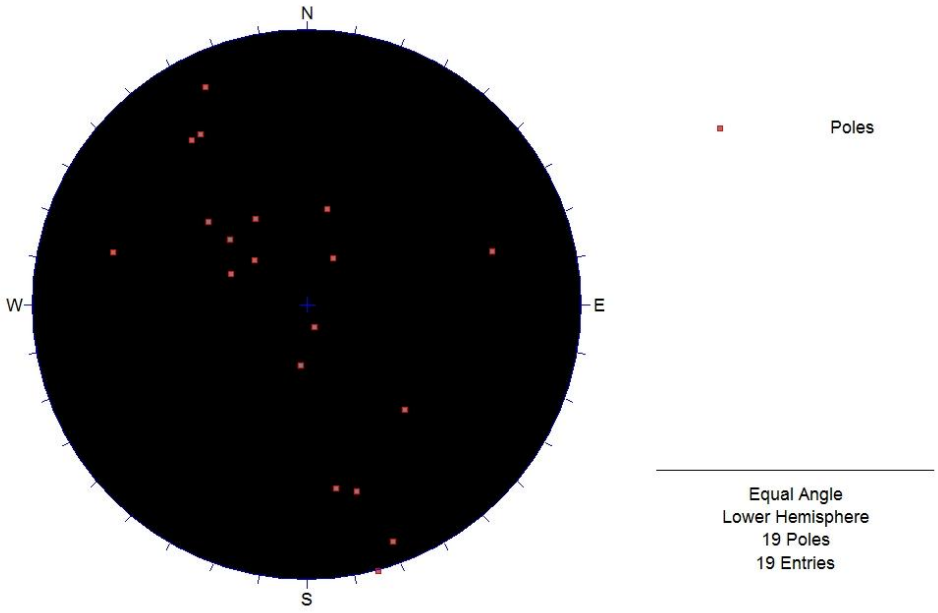

Faulting/shearing cluster

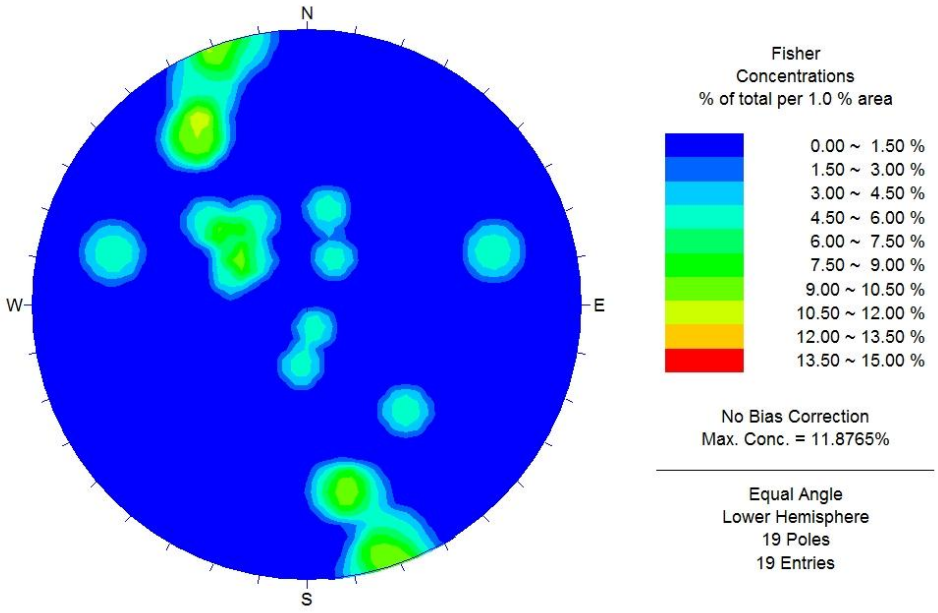

D.5 Elliott Fault UCS raw results and calculations

Unconfined Compressive Strength testing respective of sampled outcrop.

D.5 Elliott Fault - Uniaxial Compressive Strength testing

Sample ID	Height (mm)	Height (M)	Mass (g)	Mass (Kg)	Diameter (mm)	Failure Load (kN)	Failure Load (N)	Area (mm^2)	Area (M)	Stress (MPa)	Lithology	Failure mode (Szwedzicki, 2007)	Notes
6a	102.46	0.10246	517.9	0.5179	49.34	316.5	316500	1912.001249	1.912001249	165.5333647	F-M sandstone	Clean multi extension with some multi fracture	
6a	101.4	0.1014	499.2	0.4992	49.27	249.4	249400	1906.579881	1.906579881	130.8101499	F-M sandstone	Clean multi extension with some multi fracture	
5k	101.6	0.1016	498.7	0.4987	49.25	167.4	167400	1905.032333	1.905032333	87.87252433	F-M sandstone	Clean multi extension with some shear powder	Some break along existing 5-10%
4a	100.995	0.1010	512.6	0.5126	49.21	286.4	286400	1901.681466	1.901681466	150.6035606	F-M sandstone	Simple extension with some multi extension	100% break along existing quartz

D.6 Elliott Fault BTS raw results and calculations

Brazilian Tensile Strength testing respective of sampled outcrop.

D.6 Elliott Fault - Brazilian Tensile Strength testing

Outcrop	Load (Kn)	Load (N)	Diameter (mm)	Thickness (mm)	MPa	Lithology	Clean?	Failure mode (Szwedzicki, 2007)	Failure time (sec)	Notes
1e	19.1	19100	49.75	25	9.77	Fine sandstone	10% oxide	Simple extension	50.8	Perpendicular discontinuity to load
1e	53.4	53400	49.75	25	27.31	Fine sandstone	Clean	Multi extension	91.02	
1e	40.2	40200	49.75	25	20.56	Fine sandstone	Clean	Multi extension w/ some multi fracture	79.2	
1e	37.3	37300	49.75	25	19.07	Fine sandstone	5% existing	Multi extension w/ some multi fracture	89.04	Some small fractures in breakage
2a	31.8	31800	49.75	25	16.26	Fine sandstone	Clean	Simple extension w/ multi fracture	60.88	
3a	36	36000	49.75	25	18.41	Fine sandstone	20% quartz	Simple extension w/ some shear powder	N/A	
3a	15.7	15700	49.75	25	8.03	F-M sandstone	Clean	Simple extension	N/A	45° existing discontinuity to load
3a	28.2	28200	49.75	25	14.42	Fine sandstone	20% quartz	Multi fracture w/ some multi shear	N/A	
3a	13.6	13600	49.75	25	6.95	F-M sandstone	Clean	Multi fracture	N/A	
3a	15.5	15500	49.75	25	7.93	F-M sandstone	Clean	Simple extension	36.8	Perpendicular discontinuity to load
3a	19.2	19200	49.75	25	9.82	Fine sandstone	50% quartz	Multi fracture w/ some multi shear	45.6	Parallel discontinuity to load
3a	26.1	26100	49.75	25	13.35	Fine sandstone	Clean	Multi extension	53.2	
3a	11.4	11400	49.75	25	5.83	F-M sandstone	50% quartz	Simple extension	28.38	Number of discontinuities in sample
4a	20.9	20900	49.75	25	10.69	F-M sandstone	60% existing	Simple fracture	38.79	
4a	33.6	33600	49.75	25	17.18	F-M sandstone	Clean	Simple extension	53.5	
5a	31.8	31800	49.75	25	16.26	Fine sandstone	Clean	Multi extension	64.05	
5c	35.6	35600	49.75	25	18.20	F-M sandstone	Clean	Multi extension	60.75	
5c	23.5	23500	49.75	25	12.02	F-M sandstone	Clean	Simple extension	52.82	
5k	20.3	20300	49.75	25	10.38	F-M sandstone	Clean	Simple extension	N/A	Perpendicular discontinuity to load
5k	13.1	13100	49.75	25	6.70	F-M sandstone	Clean	Simple extension	38.53	
5k	22.6	22600	49.75	25	11.56	F-M sandstone	Clean	Multi extension	48.44	
5k	28.5	28500	49.75	25	14.57	F-M sandstone	Clean	Simple extension	54.74	Perpendicular discontinuity to load
5k	15.3	15300	49.75	25	7.82	F-M sandstone	50% oxide	Simple extension w/ multi fracture	34.52	Simultaneous break along existing and clean at right angles to each other
6a	41	41000	49.75	25	20.97	Fine sandstone	Clean	Simple extension	N/A	
6a	44.4	44400	49.75	25	22.70	Fine sandstone	Clean	Multi extension	N/A	Perpendicular discontinuity to load
6a	50.8	50800	49.75	25	25.98	Fine sandstone	Clean	Multi extension	N/A	Perpendicular discontinuity to load
6a	39.6	39600	49.75	25	20.25	Fine sandstone	Clean	Multi extension	N/A	
6a	16.9	16900	49.75	25	8.64	Fine sandstone	65% oxide	Multi fracture	39.93	Perpendicular discontinuity to load
10e	47.4	47400	49.75	25	24.24	Fine sandstone	Clean	Multi extension	61.07	
10e	29.1	29100	49.75	25	14.88	Fine sandstone	Clean	Multi extension	43.09	

D.7 Elliott Fault Point Load testing raw results and calculations

Point Load Index testing per sample outcrop.

D.7 Elliott Fault - Point Load testing

SAMPLE: 1a

Test No.	Type	P (kN)	D (mm)	W (mm)	A = WD (mm^2)	D_e^2	D_e	I_s	F	$I_{s(50)}$ (MPa)	Lithology	Weathering	Notes
1		1.58	47.0	87	4089	5206	72.2	0.30	1.179	0.36	F-M Sandstone	Sw	Break along existing quartz joint
2		17.59	42.0	45	1890	2406	49.1	7.31	0.991	7.25	F-M Sandstone	Sw	
3		5.59	28.0	55	1540	1961	44.3	2.85	0.947	2.70	F-M Sandstone	Sw	Break along existing
4		18.21	55.0	64	3520	4482	66.9	4.06	1.140	4.63	F-M Sandstone	Sw	
5		21.02	47.0	47	2209	2813	53.0	7.47	1.027	7.67	F-M Sandstone	Sw	
6		1.50	44.0	89	3916	4986	70.6	0.30	1.168	0.35	F-M Sandstone	Sw-Mw	Break along existing
7		3.58	43.0	31	1333	1697	41.2	2.11	0.917	1.93	F-M Sandstone	Sw-Mw	
8		6.96	48.0	44	2112	2689	51.9	2.59	1.017	2.63	F-M Sandstone	Sw	Break along existing quartz joint
9		11.56	52.0	84	4368	5562	74.6	2.08	1.197	2.49	F-M Sandstone	Sw	
10		5.00	29.0	59	1711	2179	46.7	2.30	0.970	2.23	F-M Sandstone	Sw	Break along existing quartz joint
11		0.75	22.0	30	660	840	29.0	0.89	0.782	0.70	F-M Sandstone	Sw-Mw	Break along existing
12		2.09	12.0	35	420	535	23.1	3.91	0.707	2.76	F-M Sandstone	Sw	
13		6.87	46.0	60	2760	3514	59.3	1.95	1.080	2.11	Mudstone	Sw	
14		5.87	45.0	22	990	1261	35.5	4.66	0.857	3.99	Mudstone	Sw	
15		6.09	30.0	50	1500	1910	43.7	3.19	0.941	3.00	Mudstone	Sw	
16		4.90	34.0	32	1088	1385	37.2	3.54	0.876	3.10	Mudstone	Sw	
17		6.03	32.0	27	864	1100	33.2	5.48	0.831	4.56	Mudstone	Sw	
18		3.45	17.0	29	493	628	25.1	5.50	0.733	4.03	Mudstone	Sw	
19		9.46	36.0	43	1548	1971	44.4	4.80	0.948	4.55	F-M Sandstone	Sw	
20		10.81	40.0	47	1880	2394	48.9	4.52	0.990	4.47	F-M Sandstone	Sw	
21		6.59	24.0	55	1320	1681	41.0	3.92	0.915	3.59	F-M Sandstone	Sw	
22		7.92	21.0	59	1239	1578	39.7	5.02	0.902	4.53	F-M Sandstone	Sw	
23		10.83	22.0	59	1298	1653	40.7	6.55	0.911	5.97	F-M Sandstone	Sw	
24		11.36	45.0	94	4230	5386	73.4	2.11	1.188	2.51	F-M Sandstone	Sw	
25		6.01	15.0	50	750	955	30.9	6.29	0.805	5.07	F-M Sandstone	Sw	
26		5.40	13.0	50	650	828	28.8	6.52	0.780	5.09	F-M Sandstone	Sw	
27		8.69	36.0	50	1800	2292	47.9	3.79	0.981	3.72	F-M Sandstone	Sw	
28		4.80	42.0	84	3528	4492	67.0	1.07	1.141	1.22	F-M Sandstone	Sw	Break along existing with iron oxide
29		5.85	18.0	50	900	1146	33.9	5.11	0.839	4.28	F-M Sandstone	Sw	
30		4.04	14.0	49	686	873	29.6	4.63	0.789	3.65	F-M Sandstone	Sw	

SAMPLE: 2a

Test No.	Type	P (kN)	D (mm)	W (mm)	A = WD (mm^2)	D_e^2	D_e	I_s	F	$I_{s(50)}$ (MPa)	Lithology	Weathering	Notes
1		5.12	45.0	48	2160	2750	52.4	1.86	1.022	1.90	F-M Sandstone	Mw	
2		9.44	20.0	55	1100	1401	37.4	6.74	0.878	5.92	F-M Sandstone	Sw-Mw	
3		12.04	37.0	75	2775	3533	59.4	3.41	1.081	3.68	F-M Sandstone	Sw	
4		2.70	29.0	40	1160	1477	38.4	1.83	0.888	1.62	Fine Sandstone	Mw	
5		9.39	30.0	50	1500	1910	43.7	4.92	0.941	4.63	F-M Sandstone	Sw	
6		12.15	32.0	66	2112	2689	51.9	4.52	1.017	4.59	F-M Sandstone	Sw	
7		3.82	32.0	76	2432	3097	55.6	1.23	1.049	1.29	F-M Sandstone	Sw	
8		5.24	14.0	37	518	660	25.7	7.94	0.741	5.89	F-M Sandstone	Sw	
9		2.11	35.0	25	875	1114	33.4	1.89	0.834	1.58	F-M Sandstone	Sw-Mw	Break along existing quartz vein
10		6.17	14.0	26	364	463	21.5	13.31	0.684	9.11	F-M Sandstone	Sw	
11		1.02	13.0	50	650	828	28.8	1.23	0.780	0.96	F-M Sandstone	Sw	Break along existing quartz vein
12		7.16	18.0	25	450	573	23.9	12.50	0.718	8.97	F-M Sandstone	Sw	
13		8.18	28.0	46	1288	1640	40.5	4.99	0.909	4.54	F-M Sandstone	Sw	
14		11.03	24.0	30	720	917	30.3	12.03	0.798	9.60	Fine Sandstone	Sw	

SAMPLE: 3a

Test No.	Type	P (kN)	D (mm)	W (mm)	A = WD (mm^2)	D_e^2	D_e	I_s	F	$I_{s(50)}$ (MPa)	Lithology	Weathering	Notes
1		3.58	22.0	37	814	1036	32.2	3.45	0.820	2.83	Sandstone	Mw-Sw	
2		2.15	36.0	35	1260	1604	40.1	1.34	0.905	1.21	Sandstone	Mw-Sw	
3		12.15	43.0	72	3096	3942	62.8	3.08	1.108	3.41	Sandstone	Sw	
4		5.79	63.0	80	5040	6417	80.1	0.90	1.236	1.12	Sandstone	Mw-Sw	Quartz vein
5		6.23	51.0	39	1989	2532	50.3	2.46	1.003	2.47	Mudstone	Sw	
6		5.95	51.0	70	3570	4545	67.4	1.31	1.144	1.50	Fine Sandstone	Sw	
7		10.95	36.0	39	1404	1788	42.3	6.13	0.927	5.68	Sandstone	Sw	
8		10.93	44.0	30	1320	1681	41.0	6.50	0.915	5.95	Sandstone	Sw	
9		1.97	20.0	35	700	891	29.9	2.21	0.793	1.75	Sandstone	Sw	Quartz vein
10		6.91	37.0	38	1406	1790	42.3	3.86	0.928	3.58	Sandstone	Sw	
11		3.09	15.0	58	870	1108	33.3	2.79	0.833	2.32	Mudstone	Uw-Sw	
12		6.31	30.0	28	840	1070	32.7	5.90	0.826	4.87	Mudstone	Uw-Sw	
13		3.11	26.0	60	1560	1986	44.6	1.57	0.950	1.49	Sandstone	Sw	
14		8.63	48.0	43	2064	2628	51.3	3.28	1.011	3.32	Mudstone	Uw-Sw	
15		1.54	34.0	45	1530	1948	44.1	0.79	0.945	0.75	Mudstone	Sw	
16		13.72	28.0	50	1400	1783	42.2	7.70	0.927	7.13	Mudstone	Sw	
17		6.31	33.0	55	1815	2311	48.1	2.73	0.982	2.68	Mudstone	Sw	
18		3.84	35.0	37	1295	1649	40.6	2.33	0.911	2.12	Sandstone	Sw	

D.7 Elliott Fault - Point Load testing

SAMPLE: 4a

Test No.	Type	P (kN)	D (mm)	W (mm)	A = WD (mm^2)	D_e^2	D_e	I_s	F	$I_{s(50)}$ (MPa)	Lithology	Weathering	Notes
1		3.09	37.0	60	2220	2827	53.2	1.09	1.028	1.12	Mudstone	Mw	Break along existing - shatter
2		1.97	46.0	50	2300	2928	54.1	0.67	1.036	0.70	Mudstone	Mw	Break along existing - shatter
3		8.37	41.0	38	1558	1984	44.5	4.22	0.949	4.01	F-M Sandstone	Sw	
4		6.25	44.0	48	2112	2689	51.9	2.32	1.017	2.36	F-M Sandstone	Sw-Mw	Some break along existing
5		2.19	35.0	42	1470	1872	43.3	1.17	0.937	1.10	Mudstone	Sw-Mw	
6		5.60	21.0	34	714	909	30.2	6.16	0.796	4.91	Mudstone	Sw	
7		2.42	39.0	70	2730	3476	59.0	0.70	1.077	0.75	Mudstone	Sw	Some break along existing
8		1.03	26.0	35	910	1159	34.0	0.89	0.841	0.75	Mudstone	Sw	
9		3.60	60.0	45	2700	3438	58.6	1.05	1.074	1.13	Mudstone	Sw-Mw	Some break along existing
10		1.67	24.0	65	1560	1986	44.6	0.84	0.950	0.80	Mudstone	Sw	
11		4.59	22.0	53	1166	1485	38.5	3.09	0.889	2.75	Mudstone	Sw	
12		5.91	42.0	35	1470	1872	43.3	3.16	0.937	2.96	F-M Sandstone	Sw	
13		1.77	52.0	60	3120	3973	63.0	0.45	1.110	0.49	F-M Sandstone	Sw	Break along existing quartz vein
14		11.82	39.0	31	1209	1539	39.2	7.68	0.897	6.88	F-M Sandstone	Sw	
15		9.80	29.0	45	1305	1662	40.8	5.90	0.912	5.38	F-M Sandstone	Sw	
16		6.27	35.0	35	1225	1560	39.5	4.02	0.899	3.62	F-M Sandstone	Sw	
17		3.19	51.0	44	2244	2857	53.5	1.12	1.031	1.15	F-M Sandstone	Sw	Break along existing quartz vein
18		8.93	26.0	45	1170	1490	38.6	5.99	0.890	5.34	F-M Sandstone	Sw	
19		6.51	28.0	74	2072	2638	51.4	2.47	1.012	2.50	F-M Sandstone	Sw	Some break along existing
20		3.13	39.0	48	1872	2384	48.8	1.31	0.989	1.30	F-M Sandstone	Sw	Break along existing
21		6.85	39.0	50	1950	2483	49.8	2.76	0.998	2.75	F-M Sandstone	Sw	

SAMPLE: 5a

Test No.	Type	P (kN)	D (mm)	W (mm)	A = WD (mm^2)	D_e^2	D_e	I_s	F	$I_{s(50)}$ (MPa)	Lithology	Weathering	Notes
1		10.46	50.0	81	4050	5157	71.8	2.03	1.177	2.39	F-M Sandstone	Sw-Mw	
2		16.04	59.0	70	4130	5258	72.5	3.05	1.182	3.61	F-M Sandstone	Sw	
3		17.49	53.0	89	4717	6006	77.5	2.91	1.218	3.55	F-M Sandstone	Sw	
4		16.24	42.0	90	3780	4813	69.4	3.37	1.159	3.91	F-M Sandstone	Sw	
5		14.70	42.0	55	2310	2941	54.2	5.00	1.037	5.18	F-M Sandstone	Sw	
6		11.27	37.0	58	2146	2732	52.3	4.12	1.020	4.21	F-M Sandstone	Sw	
7		8.63	32.0	54	1728	2200	46.9	3.92	0.972	3.81	F-M Sandstone	Sw	
8		17.39	54.0	51	2754	3507	59.2	4.96	1.079	5.35	F-M Sandstone	Sw	
9		7.58	28.0	55	1540	1961	44.3	3.87	0.947	3.66	F-M Sandstone	Sw	
10		7.82	24.0	66	1584	2017	44.9	3.88	0.953	3.69	F-M Sandstone	Sw	
11		6.03	26.0	37	962	1225	35.0	4.92	0.852	4.19	F-M Sandstone	Sw	
12		3.50	10.0	47	470	598	24.5	5.85	0.725	4.24	F-M Sandstone	Sw	
13		6.77	17.8	50.2	894	1138	33.7	5.95	0.838	4.98	F-M Sandstone	Sw	
14		6.37	19.2	41.7	801	1019	31.9	6.25	0.817	5.11	F-M Sandstone	Sw	
15		10.73	22.1	52	1149	1463	38.3	7.33	0.886	6.50	F-M Sandstone	Sw	

SAMPLE: 5b

Test No.	Type	P (kN)	D (mm)	W (mm)	A = WD (mm^2)	D_e^2	D_e	I_s	F	$I_{s(50)}$ (MPa)	Lithology	Weathering	Notes
1		8.89	37.0	24	888	1131	33.6	7.86	0.836	6.58	F-M Sandstone	Sw	
2		7.40	41.0	43	1763	2245	47.4	3.30	0.976	3.22	F-M Sandstone	Sw	
3		10.55	29.0	35	1015	1292	35.9	8.16	0.862	7.04	F-M Sandstone	Sw	
4		2.44	27.0	60	1620	2063	45.4	1.18	0.958	1.13	F-M Sandstone	Mw	Some break along existing
5		9.25	24.0	36	864	1100	33.2	8.41	0.831	6.99	F-M Sandstone	Sw	
6		6.57	17.0	44	748	952	30.9	6.90	0.805	5.55	F-M Sandstone	Sw-Mw	
7		2.72	7.0	27	189	241	15.5	11.30	0.591	6.68	F-M Sandstone	Sw	
8		6.49	18.0	31	558	710	26.7	9.13	0.753	6.88	F-M Sandstone	Sw	

SAMPLE: 5c

Test No.	Type	P (kN)	D (mm)	W (mm)	A = WD (mm^2)	D_e^2	D_e	I_s	F	$I_{s(50)}$ (MPa)	Lithology	Weathering	Notes
1		7.62	20.0	41	820	1044	32.3	7.30	0.822	6.00	F-M Sandstone	Sw-Mw	
2		9.68	45.0	44	1980	2521	50.2	3.84	1.002	3.85	F-M Sandstone	Sw-Mw	
3		11.25	28.0	46	1288	1640	40.5	6.86	0.909	6.24	F-M Sandstone	Sw	
4		11.94	40.0	55	2200	2801	52.9	4.26	1.026	4.37	F-M Sandstone	Sw-Mw	
5		1.59	46.0	47	2162	2753	52.5	0.58	1.022	0.59	F-M Sandstone	Mw	Break along existing
6		2.48	27.0	42	1134	1444	38.0	1.72	0.884	1.52	F-M Sandstone	Mw	Break along existing
7		3.11	32.0	38	1216	1548	39.3	2.01	0.898	1.80	F-M Sandstone	Mw	Crumbles
8		0.95	14.0	36	504	642	25.3	1.48	0.736	1.09	F-M Sandstone	Mw	Crumbles
9		2.54	50.0	21	1050	1337	36.6	1.90	0.869	1.65	F-M Sandstone	Mw	Break along existing
10		1.83	26.0	36	936	1192	34.5	1.54	0.846	1.30	F-M Sandstone	Mw	Crumbles
11		14.64	44.0	60	2640	3361	58.0	4.36	1.069	4.66	F-M Sandstone	Sw	
12		12.31	30.0	57	1710	2177	46.7	5.65	0.969	5.48	F-M Sandstone	Sw	
13		18.77	51.0	69	3519	4481	66.9	4.19	1.140	4.78	F-M Sandstone	Sw	
14		3.74	11.0	53	583	742	27.2	5.04	0.761	3.83	F-M Sandstone	Sw	
15		9.52	22.0	59	1298	1653	40.7	5.76	0.911	5.25	F-M Sandstone	Sw	

SAMPLE: 5d

Test No.	Type	P (kN)	D (mm)	W (mm)	A = WD (mm^2)	D_e^2	D_e	I_s	F	$I_{s(50)}$ (MPa)	Lithology	Weathering	Notes
1		1.99	26.0	54	1404	1788	42.3	1.11	0.927	1.03	F-M Sandstone	Mw-Hw	
2		0.53	30.0	47	1410	1795	42.4	0.30	0.928	0.27	Fine Sandstone	Hw	
3		0.79	20.0	45	900	1146	33.9	0.69	0.839	0.58	Fine Sandstone	Hw	
4		1.26	19.0	40	760	968	31.1	1.30	0.808	1.05	Fine Sandstone	Hw	
5		0.34	24.0	51	1224	1558	39.5	0.22	0.899	0.20	Fine Sandstone	Hw	Quartz veining
6		2.34	25.0	25	625	796	28.2	2.94	0.773	2.27	F-M Sandstone	Mw-Hw	

D.7 Elliott Fault - Point Load testing

SAMPLE: 6a

Test No.	Type	P (kN)	D (mm)	W (mm)	A = WD (mm^2)	D_e^2	D_e	I_s	F	$I_{s(50)}$ (MPa)	Lithology	Weathering	Notes
1		17.31	49.0	41	2009	2558	50.6	6.77	1.005	6.80	F-M Sandstone	Sw	
2		8.33	37.0	23	851	1084	32.9	7.69	0.829	6.37	F-M Sandstone	Sw	
3		5.60	9.0	49	441	561	23.7	9.97	0.715	7.13	F-M Sandstone	Uw-Sw	
4		6.37	12.0	47	564	718	26.8	8.87	0.755	6.70	F-M Sandstone	Uw-Sw	
5		5.30	11.0	47	517	658	25.7	8.05	0.741	5.96	F-M Sandstone	Uw-Sw	Some quartz veining
6		16.18	30.0	46	1380	1757	41.9	9.21	0.924	8.51	F-M Sandstone	Uw-Sw	
7		6.45	21.0	59	1239	1578	39.7	4.09	0.902	3.69	F-M Sandstone	Uw-Sw	Break along existing
8		15.36	25.0	74	1850	2355	48.5	6.52	0.987	6.43	F-M Sandstone	Uw-Sw	
9		23.07	40.0	52	2080	2648	51.5	8.71	1.013	8.82	F-M Sandstone	Uw-Sw	Some quartz veining
10		7.16	14.0	83	1162	1480	38.5	4.84	0.889	4.30	F-M Sandstone	Uw-Sw	
11		13.52	53.0	80	4240	5399	73.5	2.50	1.189	2.98	F-M Sandstone	Uw-Sw	Break along existing quartz vein
12		7.24	45.0	38	1710	2177	46.7	3.33	0.969	3.22	F-M Sandstone	Uw-Sw	Break along existing
13		9.31	16.0	80	1280	1630	40.4	5.71	0.908	5.19	F-M Sandstone	Uw-Sw	
14		6.63	15.0	41	615	783	28.0	8.47	0.770	6.52	F-M Sandstone	Uw-Sw	
15		6.45	32.0	32	1024	1304	36.1	4.95	0.864	4.27	F-M Sandstone	Uw-Sw	

SAMPLE: 5k

Test No.	Type	P (kN)	D (mm)	W (mm)	A = WD (mm^2)	D_e^2	D_e	I_s	F	$I_{s(50)}$ (MPa)	Lithology	Weathering	Notes
1		4.92	13.0	76	988	1258	35.5	3.91	0.857	3.35	M Sandstone	Sw	
2		5.38	26.0	47	1222	1556	39.4	3.46	0.899	3.11	M Sandstone	Sw	
3		5.36	17.0	38	646	823	28.7	6.52	0.779	5.07	M Sandstone	Sw	
4		2.56	14.0	47	658	838	28.9	3.06	0.782	2.39	M Sandstone	Sw	Break along existing
5		2.95	27.0	37	999	1272	35.7	2.32	0.859	1.99	M Sandstone	Sw-Mw	Break along existing
6		13.32	49.0	78	3822	4866	69.8	2.74	1.162	3.18	M Sandstone	Sw	
7		5.26	27.0	60	1620	2063	45.4	2.55	0.958	2.44	M Sandstone	Sw	
8		10.26	50.0	72	3600	4584	67.7	2.24	1.146	2.57	M Sandstone	Sw	
9		11.05	45.0	88	3960	5042	71.0	2.19	1.171	2.57	M Sandstone	Sw	

SAMPLE: 7a

Test No.	Type	P (kN)	D (mm)	W (mm)	A = WD (mm^2)	D_e^2	D_e	I_s	F	$I_{s(50)}$ (MPa)	Lithology	Weathering	Notes
1		6.55	22.0	69	1518	1933	44.0	3.39	0.944	3.20	F-M Sandstone	Sw-Mw	
2		5.73	37.0	45	1665	2120	46.0	2.70	0.964	2.60	F-M Sandstone	Mw	
3		9.66	45.0	60	2700	3438	58.6	2.81	1.074	3.02	M Sandstone	Sw-Mw	
4		7.42	39.0	74	2886	3675	60.6	2.02	1.091	2.20	M Sandstone	Mw	
5		6.59	47.0	35	1645	2094	45.8	3.15	0.961	3.02	M Sandstone	Sw-Mw	
6		2.44	20.0	41	820	1044	32.3	2.34	0.822	1.92	M Sandstone	Mw	Break along existing joint
7		3.33	22.0	53	1166	1485	38.5	2.24	0.889	1.99	M Sandstone	Mw	
8		12.02	40.0	111	4440	5653	75.2	2.13	1.202	2.55	M Sandstone	Sw-Mw	
9		4.08	25.0	50	1250	1592	39.9	2.56	0.903	2.32	M Sandstone	Sw-Mw	
10		5.85	40.0	60	2400	3056	55.3	1.91	1.046	2.00	M Sandstone	Sw-Mw	Break along existing iron oxide joint
11		1.54	33.0	40	1320	1681	41.0	0.92	0.915	0.84	M Sandstone	Mw	Break along existing joint

SAMPLE: 8a

Test No.	Type	P (kN)	D (mm)	W (mm)	A = WD (mm^2)	D_e^2	D_e	I_s	F	$I_{s(50)}$ (MPa)	Lithology	Weathering	Notes
1		3.11	27.0	47	1269	1616	40.2	1.92	0.906	1.74	M Sandstone	Mw - Hw	
2		0.89	30.0	40	1200	1528	39.1	0.58	0.895	0.52	M Sandstone	Mw - Hw	Break along existing
3		2.89	27.0	38	1026	1306	36.1	2.21	0.864	1.91	M Sandstone	Mw - Hw	
4		2.42	33.0	34	1122	1429	37.8	1.69	0.882	1.49	M Sandstone	Mw - Hw	Some break along existing
5		2.80	39.0	54	2106	2681	51.8	1.04	1.016	1.06	M Sandstone	Mw - Hw	
6		4.74	27.0	59	1593	2028	45.0	2.34	0.954	2.23	M Sandstone	Mw - Hw	
7		4.63	37.0	120	4440	5653	75.2	0.82	1.202	0.98	M Sandstone	Mw - Hw	
8		3.13	36.0	30	1080	1375	37.1	2.28	0.874	1.99	M Sandstone	Mw - Hw	
9		1.99	27.0	50	1350	1719	41.5	1.16	0.919	1.06	M Sandstone	Mw - Hw	

SAMPLE: 9a

Test No.	Type	P (kN)	D (mm)	W (mm)	A = WD (mm^2)	D_e^2	D_e	I_s	F	$I_{s(50)}$ (MPa)	Lithology	Weathering	Notes
1		8.85	42.0	22	924	1176	34.3	7.52	0.844	6.35	Fine Sandstone	Sw	Some break along oxidised fracture
2		23.17	59.0	53	3127	3981	63.1	5.82	1.110	6.46	Fine Sandstone	Sw	Rock shatter
3		7.70	43.0	38	1634	2080	45.6	3.70	0.960	3.55	Fine Sandstone	Sw	
4		4.49	28.0	27	756	963	31.0	4.66	0.807	3.76	Fine Sandstone	Sw	
5		5.30	27.0	36	972	1238	35.2	4.28	0.854	3.66	Fine Sandstone	Sw	
6		0.79	16.0	40	640	815	28.5	0.97	0.777	0.75	Breccia clast	Hw	Other breccia clasts fail without reading
7		6.01	13.0	24	312	397	19.9	15.13	0.661	10.00	Fine Sandstone	Sw	
8		2.99	45.0	52	2340	2979	54.6	1.00	1.040	1.04	Mudstone	Sw	
9		1.08	40.0	46	1840	2343	48.4	0.46	0.985	0.45	Mudstone	Sw	Breaks along existing
10		0.59	22.0	50	1100	1401	37.4	0.42	0.878	0.37	Mudstone	Sw	Breaks along existing
11		5.64	26.0	47	1222	1556	39.4	3.62	0.899	3.26	Mudstone	Sw	
12		8.14	40.0	46	1840	2343	48.4	3.47	0.985	3.42	Mudstone	Sw	
13		4.63	22.0	33	726	924	30.4	5.01	0.799	4.00	Mudstone	Sw	
14		6.47	30.0	26	780	993	31.5	6.51	0.812	5.29	Mudstone	Sw	
15		0.91	18.0	34	612	779	27.9	1.17	0.769	0.90	Mudstone	Sw	Break along existing

SAMPLE: 10d

Test No.	Type	P (kN)	D (mm)	W (mm)	A = WD (mm^2)	D_e^2	D_e	I_s	F	$I_{s(50)}$ (MPa)	Lithology	Weathering	Notes
1	parallel	6.65	58.0	80	4640	5908	76.9	1.13	1.213	1.37	Fine Sandstone	Mw	Break along existing
2		2.21	32.0	43	1376	1752	41.9	1.26	0.923	1.16	Fine Sandstone	Mw	Break along existing
3		1.52	44.0	40	1760	2241	47.3	0.68	0.976	0.66	Fine Sandstone	Mw	Soft shatter
4		0.51	20.0	33	660	840	29.0	0.61	0.782	0.47	Fine Sandstone	Mw	Soft shatter - incipient fracturing
5		0.53	34.0	22	748	952	30.9	0.56	0.805	0.45	Fine Sandstone	Mw	Soft shatter
6		0.91	40.0	24	960	1222	35.0	0.74	0.851	0.63	Fine Sandstone	Mw	Soft shatter
7		20.90	38.0	62	2356	3000	54.8	6.97	1.042	7.26	Fine Sandstone	Sw	
8		7.50	27.0	74	1998	2544	50.4	2.95	1.004	2.96	Fine Sandstone	Sw	
9		4.67	36.0	38	1368	1742	41.7	2.68	0.922	2.47	Fine Sandstone	Sw-Mw	
10		1.12	28.0	39	1092	1390	37.3	0.81	0.876	0.71	Mudstone	Mw	Break along existing
11		2.03	16.0	32	512	652	25.5	3.11	0.739	2.30	Mudstone	Sw-Mw	Shatter
12		3.09	65.0	26	1690	2152	46.4	1.44	0.967	1.39	Mudstone	Mw	
13		9.21	30.0	45	1350	1719	41.5	5.36	0.919	4.93	Fine Sandstone	Sw	

D.7 Elliott Fault - Point Load testing

SAMPLE: 10e

Test No.	Type	P (kN)	D (mm)	W (mm)	A = WD (mm^2)	D_e^2	D_e	I_s	F	$I_{s(50)}$ (MPa)	Lithology	Weathering	Notes
1		3.48	32.0	45	1440	1833	42.8	1.90	0.933	1.77	Mudstone	Sw	Shatter along existing
2		9.21	33.0	32	1056	1345	36.7	6.85	0.870	5.96	Fine Sandstone	Sw	
3		1.75	28.0	39	1092	1390	37.3	1.26	0.876	1.10	F-M Sandstone	Sw	Break along existing
4		4.00	35.0	50	1750	2228	47.2	1.80	0.974	1.75	Mudstone	Sw-Mw	Break along existing
5		7.84	35.0	68	2380	3030	55.0	2.59	1.044	2.70	Fine Sandstone	Sw	
6		2.99	18.0	58	1044	1329	36.5	2.25	0.868	1.95	Fine Sandstone	Sw	
7		3.43	21.0	22	462	588	24.3	5.83	0.722	4.21	Mudstone	Sw	
8		1.81	26.0	35	910	1159	34.0	1.56	0.841	1.31	Mudstone	Sw	
9		28.74	48.0	94	4512	5745	75.8	5.00	1.206	6.03	F-M Sandstone	Sw	
10		1.89	53.0	60	3180	4049	63.6	0.47	1.115	0.52	F-M Sandstone	Sw	Break along existing
11		11.76	31.0	49	1519	1934	44.0	6.08	0.944	5.74	F-M Sandstone	Sw	
12		9.41	42.0	31	1302	1658	40.7	5.68	0.912	5.18	F-M Sandstone	Sw	
13		7.36	16.0	42	672	856	29.3	8.60	0.786	6.76	F-M Sandstone	Sw	
14		21.85	49.0	70	3430	4367	66.1	5.00	1.134	5.67	F-M Sandstone	Sw	
15		18.65	34.0	47	1598	2035	45.1	9.17	0.955	8.75	F-M Sandstone	Sw	
16		2.38	27.0	29	783	997	31.6	2.39	0.813	1.94	Mudstone	Sw	
17		4.90	20.0	55	1100	1401	37.4	3.50	0.878	3.07	Mudstone	Sw	
18		2.11	52.0	78	4056	5164	71.9	0.41	1.177	0.48	Mudstone	Sw	Break along existing
19		3.56	15.0	39	585	745	27.3	4.78	0.762	3.64	Mudstone	Sw	
20		10.00	38.0	35	1330	1693	41.2	5.91	0.916	5.41	Fine Sandstone	Sw	
21		5.12	17.0	49	833	1061	32.6	4.83	0.825	3.98	Fine Sandstone	Sw	Break along existing

SAMPLE: 11a

Test No.	Type	P (kN)	D (mm)	W (mm)	A = WD (mm^2)	D_e^2	D_e	I_s	F	$I_{s(50)}$ (MPa)	Lithology	Weathering	Notes
1	parallel	4.71	27.0	39	1053	1341	36.6	3.51	0.869	3.05	Fine Sandstone	Sw-Mw	
2		1.54	28.0	60	1680	2139	46.2	0.72	0.966	0.70	Fine Sandstone	Mw	Break along existing
3		5.91	22.0	40	880	1120	33.5	5.27	0.835	4.40	Fine Sandstone	Sw-Mw	
4		1.95	53.0	55	2915	3711	60.9	0.53	1.093	0.57	Fine Sandstone	Mw	Break along existing
5		13.95	27.0	35	945	1203	34.7	11.59	0.848	9.83	Fine Sandstone	Sw	
6		1.77	24.0	45	1080	1375	37.1	1.29	0.874	1.13	Fine Sandstone	Sw-Mw	Some break along existing quartz vein
7		1.36	28.0	35	980	1248	35.3	1.09	0.855	0.93	Fine Sandstone	Mw	Break along existing
8		7.94	24.0	40	960	1222	35.0	6.50	0.851	5.53	Fine Sandstone	Sw	
9		4.25	52.0	60	3120	3973	63.0	1.07	1.110	1.19	Fine Sandstone	Sw	
10		2.46	38.0	54	2052	2613	51.1	0.94	1.010	0.95	Fine Sandstone	Mw	Some break along existing
11		5.52	10.0	50	500	637	25.2	8.67	0.735	6.37	Fine Sandstone	Sw	

D.8 Elliott Fault fines index test results and calculations

Fines content results and calculation tables produced from wet sieving and laser size analysis per sample outcrop.

D.8 Elliott Fault - fines index testing

5D				
Passing (wet sieve)	**Raw weight (g)**	**Container weight (g)**	**Sample weight (g)**	**Sample fines division (%)**
>4mm	1062.76	13.64	1049.12	74.67
>2mm (gravel)	343.71	182.63	161.08	11.47
>1mm (coarse sand)	218.15	182.63	35.52	2.53
Remaining fraction (<1mm)	197.76	38.51	159.25	11.33
Total sample weight (g)			1404.97	
Matrix (lasersizer)	**Average diameter (µm)**	**Cumulative %**	**Actual %**	**% of total <1mm fraction**
<2 microns (clay)	2	2.9	2.90	0.33
<60 microns (silt)	59.57	18.2	15.30	1.73
<200 microns (fine sand)	199.53	34.3	16.10	1.82
Remaining fraction (medium/coarse sand)		100	65.70	7.45

5G				
Passing (wet sieve)	**Raw weight (g)**	**Container weight (g)**	**Sample weight (g)**	**Sample fines division (%)**
>4mm	827.35	13.64	813.71	51.81
>2mm (gravel)	479.39	182.63	296.76	18.90
>1mm (coarse sand)	289.53	182.63	106.9	6.81
Remaining fraction (<1mm)	391.57	38.51	353.06	22.48
Total sample weight (g)			1570.43	
Matrix (lasersizer)	**Average diameter (µm)**	**Cumulative %**	**Actual %**	**% of total <1mm fraction**
<2 microns (clay)	2	5.07	5.07	1.14
<60 microns (silt)	59.57	26.97	21.90	4.92
<200 microns (fine sand)	199.53	34.2	7.23	1.63
Remaining fraction (medium/coarse sand)		100	65.80	14.79

5I				
Passing (wet sieve)	**Raw weight (g)**	**Container weight (g)**	**Sample weight (g)**	**Sample fines division (%)**
>4mm	1298.16	13.73	1284.43	59.92
>2mm (gravel)	604.05	188.27	415.78	19.40
>1mm (coarse sand)	299.09	188.29	110.8	5.17
Remaining fraction (<1mm)	371.22	38.51	332.71	15.52
Total sample weight (g)			2143.72	
Matrix (lasersizer)	**Average diameter (µm)**	**Cumulative %**	**Actual %**	**% of total <1mm fraction**
<2 microns (clay)	2	5.01	5.01	0.78
<60 microns (silt)	59.57	22.63	17.62	2.73
<200 microns (fine sand)	199.53	30.53	7.90	1.23
Remaining fraction (medium/coarse sand)		100	69.47	10.78

10e				
Passing (wet sieve)	**Raw weight (g)**	**Container weight (g)**	**Sample weight (g)**	**Sample fines division (%)**
>4mm	738.39	13.64	724.75	56.41
>2mm (gravel)	396.25	182.63	213.62	16.63
>1mm (coarse sand)	231.52	182.63	48.89	3.80
Remaining fraction (<1mm)	336.14	38.51	297.63	23.16
Total sample weight (g)			1284.89	
Matrix (lasersizer)	**Average diameter (µm)**	**Cumulative %**	**Actual %**	**% of total <1mm fraction**
<2 microns (clay)	2	12.4	12.40	2.87
<60 microns (silt)	59.57	54.7	42.30	9.80
<200 microns (fine sand)	199.53	54.7	0.00	0.00
Remaining fraction (medium/coarse sand)		100	45.30	10.49

D.8 Elliott Fault - fines index testing

5C				
Passing (wet sieve)	**Raw weight (g)**	**Container weight (g)**	**Sample weight (g)**	**Sample fines division (%)**
>4mm	782.52	14.67	767.85	78.16
>2mm	290.87	206.96	83.91	8.54
>1mm	221.3	206.96	14.34	1.46
Remaining fraction (<1mm)	154.7	38.43	116.27	11.84
Total sample weight			982.37	
Matrix (lasersizer)	**Average diameter (µm)**	**Cumulative %**	**Actual %**	**% of total <1mm fraction**
<2 microns (clay)	2	6.7	6.70	0.79
<60 microns (silt)	59.57	34.73	28.03	3.32
<200 microns (fine sand)	199.53	44.9	10.17	1.20
Remaining fraction (medium/coarse sand)		100	55.10	6.52

5E				
Passing (wet sieve)	**Raw weight (g)**	**Container weight (g)**	**Sample weight (g)**	**Sample fines division (%)**
>4mm	376.77	9.54	367.23	43.32
>2mm	287.02	174.06	112.96	13.33
>1mm	264.41	188.38	76.03	8.97
Remaining fraction (<1mm)	330.21	38.73	291.48	34.38
Total sample weight			847.7	
Matrix (lasersizer)	**Average diameter (µm)**	**Cumulative %**	**Actual %**	**% of total <1mm fraction**
<2 microns (clay)	2	13.33	13.33	4.58
<60 microns (silt)	59.57	68.83	55.50	19.08
<200 microns (fine sand)	199.53	81.53	12.70	4.37
Remaining fraction (medium/coarse sand)		100	18.47	6.35

5F				
Passing (wet sieve)	**Raw weight (g)**	**Container weight (g)**	**Sample weight (g)**	**Sample fines division (%)**
>4mm	389.76	10.67	379.09	51.57
>2mm	253.35	176.91	76.44	10.40
>1mm	264.55	206.95	57.6	7.84
Remaining fraction (<1mm)	261.44	39.42	222.02	30.20
Total sample weight			735.15	
Matrix (lasersizer)	**Average diameter (µm)**	**Cumulative %**	**Actual %**	**% of total <1mm fraction**
<2 microns (clay)	2	10.17	10.17	3.07
<60 microns (silt)	59.57	52.83	42.66	12.88
<200 microns (fine sand)	199.53	92.1	39.27	11.86
Remaining fraction (medium/coarse sand)		100	7.90	2.39

5H				
Passing (wet sieve)	**Raw weight (g)**	**Container weight (g)**	**Sample weight (g)**	**Sample fines division (%)**
>4mm	383.47	10.73	372.74	41.38
>2mm	268.38	176.8	91.58	10.17
>1mm	282.36	206.94	75.42	8.37
Remaining fraction (<1mm)	399.37	38.43	360.94	40.07
Total sample weight			900.68	
Matrix (lasersizer)	**Average diameter (µm)**	**Cumulative %**	**Actual %**	**% of total <1mm fraction**
<2 microns (clay)	2	12.83	12.83	5.14
<60 microns (silt)	59.57	59.57	46.74	18.73
<200 microns (fine sand)	199.53	83.2	23.63	9.47
Remaining fraction (medium/coarse sand)		100	16.80	6.73

D.8 Elliott Fault - fines index testing

5J				
Passing (wet sieve)	**Raw weight (g)**	**Container weight (g)**	**Sample weight (g)**	**Sample fines division (%)**
>4mm	386.49	9.61	376.88	40.56
>2mm	279.73	188.32	91.41	9.84
>1mm	256.92	174.01	82.91	8.92
Remaining fraction (<1mm)	417.73	39.65	378.08	40.69
Total sample weight			929.28	
Matrix (lasersizer)	**Average diameter (µm)**	**Cumulative %**	**Actual %**	**% of total <1mm fraction**
<2 microns (clay)	2	9.87	9.87	4.02
<60 microns (silt)	59.57	64.5	54.63	22.23
<200 microns (fine sand)	199.53	93.53	29.03	11.81
Remaining fraction (medium/coarse sand)		100	6.47	2.63

9A				
Passing (wet sieve)	**Raw weight (g)**	**Container weight (g)**	**Sample weight (g)**	**Sample fines division (%)**
>4mm	2596.48	13.81	2582.67	88.18
>2mm	324.28	207.13	117.15	4.00
>1mm	254.61	207.13	47.48	1.62
Remaining fraction (<1mm)	220.07	38.43	181.64	6.20
Total sample weight			2928.94	
Matrix (lasersizer)	**Average diameter (µm)**	**Cumulative %**	**Actual %**	**% of total <1mm fraction**
<2 microns (clay)	2	6.1	6.10	0.38
<60 microns (silt)	59.57	27.27	21.17	1.31
<200 microns (fine sand)	199.53	37.93	10.66	0.66
Remaining fraction (medium/coarse sand)		100	62.07	3.85

10A				
Passing (wet sieve)	**Raw weight (g)**	**Container weight (g)**	**Sample weight (g)**	**Sample fines division (%)**
>4mm	932.14	13.86	918.28	59.49
>2mm	442.92	207.17	235.75	15.27
>1mm	310.59	207.17	103.42	6.70
Remaining fraction (<1mm)	299.92	13.79	286.13	18.54
Total sample weight			1543.58	
Matrix (lasersizer)	**Average diameter (µm)**	**Cumulative %**	**Actual %**	**% of total <1mm fraction**
<2 microns (clay)	2	6.63	6.63	1.23
<60 microns (silt)	59.57	31.57	24.94	4.62
<200 microns (fine sand)	199.53	35.33	3.76	0.70
Remaining fraction (medium/coarse sand)		100	64.67	11.99

10B				
Passing (wet sieve)	**Raw weight (g)**	**Container weight (g)**	**Sample weight (g)**	**Sample fines division (%)**
>4mm	849.37	9.89	839.48	45.27
>2mm	708.8	427.99	280.81	15.14
>1mm	525.93	427.99	97.94	5.28
Remaining fraction (<1mm)	675.3	39.29	636.01	34.30
Total sample weight			1854.24	
Matrix (lasersizer)	**Average diameter (µm)**	**Cumulative %**	**Actual %**	**% of total <1mm fraction**
<2 microns (clay)	2	3.13	3.13	1.07
<60 microns (silt)	59.57	15.67	12.54	4.30
<200 microns (fine sand)	199.53	28.67	13.00	4.46
Remaining fraction (medium/coarse sand)		100	71.33	24.47

D.8 Elliott Fault - fines index testing

10C				
Passing (wet sieve)	**Raw weight (g)**	**Container weight (g)**	**Sample weight (g)**	**Sample fines division (%)**
>4mm	391.88	10.81	381.07	39.20
>2mm	328.65	182.45	146.2	15.04
>1mm	280.77	188.28	92.49	9.52
Remaining fraction (<1mm)	390.7	38.43	352.27	36.24
Total sample weight			972.03	
Matrix (Lasersizer)	**Average diameter (µm)**	**Cumulative %**	**Actual %**	**% of total <1mm fraction**
<2 microns (clay)	2	6.03	6.03	2.19
<60 microns (silt)	59.57	36.1	30.07	10.90
<200 microns (fine sand)	199.53	73.63	37.53	13.60
Remaining fraction (medium/coarse sand)		100	26.37	9.56

11A				
Passing (wet sieve)	**Raw weight (g)**	**Container weight (g)**	**Sample weight (g)**	**Sample fines division (%)**
>4mm	1855.11	13.79	1841.32	71.37
>2mm	485.5	207.13	278.37	10.79
>1mm	292.4	207.13	85.27	3.31
Remaining fraction (<1mm)	438.66	63.63	375.03	14.54
Total sample weight			2579.99	
Matrix (Lasersizer)	**Average diameter (µm)**	**Cumulative %**	**Actual %**	**% of total <1mm fraction**
<2 microns (clay)	2	4.97	4.97	0.72
<60 microns (silt)	59.57	32.3	27.33	3.97
<200 microns (fine sand)	199.53	48.53	16.23	2.36
Remaining fraction (medium/coarse sand)		100	51.47	7.48

Appendix E: Hurunui River

Results derived from the lineation analysis, raw mapping data, analysis, raw lab testing data and calculations for the Hurunui River study site.

E.1 Hurunui River lineation analysis

Landscape lineation derived from aerial photography and DEM analysis.

E.1 Hurunui River - lineation analysis

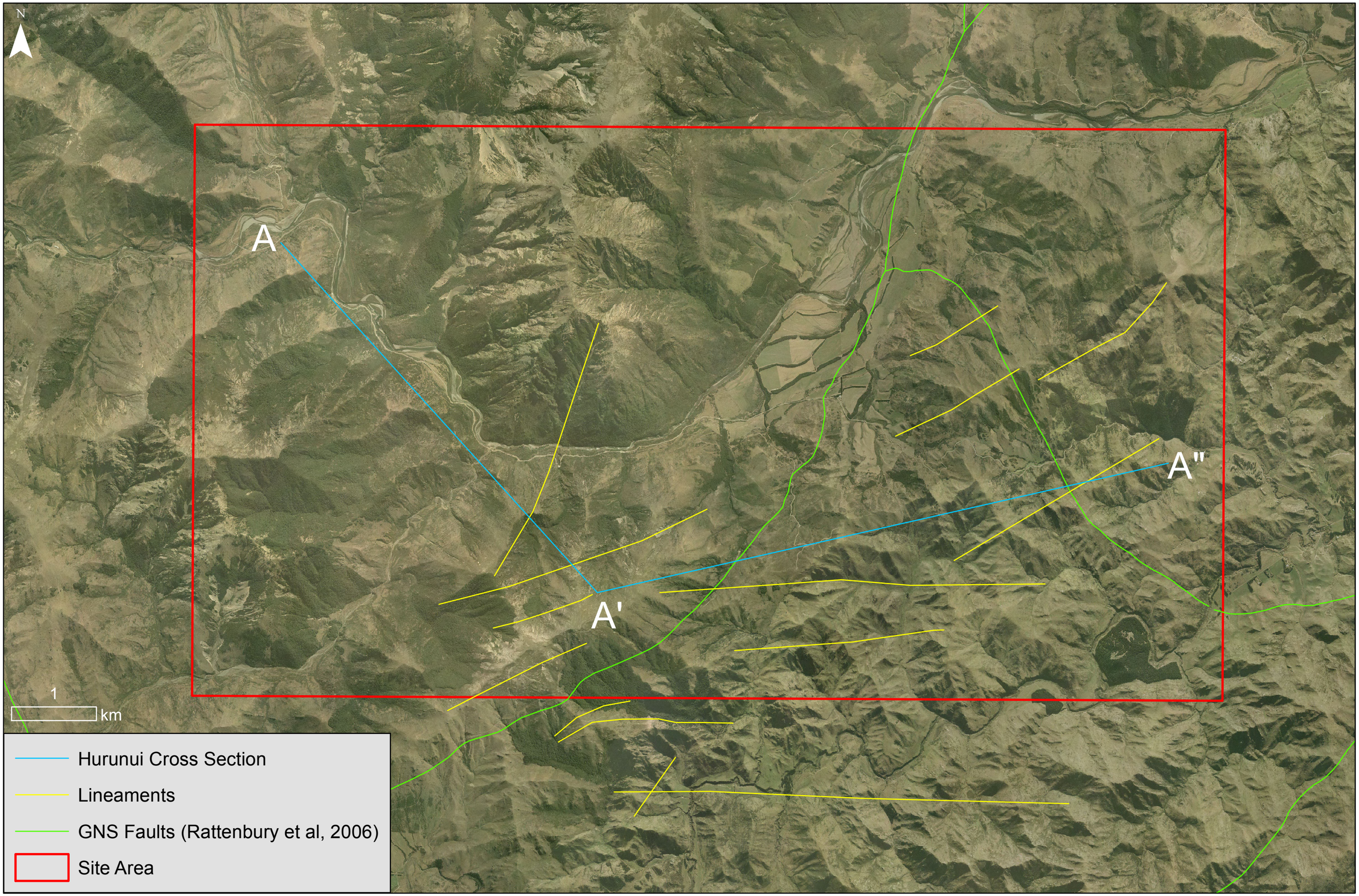

Imagery Source: Canterbury Aerial Photo

E.2 Hurunui River raw mapping data

Mapping per field data sheets (Appendix A). Where data is missing, blanked out or ranges from other sites, information has been unobtainable due to access issues, poor rock/defect conditions, recording prior to the continual modification of the field sheets or previous recording of the defect (i.e. 1 x bedding plane between two lithologies).

E.2.1 Hurunui River - Coherent rock and bedding

Outcrop #	Weathering	Colour	Bedding fabric	Bedding thickness	Bedding development	Grain Size	Rock name	Strength (schmidt intact rock rebound)	Strength (Hammer)	Wavelength (m)	Interlimb angle (ILA, °)	Degree of fracture	Dip	Dip direction	Bedding roughness	Raw field notes
1a	Sw-Mw	L-GY	Massive	V thick	M	F-M	Sandstone	56, 50, 48	VS	2.6	150					
1a	Sw-Mw	D-GY	Massive	Thick	D		Mudstone	10	VW							Friable, fragmented, heavily sheared mudstone
1b	Sw	L-GY	Massive	Massive	M	F-M	Sandstone	20, 56, 54	VS							
1c	Mw-Hw	D-GY	Massive	Massive	M		Mudstone		VW							Bedding becomes evident, heavy oxidisation in mudstone layers
1d	Sw-Mw	L-GY	Massive	Medium	WD	F-M	Sandstone	20, 40, 34	S	2	175		89	271		
1d	Hw	D-GY	Massive	Thin	WD		Mudstone	10, 14, 10	W				78	285		mudstone = friable
2a	Sw	L-GY	Massive	Medium	WD	F-M	Sandstone	36, 38, 46	S	2.8	165		27	59		
2a	Mw	D-GY	Massive	Thin	VWD		Mudstone	9	VW				48	70		
2b	Sw	L-GY	Massive	V thick	D	F-M	Sandstone	44, 59, 39	VS	4	175		81	113		multiple small scale faults
2b	Mw	D-GY	Massive	V thick	D		Mudstone	16, 25, 12	W				81	133		
3a	Sw	L-GY	Massive	V thick	D	F-M	Sandstone	47, 53, 29	VS	0	180		74	129		
3a	Sw-Mw	D-GY	Massive	Thin	WD		Mudstone	32, 26, 10, 17	MS				81	128		
3b	Sw	L-GY	Massive	Thick	WD	F-M	Sandstone	51, 62, 49, 60	ES	0	180		70	136		
3b	Sw-Mw	D-GY	Massive	Thin	VWD		Mudstone	10, 12	VW				70	134		
4a	Sw-Mw	L-GY	Massive	Thick	WD	F-M	Sandstone	54, 32, 36	VS	0	180		81	290		Difficult to see due to over wash from soil above
4a	Mw	D-GY	Massive	Thin	VWD		Mudstone	14, 18, 24	W				72	294		
4a	Sw-Mw	L/D-GY	Massive	Medium	D	F-M	Sandstone	68, 18, 26	VS				71	292		
5a	Sw	D-GY	Massive	V thick	WD	F-M	Sandstone	50, 46, 42, 44	VS	0	180		45	71		
5a	Sw	D-GY	Massive	Thin	VWD		Mudstone	13, 19	VW				48	68		
5b	Uw-Sw	D-GY	Massive	Massive	M	F-M	Sandstone	52, 56, 56	VS							Outcrop is of a massive nature
6a	Uw-Sw	L-GY	Massive	Thick	D	F-M	Sandstone	46, 52, 30, 46	VS				55	299		
6a	Mw	D-GY	Massive	Thin	WD		Mudstone	10, 14, 16, 16	W				61	299		
7a	Sw-Mw	L-GY	Massive	V thick	D	F-M	Sandstone	39, 39, 19	S	3.1	165		78	114		
7a	Mw-Hw	D-GY	Massive	Thin	VWD		Mudstone	9, 11,	VW				74	110		
8a	Sw-Mw	L-GY	Massive	V thick	D	F-M	Sandstone	46, 45, 48	VS	0	180		75	87		
8a	Mw-Hw	D-GY (red oxide)	Massive	V thin	D		Mudstone	11, 10, 13	W				78	91		mudstone beds at different orientations - lineated
8b	Sw-Mw	L-GY	Massive	V thick	D	F-M	Sandstone	38, 35, 36	S	0	180		71	63		
8b	Mw	D-GY	Massive	V thin	D		Mudstone	10, 9	VW				70	69		Lineated mudstone = reflects intense shear/stress on mudstone - beds squashed v thin
9a	Sw	L-GY	Massive	V thick	D	F-M	Sandstone	34, 38, 51	VS			MOD-HF	71	134	UR	
9a	Sw-Mw	D-GY - BLACK	Massive	V thin	D		Mudstone	14, 18, 16	MS	0.4	155	FRAG	86	139	UR	
10a	Sw-Mw	L-D GY	Massive	V thick	D	F-M	Sandstone	28, 14, 46, 21	S	1.5	175		54	30		mudstone heavily deformed flowing around sandstone (boudin) - no consistent D/DD
10a	Mw	D-GY	Massive	Thin	D		Mudstone	13, 11	VW	0.8	140		50	79		
11a	Mw	L-GY	Massive	Thick	WD	F-M	Sandstone	49, 38, 44	VS	2.8	170		83	80		mudstone heavily fragmented and oxidised, mudstone beginning to boudin sandstone but not as bad
11a	Mw	D-GY (red oxide)	Massive	Thin	WD		Mudstone	10	VW				70	80		Thin interbeds are HF vs. MF V thick sandstone
12a	Mw-Hw	L-GY	Massive	Thick	D	F-M	Sandstone	50, 56, 51, 42	VS				72	275		mudstone bed is heavily friable/fragmented with small scale (cm) blocks of intact sandstone and mudstone inside
12a	Mw-Hw	D-GY	Massive	Thick	WD		Mudstone	16, 10, 10	VW				84	302		Bedding is defined by sharp contacts with sandstone but may be boudinage
13a	Mw-Hw	L-GY (yellow)	Massive	Thin	VWD	F-M	Sandstone	35, 16, 20, 35	S	0.9	90		84	294		Note: bedding folded - D/DD = dominant orientation - tight heavy folds
13a	Mw-Hw	D-GY	Massive	Thin	VWD		Mudstone	39, 16, 25	MS				62	345		
13b	Mw-Hw	L-GY	Massive	Thin	VWD	Fine	Sandstone	22, 23, 15, 24	MS	2.9	175		53	146		
13b	Mw-Hw	D-GY	Massive	Thin	VWD		Mudstone	32, 34, 17	MS				46	160		
13c	Mw	L-GY	Massive	Thin	WD	Fine	Sandstone	49, 32, 27	S	0	180		61	86		Blocky appearance
13c	Mw	D-GY	Massive	V thin	WD		Mudstone	18, 17, 31, 39	MS				59	62		Bed structure looks like it has been tectonically compressed
14a	Sw-Mw	L-GY	Massive	V thin	WD	Fine	Sandstone	32, 20, 14	MS				61	73		
14a	Mw	D-GY	Massive	V thin	WD		Mudstone		VW				60	74		
14b	Mw	L-GY	Massive	V thin	WD	Fine	Sandstone	30, 22, 33	S				45	74		D/DD for normal bedding, deformed block in middle bound by faults
14b	Mw	D-GY	Massive	V thin	WD		Mudstone	14, 15	W				51	76		sandstone interbedding is fine-v fine sandstone in v thin - thin interbeds - a number of small scale boudins
14c	Sw-Mw	L-GY	Massive	V thick	WD	F-M	Sandstone	61, 57, 49, 52	ES	0	180		46	61		Massive sandstone on top of thin interbedding
15a	Sw	L-GY	Massive	Massive	D	F-M	Sandstone	50, 56, 42, 60	ES				61	221		Folded bedding enough so hard to recognise mudstone thus massive in appearance
16a	Sw-Mw	L-GY	Massive	V thick	WD	F-M	Sandstone	20, 47, 51, 37	VS	0	180		62	42		mudstone beds deformed with no consistent D/DD
16a	Sw-Mw	D-GY	Massive	Thin	WD		Mudstone		VW				78	65		
17a	Sw-Mw	L-GY	Massive	V thick	WD	F-M	Sandstone	51, 57, 44, 44	VS	4.2	170		76	80		More or less same as before but more joint sets
17a	Sw-Mw	D-GY	Massive	Thin	WD		Mudstone		VW				76	77		
18a	Hw	D-GY (red oxide)	Massive	V thick	D	F-M	Sandstone	42, 34, 25, 32	VS	0	180					Heavily weathered, hard to see, one uniform oxidised colour
18a	Hw-Cw	D-GY (red oxide)	Massive	Medium	D		Mudstone		H-VW				61	296		
19a	Hw	L-GY (red oxide)	Massive	Medium	D	F-M	Sandstone	18, 26, 19, 17	MS	1.2	155		80	208		sandstone in thin interbed = fine sandstone
19a	Hw	D-GY (red oxide)	Massive	Medium	D		Mudstone		VW							D/DD changes i.e. Highly disturbed
20a	Hw	L-GY (red oxide)	Massive	Medium	D	F-M	Sandstone	42, 35, 33, 31	S	0.5	160					D/DD changes i.e. Highly disturbed. mudstone at large thickness is highly shattered/fragmented, no sample for testing
20a	Hw	D-GY (red oxide)	Massive	Thick	WD		Mudstone	15, 8, 9	VW	0.65	135					D/DD changes i.e. Highly disturbed. Changing D/DD across outcrop changing from 65/230 to 75/025. Many small scale faults altering beds - hard to identify due to weathering
21a	Mw-Hw	L-GY (red oxide)	Massive	Medium	VWD	F-F-M	Sandstone	43, 53, 38, 50		4.1	165		63	220		Same as before - no consistent D/DD, heavily deformed, mudstone appears wavy
21a	Mw-Hw	D-GY (red oxide)	Massive	Medium	VWD		Mudstone		VW	0.65	155		56	224		Note: flowing of mudstone around sandstone makes mudstone look massive but thin/medium
22a	Mw-Hw	L-GY (red oxide)	Massive	Thick	D	F-M	Sandstone	18, 36, 39, 49	VS	0	180		72	210		Good example of boudinage, mudstone flows around sandstone parcels however main bedding defect holds strong i.e. 0, 180 shape
22a	Mw-Hw	D-GY (red oxide)	Massive	Thin	D		Mudstone		VW				85	235		Too disturbed for sampling/consistent D/DD, whole rock mass is MF-HF
23a	Mw	L-GY	Massive	Thin	VWD	F-FM	Sandstone	16, 25, 14	S	1.2	170	HF	82	252	UR	
23a	Mw	D-GY	Massive	Thin	VWD		Mudstone		VW			FRAG				
23b	Hw	L-GY	Massive	Thin	D	F-FM	Sandstone	21, 19, 22	MS			FRAG			SR	Heavily fragmented with boudinage
23b	Hw	D-GY	Massive	Thin	D		Mudstone		VW			FRAG				No bedding recognisable
23c	Mw-Hw	L-GY	Massive	Thin	VWD	Fine	Sandstone	40, 38, 32	VS	1	175	HF-FRAG	84	36	UR	
23c	Mw-Hw	D-GY	Massive	Thin	VWD		Mudstone		VW			FRAG				

23d	Mw	L-GY	Massive	Massive	WD	F-M	Sandstone	39, 38, 33	MS			MOD-HF			UR	
24a	Hw	L/D-GY	Massive	V thin	D	Fine	Sandstone		VW	2	175	FRAG	51	246	SR	Roughness due to fracture pattern
24a	Hw	D-GY	Massive	Medium	D		Mudstone		VW			FRAG				V thick bed of mudstone (frag) within thin fragmented mess
24b	Sw	L-GY	Massive	V thick	WD	F-M	Sandstone	31, 28, 25	S	2.5	170	FRAC-MOD	85	219	US	
25a	Sw	L-GY	Massive	Massive		F-M	Sandstone	20, 35, 30	S			S-FRAC-FRAC				
26a	Sw-Mw	L-GY	Massive	Medium	VWD	F-M	Sandstone	48, 46, 28	S	0	180	MOD	45	10	SR	
26a	Mw-Hw	D-GY	Massive	Thin	VWD		Mudstone		VW	1	175	FRAG	51	40	UR	Note: fragmented mudstone = bedding shear
27a	Sw-Mw	L-GY	Massive	Thick	WD	F-M	Sandstone	27, 37, 34	S	0	180	MOD-HF	75	60	US	All mudstone has been subject to bedding plane movement and subsequent lineation
27a	Mw	D-GY	Massive	Thin	VWD		Mudstone	9, 11	VW	0	180	FRAG	78	54	UR	
27b	Mw	L-GY (oxide)	Massive	Thin	WD	Fine	Sandstone	29, 31, 19	MS	0	180	HF-FRAG	85	64	SR	
27b	Mw	D-GY (oxide)	Massive	Thin	WD		Mudstone		VW	0	180	FRAG	83	59	UR	
27c	Sw	L-GY	Massive	Massive		F-M	Sandstone	32, 37, 34				MOD				Blocky appearance
28a	Sw	L-GY	Massive	Thick	VWD	Fine-F-M	Sandstone	25, 34, 20	S	0	180	MOD	59	208	UR	Strength = thin. Thick beds = 43, 40, 50, 52. D/DD changes between thin beds
28a	Sw	D-GY	Massive	Thin	VWD		Mudstone			0	180	FRAG	63	211	UR	
28b	Sw-Mw	D-GY	Massive	Thin	VWD		Mudstone	12	W-VW	0	180	FRAG	73	222	UR	sandstone and thin mudstone interbeds, some thin sandstone interbeds are f-m but most are fine - not uncommon
28b	Sw-Mw	L-GY	Massive	Thin	VWD	Fine-F-M	Sandstone			0	180	HF-FRAG	75	221	US	
29a	Mw-Hw	L-GY (oxide)	Massive	Medium	WD	Fine-F-M	Sandstone	26, 38, 42	S	3	175	HF-FRAG	87	220	SS	
29a	Mw-Hw	D-GY (oxide)	Massive	Thin	WD		Mudstone		VW-H	1.2	160	FRAG	86	41	SS	Thin beds - heavily folded with no consistent D/DD - beds at vertical so alternating D/DD
30a	Mw-Hw	L-GY	Massive	Medium	D	F-M	Sandstone	29, 37, 21	MS-S	1	175	FRAC-HF	35	25	SU	THIN = MOD/HIGH, THICK = FRAC-MOD
30a	Mw-Hw	D-GY	Massive	Thin	D		Mudstone		VW	1.2	170	FRAG			UR	
31a	Uw-Sw	L-GY	Massive	Massive		F-M	Sandstone					MF				Rock in quite good nick - mostly MF but MF-HF in places
32a	Mw-Hw	L-GY	Massive	Massive			Sandstone					HF				Closeness of joints make it highly fractured
33a	Sw	L-GY	Massive	Massive		F-M	Sandstone					F-MF				
34a	Mw-Hw	D-GY	Massive	Thin	D		Mudstone			1	155	HF-FRAG	60	80	UR	
34a	Mw-Hw	L-GY	Massive	Medium	D		Sandstone			4	175	MF-HF	60	80	UR	
35a	Sw	L-GY	Massive	Massive		F-M	Sandstone	46, 61, 56	ES			F-MF				
36a	Sw	L-GY	Massive	Massive		F-M	Sandstone	48, 47, 46	VS			FRACT				
37a	Mw	L-GY	Massive	Massive		F-M	Sandstone					HF				
38a	Sw-Mw	L-GY	Massive	Massive		F-M	Sandstone					HF				

E.2.2 Hurunui River - Defect structure

		Orientation								Waviness									
Outcrop #	Defect type	Dip	Dip direction	Spacing (m)	Persistence (m)	Aperture (cm)	Infilling type	Infilling strength	Defect roughness	Wavelength (m)	Interlimb angle (ILA, °)	Ends	End termination	Strength (schmidt intact rebound)	Strength (hammer)	Water	Weathering	Degree of fracture	Raw field notes
1a	Joint	45	275	0.25	8				UR	1	170	2	C	50, 18, 28, 53	VS	Dry	Sw-Mw	MF-HF	
1a	Joint	60	25	0.04	8				US	2.8	170	2	C	28, 36, 48, 54	VS	Dry	Sw-Mw	MF	
1a	Joint	30	130	0.06	3.8				US	3	175	2	C	42, 68, 48, 59	VS	Dry	Sw-Mw	MF-HF	
1a	Shear	85	105		2.8		Silt with a trace of clay	Hard	SS	1.2	155	1	D	25, 12, 10	MS	Dry	Mw-Hw	HF-FRAG	
1b	Joint	75	153	0.25	3				US	2.1	175	2	C	56, 57, 31	VS	Dry	Sw	MF	Blocky intact rock
1b	Joint	90	314	0.2	2				PR	2	175	2	C	43, 37, 36	S	Dry	Sw	MF	
1b	Joint	75	334	0.25	2.1				US	1.8	175	2	C	45, 40, 59	VS	Dry	Sw	MF	Massive beds
1b	Joint	30	236		9	1.5	Medium Sand	Hard	US	3	175	2	C	60, 46, 49, 54	VS	Dry	Sw	MF-HF	
1c	Shear				3		Sandy silt	Hard	UR	1.8	170	2,1	C,D		VW	Dry	Mw-Hw	FRAG	
1d	Shear	56	126		3.8		Sandy silt	Hard	UR	3.1	150	1	D	15, 20, 14	MS	Dry	Mw-Hw	HF-FRAG	Mudstone fragmented
1d	Joint	71	80	0.8	2				US	1.8	175	2	C	39, 27, 28	S	Dry	Mw	MF-HF	Bedding becomes apparent, oxide staining
2a	Fault	40	100		2.8		Sandy silt	Hard	UR	3.2	155	2	C	54, 15, 40	VS	Dry	Mw	HF-FRAG	
2a	Joint	35	294	0.3	2.6				US	0	180	2	C	58, 55, 34	VS	Dry	Sw	MF	
2b	Fault	See other	See other		20		Sandy silt	Hard	SS	3.4	160	2	C	32, 51, 42	VS	Dry	Sw	MF-HF	MF in sand, HF in mud, displacement observed - two D/DD 35/039 & 40/270
2b	Joint	40	271	0.5	3.1				UR	0	180	2	C	55, 54, 48	VS	Dry	Sw	MF	
2b	Joint	46	185	0.5	2.5				US	2	175	2	C	50, 52, 60	VS	Dry	Sw	MF	
3a	Joint	65	132	0.35	4.2				SR	1.5	170	2	C	52, 59, 50, 51	VS	Dry	Sw	MF	HF at top of outcrop - relaxation/movement/weathering
3a	Joint	56	58	0.3	7.5				UR	0	180	2	C	45, 56, 53	VS	Dry	Sw-Mw	MF	
3b	Joint	88	344	0.4	2.8				US	2	175	2	C	56, 57, 56, 32	VS	Dry	Sw	MF-HF	Average MF
3b	Joint	89	39	0.3	3				SS	2.5	175	2	C	55, 56, 59, 52	VS	Dry	Sw	MF-HF	
4a	Joint	61	41	0.55	4.6				PR	0	180	2	C	24, 22, 41	S	Dry	Sw-Mw	MF-HF	
4a	Joint	62	225	0.4	2.3				US	1.2	175	1	D	48, 28, 52	VS	Dry	Sw-Mw	MF-HF	Cut by fault - displacement and out of place mudstone
4a	Joint	75	303	0.3	2				US	0	180	2	C	36, 36, 57	S	Dry	Sw-Mw	MF-HF	
4a	Fault	60	280				Sandy silt	Hard	UR	3.1	170	0	O	29, 16, 20	MS	Dry	Mw	HF	Persistence hidden
5a	Joint	55	355	0.45	2				SS	2.8	170	2	C	40, 47, 55, 52	VS	Dry	Sw	F-MF	Note: bed shearing along mudstone - lineated parallel to strike coarse sand size (H-VW strength)
5a	Shear	49	176		5.2		Coarse Sand	V Stiff-Hard	UR	3.1	175	2	C	30, 29, 51, 50	VS	Dry	Mw	MF	
5a	Joint	61	170		4.8				UR	0.7	175	2	C	54, 49, 42	VS	Dry	Sw	MF	
5b	Joint	40	1	0.42	4				US	3	165	2	C	44, 58, 59	VS	Dry	Uw-Sw	SF-F	
5b	Joint	74	186	1	2				US	0	180	2	C	54, 45, 56	VS	Dry	Uw-Sw	SF-F	
6a	Joint								US							Dry	Sw	MF-HF	Heavy incipient fractures in clean greywacke - able to get mudstone sample
7a	Joint	87	5	0.45	3.1				US	0	180	1	D	58, 62, 58	VS	Dry	Sw	MF	
7a	Joint	65	357	0.4	2.8				UR	1.8	175	2	C	53, 56, 48	VS	Dry	Sw	MF	
7a	Joint	65	219	0.55	3.9				US	0	180	2	C	34, 52, 50	VS	Dry	Sw	MF	
8a	Joint	67	300	0.5	3.5				UR	3	175	2	C	56, 37, 46, 43	VS	Dry	Sw	MF-HF	Blocky shattered appearance in middle of outcrop - near fault (HF-F)
8a	Joint	80	211	0.3	2				PR	0	180	1	R	56, 42, 58	VS	Dry	Sw	MF-HF	
8a	Joint	58	68	0.25	6.2				US	3.2	175	2	C	36, 42, 39	VS	Dry	Sw-Mw	HF	
8b	Joint	40	290	0.45	2.8				SS	0	180	2	C	38, 56, 53, 53	VS	Dry	Sw	MF	
8b	Joint	88	20	0.55	4.5				PR	0	180	2	C	42, 56, 53	VS	Dry	Sw	HF	
8b	Joint	54	196	0.2	2				US	1	170	0	D	58, 54, 52, 46	VS	Dry	Sw	MF-HF	
9a	Joint	86	195	1	2.8				Uslick	0	180	2	C	55, 32, 48, 51	VS	Moist	Sw-Mw	MF	Rock mass controlled 50/50 by main joints and incipient fracturing
9a	Joint	85	103	0.45	2.7				Uslick	1	165	2	C	49, 56, 61, 36	VS	Dry	Sw	MF-HF	Blocky appearance
9a	Joint	75	40	0.2	4.2	1			US	0	180	2	C	32, 48, 33, 47	VS	Dry	Sw	HF	
9a	Fault	50	197		3.5	2			UR	0	180	2	C	23, 40, 43, 52	S	Dry	Sw-Mw	HF	
10a	Joint	54	152	0.2	10.5				UR	2.8	170	2	C	23, 37, 52, 40	S	Dry	Sw	MF-HF	Half barrels from drill blasting that are intact with minimal damage to rock, mudstone not on major joints is FRAG
10a	Joint	75	197	0.9	5.8				US	3.5	175	2	C	20, 46, 22	S	Dry	Sw	MF	
10a	Joint	36	24	0.35	4				US	2	165	2	C	38, 50, 32	S	Dry	Sw-Mw	MF-HF	
11a	Joint	65	151		3				UR	0	180	2	C	56, 54, 38, 39	VS	Dry	Mw	MF-HF	
11a	Joint	49	11		5.8				UR	1.6	170	2	C	41, 34, 39	S	Dry	Mw	MF-HF	
11a	Joint	32	300		2				UR	0.9	165	1	D	51, 40, 42, 40	VS	Dry	Mw	MF-HF	
13a	Fault				3.3				UR	1.5	145	1	R			Dry	Mw-Hw	HF-FRAG	Outcrop is tightly interbedded sand and mud
13a	Fault				2		Silt	Hard	UR	1.5	175	1	R			Dry	Mw-Hw	HF-FRAG	Frag due to sheared mud and thinness of beds taking most of the strain
13b	Joint	72	276	0.4	3.5	2	Silt	V stiff - Hard	UR	2	155	2	C			Dry	Mw-Hw	HF-FRAG	
13b	Joint	64	188	0.45	2.8				SR	1	175	2	C	32, 27, 14, 20	MS	Dry	Mw-Hw	HF-FRAG	
13c	Fault	40	320		5.2	2	Sandy silt	Hard - VW	UR	3.8	155	2	C			Dry	Mw-Hw	HF-FRAG	Infilling strength = abundance of quartz
13c	Fault	87	291		6	3.1	Silt	Stiff - V stiff	US	2	130	2	C	14, 31, 30	S	Dry	Mw-Hw	HF-FRAG	
13c	Fault				3.8	0.5	Silt		US	1.8	140	1	D			Dry	Mw-Hw	HF-FRAG	Blocky appearance with mud appearing to be squashed between more competent sand
13c	Fault				4.1	0.2			PR	2.7	165	1	D			Dry	Mw-Hw	HF-FRAG	Multiple faults with small offset, beds have a slight curve, folded slightly due to tectonic setting
14a	Joint	31	130	0.9	4.8				UR	2.5	170	2	C	16, 18, 12	MS	Dry	Sw-Mw	FRAG	No frequent joint set but many incipient fractures controlling the rock mass
14a	Joint	78	69	0.35	2.8				UR	2.7	165	2	C	24, 18, 20	MS	Dry	Sw-Mw	FRAG	
14b	Joint	85	220	1.2	3.9				US	3.6	175	2	C	44, 27, 48	VS	Dry	Sw-Mw	HF-FRAG	A number of faults that displace bedding in different D/DD
14b	Fault	69	213		9		Lineated Mud	VW	UR	4	160	2	C	26, 16, 26	MS	Dry	Sw-Mw	FRAG	
14b	Fault				7					1.2	160	2	C			Dry	Sw-Mw	FRAG	Frag by definition - a number of small scale faults intersecting
14b	Fault	71	186		12		Lineated Mud	VW	US	3	165	2	C	12, 10	W	Dry	Sw-Mw	FRAG	
14b	Fault	79	160		2.7		Lineated Mud	VW	US	0	180	1	D - against fault			Dry	Sw-Mw	FRAG	
14c	Joint	60	157	0.21	3.7	0.3			PR	0	180	2	C	21, 59, 46	VS	Dry	Sw	HF	Sandstone joints = straight 180°
14c	Joint	65	165	0.26	4.9	0.2			PR	0	180	2	C	46, 51, 32	VS	Dry	Sw	HF	
14c	Joint	69	50	0.8	2	0.1			US	0	180	2	C	56, 34, 37	VS	Dry	Sw	HF	Very blocky appearance, hard to get a good unweathered sample
14c	Joint	90	275	0.2	3.1				UR	2	175	2	C	56, 28, 40	VS	Dry	Sw-Mw	MF-HF	
15a	Joint	15	302	0.28	10	0.1-0.2			US	0	180	2	C	53, 52, 48, 49	VS	Wet (dripping)	Sw	FRACTURED-MF	Joints are wet with some dripping - slightly open 1-2mm to allow flow

16a	Joint	38	22	0.075	7				US	3.1	175	2	C	9, 27, 32, 40	S	Dry	Sw-Mw	MF-HF	
16a	Joint	90	353	0.14	4.2				US	2	170	2	C	34, 26, 53, 49	S	Dry	Sw-Mw	MF-HF	
17a	Joint	67	109	0.22	7	0.2			US	0	180	2	C	38, 33, 32, 40	S	Dry	Sw-Mw	HF	
17a	Joint			0.23	8.5				US	3	175	2	C			Dry	Sw-Mw	HF	
18a	Joint	54	87	0.35	2.8				UR	0	180	2	C	18, 28, 28	MS	Dry	Hw	HF-FRAG	Frag - potentially due to high degree of weathering
19a																Dry	Hw	HF-FRAG	Frag - potentially due to high degree of weathering
20a																Dry	Hw	MF-HF-FRAG	Sand = MF-HF, Mud = FRAG
21a	Joint	45	194		7.8				UR	0	180	2	C	13, 9, 33, 34	MS	Dry	Mw-Hw	HF-FRAG	Sand = HF, Mud = FRAG
21a	Fault	75	160		4.8				SS	0.2	165	2	C			Dry	Mw-Hw	HF-FRAG	
22a																Dry	Mw-Hw	MF-HF	
23a	Fault	34	259		3.1		Clay with some Sand	Soft	UR	2.2	175	2	C	27, 18	MS	Moist	Mw-Hw	FRAG	
23a	Fault	36	255		3.9		Clay with some Sand	Soft	PR	2	125	2	C	15, 24	MS	Moist	Mw-Hw	FRAG	Fault bounds 23a to 23b = frag non intact soil
23b	Fault	84	222		2		Clay with some Sand	Soft	UR	0.5	160	2	C	20, 11, 10	MS	Moist	Mw-Hw	FRAG	
23b	Fault	21	205		10.2		Silty Sand	Stiff	US	4.5	170	2	C	18, 15, 15	MS	Moist	Mw-Hw	FRAG	Note: persistence = 10.2m across 23b-23d
23b	Fault				3.3		Silty Sand	Stiff	UR	2.5	175	1	D	9, 13, 12	W	Moist	Mw-Hw	FRAG	
23c	Shear	52	238		3.2		Lineated Mud	VW	UR							Moist	Mw-Hw	FRAG	
23c	Fault	34	245		10.2		Silty Sand	Stiff	US	0	180	1	O	13, 21, 42	MS	Moist	Mw-Hw	HF-FRAG	
23d	Shear	45	300		4.7		Silty Sand	Firm	UR	2	175	2	C	26, 18, 10	MS	Moist	Mw-Hw	FRAG	Mudstone bed at top pinched out into massive sand on shear - no indication of bedding but maybe bedding shear
24a	Joint	77	112		2				US	0	180	1	O	30, 40, 42	S	Dry	Sw	FRAC-MOD	
25a	Joint	50	245	1.6	9.5				US	3.1	175	2	C			Dry	Sw	FRAC	
25a	Joint	65	184	2	9		Silty Sand	Stiff	US	4.5	165	2	C	38, 30, 34	S	Dry	Sw	FRAC	
25a	Joint	61	347	0.8	2.8				US	1	175	2	C	29, 30, 18	S	Dry	Sw	FRAC	
25a	Joint	21	164	0.3	5.2				US	0.3	160	2	C	25, 22, 38	S	Dry	Sw-Mw	FRAC-MOD	
26a	Joint	46	241	0.65	4				US	0	180	2	C	40, 21,25	S	Dry	Sw-Mw	MOD	
27a	Joint	45	290	0.35	3.5				US	3.2	175	2	C	23, 31, 25	S	Dry	Sw-Mw	MF-HF	
27a	Joint	40	55	0.55	6.5		Silty Sand with a trace of clay	Soft-firm	UR	2	165	2	C	39, 22, 32	S	Dry	Sw-Mw	MF-HF	
27a	Joint	21	180	0.6	5				US	0	180	2	C	38, 28, 34	S	Dry	Sw-Mw	HF	
27b	Fault	56	127		3.5		Sandy silt with a trace of clay	very stiff	UR	0	180	2	C	28, 25, 22	MS	Moist	Mw	FRAG	Shear fabric and beds cut by massive sand unit not in same orientation, fault bounds 27b to 27c
27c	Joint	48	340	0.4	3.1				US	2.8	170	2	C	46, 34, 43	VS	Dry	Sw	MF	
27c	Joint	76	80	0.45	3.2				US	2.5	175	1	D	41, 37, 31	S	Dry	Sw	MF-HF	
27c	Joint	42	269	0.3	4.9				UR	2.6	165	2	C	44, 41, 40	VS	Dry	Sw	MF-HF	
27c	Joint	51	77	0.3	3.6				US	0	180	1	D	28, 35, 28	S	Dry	Sw-Mw	HF	
28a	Fault	88	125		6.5				PR	2.6	155	2	C	25, 37, 48	VS	Dry	Sw	MF-HF	Fault appears to jump between joints i.e. Noticeable offsets, jumps between both joint sets
28a	Joint	83	83	0.75	3.2	0.35			US	1.8	160	2	C	42, 42, 41	VS	Dry	Sw	MF-HF	Aperture due to relax?
28a	Joint	11	142	0.5	6	1			US	0.4	160	2	C	22, 48, 39	S	Dry	Sw	MF-HF	
28a	Joint	38	75	0.6	3	0.1			US	0	180	2	C	34, 31, 34	S	Dry	Sw	MF-HF	
29a	Joint	30	344	0.55	7.8				UR	0	180	2	C	35, 20, 14	S	Dry	Mw	HF-FRAG	Straight joint - maybe due to weakness of thin bedding
30a	Shear	38	310		2		Silt with some sand	very stiff	US	1.6	175	1	R	16, 34, 26	S	Moist	Hw	HF	
31a	Joint	41	214	0.3	12				US	0	180	2	C			Dry	Uw-Sw	MF-HF	Dominant joint set, potentially bedding but can't get across the valley gorge
32a	Joint	57	210	0.25	18					3.5	165	2	C			Dry	Mw-Hw	HF	
33a	Joint	21	114	1	5				US	0	180	2	C			Dry	Sw	MF	
33a	Joint	89	116	0.35	2.8				US	2	175	2	C			Dry	Sw	MF	
35a	Joint	74	24	0.2	4.8				UR	2	175	2	C	42, 45, 39	VS	Dry	Sw-Mw	MF-HF	
35a	Joint	20	284	0.4	4				PR	0	180	2	C	42, 38, 35	VS	Dry	Sw-Mw	MF-HF	
35a	Joint	79	19	0.6	8.5				US	0	180	2	C	32, 42, 35	VS	Dry	Sw	FRAC	Open joint but rock inside - potentially two random closely spaced joints, REMEMBER rivers only have best rock
36a	Joint	56	80	0.4	2.9				US	0	180	2	C	48, 46, 49	VS	Dry	Sw	FRAC	
37a	Shear	25	42	0.2	5.2				SR	1.5	175	2	C			Dry	Mw	HF	
38a	Joint	30	35	0.2	9				UR	3.4	170	2	C			Wet (dripping)	Sw-Mw	HF	
38a	Joint	10	185	0.45	10				UR	0	180	2	C			Wet (dripping)	Sw-Mw	HF	Bottom joint/fracture is source for surface flow of other described joints
38a	Joint	28	80		27	4			UR	6	155	2	C			Wet (dripping)	Mw	HF	Potential fault but by definition no offset so open fracture/joint

E.2.3 Hurunui River - Soil descriptions of infill

				Strength							
Outcrop #	Fraction (name)	Colour	Structure	NZGS	PSM Non-cohs	Moisture	Grading	Sorting	Plasticity	Weathering	Raw field notes
1a	Silt with a trace of clay		HOMO	Hard	Loose						
1b	Medium Sand		HOMO	Hard	Loose						
1c	Sandy silt		HOMO	Hard	Loose						
1d	Sandy silt		HOMO	Hard	Loose						
2a	Sandy silt		HOMO	Hard	Loose						
2b	Sandy silt		HOMO	Hard	Loose						
4a	Sandy silt		HOMO	Hard	Loose						
5a	Coarse Sand		HOMO	V stiff-Hard	Loose						
13a	Silt		HOMO	Hard	Loose						
13b	Silt		HOMO	V stiff - Hard	Loose						
13c	Sandy silt		HOMO	Hard - VW	Loose						
13c	Silt		HOMO	Stiff - V stiff	Loose						
13c	Silt		HOMO		Loose						
18a	Clay with some silt	L/D-GY	Bedding	Soft-Firm	Compact	Moist			Moderate	Hw-Cw	15-20cm clay zone
23a	Clay with some Sand		HOMO	Soft	Loose						
23a	Clay with some Sand		HOMO	Soft	Loose						
23b	Clay with some Sand		HOMO	Soft	Loose						
23b	Silty Sand		HOMO	Stiff	Loose						
23b	Silty Sand		HOMO	Stiff	Loose						
23c	Lineated Mud		HOMO	VW	Loose						
23d	Silty Sand		HOMO	Stiff	Loose						
25a	Silty Sand		HOMO	Firm	Loose						
27a	Silty Sand with a trace of clay		HOMO	Soft-firm	Loose						
27b	Sandy silt with a trace of clay		HOMO	very stiff	Loose						
30a	Silt with some sand		HOMO	very stiff	Loose						

E.3 Bedding thickness portions with joint and fault occurrence

Bedding thickness across the study site with joints and faults/shears presented as percentage occurrence respective of bedding thickness.

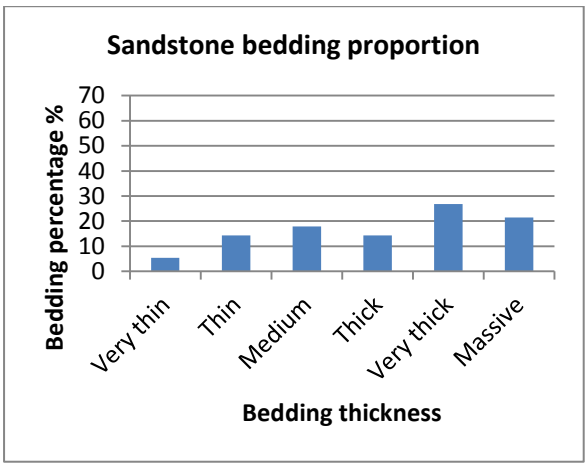

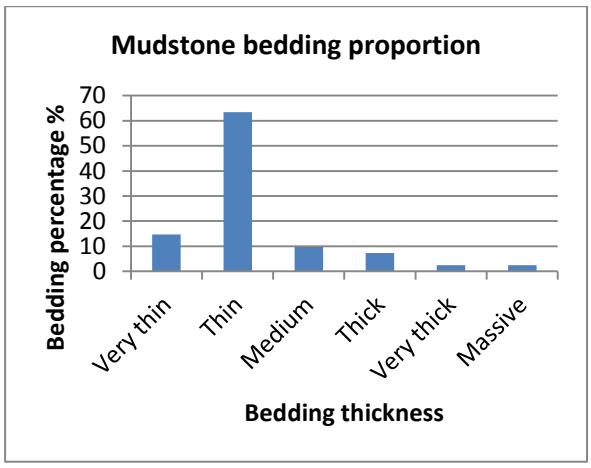

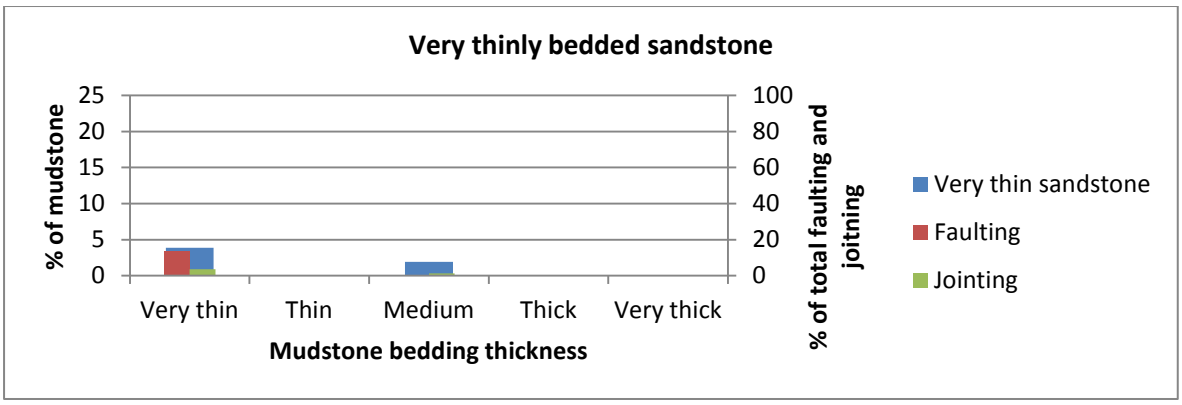

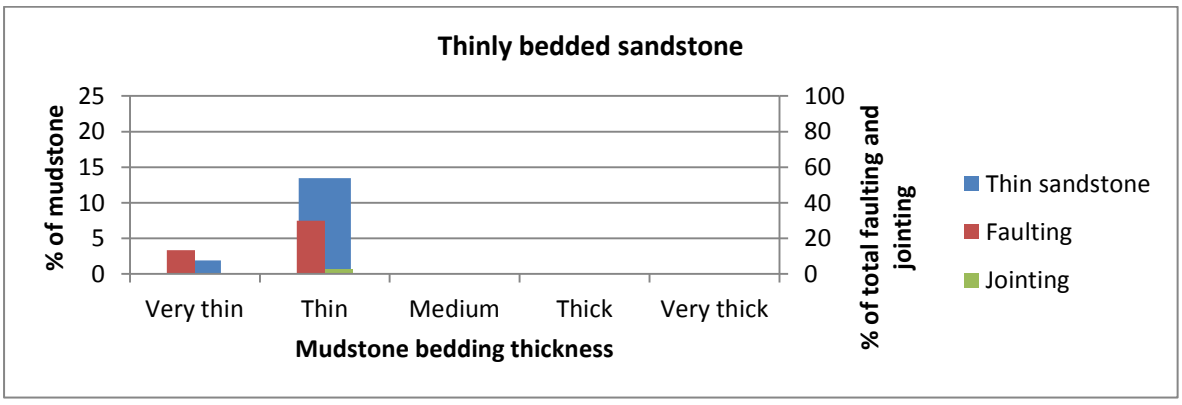

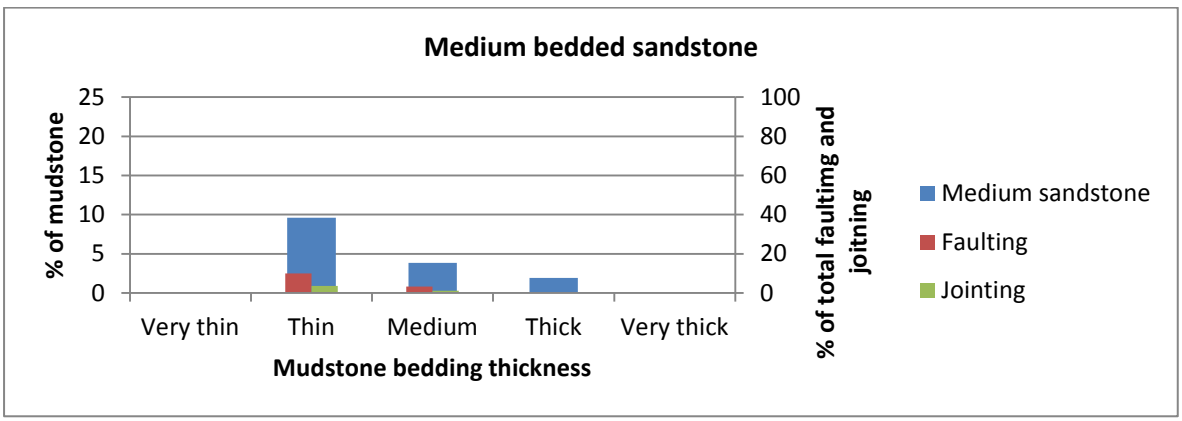

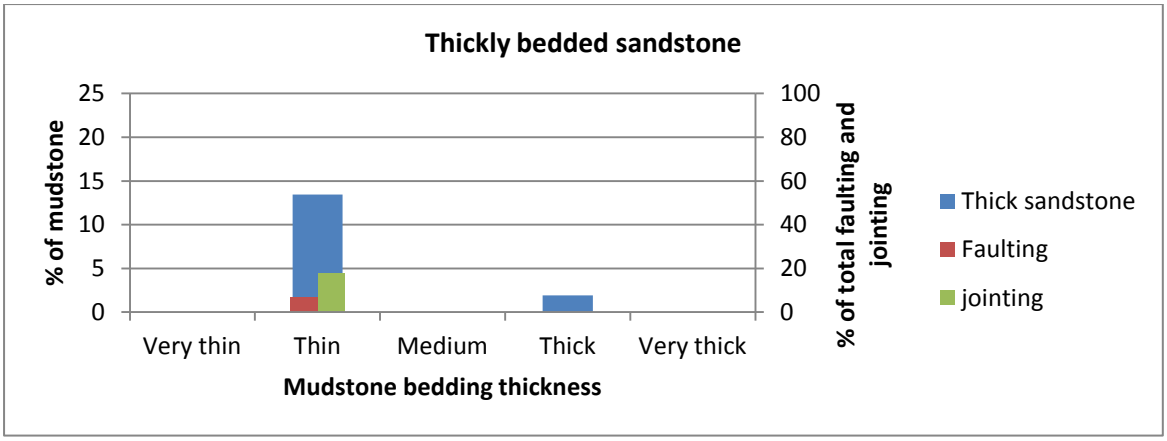
Thickly bedded sandstone
% of mudstone
25
20
15
10
5
0
100
80
60
40
20
0
% of total faulting and jointing
Very thin
Thin
Medium
Thick
Very thick
Mudstone bedding thickness
Thick sandstone
Faulting
jointing

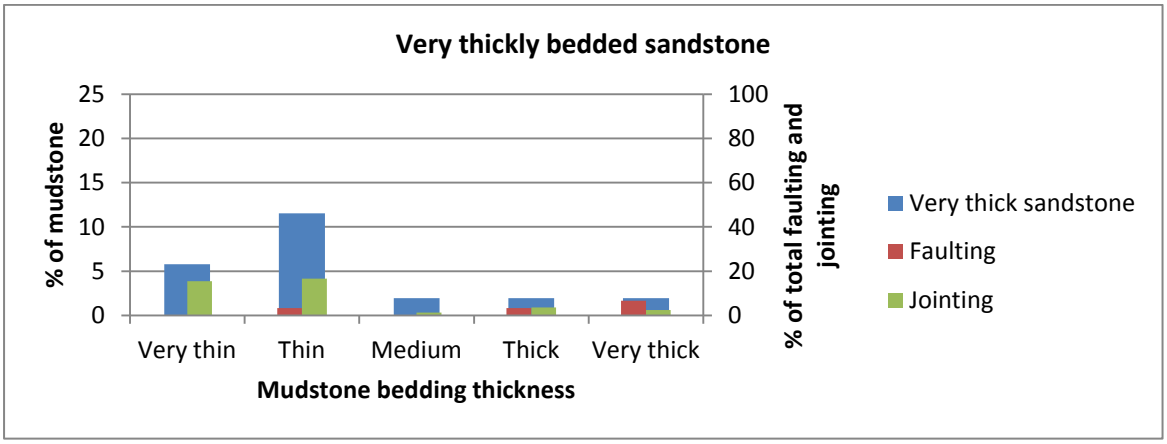
Very thickly bedded sandstone
% of mudstone
25
20
15
10
5
0
100
80
60
40
20
0
% of total faulting and jointing
Very thin
Thin
Medium
Thick
Very thick
Mudstone bedding thickness
Very thick sandstone
Faulting
Jointing

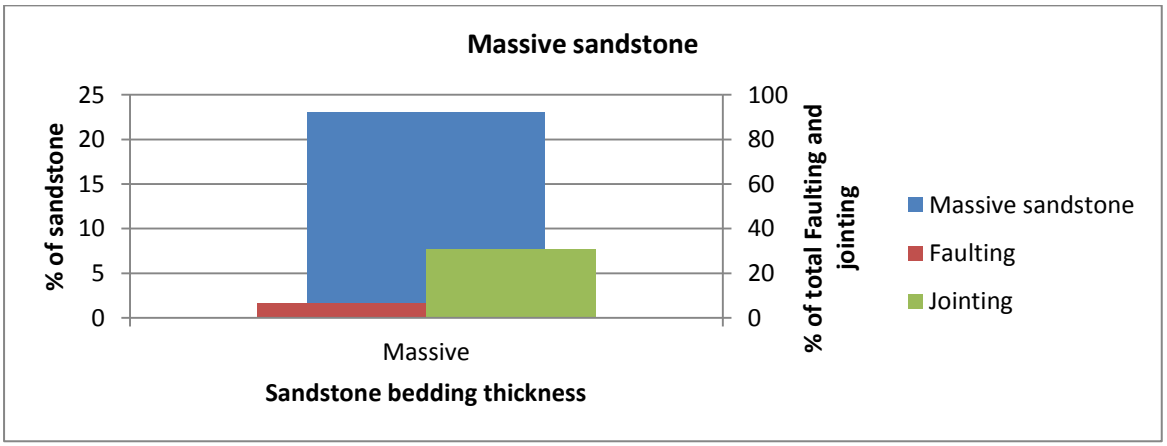
Massive sandstone
% of sandstone
25
20
15
10
5
0
100
80
60
40
20
0
% of total Faulting and jointing
Massive
Sandstone bedding thickness
Massive sandstone
Faulting
Jointing

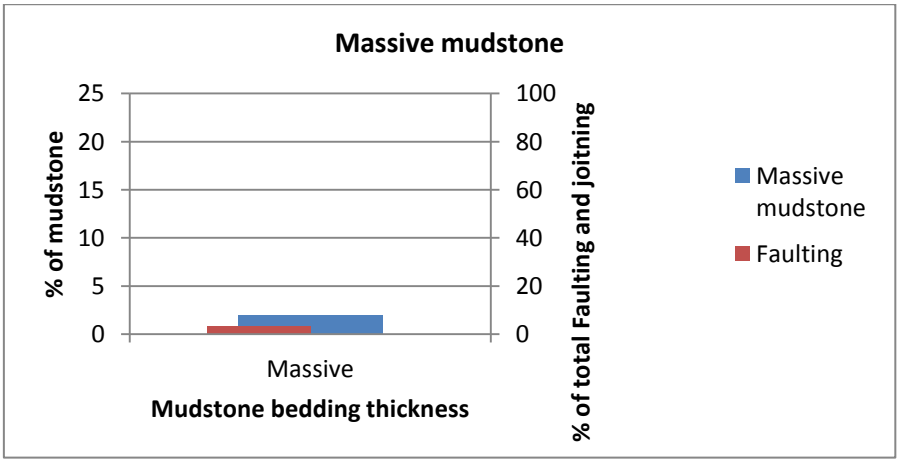
Massive mudstone
% of mudstone
25
20
15
10
5
0
100
80
60
40
20
0
% of total Faulting and joitning
Massive
Mudstone bedding thickness
Massive mudstone
Faulting

E.4 Hurunui River steronet analysis

Steronet dip/dip direction analysis of bedding, jointing and faults/shears respectively.

Overall bedding poles

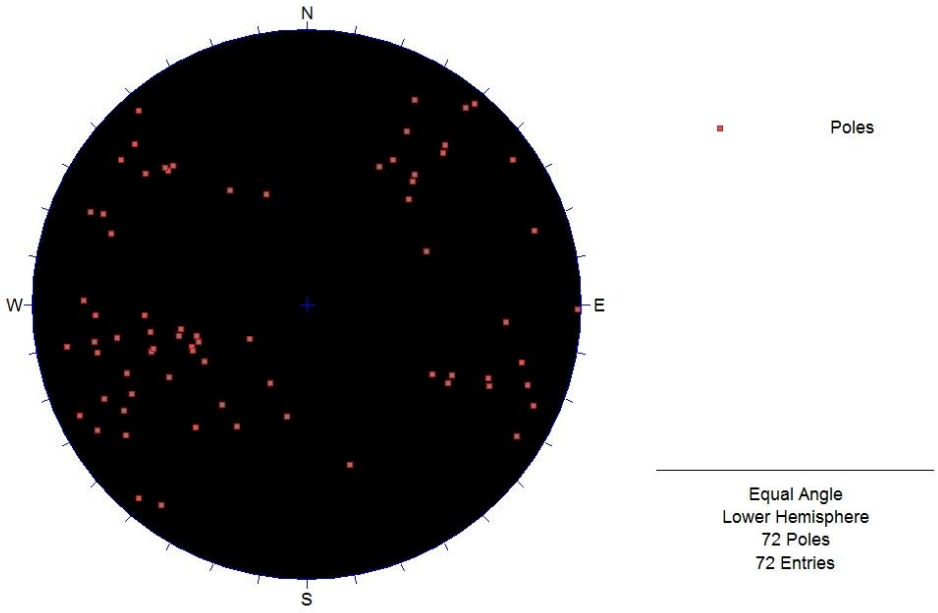

Overall bedding cluster

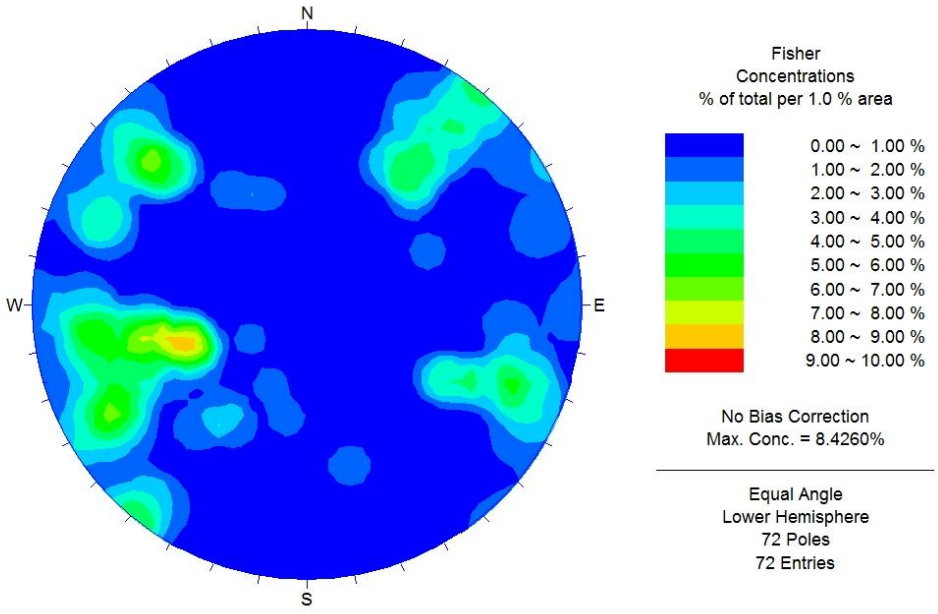

Jointing poles

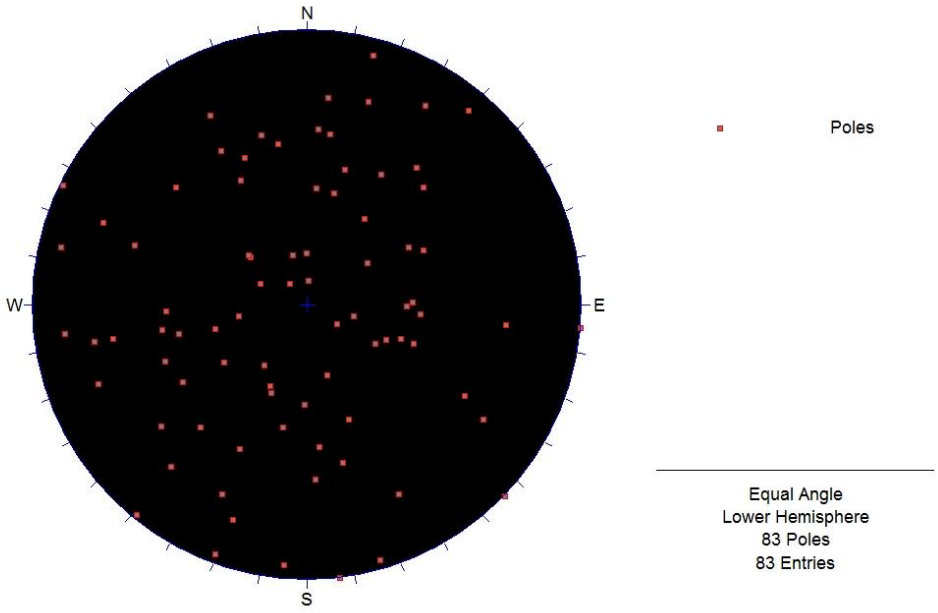

Jointing cluster

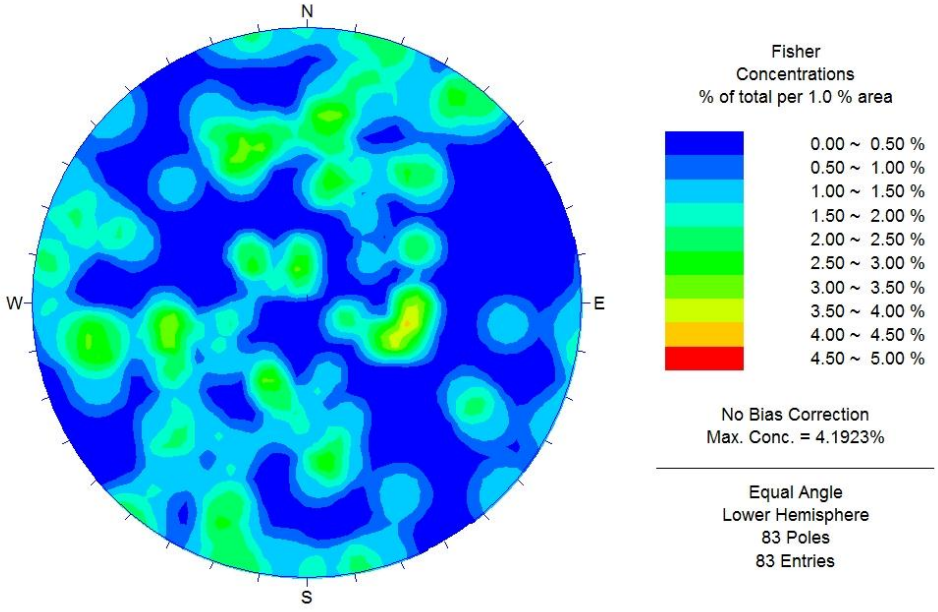

Faulting/shearing poles

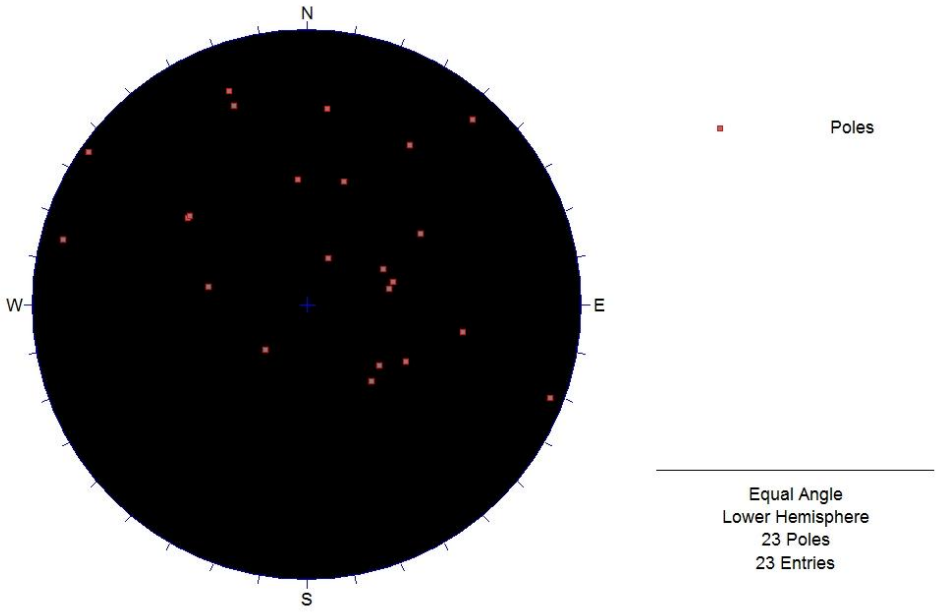

Faulting/shearing cluster

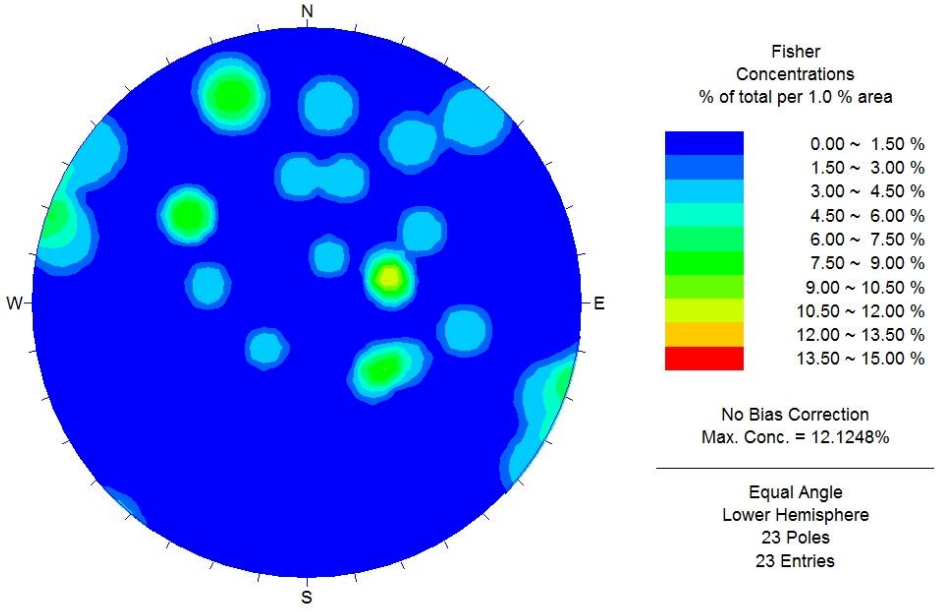

HRB bedding poles

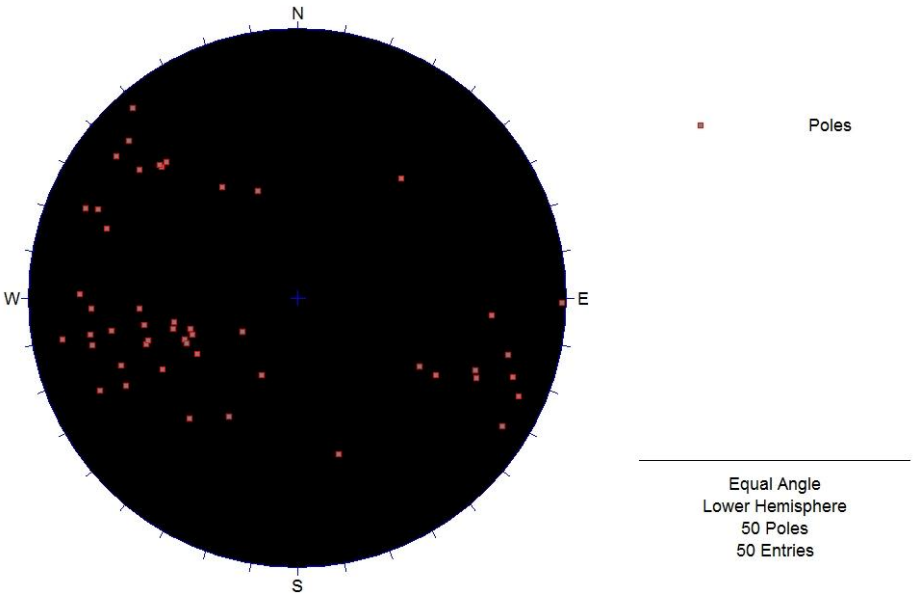

HRB bedding cluster

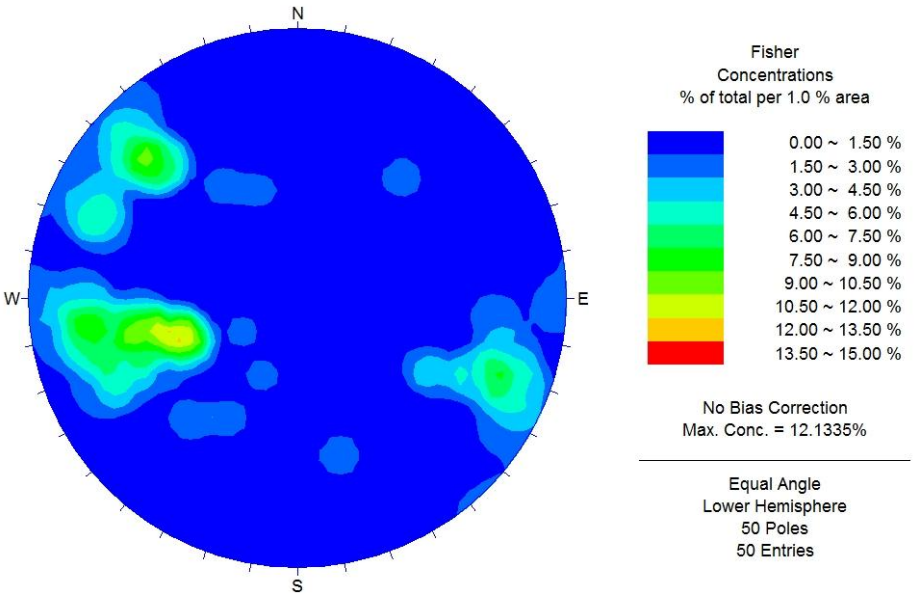

MNSZ bedding poles

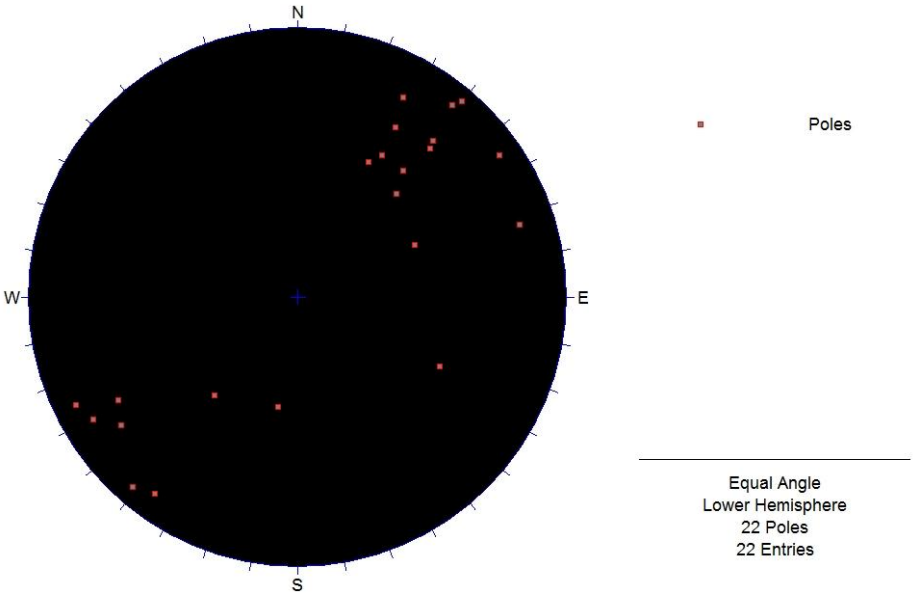

MNSZ bedding cluster

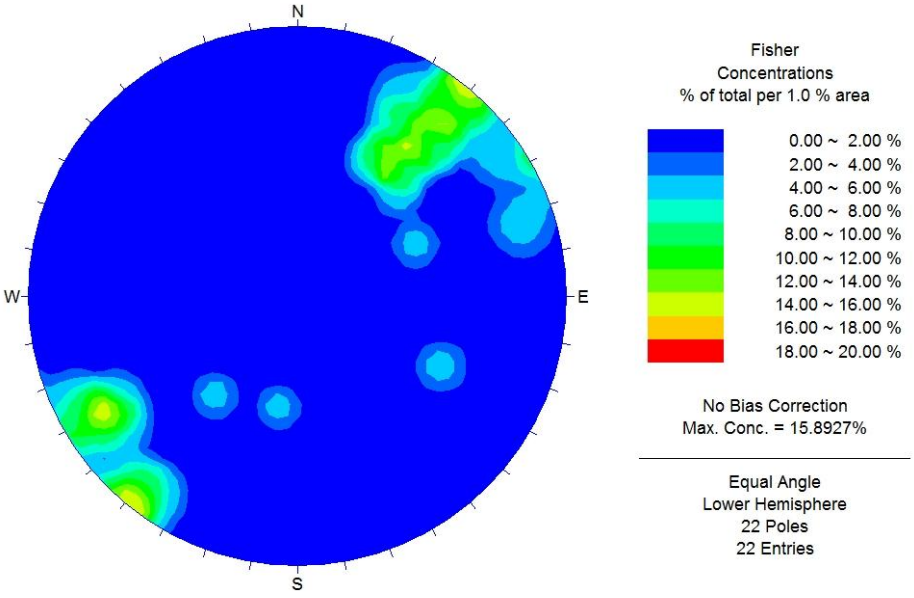

E.5 Hurunui River UCS raw results and calculations

Unconfined Compressive Strength testing respective of sampled outcrop.

E.5 Hurunui River - Uniaxial Compressive Strength testing

Sample ID	Height (mm)	Height (M)	Mass (g)	Mass (Kg)	Diameter (mm)	Failure Load (kN)	Failure Load (N)	Area (mm^2)	Area (M)	Stress (MPa)	Lithology	Failure mode (Szwedzicki, 2007)	Notes
2a	99.75	0.09975	509	0.509	49.38	481.6	481600	1915.102629	1.915102629	251.47	F-M sandstone	Clean multi extension	Disintegration - some shear powder
1b	101.60	0.1016	513.6	0.5136	49.46	311.3	311300	1921.31293	1.92131293	162.02	F-M sandstone	Clean multi extension with some multi fracture	Note: no fracture along bottom disk
2b	101.45	0.10145	512.3	0.5123	49.43	318	318000	1918.724083	1.918724083	165.74	F-M sandstone	Clean with indication of breakage along perpendicular to load quartz	Disintegration
4a	99.58	0.09958	504.4	0.5044	49.42	376.4	376400	1917.947769	1.917947769	196.25	F-M sandstone	Clean multi extension with some multi fracture from disintegration	Disintegration
5b	101.65	0.10165	514.3	0.5143	49.34	423.7	423700	1912.001249	1.912001249	221.60	F-M sandstone	Clean multi extension	Disintegration
7a	100.18	0.10018	501.8	0.5018	49.37	231.6	231600	1914.068557	1.914068557	121.00	F-M sandstone	20% break along existing oxide joint - mostly clean mutli extension	Most of sample still intact - some shear powder at bottom
10a	101.92	0.10192	521.8	0.5218	49.46	185.6	185600	1921.31293	1.92131293	96.60	F-M sandstone	Break along existing quartz vein - simple extension	Moderate quartz veining - some shear powder
11a	99.30	0.0993	504	0.504	49.44	211.4	211400	1919.500554	1.919500554	110.13	F-M sandstone	80% break along existing quartz & oxide - mutli fracture	Some quartz veining, heavy fracture
13c	99.63	0.09963	500.1	0.5001	49.37	68.2	68200	1914.327049	1.914327049	35.63	F sandstone	80% break along existing oxide - multi fracture	
16a	99.48	0.09963	509.5	0.5095	49.27	395.3	395300	1906.321913	1.906321913	207.36	F-M sandstone	Multi fracture with some shear powder	Large piece broke off at 145.3kN - registered as break, sample reloaded

E.6 Hurunui River BTS raw results and calculations

Brazilian Tensile Strength testing respective of sampled outcrop.

E.6 Hurunui River - Brazilian Tensile Strength testing

Outcrop	Load (Kn)	Load (N)	Diameter (mm)	Thickness (mm)	MPa	Lithology	Clean?	Failure mode (Szwedzicki, 2007)	Failure time (sec)	Notes
1B	55.4	55400	49.75	25	28.33	F-M sandstone	Clean	Multi extension	116.44	
8B	41.9	41900	49.75	25	21.43	F-M sandstone	Clean	Single extension	106.14	Some shear defined by powder
5B	47.6	47600	49.75	25	24.34	F-M sandstone	Clean	Multi extension	103.82	
2B	53.9	53900	49.75	25	27.56	F-M sandstone	Clean	Multi extension	92.76	Some multi fracture
5A	56.5	56500	49.75	25	28.89	F-M sandstone	Clean	Multi extension	90.64	
1A	33.9	33900	49.75	25	17.33	F-M sandstone	80% oxide	Multi fracture	44.94	Discontinuity perpendicular to load
7A	24.3	24300	49.75	25	12.43	F-M sandstone	80% quartz	Multi extension	63.49	Discontinuity perpendicular to load
3A	44.9	44900	49.75	25	22.96	F-M sandstone	Clean	Multi extension	75.63	Discontinuity perpendicular to load
4A	50.7	50700	49.75	25	25.93	F-M sandstone	Clean	Multi extension	74.07	Discontinuity 45° to load
4A	34.5	34500	49.75	25	17.64	F-M sandstone	Clean	Multi extension	69.14	Discontinuity perpendicular and 45° to load
3A	13.6	13600	49.75	25	6.95	F-M sandstone	20% oxide	Multi extension	30.52	Discontinuity perpendicular to load
4A	34.4	34400	49.75	25	17.59	F-M sandstone	40% quartz	Single extension	60.62	Single extension cut by major quartz vein
3A	52.57	52570	49.75	25	26.88	F-M sandstone	50% quartz	Multi extension	72.45	
11A	15.5	15500	49.75	25	7.93	F-M sandstone	50% oxide	Single extension	37.05	Heavy discontinuities perpendicular to load
6A	6.9	6900	49.75	25	3.53	F-M sandstone	100% existing	Multi fracture	N/A	Heavy discontinuities perpendicular and parallel to load - rock shatter
6A	6.4	6400	49.75	25	3.27	F-M sandstone	100% existing	Multi fracture	N/A	Heavy discontinuities perpendicular and parallel to load - rock shatter
2A	58.9	58900	49.75	25	30.12	F-M sandstone	Clean	Multi extension	117.38	
13C	8.6	8600	49.75	25	4.40	Fine sandstone	70% oxide	Single extension	23.8	Discontinuity perpendicular to load
23a	25.8	25800	49.46	24.48	13.55	F-M sandstone	30% existing	Single extension	71	Discontinuity perpendicular to load
23a	21.6	21600	49.44	25.51	10.89	F-M sandstone	60% existing	Multi extension	60.4	Discontinuity 45° to load
23a	14.9	14900	49.51	24.84	7.71	F-M sandstone	25% existing	Simple extension	46.3	Heavy discontinuities 45° and perpendicular to load
26a	13	13000	49.44	24.33	6.87	F-M sandstone	50% existing	Simple extension	45.1	Discontinuity perpendicular to load
26a	21.7	21700	49.46	25.9	10.77	F-M sandstone	20% existing	Multi fracture	87	Hairline discontinuities 45° and perpendicular to load
26a	21.3	21300	49.45	24.34	11.26	F-M sandstone	10% existing	Multi extension w/ some multi fracture	60	
26a	15.1	15100	49.46	23.16	8.38	F-M sandstone	75% existing	Multi fracture	38.95	Heavy discontinuities parallel and perpendicular to load
27c	27.7	27700	49.4	24.75	14.41	F-M sandstone	5% existing	Simple extension	N/A	Discontinuity perpendicular to load
27c	26.9	26900	49.44	24.53	14.11	F-M sandstone	Clean	Simple extension	67	Hairline discontinuity perpendicular to load

E.7 Hurunui River Point Load testing raw results and calculations

Point Load Index testing per sample outcrop.

E.7 Hurunui River - Point Load testing

SAMPLE: 1a

Test No.	Type	P (kN)	D (mm)	W (mm)	A = WD (mm^2)	D_e^2	D_e	I_s	F	$I_{s(50)}$ (MPa)	Lithology	Weathering	Notes
1		4.33	25.5	49.1	1252	1594	39.9	2.72	0.904	2.45	F-M sandstone	Sw-Mw	Break along existing
2		2.89	9.5	48.6	462	588	24.2	4.92	0.722	3.55	F-M sandstone	Sw-Mw	
3		5.40	52.6	78	4103	5224	72.3	1.03	1.180	1.22	F-M sandstone	Sw-Mw	Break along existing quartz
4		6.96	46.0	77.4	3560	4533	67.3	1.54	1.143	1.76	F-M sandstone	Sw-Mw	Some break along existing
5		4.19	21.3	46.7	995	1267	35.6	3.31	0.858	2.84	F-M sandstone	Sw-Mw	Some break along existing
6		5.85	29.8	45.4	1353	1723	41.5	3.40	0.920	3.12	F-M sandstone	Sw-Mw	Some break along existing
7		6.41	53.4	122.1	6520	8302	91.1	0.77	1.310	1.01	F-M sandstone	Sw-Mw	Break along existing iron oxide joint
8		19.58	30.8	56.4	1737	2212	47.0	8.85	0.973	8.61	F-M sandstone	Sw-Mw	
9		11.34	28.9	41.4	1196	1523	39.0	7.44	0.895	6.66	F-M sandstone	Sw-Mw	
10		16.67	34.2	47.5	1625	2068	45.5	8.06	0.958	7.72	F-M sandstone	Sw-Mw	
11		13.56	66.1	48.3	3193	4065	63.8	3.34	1.116	3.72	F-M sandstone	Sw-Mw	Some break along existing
12		13.30	30.0	34.8	1044	1329	36.5	10.01	0.868	8.68	F-M sandstone	Sw-Mw	

SAMPLE: 1b

Test No.	Type	P (kN)	D (mm)	W (mm)	A = WD (mm^2)	D_e^2	D_e	I_s	F	$I_{s(50)}$ (MPa)	Lithology	Weathering	Notes
1		7.54	28.7	68	1952	2485	49.8	3.03	0.999	3.03	F-M sandstone	Sw-Mw	Some break along existing quartz
2		14.33	31.4	31.6	992	1263	35.5	11.34	0.858	9.73	F-M sandstone	Sw	
3		10.73	31.0	43.1	1336	1701	41.2	6.31	0.917	5.78	F-M sandstone	Sw	
4		11.48	24.1	51.5	1241	1580	39.8	7.26	0.902	6.55	F-M sandstone	Sw	
5		14.15	39.0	72.5	2828	3600	60.0	3.93	1.086	4.27	F-M sandstone	Sw	
6		13.36	36.8	49.7	1829	2329	48.3	5.74	0.984	5.65	F-M sandstone	Sw	
7		5.30	18.0	39.5	711	905	30.1	5.85	0.796	4.66	F-M sandstone	Sw	
8		7.10	16.0	31.3	501	638	25.3	11.13	0.735	8.19	F-M sandstone	Sw	
9		3.05	17.7	47.8	846	1077	32.8	2.83	0.827	2.34	F-M sandstone	Sw	Some break along existing oxide
10		7.42	17.1	48.7	833	1060	32.6	7.00	0.824	5.77	F-M sandstone	Sw	
11		9.09	18.6	48.5	902	1149	33.9	7.91	0.839	6.64	F-M sandstone	Sw	

SAMPLE: 1c

Test No.	Type	P (kN)	D (mm)	W (mm)	A = WD (mm^2)	D_e^2	D_e	I_s	F	$I_{s(50)}$ (MPa)	Lithology	Weathering	Notes
1		1.34	28.0	24.5	686	873	29.6	1.53	0.789	1.21	Mudstone	Sw-Mw	
2		1.20	18.1	40.2	728	926	30.4	1.30	0.800	1.04	Mudstone	Sw-Mw	
3		1.81	15.3	24.5	375	477	21.8	3.79	0.689	2.61	Mudstone	Sw-Mw	
4		4.96	16.2	51.5	834	1062	32.6	4.67	0.825	3.85	Mudstone	Sw	
5		3.54	14.6	52.7	769	980	31.3	3.61	0.810	2.93	Mudstone	Sw	
6		1.16	23.0	22.4	515	656	25.6	1.77	0.740	1.31	Mudstone	Sw-Mw	Shatter - break along existing
7		0.28	23.7	39.2	929	1183	34.4	0.24	0.845	0.20	Mudstone	Sw-Mw	Break along existing - oxide
8		0.63	20.9	34.6	723	921	30.3	0.68	0.799	0.55	Mudstone	Sw-Mw	Break along existing
9		0.43	24.1	43	1036	1319	36.3	0.33	0.866	0.28	Mudstone	Sw-Mw	Break along existing
10		0.24	25.6	58.6	1500	1910	43.7	0.13	0.941	0.12	Mudstone	Sw-Mw	Break along existing - oxide
11		1.08	21.9	29.5	646	823	28.7	1.31	0.779	1.02	Mudstone	Sw-Mw	
12		1.83	11.9	32.5	387	492	22.2	3.72	0.694	2.58	Mudstone	Sw	
13		0.08	26.8	29.2	783	996	31.6	0.08	0.813	0.07	Mudstone	Sw-Mw	Shatter - break along existing
14		0.14	21.1	63.7	1344	1711	41.4	0.08	0.918	0.08	Mudstone	Sw-Mw	Break along existing - oxide
15		2.66	15.4	22.3	343	437	20.9	6.08	0.676	4.11	Mudstone	Sw	

SAMPLE: 1d

Test No.	Type	P (kN)	D (mm)	W (mm)	A = WD (mm^2)	D_e^2	D_e	I_s	F	$I_{s(50)}$ (MPa)	Lithology	Weathering	Notes
1		1.20	29.4	31.5	926	1179	34.3	1.02	0.844	0.86	F-M sandstone	Sw-Mw	Break along existing oxide
2		9.33	32.9	29.4	967	1232	35.1	7.58	0.853	6.46	F-M sandstone	Sw	
3		5.10	32.7	27.4	896	1141	33.8	4.47	0.838	3.75	F-M sandstone	Sw-Mw	
4		0.12	32.5	26.3	855	1088	33.0	0.11	0.829	0.09	Mudstone	Mw-Hw	Shatter, break along existing
5		16.30	35.5	87.2	3096	3941	62.8	4.14	1.108	4.58	F-M sandstone	Sw	
6		11.01	42.8	38.7	1656	2109	45.9	5.22	0.962	5.02	F-M sandstone	Sw	
7		10.46	25.1	42.8	1074	1368	37.0	7.65	0.873	6.68	F-M sandstone	Sw	
8		13.40	27.1	36.3	984	1253	35.4	10.70	0.856	9.16	F-M sandstone	Sw	
9		9.92	32.8	57.5	1886	2401	49.0	4.13	0.991	4.09	F-M sandstone	Sw	Some break along existing
10		17.89	39.7	51.2	2033	2588	50.9	6.91	1.008	6.97	F-M sandstone	Sw	
11		8.79	27.0	37.2	1004	1279	35.8	6.87	0.860	5.91	F-M sandstone	Sw	
12		4.35	32.4	54.5	1766	2248	47.4	1.93	0.976	1.89	F-M sandstone	Sw	Break along existing oxide
13		13.60	33.2	30.1	999	1272	35.7	10.69	0.859	9.18	F-M sandstone	Sw	
14		14.72	33.3	31.3	1042	1327	36.4	11.09	0.867	9.62	F-M sandstone	Sw	

SAMPLE: 2a

Test No.	Type	P (kN)	D (mm)	W (mm)	A = WD (mm^2)	D_e^2	D_e	I_s	F	$I_{s(50)}$ (MPa)	Lithology	Weathering	Notes
1		19.72	39.8	35.1	1397	1779	42.2	11.09	0.926	10.27	F-M sandstone	Sw	
2		1.48	38.9	31.4	1221	1555	39.4	0.95	0.899	0.86	F-M sandstone	Sw	Break along existing oxide
3		19.38	48.6	59	2867	3651	60.4	5.31	1.089	5.78	F-M sandstone	Sw	
4		11.01	46.9	38.8	1820	2317	48.1	4.75	0.983	4.67	F-M sandstone	Sw	
5		2.22	38.8	62.3	2417	3078	55.5	0.72	1.048	0.76	F-M sandstone	Sw	Break along existing oxide
6		16.02	38.7	43.5	1683	2143	46.3	7.47	0.966	7.22	F-M sandstone	Sw	
7		8.81	40.0	54.4	2176	2771	52.6	3.18	1.023	3.25	F-M sandstone	Sw	Some break along existing
8		8.65	37.2	33.4	1242	1582	39.8	5.47	0.902	4.93	F-M sandstone	Sw	Some break along existing
9		12.06	23.0	41.5	955	1215	34.9	9.92	0.850	8.44	F-M sandstone	Sw	
10		8.10	14.8	57.1	845	1076	32.8	7.53	0.827	6.23	F-M sandstone	Sw	
11		11.17	24.5	47.3	1159	1475	38.4	7.57	0.888	6.72	F-M sandstone	Sw	
12		15.06	17.0	49.1	835	1063	32.6	14.17	0.825	11.69	F-M sandstone	Sw	
13		4.53	34.0	21.5	731	931	30.5	4.87	0.801	3.90	F-M sandstone	Sw	Some break along existing
14		11.92	34.4	41.7	1434	1826	42.7	6.53	0.932	6.08	F-M sandstone	Sw	
15		9.33	19.9	51.3	1021	1300	36.1	7.18	0.863	6.20	F-M sandstone	Sw	

E.7 Hurunui River - Point Load testing

SAMPLE: 2b

Test No.	Type	P (kN)	D (mm)	W (mm)	A = WD (mm^2)	D_e^2	D_e	I_s	F	$I_{s(50)}$ (MPa)	Lithology	Weathering	Notes
1		4.25	7.8	49.1	383	488	22.1	8.72	0.692	6.03	F-M Sandstone	Sw	
2		5.12	9.7	47.8	464	590	24.3	8.67	0.723	6.27	F-M Sandstone	Sw	
3		6.25	13.4	51.7	693	882	29.7	7.09	0.791	5.61	Fine Sandstone	Sw	
4		4.35	12.6	64.8	816	1040	32.2	4.18	0.821	3.43	Fine Sandstone	Sw	
5		6.23	27.6	87	2401	3057	55.3	2.04	1.046	2.13	Fine Sandstone	Sw	
6		5.68	31.6	56.7	1792	2281	47.8	2.49	0.980	2.44	Fine Sandstone	Sw	
7		2.93	28.0	74.4	2083	2652	51.5	1.10	1.013	1.12	Fine Sandstone	Sw	Break along existing
8		2.21	30.1	77.5	2333	2970	54.5	0.74	1.040	0.77	Fine Sandstone	Sw	Break along existing
9		3.92	15.9	33.5	533	678	26.0	5.78	0.746	4.31	Fine Sandstone	Sw	
10		16.39	26.6	59.9	1593	2029	45.0	8.08	0.954	7.71	F-M Sandstone	Sw	
11		9.90	20.6	49.8	1026	1306	36.1	7.58	0.864	6.55	F-M Sandstone	Sw	
12		12.35	24.1	43.6	1051	1338	36.6	9.23	0.869	8.02	F-M Sandstone	Sw	
13		13.56	21.0	48.5	1019	1297	36.0	10.46	0.863	9.02	F-M Sandstone	Sw	
14		10.10	34.9	26.8	935	1191	34.5	8.48	0.846	7.18	F-M Sandstone	Sw	
15		6.69	26.4	90.5	2389	3042	55.2	2.20	1.045	2.30	Fine Sandstone	Sw	

SAMPLE: 3a

Test No.	Type	P (kN)	D (mm)	W (mm)	A = WD (mm^2)	D_e^2	D_e	I_s	F	$I_{s(50)}$ (MPa)	Lithology	Weathering	Notes
1		4.13	25.8	41.8	1078	1373	37.1	3.01	0.874	2.63	M Sandstone	Sw	Some break along existing
2		8.61	17.6	49.1	864	1100	33.2	7.83	0.831	6.51	M Sandstone	Sw	
3		8.91	14.2	44.9	638	812	28.5	10.98	0.776	8.52	M Sandstone	Sw	
4		10.85	29.1	40.6	1181	1504	38.8	7.21	0.892	6.43	M Sandstone	Sw	
5		11.66	27.0	40	1080	1375	37.1	8.48	0.874	7.41	M Sandstone	Sw	
6		11.50	33.0	37.6	1241	1580	39.7	7.28	0.902	6.57	M Sandstone	Sw	
7		11.96	51.8	81.8	4237	5395	73.5	2.22	1.189	2.64	M Sandstone	Sw	Break along tight existing - oxide
8		7.10	30.7	89.5	2748	3498	59.1	2.03	1.079	2.19	M Sandstone	Sw	Some break along existing
9		2.21	17.9	24.5	439	558	23.6	3.96	0.714	2.82	M Sandstone	Sw	Some break along existing
10		8.25	34.7	54.1	1877	2390	48.9	3.45	0.990	3.42	M Sandstone	Sw	Some break along existing
11		20.54	43.6	45.3	1975	2515	50.1	8.17	1.001	8.18	M Sandstone	Sw	
12		21.12	43.7	51.2	2237	2849	53.4	7.41	1.030	7.63	M Sandstone	Sw	
13		18.90	54.0	65.5	3537	4503	67.1	4.20	1.142	4.79	M Sandstone	Sw	

SAMPLE: 3b

Test No.	Type	P (kN)	D (mm)	W (mm)	A = WD (mm^2)	D_e^2	D_e	I_s	F	$I_{s(50)}$ (MPa)	Lithology	Weathering	Notes
1		14.51	42.0	63.4	2663	3390	58.2	4.28	1.071	4.58	F-M Sandstone	Sw	
2		16.38	33.2	65.7	2181	2777	52.7	5.90	1.024	6.04	F-M Sandstone	Sw	
3		6.59	18.6	41.8	777	990	31.5	6.66	0.812	5.40	F-M Sandstone	Sw	Some break along existing
4		9.60	17.8	28.8	513	653	25.5	14.71	0.739	10.87	F-M Sandstone	Sw	
5		23.89	45.4	73.1	3319	4226	65.0	5.65	1.125	6.36	F-M Sandstone	Sw	
6		14.45	32.8	45.1	1479	1883	43.4	7.67	0.938	7.20	F-M Sandstone	Sw	
7		5.04	38.6	63.7	2459	3131	56.0	1.61	1.052	1.69	F-M Sandstone	Sw	Break along existing
8		4.33	73.5	49.7	3653	4651	68.2	0.93	1.150	1.07	F-M Sandstone	Sw	Break along existing
9		14.27	47.9	56.5	2706	3446	58.7	4.14	1.075	4.45	F-M Sandstone	Sw	Some break along existing
10		7.84	16.0	25.1	402	511	22.6	15.33	0.700	10.73	F-M Sandstone	Sw	
11		22.61	55.7	64.3	3582	4560	67.5	4.96	1.145	5.68	F-M Sandstone	Sw	Some break along existing
12		9.09	26.3	46	1210	1540	39.2	5.90	0.897	5.29	F-M Sandstone	Sw	
13		17.35	29.8	75.3	2244	2857	53.5	6.07	1.030	6.26	F-M Sandstone	Sw	
14		15.36	32.4	39.6	1283	1634	40.4	9.40	0.909	8.54	F-M Sandstone	Sw	
15		10.61	18.4	31.5	580	738	27.2	14.38	0.760	10.93	F-M Sandstone	Sw	

SAMPLE: 4a

Test No.	Type	P (kN)	D (mm)	W (mm)	A = WD (mm^2)	D_e^2	D_e	I_s	F	$I_{s(50)}$ (MPa)	Lithology	Weathering	Notes
1		7.06	22.2	35.5	788	1003	31.7	7.04	0.814	5.73	F-M Sandstone	Sw	
2		7.00	13.7	39.9	547	696	26.4	10.06	0.750	7.54	F-M Sandstone	Sw	
3		2.91	17.1	47.5	812	1034	32.2	2.81	0.820	2.31	F-M Sandstone	Sw	Some break along existing
4		0.35	34.7	48.9	1697	2160	46.5	0.16	0.968	0.16	F-M Sandstone	Sw	Break along existing quartz
5		13.54	32.0	48.3	1546	1968	44.4	6.88	0.948	6.52	F-M Sandstone	Sw	
6		7.74	20.7	46.5	963	1226	35.0	6.32	0.852	5.38	F-M Sandstone	Sw	
7		1.08	35.6	32.5	1157	1473	38.4	0.73	0.888	0.65	Fine Sandstone	Sw-Mw	Some break along existing
8		0.14	18.7	32.9	615	783	28.0	0.18	0.770	0.14	Fine Sandstone	Sw-Mw	Break along existing
9		1.50	16.9	35.6	602	766	27.7	1.96	0.766	1.50	Fine Sandstone	Sw-Mw	
10		0.57	29.9	45	1346	1713	41.4	0.33	0.918	0.31	Mudstone	Mw-Hw	Shatter
11		0.47	24.4	53.2	1298	1653	40.7	0.28	0.911	0.26	Mudstone	Mw-Hw	Shatter
12		0.30	24.4	34.9	852	1084	32.9	0.28	0.829	0.23	Mudstone	Mw-Hw	Shatter
13		5.83	20.5	32.8	672	856	29.3	6.81	0.786	5.35	F-M Sandstone	Sw	
14		8.75	26.7	41.6	1111	1414	37.6	6.19	0.880	5.44	F-M Sandstone	Sw	Break along existing
15		10.22	57.0	42	2394	3048	55.2	3.35	1.046	3.51	F-M Sandstone	Sw	Some break along existing

SAMPLE: 5a

Test No.	Type	P (kN)	D (mm)	W (mm)	A = WD (mm^2)	D_e^2	D_e	I_s	F	$I_{s(50)}$ (MPa)	Lithology	Weathering	Notes
1		8.33	17.8	49.5	881	1122	33.5	7.43	0.835	6.20	F-M sandstone	Sw	
2		4.96	9.8	50.4	494	629	25.1	7.89	0.733	5.78	F-M sandstone	Sw	
3		6.43	17.5	45.5	796	1014	31.8	6.34	0.816	5.18	F-M sandstone	Sw	
4		6.19	29.8	69.9	2083	2652	51.5	2.33	1.013	2.37	F-M sandstone	Sw-Mw	Break along existing oxidised
5		6.83	13.4	47.2	632	805	28.4	8.48	0.775	6.57	F-M sandstone	Sw	
6		4.71	42.3	45.6	1929	2456	49.6	1.92	0.996	1.91	F-M sandstone	Sw	Break along existing quartz
7		12.33	28.5	35	998	1270	35.6	9.71	0.859	8.34	F-M sandstone	Sw	
8		5.18	31.2	24.1	752	957	30.9	5.41	0.806	4.36	F-M sandstone	Sw-Mw	Break along existing oxide
9		8.27	34.5	54.6	1884	2398	49.0	3.45	0.991	3.42	F-M sandstone	Sw-Mw	Some break along existing oxide
10		9.98	26.5	30.7	814	1036	32.2	9.63	0.820	7.90	F-M sandstone	Sw	
11		8.61	22.9	43.7	1001	1274	35.7	6.76	0.859	5.81	F-M sandstone	Sw	
12		5.99	31.0	46.8	1451	1847	43.0	3.24	0.934	3.03	F-M sandstone	Sw-Mw	Break along existing

SAMPLE: 5b

Test No.	Type	P (kN)	D (mm)	W (mm)	A = WD (mm^2)	D_e^2	D_e	I_s	F	$I_{s(50)}$ (MPa)	Lithology	Weathering	Notes
1		7.22	23.0	35.3	812	1034	32.2	6.98	0.820	5.73	F-M sandstone	Sw	
2		4.00	9.3	48.9	455	579	24.1	6.91	0.720	4.97	F-M sandstone	Sw	
3		14.25	40.4	55.3	2234	2845	53.3	5.01	1.029	5.16	F-M sandstone	Sw	
4		6.61	32.8	42.9	1407	1792	42.3	3.69	0.928	3.42	F-M sandstone	Sw	Some break along existing
5		13.24	31.4	49.3	1548	1971	44.4	6.72	0.948	6.37	F-M sandstone	Sw	
6		7.48	17.9	48.8	874	1112	33.3	6.73	0.833	5.60	F-M sandstone	Sw	
7		5.16	31.5	40	1260	1604	40.1	3.22	0.905	2.91	F-M sandstone	Sw	Some break along existing
8		10.02	24.9	54.7	1362	1734	41.6	5.78	0.921	5.32	F-M sandstone	Sw	
9		12.59	29.8	41.7	1243	1582	39.8	7.96	0.902	7.18	F-M sandstone	Sw	

E.7 Hurunui River - Point Load testing

SAMPLE: 6a

Test No.	Type	P (kN)	D (mm)	W (mm)	A = WD (mm^2)	D_e^2	D_e	I_s	F	$I_{s(50)}$ (MPa)	Lithology	Weathering	Notes
1		0.12	23.9	33.5	801	1019	31.9	0.12	0.817	0.10	Mudstone	Mw	Shatter
2		0.35	25.5	61.1	1558	1984	44.5	0.18	0.949	0.17	Mudstone	Mw	Shatter
3		0.37	30.8	28	862	1098	33.1	0.34	0.831	0.28	Mudstone	Mw	Shatter
4		0.69	30.9	38.7	1196	1523	39.0	0.45	0.894	0.41	Mudstone	Mw	Shatter
5		0.34	37.5	51	1913	2435	49.3	0.14	0.994	0.14	Mudstone	Mw	Shatter
6		0.67	25.0	32.8	820	1044	32.3	0.64	0.822	0.53	Fine Sandstone	Sw-Mw	Break along existing
7		4.49	23.4	45.05	1054	1342	36.6	3.35	0.869	2.91	Fine Sandstone	Sw-Mw	
8		3.11	18.1	32.4	586	747	27.3	4.17	0.762	3.17	Fine Sandstone	Mw	
9		3.09	20.7	47.5	983	1252	35.4	2.47	0.856	2.11	Fine Sandstone	Mw	
10		1.87	44.5	56.6	2519	3207	56.6	0.58	1.058	0.62	Fine Sandstone	Mw	Break along existing
11		8.04	29.3	53.2	1559	1985	44.5	4.05	0.949	3.85	Fine Sandstone	Sw-Mw	
12		0.32	30.8	45.3	1395	1776	42.1	0.18	0.926	0.17	Mudstone	Mw	Break along existing
13		2.54	47.0	62	2914	3710	60.9	0.68	1.093	0.75	Fine Sandstone	Sw-Mw	Break along existing
14		7.24	35.0	61.5	2153	2741	52.4	2.64	1.021	2.70	Fine Sandstone	Sw-Mw	
15		1.73	33.0	23.3	769	979	31.3	1.77	0.810	1.43	Fine Sandstone	Sw-Mw	Break along existing quartz

SAMPLE: 7a

Test No.	Type	P (kN)	D (mm)	W (mm)	A = WD (mm^2)	D_e^2	D_e	I_s	F	$I_{s(50)}$ (MPa)	Lithology	Weathering	Notes
1		3.45	9.3	46.7	434	553	23.5	6.24	0.712	4.44	F-M Sandstone	Sw	
2		3.62	20.1	35.5	714	909	30.1	3.98	0.796	3.17	F-M Sandstone	Sw	
3		1.85	23.8	47.9	1140	1452	38.1	1.27	0.885	1.13	F-M Sandstone	Sw	Break along existing oxide
4		11.21	23.8	48.9	1164	1482	38.5	7.57	0.889	6.73	F-M Sandstone	Sw	
5		7.82	42.9	77.5	3325	4233	65.1	1.85	1.126	2.08	F-M Sandstone	Sw	Some break along existing quartz
6		5.02	26.6	42.6	1133	1443	38.0	3.48	0.884	3.07	F-M Sandstone	Sw	Break along existing quartz
7		3.98	21.8	54.5	1188	1513	38.9	2.63	0.893	2.35	F-M Sandstone	Sw	Break along existing quartz
8		13.74	34.1	71.3	2431	3096	55.6	4.44	1.049	4.66	F-M Sandstone	Sw	
9		8.37	30.5	45.4	1385	1763	42.0	4.75	0.924	4.39	F-M Sandstone	Sw	
10		1.40	18.8	41.3	776	989	31.4	1.42	0.812	1.15	Mudstone	Mw	
11		1.20	18.0	49.5	891	1134	33.7	1.06	0.837	0.89	Mudstone	Mw	Some break along existing oxide
12		0.85	16.3	23.5	383	488	22.1	1.74	0.692	1.21	Mudstone	Mw	Some break along existing oxide
13		1.24	23.4	39.7	929	1183	34.4	1.05	0.845	0.89	Mudstone	Mw	Break along existing - shatter
14		1.73	14.2	47.4	673	857	29.3	2.02	0.786	1.59	Mudstone	Mw	Break along existing oxide
15		0.75	19.1	64.8	1238	1576	39.7	0.48	0.901	0.43	Mudstone	Mw	Most break along existing

SAMPLE: 8a

Test No.	Type	P (kN)	D (mm)	W (mm)	A = WD (mm^2)	D_e^2	D_e	I_s	F	$I_{s(50)}$ (MPa)	Lithology	Weathering	Notes
1		9.17	36.0	51.3	1847	2351	48.5	3.90	0.986	3.85	F-M Sandstone	Sw	
2		5.91	40.6	57.7	2343	2983	54.6	1.98	1.041	2.06	F-M Sandstone	Sw	Break along existing quartz
3		2.11	37.5	51.3	1924	2449	49.5	0.86	0.995	0.86	F-M Sandstone	Sw	Break along existing quartz and oxide
4		19.82	44.0	59.2	2605	3317	57.6	5.98	1.066	6.37	F-M Sandstone	Sw	
5		12.17	28.2	48.1	1356	1727	41.6	7.05	0.920	6.48	F-M Sandstone	Sw	
6		14.90	41.9	55.1	2309	2940	54.2	5.07	1.037	5.26	F-M Sandstone	Sw	
7		13.79	27.3	38.7	1057	1345	36.7	10.25	0.870	8.92	F-M Sandstone	Sw	
8		1.14	14.6	43.5	635	809	28.4	1.41	0.776	1.09	Mudstone	Mw-Hw	Break along existing oxide
9		0.34	24.7	16.7	412	525	22.9	0.65	0.704	0.46	Mudstone	Mw-Hw	Break along existing oxide
10		0.91	21.0	24.5	515	655	25.6	1.39	0.740	1.03	Mudstone	Mw-Hw	Some break along existing
11		0.71	27.7	24.6	681	868	29.5	0.82	0.788	0.64	Mudstone	Mw-Hw	Break along existing oxide
12		0.89	16.2	35.8	580	738	27.2	1.21	0.760	0.92	Mudstone	Mw-Hw	Some break along existing
13		0.75	35.8	33.6	1203	1532	39.1	0.49	0.896	0.44	Mudstone	Mw-Hw	Break along existing oxide
14		15.00	27.3	40.56	1107	1410	37.5	10.64	0.879	9.35	F-M Sandstone	Sw	
15		13.56	27.4	53.7	1471	1873	43.3	7.24	0.937	6.78	F-M Sandstone	Sw	

SAMPLE: 8b

Test No.	Type	P (kN)	D (mm)	W (mm)	A = WD (mm^2)	D_e^2	D_e	I_s	F	$I_{s(50)}$ (MPa)	Lithology	Weathering	Notes
1		19.18	46.5	80.3	3734	4754	69.0	4.03	1.156	4.66	F-M Sandstone	Sw	Some break along existing quartz
2		10.89	31.6	50.8	1605	2044	45.2	5.33	0.956	5.09	F-M Sandstone	Sw	Note: quite heavy quartz veining
3		19.34	52.8	58.3	3078	3919	62.6	4.93	1.106	5.46	F-M Sandstone	Sw	Some break along existing oxide
4		15.64	47.2	61.4	2898	3690	60.7	4.24	1.092	4.63	F-M Sandstone	Sw	
5		8.81	17.0	48.4	823	1048	32.4	8.41	0.822	6.91	F-M Sandstone	Sw	
6		3.15	8.5	48.1	409	521	22.8	6.05	0.703	4.25	F-M Sandstone	Sw	
7		18.98	34.5	70.4	2429	3092	55.6	6.14	1.049	6.44	F-M Sandstone	Sw	
8		13.95	19.7	87.1	1716	2185	46.7	6.39	0.970	6.19	F-M Sandstone	Sw	
9		9.80	51.2	49.7	2545	3240	56.9	3.02	1.060	3.21	F-M Sandstone	Sw	Some break along existing quartz
10		1.65	58.6	61.2	3586	4566	67.6	0.36	1.145	0.41	F-M Sandstone	Sw	Break along existing oxide
11		8.49	47.7	59.6	2843	3620	60.2	2.35	1.087	2.55	F-M Sandstone	Sw	Some break along existing quartz
12		5.66	30.5	35.5	1083	1379	37.1	4.11	0.875	3.59	F-M Sandstone	Sw	Some break along existing quartz
13		5.16	28.3	27.9	790	1005	31.7	5.13	0.815	4.18	F-M Sandstone	Sw	
14		3.45	19.8	61.7	1222	1555	39.4	2.22	0.899	1.99	F-M Sandstone	Sw	Break along existing quartz
15		4.69	18.8	38.3	720	917	30.3	5.12	0.798	4.08	F-M Sandstone	Sw	Some break along existing oxide

SAMPLE: 10a

Test No.	Type	P (kN)	D (mm)	W (mm)	A = WD (mm^2)	D_e^2	D_e	I_s	F	$I_{s(50)}$ (MPa)	Lithology	Weathering	Notes
1		1.44	30.3	47.4	1436	1829	42.8	0.79	0.932	0.73	Mudstone	Mw-Hw	Break along existing
2		0.37	15.6	39.9	622	793	28.2	0.47	0.772	0.36	Mudstone	Mw-Hw	Break along existing
3		0.51	31.6	58.4	1845	2350	48.5	0.22	0.986	0.21	Mudstone	Mw-Hw	Break along existing
4		2.01	35.2	25.9	912	1161	34.1	1.73	0.841	1.46	Mudstone	Mw-Hw	Most break along existing
5		0.67	11.8	18	212	270	16.4	2.48	0.606	1.50	Mudstone	Mw-Hw	Most break along existing
6		1.42	42.5	35.7	1517	1932	44.0	0.74	0.944	0.69	Mudstone	Mw-Hw	Break along existing
7		1.38	22.6	27	610	777	27.9	1.78	0.769	1.37	Mudstone	Mw-Hw	Most break along existing
8		4.09	45.8	49.4	2263	2881	53.7	1.42	1.032	1.47	F-M Sandstone	Mw	Break along existing - quartz and oxide
9		9.56	32.5	40.2	1307	1663	40.8	5.75	0.912	5.24	F-M Sandstone	Sw-Mw	
10		4.90	14.4	37.3	537	684	26.2	7.16	0.747	5.35	F-M Sandstone	Sw-Mw	
11		4.33	24.1	84.2	2029	2584	50.8	1.68	1.007	1.69	F-M Sandstone	Sw-Mw	Most break along existing
12		5.24	25.0	43.7	1093	1391	37.3	3.77	0.876	3.30	F-M Sandstone	Sw-Mw	Some break along existing
13		7.32	52.6	47.6	2504	3188	56.5	2.30	1.056	2.43	F-M Sandstone	Sw-Mw	Some break along existing quartz
14		10.79	51.0	53.8	2744	3494	59.1	3.09	1.078	3.33	F-M Sandstone	Sw-Mw	Some break along existing quartz
15		12.17	52.0	55.6	2891	3681	60.7	3.31	1.091	3.61	F-M Sandstone	Sw-Mw	Some break along existing oxide

E.7 Hurunui River - Point Load testing

SAMPLE: 11a

Test No.	Type	P (kN)	D (mm)	W (mm)	A = WD (mm^2)	D_e^2	D_e	I_s	F	$I_{s(50)}$ (MPa)	Lithology	Weathering	Notes
1		2.89	48.1	79.2	3810	4850	69.6	0.60	1.161	0.69	F-M Sandstone	Sw-Mw	Break along existing oxide
2		11.86	39.2	48.3	1893	2411	49.1	4.92	0.992	4.88	F-M Sandstone	Sw-Mw	
3		2.74	24.6	60	1476	1879	43.4	1.46	0.938	1.37	F-M Sandstone	Sw-Mw	Break along existing some oxide
4		4.63	26.6	25.5	678	864	29.4	5.36	0.787	4.22	F-M Sandstone	Sw-Mw	Some break along existing quartz
5		9.09	61.0	89.7	5472	6967	83.5	1.30	1.259	1.64	F-M Sandstone	Sw-Mw	Break along existing oxide
6		12.35	58.0	38.6	2239	2851	53.4	4.33	1.030	4.46	F-M Sandstone	Sw-Mw	Some break along existing
7		9.76	35.4	65	2301	2930	54.1	3.33	1.036	3.45	F-M Sandstone	Sw-Mw	
8		12.59	29.6	39.5	1169	1489	38.6	8.46	0.890	7.53	F-M Sandstone	Sw	
9		4.27	25.5	41.1	1048	1334	36.5	3.20	0.868	2.78	F-M Sandstone	Sw-Mw	Some break along existing
10		8.93	25.1	33	828	1055	32.5	8.47	0.823	6.97	F-M Sandstone	Sw	
11		5.46	26.4	29.6	781	995	31.5	5.49	0.813	4.46	Fine Sandstone	Sw-Mw	
12		2.84	41.7	43.3	1806	2299	47.9	1.24	0.981	1.21	F-M Sandstone	Sw-Mw	Break along existing oxide
13		3.92	32.9	28.4	934	1190	34.5	3.30	0.846	2.79	Fine Sandstone	Sw-Mw	Some break along existing
14		7.30	28.9	22.3	644	821	28.6	8.90	0.778	6.92	F-M Sandstone	Sw	
15		5.12	23.6	27.5	649	826	28.7	6.20	0.780	4.83	Fine Sandstone	Sw-Mw	

SAMPLE: 13a

Test No.	Type	P (kN)	D (mm)	W (mm)	A = WD (mm^2)	D_e^2	D_e	I_s	F	$I_{s(50)}$ (MPa)	Lithology	Weathering	Notes
1		2.54	23.5	25.1	590	751	27.4	3.38	0.763	2.58	Fine Sandstone	Mw	
2		5.16	49.8	79.9	3979	5066	71.2	1.02	1.172	1.19	Fine Sandstone	Mw	Most break along existing oxide
3		1.46	18.6	36.1	671	855	29.2	1.71	0.786	1.34	Fine Sandstone	Mw	Break along existing
4		2.60	27.4	38.4	1052	1340	36.6	1.94	0.869	1.69	Fine Sandstone	Mw	Break along existing
5		1.89	19.8	61.3	1214	1545	39.3	1.22	0.897	1.10	Fine Sandstone	Mw	Break along existing
6		5.60	34.0	45.1	1533	1952	44.2	2.87	0.946	2.71	Fine Sandstone	Mw	Break along existing
7		1.75	20.1	37.8	760	967	31.1	1.81	0.808	1.46	Fine Sandstone	Mw	Most break along existing oxide
8		1.00	32.4	43.8	1419	1807	42.5	0.55	0.930	0.51	Fine Sandstone	Mw-Hw	Break along existing
9		0.22	20.0	33.4	668	851	29.2	0.26	0.785	0.20	Fine Sandstone	Mw	Break along existing
10		0.08	14.2	25.8	366	466	21.6	0.17	0.685	0.12	Fine Sandstone	Mw	Break along existing
11		1.71	9.2	22.5	207	264	16.2	6.49	0.603	3.91	Fine Sandstone	Sw-Mw	
12		2.89	22.8	43.3	987	1257	35.5	2.30	0.857	1.97	Fine Sandstone	Mw	Some break along existing
13		2.84	55.9	50.7	2834	3609	60.1	0.79	1.086	0.85	Fine Sandstone	Mw-Hw	Break along existing
14		1.12	38.4	49.3	1893	2410	49.1	0.46	0.992	0.46	Fine Sandstone	Mw-Hw	Break along existing
15		2.13	21.4	47.9	1025	1305	36.1	1.63	0.864	1.41	Fine Sandstone	Mw	Some break along existing

SAMPLE: 13b

Test No.	Type	P (kN)	D (mm)	W (mm)	A = WD (mm^2)	D_e^2	D_e	I_s	F	$I_{s(50)}$ (MPa)	Lithology	Weathering	Notes
1		5.93	30.0	44.5	1335	1700	41.2	3.49	0.917	3.20	Fine Sandstone	Sw-Mw	
2		2.46	34.0	48.5	1649	2100	45.8	1.17	0.961	1.13	Fine Sandstone	Sw-Mw	Most break along existing
3		3.37	23.8	29.2	695	885	29.7	3.81	0.792	3.01	Fine Sandstone	Sw-Mw	Some break along existing
4		1.40	17.2	46.9	807	1027	32.0	1.36	0.819	1.12	Fine Sandstone	Sw-Mw	Some break along existing
5		1.12	10.5	34.7	364	464	21.5	2.41	0.685	1.65	Fine Sandstone	Sw-Mw	Most break along existing
6		5.34	31.6	55.8	1763	2245	47.4	2.38	0.976	2.32	Fine Sandstone	Sw-Mw	Some break along existing
7		0.89	34.7	55.3	1919	2443	49.4	0.36	0.995	0.36	Fine Sandstone	Sw-Mw	Break along existing
8		6.13	24.6	36.8	905	1153	34.0	5.32	0.840	4.47	Fine Sandstone	Sw-Mw	
9		0.89	29.2	39.7	1159	1476	38.4	0.60	0.888	0.54	Fine Sandstone	Sw-Mw	Break along existing
10		1.93	11.1	24	266	339	18.4	5.69	0.638	3.63	Fine Sandstone	Sw-Mw	Some break along existing
11		6.17	50.8	42	2134	2717	52.1	2.27	1.019	2.31	Fine Sandstone	Sw-Mw	
12		10.85	32.0	54	1728	2200	46.9	4.93	0.972	4.79	Fine Sandstone	Sw-Mw	
13		7.76	36.5	37.2	1358	1729	41.6	4.49	0.920	4.13	Fine Sandstone	Sw-Mw	Some break along existing
14		8.35	27.6	39	1076	1371	37.0	6.09	0.873	5.32	Fine Sandstone	Sw-Mw	
15		2.34	25.2	24.7	622	793	28.2	2.95	0.772	2.28	Fine Sandstone	Sw-Mw	

SAMPLE: 13c

Test No.	Type	P (kN)	D (mm)	W (mm)	A = WD (mm^2)	D_e^2	D_e	I_s	F	$I_{s(50)}$ (MPa)	Lithology	Weathering	Notes
1		13.02	61.7	80.2	4948	6300	79.4	2.07	1.231	2.54	Fine Sandstone	Sw-Mw	Break along existing oxide
2		3.52	30.5	57.3	1748	2225	47.2	1.58	0.974	1.54	Fine Sandstone	Sw-Mw	Break along existing oxide
3		4.90	24.5	41.4	1014	1291	35.9	3.79	0.862	3.27	Fine Sandstone	Sw-Mw	Some break along existing
4		10.24	50.1	55.9	2801	3566	59.7	2.87	1.083	3.11	Fine Sandstone	Sw-Mw	
5		18.17	35.2	51.7	1820	2317	48.1	7.84	0.983	7.71	Fine Sandstone	Sw	
6		7.78	24.1	38	916	1166	34.1	6.67	0.842	5.62	Fine Sandstone	Sw	
7		5.42	60.0	60.1	3606	4591	67.8	1.18	1.147	1.35	Fine Sandstone	Sw-Mw	Break along existing oxide
8		1.79	31.9	54.8	1748	2226	47.2	0.80	0.974	0.78	Mudstone	Sw-Mw	Some break along existing
9		4.06	14.8	46.7	692	881	29.7	4.61	0.791	3.64	Mudstone	Sw	
10		10.26	22.0	88.3	1943	2473	49.7	4.15	0.998	4.14	Mudstone	Sw	
11		2.68	13.9	39.3	546	696	26.4	3.85	0.750	2.89	Mudstone	Sw	
12		2.44	21.4	40.8	873	1112	33.3	2.19	0.833	1.83	Mudstone	Sw-Mw	Some break along existing
13		2.89	36.8	50.6	1862	2371	48.7	1.22	0.988	1.20	Mudstone	Sw-Mw	Some break along existing
14		4.04	47.5	76	3610	4596	67.8	0.88	1.147	1.01	Mudstone	Sw-Mw	Shatter along existing
15		2.84	13.0	41.2	536	682	26.1	4.16	0.747	3.11	Mudstone	Sw	

SAMPLE: 14a

Test No.	Type	P (kN)	D (mm)	W (mm)	A = WD (mm^2)	D_e^2	D_e	I_s	F	$I_{s(50)}$ (MPa)	Lithology	Weathering	Notes
1		0.28	19.9	54.13	1075	1369	37.0	0.20	0.873	0.18	Mudstone	Mw	Most break along existing oxide
2		3.90	13.1	33.8	442	562	23.7	6.93	0.715	4.96	Mudstone	Sw	
3		11.36	33.7	56.34	1898	2416	49.2	4.70	0.992	4.67	Fine Sandstone	Sw-Mw	
4		4.88	43.4	46.33	2011	2560	50.6	1.91	1.005	1.92	Fine Sandstone	Sw-Mw	Most break along existing oxide
5		0.30	22.8	41.63	949	1209	34.8	0.25	0.849	0.21	Mudstone	Mw	Most break along existing oxide
6		10.10	28.5	57.6	1644	2093	45.8	4.83	0.961	4.64	Fine Sandstone	Sw	
7		2.84	28.8	42.48	1223	1558	39.5	1.82	0.899	1.64	Fine Sandstone	Sw	Break along existing oxide
8		3.19	13.8	31.98	441	562	23.7	5.68	0.715	4.06	Mudstone	Sw	

SAMPLE: 14b

Test No.	Type	P (kN)	D (mm)	W (mm)	A = WD (mm^2)	D_e^2	D_e	I_s	F	$I_{s(50)}$ (MPa)	Lithology	Weathering	Notes
1		1.67	20.8	29.42	611	778	27.9	2.15	0.769	1.65	Mudstone	Sw-Mw	
2		0.91	17.2	44.33	761	969	31.1	0.94	0.808	0.76	Mudstone	Mw	Most break along existing
3		0.67	16.2	51.82	837	1066	32.6	0.63	0.825	0.52	Mudstone	Mw	Most break along existing
4		4.49	21.7	52.9	1147	1460	38.2	3.07	0.886	2.72	Mudstone	Sw-Mw	
5		0.10	34.6	61.6	2130	2712	52.1	0.04	1.018	0.04	Mudstone	Mw	Break along existing
6		3.31	42.9	54.22	2326	2962	54.4	1.12	1.039	1.16	Mudstone	Sw-Mw	Some break along existing
7		1.12	22.6	36.27	820	1044	32.3	1.07	0.822	0.88	Mudstone	Sw-Mw	Most break along existing

E.7 Hurunui River - Point Load testing

SAMPLE: 14c

Test No.	Type	P (kN)	D (mm)	W (mm)	A = WD (mm^2)	D_e^2	D_e	I_s	F	$I_{s(50)}$ (MPa)	Lithology	Weathering	Notes
1		25.32	55.3	66.6	3682	4688	68.5	5.40	1.152	6.22	F-M Sandstone	Sw	
2		13.62	27.5	74.6	2054	2616	51.1	5.21	1.010	5.26	F-M Sandstone	Sw	
3		22.47	50.2	77.8	3906	4973	70.5	4.52	1.167	5.27	F-M Sandstone	Sw	
4		28.08	40.2	79.9	3214	4092	64.0	6.86	1.117	7.67	F-M Sandstone	Sw	
5		17.41	24.0	59.4	1426	1815	42.6	9.59	0.931	8.93	F-M Sandstone	Sw	
6		10.02	20.2	35.48	718	914	30.2	10.96	0.797	8.74	F-M Sandstone	Sw	

SAMPLE: 16a

Test No.	Type	P (kN)	D (mm)	W (mm)	A = WD (mm^2)	D_e^2	D_e	I_s	F	$I_{s(50)}$ (MPa)	Lithology	Weathering	Notes
1		11.62	48.2	75.14	3623	4613	67.9	2.52	1.148	2.89	F-M Sandstone	Sw	
2		9.74	43.5	50.59	2198	2799	52.9	3.48	1.026	3.57	F-M Sandstone	Sw	Some break along existing oxide
3		26.09	62.5	71.2	4449	5664	75.3	4.61	1.202	5.54	F-M Sandstone	Sw	
4		7.86	13.7	50.55	690	879	29.6	8.95	0.790	7.07	F-M Sandstone	Sw	
5		23.68	51.4	42.9	2206	2809	53.0	8.43	1.027	8.65	F-M Sandstone	Sw	
6		6.94	13.6	36.1	491	626	25.0	11.09	0.732	8.12	F-M Sandstone	Sw	
7		0.75	17.6	29.8	524	668	25.8	1.12	0.743	0.83	Mudstone	Mw-Hw	Some break along existing oxide

SAMPLE: 18a

Test No.	Type	P (kN)	D (mm)	W (mm)	A = WD (mm^2)	D_e^2	D_e	I_s	F	$I_{s(50)}$ (MPa)	Lithology	Weathering	Notes
1		16.95	40.1	88.56	3551	4522	67.2	3.75	1.143	4.28	F-M Sandstone	Sw-Mw	
2		0.30	37.7	53.8	2028	2582	50.8	0.12	1.007	0.12	F-M Sandstone	Mw	Break along existing oxide
3		3.52	36.4	38.89	1416	1802	42.5	1.95	0.929	1.81	F-M Sandstone	Sw-Mw	Some break along existing
4		7.10	27.2	73.06	1989	2532	50.3	2.80	1.003	2.81	F-M Sandstone	Sw-Mw	
5		10.12	21.5	43.99	947	1206	34.7	8.39	0.849	7.12	F-M Sandstone	Sw-Mw	
6		12.13	24.8	68.34	1691	2154	46.4	5.63	0.967	5.45	F-M Sandstone	Sw-Mw	
7		7.24	22.8	37	844	1075	32.8	6.73	0.827	5.57	F-M Sandstone	Sw-Mw	

SAMPLE: 19a

Test No.	Type	P (kN)	D (mm)	W (mm)	A = WD (mm^2)	D_e^2	D_e	I_s	F	$I_{s(50)}$ (MPa)	Lithology	Weathering	Notes
1		3.39	35.8	58.12	2083	2652	51.5	1.28	1.013	1.30	F-M Sandstone	Mw-Hw	
2		13.26	26.4	63.9	1686	2147	46.3	6.18	0.966	5.97	F-M Sandstone	Mw	
3		1.58	14.9	27.49	410	522	22.8	3.03	0.703	2.13	F-M Sandstone	Mw-Hw	
4		1.06	36.0	112.53	4051	5158	71.8	0.21	1.177	0.24	F-M Sandstone	Mw-Hw	Break along existing oxide
5		5.99	15.6	39.73	618	787	28.1	7.61	0.771	5.87	F-M Sandstone	Mw	
6		11.72	19.6	55.5	1089	1387	37.2	8.45	0.876	7.40	F-M Sandstone	Mw	
7		1.52	42.2	47.48	2001	2548	50.5	0.60	1.004	0.60	F-M Sandstone	Hw	Break along existing oxide

SAMPLE: 20a

Test No.	Type	P (kN)	D (mm)	W (mm)	A = WD (mm^2)	D_e^2	D_e	I_s	F	$I_{s(50)}$ (MPa)	Lithology	Weathering	Notes
1		1.54	21.6	26.04	561	714	26.7	2.16	0.754	1.63	F-M Sandstone	Mw	
2		11.52	22.3	46.09	1028	1309	36.2	8.80	0.864	7.61	F-M Sandstone	Sw-Mw	
3		16.02	32.7	60.78	1985	2527	50.3	6.34	1.002	6.35	F-M Sandstone	Sw-Mw	
4		12.02	21.6	69.05	1491	1899	43.6	6.33	0.940	5.95	F-M Sandstone	Sw-Mw	
5		13.52	28.2	57.7	1624	2068	45.5	6.54	0.958	6.26	F-M Sandstone	Sw-Mw	
6		9.50	26.0	58.74	1525	1942	44.1	4.89	0.945	4.62	F-M Sandstone	Sw-Mw	

SAMPLE: 21a

Test No.	Type	P (kN)	D (mm)	W (mm)	A = WD (mm^2)	D_e^2	D_e	I_s	F	$I_{s(50)}$ (MPa)	Lithology	Weathering	Notes
1		5.66	26.6	55.09	1463	1863	43.2	3.04	0.936	2.84	F-M Sandstone	Mw	
2		2.58	23.6	30.9	729	928	30.5	2.78	0.800	2.22	F-M Sandstone	Mw	
3		9.80	45.4	44.7	2031	2586	50.8	3.79	1.008	3.82	F-M Sandstone	Mw	
4		18.63	27.6	58.79	1623	2066	45.5	9.02	0.958	8.64	F-M Sandstone	Sw	
5		19.30	29.2	61.9	1809	2303	48.0	8.38	0.982	8.23	F-M Sandstone	Sw	
6		8.85	21.0	68.23	1433	1824	42.7	4.85	0.932	4.52	F-M Sandstone	Sw	
7		15.06	27.9	48.29	1347	1715	41.4	8.78	0.919	8.07	F-M Sandstone	Sw	

SAMPLE: 23a

Test No.	Type	P (kN)	D (mm)	W (mm)	A = WD (mm^2)	D_e^2	D_e	I_s	F	$I_{s(50)}$ (MPa)	Lithology	Weathering	Notes
1		13.71	34.8	58.8	2046	2605	51.0	5.26	1.009	5.31	F-M Sandstone	Sw-Mw	
2		9.86	27.2	58.4	1588	2023	45.0	4.88	0.953	4.65	F-M Sandstone	Sw-Mw	Some break along existing
3		19.17	51.5	56.6	2915	3711	60.9	5.17	1.093	5.65	F-M Sandstone	Sw	
4		11.26	24.9	37.7	939	1195	34.6	9.42	0.847	7.98	F-M Sandstone	Sw	
5		2.30	8.8	21.1	186	236	15.4	9.73	0.588	5.72	F-M Sandstone	Sw-Mw	
6		5.95	18.7	51.6	965	1229	35.1	4.84	0.852	4.13	F-M Sandstone	Sw-Mw	
7		16.93	28.1	56.3	1582	2014	44.9	8.40	0.953	8.01	F-M Sandstone	Sw	
8		5.93	21.1	35.7	753	959	31.0	6.18	0.806	4.98	F-M Sandstone	Sw-Mw	
9		7.27	34.8	52.6	1830	2331	48.3	3.12	0.984	3.07	F-M Sandstone	Sw-Mw	

SAMPLE: 26a

Test No.	Type	P (kN)	D (mm)	W (mm)	A = WD (mm^2)	D_e^2	D_e	I_s	F	$I_{s(50)}$ (MPa)	Lithology	Weathering	Notes
1		17.03	31.7	73.5	2330	2967	54.5	5.74	1.039	5.97	F-M Sandstone	Sw	
2		2.22	12.3	40	492	626	25.0	3.54	0.732	2.60	F-M Sandstone	Mw	
3		18.54	38.2	57.3	2189	2787	52.8	6.65	1.025	6.82	F-M Sandstone	Sw	
4		1.81	45.3	64	2899	3691	60.8	0.49	1.092	0.54	F-M Sandstone	Mw	Break along existing
5		4.45	53.1	52.5	2788	3549	59.6	1.25	1.082	1.36	F-M Sandstone	Mw	Break along existing
6		10.04	27.2	29.2	794	1011	31.8	9.93	0.816	8.10	F-M Sandstone	Sw	
7		11.31	37.9	44	1668	2123	46.1	5.33	0.964	5.13	F-M Sandstone	Sw	
8		15.18	31.9	65.6	2093	2664	51.6	5.70	1.014	5.78	F-M Sandstone	Sw	
9		5.85	22.2	32.3	717	913	30.2	6.41	0.797	5.11	F-M Sandstone	Sw	Break along existing quartz
10		7.59	26.9	25.4	683	870	29.5	8.72	0.789	6.88	F-M Sandstone	Sw	
11		2.48	24.6	47.1	1159	1475	38.4	1.68	0.888	1.49	F-M Sandstone	Sw	Break along existing
12		3.33	17.3	39	675	859	29.3	3.88	0.786	3.05	F-M Sandstone	Sw	
13		1.65	7.0	31.4	220	280	16.7	5.90	0.611	3.60	F-M Sandstone	Sw	
14		2.78	11.1	37.3	414	527	23.0	5.27	0.705	3.72	F-M Sandstone	Sw	
15		3.94	14.5	45.8	664	846	29.1	4.66	0.784	3.65	F-M Sandstone	Sw	

E.7 Hurunui River - Point Load testing

SAMPLE: 27b

Test No.	Type	P (kN)	D (mm)	W (mm)	A = WD (mm^2)	D_e^2	D_e	I_s	F	$I_{s(50)}$ (MPa)	Lithology	Weathering	Notes
1		11.49	25.8	46.9	1210	1541	39.3	7.46	0.897	6.69	F-M Sandstone	Sw	
2		15.83	26.4	40.8	1075	1369	37.0	11.56	0.873	10.10	F-M Sandstone	Sw	
3		11.26	33.9	36.4	1234	1571	39.6	7.17	0.901	6.46	F-M Sandstone	Sw	
4		6.66	35.2	31.9	1123	1430	37.8	4.66	0.882	4.11	F-M Sandstone	Sw	Some break along existing oxide
5		8.02	43.6	59.1	2577	3281	57.3	2.44	1.063	2.60	F-M Sandstone	Sw	Break along existing
6		5.77	28.5	31.5	898	1143	33.8	5.05	0.839	4.23	F-M Sandstone	Sw	
7		1.99	29.0	31.5	914	1163	34.1	1.71	0.842	1.44	F-M Sandstone	Sw	Some break along existing oxide

SAMPLE: 27c

Test No.	Type	P (kN)	D (mm)	W (mm)	A = WD (mm^2)	D_e^2	D_e	I_s	F	$I_{s(50)}$ (MPa)	Lithology	Weathering	Notes
1		4.04	13.5	41.8	564	718	26.8	5.62	0.755	4.25	F-M Sandstone	Sw-Mw	
2		0.81	13.8	27.8	384	488	22.1	1.66	0.693	1.15	F-M Sandstone	Mw	Break along existing
3		3.80	21.7	54.7	1187	1511	38.9	2.51	0.893	2.25	F-M Sandstone	Sw-Mw	
4		2.97	11.7	26.5	310	395	19.9	7.52	0.660	4.97	F-M Sandstone	Sw-Mw	
5		4.45	26.5	27.9	739	941	30.7	4.73	0.803	3.79	F-M Sandstone	Sw-Mw	
6		13.94	22.5	68.8	1548	1971	44.4	7.07	0.948	6.70	F-M Sandstone	Sw	
7		3.62	21.7	33.4	725	923	30.4	3.92	0.799	3.13	F-M Sandstone	Sw-Mw	
8		5.34	24.5	38.7	948	1207	34.7	4.42	0.849	3.76	F-M Sandstone	Sw-Mw	
9		16.82	40.9	67.4	2757	3510	59.2	4.79	1.079	5.17	F-M Sandstone	Sw	
10		3.09	18.5	26.2	485	617	24.8	5.01	0.730	3.65	F-M Sandstone	Sw-Mw	
11		8.74	21.6	49.3	1065	1356	36.8	6.45	0.871	5.62	F-M Sandstone	Sw	

SAMPLE: 28a

Test No.	Type	P (kN)	D (mm)	W (mm)	A = WD (mm^2)	D_e^2	D_e	I_s	F	$I_{s(50)}$ (MPa)	Lithology	Weathering	Notes
1		3.31	31.0	24.9	772	983	31.3	3.37	0.811	2.73	Fine Sandstone	Sw-Mw	
2		4.59	24.2	22.4	542	690	26.3	6.65	0.749	4.98	Fine Sandstone	Sw-Mw	
3		3.47	20.1	31.6	635	809	28.4	4.29	0.776	3.33	Fine Sandstone	Sw-Mw	
4		4.13	56.6	48.1	2722	3466	58.9	1.19	1.076	1.28	F-M Sandstone	Sw-Mw	Break along existing oxide
5		4.27	27.9	58.7	1638	2085	45.7	2.05	0.960	1.97	F-M Sandstone	Sw-Mw	Break along existing oxide
6		13.41	30.9	45.8	1415	1802	42.4	7.44	0.929	6.91	F-M Sandstone	Sw-Mw	
7		6.70	24.6	25.6	630	802	28.3	8.36	0.774	6.47	F-M Sandstone	Sw-Mw	
8		7.23	19.4	53.5	1038	1321	36.4	5.47	0.866	4.74	F-M Sandstone	Sw-Mw	
9		8.56	20.5	53.8	1103	1404	37.5	6.10	0.878	5.35	F-M Sandstone	Sw-Mw	
10		7.17	24.0	43.9	1054	1341	36.6	5.34	0.869	4.65	F-M Sandstone	Sw-Mw	
11		4.27	14.3	49.3	705	898	30.0	4.76	0.794	3.78	F-M Sandstone	Mw	
12		3.88	13.5	30.2	408	519	22.8	7.47	0.702	5.25	F-M Sandstone	Mw	
13		0.53	19.3	39.2	757	963	31.0	0.55	0.807	0.44	Fine Sandstone	Mw	Break along existing oxide
14		1.87	15.1	20.1	304	386	19.7	4.84	0.657	3.18	Fine Sandstone	Sw-Mw	
15		5.75	17.9	99.7	1785	2272	47.7	2.53	0.979	2.48	Fine Sandstone	Sw	

SAMPLE: 30a

Test No.	Type	P (kN)	D (mm)	W (mm)	A = WD (mm^2)	D_e^2	D_e	I_s	F	$I_{s(50)}$ (MPa)	Lithology	Weathering	Notes
1		12.94	22.0	47.98	1053	1341	36.6	9.65	0.869	8.39	F-M Sandstone	Sw	
2		1.87	16.7	46.7	779	992	31.5	1.89	0.812	1.53	F-M Sandstone	Mw	Break along existing
3		3.01	36.3	56.7	2058	2621	51.2	1.15	1.011	1.16	F-M Sandstone	Mw	Break along existing
4		3.70	29.7	24	713	908	30.1	4.08	0.796	3.25	F-M Sandstone	Mw	Break along existing
5		2.80	16.8	48.4	813	1035	32.2	2.70	0.820	2.22	F-M Sandstone	Mw	Break along existing
6		9.86	18.6	31.5	586	746	27.3	13.22	0.762	10.07	F-M Sandstone	Sw	
7		10.18	23.8	30.5	726	924	30.4	11.01	0.799	8.80	F-M Sandstone	Sw	

E.8 Hurunui River fines index test results and calculations

Fines content results and calculation tables produced from wet sieving and laser size analysis per sample outcrop.

E.8 Hurunui River - fines index testing

23b				
Passing (wet sieve)	**Raw weight (g)**	**Container weight (g)**	**Sample weight (g)**	**Sample fines division (%)**
>4mm	454.5	285	169.5	23.70
>2mm (gravel)	114.4	10.2	104.2	14.57
>1mm (coarse sand)	84.5	10.6	73.9	10.33
Remaining fraction (<1mm)	1643.5	1275.79	367.71	51.41
Total sample weight (g)			715.31	
Matrix (lasersizer)	**Average diameter (µm)**	**Cumulative %**	**Actual %**	**% of total <1mm fraction**
<2 microns (clay)	2	8.1	8.1	4.16
<60 microns (silt)	59.57	50.7	42.6	21.90
<200 microns (fine sand)	199.53	69.5	18.8	9.66
Remaining fraction (medium/coarse sand)		100	30.5	15.68

30a				
Passing (wet sieve)	**Raw weight (g)**	**Container weight (g)**	**Sample weight (g)**	**Sample fines division (%)**
>4mm	52.1	14.1	38	37.34
>2mm (gravel)	28.1	10.6	17.5	17.19
>1mm (coarse sand)	22.9	10.8	12.1	11.89
Remaining fraction (<1mm)	337.79	303.61	34.18	33.58
Total sample weight (g)			101.78	
Matrix (lasersizer)	**Average diameter (µm)**	**Cumulative %**	**Actual %**	**% of total <1mm fraction**
<2 microns (clay)	2	5.9	5.90	1.98
<60 microns (silt)	59.57	48.9	43.00	14.44
<200 microns (fine sand)	199.53	66.1	17.20	5.78
Remaining fraction (medium/coarse sand)		100	33.90	11.38

23b - Clay				
Matrix (lasersizer)	**Average diameter (µm)**	**Cumulative %**	**Actual %**	**% of total sample**
<2 microns (clay)	2	15.2	15.2	15.20
<60 microns (silt)	59.57	70.9	55.7	55.70
<200 microns (fine sand)	199.53	85	14.1	14.10
Remaining fraction (medium/coarse sand)		100	15	15.00

Appendix F: Ashley River Gorge

Results derived from the lineation analysis, raw mapping data, analysis, raw lab testing data and calculations for the Ashley River Gorge study site.

F.1 Ashley River Gorge lineation analysis

Landscape lineation derived from aerial photography and DEM analysis. Note the occurrence of river morphology between the two defined structural zones i.e. the upper, relatively linear LHB meander vs. the downstream LAGB large lopping meanders likely related to rock mass condition.

F.1 Ashley River Gorge - lineation analysis

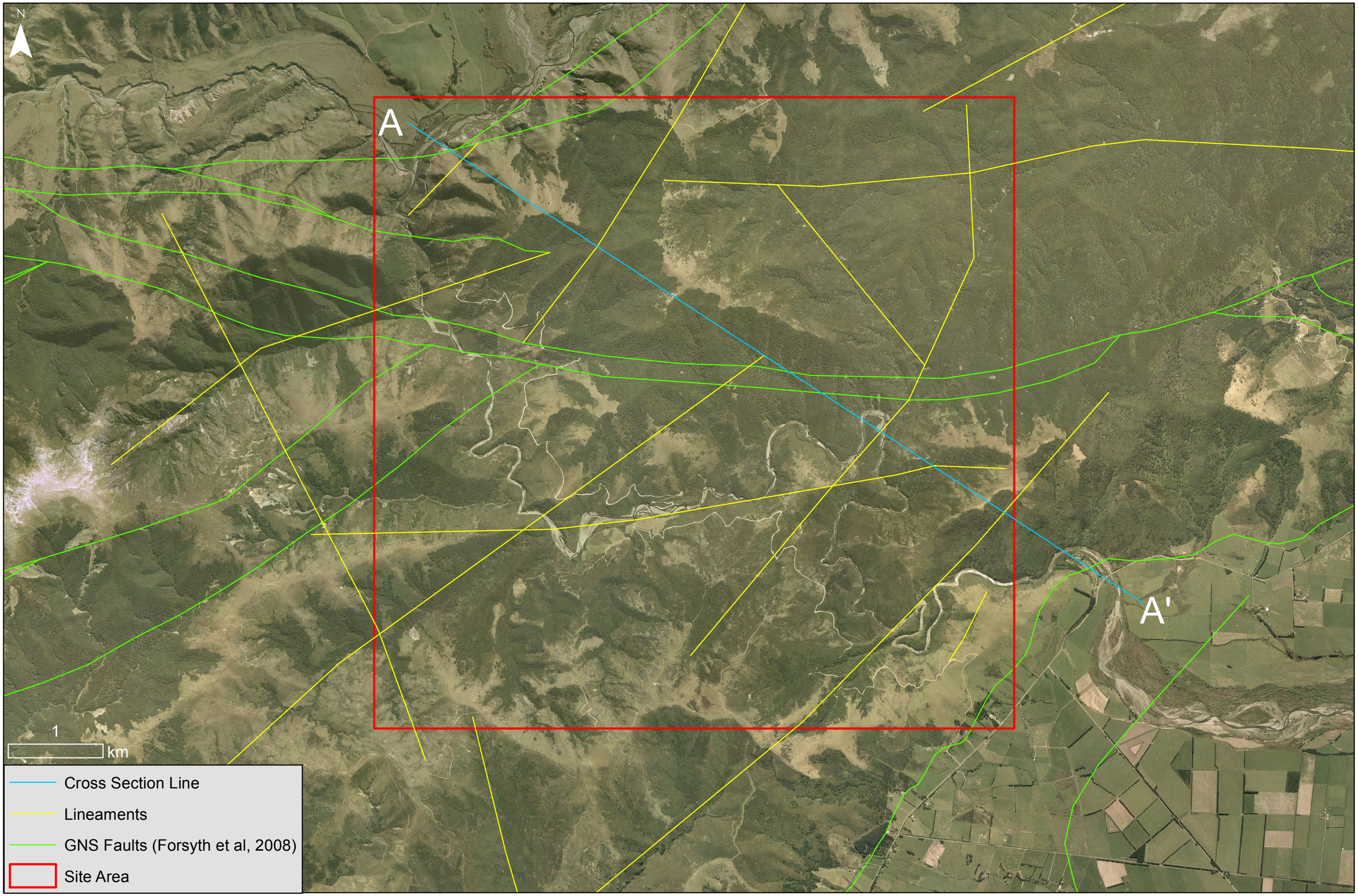

Imagery Source: Canterbury Aerial Photo

F.2 Ashley River Gorge raw mapping data

Mapping per field data sheets (Appendix A). Where data is missing, blanked out or ranges from other sites, information has been unobtainable due to access issues, poor rock/defect conditions, recording prior to the continual modification of the field sheets or previous recording of the defect (i.e. 1 x bedding plane between two lithologies).

F.2.1 Ashley River Gorge - Coherent Rock and bedding

													Waviness			
Outcrop #	Weathering	Colour	Bedding fabric	Bedding structure	Bedding development	Grain size	Rock name	Strength (rock)	Strength (bed)	Dip	Dip direction	Bedding roughness	Interlimb angle (ILA, °)	Wavelength (m)	Degree of fracture	Raw field notes
1a	Hw	L-GY	M	V thick	D	F-M	Sandstone	MS	MS	70	115	NO SURFACE	180	0	FRAG	Heavy quartz infill. This outcrop is more or less on the trace of the Lees Valley Fault
1a	Hw	D-GY	M	V thin	D		Mudstone	WEAK	WEAK				125	0.6	FRAG	
2a	Sw	L-GY	M	V thick	D	F-M	Sandstone	VS	S	34	144	PR	160	6.2	HF	
2a	Hw	D-GY	M	Thin	D		Mudstone	V STIFF	V STIFF				140	0.9	FRAG	
3a	Sw	L-GY	M	Thick	D	F-M	Sandstone	VS	VS	31	159	PR	180	0	HF	
3a	Hw	D-GY	M	Thin	D		Mudstone	VW	VW				150	4.1	FRAG	Slight boudin deforms mudstone shape but not sandstone
4a	Sw	L-GY	M	Thick	WD	F-M	Sandstone	VS	S	72	126	SS	180	0	MF	Same as above, mudstone is still frag and lineated with bedding
4a	Hw	D-GY	M	Thin	WD		Mudstone	VW	VW				130	1.1	FRAG	Boudin developing
5a	Sw	L-GY	M	Thick	D	F-M	Sandstone	S	S	45	116	UR	160	1	HF	
5a	Hw	L-GY	M	V thick	D	F-M	Sandstone	VS	VS	74	128	UR	180	0	FRACT	
5a	Sw	D-GY	M	V Thin	D		Mudstone	VW	VW	64	136		180	0	FRAG	
6a	Sw	L-GY	M	V thick	WD	F-M	Sandstone	VS	VS	52	162	US	180	0	MF	
6a	Hw	D-GY	M	Thin	WD		Mudstone	VW	MS				155	5.6	FRAG	Boudin in thin interbedding sequence
7a	Sw	L-GY	M	V thick	D	F-M	Sandstone	VS	VS	66	185				MF	Rock in V good condition
7a	Hw	D-GY	M	V thin	D		Mudstone	WEAK	VW			SS	160	4.3	FRAG	
7b	Sw	L-GY	M	V thick	WD	F-M	Sandstone	VS	S	79	171	PR	175	1	HF	Thin interbedding here is very altered by quartz fluid flow
7b	Mw	D-GY	M	Thin	WD		Mudstone	VW	VW				115	0.4	FRAG	Boudins enclosing sandstone parcels. There is clear evidence of shearing through notable lineation of material
7b	Hw	L-GY	M	Thin	D		Sandstone	VW	VW				130	0.75	FRAG	
8a	Mw	L-GY	M	V thick	WD	F-M	Sandstone	S	S	86	151		170	0.55	FRAG	GNS says a fault goes through here - no surface but mudstone is relatively fragmented and boudins around sandstone - shape is very wavy
8a	Hw	D-GY	M	Thin	WD		Mudstone	VW	VW			NO SURFACE	105	0.9	FRAG	Clear shearing in boudins
8a	Hw	L-GY	M	Medium	D	F-M	Sandstone	MS	MS	77	157		160	0.75	FRAG	
9a	Sw	L-GRN	M	V thick			Mudstone	S	S	84	239	US	175	1.8	HF	
9a	Sw	BLCK	M	V thick			Mudstone	MS	MS	76	47	PR	180	0	FRAG	
10a	Mw	L-GRN	M	V thick	D		Mudstone	VS		75	161	US	160	2.7	HF	Outcrop somewhat blends together with only one section of rock with evident bedding
10a	Mw	D-RED	M	Thin	D		Mudstone	VS					120	0.9	FRAG	
11a	Mw	L-GY	M	Medium	D	F-M	Sandstone	S	S	79	103	US	175	0.8	MF	D/DD variance is due to folding at an outcrop level
11a	Mw	D-GY	M	V thin	D		Mudstone	MS	MS	88	125		160	1.3	FRAG	Relatively fractured but rock is mainly controlled by bedding defect so is in quite good condition
12a	Hw	L-GY (Ox)	M	V thick	D	F-M	Sandstone	S	S	68	341		180	0	HF	One fault in thick mudstone v thick sandstone, 3 others go through v thick sandstone and v thin mudstone
12a	Hw	D-GY (Ox)	M	V thin	D		Mudstone	WEAK	WEAK				105	5.5	FRAG	
12a	Hw	L-GY (Ox)	M	Medium	D	F-M	Sandstone	MS	MS	NOT		TOO	135	1.2	FRAG	
12a	Hw	D-GY (Ox)	M	Thick	D		Mudstone	WEAK	WEAK	CONSISTENT		WEATHERED	180	0	FRAG	No consistent D/DD for thin mudstone beds
13a	Hw	L-GY	M	V thick	WD	F-M	Sandstone	MS	MS				170	2	FRAG	Crush zone ~4m thick on the hanging wall side of fault. Outside 4m rock is still frag but better quality. Rock on the footwall is similar to rest of the outcrop mostly hf with zones of frag
13a	Hw	BLCK	M	Thick	WD		Mudstone	FIRM	FIRM	66	345		180	0	FRAG	Fracture pattern is too intense to get any good surface for roughness and same above for D/DD
14a	Sw	L-GY	M	Medium	D	F-M	Sandstone	S	S	35	327	PR	170	1.1	MF	
14a	Mw	D-GY	M	V thick	D		Mudstone	WEAK	WEAK	36	317	PR	180	0	FRAG	
15a	Mw	L-GY	M	V thick	WD	F-M	Sandstone	S	S	78	153	PR	160	3.7	HF	Gradational boundaries between sandstone and mudstone, Some boudin along sheared mudstone that is lineated with bedding
15a	Hw	D-GY	M	Thin	WD		Mudstone	WEAK	WEAK	81	121	PR	110	0.45	FRAG	Many faults cutting perpendicular to bedding which offset and cause random patches of mudstone within sandstone
16a	Sw	L-GY	M	Medium	V	F-M	Sandstone	V	VS	85	306	PR	180	0	MF	
16a	Mw	D-GY	M	Thin	V		Mudstone	MS	MS				180	0	FRAG	
17a	Sw	L-GY	M	Thin	WD	Fine	Sandstone	S	S	44	309	PS	140	7.1	HF	Good shape shown on the road - appears 180/0 on outcrop
17a	Sw	D-GY	M	Thin	WD		Mudstone	MS	MS	50	309		180	0	FRAG	
18a	Sw	L-GY	M	Massive		F-M	Sandstone	VS							FRACT	Rock in V good condition
19a	Sw	L-GY	M	Massive		F-M	Sandstone	VS							MF	Demonstrates how across ~20m conditions can change from a fract rock mass controlled by persistent jointing to a more blocky rock mass controlled by <2m joints of MF
20a	Hw	L-GY	M	V thin	VWD	F-M	Sandstone	MS	MS	70	311	PR	140	0.6	FRAG	
20a	Hw	D-GY	M	V thin	VWD		Mudstone	WEAK	WEAK				155	0.9	FRAG	
21a	Sw	L-GY	M	V thick	WD	F-M	Sandstone	VS	VS	70	139	PR	180	0	HF	Gradational boundary between mudstone-fine sandstone-medium sandstone but all definable layers
21a	Mw	D-GY	M	Medium	WD		Mudstone	MS	MS			SS	180	0	FRAG	
21a	Mw	L-GY	M	Thin	WD	Fine	Sandstone	S	S	71	133	US	180	0	FRAG	FRAG but in a better condition than mudstone
22a	Mw	L-GY	M	V thin	VWD	Fine	Sandstone	S	S	61	149	PR	155	1.7	FRAG	
22a	Mw	D-GY	M	V thin	VWD		Mudstone	MS	MS			US	105	1.3	FRAG	Shape = average for the outcrop bedding
23a	Hw	L-GY (Ox)	M	V thick	WD	F-M	Sandstone	VS	S				175	1.5	FRAG	Infill: Silty sandstone, 2cm along with heavy lineation and crush of both mudstone and sandstone
23a	Hw	D-GY (Ox)	M	Medium	WD		Mudstone	MS	MS	56	329	PR	165	0.45	FRAG	
23a	Hw	D-GY (Ox)	M	Thick	WD		Mudstone	MS	MS	35	259				FRAG	
24a	Sw	L-GY	M	V thick	WD	F-M	Sandstone	VS	VS	56	241	PR	160	3	HF	
24a	Mw	D-GY	M	V thin	WD		Mudstone	MS	MS				150	0.8	FRAG	
24a	Mw	L-GY	M	Thin	WD	Fine	Sandstone	S	S				160	0.8	FRAG	
25a	Mw	L-GY	M	Thin	VWD	Fine	Sandstone	S	S	75	109	PR	135	2.7	HF	sandstone is in relatively good condition for thin interbedding
25a	Mw	D-GY	M	Thin	VWD		Mudstone	WEAK	WEAK	67	109		120	0.8	FRAG	
26a	Mw	L-GY	M	V thick	WD	F-M	Sandstone	VS	VS			PR	180	0	HF	Fracturing is average for the whole outcrop - some MF and FRAG away from structures
26a	Mw	D-GY	M	Thin	VWD		Mudstone	WEAK	WEAK	37	271		180	0	FRAG	Many small scale faults cut the thin interbedding offsetting it
26a	Mw	L-GY	M	Thin	VWD	FINE	Sandstone	VS	S	35	265	US	180	0	HF	
27a	Mw	L-GY	M	Massive		F-M	Sandstone	VS							HF	Massive sandstone dissected by heavy shearing which around shears fragments rock - see picture of two intersecting faults and material between
27b	Hw	L-GY	M	Massive		F-M	Sandstone	S							FRAG	
28a	Uw	L-GY	M	Thin	VWD	F-M	Sandstone	VS	VS	83	4	US	170	1.2	MF	Unweathered nature allows the nature of thin interbedding to be observed - shows different bands of fine sandstone to medium sandstone to mudstone
28a	Uw	D-GY	M	Thin	VWD		Mudstone	MS	MS			PS			HF	Not uncommon to see different banding and grain sizes within a bed with no defined bedding plane
28a	Uw	D-GY	M	Thin	VWD	Fine	Sandstone	S	S	85	20	PS	175	1	MF	
29a	Sw	L-GY	M	Thin	D	F-M	Sandstone	VS	VS	31	296	US	120	3.7	MF	Fine sandstone is slightly darker
29a	Sw	L-GY	M	Thin	D	Fine	Sandstone	VS	VS				115	3.6	FRAG	
30a	Sw	L-GY	M	Thin	D	F-M	Sandstone			61	300	US	125	3.1	HF	
30a	Sw	D-GY	M	Thin	D		Mudstone								FRAG	
30a	Sw	L-GY	M	Thin	D	Fine	Sandstone								FRAG	All but the same as 29a thus not described to the same vigour. F-M sandstone beds are not consistent and are boudin by the fine sandstone and mudstone

31a	Sw	L-GY	M	Massive		F-M	Sandstone	VS							FRACT	Marks a change in lithotype. Intense quartz veining small <4mm veins
32a	Sw	L-GY	M	V thick	D	F-M	Sandstone	VS	VS	86	5	PR	180	0	MF	
32a	Sw	L-GY	M	Medium	D	Fine	Sandstone	S	S				180	0	FRAG	Hard to distinguish between fine sandstone and mudstone in field due to weathering and gradational bedding planes
33a	Sw	L-GY	M	V thin	D	F-M	Sandstone	VS	VS	36	265	PR	165	0.2	HF	Could be classed as a massive sandstone but clear breaks along gradational boundaries between sandstone of varying sizes. Intense quartz veining similar to massive sandstone above
33a	Sw	L-GY	M	V thin	D	Fine	Sandstone	VS	VS	45	272				HF	
33b		L-GY	M	V thin	D	F-M	Sandstone	S	S	84	340		135	42	HF	Across the river from 33b is 33a at 45/272 then 20m down a measurement of 49/301 potential structure up the river valley?????
33b	Uw	L-GY	M	V thin	D	Fine	Sandstone	S	S						HF	
34a	Sw	L-GY	M	Thin	WD	F-M	Sandstone	VS	VS	79	338	PS	180	0	MF	
34a	Sw	L-GY	M	Thin	WD	Fine	Sandstone	VS	VS	70	341	PS	160	1	MF	
34a	Sw	D-GY	M	V thin	WD		Mudstone	MS	MS				160	1.2	FRAG	
35a																Exact same as 34a - just marked for lithotype mapping - 75/349
36a	Mw	L-GY	M	V thick	WD	F-M	Sandstone	VS	S	NO SURFACE			160	14	HF	60m cliff. Mix of v thick / medium sandstone with v thin mudstone. Whole cliff is very damaged. No consistent D/DD with mudstone tending to follow the shears in different orientations
36a	Hw	D-GY	M	Thin	WD		Mudstone	S	S				115	4.4	FRAG	5 main faults dissect the cliff and cause heavy FRAG. V thick beds remain relatively intact.
36a	Mw	L-GY	M	Medium	WD	F-M	Sandstone	FIRM	FIRM				145	5.9	FRAG	Note: heavy level of quartz infill around defects (especially shears). Closer to the outcrop hundreds of small scale shears and faults can be observed
37a	Sw	L-GY	M	Thick	VWD	F-M	Sandstone	VS	VS	89	140	PS	180	0	MF	D/DD similar to faulting with moderate infill
37a	Mw	D-GY	M	Thin	VWD		Mudstone	MS	WEAK				180	0	FRAG	
38a	Sw	L-GY	M	V thick	VWD	F-M	Sandstone	VS	VS	86	150	PS	170	2.8	HF	Fault zone with approx 3.5m of shear material - either side of this material is heavily disturbed.
38a	Mw	D-GY	M	V thin	VWD		Mudstone	MS	MS	NO SURFACE			120	1	FRAG	Some thin interbeds with v thick sandstone are fragmented & folded. Note the level of offset & intense grouping of shears around fault zone.
38a	Mw	L-GY	M	Thin	VWD	F-M	Sandstone	VS	S				85	0.7	FRAG	Heavy quartz veining and tight folding is observed
39a	Sw	L-GY	M	Massive		F-M	Sandstone	VS							MF	
40a	Sw	L-GY	M	Massive		F-M	Sandstone	VS							FRACT	
41a	Sw	L-GY	M	V thick	VWD	F-M	Sandstone	VS	VS	68	330	US	180	0	MF	
41a	Sw	D-GY	M	Thin	VWD		Mudstone	S	S				160	1	FRAG	FRAG but has a high strength considering
41a	Sw	L-GY	M	Thin	VWD	F-M	Sandstone	S	S	63	320	PR	155	0.9	FRAG	
42a	Sw	L-GY	M	V thick	WD	F-M	Sandstone	VS	NO SURFACE						MF	
42a	Hw	D-GY	M	V thin	WD		Mudstone	MS							FRAG	
42a	Hw	L-GY	M	Thin	WD	F-M	Sandstone	S							FRAG	
43a	Sw	L-GY	M	V thick	VWD	F-M	Sandstone	VS		CAN'T REACH					HF	
43a	Sw	L-GY	M	Thick	VWD		Sandstone								HF	
43a	Sw	D-GY	M	Thin	VWD		Mudstone						95	1.3	FRAG	Shape is dictated by a fault offset
43b	Sw	L-GY	M	Thin	VWD		Sandstone	CAN'T REACH					150	0.9	HF	
43b	Sw	L-GY	M	V thin	VWD		Sandstone						160	0.2	FRAG	
43b	Sw	D-GY	M	Thin	VWD		Mudstone						160	0.2	FRAG	
44a	Sw	L-GY	M	V thick	WD	F-M	Sandstone	VS	VS	55	179	US	180	0	MF	
44a	Mw	D-GY	M	Thin	WD		Mudstone	MS	MS						HF	
45a	Mw	L-GY	M	V thick	WD	F-M	Sandstone	S	S	CAN'T REACH			170	0.7	FRAG	Heaps of shears - mainly through the thin interbedding but throughout all lithotypes
45a	Hw	D-GY	M	Thin	WD		Mudstone	WEAK	WEAK				155	0.5	FRAG	
45a	Mw	L-GY	M	Thin	WD	F-M	Sandstone	MS	MS				140	1.7	FRAG	
46a	Sw	GRN/RED	M	Massive			Mudstone	VS							HF	Red and green mudstone are merged together with no evidence of bedding - likely the result of faulting. Rock is relatively sheared and heavy quartz infill is common.
47a	Sw	L-GRN	M	V thick	WD		Mudstone	VS	VS	84	138	SR	120	3.5	HF	50a is the last occurrence of green mudstone along the river.
47a	Mw	BLCK	M	Thick	WD		Mudstone	MS	MS	89	287	US			FRAG	mudstone (black) appears in sheared condition lineated with bedding. Bedding shape is not consistent.
48a	Sw	L-GY	M	Thick	D	F-M	Sandstone	VS		66	290		170	2.9	HF	
48a	Mw	D-GY	M	V thin	D		Mudstone	CAN'T REACH							FRAG	
49a	Sw	L-GY	M	Thick	D	F-M	Sandstone	VS	VS	40	310	SR	180	0	MF	Noticeable shearing along mudstone beds and random quartz veining along thick sandstone however not as intense as previously seen
49a	Mw	D-GY	M	V thin	D		Mudstone	MS	MS	87	187	US	175	6	FRAG	
50a	Sw	L-GY	M	Thick	D	F-M	Sandstone	VS	VS			US			MF	
50a	Mw	D-GY	M	V thin	D		Mudstone	WEAK	WEAK	47	227		180	0	FRAG	Two separate bedding directions over 10m of rock
51a	Mw	L-GY	M	V thick	D	F-M	Sandstone	S				PS			FRAG	
51a	Hw	D-GY	M	Thin	D		Mudstone	HARD	HARD			PS	125	0.25	FRAG	Similar character to 41a - continuation??? Same applies with many small scale faults and shears including in thick sandstone with reworked mudstone along shears
51a	Mw	L-GY	M	V thin	D	F-M	Sandstone	MS	MS	75	300	PS	100	0.3	FRAG	
52a	Sw	L-GY	M	Thin	D	F-M	Sandstone	VS	S	86	326	UR	165	2.8	MF	
52a	Mw	D-GY	M	Thin	D		Mudstone	MS	MS				180	0	FRAG	Notable shearing
53a	Sw	L-GY	M	Massive	D	F-M	Sandstone	VS							MF	
54a	Sw	L-GY	M	Thick	D	F-M	Sandstone	VS	VS	74	319	PS	180	0	MF	
54a	Sw	D-GY	M	Thin	D		Mudstone	S	S				165	1.2	FRAG	
54a	Sw	L-GY	M	Medium	D	F-M	Sandstone	VS	VS	79	340	US	165	1	MF	
55a	Mw	L-GY	M	Massive	D	F-M	Sandstone	S							FRAG	Intact non fault rock but fragmented with no major jointing
56a	Sw	L-GY	M	Massive	D	F-M	Sandstone	VS							HF	
57a	Sw	L-GY	M	V thick	D	F-M	Sandstone	VS	VS	79	189	US	160	2.9	MF	Rock is fragmented in some spots - in one spot quartz veining is so intense it looks to have fragmented the rock itself. In other areas of the outcrop no quartz veining is observed
57a	Mw	D-GY	M	Thin	D		Mudstone	WEAK	WEAK				175	2	FRAG	Rock is fragmented in some spots - in one spot quartz veining is so intense it looks to have fragmented the rock itself. In other areas of the outcrop no quartz veining is observed
57a	Sw	L-GY	M	Medium	D	F-M	Sandstone	VS	S				180	0	MF	

F.2.2 Ashley River Gorge - Defect structure

		Orientation										Waviness									
Outcrop #	Defect type	Dip	Dip direction	Spacing (m)	Persistence (m)	Aperture (cm)	Infilling type	Infilling strength	Infill moisture	Infill thickness (mm)	Defect roughness	Interlimb angle (ILA, °)	Wavelength (m)	Ends	End termination	Strength (rebound)	Strength (hammer)	Strength (MPa)	Water	Weathering	Degree of fracture	Raw field notes
1a	Shear	64	120		2.1		Silty sand with some gravel	V stiff	D	5	NO SURFACE	170	1.8	2	C		MS		D	Hw	FRAG	Part of Lees Valley fault trace???
1a	Fault	28	219		2.2							180	0	2	C		MS		D	Hw	FRAG	
2a	Joint	48	328	1	4.1		Stain			<1mm	US	180	0	1	O		VS		D	Sw	MF	
2a	Joint	54	285	0.7	3.6						US	180	0	1	O		VS		D	Sw	HF	
2a	Joint	30	335	2.3	11.1						PR	175	3	2	C		VS		D	Sw	MF	
2a	Joint	67	31	0.3	4.7	0.2					PR	180	0	2	C		VS		D	Sw	MF	
2a	Joint	36	338	0.65	6						UR	180	0	2	C		VS		D	Sw	MF	
2a	Shear	55	213		18		Sandy silt	Stiff	D	30	US	175	8	2	C		S		D	Mw	HF	
2a	Shear	NO SURFACE			5.9		Sandy silt with some gravel	Stiff	D	100		120	2.9	2	C		MS		D	Hw	FRAG	Note: includes all frag rock in the shear
2a	Shear				3.8		Sandy silt with some gravel	Stiff	D	200		105	1.1	1	D		MS		D	Hw	FRAG	Shears bound a block, boudin almost, where the block is more frag than surrounding rock. Surfaces too frag for surface conditions
2a	Shear	59	15		19		Sandy silt with some gravel	Stiff	D	160		140	11.5	2	C		MS		D	Hw	FRAG	
4a	Joint	35	281	0.3	2.9						PS	180	0	2	C		S		D	Sw	MF	
5a	Shear	62	175		3.4		Silt with some Sand	Stiff	Moist	220	PS	180	0	2	C		VS		D	Sw	HF	
5a	Shear	SAME AS SHEAR ABOVE					Clay	Firm	Moist	15	SAME AS SHEAR ABOVE - MADE FOR DIFFERENT INFILL											Shear has a small 2cm D-GY clay seam before bigger 20cm silt shear fabric - shear fabric has heavy quartz veining
5a	Joint	34	161	1.2	4.3						SR	165	2	2	C		VS		D	Sw	MF	
6a	Joint	74	221	1.2	2.9						SR	175	0.4	2	C		S		D	Sw	MF	
6a	Joint	28	218	0.4	2						PS	180	0	1	O		VS		D	Sw	MF	
6a	Joint	21	112	1.1	12						US	180	0	2	C		VS		D	Sw	MF	Rock is blocky in appearance but in good quality - NOTE: despite blockiness there are not many joints >2m to measure
6a	Fault	56	30		4						PS	110	1.1	1	R		VS		D	Sw	MF	Notable offset of a mudstone bed with a random parcel of mudstone observed within the sandstone
6a	Shear	71	115		4.6		Sandy silt	V stiff	D	25	US	160	1.7	2	C		VS		D	Sw	HF	
6a	Shear	89	1		3.3		Silty sandy gravel	VW	D	190	US	180	0	1	O		VS		D	Sw	MF	
7a	Joint	24	262	0.7	3						UR	160	2.9	1	R		VS		D	Sw	MF	Random parcels of mudstone and shears with lineated mudstone in other orientations away from bedding
7a	Joint	70	278	0.6	4.1						US	180	0	2	C		VS		D	Sw	MF	Shears concentrated around thin mudstone beds - i.e. No cross shearing linking up bedding in thick sandstone
7a	Joint	78	151	0.48	4.1		Stain			<1	PR	180	0	2	C		VS		D	Sw	MF	Rock is dominated by systematic jointing
7a	Joint	69	40	0.85	10.3		Stain			<1	UR	170	4	2	C		VS		D	Sw	MF	
7a	Shear	43	206		9.3		Crush rock	VW	D	100		155	2.7	1	D		MS		D	Sw	FRAG	Heavy quartz infill 20-30cm around shear
7a	Shear	71	175		2		Lineated mudstone	VW	D	8	PR	135	2.9	2	C		S		D	Mw	HF	
7a	Shear	66	185		8.1		Lineated mudstone	VW	D	30	SS	160	4.3	2	C		VS		D	Sw	HF	
7b	Joint	87	127	0.2	4.4						PR	170	3	2	C		VS		D	Sw	HF	
7b	Shear	28	229		19		Sandy silt	V stiff	D	10	UR	155	3.6	1	D		VS		D	Sw	HF	
7b	Shear	48	228		4.7		Crush quartz rocks	VW	D	240	PR	165	3	2	C		S		D	Sw	HF	Heavy quartz veining in infill
7b	Shear	88	333		4.4		Silt with some sand and gravel	Hard	D	40	PR	170	1.6	2	C		S		D	Mw	HF	
7b	Shear	64	305		4.3		Sandy silt with minor gravel	V stiff	D	22	UR	180	0	2	C		S		D	Mw	FRAG	
7b	Shear	86	319		4.6		Silt with some sand	Stiff	Moist	110	US	170	2	2	C		MS		D	Mw	FRAG	
7b	Fault	15	41		6.8	1.2					US	165	4	2	C		VS		D	Sw	HF	Notable offset
9a	Cleavage	76	47	0.001	2						PR	180	0	2	C		MS		D	Sw	FRAG	Platy mudstone cleavage present - In better condition than other mudstone observed
9a	Cleavage	84	239	0.05	3.2						US	175	1.8	2	C		S		D	Sw	HF	Quartz veining is observed in both lithologies although is v thin ~1mm and is restricted to cleavage planes
9a	Joint	56	296	0.45	3.2						US	175	3	2	C		S		D	Sw	HF	
10a	Joint	69	6	0.25	2.7						US	175	1	2	C		S		D	Mw	HF	
10a	Fault	37	135		9.5						PR	130	1.8	2	C		S		D	Mw	HF	
11a	Joint	58	178	0.55	7.3		Silty sand	Firm	D	3	US	170	2.8	2	C		VS		D	Mw	MF	
12a	Joint	50	290	0.3	2.9		Stain			<1	US	170	1.3	2	C		S		D	Hw	HF	
12a	Joint	54	330	1	3.4		Quartz		D	1	UR	180	0	1	R		MS		D	Hw	FRAG	
12a	Fault	CAN'T REACH			6.5							160	3.2	2	C		MS		D	Hw	FRAG	
12a	Fault	36	205		8						PR	175	3	2	C		MS		D	Hw	FRAG	
12a	Fault	76	60		4.5		Sandy silt	Firm	D	12	PR	180	0	1	O		S		D	Hw	HF	
12a	Shear	31	201		4		Crush rock	MS	D	250	PR	155	2.8	1	O		MS		D	Hw	FRAG	
13a	Rock here is similar to 12a (same spatial proximity) but recorded due to the soft breccia like mudstone where it is likely a fault runs																					
15a	Fault	31	10		6.7		Silty sand	V stiff	D	9	US	170	5	2	C		S		D	Mw	HF	
15a	Fault	30	1		7.1		Silty sand	V stiff	D	7	PR	170	7	2	C		S		D	Mw	HF	This defect cuts the bottom fault into two with an offset around 30cm
15a	Shear	55	147		5.4		Silty sand	Hard	D	8	PR	180	0	2	C		MS		D	Mw	FRAG	
15a	Fault	62	160		2		Silty sandy gravel	Hard	D	28	US	180	0	2	C		MS		D	Mw	FRAG	
17a	Joint	88	236	1.4	2						SR	180	0	2	C		S		D	Sw	FRAG	
17a	Joint	74	57	0.25	2						PS	180	0	2	C		S		D	Sw	FRAG	Many small scale <2m faults/shears/joints cut the rock, mudstone is in good overall frag condition
17a	Joint	65	225	0.45	2						PS	180	0	2	C		S		D	Mw	FRAG	NOTE: Defects are relatively straight however rock mass still heavily controlled by fragmented mudstone
17a	Fault	86	64		3.3		Sandy silt	Firm	D	6	PR	180	0	2	C		S		D	Mw	FRAG	
18a	Joint	79	225	0.3	6.1						PR	180	0	2	C		VS		D	Sw	FRACT	
19a	Joint	68	20	0.4	2		Stain			<1	US	180	0	2	C		VS		D	Sw	MF	
19a	Joint	13	182	0.95	5.5						US	155	4.2	2	C		VS		D	Sw	MF	
19a	Shear	23	99		5.9		Crush rock	MS	D	23	PR	170	4.5	2	C		S		D	Sw	HF	
21a	Shear	17	310		6.9		Sandy silt	Firm	D	11	PS	170	5	2	C		S		D	Sw	MF	Note: Moderate fracturing around major joints, away from this we see a HF rock mass
21a	Joint	46	338	1.4	2.8						PS	180	0	1	R		VS		D	Mw	HF	
22a	Fault	NO SURFACE			3							175	1	1	R		S		D	Mw	FRAG	Offset thin interbedding by up to 10cm. Surface too weathered for roughness
22a	Fault	29	46		15.3						PR	165	11	2	C		S		D	Mw	FRAG	
22a	Fault	38	123		2.5						UR	180	0	1	R		S		D	Mw	FRAG	
23a	Joint	79	277	0.35	4.1						US	165	0.9	2	C		S		D	Mw	FRAG	
23a	Joint	46	340	0.5	3		Too weathered to see infill				US	180	0	2	C		VS		D	Mw	MF	
23a	Joint	41	350	0.6	2.5						US	175	2.5	1	O		S		D	Mw	FRAG	
23a	Joint	33	13	0.35	2.2						UR	175	1.7	2	C		VS		D	Mw	HF	
25a	Fault	NO SURFACE			4.2		Crush rock	VW	D	27	NO SURFACE	180	0	2	C		S		D	Hw	FRAG	
25a	Fault				4.3		Silty sand	Firm	D	7		170	2.8	2	C		VW		D	Hw	FRAG	Note: Many small scale faults cut thin interbedding by a few cm that are <2m
25a	Fault	72	178		4		Silt with some sand	Stiff	D	29	PS	145	1.6	2	C		MS		D	Hw	FRAG	Around all faults here a region in excess of 20cm is completely fragmented and lineated parallel with movement.

25a	Fault	75	161		4.7						US	135	1.2	2	C		MS		D	Hw	FRAG	FRAG is of lesser extent than others
26a	Joint	72	36	0.25	5.1		Stain			<1	US	160	3.3	2	C		VS		D	Sw	MF	Waviness changes D/DD
26a	Joint	42	252	0.23	2.7		Stain			<1	PR	165	2	1	D		VS		D	Sw	MF	
26a	Shear	87	205		5.2		Silt with minor sand	Firm	D	9	UR	170	0.55	2	C		MS		D	Mw	FRAG	40cm of crush rock along shear beside infill
26a	Fault	77	51		5.4						US	155	2.1	2	C		MS		D	Mw	FRAG	
26a	Shear	58	231		2.1		Silt	Firm	D	3	UR	180	0	1	O		VS		D	Mw	HF	
26a	Shear	59	349		2.5		Sandy silt	Firm	D	8	PR	165	1	1	O		S		D	Mw	FRAG	
26a	Shear	69	357		2.2		Silt minor sand and clay	Firm	D	21	PS	175	2	1	O		S		D	Mw	FRAG	
27a	Shear	76	147		12.2		Sand some silt	V stiff	D	38	US	165	9	2	C		S		D	Mw	HF	Note: More quartz infilling observed in 27a and 27b than observed at other outcrop localities
27a	Shear	75	144		10.8		Sandy silt	V stiff	D	14	US	125	5.5	1	D		S		D	Mw	HF	27a & 27b faults appear to orientate in a similar direction to potential fault scarp across the valley.
27a	Fault	51	327		4.2		Crush rock	Hard	D	19	UR	160	1.1	1	R		VS		D	Mw	HF	Outcrop has a higher % of shearing, increased quartz veining and fracture
27b	Shear	CAN'T REACH			3.8		CAN'T REACH					175	3	2	C		MS		D	Hw	FRAG	This shear is a continuation of the first 27a shear - discount for analysis
27b	Shear	74	52		3.1		Sand with some silt and gravel	Hard	D	210	US	180	0	1	R		S		D	Hw	FRAG	Heavy crush zone
27b	Shear	52	63		6.3		Sandy silt	Firm	D	60	PR	180	0	2	C		S		D	Hw	FRAG	Shear material has quartz veining inside
27b	Shear	20	52		5.7						U slick	175	2.2	1	R		MS		D	Hw	FRAG	
27b	Shear	50	294		2.9		Silt with a trace of clay	Firm	D	19	PR	160	2.5	1	O		S		D	Hw	FRAG	Shears have intact clasts within the shear matrix - only small amounts as matrix flows around rock in movement as the clast potentially rotates
28a	Fault	CAN'T REACH			3.8		CAN'T REACH					170	3.8	2	C		VS		D	Uw	MF	mudstone is straighter and intact - incipient fracturing still exists but are tightly closed giving mudstone a HF description.
28a	Joint	32	127	1.3	3.1						US	140	1.6	1	D		VS		D	Uw	HF	The mudstone is also a lot more indurated as a result
29a	Fault	71	85		3.4						US	175	0.3	2	C		VS		D	Sw	MF	Bedding doesn't allow for rock mass to be controlled systematically
29a	Fault	51	90		2.5						US	180	0	1	R		VS		D	Sw	FRAG	
36a	Fault	NO SURFACE			14		NO SURFACE					180	0	1	O				D	Mw	FRAG	
36a	Fault	CAN'T REACH			70		Cannot reach too high					155	50	2	C				D	Mw	FRAG	
36a	Fault	86	124		30		Lineated mudstone	Soft	Moist	70	NO SURFACE	180	0	1	D		N/A		D	Mw	FRAG	Roughness - too fractured and weak. Strength - some rock too high to reach others without a surface.
36a	Fault	CAN'T REACH			42		CAN'T REACH					180	0	1	D				D	Mw	HF	
36a	Fault	70	129		6.5		Silty sand	Firm	Moist	9	NO SURFACE	180	0	1	R				D	Mw	HF	
38a	Fault (main)	80	311		2		Sandy silt with some gravel	V stiff	D	1000		180	0	2	C				D	Hw	FRAG	Infill has silty sandstone between lineated clasts of rock
39a	Joint	40	181	0.4	3.5						US	180	0	2	C		VS		D	Sw	MF	
39a	Joint	52	205	1.8	3.8						US	180	0	2	C		VS		D	Sw	MF	
39a	Joint			1.7	2							180	0	2	C		VS		D	Sw	MF	
40a	Joint	CAN'T REACH		2.2	4.9						CAN'T	180	0	2	C		VS		D	Sw	FRACT	
40a	Joint			2.5	4.5						REACH	180	0	2	C		VS		D	Sw	FRACT	
40a	Joint			1	6.9							155	2.7	2	C		VS		D	Sw	FRACT	
42a	Fault	61	86		17		Sandy silt with some reworked mudstone	VW	D	250	PR	175	9	2	C		S		D	Sw	HF	
42a	Note: Major fault comes through bounding intact v thick sand to thin interbeds. The fault does all the damage to the thin interbedding causing distortion and waviness. The rock is very fragmented with 20cm infill and 3.5m of fragmented damage whose bedding is only recognisable in small discontinuous lumps that are very sheared and orientated in a similar orientation to the fault.																					
43a	Joint			0.65	3.9							180	0	2	C				D	Sw	HF	
43a	Joint			0.75	4.6							175	3	2	C				D	Sw	HF	
43a	Joint	CAN'T REACH		0.2	4		CAN'T REACH					180	0	2	C		CAN'T		D	Sw	HF	Main joint set controlling outcrop rock mass
43a	Joint			0.35	2.9							180	0	2	C		REACH		D	Sw	HF	
43a	Fault				4.6							170	0.8	2	C				D	Sw	HF	
43b	Fault				4.6							170	0.8	2	C				D	Sw	FRAG	Note: fault is same as above that goes through A & B
44a	Joint	86	39	0.65	3.4						US	180	0	1	R		VS		D	Sw	FRACT	
44a	Joint	80	305	2.3	2		Quartz			<1	US	180	0	1	R		VS		D	Sw	FRACT	Very thin coat of quartz
44a	Joint	56	341	0.8	2		Quartz			<1	PR	180	0	2	C		VS		D	Sw	FRACT	
44a	Joint	80	53	1.2	4.5						US	175	2.2	2	C		VS		D	Sw	MF	
45a	Shear				3.1							160	1.1	2	C		MS		D	Mw	FRAG	1 shear runs through thin - rest run through v thick sandstone
45a	Shear	CAN'T REACH			2.8		CAN'T REACH					170	0.8	2	C		S		D	Mw	FRAG	
45a	Shear				4.3							135	4	2	C		S		D	Mw	FRAG	
45a	Shear (main)	54	255		2.8							180	0	2	C		VW		D	Mw	FRAG	Looks to follow the thin interbedding. Example of shear infill with 80cm crush around it concentrated to one side of the shear
45a	Shear	36	225		3.2		Silty clay	V stiff	D	8mm	PR	180	0	2	C		S		D	Mw	FRAG	
46a	Shear	80	330		2		Silt with some sand	V stiff	D	70	PR	170	1.3	2	C		VS		D	Sw	HF	No infill but rock has a shear system similar to jointing
46a	Joint	21	251	2.4	6						US	180	0	2	C		VS		D	Sw	MF	
46a	Joint	89	5	0.55	3.7						PR	175	2.5	2	C		VS		D	Sw	HF	
46a	Joint	51	210	1.1	4.1						US	180	0	2	C		VS		D	Sw	MF	
47a	Joint	21	48	1	6.5						US	165	7	2	C		VS		D	Sw	HF	Green bed beside mudstone is completely quartz infilled along ALL small incipient fractures
47a	Joint	44	338	2.4	7.5						UR	180	0	2	C		VS		D	Sw	HF	
48a	Fault				19							180	0	2	C		VS		D	Sw	HF	
48a	Fault	CAN'T REACH			21		CAN'T REACH					180	0	2	C		VS		D	Sw	HF	
48a	Fault				19							165	8	2	C		VS		D	Sw	HF	
49a	Joint	42	14	1.3	4.9		Quartz			<1	US	180	0	2	C		VS		D	Sw	MF	
51a	Fault (main)	62	275		4.2		Silty clay	Firm	Moist	9	PS	180	0	2	C		VW		Moist	Hw	FRAG	
52a	Joint	34	124	0.9	7						PR	180	0	2	C		VS		D	Sw	MF	
52a	Joint	85	121	0.55	3.8						PR	175	1.7	2	C		VS		D	Sw	MF	
52a	Joint	54	205	0.4	2						US	180	0	1	R		VS		D	Sw	MF	
53a	Joint	CAN'T REACH		2.1	11		CAN'T REACH					165	9.5	2	C		VS		D	Sw	MF	
53a	Joint			2	3.8							180	0	1	D		VS		D	Sw	MF	
54a	Joint	32	155	0.9	5						PS	180	0	2	C		VS		D	Sw	MF	
56a	Joint	23	308	2.3	4.8							180	0	2	C		VS		D	Sw	HF	Jointing creates a boundary from the better HF rock away from the FRAG rock
56a	Joint	35	355	1.2	3.5						CAN'T REACH	180	0	1	R		VS		D	Sw	HF	Discrete jointing can be seen behind the incipient fractured rock mass
56a	Joint	71	44	2	4.3							170	2.5	2	C		VS		D	Sw	HF	
57a	Joint	54	45	0.65	4.1	0.6					UR	170	2.8	2	C		VS		D	Sw	MF	
57a	Joint	58	321	0.4	2.9						PR	170	2.5	2	C		VS		D	Sw	MF	

F.2.3 Ashley River Gorge - Soil descriptions of infill

				Strength							
Outcrop #	Fraction (name)	Colour	Structure	NZGS	PSM Non-cohs	Moisture	Grading	Sorting	Plasticity*	Weathering	Raw field notes
1a	Silty sand with some gravel		HOMO	V stiff	Loose	D				Hw	
2a	Sandy silt		HOMO	Stiff	Loose	D				Hw	
2a	Sandy silt with some gravel		HOMO	Stiff	Loose	D				Hw	
2a	Sandy silt with some gravel		HOMO	Stiff	Loose	D				Hw	
2a	Sandy silt with some gravel		HOMO	Stiff	Loose	D				Hw	
5a	Silt with some Sand		HOMO	Stiff	Loose	Moist				Sw	
5a	Clay		HOMO	Firm	Loose	Moist			SP	Sw	
6a	Sandy silt		HOMO	V stiff	Loose	D				Sw	
6a	Silty sandy gravel		HOMO	VW	Loose	D				Mw	
7a	Crush rock		HOMO	VW	Loose	D				Mw	
7b	Sandy silt		HOMO	V stiff	Loose	D				Mw	
7b	Crush quartz rocks		HOMO	VW	Loose	D				Mw	
7b	Silt with some sand and gravel		HOMO	Hard	Loose	D				Mw	
7b	Sandy silt with minor gravel		HOMO	V stiff	Loose	D				Mw	
7b	Silt with some sand		HOMO	Stiff	Loose	Moist				Mw	
11a	Silty sand		HOMO	Firm	Loose	D				Mw	
12a	Sandy silt		HOMO	Firm	Loose	D				Hw	
12a	Crush rock		HOMO	MS	Loose	D				Hw	
15a	Silty sand		HOMO	V stiff	Loose	D				Mw	
15a	Silty sand		HOMO	V stiff	Loose	D				Mw	
15a	Silty sand		HOMO	Hard	Loose	D				Mw	
15a	Silty sandy gravel		HOMO	Hard	Loose	D				Mw	
17a	Sandy silt		HOMO	Firm	Loose	D				Mw	
19a	Crush rock		HOMO	MS	Loose	D				Sw	
21a	Sandy silt		HOMO	Firm	Loose	D				Hw	
25a	Crush rock		HOMO	VW	Loose	D				Hw	
25a	Silty sand		HOMO	Firm	Loose	D				Hw	
25a	Silt with some sand		HOMO	Stiff	Loose	D				Hw	
26a	Silt with minor sand		HOMO	Firm	Loose	D				Mw	
26a	Silt		HOMO	Firm	Loose	D				Mw	
26a	Sandy silt		HOMO	Firm	Loose	D				Mw	
26a	Silt minor sand and clay		HOMO	Firm	Loose	D			SP	Mw	
27a	Sand some silt		HOMO	V stiff	Loose	D				Hw	
27a	Sandy silt		HOMO	V stiff	Loose	D				Hw	
27a	Crush rock		HOMO	Hard	Loose	D				Hw	
27b	Sand with some silt and gravel		HOMO	Hard	Loose	D				Hw	
27b	Sandy silt		HOMO	Firm	Loose	D				Hw	
27b	Silt with a trace of clay		HOMO	Firm	Loose	D			SP	Hw	
36a	Silty sand		HOMO	Firm	Loose	Moist				Mw	
38a	Sandy silt with some gravel		HOMO	V stiff	Loose	D				Mw	
45a	Silty clay	Black	HOMO	V stiff	Loose	D			MP	Sw	
46a	Silt with some sand		HOMO	V stiff	Loose	D				Sw	
51a	Silty clay	Black	HOMO	Firm	Loose	Moist			MP	Sw	

F.2.4 Ashley River Gorge - Breccia fabric descriptions

Outcrop	Fabric support	Fabric arrangment	Fabric (random - lineated?)	% Clast >1mm to matrix	% of Clasts >2mm	Matrix vs. cement	Rotation angle	Rounding	Clast size	Alteration	Grain size*	Other
1a	Clast	Crackle	Random			Matrix		Angular				
13a	Clast	Crackle	Lineated			Matrix		Angular				
38a	Clast	Choatic	Random			Matrix		Angular				
42a	Matrix	Mosaic	Random			Matrix		Angular				
45a	Matrix	Choatic	Random			Matrix		Angular				
51a	Matrix	Choatic	Random			Matrix		Angular				

F.3 Bedding thickness portions with joint and fault occurrence

Bedding thickness and nature across the study site with joints and faults/shears presented as percentage occurrence respective of bedding thickness.

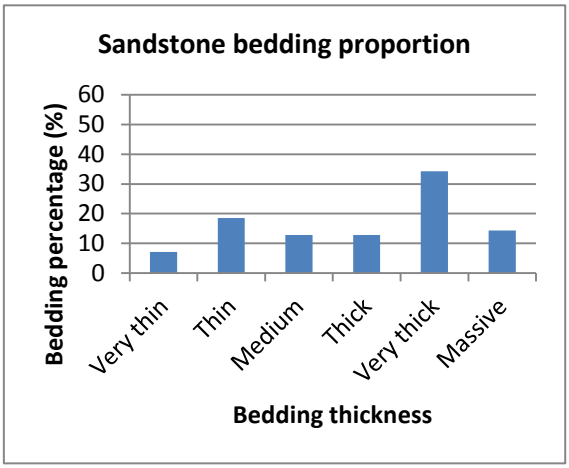

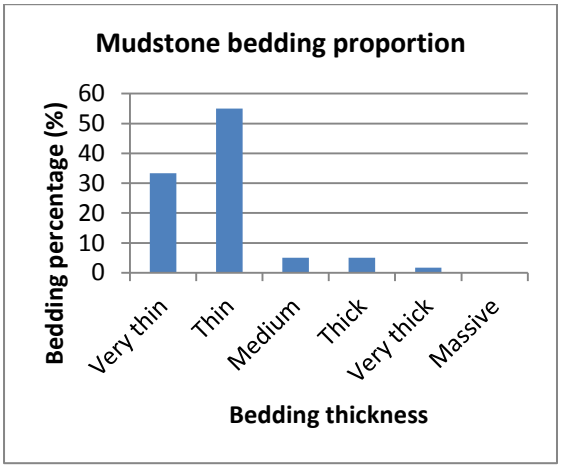

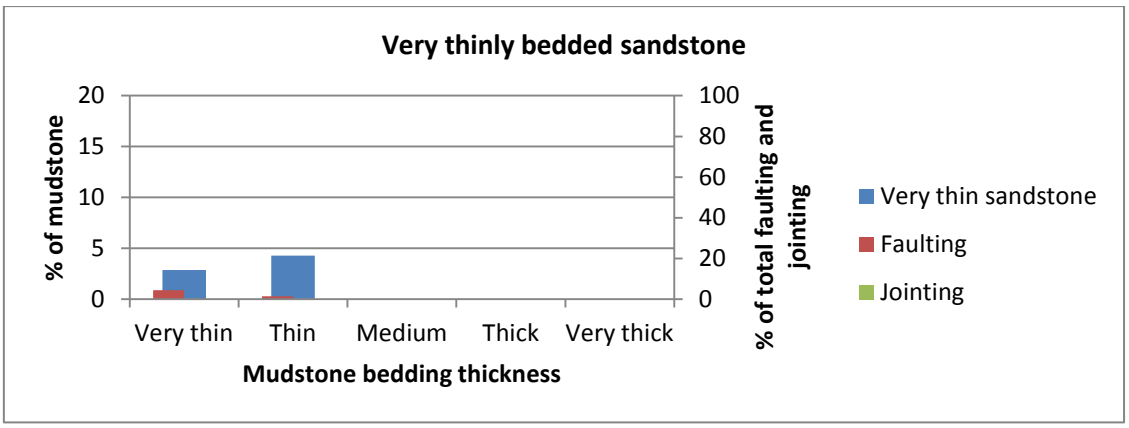

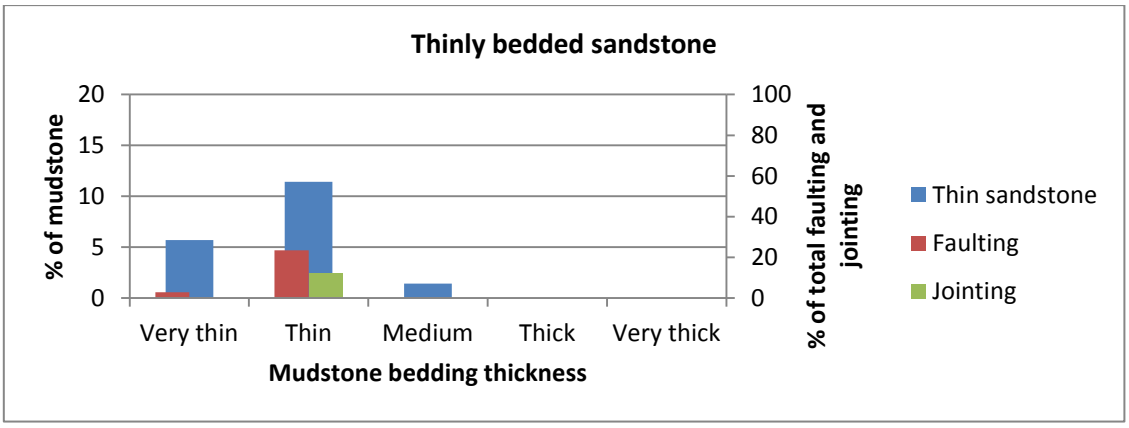

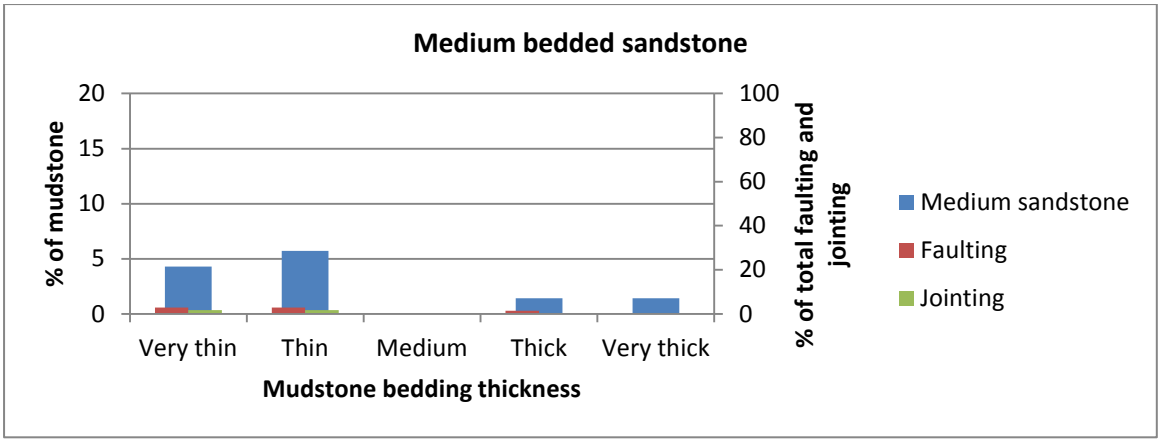
Medium bedded sandstone
% of mudstone
20
15
10
5
0
100
80
60
40
20
0
% of total faulting and jointing
Very thin
Thin
Medium
Thick
Very thick
Mudstone bedding thickness
Medium sandstone
Faulting
Jointing

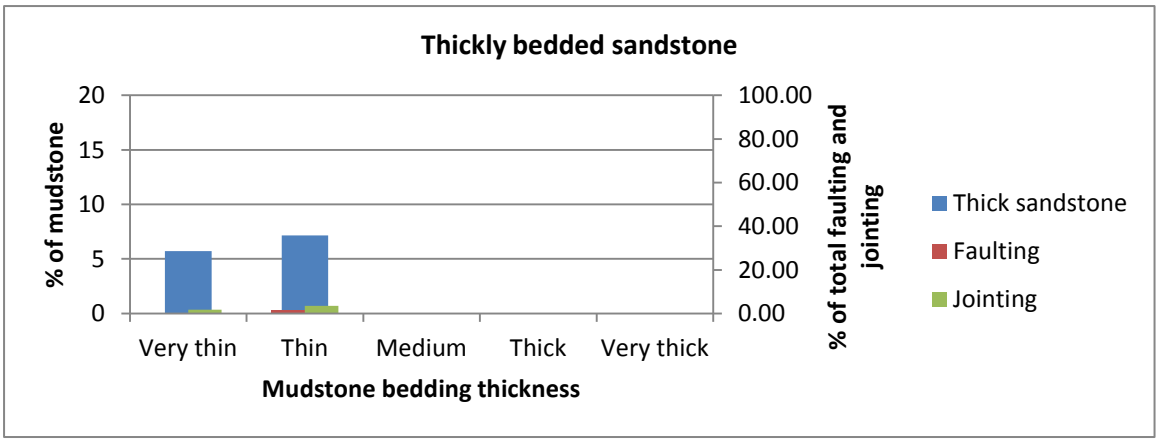
Thickly bedded sandstone
% of mudstone
20
15
10
5
0
100.00
80.00
60.00
40.00
20.00
0.00
% of total faulting and jointing
Very thin
Thin
Medium
Thick
Very thick
Mudstone bedding thickness
Thick sandstone
Faulting
Jointing

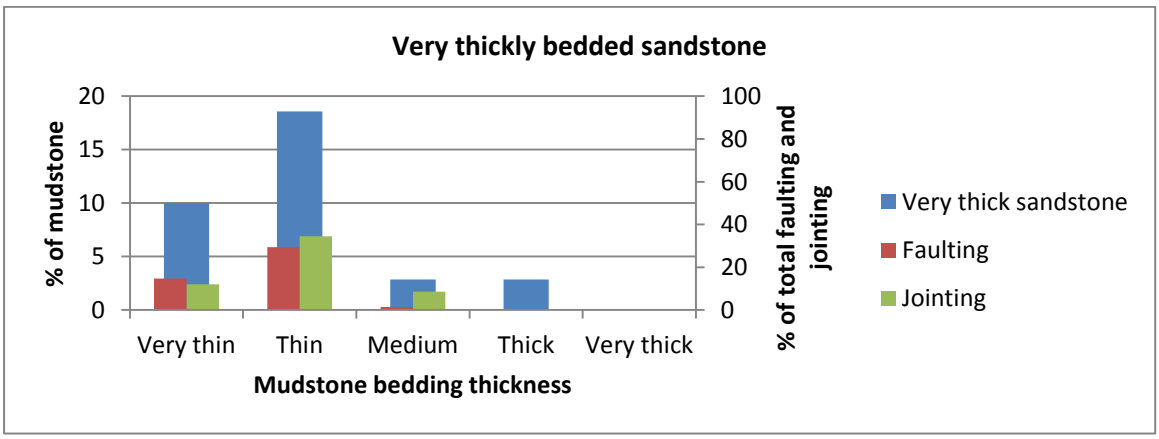
Very thickly bedded sandstone
% of mudstone
20
15
10
5
0
100
80
60
40
20
0
% of total faulting and jointing
Very thin
Thin
Medium
Thick
Very thick
Mudstone bedding thickness
Very thick sandstone
Faulting
Jointing

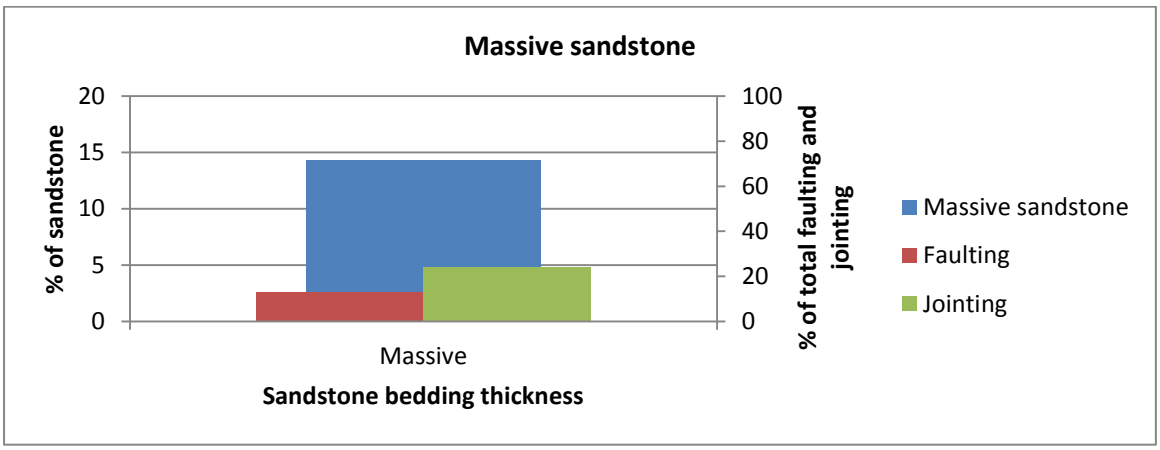
Massive sandstone
% of sandstone
20
15
10
5
0
100
80
60
40
20
0
% of total faulting and jointing
Massive
Sandstone bedding thickness
Massive sandstone
Faulting
Jointing

F.4 Ashley River Gorge steronet analysis

Steronet dip/dip direction analysis of bedding, jointing and faults/shears respectively.

Bedding poles

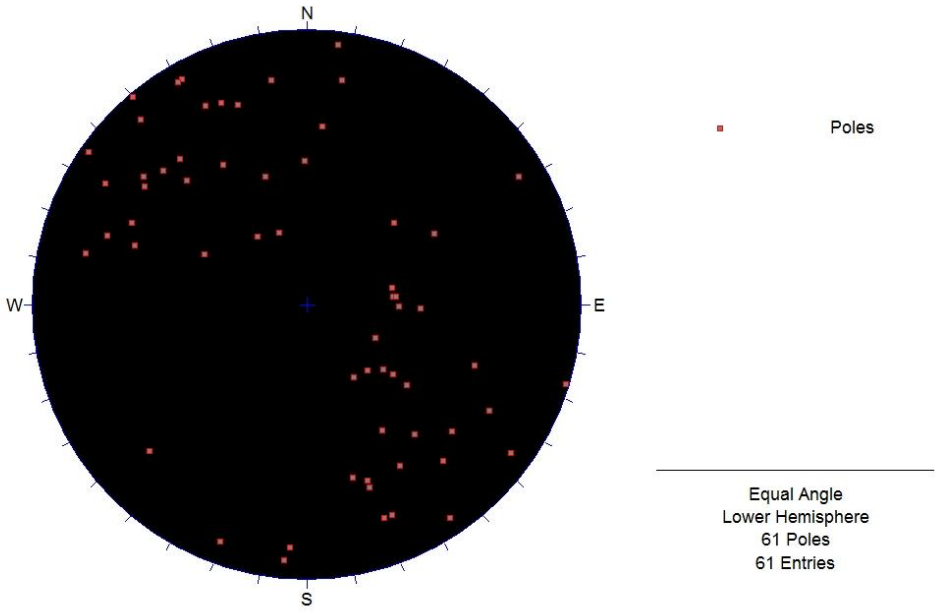

Bedding cluster

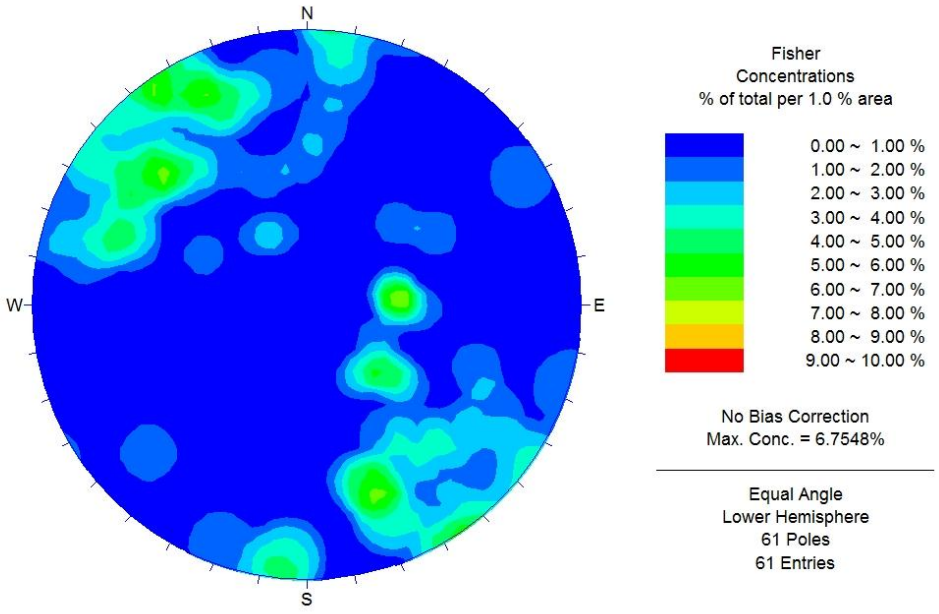

Jointing poles

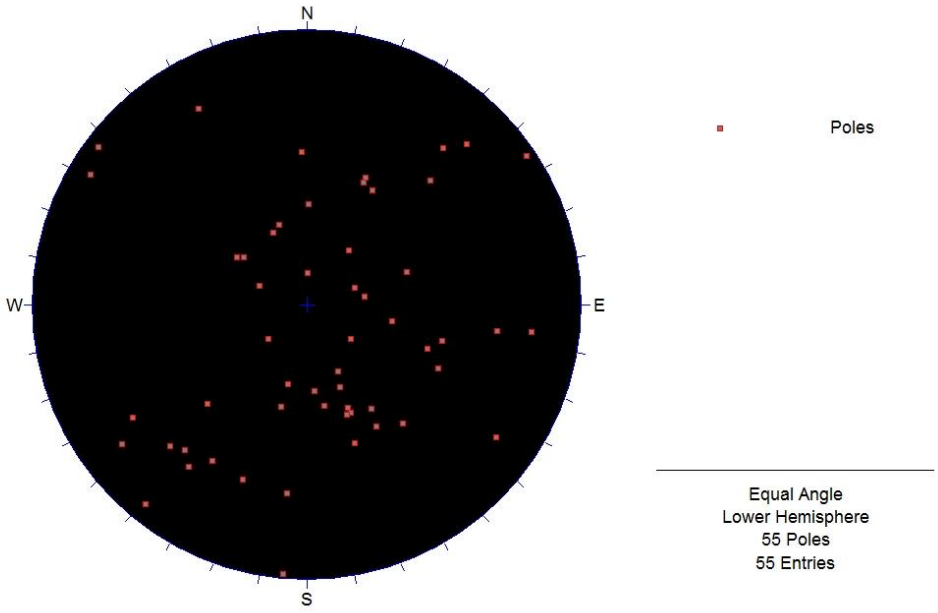

Jointing cluster

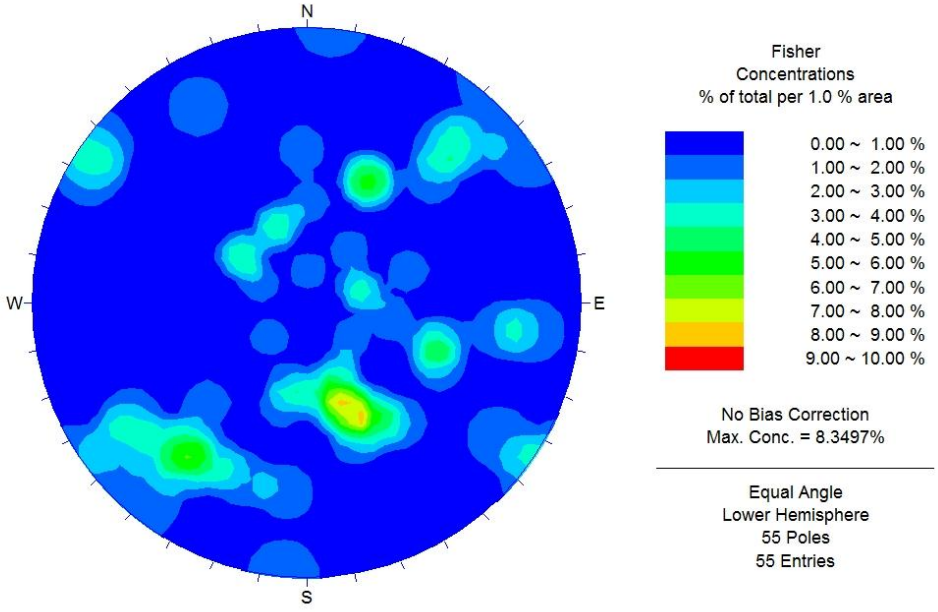

Faulting/shearing poles

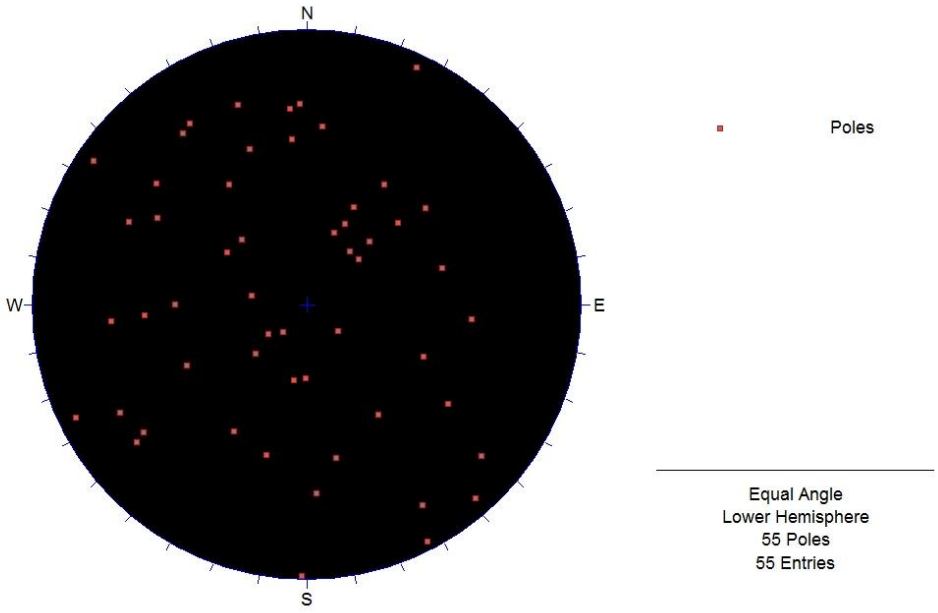

Faulting/shearing cluster

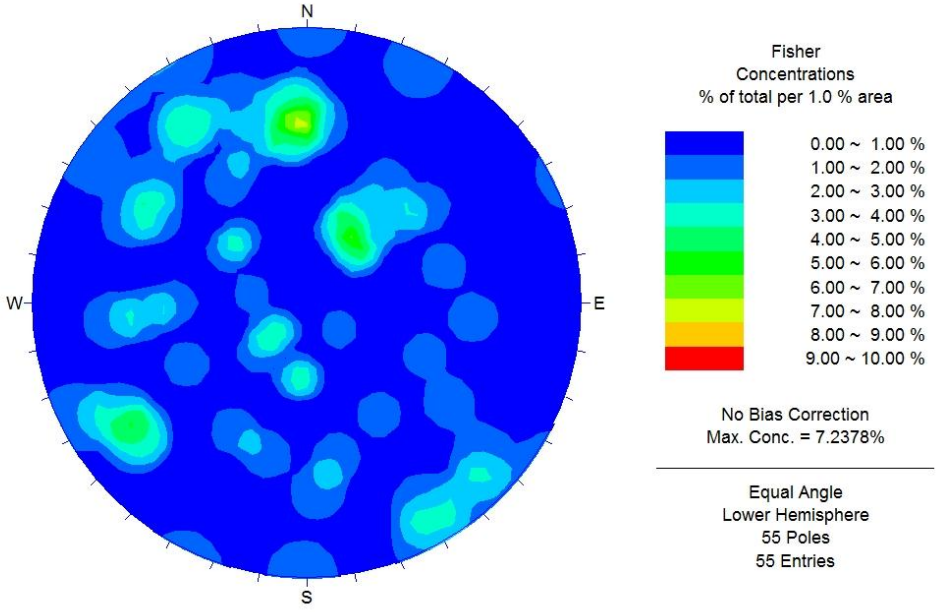

F.5 Ashley River Gorge BTS raw results and calculations

Brazilian Tensile Strength testing respective of sampled outcrop.

F.5 Ashley River Gorge - Brazilian Tensile Strength testing

Outcrop	Load (Kn)	Load (N)	Diameter (mm)	Thickness (mm)	MPa	Lithology	Clean?	Failure mode (Szwedzicki, 2007)	Failure time (sec)	Notes
5a	21.8	21800	49.26	24.14	11.66	F-M sandstone	Clean	Simple extension	50.9	
5a	28.8	28800	49.16	24.44	15.25	F-M sandstone	Clean	Simple extension	77	Discontinuities at 45° to load
4a	25	25000	49.34	25.08	12.85	F-M sandstone	40% existing	Simple extension	68	
4a	22.4	22400	49.36	24.75	11.66	F-M sandstone	10% existing	Multi extension	44.6	Discontinuity perpendicular to load
14a	15.7	15700	49.44	24.27	8.32	Fine sandstone	30% existing	Simple extension	37.6	Discontinuity perpendicular to load
14a	20.7	20700	49.51	24.34	10.92	Fine sandstone	Clean	Simple extension	53.3	Discontinuity at 45° degrees to load
21a	9.2	9200	49.1	24.17	4.93	Fine sandstone	Clean	Multi extension	26.21	
21a	21.3	21300	49.4	25.59	10.72	F-M sandstone	Clean	Simple extension	57.3	
21a	14.6	14600	49.2	24.02	7.86	F-M sandstone	Clean	Simple extension	41.66	Discontinuity perpendicular to load
21a	25.8	25800	49.44	24.51	13.54	F-M sandstone	Clean	Simple extension	69	
11a	18.9	18900	49.44	24.19	10.05	F-M sandstone	35% existing	Simple extension	56.3	Multiple discontinuities perpendicular, 45° and parallel with load
11a	23.7	23700	49.45	25.01	12.19	F-M sandstone	10% existing	Multi extension	59.39	
9a	12.2	12200	49.4	25.65	6.12	GRN mudstone	100% existing	Simple extension w/ multi fracture	39.07	Multiple discontinuities perpendicular, 45° and parallel with load
10a	6.7	6700	49.38	25.95	3.33	RED mudstone	Clean	Simple extension	25.15	Multiple discontinuities perpendicular to load
10a	6.1	6100	49.4	24.1	3.26	RED mudstone	100% existing	Multi extension	25.2	Multiple discontinuities parallel to load
5a	20.3	20300	49.58	24.3	10.72	F-M sandstone	60% existing	Simple extension	58.8	Discontinuity at 45° to load
5a	32.5	32500	49.62	24.5	17.00	F-M sandstone	Clean	Multi extension	77	
5a	25.6	25600	49.42	25.72	12.81	F-M sandstone	Clean	Simple extension	69	Discontinuity perpendicular to load

F.6 Ashley River Gorge Point Load testing raw results and calculations

Point Load Index testing per sample outcrop.

F.6 Ashley River Gorge - Point Load testing

SAMPLE: 2a

Test No.	Type	P (kN)	D (mm)	W (mm)	A = WD (mm^2)	D_e^2	D_e	I_s	F	$I_{s(50)}$ (MPa)	Lithology	Weathering	Notes
1		8.40	26.7	49.6	1323	1684	41.0	4.99	0.915	4.56	F-M Sandstone	Sw	
2		8.08	23.9	34.35	822	1047	32.4	7.72	0.822	6.34	F-M Sandstone	Sw	
3		14.04	49.9	45.25	2257	2873	53.6	4.89	1.032	5.04	F-M Sandstone	Sw	
4		10.00	18.1	50.3	911	1160	34.1	8.62	0.841	7.25	F-M Sandstone	Sw	
5		13.84	21.9	57.6	1261	1606	40.1	8.62	0.905	7.80	Fine Sandstone	Sw	Fine sandstone with small mudstone banding
6	perpendicular	10.73	20.8	29.16	605	771	27.8	13.92	0.767	10.68	Fine Sandstone	Sw	
7	parallel	0.83	36.4	27.94	1017	1295	36.0	0.64	0.862	0.55	Fine Sandstone	Sw	Some break along existing oxide
8	perpendicular	1.81	14.5	50.17	727	926	30.4	1.96	0.800	1.56	Fine Sandstone	Sw	Break along existing
9		3.05	14.0	19.8	277	352	18.8	8.66	0.643	5.57	Fine Sandstone	Sw	
10		0.89	37.9	53.46	2028	2582	50.8	0.34	1.007	0.35	Mudstone	Sw	Most break along existing
11		1.83	21.2	38.97	828	1054	32.5	1.74	0.823	1.43	Mudstone	Sw	Some break along existing oxide
12		0.67	21.8	30.43	662	843	29.0	0.79	0.783	0.62	Mudstone	Sw	Some break along existing oxide
13	perpendicular	6.01	13.9	26.68	371	472	21.7	12.74	0.687	8.75	Fine Sandstone	Sw	
14		5.59	17.4	29.42	511	651	25.5	8.59	0.739	6.34	F-M Sandstone	Sw	
15		6.58	19.3	49.26	950	1210	34.8	5.44	0.849	4.62	F-M Sandstone	Sw	

SAMPLE: 4a

Test No.	Type	P (kN)	D (mm)	W (mm)	A = WD (mm^2)	D_e^2	D_e	I_s	F	$I_{s(50)}$ (MPa)	Lithology	Weathering	Notes
1		11.92	54.6	64.4	3516	4477	66.9	2.66	1.140	3.04	F-M Sandstone	Mw	Some break along existing
2		3.41	28.6	61.19	1751	2229	47.2	1.53	0.975	1.49	F-M Sandstone	Mw	Break along existing oxide
3		9.45	22.1	61.4	1359	1730	41.6	5.46	0.921	5.03	F-M Sandstone	Sw	
4		10.45	29.8	52.96	1577	2008	44.8	5.20	0.952	4.95	F-M Sandstone	Sw	
5		20.51	40.2	83.74	3370	4290	65.5	4.78	1.129	5.40	F-M Sandstone	Sw	
6		11.90	37.8	47.04	1780	2266	47.6	5.25	0.978	5.14	F-M Sandstone	Sw	
7		7.10	31.2	59.48	1855	2361	48.6	3.01	0.987	2.97	F-M Sandstone	Sw	Break along existing oxide
8		9.86	20.0	56.8	1137	1448	38.1	6.81	0.884	6.02	F-M Sandstone	Sw	
9		18.39	32.3	73.3	2364	3010	54.9	6.11	1.043	6.37	F-M Sandstone	Sw	
10		6.00	17.7	39.63	700	892	29.9	6.73	0.793	5.34	F-M Sandstone	Sw	

SAMPLE: 5a

Test No.	Type	P (kN)	D (mm)	W (mm)	A = WD (mm^2)	D_e^2	D_e	I_s	F	$I_{s(50)}$ (MPa)	Lithology	Weathering	Notes
1		8.26	30.0	38.13	1143	1455	38.2	5.68	0.885	5.02	F-M Sandstone	Sw	Some break along existing
2		7.35	23.3	31.78	741	944	30.7	7.79	0.803	6.26	F-M Sandstone	Sw	
3		4.71	10.6	43.17	456	581	24.1	8.11	0.720	5.84	F-M Sandstone	Sw	
4		2.32	8.2	44.1	359	458	21.4	5.07	0.682	3.46	F-M Sandstone	Sw	
5		12.28	25.5	47.66	1213	1544	39.3	7.95	0.897	7.13	F-M Sandstone	Sw	
6		2.78	21.4	47.36	1014	1290	35.9	2.15	0.862	1.86	F-M Sandstone	Sw	Most break along existing oxide
7		13.88	48.7	47.74	2327	2963	54.4	4.69	1.039	4.87	F-M Sandstone	Sw	Some break along existing oxide
8		17.15	42.2	53.78	2272	2892	53.8	5.93	1.033	6.13	F-M Sandstone	Sw	
9		5.12	30.6	39.53	1210	1541	39.3	3.32	0.897	2.98	F-M Sandstone	Mw	Break along existing oxide
10		5.24	11.7	43.88	513	653	25.5	8.03	0.739	5.94	F-M Sandstone	Sw	
11		7.39	26.3	43.81	1154	1469	38.3	5.03	0.887	4.46	F-M Sandstone	Sw	Some break along existing oxide

SAMPLE: 11a

Test No.	Type	P (kN)	D (mm)	W (mm)	A = WD (mm^2)	D_e^2	D_e	I_s	F	$I_{s(50)}$ (MPa)	Lithology	Weathering	Notes
1		7.29	15.1	45.68	691	880	29.7	8.28	0.791	6.55	F-M Sandstone	Sw	
2		3.01	12.2	47	573	729	27.0	4.13	0.758	3.13	F-M Sandstone	Sw	Some break along existing
3		6.17	34.7	43.87	1522	1938	44.0	3.18	0.944	3.01	F-M Sandstone	Mw	Most break along existing
4		11.69	29.1	67.19	1952	2485	49.9	4.70	0.999	4.70	F-M Sandstone	Mw	
5		11.41	29.0	57.08	1654	2106	45.9	5.42	0.962	5.21	F-M Sandstone	Mw	
6		12.12	24.9	57.02	1417	1804	42.5	6.72	0.929	6.24	F-M Sandstone	Sw	
7		8.58	35.2	94.84	3338	4251	65.2	2.02	1.127	2.27	F-M Sandstone	Mw	Most break along existing
8		4.33	25.2	32.52	818	1042	32.3	4.16	0.821	3.41	F-M Sandstone	Mw	
9		7.00	24.6	56.7	1394	1775	42.1	3.94	0.926	3.65	F-M Sandstone	Mw	
10		6.50	15.5	48.23	748	952	30.9	6.83	0.805	5.50	F-M Sandstone	Sw	

SAMPLE: 13a

Test No.	Type	P (kN)	D (mm)	W (mm)	A = WD (mm^2)	D_e^2	D_e	I_s	F	$I_{s(50)}$ (MPa)	Lithology	Weathering	Notes
1		1.08	32.0	41.25	1320	1680	41.0	0.64	0.914	0.59	F-M Sandstone	Mw	50% break along existing
2		1.14	30.9	52.86	1631	2077	45.6	0.55	0.959	0.53	F-M Sandstone	Mw	Break along existing
3		0.55	18.0	37.37	674	858	29.3	0.64	0.786	0.50	F-M Sandstone	Mw	Break along existing quartz
4		0.14	23.1	34.38	793	1010	31.8	0.14	0.816	0.11	F-M Sandstone	Mw	Break along existing
5		1.00	23.9	28.14	672	855	29.2	1.17	0.786	0.92	F-M Sandstone	Mw	Most break along existing quartz
6		1.50	28.6	73.35	2101	2675	51.7	0.56	1.015	0.57	F-M Sandstone	Mw	Most break along existing quartz

SAMPLE: 14a

Test No.	Type	P (kN)	D (mm)	W (mm)	A = WD (mm^2)	D_e^2	D_e	I_s	F	$I_{s(50)}$ (MPa)	Lithology	Weathering	Notes
1	perpendicular	1.24	8.7	59.18	517	659	25.7	1.88	0.741	1.39	Mudstone	Sw	Small fine sandstone interbeds
2	perpendicular	3.66	28.1	34.69	974	1241	35.2	2.95	0.854	2.52	Fine Sandstone	Sw	Small Mudstone interbeds/banding
3		0.65	31.9	78.71	2514	3201	56.6	0.20	1.057	0.21	Mudstone	Sw	Break along existing
4		1.24	39.3	36.36	1427	1818	42.6	0.68	0.931	0.64	Mudstone	Sw	Break along existing
5	perpendicular	5.44	38.1	43.61	1661	2115	46.0	2.57	0.963	2.48	Fine Sandstone	Sw	Small Mudstone interbeds/banding
6	Parallel	0.22	35.3	60.13	2120	2700	52.0	0.08	1.017	0.08	Fine Sandstone	Sw	Break along banding
7	Parallel	1.71	23.2	45.77	1060	1349	36.7	1.27	0.870	1.10	Mudstone	Sw	Small fine sandstone interbeds
8	perpendicular	1.71	26.3	73.23	1928	2455	49.5	0.70	0.996	0.69	Mudstone	Sw	Break along existing
9	Parallel	0.39	27.6	73.21	2024	2576	50.8	0.15	1.007	0.15	Mudstone	Sw	Break along banding
10		9.31	46.7	71.73	3352	4268	65.3	2.18	1.128	2.46	Fine Sandstone	Sw	
11		7.81	38.5	60	2311	2942	54.2	2.65	1.037	2.75	F-M Sandstone	Mw	Some break along existing
12		5.49	27.9	90.99	2534	3226	56.8	1.70	1.059	1.80	F-M Sandstone	Mw	Some break along existing
13		4.06	18.0	37.46	676	860	29.3	4.72	0.787	3.71	F-M Sandstone	Sw	
14		8.38	25.1	40.38	1012	1288	35.9	6.50	0.861	5.60	F-M Sandstone	Sw	
15		7.75	22.0	41.08	904	1151	33.9	6.73	0.840	5.65	F-M Sandstone	Sw	

F.6 Ashley River Gorge - Point Load testing

SAMPLE: 17a

Test No.	Type	P (kN)	D (mm)	W (mm)	A = WD (mm^2)	D_e^2	D_e	I_s	F	$I_{s(50)}$ (MPa)	Lithology	Weathering	Notes
1		2.50	37.1	56.45	2096	2669	51.7	0.94	1.015	0.95	Fine Sandstone	Mw	Break along existing oxide
2		6.72	38.7	103.88	4016	5113	71.5	1.31	1.175	1.54	Fine Sandstone	Mw	Break along existing oxide
3		11.12	47.5	43.55	2068	2633	51.3	4.22	1.012	4.27	Fine Sandstone	Mw	
4		6.19	32.4	73.61	2386	3039	55.1	2.04	1.045	2.13	Fine Sandstone	Mw	Break along existing oxide
5		1.50	20.2	40.42	815	1038	32.2	1.45	0.821	1.19	Mudstone	Sw	Note: other mudstones do not register
6		1.14	22.6	28.9	652	830	28.8	1.37	0.780	1.07	Mudstone	Sw	
7	perpendicular	2.22	16.9	25.6	432	550	23.4	4.04	0.711	2.87	Mudstone	Sw	Small fine sandstone band
8	perpendicular	0.12	28.6	64.06	1829	2329	48.3	0.05	0.984	0.05	Mudstone	Sw	Mudstone breaks along existing with fine sandstone banding
9	perpendicular	1.28	19.2	63.05	1209	1539	39.2	0.83	0.897	0.75	Mudstone	Sw	
10		6.78	36.6	51.55	1887	2402	49.0	2.82	0.991	2.80	Fine Sandstone	Sw	Some break along existing oxide
11	perpendicular	5.40	25.1	31.3	787	1001	31.6	5.39	0.814	4.39	Fine Sandstone	Sw	
12	perpendicular	1.32	28.1	36.4	1021	1300	36.1	1.02	0.863	0.88	Mudstone	Sw	

SAMPLE: 21a

Test No.	Type	P (kN)	D (mm)	W (mm)	A = WD (mm^2)	D_e^2	D_e	I_s	F	$I_{s(50)}$ (MPa)	Lithology	Weathering	Notes
1		8.68	29.0	47.56	1378	1754	41.9	4.95	0.923	4.57	Fine Sandstone	Sw	
2		0.39	8.3	40.34	333	424	20.6	0.92	0.671	0.62	Fine Sandstone	Sw	Break along existing
3		3.23	26.8	27.42	734	934	30.6	3.46	0.801	2.77	Fine Sandstone	Sw	
4		1.42	25.6	45.06	1154	1469	38.3	0.97	0.887	0.86	Fine Sandstone	Sw	Break along existing
5		0.93	6.7	48.47	325	413	20.3	2.25	0.667	1.50	Fine Sandstone	Sw	
6		1.50	8.0	41.88	337	429	20.7	3.50	0.673	2.35	Fine Sandstone	Sw	
7		3.03	15.7	32.18	504	641	25.3	4.73	0.736	3.48	Fine Sandstone	Sw	
8		5.00	24.2	60.5	1465	1866	43.2	2.68	0.936	2.51	Fine Sandstone	Sw	
9		2.40	30.0	63.92	1918	2442	49.4	0.98	0.995	0.98	Fine Sandstone	Sw	
10		2.11	17.2	66.26	1141	1453	38.1	1.45	0.885	1.29	Fine Sandstone	Sw	
11		27.15	42.2	61.09	2577	3281	57.3	8.28	1.063	8.80	F-M Sandstone	Sw	
12		17.99	34.9	58.39	2039	2596	51.0	6.93	1.009	6.99	F-M Sandstone	Sw	
13		18.25	33.7	57.61	1940	2470	49.7	7.39	0.997	7.37	F-M Sandstone	Sw	
14		17.15	34.2	56.76	1939	2469	49.7	6.94	0.997	6.93	F-M Sandstone	Sw	
15		7.25	18.8	46.76	878	1118	33.4	6.48	0.834	5.41	F-M Sandstone	Sw	Break along existing

SAMPLE: 28a

Test No.	Type	P (kN)	D (mm)	W (mm)	A = WD (mm^2)	D_e^2	D_e	I_s	F	$I_{s(50)}$ (MPa)	Lithology	Weathering	Notes
1	perpendicular	9.13	27.8	36.9	1026	1306	36.1	6.99	0.864	6.04	Fine Sandstone	Sw	Fine sandstone with cross bedded mudstone
2	parallel	3.21	14.0	21.51	300	383	19.6	8.39	0.656	5.50	Fine Sandstone	Sw	
3		0.59	23.6	29.42	694	884	29.7	0.67	0.791	0.53	Mudstone	Sw	Note heavy incipient fracturing - break along multiple existing
4	parallel	7.08	15.6	46.03	718	914	30.2	7.75	0.797	6.18	Mudstone	Sw	
5	parallel	3.98	14.1	32.05	452	575	24.0	6.92	0.718	4.97	Mudstone	Sw	
6		6.30	20.6	71.86	1482	1887	43.4	3.34	0.939	3.13	F-M Sandstone	Sw	Some break along existing quartz
7		6.92	13.5	23.48	317	404	20.1	17.13	0.664	11.37	F-M Sandstone	Sw	
8		4.25	15.8	26.85	425	541	23.3	7.86	0.709	5.57	F-M Sandstone	Sw	
9		5.79	15.0	32.68	489	622	24.9	9.31	0.731	6.81	F-M Sandstone	Sw	
10	parallel	7.19	19.4	35.99	697	887	29.8	8.10	0.792	6.42	Fine Sandstone	Sw	
11		5.79	15.0	37.89	568	723	26.9	8.01	0.756	6.06	F-M Sandstone	Sw	
12	parallel	4.29	19.1	42.03	801	1020	31.9	4.21	0.817	3.44	Fine Sandstone	Sw	Some break along existing
13	parallel	3.76	12.9	39.77	511	651	25.5	5.77	0.739	4.27	Fine Sandstone	Sw	
14	parallel	4.80	18.0	47.39	851	1084	32.9	4.43	0.829	3.67	Fine Sandstone	Sw	
15		7.96	19.7	39.9	784	998	31.6	7.97	0.813	6.49	F-M Sandstone	Sw	

SAMPLE: 39a

Test No.	Type	P (kN)	D (mm)	W (mm)	A = WD (mm^2)	D_e^2	D_e	I_s	F	$I_{s(50)}$ (MPa)	Lithology	Weathering	Notes
1		7.61	30.8	37	1138	1450	38.1	5.25	0.885	4.64	F-M Sandstone	Sw	
2		3.80	13.6	37.95	518	659	25.7	5.77	0.741	4.27	F-M Sandstone	Sw	
3		4.35	40.4	54.1	2183	2779	52.7	1.57	1.024	1.60	F-M Sandstone	Sw	Some break along existing quartz
4		6.90	32.3	40.12	1297	1652	40.6	4.18	0.911	3.80	F-M Sandstone	Sw	
5		8.26	21.3	39.5	843	1073	32.8	7.70	0.827	6.36	F-M Sandstone	Sw	
6		6.25	23.6	65.4	1541	1962	44.3	3.19	0.947	3.02	F-M Sandstone	Sw	Some break along existing quartz
7		2.80	34.6	50.03	1729	2201	46.9	1.27	0.972	1.24	Fine Sandstone	Sw	
8		4.04	19.1	55.49	1060	1349	36.7	2.99	0.870	2.61	Fine Sandstone	Sw	
9		6.05	35.3	52.18	1841	2344	48.4	2.58	0.986	2.54	F-M Sandstone	Sw	
10		0.35	10.8	47.05	508	647	25.4	0.54	0.738	0.40	Fine Sandstone	Sw	Most break along existing quartz
11		2.56	26.7	33.84	905	1152	33.9	2.22	0.840	1.87	Fine Sandstone	Sw	
12		3.56	18.2	53.78	977	1244	35.3	2.86	0.855	2.45	Fine Sandstone	Sw	

SAMPLE: 41a

Test No.	Type	P (kN)	D (mm)	W (mm)	A = WD (mm^2)	D_e^2	D_e	I_s	F	$I_{s(50)}$ (MPa)	Lithology	Weathering	Notes
1		2.82	21.4	36.68	786	1001	31.6	2.82	0.814	2.29	F-M Sandstone	Sw	
2		0.61	19.0	24.57	467	595	24.4	1.03	0.724	0.74	F-M Sandstone	Sw	
3		2.42	15.9	35.33	561	715	26.7	3.39	0.754	2.55	F-M Sandstone	Sw	
4		2.70	21.3	42.02	893	1137	33.7	2.37	0.838	1.99	F-M Sandstone	Sw	
5		6.84	21.7	25.2	547	697	26.4	9.81	0.750	7.36	F-M Sandstone	Sw	
6		6.17	21.1	25.55	538	685	26.2	9.01	0.747	6.73	F-M Sandstone	Sw	

SAMPLE: 44a

Test No.	Type	P (kN)	D (mm)	W (mm)	A = WD (mm^2)	D_e^2	D_e	I_s	F	$I_{s(50)}$ (MPa)	Lithology	Weathering	Notes
1		6.48	23.6	50.67	1198	1525	39.1	4.25	0.895	3.80	Mudstone	Sw	
2		4.27	14.9	55.73	832	1059	32.5	4.03	0.824	3.32	Mudstone	Sw	
3		3.92	17.7	43.73	774	985	31.4	3.98	0.811	3.23	Mudstone	Sw	
4		1.71	6.6	40.33	266	338	18.4	5.05	0.638	3.22	Mudstone	Sw	
5		7.27	12.2	30.68	375	478	21.9	15.22	0.689	10.49	Mudstone	Sw	
6		7.75	30.2	37.65	1137	1448	38.0	5.35	0.884	4.73	F-M Sandstone	Sw	
7		2.68	26.7	52.94	1415	1802	42.4	1.49	0.929	1.38	F-M Sandstone	Sw	Some break along existing quartz
8		5.10	23.6	42.39	998	1271	35.7	4.01	0.859	3.45	F-M Sandstone	Sw	50% break along existing quartz
9		10.77	20.2	74.79	1508	1920	43.8	5.61	0.942	5.29	F-M Sandstone	Sw	
10		8.22	19.3	61.18	1181	1503	38.8	5.47	0.892	4.88	F-M Sandstone	Sw	
11		5.02	26.2	45.8	1201	1530	39.1	3.28	0.895	2.94	F-M Sandstone	Sw	
12		8.04	22.0	35.24	775	987	31.4	8.14	0.811	6.61	F-M Sandstone	Sw	
13		5.36	19.5	24.19	472	602	24.5	8.91	0.726	6.47	F-M Sandstone	Sw	

F.7 Ashley River Gorge fines index test results and calculations

Fines content results and calculation tables produced from wet sieving and laser size analysis per sample outcrop.

F.7 Ashley River Gorge - fines index testing

1a				
Passing (wet sieve)	**Raw weight (g)**	**Container weight (g)**	**Sample weight (g)**	**Sample fines division (%)**
>4mm	753.5	275.1	478.4	63.66
>2mm (gravel)	299.4	186.1	113.3	15.08
>1mm (coarse sand)	252	195.2	56.8	7.56
Remaining fraction (<1mm)	141.66	38.67	102.99	13.70
Total sample weight (g)			751.49	
Matrix (lasersizer)	**Average diameter (µm)**	**Cumulative %**	**Actual %**	**% of total <1mm fraction**
<2 microns (clay)	2	7.5	7.50	1.03
<60 microns (silt)	59.57	44.7	37.20	5.10
<200 microns (fine sand)	199.53	66.2	21.50	2.95
Remaining fraction (medium/coarse sand)		100	33.80	4.63

38a				
Passing (wet sieve)	**Raw weight (g)**	**Container weight (g)**	**Sample weight (g)**	**Sample fines division (%)**
>2mm (gravel)	382.64	194.61	188.03	32.17
>2mm (gravel)	293.08	224.84	68.24	11.68
>1mm (coarse sand)	212.18	174.11	38.07	6.51
Remaining fraction (<1mm)	329.78	39.66	290.12	49.64
Total sample weight (g)			584.46	
Matrix (lasersizer)	**Average diameter (µm)**	**Cumulative %**	**Actual %**	**% of total <1mm fraction**
<2 microns (clay)	2	7.7	7.70	3.82
<60 microns (silt)	59.57	60.1	52.40	26.01
<200 microns (fine sand)	199.53	78.7	18.60	9.23
Remaining fraction (medium/coarse sand)		100	21.30	10.57

42a				
Passing (wet sieve)	**Raw weight (g)**	**Container weight (g)**	**Sample weight (g)**	**Sample fines division (%)**
>2mm (gravel)	240.5	217.6	22.9	5.73
>2mm (gravel)	285	252.1	32.9	8.23
>1mm (coarse sand)	461	424.2	36.8	9.21
Remaining fraction (<1mm)	346.25	39.32	306.93	76.82
Total sample weight (g)			399.53	
Matrix (lasersizer)	**Average diameter (µm)**	**Cumulative %**	**Actual %**	**% of total <1mm fraction**
<2 microns (clay)	2	7.8	7.80	5.99
<60 microns (silt)	59.57	45.9	38.10	29.27
<200 microns (fine sand)	199.53	72.7	26.80	20.59
Remaining fraction (medium/coarse sand)		100	27.30	20.97

51a				
Passing (wet sieve)	**Raw weight (g)**	**Container weight (g)**	**Sample weight (g)**	**Sample fines division (%)**
>2mm (gravel)	481.16	399.64	81.52	11.02
>2mm (gravel)	261.54	188.4	73.14	9.89
>1mm (coarse sand)	231.2	190.49	40.71	5.50
Remaining fraction (<1mm)	608.23	64.01	544.22	73.58
Total sample weight (g)			739.59	
Matrix (lasersizer)	**Average diameter (µm)**	**Cumulative %**	**Actual %**	**% of total <1mm fraction**
<2 microns (clay)	2	6.5	6.50	4.78
<60 microns (silt)	59.57	34	27.50	20.24
<200 microns (fine sand)	199.53	50.6	16.60	12.21
Remaining fraction (medium/coarse sand)		100	49.40	36.35

F.7 Ashley River Gorge - fines index testing

5a - Clay				
Matrix (lasersizer)	**Average diameter (µm)**	**Cumulative %**	**Actual %**	**% of total sample**
<2 microns (clay)	2	31.4	31.4	31.4
<60 microns (silt)	59.57	100	68.6	68.6
<200 microns (fine sand)	199.53	0	0	0
Remaining fraction (medium/coarse sand)		0	0	0

13a - Clay				
Matrix (lasersizer)	**Average diameter (µm)**	**Cumulative %**	**Actual %**	**% of total sample**
<2 microns (clay)	2	45.3	45.30	45.30
<60 microns (silt)	59.57	100	54.70	54.70
<200 microns (fine sand)	199.53	0	0.00	0.00
Remaining fraction (medium/coarse sand)		0	0.00	0.00

45a - Clay				
Matrix (lasersizer)	**Average diameter (µm)**	**Cumulative %**	**Actual %**	**% of total sample**
<2 microns (clay)	2	33.9	33.90	33.90
<60 microns (silt)	59.57	100	66.10	66.10
<200 microns (fine sand)	199.53	0	0.00	0.00
Remaining fraction (medium/coarse sand)		0	0.00	0.00

Appendix G: Opuha Dam

Results derived from the lineation analysis, raw mapping data, analysis, raw lab testing data and calculations for the Opuha Dam study site.

G.1 Opuha Dam raw mapping data

Mapping per field data sheets (Appendix A). Where data is missing, blanked out or ranges from other sites, information has been unobtainable due to access issues, poor rock/defect conditions, recording prior to the continual modification of the field sheets or previous recording of the defect (i.e. 1 x bedding plane between two lithologies).

G.1.1 Opuha Dam - Coherent rock and bedding

													Waviness			
Outcrop #	Weathering	Colour	Bedding fabric	Bedding thickness	Bedding development	Grain Size	Rock name	Strength (rock)	Strength (bed)	Dip	Dip direction	Bedding roughness	Wavelength (m)	Interlimb angle (ILA, °)	Degree of fracture	Raw field notes
1a	Sw	L-GY	M	V thick	WD	F-M	Sandstone	S	S	66	217	UR	175	3.6	MF	
1b	Mw	L-GY	M	Thin	VWD	FINE	Sandstone	W	W	69	194	SS	165	0.4	FRAG	Boudin developing
1b	Mw	D-GY	M	Thin	VWD		Mudstone	VW	VW						FRAG	Below 1b ~2m thick breccia zone with 6mm observable clay seam within interbedding
1c	Mw	L-GY	M	Massive		F-M	Sandstone	MS							HF	
1d	Mw	L-GY	M	Thin	WD	F-M	Sandstone	W	W	53	234	UR	160	1.8	FRAG	
1d	Mw	D-GY	M	V thin	WD		Mudstone	VW	VW			UR			FRAG	1d = same outcrop different sections
1d	Sw	L-GY	M	V thick	D	F-M	Sandstone	S	MS	48	240	UR	170	1.2	HF	
1e	Sw	L-GY	M	V thick	D	F-M	Sandstone	VS		72	235	UR	180	0	MF	
1e	Hw	L-GY	M	Medium	D	F-M	Sandstone	VW	VW	68	230		160	1	FRAG	Heavy quartz veining leaving material very weak
1e	Hw	D-GY	M	Thin	D		Mudstone	VW	VW						FRAG	
1f	Hw	L-GY	M	Thin	D	FINE	Sandstone	W	W	76	237	UR	165	1	FRAG	Boudins observed as mud flows and isolates parcels of sand
1f	Hw	D-GY	M	Thin	D		Mudstone	W	W			UR	155	0.4	FRAG	
1g	Sw	L-GY	M	Massive		F-M	Sandstone	CS							FRACT	
1h	Sw	L-GY	M	V thick	D	F-M	Sandstone	S	S	70	218	UR	175	3.4	HF	
1h	Mw	D-GY	M	V thin	D		Mudstone	VW	VW						FRAG	
2a	Sw	L-GY	M	Massive		F-M	Sandstone	VS							FRAG	Multiple small scale >1cm shears with one large 1.4m shear with 4cm clay infill
2b	Mw	L-GY	M	Massive		F-M	Sandstone	VS							HF	
3a	Mw	L-GY	M	Massive		F-M	Sandstone	VS							MF	Middle of outcrop MF, either side = HF. Heavy amount of fluid flow shown by heavy quartz veining tends to follow existing defects
4a	Sw	L-GY	M	V thick	D	F-M	Sandstone	VS	S	88	210	US	175	0.7	MF	
4a	Hw	D-GY	M	Medium	D	FINE	Sandstone	MS	W			US			HF	Bedding strength affected by weathering control
4a	Hw	D-GY	M	V thin	D		Mudstone	VW	W	84	212	UR	170	0.45	FRAG	
4b	Sw	L-GY	M	V thick	D	F-M	Sandstone	VS	VS	86	221	SS	180	0	FRAG	Note: Roughness maybe due to fracture pattern and relaxation. Mudstone and fine sandstone has also been squeezed between thick sandstone and is thus lineated parallel to bedding
4b	Sw	D-GY	M	Thin	D		Mudstone	MS	W	75	246	PR	175	4	FRAG	Note: Whole area is dominated by heavy quartz veining, ~1mm-12cm in random orientation through incipient fracturing and main jointing
4b	Sw	L-GY	M	Medium	D	FINE	Sandstone	S	S	76	238	US	165	5	FRAG	Thicker veining occurs in areas parallel with bedding, this tends to brecciate the sandstone which is not observed in jointing quartz. However some evidence in hand sample that the veining makes its own path along non-existing
5a	Sw	L-GY	M	Massive		F-M	Sandstone	VS							MF	
5b	Mw	L-GY	M	Massive	WD	F-M	Sandstone	S							FRAG	No bedding plane recognisable between Sand and Mud - fault related
5b	Hw	D-GY	M	Thin	WD		Mudstone	Firm	Firm	71	211	UR	170	2	FRAG	Breccia - Wet
5b	Hw	L-GY	M	Thin	WD	F-M	Sandstone	Firm	Firm	75	209	UR	90	1.1	FRAG	Breccia - Moist. Note: Heavy weathering mostly mechanical deems material a soil with Firm strength
6a	Mw	L-GY	M	Medium	WD	F-M	Sandstone	S	S	57	238	US	170	0.5	HF	
6a	Mw	D-GY	M	Thin	WD		Mudstone	W	W	49	235	SS			FRAG	
6b	Mw	L-GY	M	Medium	WD	F-M	Sandstone	VS	VS	54	246	US	175	0.8	HF	
6b	Mw	D-GY	M	Thin	WD		Mudstone	W	W	45	253	US	170	0.7	FRAG	
7a	Hw	L-GY	M	Massive		F-M	Sandstone	MS							FRAG	Huge level of quartz infilling in intact rock bordering the main fault zone, nearly every defect is coated with 1-2mm of quartz
7b	Mw	L-GY	M	V thick	D	F-M	Sandstone	VS	S	89	340	US	165	2.2	HF	
7b	Mw	D-GY	M	Thin	D		Mudstone	W	W			UR			FRAG	
7c	Sw	L-GY	M	V thick	VWD	F-M	Sandstone	VS	S	73	209	UR	180	0	MF	Note the difference between the top level of 7c controlled by systematic controls vs. the bottom controlled non-systematically
7c	Sw	D-GY	M	V thick	VWD		Mudstone	MS	MS			UR	180	0	FRAG	
8a	Sw	L-GY	M	V thick	WD	F-M	Sandstone	VS	S			US			MF	Note: mudstone still fragmented but in better condition than observed away from Opuha
8a	Mw	D-GY	M	Thick	WD		Mudstone	S	MS	74	206	UR	180	0	HF	
9a	Sw	L-GY	M	Massive		F-M	Sandstone	VS							FRACT	rock mass controlled completely systematically
10a	Sw	L-GY	M	Massive		F-M	Sandstone	VS							HF	
11a	Sw	L-GY	M	V thick	VWD	F-M	Sandstone	VS					175	3.8	MF	Other side of the highway with no room to get accurate data
11a	Sw	D-GY	M	Thin	VWD		Mudstone	Weak					170	3.8	FRAG	Jointing here is somewhat straight 180°/0m, 170°/3m, 180°/0m with 2 x shears 180°/0m

G.1.2 Opuha Dam - Defect structure

		Orientation										Waviness								
Outcrop #	Defect type	Dip	Dip direction	Spacing (m)	Persistence (m)	Aperture (cm)	Infilling type	Infilling strength	Infill moisture	Infill thickness (mm)	Roughness	Interlimb angle (ILA, °)	Wavelength (m)	Ends	End termination	Strength (Rock hammer)	Water	Weathering	Degree of fracture	Raw field notes
1a	Joint	27	50	0.4	8						US	180	0	2	C	S	D	Mw	MF	
1a	Joint	30	85	0.8	4.2						US	180	0	2	C	VS	D	Sw	MF	
1a	Joint	39	44	0.45	2.8		Quartz	MS	D	8	SR	170	1.8	2	C	VS	D	Sw	MF	
1b	Joint	31	12	1	16	0.2					US	180	0	2	C	MS	D	Sw	HF	
1b	Fault	59	209		12		Breccia/clay	V stiff/Soft	Moist	1500	UR	170	1	1	O	FIRM	D	Mw	FRAG	No offset observed but crush zone 1-2m below thin interbedding
1c	Joint	40	86	0.45	6.2		Quartz	MS	D	2	SS	170	3.1	1	O	FIRM	D	Mw	HF	
1c	Shear	85	150		3.7						UR	175	3	1	O	MS	Moist	Hw	FRAG	Left of shear more fractured than right
1c	Joint	30	31	0.45	3.5	2.5					PR	180	0	2	C	VS	Wet	Mw	MF	
1c	Joint	68	294	0.2	2	0.8					US	170	0.4	1	O	MS	D	Sw	HF	
1c	Joint	60	21	0.28	2	0.8					UR	165	0.25	1	O	S	D	Sw	MF	
1d	Joint	32	46	1.1	5.1		Quartz	MS	D	4	US	180	0	2	C	MS	D	Sw	MF	
1d	Joint	59	333	0.6	20						SS	175	1	1	O	S	D	Sw	MF	
1d	Shear	73	324		2.9		Silt with some clay	Soft	Moist	300	SS	160	1.2	1	O	FIRM	Moist	Hw	FRAG	
1e	Joint	72	335	1.5	3.2	0.3					SS	170	2.2	2	C	S	D	Mw	MF	
1e	Joint	32	36	0.45	10						US	180	0	1	D	VS	Wet	Sw	MF	
1f	Joint	11	359	0.4	4.1	1.2	Lineated Mud	VW	D	20	UR	145	2.1	0	C	W	Wet	Hw	FRAG	1 litre/min, low pressure. Bottom mud appears to flow below joint, above joint mudstone is better condition, some rotation of sand unit boudins away from normal bedding
1g	Joint	26	38	2	33	0.6					PS	180	0	2	C	VS	Wet	Sw	FRACT	
1g	Joint	63	211	0.55	2						US	180	0	1	D	VS	D	Sw	FRACT	
1g	Joint	89	348	1.2	2						US	170	2.3	1	D	VS	D	Sw	FRACT	
1h	Joint	58	30	1.2	3.3	0.7					PS	180	0	2	C	VS	Wet	Sw	MF	
1h	Joint	78	174	0.3	2	0.2	Stain			<1	PR	180	0	2	C	VS	D	Sw	MF	1h = blocky appearance
1h	Joint	80	331	0.5	2	0.1	Stain			<1	UR	175	1	1	C	VS	D	Sw	HF	
1h	Shear	64	194		3.7		Sandy silt with minor clay	Soft	Moist	25	UR	175	2	1	O	MS	Moist	Hw	FRAG	Appears as if fluid movement has degraded rock along bedding, rock appears as soil heavy in quartz
2a	Shear	65	134		2		Sand with some gravel & silt/ 4cm clay seam	V stiff/Soft	Moist	1400	PR	160	0.8	1	O	WEAK	D	Hw	HF	NOTE: INFILL IS MOIST, DEFECT WALLS ARE DRY, SAME WITH DEGREE OF FRACTURE FOR DEFECT SURFACE
2a	Shear	80	143		2		Silty sand with minor clay	Firm	Moist	9	PR	160	0.7	1	O	MS	D	Hw	FRAG	Note: some free water developing on clay surface of the first shear zone clay
2a	Shear	60	280		2		Silty sand with minor clay	Soft	Moist	4	SS	165	1	1	D	MS	D	Hw	MF	
2a	Shear	63	135		2		Silty sand with minor clay	Firm	Moist	8	PR	165	1	1	O	VS	D	Hw	MF	
2a	Shear	76	94		2		Silt with some sand & minor clay	Soft	D	6	UR	180	0	2	C	VS	D	Hw	HF	
2a	Shear	78	264		2		Silt with some clay	Firm	Moist	9	US	155	1.3	1	O	S	D	Hw	HF	
2a	Shear	83	137		2		Silt with some clay	Soft	Moist	10	SR	170	2	2	C	S	Wet	Hw	MF	Some free water developing on shear
2b	Joint	48	180	1.1	2						PR	175	1	1	O	VS	D	Mw	MF	Boarder between rock mass being systematically controlled and non-systematically controlled
2b	Joint	85	155	0.3	3.7						PR	180	0	0	O	S	D	Mw	HF	
2b	Joint	79	234	1.3	4.2						UR	175	2.5	2	C	VS	D	Mw	MF	
3a	Joint	78	150	1.1	2.7						UR	170	1	2	C	VS	D	Mw	MF	Potential shearing along joints with heavy quartz infill, makes rock mass weaker?
3a	Joint	36	231	0.25	4.9						PR	175	3	2	C	VS	D	Mw	MF	
3a	Shear	81	121		3.5		Silt with some clay	Stiff	Moist	7	PR	155	1.1	2	C	WEAK	D	Mw	MF	
3a	Shear	81	136		4.1		Silt with some sand	Stiff	D	60	UR	170	3	2	C	MS	D	Mw	HF	
3a	Shear	56	343		10		Coarse sand with some silt & minor clay	V stiff	Moist	11	US	150	4	2	C	MS	D	Mw	HF	Some green infill as observed in 2a, shear appears to be completely infilled with quartz which is V stiff to hard acting as a soil
3a	Shear	6	54		3.1		Silt with some sand	V stiff	Moist	9	US	175	1	1	D	MS	D	Mw	HF	NOTE: MOIST INFILL FOR ALL SHEARS
4a	Joint	56	234	0.35	2						US	175	0.45	2	C	VS	D	Sw	MF	
4a	Joint	54	290	0.4	2	0.2					SS	175	1.5	0	C	VS	D	Sw	MF	
4a	Joint	21	344	0.28	8.9		Quartz	MS	D	1	PR	180	0	2	C	VS	D	Sw	MF	
4a	Joint	88	310	0.15	3.8	0.3	Stained			<1	US	165	2.3	2	C	S	D	Sw	HF	
4a	Shear	85	210		2		Lineated mud	VW	D	4	US	175	0.7	1	O	WEAK	D	Hw	HF	
4a	Joint	43	264	0.65	2						UR	165	1	2	C	VS	D	Sw	MF	
4b	Shear	77	51		9		Sandy silt with minor clay	Hard	D	80	US	180	0	1	R	VS	Moist	Mw	HF	Note this and quartz vein along same defect bedding
4b	Qrtz Vein	72	47		9		Quartz	Weak	D	130	SR	180	0	2	C	MS	D	Hw	HF	Note: Within quartz vein sandstone trapped and rotated within, quartz is weak and disaggregates easy - Weathering related???
4b	Fault	69	112		14		Silty Sandy Gravel	VW	Moist	450	SR	160	2.5	2	C	MS	D	Mw	FRAG	Intact Sandstone clasts within
4b	Shear	79	145		8		Silt with minor clay	Firm	Moist	25	UR	165	5	2	C	MS	Moist	Mw	FRAG	Note: These two shears/faults/movement planes intersect and between create a heavy crush zone more heavily fragmented than surrounding rock
4b	Joint	15	8	0.35	2						UR	180	0	1	C	S	D	Sw	HF	
4b	Joint	30	0	0.28	2		Quartz	MS	D	1	PR	180	0	1	C	VS	D	Sw	HF	
5a	Joint	46	125	0.15	3						UR	175	0.4	2	C	VS	D	Sw	MF	
5a	Joint	23	224	1.8	4.5	0.9					US	170	2	2	C	VS	D	Sw	MF	
5a	Joint	85	281	0.45	2	0.8					PR	180	0	2	C	VS	D	Sw	MF	
5a	Shear	58	131		3.8		Silt with minor clay	Firm	Moist	310	UR	165	2.8	2	C	VS	D	Sw	MF	
5a	Shear	89	336		2		Crush rock with heavy quartz infill	MS	Moist	310	UR	175	2	2	C	VS	D	Mw	MF	
5a	Joint	59	164	0.3	2						US	170	2	1	C	VS	D	Sw	MF	
5a	Joint	79	233	1.8	2						US	180	0	0	C	VS	Moist	Sw	MF	
5a	Joint	29	35	2.1	2						SR	155	0.7	1	D	S	D	Sw	MF	
5b	Fault	64	334		4.3		Silt with some sand	Firm	D	330	US	175	2	2	C	MS	Moist	Mw	HF	
5b	Fault	SAME AS FAULT ABOVE					Clayey Silt	Soft	Moist	10	SAME AS FAULT ABOVE - MADE FOR DIFFERENT INFILL									Bordering fault plane - rest of fault zone is crush silt with some sand
6a	Shear	74	284		4.6		Silty sand with minor clay	Stiff	Moist	20	UR	165	2.1	2	C	MS	D	Hw	FRAG	
6a	Joint	85	108	0.8	3.8		Silt with some sand	Stiff	Moist	10	UR	170	1.9	1	C	S	D	Hw	FRAG	
6a	Shear	72	120		11.5		Silt with minor clay	Firm	Moist	26	US	160	5	2	C	S	D	Mw	HF	
6a	Fault	51	67		12.8		Silt with some sand	Firm	Moist	10	US	175	6	2	C	WEAK	D	Hw	FRAG	
6a	Shear	64	339		11	0.7					UR	155	6	2	C	MS	D	Hw	HF	
6a	Shear	40	179		8.5		Silt with some sand and clay	Firm	Moist	9	SS	155	4	2	C	S	D	Mw	HF	
6a	Joint	14	1	0.27	7						PS	180	0	1	D	VS	D	Sw	MF	
6a	Shear	74	284		10.2	0.6	Sandy silt with some clay	Firm	Moist	8	UR	160	1.7	2	C	S	D	Hw	MF	
6a	Shear	59	172		11							175	5	1	D	MS	D	Hw	FRAG	
6b	Shear	84	273		5.4		Quartz, clayey silt	Soft	Moist	35	US	180	0	2	C	MS	D	Mw	FRAG	NOTE: Area dominated by small distinct shearing and incipient fracturing with little systematic control, where jointing is present it isn't dominant and has close spacing

6b	Fault	70	136		2		Sandy silt	V stiff	D	6	UR	180	0	1	D	S	D	Mw	FRAG	Note: 30cm zone accompanying 6mm infill of frag rock - fault distinguishable by offset quartz vein - see photo
6b	Shear	79	127		2.7		Silt with minor sand and minor clay	Stiff	Moist	60	SR	175	1.5	2	C	S	D	Mw	HF	Note: Shear on approx same orientation as main jointing pattern, 45cm FRAG zone around shear
6b	Shear	83	101		5.1							160	4.5	2	C	S	D	Mw	FRAG	
6b	Joint	74	123	0.2	2.8						US	160	0.5	2	C	VS	D	Sw	HF	
6b	Qrtz Vein	16	85		6.8		Quartz	Ms	D	7	PR	180	0	2	C	S	D	Sw	HF	No similar jointing so appears to have made its own defect, however vein is dissected into three blocks by faults/shears with notable offset
6b	Fault	88	112		2.9		Quartz Sandy silt	Hard	Moist	140	US	175	2.2	2	C	VS	D	Mw	HF	Frag within 14cm shear zone with heavy quartz infill
6b	Joint	73	244	0.42	2						PR	175	1	1	R	VS	D	Sw	HF	
7a	Joint	56	174	0.3	2						US	145	2	2	C	WEAK	D	Hw	FRAG	Multiple shears between coherent rock within main crush zone, NOTE: North facing shear bound structure - potentially the fault plane
7a	Shear	84	333		3.9		Silty sand with minor clay	V stiff	D	2	UR	160	3	2	C	WEAK	D	Hw	FRAG	
7a	Fault	69	311		5.3		Silt with some clay	Firm	Moist	20	UR	180	0	2	C	MS	D	Mw	FRAG	
7b	Joint	2	39	0.65	13.3	0.1					Sslick	175	3	2	C	VS	D	Mw	MF	
7b	Fault	86	25		4.7						US	155	2.6	2	C	S	D	Mw	HF	7b shows a number of joints cut by multiple faults - see photos
7b	Joint	74	341	2	3.1	0.3					UR	160	2.8	2	C	VS	D	Sw	MF	
7b	Fault	85	129		4.6		Sandy silt	V stiff	D	60	US	165	2.5	2	C	S	D	Mw	HF	
7c	Shear	53	277		7.1		Silty gravel with some sand	Hard	D	110	PR	170	3	2	C	MS	D	Sw	FRAG	Rotated breccia - intact clasts
7c	Fault	64	207		24		Sandy silt with some clay	Stiff	Moist	60	PR	165	10	2	C	S	D	Mw	FRAG	Fault suddenly cuts off mudstone bedding
7c	Shear	85	330		3		Crush rock	Weak	D	340	PR	175	1.8	2	C	VS	D	Hw	HF	Crush zone is very hard with fragmented infill - not like traditional crush zones encountered at other sites
7c	Joint	28	21	1.5	5.1		Quartz	MS	D	2	PR	180	0	2	C	VS	D	Sw	MF	
7c	Joint	40	85	1.2	2	0.2					US	180	0	2	C	VS	D	Sw	MF	
7c	Joint	87	295	0.25	2.8	2					PS	175	1.9	2	C	VS	D	Sw	MF	
8a	Joint	30	85	1.8	3.3	0.2	Quartz	MS	D	1	PR	180	0	2	C	VS	D	Sw	MF	
8a	Joint	62	286	1.2	3.4						US	175	2	2	C	VS	D	Sw	MF	
8a	Joint	21	186	2	2						SS	175	3	2	C	VS	D	Sw	MF	
8a	Joint	80	193	0.9	3						PR	180	0	2	C	VS	D	Sw	MF	
8a	Shear	70	175		2.9		Crush rock	V stiff	D			180	0	1	O	S	D	Hw	FRAG	No defect surface recognisable, no definitive infill type - to weathered to see - heavy crush rock
8a	Joint	45	175	2.9	6.1						US	180	0	2	C	VS	D	Sw	HF	
8a	Joint	82	290	0.3	8	1						175	4	2	C	S	D	Sw	MF	
9a	Joint	26	355	2.9	4.1	0.1					PR	170	4	2	C	VS	D	Sw	FRACT	
9a	Joint	25	46	2.1	6.3	0.3	Quartz	Ms	D	1	SR	180	0	2	C	VS	D	Sw	MF	
9a	Joint	60	265	0.42	7.1						PR	175	4	2	C	VS	D	Sw	FRACT	
9a	Joint	69	136	0.35	2	0.4					SS	175	1	1	D	VS	D	Sw	MF	
9a	Joint	88	356	0.45	2						PS	175	1.5	1	C	VS	D	Sw	FRACT	
10a	Joint											155	2.9							
10a	Joint											165	3.1							
10a	Joint											180	0							
10a	Shear											180	0							
10a	Shear											180	0							
10a	Shear											165	4							
11a	Joint											180	0							
11a	Joint											170	3							
11a	Joint											180	0							
11a	Shear											180	0							
11a	Shear											180	0							

G.1.3 Opuha dam - Soil descriptions of infill

				Strength							
Outcrop #	Fraction (name)	Colour	Structure	NZGS	PSM Non-cohs	Moisture	Grading	Sorting	Plasticity*	Weathering	Raw field notes
1b	Clay (seam)	L-GY	HOMO	Soft	Loose	Moist	PG	WS	MP	Hw	6mm infill
1b	Fine gravel with some sand & silt	L-GY	HOMO	Stiff	Loose	Moist	WG	PS		Hw	Massive
1c	Sandy silt with some clay	L-GY	HOMO	Firm	Loose	Moist	G	PS		Hw	
1c	Clay (seam)	L-GY	HOMO	Soft	Loose	Moist	PG	WS	MP	Hw	
1d	Clay (seam)	L-GY	HOMO	Soft	Loose	Moist	PG	WS	MP	Hw	9mm clay seam within shear
1d	Silt with some sand and gravel	L-GY	HOMO	Firm	Loose	Moist	G	PS		Hw	30cm large shear
1h	Sandy silt with minor clay	L-GY	HOMO	Soft	Loose	Moist	G	PS		Hw	
2a	Clay (seam)	D-GY	HOMO	Soft	Loose	Moist	PG	WS	MP	Hw	
2a	Sand with some silt and gravel	L-GY	HOMO	V stiff	Loose	Moist	WG	PS		Hw	~5% clay within soil
2a	Silty sand with minor clay	L-GY	HOMO	Firm	Loose	Moist	G	PS		Hw	
2a	Silty sand with minor clay	L-GY	HOMO	Soft	Loose	Moist	G	PS		Hw	
2a	Silty sand with minor clay	L-GY	HOMO	Firm	Loose	Moist	G	PS		Hw	
2a	Silt with some sand & minor clay	L-GY	HOMO	Soft	Loose	Moist	G	PS		Hw	
2a	Silt with some clay	L-GY	HOMO	Firm	Loose	Moist	PG	S	SP	Hw	
2a	Silt with some clay	L-GY	HOMO	Soft	Loose	Moist	PG	S	SP	Hw	
3a	Silt with some clay	L-GY	HOMO	Stiff	Loose	Moist	PG	S	SP	Hw	
3a	Silt with some sand	L-GY	HOMO	Stiff	Loose	Moist	G	PS		Hw	
3a	Coarse sand with some silt	L-GY	HOMO	V stiff	Loose	Moist	G	PS		Hw	
3a	Silt with some sand	L-GY	HOMO	Stiff	Loose	Moist	G	PS		Hw	
3a	Coarse sand with some silt	L-GY	HOMO	V stiff	Loose	Moist	G	PS		Hw	
3a	Silt with some sand	L-GY	HOMO	V stiff	Loose	Moist	G	PS		Hw	
4b	Sandy silt with minor clay	L-GY	HOMO	Hard	Loose	D	G	PS		Hw	
4b	Silty Sandy Gravel	L-GY	HOMO	V weak	Loose	Moist	G	PS		Hw	
4b	Silt with minor clay	L-GY	HOMO	Firm	Loose	Moist	PG	S		Hw	
5a	Silt with minor clay	L-GY	HOMO	Firm	Loose	Moist	PG	S		Hw	
5b	Silt with some sand	L-GY	HOMO	Firm	Loose	D	PG	S		Hw	
5b	Clayey Silt	D-GY	HOMO	Soft	Loose	Moist	PG	S	MP	Hw	
6a	Silty sand with minor clay	L-GY	HOMO	Stiff	Loose	Moist	G	PS		Hw	
6a	Silt with some sand	L-GY	HOMO	Stiff	Loose	Moist	PG	S		Hw	
6a	Silt with minor clay	L-GY	HOMO	Firm	Loose	Moist	PG	S		Hw	
6a	Silt with some sand	L-GY	HOMO	Firm	Loose	Moist	PG	S		Hw	
6a	Silt with some sand and clay	L-GY	HOMO	Firm	Loose	Moist	G	PS	SP	Hw	
6a	Sandy silt with some clay	L-GY	HOMO	Firm	Loose	Moist	G	PS	SP	Hw	
6b	Calcite, clayey silt	L-GY	HOMO	Soft	Loose	Moist	PG	S		Hw	Heavy weathering of calcite veining - soil appearance
6b	Sandy silt	L-GY	HOMO	V stiff	Loose	D	PG	S		Hw	
6b	Silt with minor sand and minor clay	L-GY	HOMO	Stiff	Loose	Moist	G	PS		Hw	
6b	Quartz Sandy silt	L-GY	HOMO	Hard	Loose	Moist	G	S		Hw	
7a	Sandy silt	L-GY	HOMO	Hard	Loose	D	G	S		Hw	
7a	Silty sand with minor clay	L-GY	HOMO	V stiff	Loose	D	PG	PS		Hw	
7a	Silt with some clay	L-GY	HOMO	Firm	Loose	Moist	G	S	SP	Hw	
7b	Sandy silt	L-GY	HOMO	V stiff	Loose	D	G	S		Hw	
7c	Silty gravel with some sand	L-GY	HOMO	Hard	Loose	D	PG	PS		Hw	
7c	Sandy silt with some clay	L-GY	HOMO	Stiff	Loose	Moist	PG	PS	SP	Hw	

G.1.4 Opuha Dam - Breccia fabric descriptions

Outcrop	Fabric support	Fabric arrangement	Fabric (random - lineated?)	% Clast >1mm to Matrix	% of Clasts >2mm	Matrix vs. cement	Rotation angle	Rounding	Clast size	Alteration	Grain size*	Raw field notes
1b	Matrix	Mosaic	Lineated			Matrix		Angular	6mm to silt		Gravel to silt	
1d	Matrix	Rotated	Random			Matrix		Angular	10 x 8 x 7mm		Gravel to silt	
2a	Clast	Crackle	Random			Matrix		Angular	Fine gravel to silt	Green chlorite?	Gravel to silt	
3a	Clast	Mosaic	Random			Cement (Calcite)		Angular		Calcite veining		
4b	Clast	Crackle	Random			Matrix		Angular				
4b	Matrix	Chaotic	Random			Matrix		Sub-Angular				
5a	Clast	Crackle	Random			Cement (Calcite)		Angular		Calcite veining		
5b	Clast	Crackle	Random			Matrix		Angular				
5b	Clast	Mosaic	Lineated			Matrix		Angular		Quartz veining		
6a	Clast	Mosaic	Random			Matrix		Angular				
7a	Clast	Mosaic	Random			Matrix		Angular				
7c	Clast	Crackle	Random			Matrix		Angular				
8a	Clast	Crackle	Random			Matrix		Angular				

G.2 Bedding thickness portions with joint and fault occurrence

Bedding thickness across the study site with joints and faults/shears presented as percentage occurrence respective of bedding thickness.

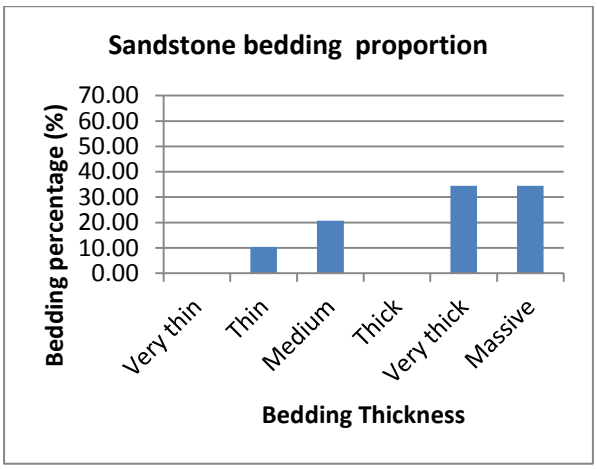

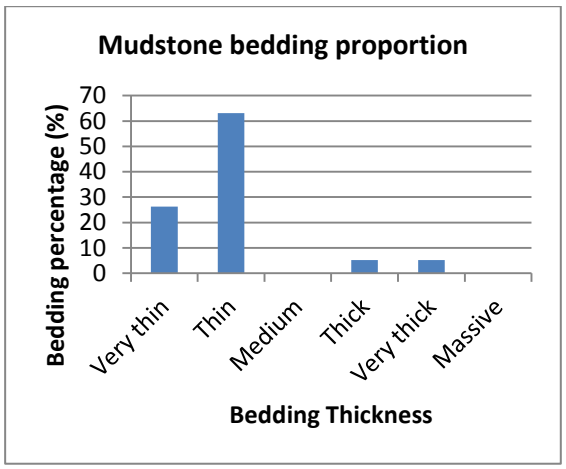

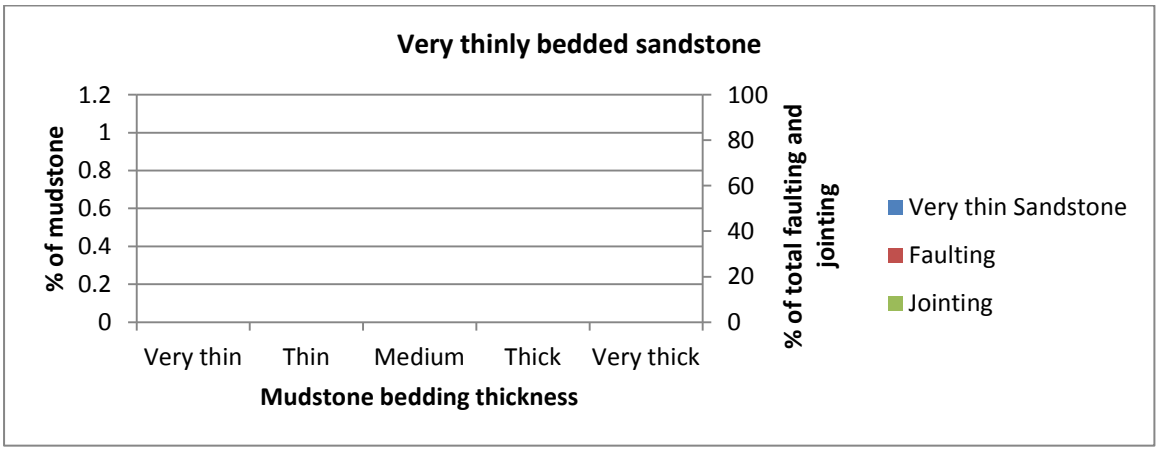

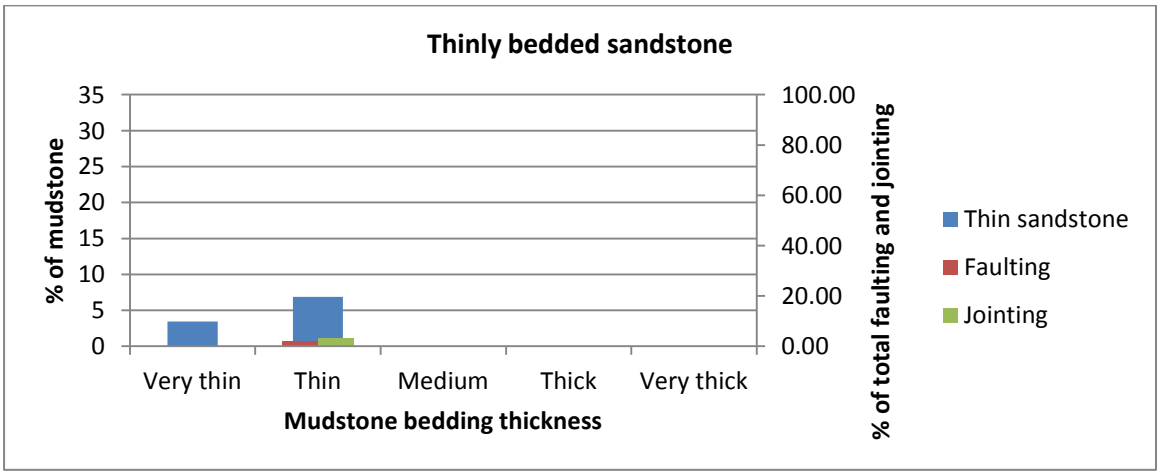

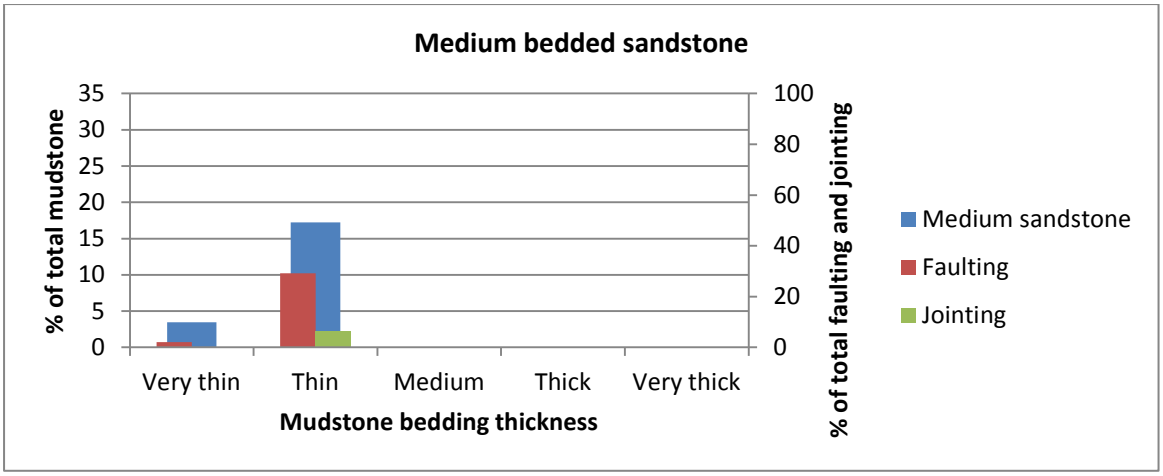
Medium bedded sandstone
% of total mudstone
35
30
25
20
15
10
5
0
100
80
60
40
20
0
% of total faulting and jointing
Very thin
Thin
Medium
Thick
Very thick
Mudstone bedding thickness
Medium sandstone
Faulting
Jointing

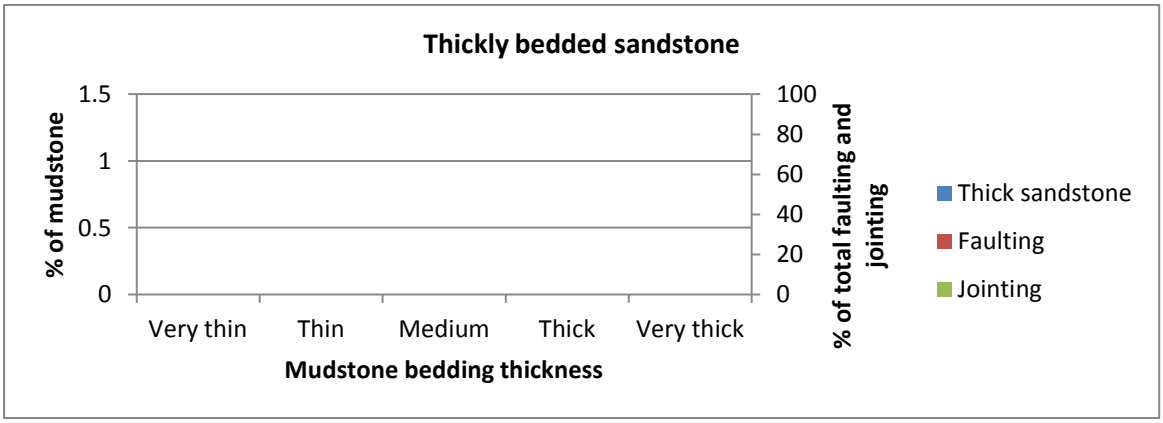
Thickly bedded sandstone
% of mudstone
1.5
1
0.5
0
100
80
60
40
20
0
% of total faulting and jointing
Very thin
Thin
Medium
Thick
Very thick
Mudstone bedding thickness
Thick sandstone
Faulting
Jointing

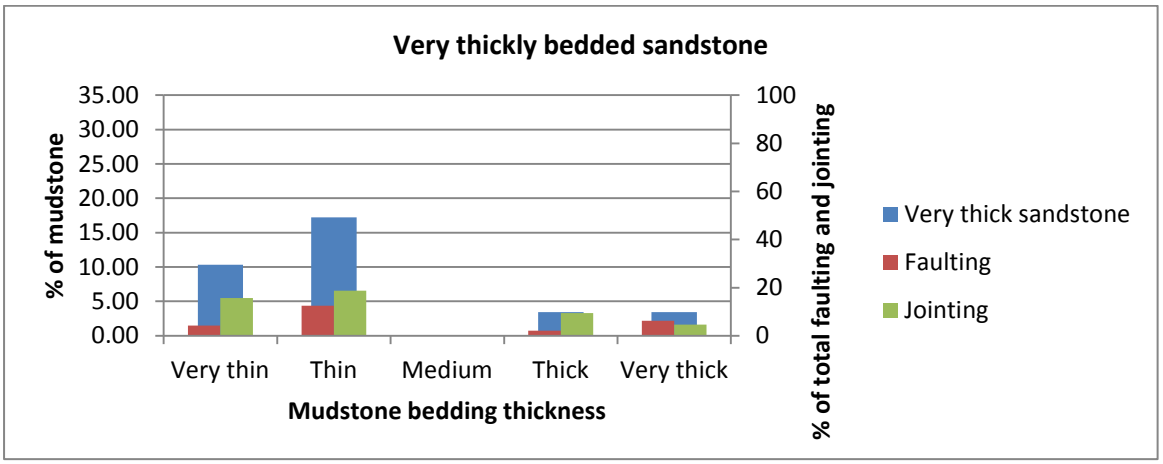
Very thickly bedded sandstone
% of mudstone
35.00
30.00
25.00
20.00
15.00
10.00
5.00
0.00
100
80
60
40
20
0
% of total faulting and jointing
Very thin
Thin
Medium
Thick
Very thick
Mudstone bedding thickness
Very thick sandstone
Faulting
Jointing

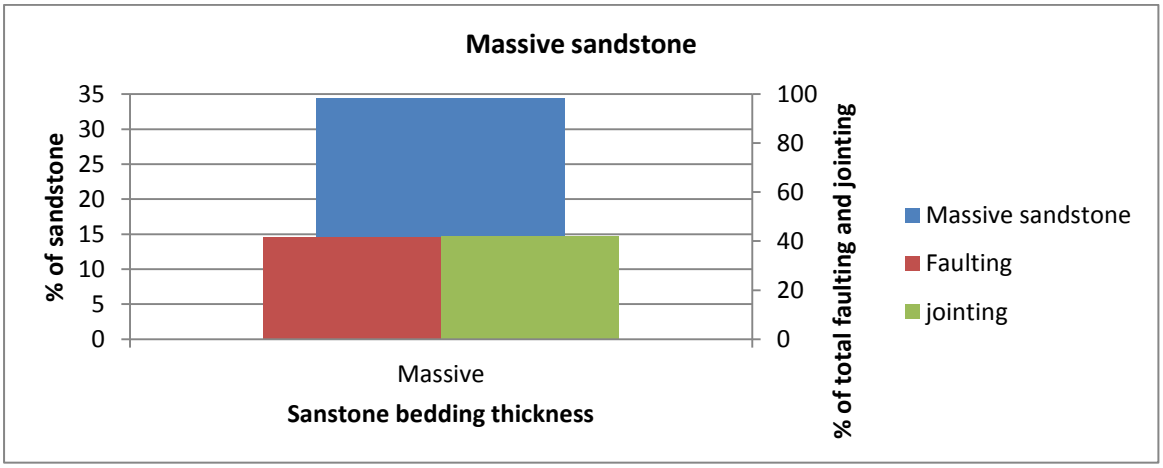
Massive sandstone
% of sandstone
35
30
25
20
15
10
5
0
100
80
60
40
20
0
% of total faulting and jointing
Massive
Sanstone bedding thickness
Massive sandstone
Faulting
jointing

G.3 Opuha Dam steronet analysis

Steronet dip/dip direction analysis of bedding, jointing and faults/shears respectively.

Bedding poles

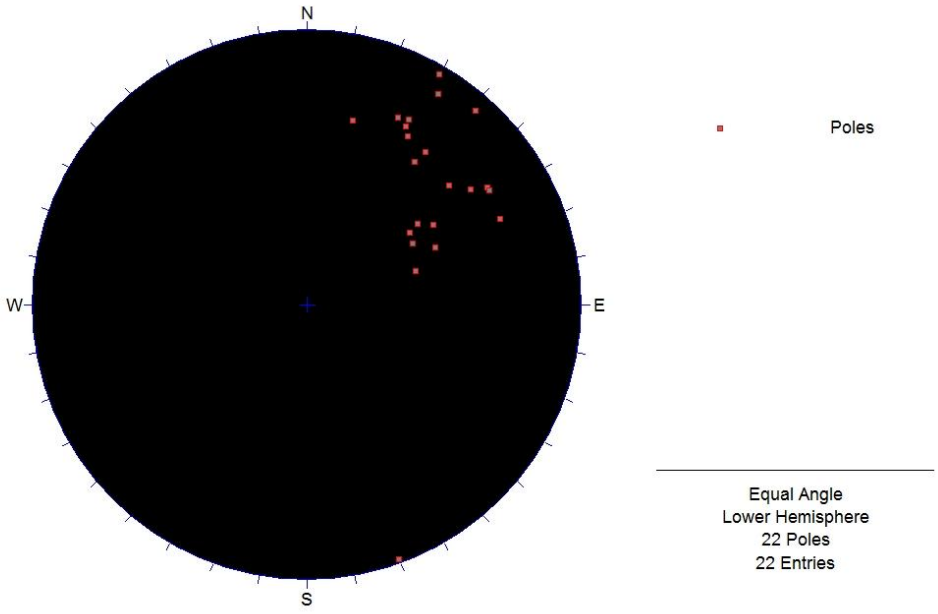

Bedding cluster

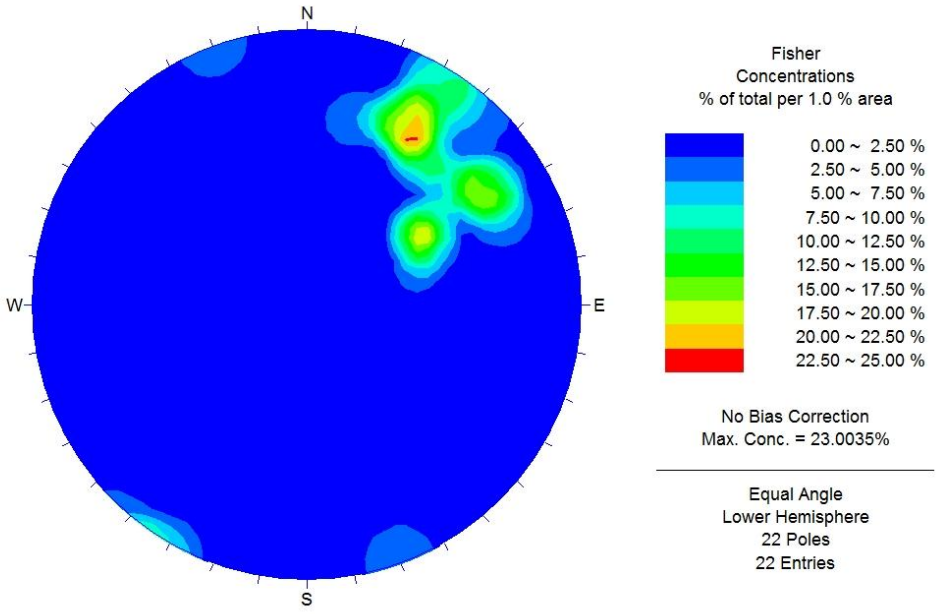

Jointing poles

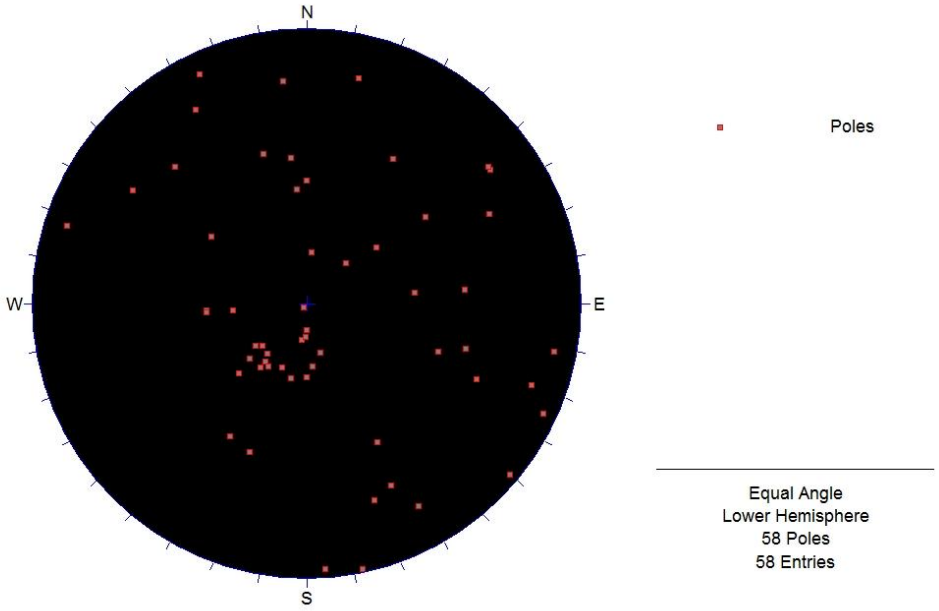

Jointing cluster

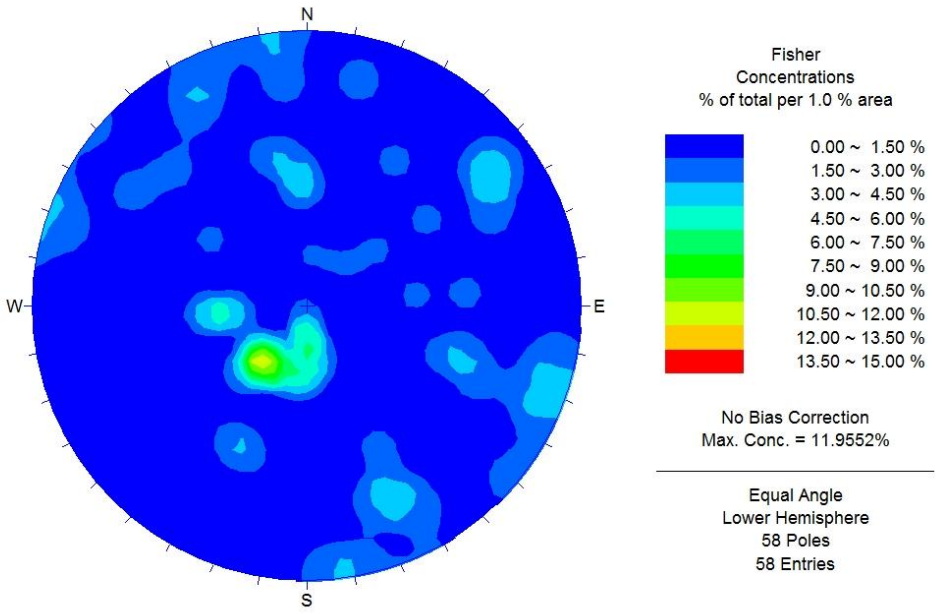

Faulting/shearing poles

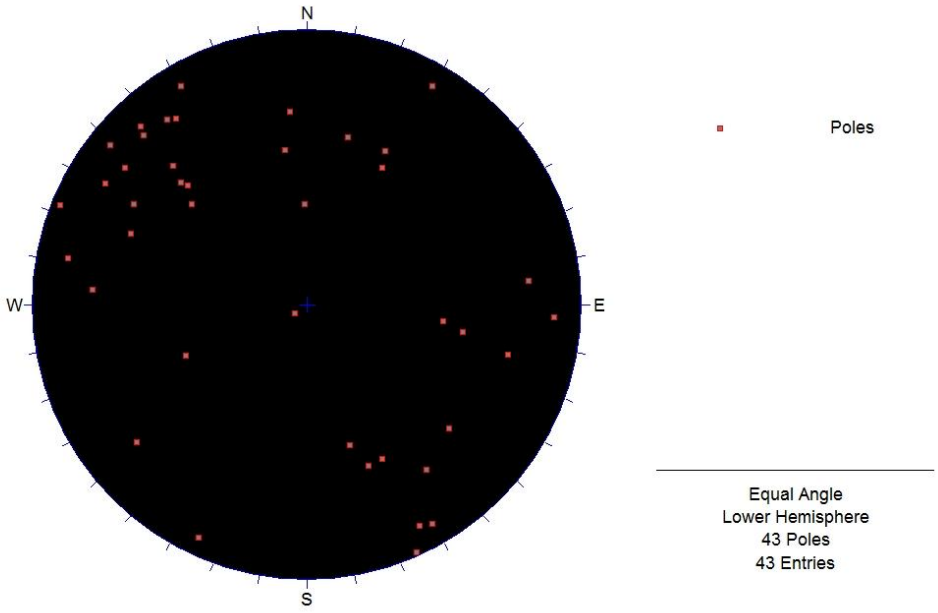

Faulting/shearing cluster

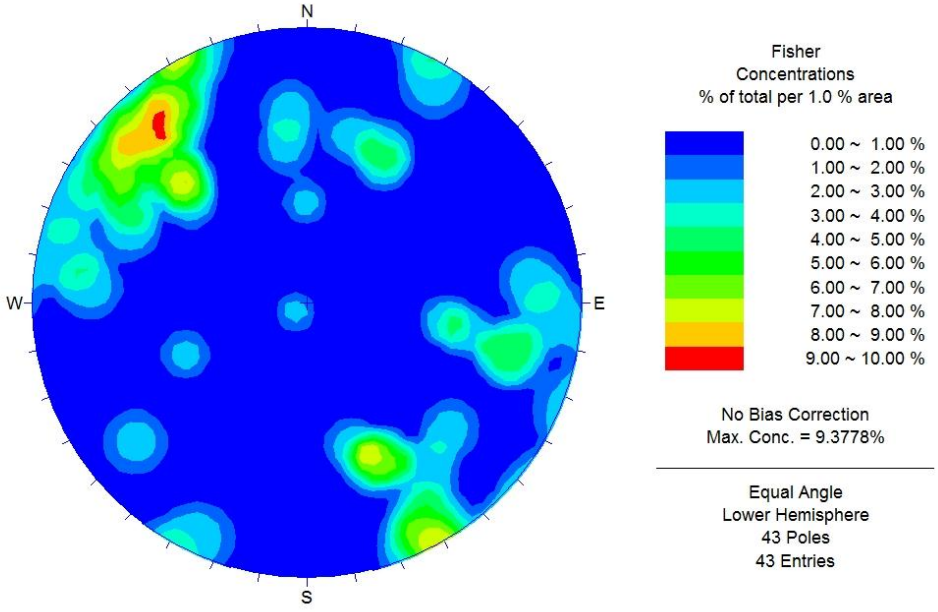

G.4 Opuha Dam BTS raw results and calculations

Brazilian Tensile Strength testing respective of sampled outcrop.

G.4 Opuha Dam - Brazilian Tensile Strength testing

Outcrop	Load (Kn)	Load (N)	Diameter (mm)	Thickness (mm)	MPa	Lithology	Clean?	Failure mode (Szwedzicki, 2007)	Failure time (sec)	Notes
2a	54.3	54300	49.49	26.14	26.70	F-M sandstone	Clean	Multi extension	101	Discontinuity at 45 degrees to load
2a	46.8	46800	49.45	25.04	24.04	F-M sandstone	Clean	Multi extension	98	Discontinuity at 45 degrees to load
2a	44.9	44900	49.27	24.32	23.83	F-M sandstone	Clean	Multi extension	95	
2a	16.5	16500	49.45	24.13	8.79	F-M sandstone	100% existing	Multi fracture	42.6	Multiple discontinuities perpendicular and parallel to load
6b	25.5	25500	49.5	23.8	13.77	F-M sandstone	Clean	Simple extension w/ multi fracture	N/A	
1H	52.1	52100	49.45	24.52	27.33	F-M sandstone	Clean	Simple extension	110	
1H	51.4	51400	49.44	25.39	26.04	F-M sandstone	Clean	Multi extension	107	Hairline discontinuities parallel with load
1H	24.2	24200	49.39	25.45	12.24	F-M sandstone	Clean	Simple extension	62	
1H	36.9	36900	49.39	25.34	18.75	F-M sandstone	Clean	Simple extension	88	Discontinuity parallel to load
5a	47.7	47700	49.38	25.78	23.83	F-M sandstone	Clean	Multi extension	100	Hairline discontinuities parallel and perpendicular with load
5a	51.4	51400	49.44	24.36	27.14	F-M sandstone	Clean	Multi extension	95	Discontinuity perpendicular to load
5a	29.1	29100	49.55	25.03	14.92	F-M sandstone	Clean	Simple extension	74	Multiple hairline discontinuities parallel, 45 and perpendicular to load
5a	35	35000	49.55	25.1	17.90	F-M sandstone	Clean	Multi extension	79	Discontinuity perpendicular to load
9a	40.5	40500	49.49	25.17	20.68	F-M sandstone	Clean	Simple extension	85	
9a	41	41000	49.52	25.12	20.96	F-M sandstone	Clean	Simple extension	88	Discontinuities parallel to load
9a	29.8	29800	49.47	26.3	14.57	F-M sandstone	Clean	Simple extension	79	Discontinuity perpendicular to load

G.5 Opuha Dam Point Load testing raw results and calculations

Point Load Index testing per sample outcrop.

G.5 Opuha Dam - Point Load testing

SAMPLE: 1a

Test No.	Type	P (kN)	D (mm)	W (mm)	A = WD (mm^2)	D_e^2	D_e	I_s	F	$I_{s(50)}$ (MPa)	Lithology	Weathering	Notes
1		1.75	25.6	37.4	956	1217	34.9	1.44	0.850	1.22	F-M Sandstone	Mw	Break along existing
2		7.81	31.9	66.46	2122	2702	52.0	2.89	1.018	2.94	F-M Sandstone	Sw	50% break along existing
3		10.69	36.1	58.72	2118	2697	51.9	3.96	1.017	4.03	F-M Sandstone	Sw	
4		12.10	33.0	57.07	1884	2399	49.0	5.04	0.991	5.00	F-M Sandstone	Sw	
5		13.26	46.4	49.59	2303	2932	54.1	4.52	1.037	4.69	F-M Sandstone	Sw	
6		8.00	17.3	68.26	1184	1507	38.8	5.31	0.892	4.74	F-M Sandstone	Sw	
7		5.51	28.2	48.29	1359	1731	41.6	3.18	0.921	2.93	F-M sandstone	Sw	
8		11.59	21.1	32.93	694	883	29.7	13.12	0.791	10.38	F-M Sandstone	Sw	
9		6.21	17.1	31.82	543	692	26.3	8.97	0.749	6.72	F-M Sandstone	Sw	
10		11.61	20.4	65.8	1342	1709	41.3	6.79	0.918	6.24	F-M sandstone	Sw	

SAMPLE: 1d

Test No.	Type	P (kN)	D (mm)	W (mm)	A = WD (mm^2)	D_e^2	D_e	I_s	F	$I_{s(50)}$ (MPa)	Lithology	Weathering	Notes
1		0.35	34.9	39.02	1361	1732	41.6	0.20	0.921	0.19	Fine Sandstone	Mw	Break along existing quartz & Oxide
2		4.67	19.8	32.17	636	809	28.4	5.77	0.776	4.48	Fine Sandstone	Mw	
3		3.82	24.5	27.68	678	863	29.4	4.42	0.787	3.48	Fine Sandstone	Mw	
4		0.73	21.3	69.5	1478	1881	43.4	0.39	0.938	0.36	Mudstone	Mw	
5		0.61	14.8	31.6	468	595	24.4	1.02	0.724	0.74	Mudstone	Mw	
6		5.85	32.5	40	1299	1654	40.7	3.54	0.911	3.22	Fine SandStone	Mw	
7		5.79	19.8	33.07	655	835	28.9	6.94	0.781	5.42	Fine SandStone	Mw	
8		0.71	33.1	39.55	1309	1667	40.8	0.43	0.913	0.39	Fine SandStone	Mw	Most break along existing
9		2.19	26.9	42.24	1136	1447	38.0	1.51	0.884	1.34	Mudstone	Mw	
10		2.40	13.8	47.08	647	824	28.7	2.91	0.779	2.27	Fine SandStone	Mw	
11		6.80	43.7	36.53	1596	2033	45.1	3.35	0.954	3.19	Fine SandStone	Mw	
12		2.09	22.5	43.75	983	1252	35.4	1.67	0.856	1.43	Fine SandStone	Mw	Break along existing
13		4.86	22.3	32.37	721	918	30.3	5.29	0.798	4.23	Fine SandStone	Mw	
14		3.17	19.6	54.21	1060	1350	36.7	2.35	0.871	2.04	Fine SandStone	Mw	Some break along existing
15		3.17	22.7	50.9	1156	1472	38.4	2.15	0.888	1.91	Fine SandStone	Mw	Some break along existing

SAMPLE: 1h

Test No.	Type	P (kN)	D (mm)	W (mm)	A = WD (mm^2)	D_e^2	D_e	I_s	F	$I_{s(50)}$ (MPa)	Lithology	Weathering	Notes
1		3.11	25.8	45.01	1159	1476	38.4	2.11	0.888	1.87	Mudstone	Sw	
2		3.64	23.3	18.06	421	536	23.2	6.79	0.707	4.80	Mudstone	Sw	
3		1.28	20.0	34.88	698	888	29.8	1.44	0.792	1.14	Mudstone	Sw	
4		14.94	24.6	49.32	1213	1544	39.3	9.68	0.897	8.68	F-M Sandstone	Sw	
5		15.18	23.7	40.83	966	1229	35.1	12.35	0.852	10.52	F-M Sandstone	Sw	
6		8.72	12.9	48.6	626	798	28.2	10.93	0.773	8.45	F-M Sandstone	Sw	
7		16.04	23.5	49.11	1154	1469	38.3	10.92	0.887	9.69	F-M Sandstone	Sw	
8		9.35	24.0	49.5	1189	1514	38.9	6.17	0.893	5.52	F-M Sandstone	Sw	
9		7.29	16.1	47.89	771	981	31.3	7.43	0.810	6.02	F-M Sandstone	Sw	
10		2.03	4.4	49.15	214	272	16.5	7.46	0.607	4.53	F-M Sandstone	Sw	
11		12.35	22.7	64.51	1466	1867	43.2	6.62	0.936	6.19	F-M Sandstone	Sw	
12		19.31	32.3	62.55	2020	2572	50.7	7.51	1.006	7.56	F-M Sandstone	Sw	

SAMPLE: 2a

Test No.	Type	P (kN)	D (mm)	W (mm)	A = WD (mm^2)	D_e^2	D_e	I_s	F	$I_{s(50)}$ (MPa)	Lithology	Weathering	Notes
1		8.64	26.0	36.29	945	1203	34.7	7.18	0.848	6.09	F-M Sandstone	Sw	
2		5.30	11.5	57.91	667	849	29.1	6.25	0.784	4.90	F-M Sandstone	Sw	
3		22.93	38.3	89.42	3424	4359	66.0	5.26	1.133	5.96	F-M Sandstone	Sw	
4		8.02	42.9	45.33	1943	2474	49.7	3.24	0.998	3.23	F-M Sandstone	Sw	Break along existing quartz
5		6.50	15.6	29.49	460	586	24.2	11.10	0.721	8.01	F-M Sandstone	Sw	
6		4.51	9.2	49.31	455	579	24.1	7.78	0.720	5.60	F-M Sandstone	Sw	
7		8.64	15.4	43.72	674	858	29.3	10.07	0.786	7.92	F-M Sandstone	Sw	
8		12.43	23.7	46.5	1104	1406	37.5	8.84	0.878	7.77	F-M Sandstone	Sw	
9		7.02	19.8	39.98	792	1008	31.7	6.96	0.815	5.68	F-M Sandstone	Sw	

SAMPLE: 4a

Test No.	Type	P (kN)	D (mm)	W (mm)	A = WD (mm^2)	D_e^2	D_e	I_s	F	$I_{s(50)}$ (MPa)	Lithology	Weathering	Notes
1	Parallel	2.95	12.5	59.22	739	941	30.7	3.13	0.803	2.52	Fine Sandstone	Sw	50% break along existing
2	Parallel	3.13	12.4	38.68	481	612	24.7	5.11	0.729	3.73	Fine Sandstone	Sw	
3		0.08	15.2	56.89	866	1103	33.2	0.07	0.832	0.06	Fine Sandstone	Sw	Break along existing oxide
4		4.31	15.1	54.48	821	1045	32.3	4.12	0.822	3.39	Fine Sandstone	Sw	Some break along existing oxide
5		10.98	17.1	41.9	716	912	30.2	12.04	0.797	9.60	F-M Sandstone	Sw	
6		9.13	18.8	41.67	783	997	31.6	9.15	0.813	7.44	F-M Sandstone	Sw	
7		8.48	13.8	39.61	546	695	26.4	12.19	0.750	9.14	F-M Sandstone	Sw	
8		11.94	21.9	34.92	765	974	31.2	12.26	0.809	9.91	F-M Sandstone	Sw	
9		13.10	20.9	53.35	1117	1422	37.7	9.21	0.881	8.11	F-M Sandstone	Sw	
10		4.19	10.4	34.91	364	463	21.5	9.05	0.684	6.19	F-M Sandstone	Sw	50% break along existing
11		5.38	17.3	39.49	683	870	29.5	6.18	0.789	4.88	F-M Sandstone	Sw	
12		3.56	7.1	46.05	327	417	20.4	8.54	0.668	5.71	F-M Sandstone	Sw	
13		3.41	13.3	37.18	493	628	25.1	5.43	0.733	3.98	F-M Sandstone	Sw	
14		1.46	19.0	52.52	999	1273	35.7	1.15	0.859	0.99	Quartz	Mw	
15		0.91	29.7	63.26	1879	2392	48.9	0.38	0.990	0.38	Quartz	Mw	

G.5 Opuha Dam - Point Load testing

SAMPLE: 4b

Test No.	Type	P (kN)	D (mm)	W (mm)	A = WD (mm^2)	D_e^2	D_e	I_s	F	$I_{s(50)}$ (MPa)	Lithology	Weathering	Notes
1		3.25	20.0	45.36	906	1154	34.0	2.82	0.840	2.37	Mudstone	Sw	
2		7.06	18.4	52.9	975	1241	35.2	5.69	0.854	4.86	Mudstone	Sw	
3		3.19	22.1	40.93	905	1152	33.9	2.77	0.840	2.33	F-M Sandstone	Sw	50% break along existing
4		2.52	17.6	35.07	618	786	28.0	3.20	0.771	2.47	Mudstone	Sw	
5		2.87	20.8	36.93	767	977	31.3	2.94	0.809	2.38	Fine Sandstone	Sw	
6		5.22	23.6	28.96	683	870	29.5	6.00	0.789	4.73	Fine Sandstone	Sw	
7		8.44	21.8	52.79	1153	1468	38.3	5.75	0.887	5.10	Mudstone	Sw	
8		0.47	28.8	35.09	1009	1285	35.8	0.37	0.861	0.31	Fine Sandstone	Sw	Break along existing
9		4.65	10.6	26.63	283	360	19.0	12.90	0.647	8.34	Mudstone	Sw	
10		1.14	10.3	18.29	188	239	15.5	4.76	0.590	2.81	Fine Sandstone	Sw	
11		9.66	21.5	54.45	1170	1489	38.6	6.49	0.890	5.77	F-M Sandstone	Sw	
12		5.00	27.7	50.25	1393	1774	42.1	2.82	0.926	2.61	F-M Sandstone	Sw	Some break along existing
13		9.96	20.9	60.71	1271	1618	40.2	6.16	0.907	5.58	F-M Sandstone	Sw	
14		5.30	19.6	63	1234	1571	39.6	3.37	0.901	3.04	F-M Sandstone	Sw	Some break along existing quartz
15		9.21	20.7	47.84	988	1258	35.5	7.32	0.857	6.27	F-M Sandstone	Sw	

SAMPLE: 4b - shear

Test No.	Type	P (kN)	D (mm)	W (mm)	A = WD (mm^2)	D_e^2	D_e	I_s	F	$I_{s(50)}$ (MPa)	Lithology	Weathering	Notes
1		3.31	42.0	32.41	1361	1732	41.6	1.91	0.921	1.76	F-M Sandstone	Sw	Heavily quartz veined
2		1.02	38.4	42.17	1618	2061	45.4	0.49	0.957	0.47	F-M Sandstone	Sw	Heavily quartz veined
3		0.26	33.4	34.6	1155	1470	38.3	0.18	0.887	0.16	F-M Sandstone	Sw	Break along existing quartz
4		0.91	21.9	33.28	730	929	30.5	0.98	0.800	0.78	F-M Sandstone	Sw	Break along existing quartz
5		0.53	28.0	56.79	1592	2027	45.0	0.26	0.954	0.25	F-M Sandstone	Sw	Break along existing quartz
6		0.75	28.9	40.85	1179	1502	38.8	0.50	0.892	0.45	F-M Sandstone	Sw	Break along existing quartz
7		0.24	32.7	43.29	1417	1804	42.5	0.13	0.929	0.12	F-M Sandstone	Sw	Break along existing quartz

SAMPLE: 5a

Test No.	Type	P (kN)	D (mm)	W (mm)	A = WD (mm^2)	D_e^2	D_e	I_s	F	$I_{s(50)}$ (MPa)	Lithology	Weathering	Notes
1		2.97	17.2	43.7	752	958	30.9	3.10	0.806	2.50	F-M Sandstone	Mw	Quartz shear rock
2		2.15	39.5	59.29	2339	2978	54.6	0.72	1.040	0.75	F-M Sandstone	Mw	Quartz shear rock - break along existing vein
3		2.89	12.8	28.03	360	458	21.4	6.31	0.683	4.31	F-M Sandstone	Mw	Quartz shear rock
4		3.11	21.0	39.47	830	1056	32.5	2.94	0.824	2.43	F-M Sandstone	Mw	Quartz shear rock
5		0.39	14.5	21.71	315	401	20.0	0.97	0.662	0.64	F-M Sandstone	Mw	Quartz shear rock
6		5.42	25.8	35.08	906	1154	34.0	4.70	0.840	3.95	F-M Sandstone	Mw	Quartz shear rock
7		1.16	9.3	22.08	204	260	16.1	4.46	0.601	2.68	F-M Sandstone	Mw	Quartz shear rock
8		2.72	13.7	30.45	416	530	23.0	5.14	0.705	3.62	F-M Sandstone	Mw	Quartz shear rock
9		14.16	34.5	49.43	1706	2172	46.6	6.52	0.969	6.32	F-M Sandstone	Sw	
10		19.63	52.4	60.29	3158	4021	63.4	4.88	1.113	5.43	F-M Sandstone	Sw	
11		22.59	44.9	83.28	3737	4758	69.0	4.75	1.156	5.49	F-M Sandstone	Sw	Some quartz break
12		26.15	51.6	67.22	3469	4416	66.5	5.92	1.137	6.73	F-M Sandstone	Sw	
13		19.71	35.3	53.15	1874	2385	48.8	8.26	0.990	8.18	F-M Sandstone	Sw	
14		14.49	31.5	46.52	1463	1863	43.2	7.78	0.936	7.28	F-M Sandstone	Sw	
15		2.97	12.6	27.32	343	437	20.9	6.79	0.676	4.59	F-M Sandstone	Sw	

SAMPLE: 5b - shear (left)

Test No.	Type	P (kN)	D (mm)	W (mm)	A = WD (mm^2)	D_e^2	D_e	I_s	F	$I_{s(50)}$ (MPa)	Lithology	Weathering	Notes
1		0.59	30.8	50.86	1566	1995	44.7	0.30	0.950	0.28	F-M Sandstone	Mw	Break along existing
2		6.72	21.3	64.23	1366	1739	41.7	3.86	0.922	3.56	F-M Sandstone	Mw	
3		1.97	25.4	37.82	959	1221	34.9	1.61	0.851	1.37	F-M Sandstone	Mw	
4		1.34	28.0	39.72	1113	1417	37.6	0.95	0.880	0.83	F-M Sandstone	Mw	Break along existing
5		0.47	17.9	34.75	622	792	28.1	0.59	0.772	0.46	F-M Sandstone	Mw	
6		1.10	13.1	43.25	567	722	26.9	1.52	0.756	1.15	F-M Sandstone	Mw	
7		1.75	19.0	36.42	691	880	29.7	1.99	0.791	1.57	F-M Sandstone	Mw	
8		4.88	17.4	51.04	887	1129	33.6	4.32	0.836	3.61	F-M Sandstone	Mw	
9		1.48	27.9	28.51	795	1013	31.8	1.46	0.816	1.19	F-M Sandstone	Mw	

SAMPLE: 5b - shear (right)

Test No.	Type	P (kN)	D (mm)	W (mm)	A = WD (mm^2)	D_e^2	D_e	I_s	F	$I_{s(50)}$ (MPa)	Lithology	Weathering	Notes
1		0.65	29.1	36.55	1063	1354	36.8	0.48	0.871	0.42	F-M Sandstone	Hw	
2		0.39	22.0	36.01	793	1010	31.8	0.39	0.815	0.32	F-M Sandstone	Hw	Break along existing quartz
3		1.12	38.0	57.28	2175	2770	52.6	0.40	1.023	0.41	F-M Sandstone	Mw	Some break along existing oxide
4		0.95	32.8	48.97	1608	2048	45.3	0.46	0.956	0.44	F-M Sandstone	Mw	Break along existing quartz
5		1.69	26.0	49.59	1291	1644	40.5	1.03	0.910	0.94	Fine Sandstone	Mw	
6		0.67	24.9	31.68	789	1005	31.7	0.67	0.815	0.54	Fine Sandstone	Mw	Break along heavy quartz veining
7		1.02	33.7	25.98	876	1116	33.4	0.91	0.834	0.76	Fine Sandstone	Mw	
8		0.95	32.3	42.17	1361	1733	41.6	0.55	0.921	0.50	F-M Sandstone	Mw	

SAMPLE: 6b

Test No.	Type	P (kN)	D (mm)	W (mm)	A = WD (mm^2)	D_e^2	D_e	I_s	F	$I_{s(50)}$ (MPa)	Lithology	Weathering	Notes
1		3.52	26.2	35.2	922	1174	34.3	3.00	0.844	2.53	F-M Sandstone	Mw	Most break along existing
2		15.77	35.1	50.54	1772	2256	47.5	6.99	0.977	6.83	F-M Sandstone	Sw	
3		7.15	24.1	38.76	935	1191	34.5	6.00	0.846	5.08	F-M Sandstone	Sw	
4		6.21	14.5	68.41	990	1260	35.5	4.93	0.857	4.22	F-M Sandstone	Sw	
5		12.29	23.1	34.5	796	1014	31.8	12.12	0.816	9.89	F-M Sandstone	Sw	
6		16.56	26.4	60.75	1601	2038	45.1	8.12	0.955	7.76	F-M Sandstone	Sw	
7		13.51	20.1	65.97	1325	1687	41.1	8.01	0.915	7.33	F-M Sandstone	Sw	
8		10.31	15.3	32.96	506	644	25.4	16.02	0.737	11.80	F-M Sandstone	Sw	
9		2.36	20.0	53.26	1063	1353	36.8	1.74	0.871	1.52	Mudstone	Mw	
10		2.26	20.1	26.08	524	667	25.8	3.39	0.743	2.52	Mudstone	Mw	
11		3.86	22.6	27.88	631	803	28.3	4.81	0.775	3.72	Fine Sandstone	Sw	
12		0.95	15.4	25.41	391	498	22.3	1.91	0.696	1.33	Mudstone	Sw	
13		1.20	6.4	42.26	272	346	18.6	3.47	0.641	2.22	Mudstone	Sw	

G.5 Opuha Dam - Point Load testing

SAMPLE: 7a - shear

Test No.	Type	P (kN)	D (mm)	W (mm)	A = WD (mm^2)	D_e^2	D_e	I_s	F	$I_{s(50)}$ (MPa)	Lithology	Weathering	Notes
1		0.85	27.3	55.25	1506	1918	43.8	0.44	0.942	0.42	F-M Sandstone	Mw	Break along existing quartz
2		4.71	19.0	42.45	805	1025	32.0	4.60	0.818	3.76	F-M Sandstone	Mw	
3		3.45	18.6	45.49	848	1080	32.9	3.20	0.828	2.65	F-M Sandstone	Mw	
4		2.22	21.1	24.68	520	662	25.7	3.35	0.742	2.49	F-M Sandstone	Mw	
5		1.04	16.5	39.43	649	827	28.8	1.26	0.780	0.98	F-M Sandstone	Mw	
6		1.71	14.0	42.2	592	754	27.5	2.27	0.764	1.73	F-M Sandstone	Mw	
7		4.39	18.2	35.08	639	814	28.5	5.39	0.777	4.19	F-M Sandstone	Mw	
8		1.20	17.3	45.48	786	1001	31.6	1.20	0.814	0.98	F-M Sandstone	Mw	Break along existing quartz
9		2.05	14.2	30.47	434	552	23.5	3.71	0.712	2.64	F-M Sandstone	Mw	

SAMPLE: 7b

Test No.	Type	P (kN)	D (mm)	W (mm)	A = WD (mm^2)	D_e^2	D_e	I_s	F	$I_{s(50)}$ (MPa)	Lithology	Weathering	Notes
1		8.30	13.0	54.15	702	894	29.9	9.28	0.793	7.36	F-M Sandstone	Sw	
2		9.01	22.7	54.74	1242	1581	39.8	5.70	0.902	5.14	F-M Sandstone	Sw	
3		8.78	22.5	39.7	892	1135	33.7	7.73	0.837	6.48	F-M Sandstone	Sw	Some break along existing quartz
4		11.06	45.2	52.94	2392	3046	55.2	3.63	1.045	3.80	F-M Sandstone	Sw	
5		3.96	14.3	47.63	681	867	29.4	4.57	0.788	3.60	F-M Sandstone	Sw	
6		9.17	22.8	49.48	1128	1436	37.9	6.38	0.883	5.64	F-M Sandstone	Sw	
7		2.82	12.5	43.78	549	699	26.4	4.03	0.751	3.03	F-M Sandstone	Sw	50% break along existing quartz

SAMPLE: 7c

Test No.	Type	P (kN)	D (mm)	W (mm)	A = WD (mm^2)	D_e^2	D_e	I_s	F	$I_{s(50)}$ (MPa)	Lithology	Weathering	Notes
1	Perpendicular	7.35	14.5	30.42	440	560	23.7	13.12	0.714	9.37	Mudstone	Sw	1mm fine sand band
2		0.98	15.9	25.15	399	508	22.5	1.93	0.699	1.35	Mudstone	Sw	
3		0.49	24.7	28.04	692	881	29.7	0.56	0.791	0.44	Mudstone	Sw	Most break along existing
4		3.94	13.8	27.42	378	481	21.9	8.19	0.690	5.65	Mudstone	Sw	
5		6.07	17.9	31.37	562	715	26.7	8.49	0.755	6.40	Mudstone	Sw	
6		2.76	15.9	26.44	420	535	23.1	5.16	0.707	3.65	Mudstone	Sw	
7		7.85	17.1	45.45	777	989	31.4	7.94	0.812	6.44	Mudstone	Sw	
8		4.59	12.9	38.58	497	633	25.2	7.25	0.734	5.33	Mudstone	Sw	
9		13.06	26.4	45.99	1214	1545	39.3	8.45	0.897	7.58	F-M Sandstone	Sw	
10		12.43	33.0	87.49	2891	3681	60.7	3.38	1.091	3.68	F-M Sandstone	Sw	50% break along existing
11		3.90	21.0	34.38	720	917	30.3	4.25	0.798	3.39	F-M Sandstone	Sw	
12		8.93	16.3	35.3	576	734	27.1	12.17	0.759	9.24	F-M Sandstone	Sw	
13		10.02	17.4	36.33	633	806	28.4	12.43	0.775	9.63	F-M Sandstone	Sw	
14		11.08	19.6	41.16	808	1028	32.1	10.78	0.819	8.82	F-M Sandstone	Sw	
15		11.59	26.3	44.34	1164	1482	38.5	7.82	0.889	6.95	F-M Sandstone	Sw	50% break along existing quartz

SAMPLE: 9a

Test No.	Type	P (kN)	D (mm)	W (mm)	A = WD (mm^2)	D_e^2	D_e	I_s	F	$I_{s(50)}$ (MPa)	Lithology	Weathering	Notes
1		6.66	16.7	75.13	1257	1600	40.0	4.16	0.905	3.76	F-M Sandstone	Sw	50% break along existing oxide
2		13.92	31.1	34.51	1072	1365	36.9	10.20	0.873	8.90	F-M Sandstone	Sw	
3		13.98	20.8	61.14	1274	1622	40.3	8.62	0.907	7.82	F-M Sandstone	Sw	
4		8.00	9.2	59.22	544	692	26.3	11.56	0.749	8.66	F-M Sandstone	Sw	
5		9.61	29.1	47.71	1389	1768	42.1	5.43	0.925	5.03	F-M Sandstone	Sw	
6		11.98	33.6	37.74	1267	1613	40.2	7.43	0.906	6.73	F-M Sandstone	Sw	
7		8.58	14.1	73.81	1039	1323	36.4	6.48	0.867	5.62	F-M Sandstone	Sw	
8		8.10	12.8	72.25	921	1173	34.2	6.91	0.843	5.82	F-M Sandstone	Sw	
9		18.80	27.6	56.69	1564	1991	44.6	9.44	0.950	8.97	F-M Sandstone	Sw	
10		3.96	10.8	36.92	400	509	22.6	7.78	0.699	5.44	F-M Sandstone	Sw	
11		8.04	10.8	42.12	456	580	24.1	13.86	0.720	9.97	F-M Sandstone	Sw	

G.6 Opuha Dam fines index test results and calculations

Fines content results and calculation tables produced from wet sieving and laser size analysis per sample outcrop.

G.6 Opuha Dam - fines index testing

1c				
Passing (wet sieve)	**Raw weight (g)**	**Container weight (g)**	**Sample weight (g)**	**Sample fines division (%)**
>4mm	253.22	200.03	53.19	11.98
>2mm (gravel)	422.64	354.29	68.35	15.39
>1mm (coarse sand)	269.53	193.92	75.61	17.03
Remaining fraction (<1mm)	280.35	33.44	246.91	55.60
Total sample weight (g)			444.06	
Matrix (lasersizer)	**Average diameter (µm)**	**Cumulative %**	**Actual %**	**% of total <1mm fraction**
<2 microns (clay)	2	9.2	9.20	5.12
<60 microns (silt)	59.57	68	58.80	32.69
<200 microns (fine sand)	199.53	90.2	22.20	12.34
Remaining fraction (medium/coarse sand)		100	9.80	5.45

2a				
Passing (wet sieve)	**Raw weight (g)**	**Container weight (g)**	**Sample weight (g)**	**Sample fines division (%)**
>4mm	307.2	115.42	191.78	25.95
>2mm (gravel)	231.57	116.98	114.59	15.50
>1mm (coarse sand)	424.6	354.29	70.31	9.51
Remaining fraction (<1mm)	396.36	33.93	362.43	49.04
Total sample weight (g)			739.11	
Matrix (lasersizer)	**Average diameter (µm)**	**Cumulative %**	**Actual %**	**% of total <1mm fraction**
<2 microns (clay)	2	10.3	10.30	5.05
<60 microns (silt)	59.57	61	50.70	24.86
<200 microns (fine sand)	199.53	84	23.00	11.28
Remaining fraction (medium/coarse sand)		100	16.00	7.85

4b				
Passing (wet sieve)	**Raw weight (g)**	**Container weight (g)**	**Sample weight (g)**	**Sample fines division (%)**
>4mm	629.06	352.51	276.55	30.96
>2mm (gravel)	468.89	357.96	110.93	12.42
>1mm (coarse sand)	279.32	212.44	66.88	7.49
Remaining fraction (<1mm)	472.82	33.82	439	49.14
Total sample weight (g)			893.36	
Matrix (lasersizer)	**Average diameter (µm)**	**Cumulative %**	**Actual %**	**% of total <1mm fraction**
<2 microns (clay)	2	9.9	9.90	4.86
<60 microns (silt)	59.57	56.9	47.00	23.10
<200 microns (fine sand)	199.53	79	22.10	10.86
Remaining fraction (medium/coarse sand)		100	21.00	10.32

5b				
Passing (wet sieve)	**Raw weight (g)**	**Container weight (g)**	**Sample weight (g)**	**Sample fines division (%)**
>4mm	613.47	352.61	260.86	31.27
>2mm (gravel)	479.52	357.96	121.56	14.57
>1mm (coarse sand)	304.41	212.44	91.97	11.02
Remaining fraction (<1mm)	423.4	63.5	359.9	43.14
Total sample weight (g)			834.29	
Matrix (lasersizer)	**Average diameter (µm)**	**Cumulative %**	**Actual %**	**% of total <1mm fraction**
<2 microns (clay)	2	5.8	5.80	2.50
<60 microns (silt)	59.57	57.7	51.90	22.39
<200 microns (fine sand)	199.53	82.8	25.10	10.83
Remaining fraction (medium/coarse sand)		100	17.20	7.42

G.6 Opuha Dam - fines index testing

7a				
Passing (wet sieve)	**Raw weight (g)**	**Container weight (g)**	**Sample weight (g)**	**Sample fines division (%)**
>4mm	715.77	603.66	112.11	14.16
>2mm (gravel)	257.06	199.97	57.09	7.21
>1mm (coarse sand)	289.67	193.89	95.78	12.10
Remaining fraction (<1mm)	560.22	33.7	526.52	66.52
Total sample weight (g)			791.5	
Matrix (lasersizer)	**Average diameter (µm)**	**Cumulative %**	**Actual %**	**% of total <1mm fraction**
<2 microns (clay)	2	10.8	10.80	7.18
<60 microns (silt)	59.57	69.2	58.40	38.85
<200 microns (fine sand)	199.53	84.8	15.60	10.38
Remaining fraction (medium/coarse sand)		100	15.20	10.11

1h - Clay				
Matrix (lasersizer)	**Average diameter (µm)**	**Cumulative %**	**Actual %**	**% of total sample**
<2 microns (clay)	2	9.8	9.80	9.80
<60 microns (silt)	59.57	54.6	44.80	44.80
<200 microns (fine sand)	199.53	55.9	1.30	1.30
Remaining fraction (medium/coarse sand)		100	44.10	44.10

2a - Clay				
Matrix (lasersizer)	**Average diameter (µm)**	**Cumulative %**	**Actual %**	**% of total sample**
<2 microns (clay)	2	13.5	13.50	13.50
<60 microns (silt)	59.57	59.1	45.60	45.60
<200 microns (fine sand)	199.53	59.5	0.40	0.40
Remaining fraction (medium/coarse sand)		100	40.50	40.50

7a - Clay				
Matrix (lasersizer)	**Average diameter (µm)**	**Cumulative %**	**Actual %**	**% of total sample**
<2 microns (clay)	2	27.1	27.10	27.10
<60 microns (silt)	59.57	100	72.90	72.90
<200 microns (fine sand)	199.53	0	0.00	0.00
Remaining fraction (medium/coarse sand)		0	0.00	0.00

Appendix H: Blockiness analysis

Bedding thickness and degree of fracture per bedding thickness for all outcrops surveyed defining blockiness. The relationship between bedding thickness and degree of fracture has been grouped into 6 representative rock mass classes that encompass the range of occurrence and make up the TRC blockiness axis.

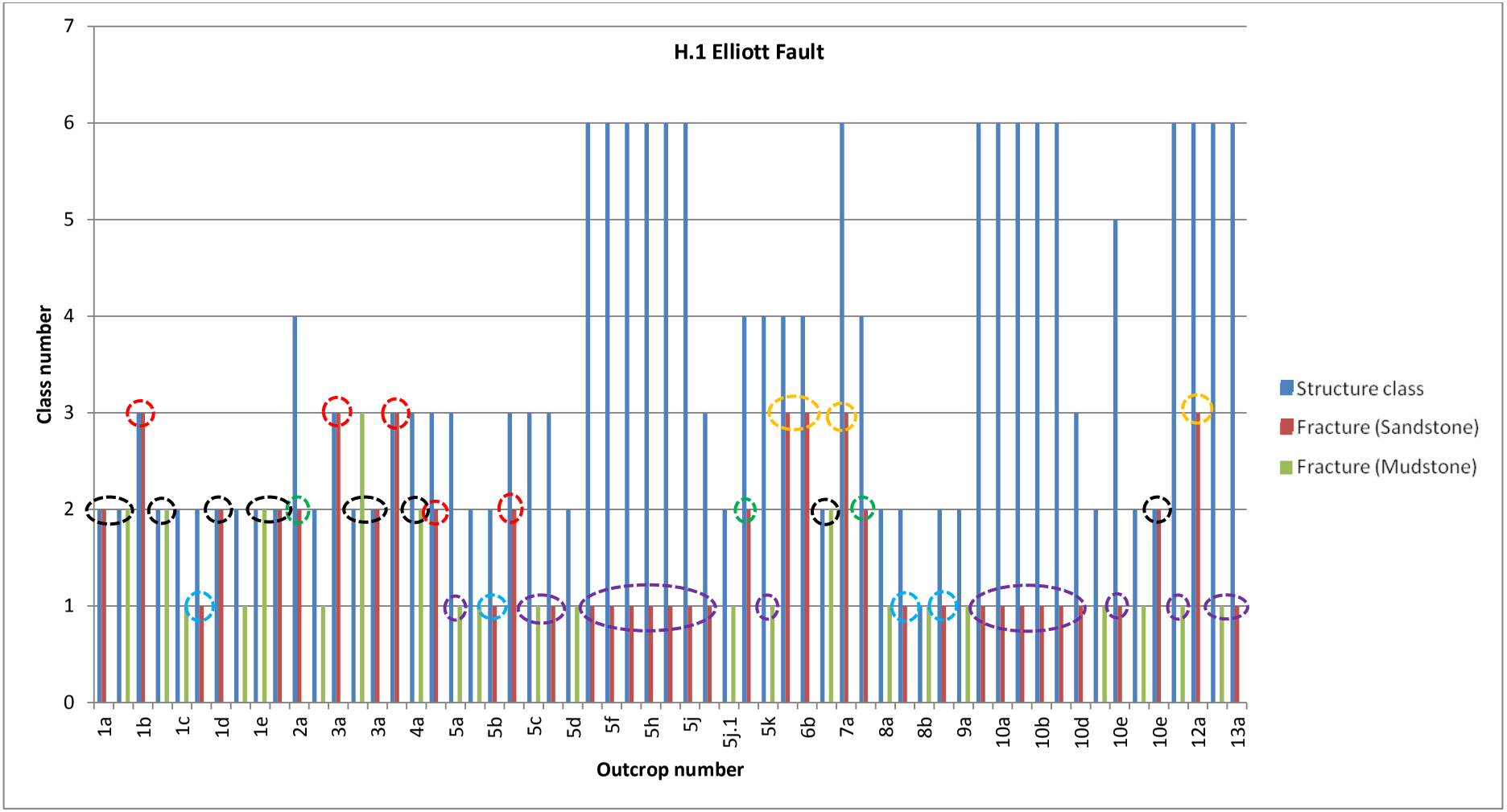

Class F – Very thin to thin bedded sandstone/mudstone that is typically fragmented
Class E – Medium bedded to massive sandstone/mudstone that is fragmented
Class D – Very thinly to thinly bedded sandstone/mudstone with moderate to high fracturing
Class C – Thickly bedded to massive sandstone/mudstone with high fracturing
Class B – Medium bedded sandstone with moderate to high fracturing
Class A – Thickly bedded to massive sandstone typically slightly to moderately fractured

Structure class	Fracture class
1 = Very thin	1 = fragmented
2 = Thin	2 = highly fractured
3 = Medium	3 = moderately fractured
4 = Thick	4 = Fractured
5 = Very thick	5 = slightly fractured
6 = Massive	6 = Unbroken

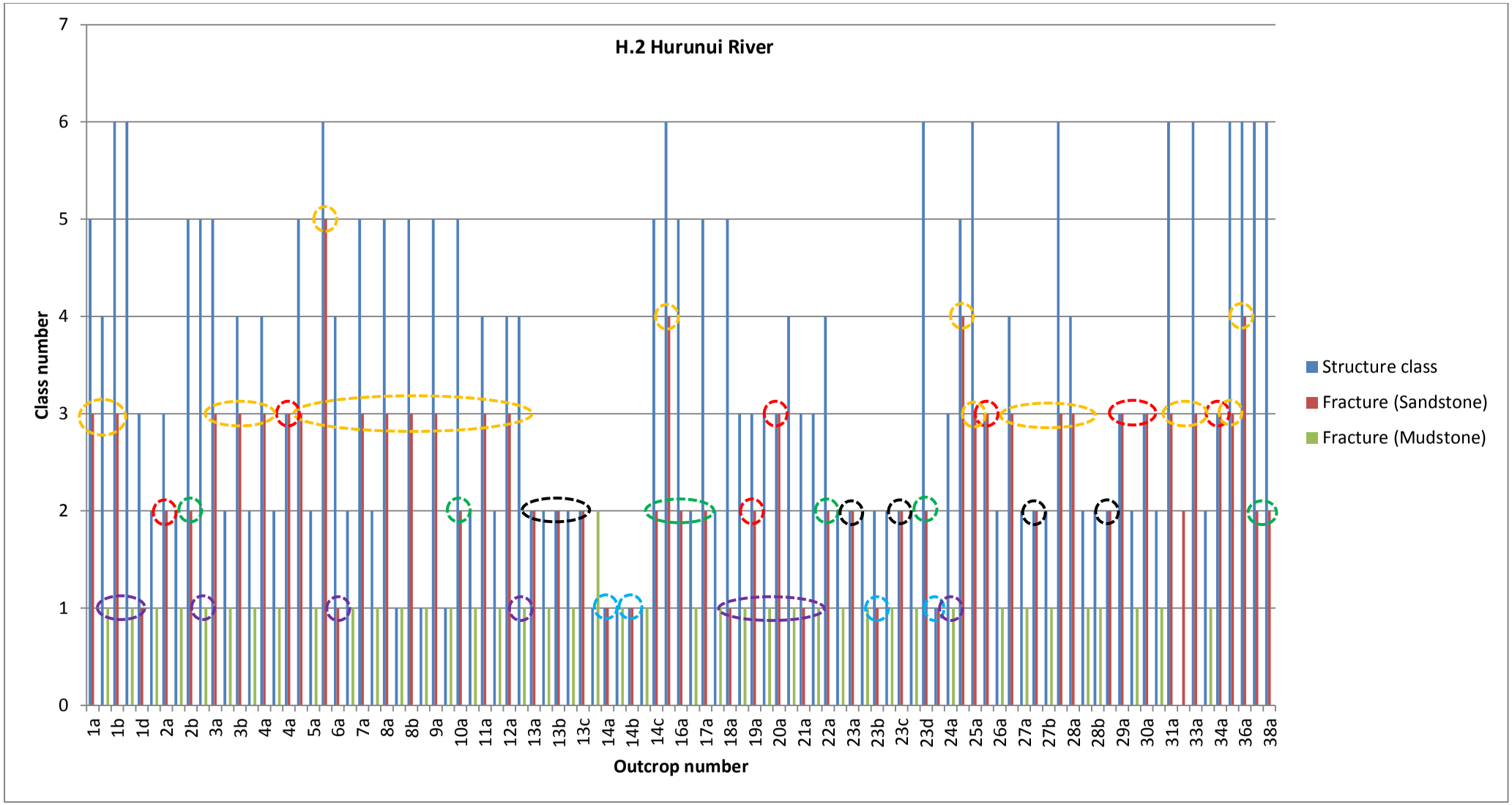

Class F – Very thin to thin bedded sandstone/mudstone that is typically fragmented

Class E – Medium bedded to massive sandstone/mudstone that is fragmented

Class D – Very thinly to thinly bedded sandstone/mudstone with moderate to high fracturing

Class C – Thickly bedded to massive sandstone/mudstone with high fracturing

Class B – Medium bedded sandstone with moderate to high fracturing

Class A – Thickly bedded to massive sandstone typically slightly to moderately fractured

Structure class

1 = Very thin
2 = Thin
3 = Medium
4 = Thick
5 = Very thick
6 = Massive

Fracture class

1 = fragmented
2 = highly fractured
3 = moderately fractured
4 = Fractured
5 = slightly fractured
6 = Unbroken

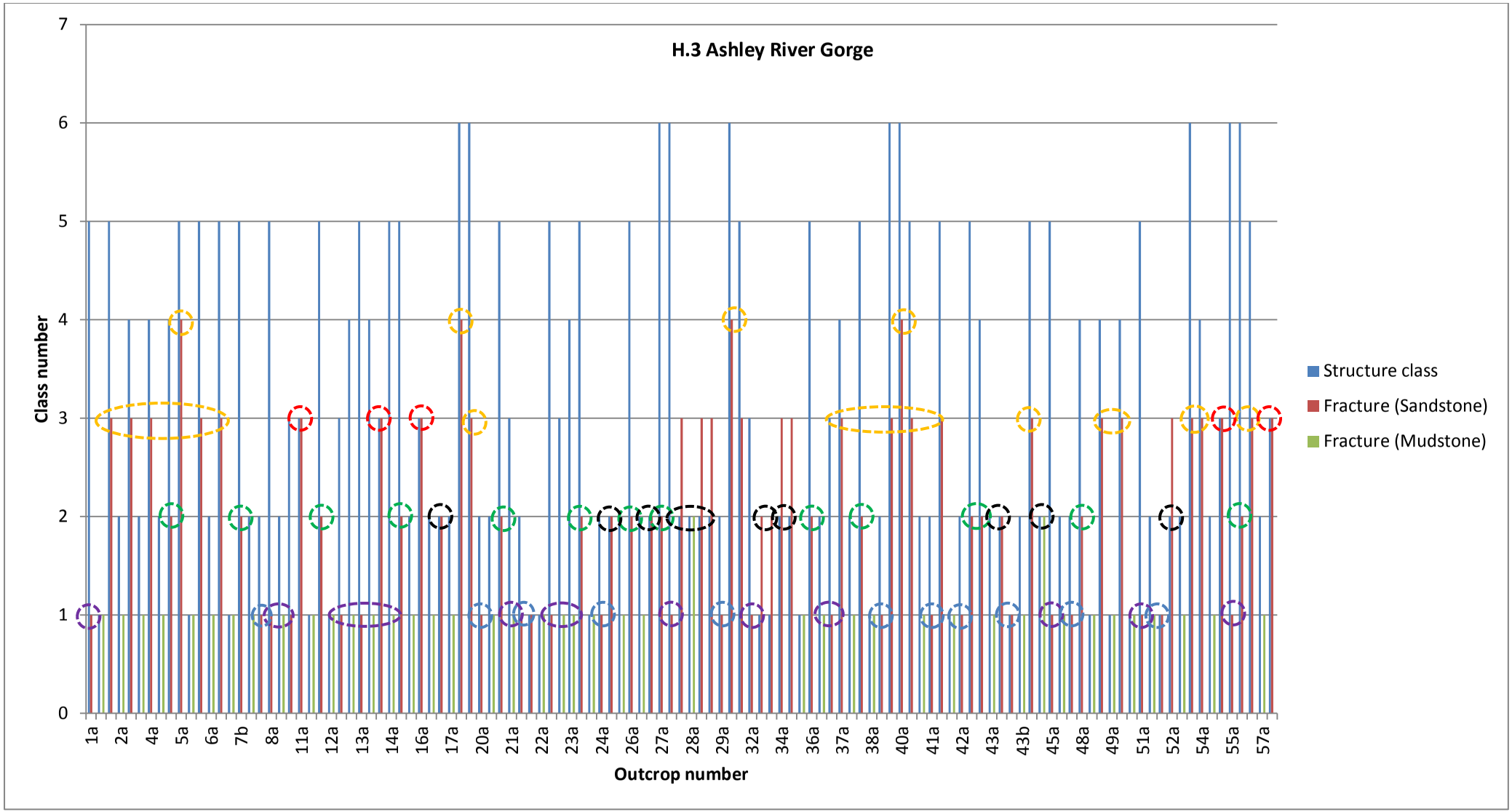

Class F – Very thin to thin bedded sandstone/mudstone that is typically fragmented

Class E – Medium bedded to massive sandstone/mudstone that is fragmented

Class D – Very thinly to thinly bedded sandstone/mudstone with moderate to high fracturing

Class C – Thickly bedded to massive sandstone/mudstone with high fracturing

Class B – Medium bedded sandstone with moderate to high fracturing

Class A – Thickly bedded to massive sandstone typically slightly to moderately fractured

Structure class	Fracture class
1 = Very thin	1 = fragmented
2 = Thin	2 = highly fractured
3 = Medium	3 = moderately fractured
4 = Thick	4 = Fractured
5 = Very thick	5 = slightly fractured
6 = Massive	6 = Unbroken

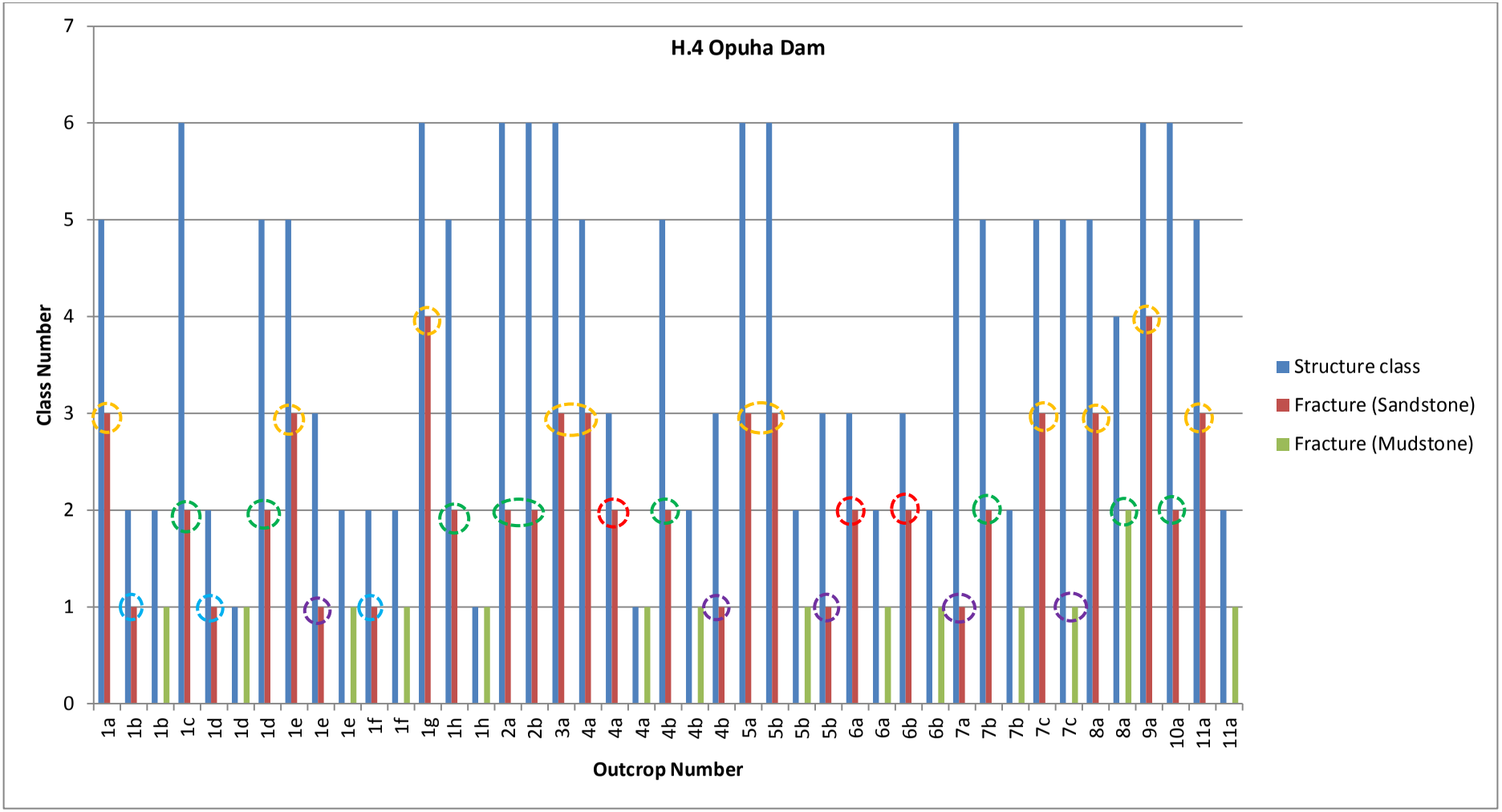

Class F – Very thin to thin bedded sandstone/mudstone that is typically fragmented

Class E – Medium bedded to massive sandstone/mudstone that is fragmented

Class D – Very thinly to thinly bedded sandstone/mudstone with moderate to high fracturing

Class C – Thickly bedded to massive sandstone/mudstone with high fracturing

Class B – Medium bedded sandstone with moderate to high fracturing

Class A – Thickly bedded to massive sandstone typically slightly to moderately fractured

Structure class

1 = Very thin
2 = Thin
3 = Medium
4 = Thick
5 = Very thick
6 = Massive

Fracture class

1 = fragmented
2 = highly fractured
3 = moderately fractured
4 = Fractured
5 = slightly fractured
6 = Unbroken

Appendix I: Defect structure pictorial gradation

Pictorial gradation of defect structure assigned values respective of individual class to allow TRC plotting. Where no defect information has enabled grouping into representative structure classes, outcrops were emplaced and assigned a number respective of overall appearance against the existing gradation.

I.1 Elliott Fault

Outcrop	Picture	Defect structure assigned class number
6a		0.6
6b	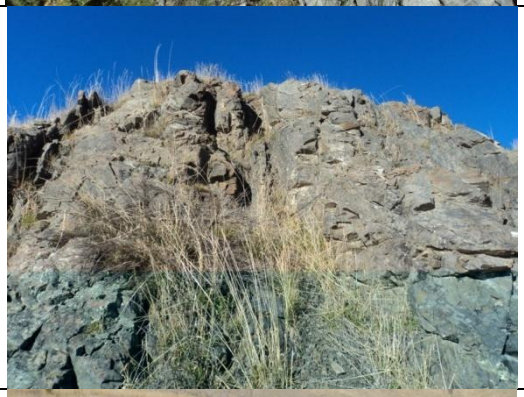	0.8
8a		0.8
7a		1.4

4a		1.4
12a		1.4
3a		1.8
1a		1.8`
1b		1.8

1e		1.8
5k		2.4
5a		2.4
1d		2.8
2a		3.4

10e		3.4
5c		4.4
9a		4.4
5b		4.6
10d		4.8

5d		4.8
11a		5
10a		5.2
8b		5.4
1c		5.6

5e		5.8
5f		5.8
13a	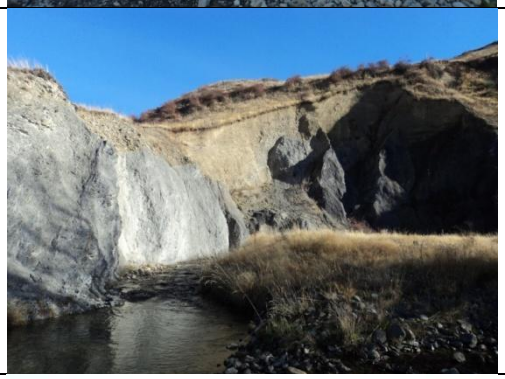	5.8
5g		6
5h	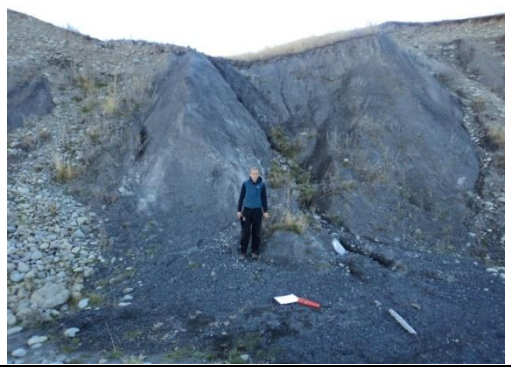	6

5i		6
5j	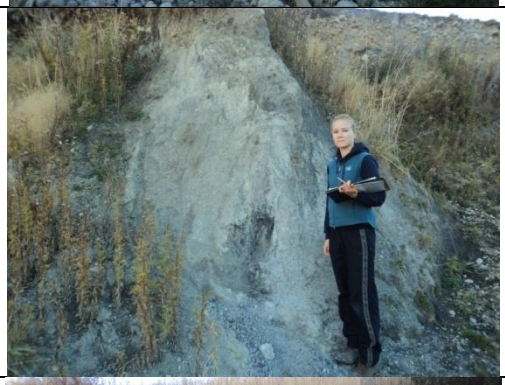	6
5j.1		6
10b		6
10c		6

I.2 Hurunui River

Outcrop	Picture	Defect structure assigned class number
5b		0.2
36a		0.2
7a		0.2
25a		0.4

5a	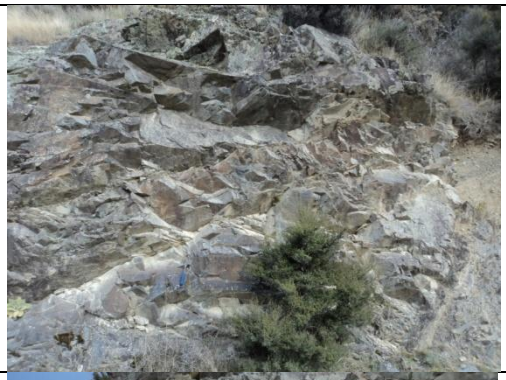	0.6
8b		0.6
33a		0.8
24b		0.8
16a		0.8

17a	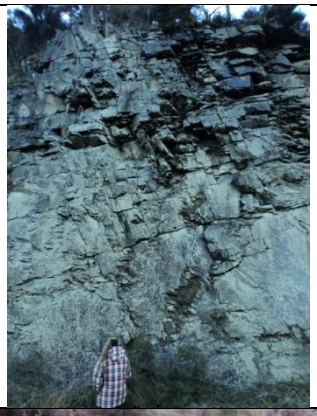	0.8
35a	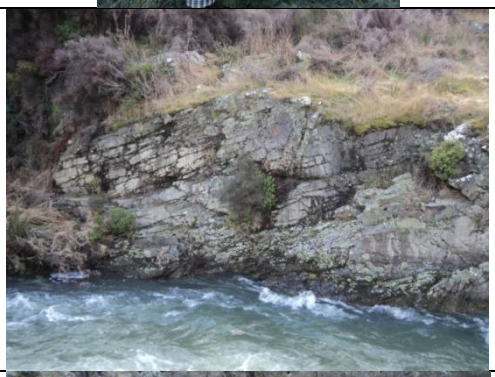	0.8
27c		1
3b		1
11a		1

13b		1.2
10a		1.2
3a		1.4
8a		1.4
38a	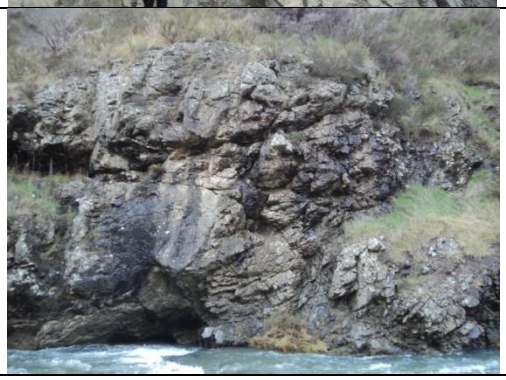	1.4

31a	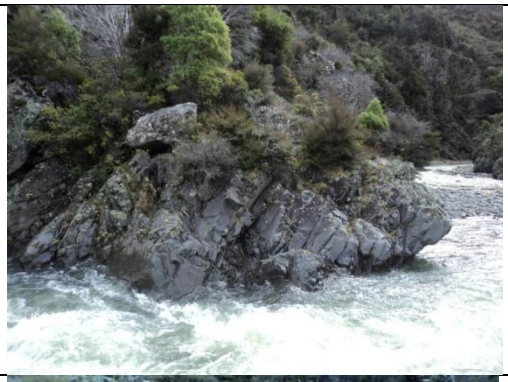	1.6
15a		1.6
28a		1.6
9a		1.6
30a		1.6

37a		1.6
22a		1.8
1b		1.8
1a		1.8
4a		1.8

34a		1.8
26a		1.8
27a		2
29a		2
32a	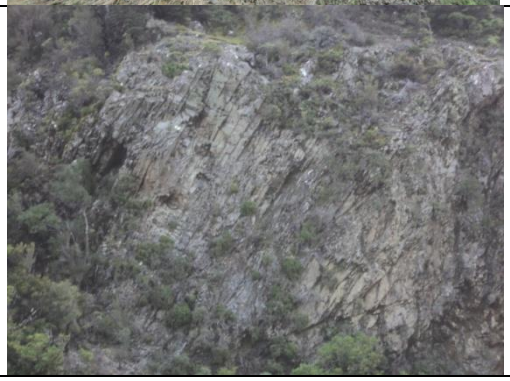	2

18a		2.2
14c		2.4
2b		2.4
12a		2.4
1d		2.6

6a		2.8
14a		3
2a		3.4
13c		3.4
20a		3.6

21a		3.6
27b		3.6
19a		3.6
14b		3.8
24a		4

23d		4.2
23c		4.2
23a		4.2
23b		4.2
28b		4.4

13a			4.6
1c			4.8

I.3 Ashley River Gorge

Outcrop	Picture	Defect structure assigned class number
31a		0.2
18a		0.6
11a		0.6
40a		0.8

53a		1.2
39a		1.2
19a		1.4
32a		1.4
44a		1.4

43a		1.4
37a		1.6
49a		1.6
50		1.8
54a		1.8

52a	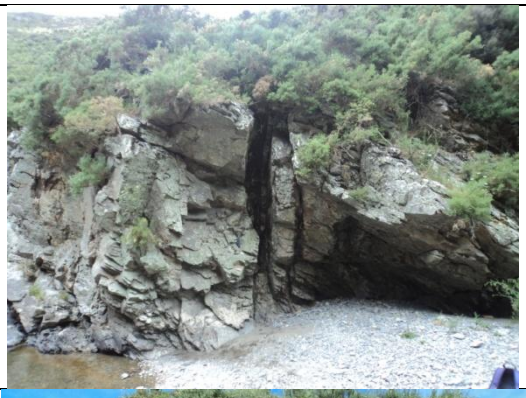	1.8
57a		1.8
4a	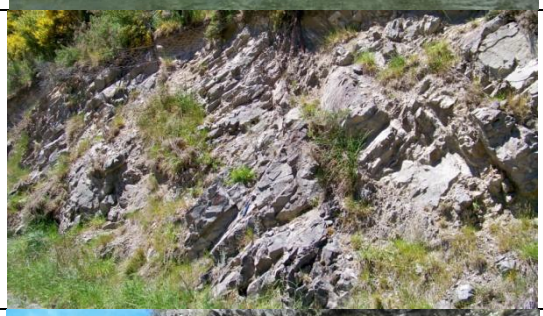	2
56a		2.2
21a		2.4

7a	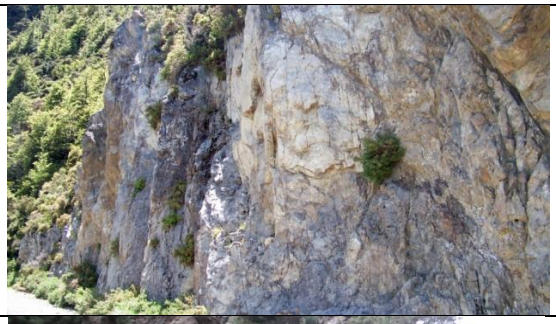	2.6
43b		2.6
5a		2.6
6a		2.6
23a		2.6

28a	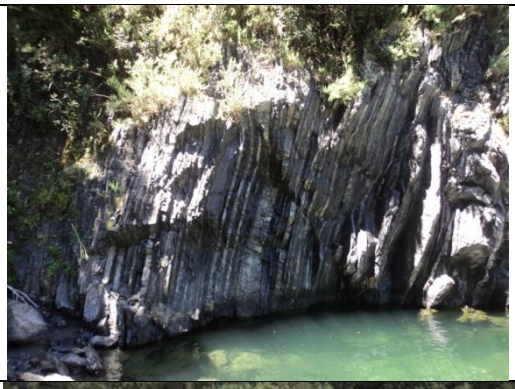	2.8
55a	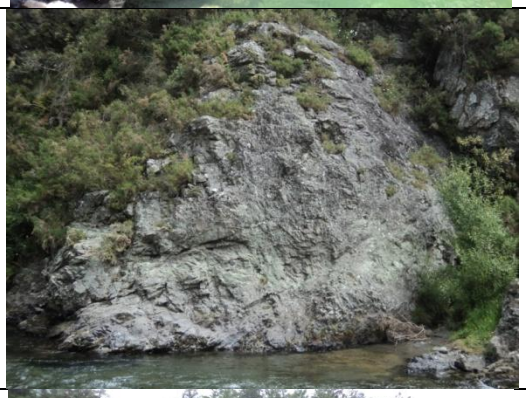	**3**
41a		3
16a		3
48a		3

29a		3.2
33b		3.2
30a		3.2
33a		3.2
34a		3.2

7b		3.4
12a		3.4
14a		3.6
17a		3.6
24a		3.8
26a		3.8

2a		4
3a		4
15a		4.2
36a		4.2
27a		4.4

25a		4.6
20a		4.6
22a		4.6
27b		4.8
8a		4.8

45a	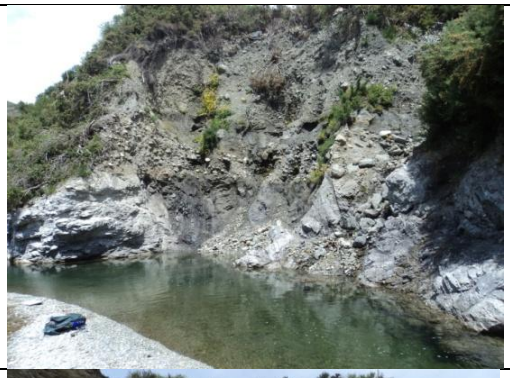	5
1a		5.2
38a		5.6
42a		5.6
51a		5.6

I.4 Opuha Dam

Outcrop	Picture	Defect structure assigned class number
1g		0.4
9a		0.6
8a		1.2
2b		1.4
1h	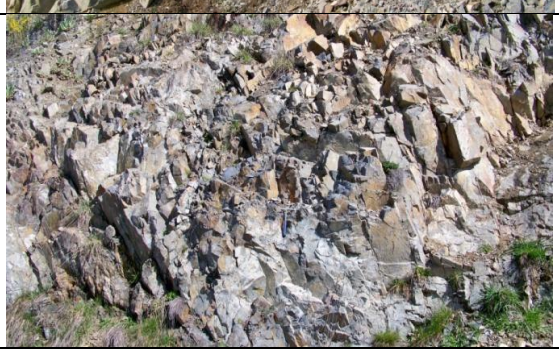	1.4

5a		2.2
7c	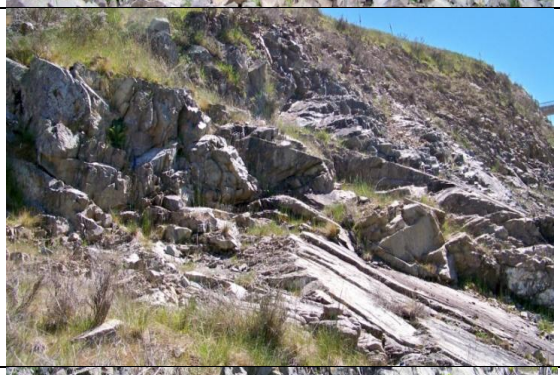	2.2
7b	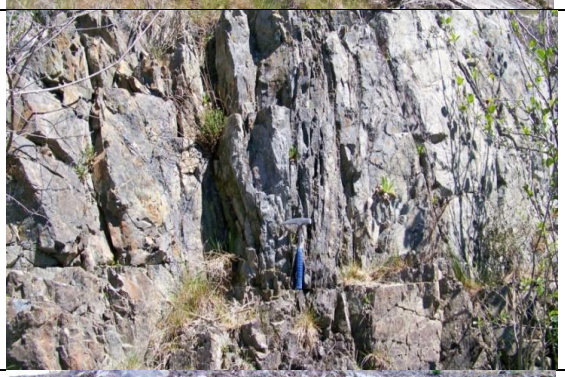	2.4
1a		2.4
1e		2.4

1c		2.6
4a		2.6
1d		2.8
3a		3
6a		3.4

6b	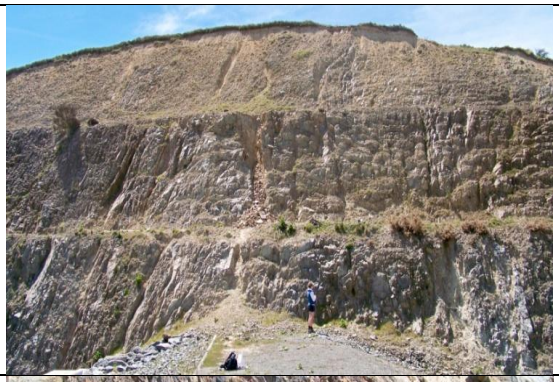	3.4
1f	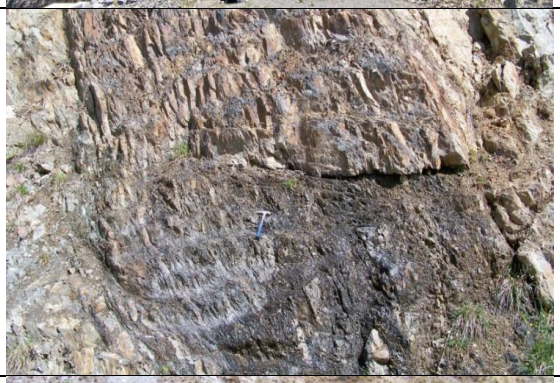	3.6
1b		4.4
4b		5
2a		5

7a		5.6
5b		5.6

Appendix J: Defect condition analysis

Defect condition analysis was carried out across all study sites to give an indication of overall surface condition to allow the TRC to be used as a predictive tool. Analysis was carried out respective of defect type and includes analysis of roughness, infill type, infill width, interlimb angle (ILA) and wavelength against defect structure. Roughness and infill lithology values used for plotting purpose are described below.

Infill lithology (main fraction)	
No infill	0
Gravel	1
Sand	2
Silt	3
Clay	4

Roughness (NZGS, 2005)	
Stepped rough	1
Stepped smooth	2
Stepped slickenside	3
Undulating rough	4
Undulating smooth	5
Undulating slickenside	6
Planar rough	7
Planar smooth	8
Planar slickenside	9

J.1 Bedding defect

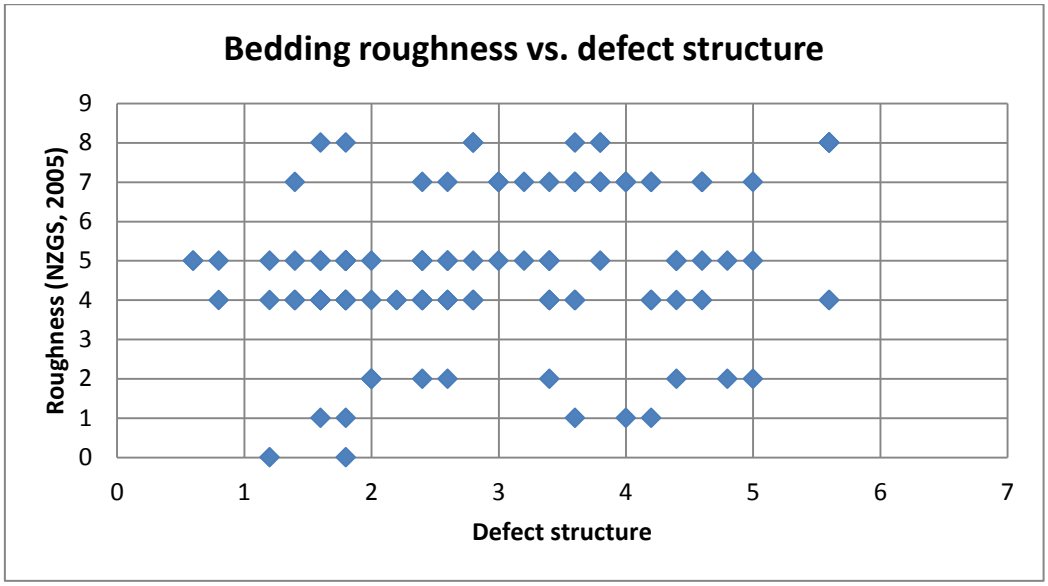

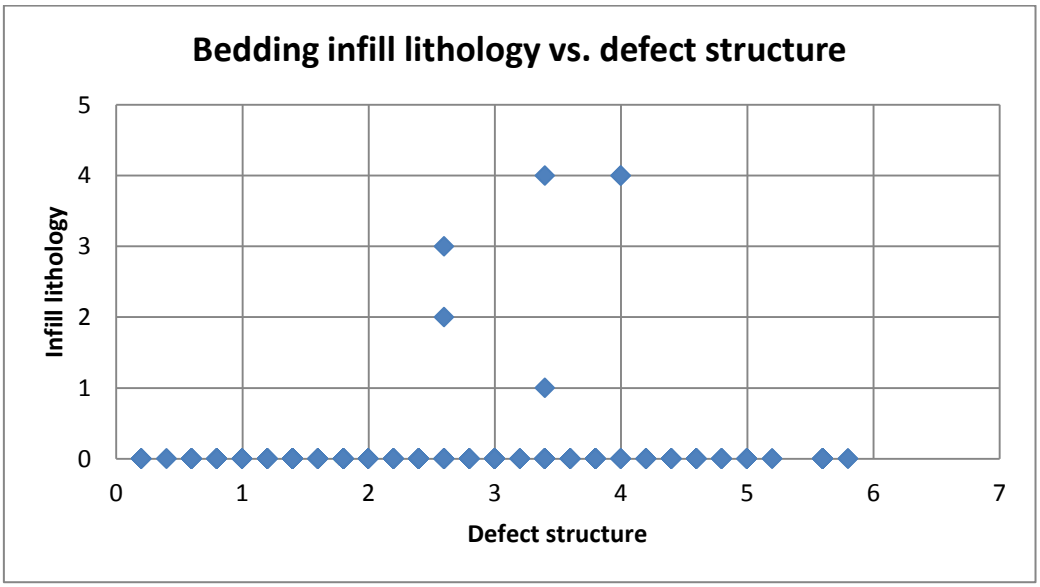

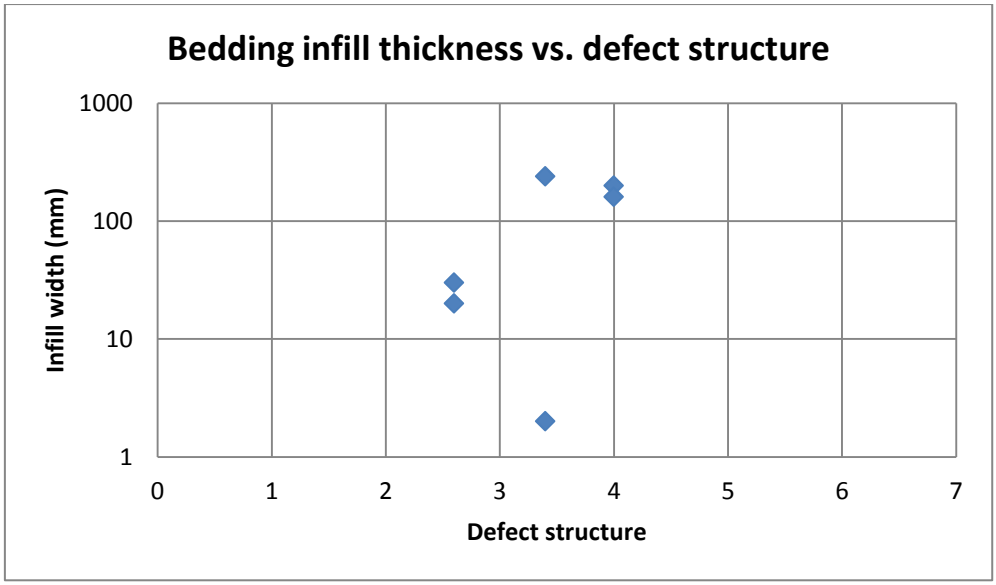
Bedding infill thickness vs. defect structure
Infill width (mm)
1000
100
10
1
0
1
2
3
4
5
6
7
Defect structure

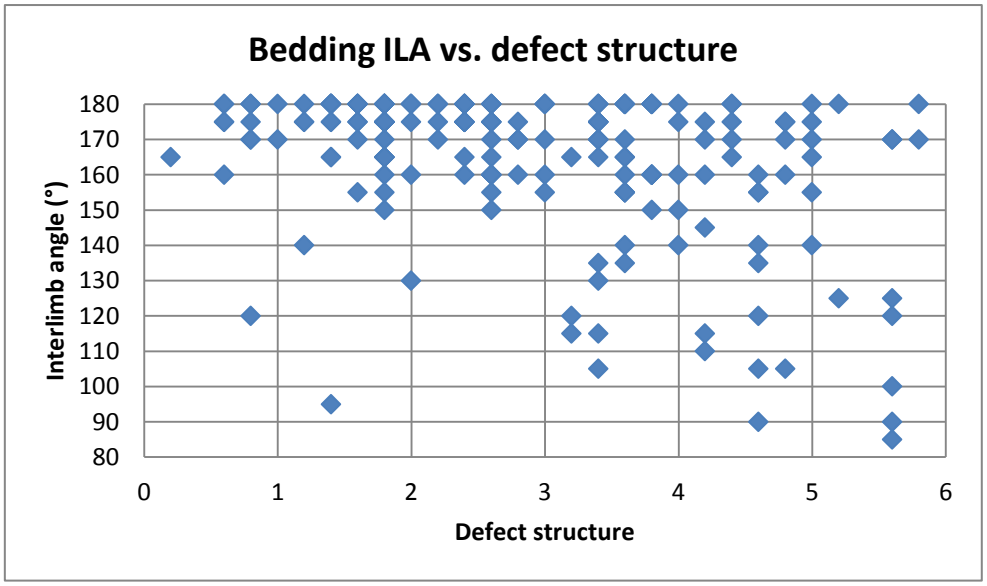
Bedding ILA vs. defect structure
Interlimb angle (°)
180
170
160
150
140
130
120
110
100
90
80
0
1
2
3
4
5
6
Defect structure

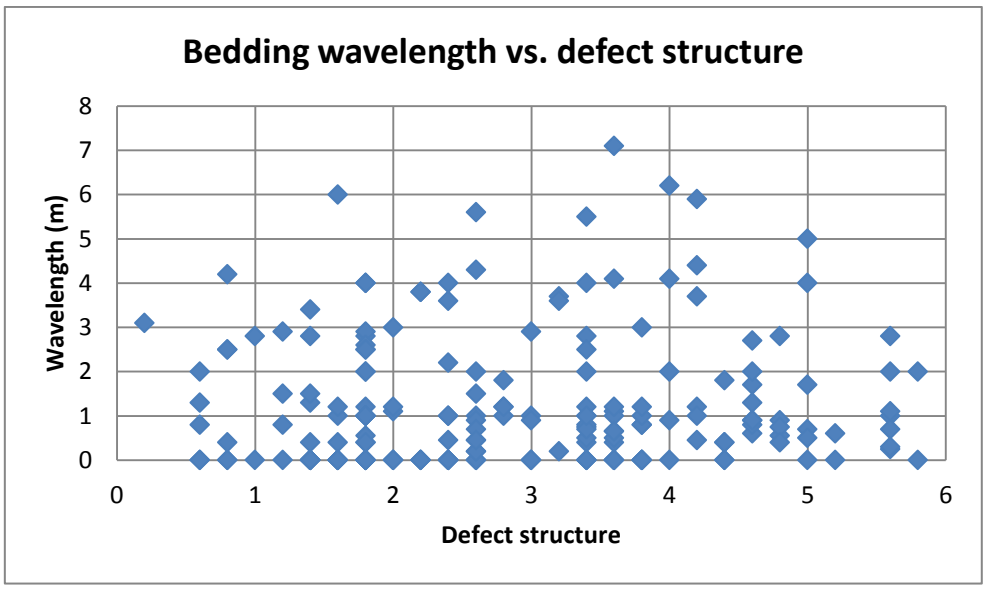
Bedding wavelength vs. defect structure
Wavelength (m)
8
7
6
5
4
3
2
1
0
0
1
2
3
4
5
6
Defect structure

J.2 Jointing defect

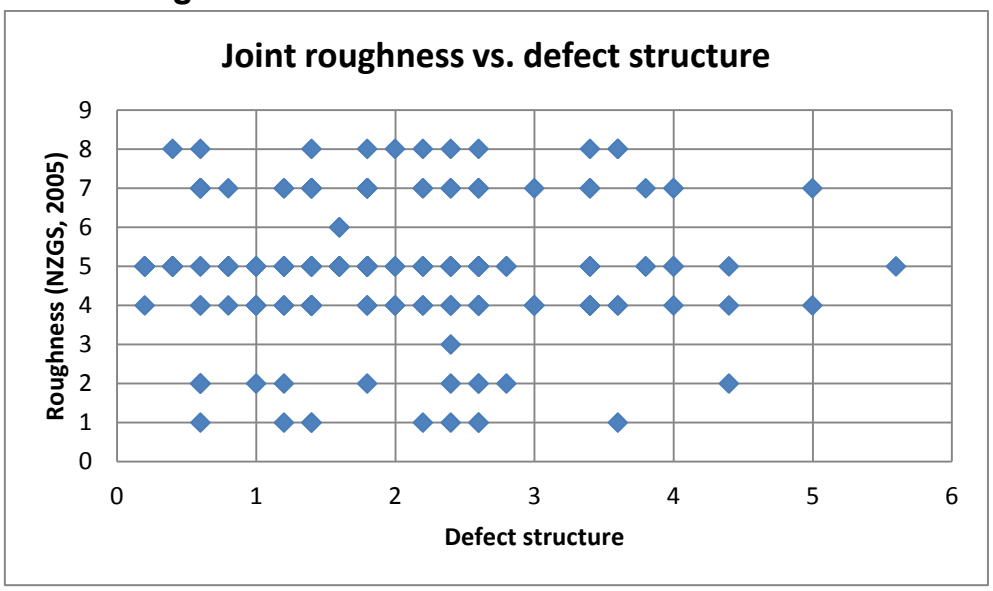

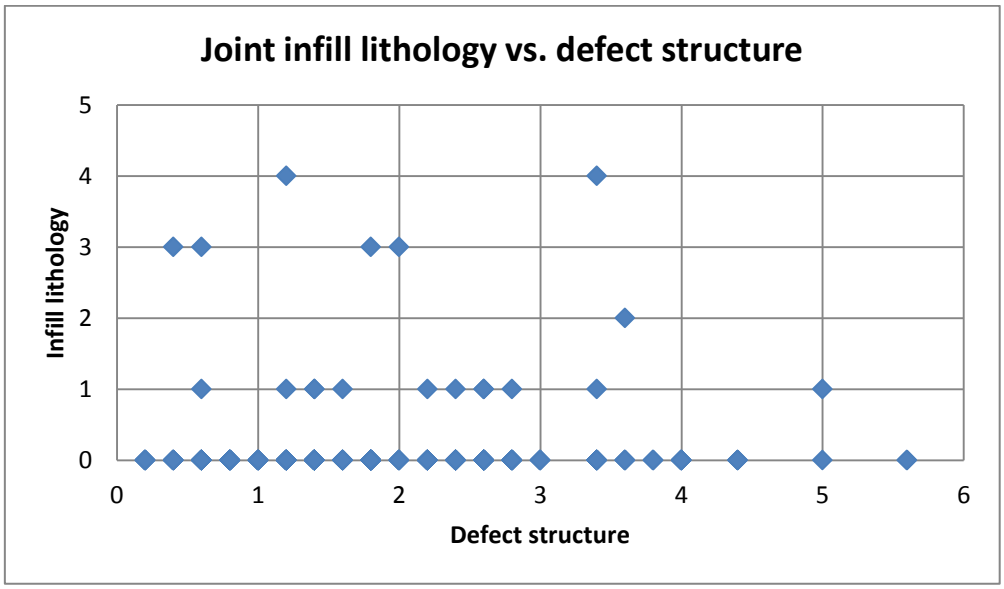

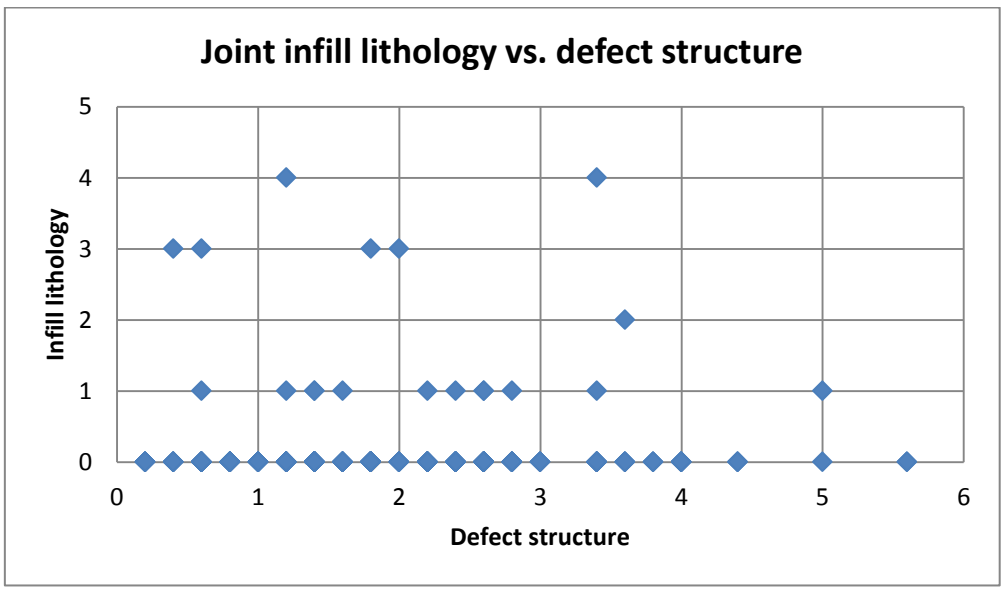

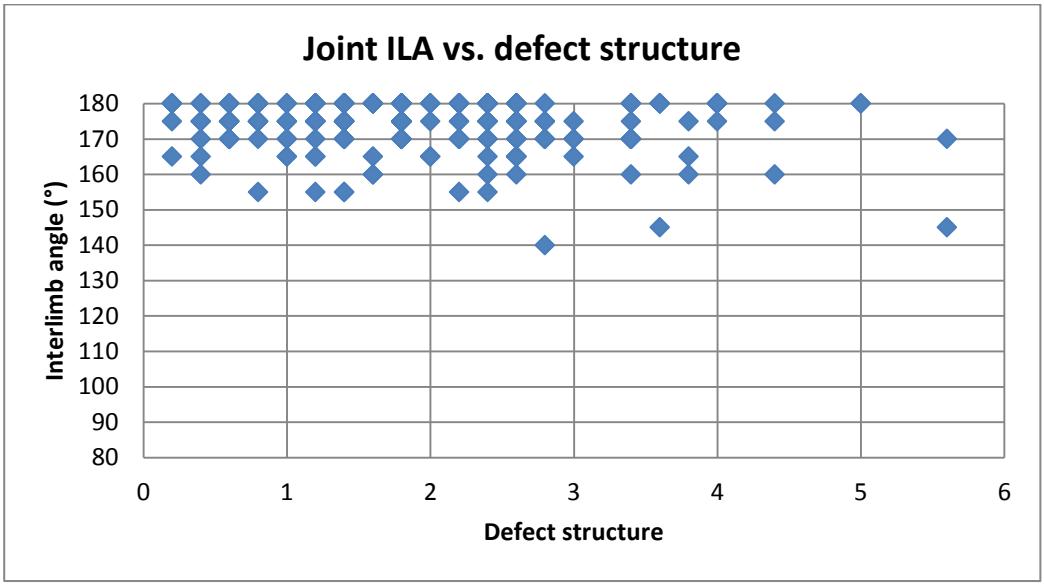
Joint ILA vs. defect structure
Interlimb angle (°)
180
170
160
150
140
130
120
110
100
90
80
0
1
2
3
4
5
6
Defect structure

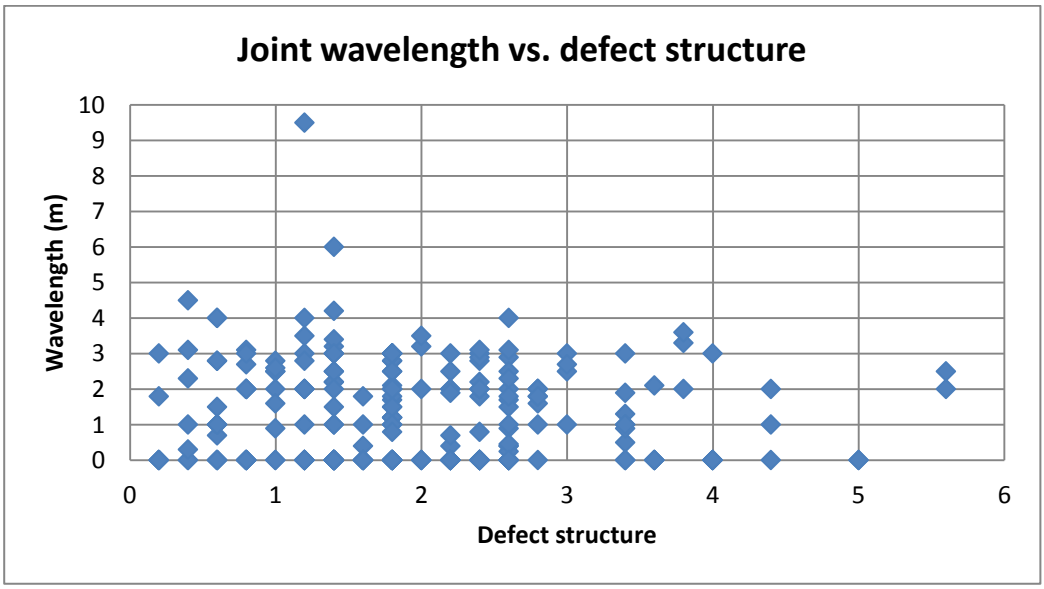
Joint wavelength vs. defect structure
Wavelength (m)
10
9
8
7
6
5
4
3
2
1
0
0
1
2
3
4
5
6
Defect structure

J.3 Fault/shear defect

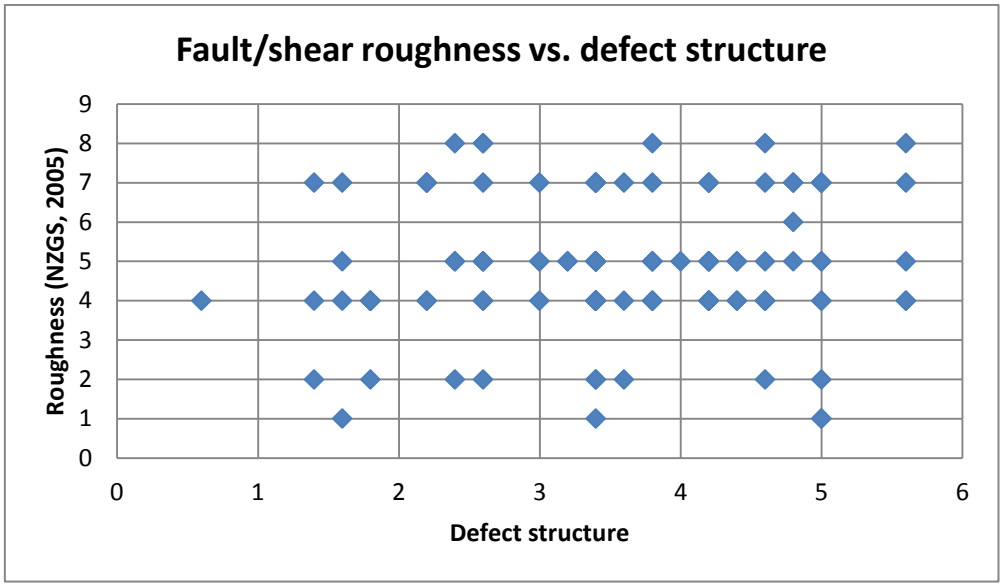

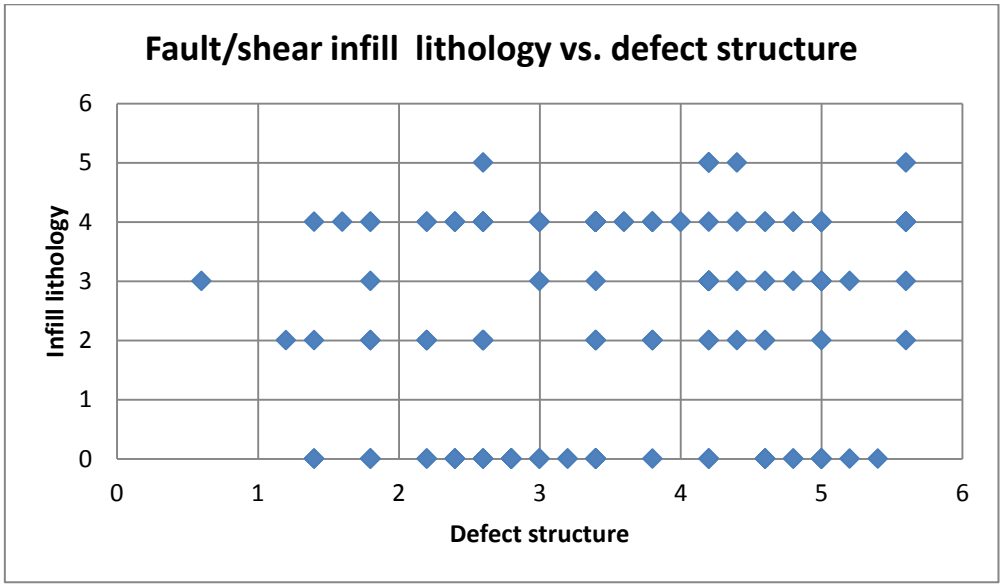

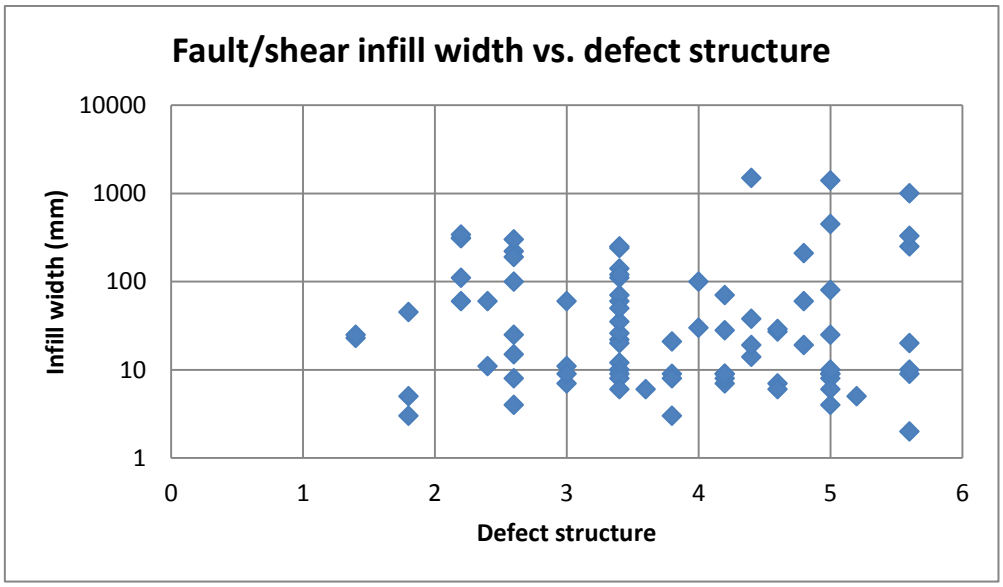

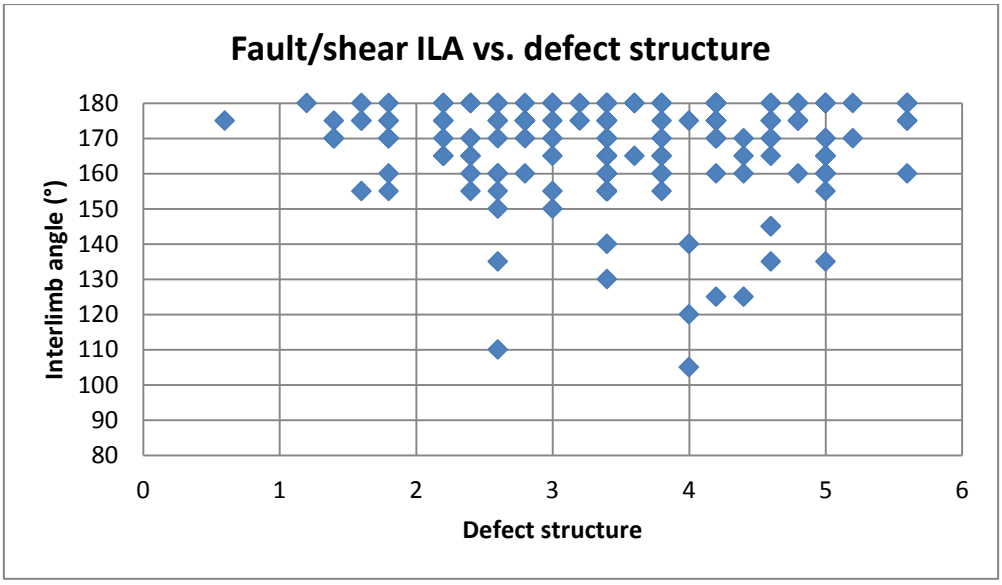
Fault/shear ILA vs. defect structure
Interlimb angle (°)
180
170
160
150
140
130
120
110
100
90
80
0
1
2
3
4
5
6
Defect structure

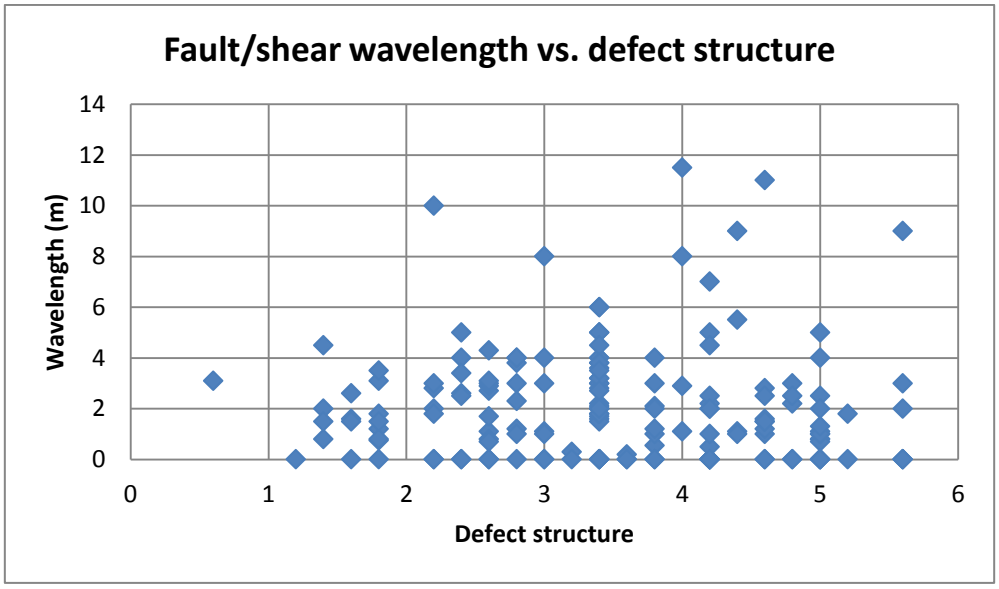
Fault/shear wavelength vs. defect structure
Wavelength (m)
14
12
10
8
6
4
2
0
0
1
2
3
4
5
6
Defect structure

Appendix K: Rock mass type mapping

Rock mass type mapping was carried out by colouring up outcrop point locations into respective rock mass types. Regions of similar rock mass types were grouped and orientated in respect to bedding or large scale fault trends.

K.1 Elliott Fault - type mapping

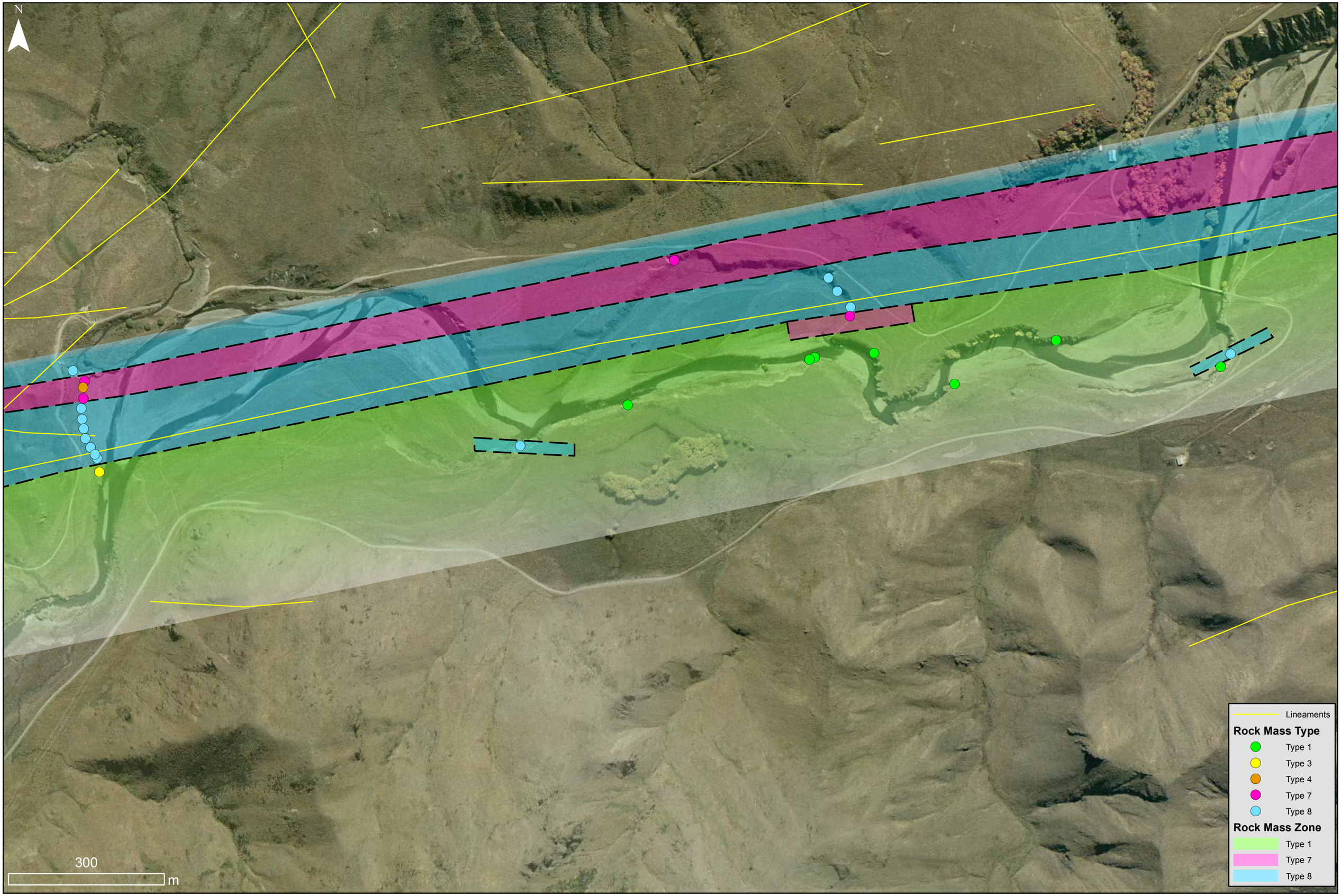

Imagery Source: Canterbury Aerial Photo

K.2 Hurunui River - type mapping

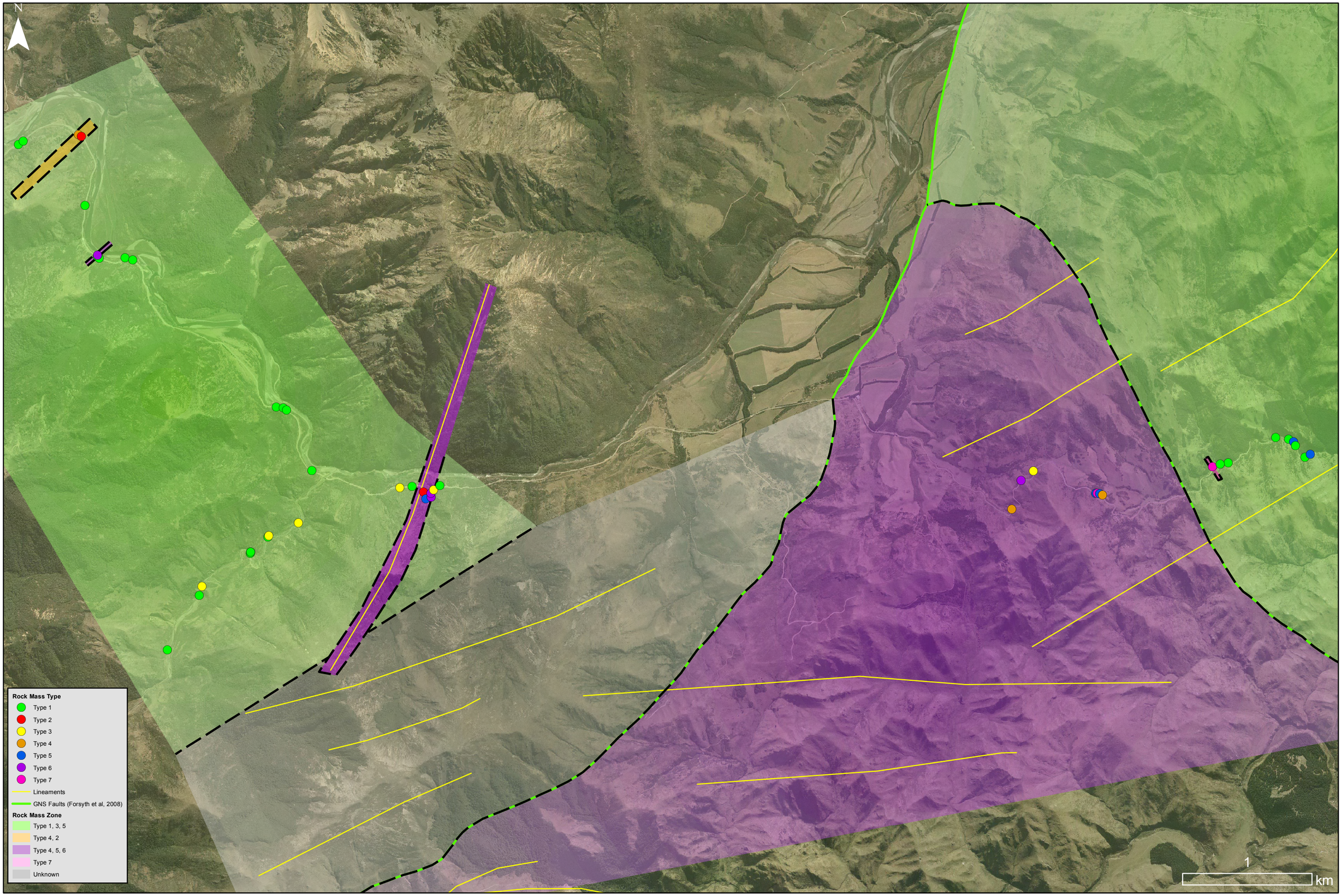

Imagery Source: Canterbury Aerial Photo

K.3 Ashley River Gorge - type mapping

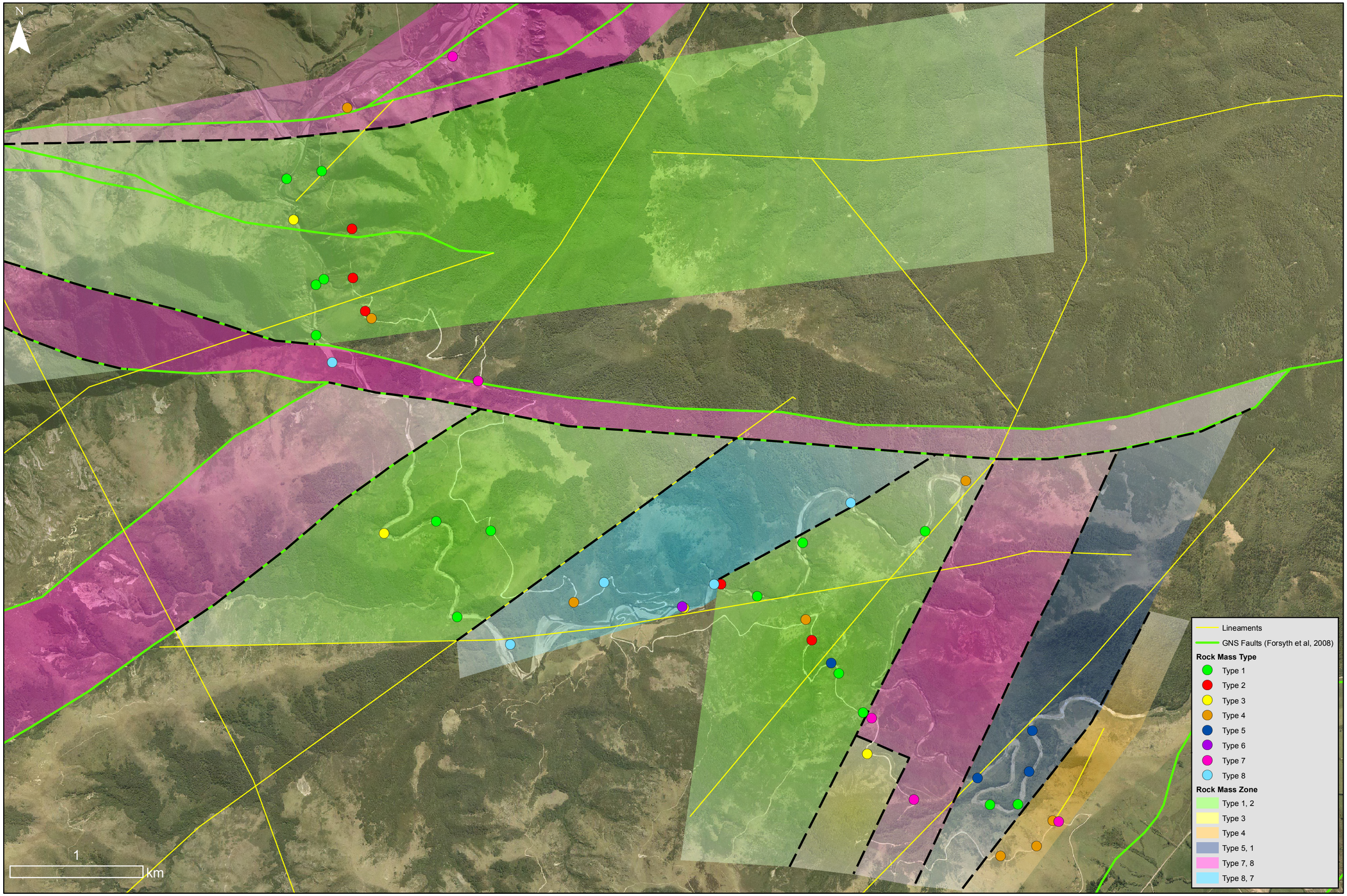

Imagery Source: Canterbury Aerial Photo

K.4 Opuha Dam - type mapping

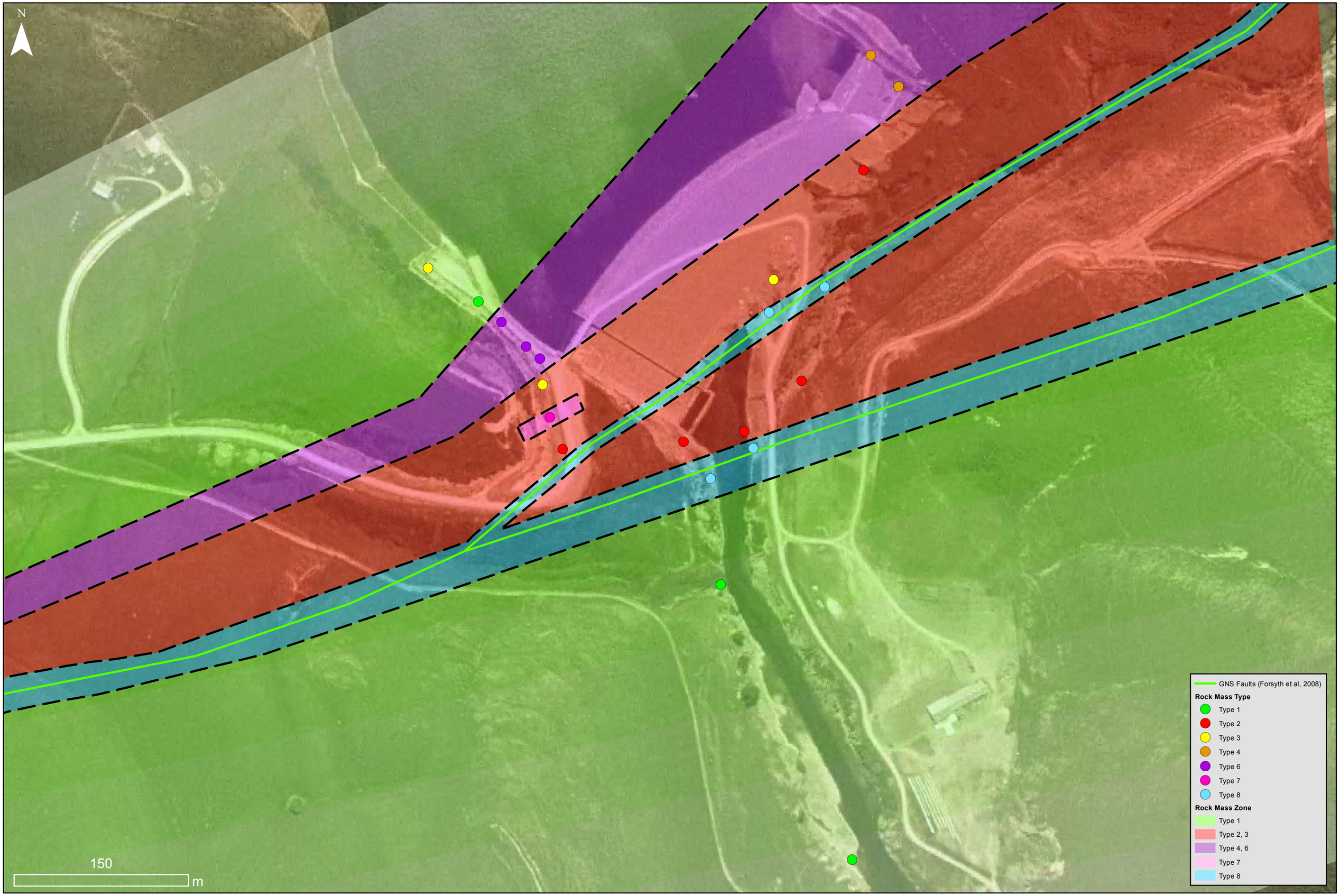

Imagery Source: Canterbury Aerial Photo

Appendix L: TRC diagram for external use

L.1 Blank TRC

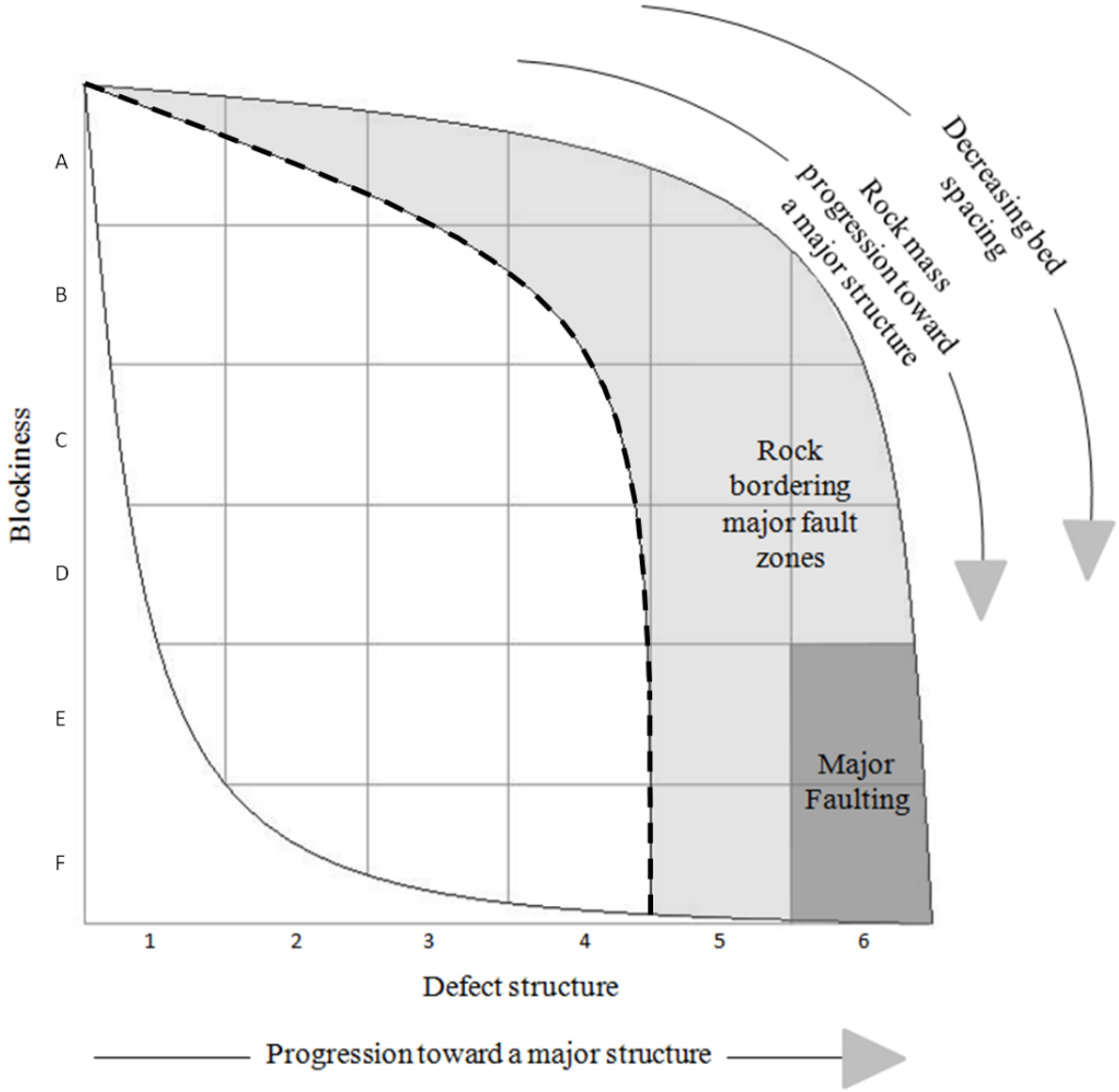

L.2 Blank TRC with rock mass type overlay from this study

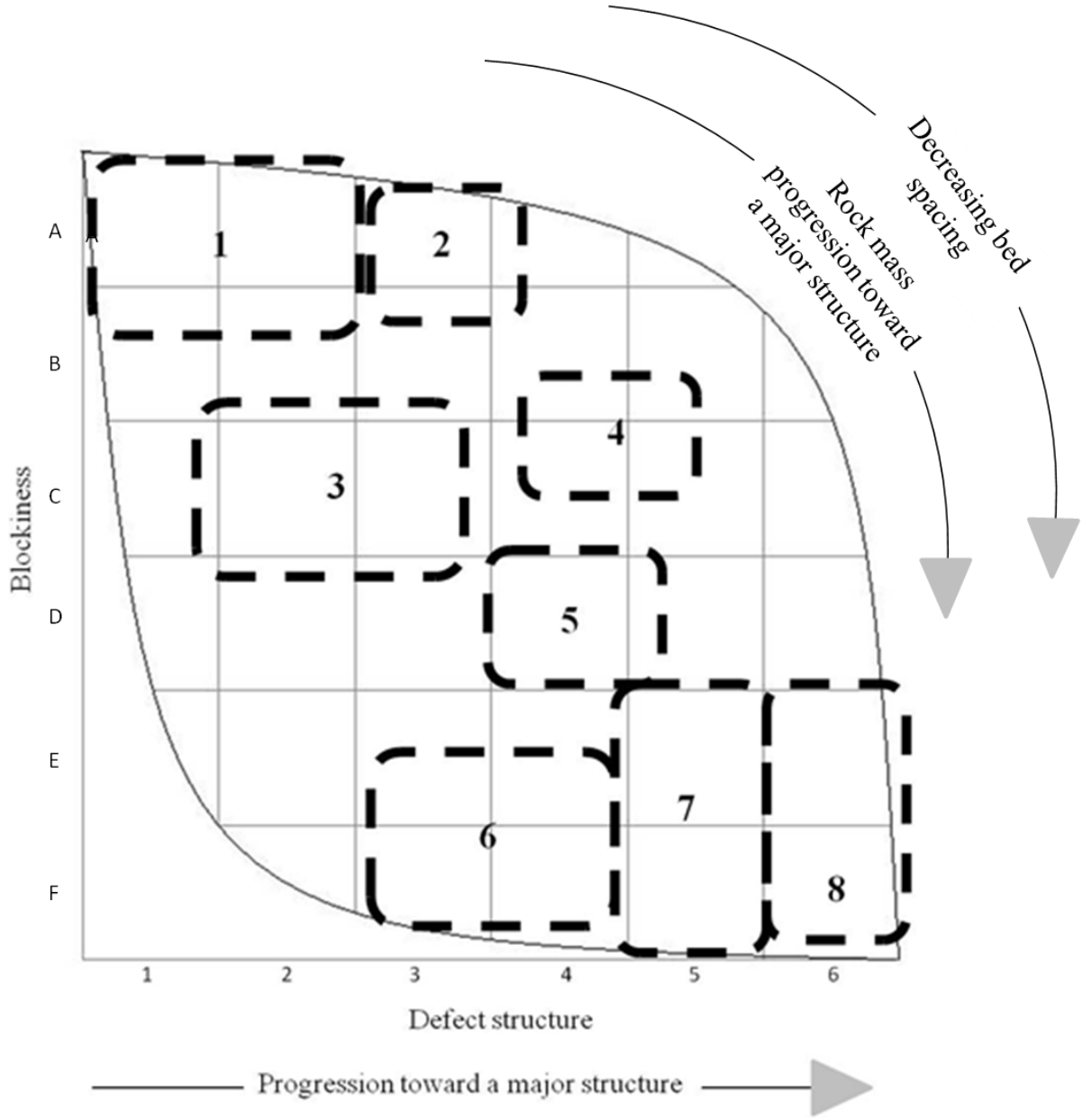

Appendix M: Engineering geological characterisation of the Torlesse Composite Terrane in Canterbury, New Zealand with reference to mechanised tunnelling

Publication produced during the thesis (produced for the New Zealand Geotechnical Society (NZGS) 19th Symposium).

Irvine, A.G., Eggers, M.J., Villeneuve, M. (2013)
Engineering geological characterisation of the Torlesse composite terrane in Canterbury, New Zealand with reference to mechanised tunnelling
Proc. 19th NZGS Geotechnical Symposium. Ed. CY Chin, Queenstown

Engineering geological characterisation of the Torlesse composite terrane in Canterbury, New Zealand with reference to mechanised tunnelling

A G Irvine
Department of Geological Sciences, University of Canterbury, New Zealand
irvineAG@gmail.com (Corresponding author)

M J Eggers
Pells Sullivan Meynink, Engineering Consultants, Sydney, Australia

M C Villeneuve
Department of Geological Sciences, University of Canterbury, New Zealand

Keywords: Torlesse; outcrop mapping; rock mass; faulting; classification

ABSTRACT
The Torlesse composite terrane is an important geological unit in Canterbury, New Zealand. It consists of a large group of rocks which exhibit a range in engineering geological condition between locations. Four sites throughout Canterbury were selected for mapping to represent all three Torlesse terrane types and a range of regional fault settings. Observed trends in the field data were used to develop a classification framework based on a series of rock mass classes that describe blockiness and defect structure conditions. Blockiness is defined by bedding thickness and density of non-systematic jointing (fractures) while defect structure is defined by the combination of systematic discontinuities such as persistent jointing and shearing. Individual outcrops were assessed using the classification and a total of eight distinctive rock mass types were derived for the four sites mapped. Major controls on rock mass conditions were found to be lithostructure and proximity to major and regional scale fault zones. Sub-dividing proposed tunnel alignments by rock mass type will allow assessment on tunnelling parameters such as support measures, equipment specification, advance rates, groundwater inflows and so on.

1 INTRODUCTION
Torlesse Composite Terrane is a dominant rock unit in the geology of New Zealand, particularly in Canterbury, and as such is encountered in many engineering projects. Despite widespread distribution there is relatively little description in the literature on the engineering geology of the Torlesse, especially for the assessment of mechanised tunnelling. Past work by Read et al. (2000), Richards and Read (2007), Read and Richards (2007) and Stewart (2007) typically address New Zealand greywacke rock mass characterisation and classification, where strength and structure has been examined mainly for input into failure criteria. To further existing knowledge to the application of tunnelling, this study undertook to characterise the range of engineering geological conditions in the Torlesse exposed in Canterbury to help assess the geological controls on tunnel selection, specification and design.

An outcome of the study includes a framework for the classification of Torlesse rock mass conditions. This conceptual classification is based on trends analysed from mapping data collected from four sites across a range of terrane types and regional structural locations in Canterbury. It differs from existing classifications such as Read et al. (2000) where lithostructure, specifically the lithological control on bedding spacing and density of short, discrete non-systemic jointing, is emphasised together with the occurrence of systematic defects. It is anticipated that as more data is collected from future studies the classification can be improved to assist engineering design of tunnels.

2 GEOLOGICAL SETTING

The Torlesse composite terrane rocks of New Zealand comprise indurated fine to medium grained, poorly sorted, sub-angular quartzo-feldspathic interbedded sandstone and mudstone (Cox and Barrell, 2007, Mortimer, 2004). The proportion between sandstone and mudstone range substantially between localities (Richards and Read, 2007). The mudstone beds are typically more susceptible to deformation and as a result significant layer parallel shearing (termed Broken Formation by Rattenbury et al. (2006)) and boudinage is common. Tectonically the Torlesse rock mass has undergone extensive deformation in the exhumation, uplift and more recently formation of the modern day plate boundary (Pettinga et al., 2001). Read and Richards (2007) discuss low persistence jointing dominates the rock mass (>90%) with ~80% terminating against other defects. They go on to discuss defect spacing between 60-200mm with planar smooth to planar rough surfaces. Infilling is reported as inactive clays (Read and Richards, 2007, Stewart, 2007). Torlesse sandstone intact strengths are high with UCS averaging ~160MPa in comparison to mudstone UCS averaging 70MPa (Stewart, 2007).

The Torlesse is sub-divided into two terrane types, distinguished by age, and a third sub-terrane (Figure 1). The older Rakaia terrane is the largest by area (Cox and Barrell, 2007). It is widely deformed and monotonous (Mortimer, 2004). The Pahau terrane is the youngest and is separated from the Rakaia terrane by the third (sub) terrane in the study region, the Esk Head Belt. The Esk Head Belt is described as a zone of more sheared rock dominantly comprising Rakaia and Pahau Torlesse (Rattenbury et al., 2006). The sandstone in the Pahau has a slightly lighter colour and induration than the Rakaia terrane ((Forsyth et al., 2008, Rattenbury et al., 2006).

3 DATA COLLECTION AND STUDY APPROACH

3.1 Study sites

Four study areas, the Elliott Fault, Hurunui River, Ashley River Gorge and Opuha Dam, were selected on the basis of obtaining representation across the suite of Torlesse (Figure 1). The four sites were chosen to represent all terrane types, metamorphic facies and structural styles.

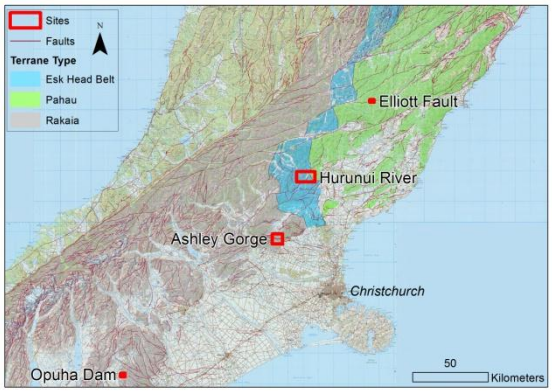

Figure 1: Torlesse terrane and study sites. Data sourced and modified from Rattenbury et al. (2006), Nathan et al. (2002), Forsyth et al. (2008) and Cox and Barrell (2007).

3.2 Methodology

Prior to field work a desktop study was carried out in association with a landscape lineation study to develop 1) a conceptual geological model at each site and 2) field mapping sheets to provide a check list to ensure consistency of information collected between outcrops and sites. Information recorded on the mapping sheets included weathering, intact strength, defect type and orientation, bedding fabric, defect roughness, spacing, persistence, aperture, infill type, strength, thickness and moisture according to NZGS (2005). Bedding thickness, degree of fracturing, defect waviness (ILA – inter-limb angle and wavelength), defect end condition and

termination parameters were collected according to PSM internal documents (2010) which are variably based on ISRM (1978). Outcrop lithology was observed including colour, lithology and grain size. Sampling for lab testing was carried out on selected outcrops to obtain a representation of rock mass characteristics and spatial extent across the entire study site.

In this study a differentiation has been made between defects which can be described as systematic and non-systematic based on their relative persistence (ISRM, 1978) and their ability to form defect sets. Non-systematic joints are short, discrete and generally of random orientation. In this study they are differentiated as fractures from persistent joints that form sets. Terminology for describing bedding thickness and degree of fracture are defined in Table 1.

Table 1: Left: Bedding thickness (PSM, 2010); right: Degree of fracture (PSM, 2010)

Term		Description	Separation of stratification planes
Stratification not recognisable		Massive	-
Stratification more than 20mm apart	Bedded	Very thickly bedded	>2m
		Thickly bedded	0.6 - 2m
		Medium bedded	0.2 - 0.6m
		Thinly bedded	60mm - 0.2m
		Very thinly bedded	20 - 60mm
Stratification planes less than 20mm apart	Laminated	Thickly laminated	6 - 20mm
		Thinly laminated	<6mm

Descriptive term	Condition of freshly drilled core
Fragmented	The core is comprised primarily of fragments of less than 20 mm and mostly of width less than the core diameter. Generally >50 breaks/metre.
Highly Fractured	Core lengths are generally 20-40 mm with occasional fragments. Generally 25-50 breaks/meter.
Moderately Fractured	Core lengths are generally 30-100 mm with occasional shorter and longer section. Generally 10-30 breaks/metre.
Fractured	Core lengths are generally 80-400 mm with occasional shorter and longer sections. Generally 3-12 breaks/metre.
Slightly Fractured	Core lengths are generally 300-1000 mm with occasional shorter and longer sections. Generally 0-3 breaks/metre.
Unbroken	The core does not contain any natural breaks.

4 CLASSIFICATION

Field data were plotted to identify trends. Trends were analysed and common characteristics grouped together to form a series of rock mass classes which combined form a conceptual classification diagram. Plotting of individual outcrop on the classification enabled clusters to be identified indicative of the Torlesse rock mass for the purpose of assessing geological and rock mass controls. An objective of the classification is to characterise the variability in condition. Observations show the mudstone has consistent thin bed thickness, is fragmented and contacts with sandstone are typically sheared. The sandstone makes up a larger portion of the rock mass by volume and displays a higher degree of variability in condition. The classification attempts to capture variability in the sandstone while incorporating the typical mudstone characteristics.

4.1 Conceptual classification system

Rock mass condition was divided into two categories: blockiness and defect structure (Table 2). Blockiness describes the shape and size of blocks defined by bed thickness and fracture density. Thicker bedding was generally associated with a better quality rock mass. Where bed thickness decreased, fracture density generally increased. Bedding distribution is closely related to lithology where bed thickness decreased as the proportion of mudstone to sandstone increased. As such lithostructure appears to be a major control on rock mass condition in the Torlesse.

Defect structure describes the occurrence of systematic jointing and localised to regional scale faulting. The best rock mass typically had little to no faulting and is controlled by persistent (>2m long) jointing. As the level of shearing and faulting increased, the occurrence of persistent, systematic jointing decreased. A higher occurrence of shearing and faulting was related to rock mass lithology with a larger proportion of mudstone to sandstone in more closely bedded rock masses. This further highlights the lithostructural control on rock mass condition.

Categories describing both blockiness and defect structure were formulated such that rock mass conditions deteriorate from Class A to F and 1 through 6, respectively. Categories were plotted against each other to form a conceptual model termed the Torlesse rock mass classification

(TRC) as shown in Figure 2 to 4. A zone termed 'rock bordering major fault zones' was implemented as an indicator of increasing proximity toward a major structure. While a vast majority of outcrop plotting in this region are related to large scale faulting, the trend does not hold true in all circumstances and as such should only be used as an indicator.

Table 2: Blockiness and defect structure classes

Blockiness		
Class	**Lithostructure**	**Fracture Density**
A	Massive to thickly bedded sandstone	Slightly to moderately fractured
B	Medium bedded sandstone	Moderately to highly fractured
C	Massive to very thickly bedded sandstone	Highly fractured
D	Thinly bedded sandstone	Moderately to highly fractured
E	Massive to medium bedded sandstone	Fragmented
F	Thinly to very thinly bedded sandstone and mudstone	Fragmented
Defect Structure		
Class	**Dominant Structure**	**Secondary Components**
1	Persistent joints, moderate (rarely close) to very wide spacing	Shears and faults are rare
2	Persistent joints, moderate (rarely close) to very wide spacing	Shears and faults, very to extremely wide spacing
3	Persistent joints (moderate to very wide spacing, rarely close) and shears/faults (very to extremely wide spacing) in approximately equal portions	
4	Shears and faults, wide to extremely wide spacing	Persistent joints, moderate to very wide spacing
5	Shears and faults, moderate to wide spacing	Persistent joints are rare
6	Brecciated rock with very close to widely spaced sheared and crushed zones typical of major fault zones	

4.2 Defect condition

Intact strength and defect condition were found to vary less across blockiness and defect structure classes and as a result are not defined as major controls in the conceptual classification system. Typical defect conditions are summarised in Table 3. Notable trends include 1) bedding – degree of waviness increases in defect Class 4 and 5 rock where shearing is the major influence, 2) persistent joints – little change in condition between defect classes and 3) shears and faults – width of sheared zones and the degree of waviness both increase as the influence of shearing and crushing intensifies from Class 1 to 6.

Table 3: Typical condition of systematic defects (fresh rock)

Defect Type	**Roughness (2^{nd} order asperities)**	**Infill**	**Waviness (1^{st} order asperities)**	
			Inter-limb angle	**Wavelength**
Bedding	Undulating smooth or rough, some planar smooth	Clean	170-180° (gentle), some 150-170° (open); becoming 90-180° from Class 4 (close to gentle)	0.5-4m, usually ~2m
Joints	Undulating smooth or rough, some planar smooth or rough	Clean	170-180° (gentle), some 150-170° (open)	0.2-3m, usually ~2m
Shears	Sheared zone contacts undulating smooth or rough	Class 2-3: fragmented rock ~10-100mm wide Class 4: fragmented rock in a silty/sandy matrix up to 300mm wide Class 5-6: clay/silt/sand up to 2m wide	Class 2: 170-180° (gentle) Class 3 & 4: 150-180° (open to gentle) Class 5 & 6: 90-180° (close to gentle)	0.5-12m, usually ~3m

4.3 Elliott Fault

The trend of the Elliott Fault TRC (Figure 2) shows a gradation in rock mass character toward a regional structure with increasing levels of shearing toward the principal slip zone. Four clusters were identified. Cluster 1 is characterised by thick sandstone with minimal shearing and persistent jointing. Cluster 2 represents a transition zone between the main zones of movement and the intact rock of cluster 1. A higher degree of shearing is present with few persistent joints. The rock mass is controlled by incipient, low persistence (<2m) jointing. Cluster 3 represents the fragmented rock mass bordering the major fault zone. Cluster 4 represents the worst rock mass conditions. Rock is completely fragmented and behaves as a soil. More intact blocks bound by shearing are common and observed from cm to meter sized blocks.

4.4 Hurunui River

The Hurunui River represents the best rock mass conditions in this study (Figure 2). Five rock mass classes are present. Cluster 1 represents the bulk of the data and presents the best rock mass. Cluster 2 presents a more fractured rock mass. The rock mass still contains some persistent joints, however, the small discrete joints have an effect on the rock mass making the cluster transitional between systematic and non-systematic joint control. Cluster 3 represents a similar rock mass with increased levels of faulting. Cluster 4 is characterised by thin bedding that is faulted and sheared. Persistent jointing is uncommon and low persistence fracturing dominates. Cluster 5 represents a fragmented rock mass with some persistent joints. The rock mass has a high degree of faulting and shearing irrespective of bedding thickness.

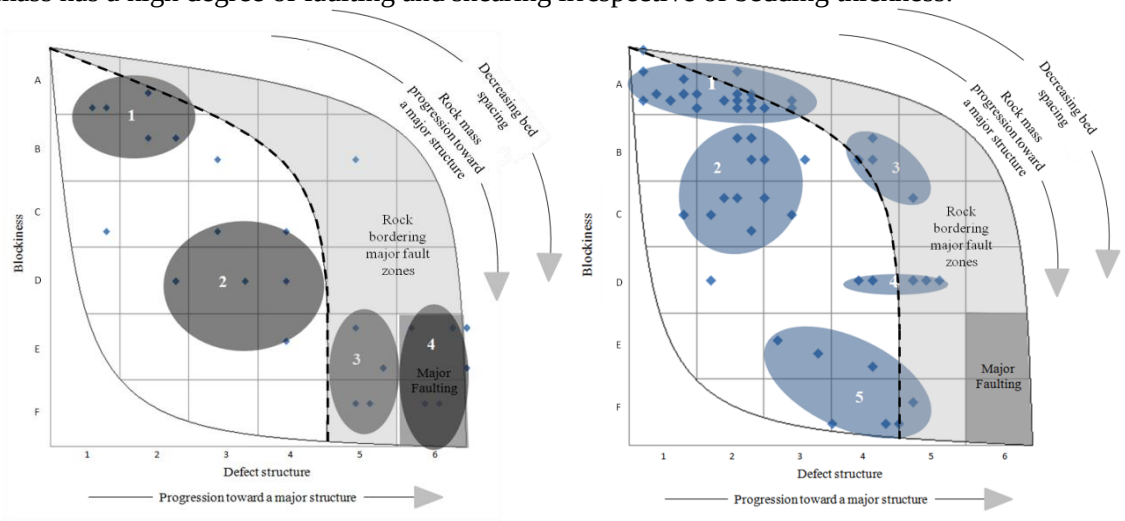

Figure 2: Left: Elliott Fault TRC plot; right: Hurunui River TRC plot.

4.5 Opuha Dam

A range of conditions were observed primarily due to the Opuha Dam Fault (Figure 3). Cluster 1 represents the best rock mass. Cluster 2 is similar to cluster 1 however an increase in the level of small scale shearing is present in close proximity to the Opuha Dam Fault. Cluster 3 has a higher degree of fracture in similar thickly bedded sandstone with similar levels of shearing. Cluster 4 is a fragmented rock mass, with numerous shears, but also contains some persistent jointing. Cluster 5 represents the fault breccia zone. Material here primarily acts as a soil with intact blocks rarely exceeding 2cm in size. Small scale (<10cm) zones of plastic, silt sized, brown gouge material can be differentiated along apparent primary slip zones.

4.6 Ashley River Gorge

The Ashley River Gorge site represents a sampling of all rock mass types exhibited in other sites (Figure 3). Eight clusters are identified in the Ashley Gorge dataset. All clusters are similar to descriptions at other sites.

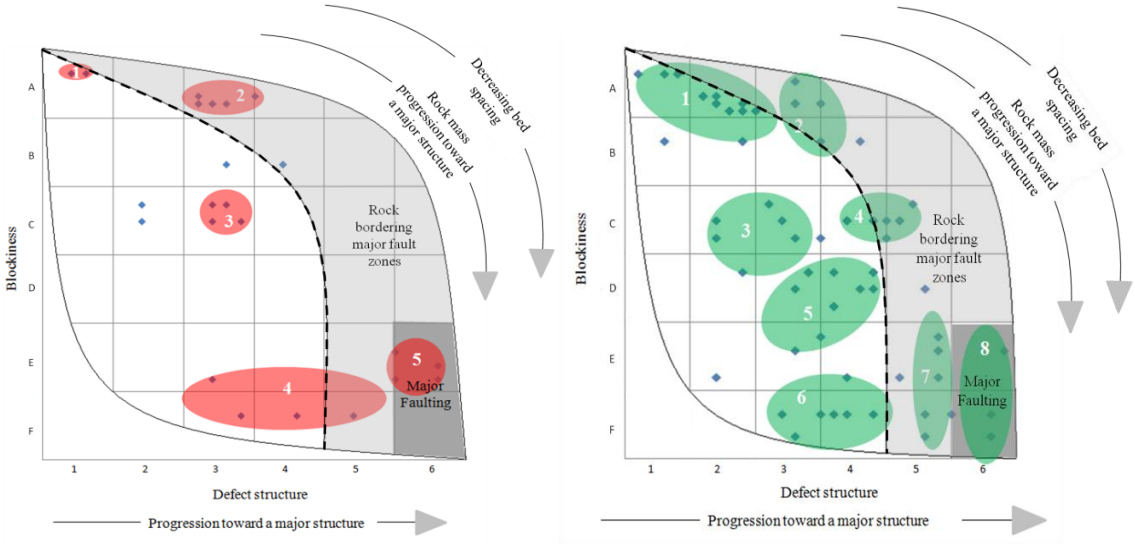

Figure 3: Left: Opuha Dam TRC plot; right: Ashley River Gorge TRC plot.

5 DISCUSSION

5.1 Application to tunnel assessment

Identifying clustering in the TRC allows characterisation of the range in rock mass conditions likely to be encountered throughout the Torlesse. Figure 4 presents eight different rock mass types identified from the overlay of TRC site clustering. Table 4 summarises the characteristics of each rock mass type. Each type has a series of geological controls that influence the nature of the rock mass. Rock mass conditions can be evaluated starting with desktop study information, lineation analysis followed by field observation. Assessment of geological controls can then aid in the prediction of rock mass conditions for tunnel alignment selection. The alignment can be divided into rock mass types to allow preliminary assessment of tunnelling conditions including implications such as support, equipment specification, advance rates, groundwater and so on.

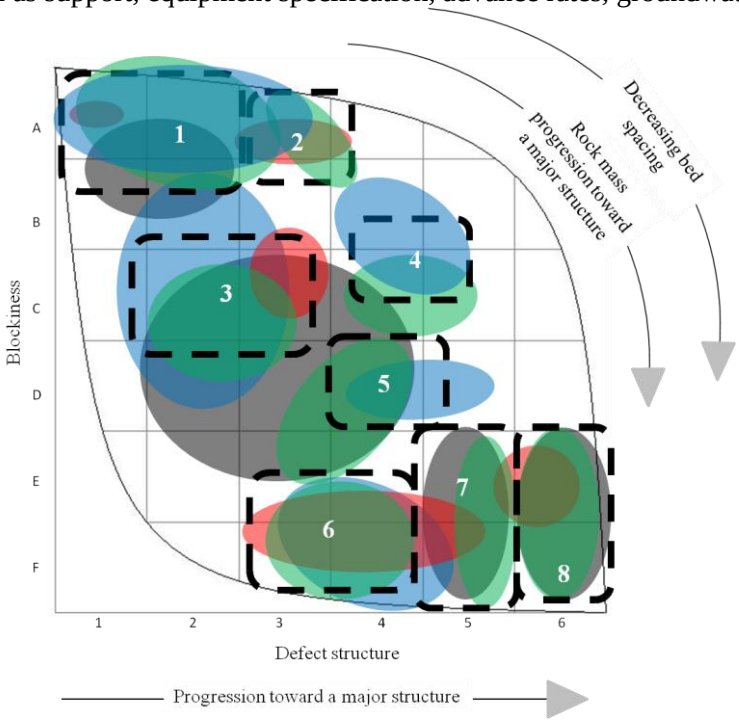

Figure 4: TRC plot of individual outcrop clusters

5.2 Geological controls on rock mass condition

Understanding geological controls can aid in the prediction of rock mass conditions. A dominant control in the Torlesse identified in this study is lithostructure, specifically the effect of lithology on bedding thickness and fracturing by non-systematic jointing. The distribution of mudstone bands is a major control on bedding thickness. Mudstone, being the weaker of the lithotypes, appears to localise and accommodate stress within the rock mass and is therefore typically highly strained. The result is fracturing to the point of fragmentation of mudstone beds and localised shearing of the contacts with the stiffer sandstone interbeds.

Medium to massive bedding as part of Types 1 and 2 (Figure 4, Table 4) result in the best rock mass. In the sandstone rich mass, systematic jointing dominates with less shearing and faulting and a lower occurrence of short, discrete, non-systematic jointing, although there is always a degree of fracturing present. Conversely, the thin bedded Torlesse represented by Type 5 lacks persistent jointing. This type, being mudstone dominant, fractures more easily, is characterised by short, discrete jointing and tends to localise faulting, shearing and some folding.

Modern tectonic stress fields are also a major control. The size of tectonic structure can impact on different volumes of rock. Rock outside the direct fault zone can also be impacted giving rise to Type 6 conditions. For example, increased levels of shearing are observed within adjacent rock at both the Elliott and Opuha Dam Faults. Proximity to major faulting is also a large influence on fracture density and is related to differences in stress fields throughout the complex tectonic history of the Torlesse. Types 3 and 4 represent a transition from the best to worst rock mass conditions. Both lithostructure and major faulting may have an influence without a definitive control being obvious.

Future studies will include differentiating conditions of sheared zones related to older, inactive fault zones from younger, active faulting. Older sheared zones can be recemented or annealed potentially giving rise to higher shear strengths relative to more recent fault related structures.

Table 4: Rock mass type characteristics

Type	Bedding & Lithology	Fracturing	Defect structure (spacing based on ISRM (1978)
1	Thick to massive sandstone	Slight to moderate	Persistent, moderate (rarely close) to very wide spaced joints with rare faults and shears
2	Thick to massive sandstone	Slight to moderate	Moderate to very wide spaced, common persistent jointing with wide to extremely wide faults/shears in equal portions
3	Medium to massive sandstone	High	Dominant, persistent joints, moderate (rarely close) to very widely spaced with shears and faults, very to extremely wide spacing, sometimes in equal portions
4	Medium to massive sandstone	High	Dominant, wide to extremely wide shears and faults, with persistent jointing (sometimes rare) moderate to very wide in spacing
5	Thin sandstone	Moderate to high	Dominant, wide to extremely wide shears and faults, with infrequent persistent jointing moderate to very wide in spacing
6	Very thin to massive sandstone & mudstone	Fragmented	Persistent, (rarely close) moderate to very widely spaced jointing with very wide to extremely wide shears/faults in both equal and shear/fault favouring portion
7	Very thin to massive sandstone & mudstone	Fragmented	Shears and faults, moderate to widely spaced, with rare occurrences of persistent jointing
8	Very thin to massive sandstone & mudstone	Fragmented	Brecciated rock with very close to widely spaced sheared and crush zones typical of major fault zones

6 CONCLUSION

Variability in engineering geological condition of the Torlesse Composite Terrane specific to Canterbury, New Zealand, has been assessed in this paper. Four sites were selected to represent all Torlesse terrane and regional structure conditions with the resulting mapping information analysed to observe rock mass trends. Bedding thickness, fracture density and defect structure were found to be the differentiating characteristics across the range of rock mass conditions. These attributes were related together to form the Torlesse rock mass classification (TRC). Each outcrop was plotted on the TRC to derive rock mass types with clustering of points used to highlight regions indicative of the range in Torlesse rock mass condition. Eight rock mass types were identified ranging from massive sandstone controlled by systematic persistent jointing to incipient fractured, brecciated and shear dominated fault rock. Lithostructure and tectonic stresses resulting in major to regional scale faults are the key influences on rock mass condition. The TRC enables assessment of geological controls for predicting rock mass conditions, which can be used for alignment selection and assessment of tunnelling implications.

REFERENCES

Cox, S. C. & Barrell, D. J. A. 2007. *Geology of the Aoraki Area*, Institute of Geological & Nuclear Sciences, Lower Hutt, New Zealand.

Forsyth, P. J., Jongens, R. & Barrell, D. J. A. 2008. *Geology of the Christchurch area*, Institute of Geological and Nuclear Sciences, Lower Hutt, New Zealand.

ISRM 1978. *Suggested methods for the quantitative description of discontinuities in rock masses*, International Society for Rock Mechanics. Pergamon Press.

Mortimer, N. 2004. New Zealand's geological foundations. *Gondwana Research,* 7**,** 261-272.

Nathan, S., Rattenbury, M. S. & Suggate, R. P. 2002. *Geology of the Greymouth area*, Institute of Geological & Nuclear Sciences, Lower Hutt, New Zealand.

NZGS 2005. Field Description of Soil and Rock. *Guidelines for the field classification and description of soil and rock for engineering purposes.* New Zealand Geotechnical Society Inc.

Pettinga, J. R., Yetton, M. D., Van Dissen, R. J. & Downes, G. 2001. Earthquake source identification and characterisation for the Canterbury region, South Island, New Zealand. *Bulletin of the New Zealand Society for Earthquake Engineering,* 34**,** 282-317.

PSM 2010. PSM Guideline Geotechnical Line Mapping. Internal document: Pells Sullivan Meynink.

Rattenbury, M., Townsend, D. & Johnston, M. 2006. *Geology of the Kaikoura area*, Institute of Geological and Nuclear Sciences, Lower Hutt, New Zealand.

Read, S. & Richards, L. 2007. Characteristics and classification of New Zealand greywackes. *Rock Mechanics: Meeting Society's Challenges and Demands, Two Volume Set.* Taylor & Francis.

Read, S. A., Richards, L. & Perrin, N. D. 2000. Assessment of New Zealand greywacke rock masses with the Hoek-Brown failure criterion. *GeoEng2000, Melbourne***,** 20-24.

Richards, L. & Read, S. 2007. New Zealand greywacke characteristics and influences on rock mass behaviour. *The Second Half Century of Rock Mechanics, Three Volume Set.* Taylor & Francis.

Stewart, S. W. 2007. *Rock mass strength and deformability of unweathered closely jointed New Zealand greywacke.* Doctor of Philosophy, unpublished thesis, University of Canterbury, Christchurch, New Zealand.